

NOTE TO USERS

This reproduction is the best copy available.

UMI[®]

**SPATIALLY-EXPLICIT HABITAT CHARACTERIZATION,
SUITABILITY ANALYSIS, VERIFICATION, AND
MODELLING OF THE YELLOW PERCH *Perca
flavescens* (Mitchell 1814) POPULATION IN LONG
POINT BAY, LAKE ERIE**

By

SUSAN ELISABETH DOKA, H.B.SC., M.SC.

**A thesis submitted to the School of Graduate Studies
in partial fulfilment
of the requirements for the Degree of**

Doctor of Philosophy

McMaster University

2004

Approved by: Dr. Charles K. Minns
Chairperson of Supervisory Committee

Dr. Jurek Kolasa

Dr. Brian Shuter

Dr. D. Gordon McDonald

Program Authorized
to Offer Degree: Biology Department

Date: May 28, 2004

**SPATIAL HABITAT ASSESSMENT OF YELLOW PERCH
IN LONG POINT BAY**

Doctor of Philosophy (2004)
(Biology)

McMaster University
Hamilton, Ontario

TITLE: Spatially Explicit Habitat Characterization, Suitability
 Analysis, Verification, and Modelling of the Yellow Perch
 Perca flavescens (Mitchell 1814) Population in Long Point
 Bay, Lake Erie

AUTHOR: Susan Elisabeth Doka, H.B.Sc. (University of Western
 Ontario), M.Sc. (University of Guelph)

SUPERVISOR: Charles K. Minns, Ph.D.

Number of pages: xxii, 250, A-67

McMaster University
Abstract

**Spatially-Explicit Habitat Characterization, Suitability Analysis,
Verification and Modelling of the Yellow Perch, *Perca flavescens*
(Mitchill 1814), Population in Long Point Bay, Lake Erie**

by Susan Elisabeth Doka

Chairperson of the Supervisory Committee: Dr. Charles K Minns
Adjunct Professor
Department of Biology

Different approaches were used to characterize, assess, test and model the fish-habitat interactions of yellow perch in Long Point Bay. Chapter 1 describes the methodologies for explicitly characterizing spatial and temporal habitat through mapping and modelling. Chapter 2 connects habitat and ontogenetic niche shifts in perch life history, with the aim of determining suitable habitat availability for the Long Point Bay perch population. Habitat suitability indices and models were used to map and identify the areas of suitable habitat, including thermal habitat. Chapter 3 compares a known distribution of yellow perch larvae with HSI predictions of habitat suitability as a validation exercise. Abundance and size distributions from the survey were compared to thermal and HSI predictions of suitable habitat to test for correspondence. The relationship between food availability and habitat characteristics, especially vegetation, were also tested. A model was developed in Chapter 4 that concentrated on the first year of life and the effect of consecutive constraints on early life stages with different habitat requirements. The purpose of the model was to compare the potential growth and survival of consecutive life stages in a spatially explicit manner when different habitat-based rules are imposed. The results highlight the importance of life history theory and knowledge of mechanisms used in habitat selection for determining limits to fish production.

ACKNOWLEDGEMENTS

Graduate Supervisor: Dr. Charles K. Minns

Your patience, direction, and support during graduate studies and at the beginning of my career are very much appreciated. Thank you for being a role model.

Advisory Committee Members: Drs. Jurek Kolasa, D. Gordon

McDonald, and Brian Shuter. Jurek, you always welcomed me on campus and at home, and provided positive feedback when I needed it most. Gord, your input on fish physiology and temperature was very much appreciated. Brian, your laughter is contagious, I never had to explain anything twice, and you helped me hone the focus of my thesis. Thank you all for your support, I could not have asked for a better committee.

Examination committee members: Drs. Edward S. Rutherford, Carl

Riehm, and Peter MacDonald. Ed, thank you so much for your thorough comments and encouragement towards publishing manuscripts. Thank you all for making my defence an enjoyable experience.

Technical & Field Help: Ron Buliung, Carolyn Bakelaar, Peter Brunette, Mike Stoneman, Christine Boston, Gale Bravener, Mandi Clark, Cindy Chu, Georgina Fodor, Bill Williston, Bud Timmins, Paul Ashley, Larry Witzel, Phil Ryan, Sarah Bartnik, Jennifer Bowman, Bill Schertzer, Mike Jones, Nigel Lester, Dan Hayes; Cristina Dimitru, Ora Johannsson, Chris Giroux, Tom MacDougall; Donna Graham; Dave Pyatt; Chris Lomas; Bob Rowsell; Bruce Petrochuk at Talisman Energy; Mike Johnston in Hydrography; Capt. Morris and the crew of the CCG Gull Isle; Tara Frezza; Mary Hollinger at NCAAS, and Nelson May at the Stennis Space Center all contributed in their own way to this document.

Family & Friends: To my husband, Timothy Pascoe, I would not have been able to accomplish what I did without your support on so many levels. Thank you for standing by me. To the extended Doka and Pascoe families, and all the friends I have met through work and school, your gentle ribbing and encouragement kept me sane and on track. Thank you all. It is done!

TABLE OF CONTENTS

Abstract	iii
Acknowledgements	iv
List of Figures	ix
List of Tables	xx
List of Appendices	xxi
List of Abbreviations	xxii
GENERAL INTRODUCTION	1
CHAPTER 1: Characterizing physical habitat from a fish's perspective	7
1.0 INTRODUCTION.....	8
1.0.1 Spatial Issues and Fish Habitat	8
1.0.2 Physical Habitat Variables	10
Bathymetry	11
Substrate Type	11
Vegetation	11
Temperature	12
Wind, Waves & Exposure	13
Other Factors.....	14
1.1 METHODS & RESULTS	14
1.1.1 Shoreline	15
1.1.2 Spatial Resolution	19
1.1.3 Bathymetry and Water Depth	20
1.1.4 Substrate Type & Vegetation.....	21
CASI survey.....	22
Offshore Substrate Surveys.....	22
Substrate Type Standardization	24
Vegetation Standardization & Time-series Modelling	25
1.1.5 Thermal Data.....	29
Lake Erie Biomonitoring Temperature Data.....	29
AVHRR Imagery	30
Nearshore Temperature Study	35
1.1.6 Thermal Structure Recreation	40
1993/94 3D Thermal Structure	40
1999 3D Thermal Structure	41
Correction of Nearshore SST Errors.....	42
Surface Temperature Temporal Interpolation	44
Temperature Profile Generation	46
1.1.7 Winds & Exposure	56
1.2 DISCUSSION.....	57

CHAPTER 2: Thermal and physical habitat assessment for yellow perch at different life stages.	60
2.0 INTRODUCTION.....	61
2.0.1 Habitat Suitability Indices and Habitat Modelling.....	61
2.0.2 Long Point Bay Yellow Perch Habitat Assessment	64
2.1 METHODS	65
2.1.1 Suitable Thermal Habitat Assessment.....	65
Egg Development & Survival	66
Age-0 Survival (Pelagic and Demersal Stages).....	67
Juveniles & Adults	68
2.1.2 Overall Habitat Suitability Assessment.....	69
2.2 SUITABLE THERMAL HABITAT RESULTS	71
2.2.1 Spawning & Egg Thermal Habitat.....	71
2.2.2 Pelagic Larva and Demersal YOY Thermal Habitat	73
2.2.3 Juvenile & Adult Thermal Habitat	75
2.3 OVERALL HABITAT SUITABILITY RESULTS.....	76
2.3.1 Overall Spawning & Egg Habitat Suitability	77
2.3.2 Overall Pelagic Larvae Habitat Suitability.....	78
2.3.3 Overall Demersal Larvae Habitat Suitability	80
2.3.4 Overall Juvenile and Adult Habitat Suitability	81
2.4 CONCLUSIONS.....	83
2.4.1 Thermal Habitat.....	83
Spawning & Egg Thermal Habitat.....	84
Larval & YOY Thermal Habitat	85
Juvenile & Adult Thermal Habitat	86
2.4.2 Overall Habitat Assessment	87
 CHAPTER 3: Does suitable habitat predict fish distributions?.....	90
3.0 INTRODUCTION.....	91
3.0.1 <i>P. flavescens</i> Early Life History and Habitat Associations...	92
3.0.2 Prey Availability, Habitat, and YOY Distributions.....	93
3.1 METHODS	94
3.1.1 Fish & Zooplankton Data	94
3.1.2 Habitat & Suitability Information	95
3.1.3 Data Analysis	97
3.2 RESULTS	97
3.2.1 YOY Perch Distributions.....	97
3.2.2 Crustacean Zooplankton Distributions.....	101
3.3 CONCLUSIONS.....	106
 CHAPTER 4: Can habitat be linked to fish population dynamics? If so, how does habitat limit fish production?	110
4.0 INTRODUCTION.....	111

4.0.1	Habitat Associations with Population Dynamics	112
4.0.2	Computer Simulation Modelling	114
4.0.3	Model Review	116
	Population Models with Environmental Relationships.....	116
	Metapopulation Models.....	117
	Reaction-diffusion Models	118
	Individual-based Models	119
	Bioenergetic-based Habitat Models	120
	Habitat Models.....	121
	Spatially Explicit Models	122
	Other Yellow Perch Models	125
4.1	METHODS	125
4.1.1	Bounding in Time, Space and Subsystems	126
4.1.2	Definition of Model Complexity	126
4.1.3	Data Requirements.....	127
4.1.4	Conceptual Diagrams	128
4.1.5	Equations	128
4.1.6	Yellow Perch Model Description	130
	Spawning and Habitat.....	130
	Egg Survival and Development	132
	YOY Stage Growth (Pelagic Phase).....	137
	YOY Stage Survival (Pelagic Phase).....	141
4.1.7	Model Output Variables	142
4.1.8	Testing Habitat Limitations Using Scenarios	143
	Spawning.....	145
	Egg Development & Survival	145
	Larval Growth and Survival.....	146
4.2	RESULTS	147
4.2.1	Uniform Spawning Scenario Combinations	147
4.2.2	Habitat-Effects Spawning, Scenario Combinations	158
	Equal Initial Egg Distribution	158
	Ideal-Free Initial Egg Distribution.....	168
4.2.3	Thermal & Habitat-Effects Spawning Scenarios.....	177
	Equal Initial Egg Distribution	177
	Ideal-Free Initial Egg Distribution.....	188
4.2.5	Final Scenario Comparisons	198
4.3	DISCUSSION & CONCLUSIONS	199
4.3.1	Life History Stages	199
	Spawning.....	200
	Egg Stage.....	201
	YOY Stage.....	201
	Individual Growth vs. Larval Production.....	202
4.3.2	Limiting Life Stage	204
4.3.3	Space & Time Limitations.....	206
4.3.4	Overwinter Survival	211
4.3.5	General Conclusions	215

OVERALL CONCLUSIONS	217
UNCERTAINTY IN THE ANALYSES	225
FUTURE ANALYSES.....	229
BIBLIOGRAPHY	233
APPENDICES	A-1

LIST OF FIGURES

Figure A: Outline of steps used in the habitat assessment of the yellow perch population	6
Figure 1.01: Grid matrix based on SST imagery resolution (1.4 km) used for standardizing habitat variables and in habitat-based modelling of the early life history stages of yellow perch.....	19
Figure 1.02: One-metre bathymetric contours of waters in Long Point Bay and Lake Erie south of Long Point spit.	21
Figure 1.03: Several scenes of CASI survey information on submergent vegetation percent cover categories for the tip of Long Point sand bar. CASI survey raster information is very detailed at 3-m resolution.	22
Figure 1.04: Several scenes of the CASI survey on substrate type for the tip of Long Point at 3-m resolution. Substrate type in dense submergent vegetation was assigned a combination of sand/muck/clay.	23
Figure 1.05: Voronoi polygons for substrate type interpolated from point survey data in Rukavina (1976) and Thomas <i>et al.</i> (1976) for an offshore survey of Lake Erie, including Long Point Bay.....	23
Figure 1.06: Comparison of the percent composition (log scale) of standardized substrate type classifications in the nearshore zone (CASI survey < 5 m) and in all of Long Point Bay, Lake Erie	24
Figure 1.07: Dominant substrate type by cell in the habitat grid of Long Point Bay, Lake Erie.....	25
Figure 1.08: Dominant submergent vegetation category by cell, standardized to the habitat matrix resolution (Long Point Bay, Lake Erie).	26
Figure 1.09: Percent composition of standardized vegetation categories in the nearshore zone compared to all of Long Point Bay, Lake Erie in July, 1995.....	26
Figure 1.10: Example of the daily vegetation category changes due to modelled growth and senescence of macrophytes in a cell of the habitat grid with 21% emergent cover , 3% moderate density and 76% high density submergent coverage during peak times in Long Point Bay.....	28
Figure 1.11: Lake Erie Biomonitoring sites for profile data (1993-1994), OMNR temperature logger locations (inner bay site is continuous through most of the 90s, other sites were 1999 only) including the Port Dover water intake, and nearshore temperature logger locations (1999) used in this thesis	30
Figure 1.12: 1993 temperature profile time-series interpolated from biweekly profile samples taken at the outer bay LEB stations (E1, E2, E3) and extrapolated using available ice cover data for Long Point Bay, Lake Erie.	31
Figure 1.13: 1994 temperature profile time-series interpolated from weekly profile samples taken at the outer bay LEB stations and extrapolated using available ice cover data for Long Point Bay, Lake.	32

Figure 1.14: Example of the lower Great Lakes scene from AVHRR SST imagery, May 10, 1993 showing the high degree of spatial variability possible at different time of the year.....	33
Figure 1.15: Daily temperature averages for the inner bay logger sites in 1999 (see Figure 1.10 for datalogger locations).	39
Figure 1.16: Daily temperature averages for the outer bay logger sites in 1999 & 2000 (see Figure 1.10 for datalogger locations).	39
Figure 1.17: Thermal layers for May 10, 1993 in Long Point Bay based in interpolation and extrapolation of SST imagery and LEB profile data.	40
Figure 1.18: Long Point bottom 1-m temperatures extrapolated and interpolated from SST imagery and LEB profiles for different dates in 1993. May 10th temperatures were draped over a TIN of Long Point Bay derived from bathymetry values.....	41
Figure 1.19: Thermal regions used in temperature modelling based on statistical analysis of satellite and dataloggers temperature data.	43
Figure 1.20: Map of significant regression coefficients ($p < 0.05$) calculated for converting temperatures at different datalogger locations in Long Point Bay. Arrows point to the independent variable in regression equations.	45
Figure 1.21: Temperature differences between 0.5-m intervals for temporally interpolated profiles at LEB Station E1 in 1993 & 1994.....	47
Figure 1.22: Temperature differences between 0.5-m intervals for temporally interpolated profiles at LEB Station E3 in 1993 & 1994.....	47
Figure 1.23: Temperature differences between 0.5-m intervals for temporally interpolated profiles at LEB Station E2 in 1993 & 1994.....	48
Figure 1.24: Logical statements to correct for predicted thermocline depths that are outside of boundary conditions.....	50
Figure 1.25: The slope of the equation for predicting the change in temperature over the mesolimnion from mesolimnion thickness was related to site depth by the relationships shown.....	52
Figure 1.26: Latitudinal cross-section of profiles through inner and outer Long Point Bay in late spring, 1999 (See Figure 1.0 for Cell IDs). Surface temperatures ranged from 20 to 9 oC.....	55
Figure 1.27: Time-series of profiles for a 40-m deep site in outer Long Point Bay in May and June, 1999 showing thermocline set-up, upwelling and downwelling events in mid-June.	55
Figure 1.28: Example of an exposure map for Long Point Bay, Lake Erie based on July 15, 1999 wind conditions. Exposure values were calculated according to Keddy (1984).....	57
Figure 1.29: Frequency distribution of exposure values calculated for all grid cells and days in 1999 in Long Point Bay, Lake Erie.	57

Figure 1.30: Structure of the habitat database used for modelling. Grid cell IDs linked the habitat attributes between tables, and date linked the daily habitat attributes.	59
Figure 2.01: Habitat suitability model framework for yellow perch from Krieger <i>et al.</i> (1983).	63
Figure 2.02: Habitat suitability of bottom temperatures (°C) for yellow perch eggs based on polynomial equation (2.1).....	66
Figure 2.03: Thermal suitability curve for planktonic and demersal stages of age-0 yellow perch (Equation 2.2)	67
Figure 2.04: Thermal suitabilities for juvenile and adult yellow perch based on (Equations 2.3 and 2.4) and estimated from a bioenergetics model	69
Figure 2.05: Perch egg thermal habitat suitabilities in May 1993 draped over a 3D-representation of bathymetry (elevation) in Long Point Bay, Lake Erie.	72
Figure 2.06: Bottom thermal suitabilities for perch eggs on selected dates between April 6 and June 23 1993, when AVHRR SST satellite imagery was available, in Long Point Bay, Lake Erie.	72
Figure 2.07: Daily time-series of epilimnetic thermal suitabilities for larval yellow perch based on the average temperature in the top 6 m of Long Point Bay from July 1 - 31, 1999.....	74
Figure 2.08: Average thermal suitabilities during the pelagic (June; 0-6m) and demersal (July – Sept; bottom) larval stages for 1993 in Long Point Bay, Lake Erie.....	75
Figure 2.09: Juvenile thermal habitat suitabilities for growth at 5-m depth intervals on selected dates (May 26, June 23, July 20, August 25, October 5, and November 21) spanning the growing season in 1993.	76
Figure 2.10: Adult thermal habitat suitabilities for growth within the top 20 m on selected dates in 1993 during the adult growing season in Long Point Bay, Lake Erie. The seasonal average for June to September is also shown.....	77
Figure 2.11: Spawning & egg suitabilities for the different habitat variables assessed in Long Point Bay, Lake Erie.	78
Figure 2.12: Pelagic larval (PL) suitabilities for the different habitat variables assessed in Long Point Bay, Lake Erie	79
Figure 2.13: Demersal larval (DL) suitabilities for the different habitat variables assessed in Long Point Bay, Lake Erie.	80
Figure 2.14: Juvenile perch suitabilities for the different habitat variables assessed in Long Point Bay, Lake Erie.	82
Figure 2.15: Adult perch suitabilities for the different habitat variables assessed in Long Point Bay, Lake Erie.	83
Figure 3.01: DFO and OMNR sampling locations on August 27-28, 1998 in the Inner Bay at Long Point, Lake Erie showing both planned and surveyed sampling locations for young-of-the-year fish and zooplankton samples.....	94

Figure 3.02: Average temperatures in August 1998 in the Inner Bay of Long Point Bay, Lake Erie converted to YOY thermal suitabilities based on survival probabilities.....	95
Figure 3.03: Physical habitat maps of the Inner Bay of Long Point, including aquatic vegetation, substrate type and bathymetry.....	96
Figure 3.04: YOY abundance (# of individuals per 10-minute trawl) and average larval weight (mg) per trawl captured during an August, 1998 larval perch survey in the Inner Bay of Long Point Bay, Lake Erie	97
Figure 3.05: YOY abundance (CPUE = # of individuals per standard-length trawl) plotted against average individual YOY weight per trawl (g) from a larval spatial survey conducted in Long Point Bay	98
Figure 3.06: YOY abundance (# of individuals per trawl) and average YOY weight per trawl (mg) from a larval spatial survey conducted in Long Point Bay plotted against the larval thermal suitability at each sampling point during August, 1998 based on average August temperatures.....	98
Figure 3.07: YOY abundance (# of individuals per standard trawl) and average YOY weight per trawl (mg) from a larval spatial survey conducted in Long Point Bay plotted against the larval habitat suitability at each sampling point during August, 1998 based on depth, vegetation and substrate type associations.....	99
Figure 3.08: YOY abundance (# of individuals per standard trawl) and average YOY weight per trawl (g) from a larval spatial survey conducted in Long Point Bay during August, 1998 plotted against the water depth (rounded to nearest 0.5 m) at each sampling point from bathymetry data.....	100
Figure 3.09: YOY abundance (# of individuals per standard trawl) and average YOY weight per trawl (g) from a larval spatial survey conducted in Long Point Bay plotted against the proportion of sand in substrates at each sampling point during August, 1998.....	100
Figure 3.10: YOY abundance (# of individuals per standard trawl) and average YOY weight per trawl (g) from a larval spatial survey conducted in Long Point Bay plotted against the proportion of submergent vegetation cover at each sampling point during August, 1998.....	101
Figure 3.11: Zooplankton densities and total biomass (1000s of individuals or milligrams per cubic metre) collected during a spatial survey of the Inner Bay in Long Point Bay, Lake Erie during August 1998	102
Figure 3.12: Zooplankton density plotted against total zooplankton biomass from a spatial survey conducted in Long Point Bay	102
Figure 3.13: Zooplankton density (# per cubic metre) and biomass (mg per cubic metre) collected during a spatial survey on August 24-25, 1998 of the Inner Bay of Long Point Bay, Lake Erie plotted against the average temperature of the site for the previous 2 weeks.....	103
Figure 3.14: Zooplankton density (# per cubic metre) and biomass (mg per cubic metre) collected during a spatial survey of the Inner Bay of Long Point Bay, Lake Erie plotted against the depth derived from bathymetric data.....	103

Figure 3.15: Zooplankton density (# per cubic metre) and biomass (mg per cubic metre) collected during a spatial survey of the Inner Bay of Long Point Bay, Lake Erie plotted against the proportion of sandy substrate at the sampling point....	104
Figure 3.16: Zooplankton density (# per cubic metre) and biomass (mg per cubic metre) collected during a spatial survey of the Inner Bay of Long Point Bay, Lake Erie plotted against the proportion of submergent vegetation cover at the sampling point.....	104
Figure 3.17: Zooplankton densities (# per cubic metre) versus YOY abundance (# per trawl) at each point in the spatial survey conducted in August 1998 in the Inner Bay of Long Point Bay, Lake Erie	105
Figure 3.18: Zooplankton densities (# per cubic metre) versus YOY abundance (# per trawl) at each point in the spatial survey conducted in August 1998 in the Inner Bay of Long Point Bay, Lake Erie	105
Figure 4.01: Flowchart of model building steps defined by Jorgensen	115
Figure 4.02: Conceptual diagram of how habitat relates to the first-year life stages of yellow perch.....	128
Figure 4.03: The frequency distribution of exposure values for all cells in the habitat matrix during 1999	132
Figure 4.04: The relationship between temperature and the time to develop in days for yellow perch eggs	134
Figure 4.05: The relationship between temperature during development and the percentage of hatched eggs that are normal for yellow perch.....	135
Figure 4.06: The relationship between temperature experienced during egg development and the hatch length of yellow perch yolk-sac fry	136
Figure 4.07: The relationship between temperature and the percent survival of yellow perch yolk-sac fry to the swim-up stage after	136
Figure 4.08: Generalised annual, maximum zooplankton density in the Long Point Bay region.....	140
Figure 4.09: Schematic diagram of order of operations in the model logic.....	143
Figure 4.10: Flow diagram outlining how the life stage-specific scenarios were combined and tested concomitantly	144
Figure 4.13: Frequency distribution of virtual eggs hatched per cell and total number of eggs hatched in Long Point Bay by spawning date in 1999 under Scenario S1E1 conditions; temperature effects after spawning	148
Figure 4.14: Frequency distribution of virtual eggs hatched per cell and the total number of eggs hatched in Long Point Bay by hatch date in 1999 under Scenario S1E1 conditions; temperature effects after spawning	149
Figure 4.15: Monthly maps of the total number of virtual eggs hatched in each cell in Long Point Bay by spawning month, March until October, 1999 under Scenario S1E1 conditions	150

Figure 4.16: Monthly maps of the total number of virtual eggs hatched in each cell in Long Point Bay by spawning month, March until October, 1999 under Scenario S1E2 conditions 150

Figure 4.17: Frequency distribution by spawning date of virtual YOYs per cell and the total number of YOYs that survived to October 31, 1999 in Long Point Bay under Scenario S1E1L1 conditions; spawning with temperature effects on eggs & larvae 151

Figure 4.18: Monthly maps of the total number of virtual YOYs that survive until October 31st in each cell in Long Point Bay by spawning month, March until October, 1999 under Scenario S1E1L1 conditions 152

Figure 4.19: Frequency distribution by spawning date of YOY average size (g) per cell and the total production of YOYs (kg) that survived to October 31, 1999 in Long Point Bay under Scenario S1E1L1 conditions; uniform spawning, temperature effects on eggs and larvae 153

Figure 4.20: Monthly maps of the average weight gain (g) of virtual YOYs that survive until October 31st in each cell in Long Point Bay by spawning month, March until October, 1999 under Scenario S1E1L1 conditions 153

Figure 4.21: Monthly maps of the total production (kg) of virtual YOYs that survived until October 31st in each cell in Long Point Bay from the month of spawning in 1999 under Scenario S1E1L1 conditions 154

Figure 4.22: Frequency distribution by spawning date of virtual YOYs per cell and the total YOYs that survived to October 31, 1999 in Long Point Bay (Scenario S1E1L2; spawning with temperature effects on eggs, temperature and habitat effects on larvae) 155

Figure 4.23: Monthly maps of the total number of virtual YOYs that survive until October 31st in each cell in Long Point Bay by spawning month, March until October, 1999 under Scenario S1E1L2 conditions 156

Figure 4.24: Frequency distribution by spawning date of YOY average size (g) per cell and the total production of YOYs (kg) that survived to October 31, 1999 in Long Point Bay under Scenario S1E1L2 conditions; spawning with temperature effects on eggs and temperature & habitat effects on larvae 156

Figure 4.25: Monthly maps of the average weight gain (g) of virtual YOYs that survive until October 31st in each cell in Long Point Bay by spawning month, March until October, 1999 under Scenario S1E1L2 conditions 157

Figure 4.26: Monthly maps of the total production (kg) of virtual YOYs that survived until October 31st in each cell in Long Point Bay from the month of spawning in 1999 under Scenario S1E1L2 conditions 157

Figure 4.27: Frequency distribution of virtual eggs spawned per cell and total number of eggs spawned in Long Point Bay by date in 1999 under Scenario S2 conditions; habitat selection 158

Figure 4.28: Monthly maps of the total number of virtual eggs spawned in each cell in Long Point Bay from March until October, 1999 under Scenario S2 conditions 159

Figure 4.29: Frequency distribution of virtual eggs hatched per cell and the total number of eggs hatched in Long Point Bay by spawning date in 1999 under Scenario S2E1 conditions; spawning site selection and temperature effects on eggs	160
Figure 4.30: Frequency distribution of virtual eggs hatched per cell and the total number of eggs hatched in Long Point Bay by hatch date in 1999 under Scenario S2E1 conditions; spawning site selection and temperature effects on eggs	160
Figure 4.31: Monthly maps of the total number of virtual eggs hatched in each cell in Long Point Bay by spawning month, March until October, 1999 under Scenario S2E1 conditions	161
Figure 4.32: Monthly maps of the total number of virtual eggs hatched in each cell in Long Point Bay by spawning month, March until October, 1999 under Scenario S2E2 conditions	161
Figure 4.33: Frequency distribution by spawning date of virtual YOYs per cell and the total number of YOYs that survived to October 31, 1999 in Long Point Bay under Scenario S2E1L1 conditions; spawning site selection with temperature effects on eggs & larvae	162
Figure 4.34: Monthly maps of the total number of virtual YOYs that survive until October 31st in each cell in Long Point Bay by spawning month, March until October, 1999 under Scenario S2E1L1 conditions	163
Figure 4.35: Frequency distribution by spawning date of YOY average size (g) per cell and the total production of YOYs (kg) that survived to October 31, 1999 in Long Point Bay under Scenario S2E1L1 conditions; spawning site selection with temperature effects on eggs and larvae	163
Figure 4.36: Monthly maps of the average weight gain (g) of virtual YOYs that survive until October 31st in each cell in Long Point Bay by spawning month, March until October, 1999 under Scenario S2E1L1 conditions	164
Figure 4.37: Monthly maps of the total production (kg) of virtual YOYs that survived until October 31st in each cell in Long Point Bay from the month of spawning in 1999 under Scenario S2E1L1 conditions	164
Figure 4.38: Frequency distribution by spawning date of virtual YOYs per cell and the total YOY survival to October 31, 1999 in Long Point Bay under S2E1L2 conditions; spawning selection with thermal effects on eggs, thermal and habitat effects on larvae	165
Figure 4.39: Monthly maps of the total number of virtual YOYs that survive until October 31st in each cell in Long Point Bay by spawning month, March until October, 1999 under Scenario S2E1L2 conditions	166
Figure 4.40: Frequency distribution by spawning date of YOY average size (g) per cell and the total production of surviving YOYs (kg) on October 31, 1999 in Long Point Bay (Scenario S2E1L2 conditions; habitat-based spawning with temperature & habitat effects on larvae.).....	166

Figure 4.41: Monthly maps of the average weight gain (g) of virtual YOYs that survive until October 31st in each cell in Long Point Bay by spawning month, March until October, 1999 under Scenario S2E1L2 conditions..... 167

Figure 4.42: Monthly maps of the total production (kg) of virtual YOYs that survived until October 31st in each cell in Long Point Bay from the month of spawning in 1999 under Scenario S2E1L2 conditions 167

Figure 4.43: Frequency distribution of virtual eggs spawned per cell and the total number of eggs spawned in Long Point Bay by date in 1999 under Scenario S2* conditions; habitat selection with IFD..... 168

Figure 4.44: Monthly maps of the total number of virtual eggs spawned in each cell in Long Point Bay from March until October, 1999 under Scenario S2* conditions 169

Figure 4.45: Frequency distribution of virtual eggs hatched per cell and the total eggs hatched in Long Point Bay by spawning date in 1999 under Scenario S2*E1 conditions; IFD spawning and temperature effects on eggs..... 169

Figure 4.46: Frequency distribution of virtual eggs hatched per cell and the total number of eggs hatched in Long Point Bay by hatch date in 1999 under Scenario S2*E1 conditions; IFD spawning site selection and temperature effects..... 170

Figure 4.47: Monthly maps of the total number of virtual eggs hatched in each cell in Long Point Bay by spawning month, March until October, 1999 under Scenario S2*E1 conditions 170

Figure 4.48: Frequency distribution by spawning date of virtual YOYs per cell and the total YOYs that survived to October 31, 1999 in Long Point Bay under Scenario S2*E1L1 conditions; IFD spawning site selection with temperature effects on eggs & larvae 172

Figure 4.49: Monthly maps of the total number of virtual YOYs that survive until October 31st in each cell in Long Point Bay by spawning month, March until October, 1999 under Scenario S2*E1L1 conditions..... 172

Figure 4.50: Frequency distribution by spawning date of YOY average size (g) per cell and the total production of YOYs (kg) by October 31, 1999 in Long Point Bay (Scenario S2*E1L1 conditions; IFD spawning with temperature effects on eggs and larvae..... 173

Figure 4.51: Monthly maps of the average weight gain (g) of virtual YOYs that survive until October 31st in each cell in Long Point Bay by spawning month, 1999 under Scenario S2*E1L1 conditions 173

Figure 4.52: Monthly maps of the total production (kg) of virtual YOYs that survived until October 31st in each cell in Long Point Bay from the month of spawning in 1999 under Scenario S2*E1L1 conditions..... 174

Figure 4.53: Frequency distribution of virtual YOYs per cell and the total number of surviving YOYs on October 31, 1999 by spawning date in Long Point Bay. (Scenario S2*E1L2; IFD habitat-based spawning, temperature & habitat effects on larvae.) 174

Figure 4.54: Monthly maps of the total number of virtual YOYs that survive until October 31st in each cell in Long Point Bay by spawning month, March until October, 1999 under Scenario S2*E1L2 conditions..... 175

Figure 4.55: Frequency distribution by spawning date of YOY average size (g) per cell and the total production of YOYs (kg) that survived to October 31, 1999 under Scenario S2*E1L2 conditions; IFD spawning site selection with temperature effects on eggs and temperature & habitat effects on larvae 176

Figure 4.56: Monthly maps of the average weight gain (g) of virtual YOYs that survive until October 31st in each cell in Long Point Bay by spawning month, March until October, 1999 under Scenario S2*E1L2 conditions..... 176

Figure 4.57: Monthly maps of the total production (kg) of virtual YOYs that survived until October 31st in each cell in Long Point Bay from the month of spawning in 1999 under Scenario S2*E1L2 conditions..... 177

Figure 4.58: Frequency distribution of virtual eggs spawned per cell and the total number of eggs spawned in Long Point Bay by date in 1999 under Scenario S3 conditions; habitat selection with thermal threshold 178

Figure 4.59: Monthly maps of the total number of virtual eggs spawned in each cell in Long Point Bay from March until October, 1999 under Scenario S3 conditions..... 178

Figure 4.60: Frequency distribution of virtual eggs hatched per cell and the total eggs hatched in Long Point Bay by spawning date in 1999 under Scenario S3E1 conditions; spawning site selection with temperature cue and temperature effects on eggs 179

Figure 4.61: Frequency distribution of virtual eggs hatched per cell and the total number of eggs hatched in Long Point Bay by hatch date in 1999 under Scenario S3E1 conditions; spawning site selection with temperature cue and temperature effects on eggs..... 180

Figure 4.62: Monthly maps of the total number of virtual eggs hatched in each cell in Long Point Bay by spawning month, March until October, 1999 under Scenario S3E1 conditions 180

Figure 4.63: Monthly maps of the total number of virtual eggs hatched in each cell in Long Point Bay by spawning month, March until October, 1999 under Scenario S3E2 conditions 181

Figure 4.64: Frequency distribution by spawning date of virtual YOYs per cell and the total number of YOYs that survived to October 31, 1999 in Long Point Bay under Scenario S3E1L1 conditions; spawning site selection with thermal cue and temperature effects on eggs & larvae 182

Figure 4.65: Monthly maps of the total number of virtual YOYs that survive until October 31st in each cell in Long Point Bay by spawning month, March until October, 1999 under Scenario S3E1L1 conditions 182

Figure 4.66: Frequency distribution by spawning date of YOY average size (g) per cell and the total production of YOYs (kg) that survived to October 31, 1999 in Long Point Bay under Scenario S3E1L1 conditions; spawning site selection with temperature cue and temperature effects on eggs and larvae..... 183

Figure 4.67: Monthly maps of the average weight gain (g) of virtual YOYs that survive until October 31st in each cell in Long Point Bay by spawning month, April until August, 1999 under Scenario S3E1L1 conditions 184

Figure 4.68: Monthly maps of the total production (kg) of virtual YOYs that survived until October 31st in each cell in Long Point Bay from the month of spawning in 1999 under Scenario S3E1L1 conditions 184

Figure 4.69: Frequency distribution by spawning date of virtual YOYs per cell and the total number of YOYs that survived to October 31, 1999 under Scenario S3E1L2 conditions; spawning site selection with temperature cue, temperature effects on eggs, and temperature & habitat effects on larvae 185

Figure 4.70: Monthly maps of the total number of virtual YOYs that survive until October 31st in each cell in Long Point Bay by spawning month, March until October, 1999 under Scenario S3E1L2 conditions 186

Figure 4.71: Frequency distribution by spawning date of YOY average size (g) per cell and the total production of YOYs (kg) that survived to October 31, 1999 in Long Point Bay under Scenario S3E1L2 conditions; spawning site selection with temperature cue, temperature effects on eggs and temperature & habitat effects on larvae 186

Figure 4.72: Monthly maps of the average weight gain (g) of virtual YOYs that survive until October 31st in each cell in Long Point Bay by spawning month, April until June, 1999 under Scenario S3E1L2 conditions 187

Figure 4.73: Monthly maps of the total production (kg) of virtual YOYs that survived until October 31st in each cell in Long Point Bay from the month of spawning in 1999 under Scenario S3E1L2 conditions 187

Figure 4.74: Frequency distribution of virtual eggs spawned per cell and the total number of eggs spawned in Long Point Bay by date in 1999 under Scenario S3* conditions; habitat selection with thermal threshold and IFD 188

Figure 4.75: Monthly maps of the total number of virtual eggs spawned in each cell in Long Point Bay from March until October, 1999 under Scenario S3* conditions 189

Figure 4.76: Monthly maps of the total number of virtual eggs hatched in each cell in Long Point Bay by spawning month, March until October, 1999 under Scenario S3*E1 conditions 190

Figure 4.77: Frequency distribution of virtual eggs hatched per cell and the total eggs hatched per spawning date in 1999 (Scenario S3*E1 ; IFD spawning site selection with thermal cue and thermal effects on eggs 190

Figure 4.78: Frequency distribution of virtual eggs hatched per cell and the total eggs hatched by hatch date in 1999 (Scenario S3*E1; IFD spawning site selection with temperature cue and temperature effects on eggs 191

Figure 4.79: Frequency distribution by spawning date of virtual YOYs per cell and the total number of YOYs that survived to October 31, 1999 in Long Point Bay under Scenario S3*E1L1 conditions; IFD spawning site selection with temperature cue, temperature effects on eggs & larvae 192

Figure 4.80: Monthly maps of the total number of virtual YOYs that survive until October 31st in each cell in Long Point Bay by spawning month, March until October, 1999 under Scenario S3*E1L1 conditions.....	192
Figure 4.81: Frequency distribution by spawning date of YOY average size (g) per cell and the total production of YOYs (kg) that survived to October 31, 1999 in Long Point Bay under Scenario S3*E1L1 conditions; IFD spawning site selection with temperature cue and temperature effects on eggs and larvae...	193
Figure 4.82: Monthly maps of the average weight gain (g) of virtual YOYs that survive until October 31st in each cell in Long Point Bay by spawning month, April until August, 1999 under Scenario S3*E1L1 conditions.....	194
Figure 4.83: Monthly maps of the total production (kg) of virtual YOYs that survived until October 31st in each cell in Long Point Bay from the month of spawning in 1999 under Scenario S3*E1L1 conditions.....	194
Figure 4.84: Frequency distribution by spawning date of virtual YOYs per cell (# of values is colour-coded) and the total number of YOYs that survived to October 31, 1999 in Long Point Bay under Scenario S3*E1L2 conditions; IFD spawning site selection with temperature cue, temperature effects on eggs, and temperature & habitat effects on larvae	195
Figure 4.85: Monthly maps of the total number of virtual YOYs that survive until October 31st in each cell in Long Point Bay by spawning month, March until October, 1999 under Scenario S3*E1L2 conditions.....	196
Figure 4.86: Frequency distribution by spawning date of YOY average size (g) per cell and the total production of YOYs (kg) that survived to October 31, 1999 in Long Point Bay under Scenario S3*E1L2 conditions; IFD spawning site selection with temperature cue and temperature effects on eggs, temperature & habitat effects on larvae	196
Figure 4.87: Monthly maps of the average weight gain (g) of virtual YOYs that survive until October 31st in each cell in Long Point Bay by spawning month, April until June, 1999 under Scenario S3*E1L2 conditions	197
Figure 4.88: Monthly maps of the total production (kg) of virtual YOYs that survived until October 31st in each cell in Long Point Bay from the month of spawning in 1999 under Scenario S3*E1L2 conditions.....	197
Figure 4.89: Scenario comparisons of the potential YOY production (kg) by October 31, 1999 in Long Point Bay plotted by spawning date. See Table 4.6 for a description of scenarios.....	198
Figure 4.90: Historical spawning and nursery areas for yellow perch in the Long Point Bay Region.....	201
Figure 4.91: The potential daily maximum abundance of successive life stages of yellow perch in the Long Point system under different scenario conditions..	204
Figure 4.92: The potential annual abundance of successive life stages of yellow perch in Long Point under different scenario conditions	205

Figure 4.93: The number of days of the year in 1999 that would have suitable habitat in the Long Point system for successive life stages under different scenario conditions... 206

Figure 4.95: The number of cells used each day for spawning under S3* conditions in 1999 compared to the abundance of swim-up larvae surviving from that day's spawn under E1 conditions 207

Figure 4.96: The number of spawning days in 1999 that successfully produced larvae by October 31st plotted against the potential annual production of larvae under different scenario conditions..... 208

Figure 4.97: The ratio of successful spawning days in 1999 compared to the production efficiency (kg of larvae produced per 1000 eggs laid) of each scenario in Long Point Bay 209

Figure 4.98: The number of grid cells in the Long Point grid that produced larvae in 1999 versus the potential annual production under different scenario conditions 210

Figure 4.99: The ratio of total annual YOY area (successful cells over successful days) to cumulative spawning area compared to production efficiency for each scenario (kg of larvae produced per 1000 eggs laid) 210

Figure 4.100: Frequency histograms of virtual size categories (weight; grams) based on annual totals (1000s of individuals) for each of the scenario results .212

Figure 4.101: The production efficiency (kg of larvae produced per 1000 eggs laid) compared to the predicted overwinter mortality production loss for each scenario based on a size criteria for overwintering 215

LIST OF TABLES

Table 1.1: A complete list of the data sources used for habitat map generation, statistics and modelling in different analyses for this study.	17
Table 1.2: List of datalogger site codes & descriptions, equipment, geographic locations, logger & site depths, deployment periods, recording intervals & deployment methods	37
Table 1.3: Correction factors for offshore grid cells determined from datalogger and satellite temperature comparisons at different pass times.....	43
Table 1.4: Offshore cell IDs used to predict nearshore cell temperatures based on regression equations developed from 1999 datalogger temperatures.....	44
Table 1.5: Sentinel sites used for each region's temperature changes (temporal interpolation)	45
Table 1.6: A list of the habitat characteristics used in this study and the years they were surveyed, the spatial and temporal resolution used in each chapter's analyses for different years of thermal data.	58
Table 2.1: The depth strata averaged for each grid cell to obtain thermal HSI calculations for each life stage.....	68
Table 2.2: HSI values used for categorical variables: maximum site depth, substrate type, and vegetation density for different life stages of yellow perch ..	70
Table 4.1: Physical habitat variables and subcategories that were assigned different habitat suitabilities based on spawning preferences that have been documented for yellow perch.....	133
Table 4.2: Daily mortality rates of yellow perch eggs in different temperature ranges	134
Table 4.3: Macrozooplankton average concentration estimates for 1993/1994 LEB sites.....	138
Table 4.4: The model scenarios were implemented and assessed in a stepwise procedure using 16 different combinations	144
Table 4.5: Comparison of the location of high larval growth and high larval production nuclei across the spawning and larval scenarios.....	203
Table 4.6: Comparisons of the percent decreases from L1 (thermal effects on larval maximum feeding and mortality) to L2 scenarios (thermal & habitat-based effects on larval food availability and mortality).....	214

LIST OF APPENDICES

Appendix 1.1: Background information for (A.) CoastWatch satellite images (or scenes) file nomenclature convention and (B.) Format options selected for this study during image file generation in the DECCON software program.....	A-2
Appendix 1.2: The following map coordinates for prominent features in Long Point Bay were used to georegister the satellite imagery to a Universal Transverse Mercator projection.	A-3
Appendix 1.3: Manuscript submitted to Photogrammetric Engineering and Remote Sensing journal on validation and matrix method	A-4
Appendix 2.1: Literature Review of Yellow Perch (<i>Perca flavescens</i>) Habitat Requirements.....	A-32
Appendix 2.2: Yellow perch habitat associations by life stage.....	A-55
Appendix 4.1: Comparison of different types of models used to evaluate different fish species.....	A-61
Appendix 4.2: Definitions and units of coefficients and variables used in calculating bioenergetic consumption rates for yellow perch	A-63
Appendix 4.3: Life stage specific coefficients used in calculating bioenergetic consumption rates for yellow perch	A-63
Appendix 4.4: Coefficients used for bioenergetic respiration rate calculations	A-63
Appendix 4.5: Definitions and units for coefficients and variables used in respiration and specific dynamic bioenergetic equations	A-63
Appendix 4.6: Annual totals table showing the number of potential spawning days that successfully reach each life stage, the minimum, maximum, mean and standard deviation for annual abundances at each stage	A-64
Appendix 4.7: Table showing the number of potential spawning cells that successfully produced each life stage on the maximum abundance date, the minimum, maximum, mean and standard deviation and total daily abundance at each stage	A-65

LIST OF ABBREVIATIONS

Acronym	Long Name
AML	Arc Macro Language
AVHRR	Advanced Very High Resolution Radiometer
CASI	Compact Airborne Spectrophotometric Imager
DECCON	Decompression and Conversion
DFO	Department of Fisheries & Oceans
EC	Environment Canada
GLERL	Great Lakes Environmental Resource Laboratory
GLLFAS	Great Lakes Laboratory for Fisheries and Aquatic Sciences
HRPT	High Resolution Picture Transmission
LEB	Lake Erie Biomonitoring Survey
NCAAS	NOAA CoastWatch Active Access System,
NESDIS	National Environmental Satellite, Data & Information Service
NOAA	National Oceanic & Atmospheric Administration
OMNR	Ontario Ministry of Natural Resources
SST	Sea Surface Temperature
TIN	Triangulated Irregular Network
UTM	Universal Transverse Mercator

[T]o interpret and predict the patterns observed in nature accurately our methods of study must embrace temporal and spatial variability as essential features of population and community dynamics.

- Sousa

(1984)

GENERAL INTRODUCTION

Four major stresses have been linked to the widespread declines in fish populations: habitat loss, species introductions, pollution, and over-exploitation (Thomas 1994). Habitat loss usually refers to culturally induced physical changes in the landscape that detrimentally affect population abundance. Habitat can be defined as a multidimensional space that exhibits the characteristics and functions required by organisms to complete their life cycle and maintain a population (*sensu* Hutchinson 1965, Odum 1971). Changes in these characteristics and functions in many areas (e.g. loss of wetland habitat and thermal changes due to global warming) can contribute to local and regional losses in animal diversity (Magnuson *et al.* 1990, Minns & Moore 1995). A clear definition of fish habitat is needed. Then the effects of habitat loss will need to be measured for different species at different life stages.

Rose (2000) advocated that the prediction of environmental quality (habitat) effects on fish populations would benefit by increased consideration of three areas: individual-based modelling, life history theory, and multidisciplinary studies. To determine the relative effect of spatial heterogeneity on populations a spatially explicit approach is needed but not necessarily an individual-based one. This approach replaced individual variability in niche requirements with spatial heterogeneity in habitat. The research investigates hypotheses concerning the productive capacity of systems, the definition of critical habitat requirements for fish populations, and limiting habitat that may constrain a population at a carrying capacity. Targets for fisheries management and habitat conservation may be more easily obtained because of the research.

Odum (1971) defined habitat as the set of places where a species (or group of species) could potentially live. Such a broad definition is further refined by stating that potential occupancy of a location is determined by the niche of a fish species. The definitions of niche and habitat are often confused. Niche is defined as the sum of all factors acting on an organism, a region of n-dimensional hyperspace, that encompasses the combination of biological, physical and chemical factors that a species (or individual) can tolerate (Odum 1971). A niche is the property of an organism determined by its phenotype (a function of genotype and environmental history), whereas habitat is a property of space. However, a fish's niche determines what is useable habitat

(tolerable), preferred habitat (selection) and optimal habitat (maximizing fitness) from the suite of available habitats. The characterization of the environment into these habitat categories can vary because of ontogenetic niche changes over an organism's life history. Early life stage habitats are usually more important to protect because change or variation in survival of young fish has a much greater impact on populations than variability in later stages. In fish, habitat requirements for spawning, and larval and juvenile survival, are usually more specific than non-spawning adult needs. Eggs and young are generally more susceptible to environmental changes, tend to live in more variable habitats, have smaller energy stores, and are also less mobile (Hayes 1999).

The common concepts of habitat-based approaches include ideal free distributions (Kennedy & Gray 1993), optimization and habit selection (Giannico & Healey 1999), and density-dependent processes (Messier *et al.* 1990). Regional differences in population performance, noted because of empirical observations of recruitment differences between years and across space, elicit questions regarding the variability of the intrinsic rate of increase of a population and the environmental factors that may extrinsically affect carrying capacity and population dynamics. Ontogenetic habitat requirements may be connected to observed spatial patterns if the population is constrained by habitat limitations at a particular life stage. The variability of important habitat factors and their interaction with the performance of different life stages need to be included in any assessment. Knowledge of bioenergetics and life history theory help bound the problems. Listing the many abiotic and biotic factors affecting individuals as they progress through successive life stages is a valuable first step in population analysis.

The limited supply of any life-stage habitat can create a productivity bottleneck, influencing population structure, competitive and predator-prey interactions, and potential yield for fisheries. Bottlenecks in productivity for different species can occur at several different stages in different habitats due to specific habitat requirements not being met (Shuter & Post 1990, Minns *et al.* 1996, Hayes *et al.* 1996). Initially, the quantification and ranking of different components of fish habitat is undertaken in habitat assessments. Then the relationship between population dynamics is determined by qualifying, or establishing suitability criteria, for particular life stages of a fish species in relation to the range of available habitat. Once this type of analysis is extended to a multidimensional representation of a population's habitat requirements, then habitat conservation and management can proceed from a reference framework before further degradation occurs.

Fish habitat is generally thought of as physical attributes of the environment; however, biological components of habitats, such as vegetation and interactions with other species, also affect habitat choice in fish. For most fish, however, vegetation functions primarily as a physical feature of the habitat as opposed to a direct food source. The interaction

of key factors, such as temperature (Casselman 2002), with other more static habitat characteristics (such as bathymetry) needs to be considered. Further, the spatial and temporal dynamics of these variables might shape the distribution of fish and affect their growth and survival rates (Tyler & Rose 1997). Potential structuring factors linked to fish populations are vegetation, substrate type, temperature, light, turbidity, dissolved oxygen, depth, and exposure.

Temperature is considered one of the important variables that defines fish habitat. Magnuson *et al.* (1979) defined a fundamental thermal niche of a fish species as “a range of temperature around a species’ final preferendum that defines the optimum conditions for activity and metabolism”. Some conflicting reports of the effects of temperature on the life cycle and distribution of fish suggest that complex and multivariate interactions are at work (Henderson 1985, Hayward & Margraf 1987), but this is consistent with the multidimensional definition of habitat. However, the link between fish bioenergetics and temperature has been well-established (Kitchell *et al.* 1977, Hanson *et al.* 1997) and the selection of specific thermal habitats by fish has been documented (Brandt *et al.* 1980).

The quantification of different components of fish habitat involves defining the geographic extent of a study area and determining the variability of certain important characteristics. Some habitat variables, such as temperature and vegetation, change significantly over time and three-dimensional (3-D) space. Therefore the traditional, static, two-dimensional (2-D) approach to mapping suitable habitat areas may not apply as it does for variables that change little over time, like bottom substrate. Water temperature varies over both vertical and horizontal space, and through time, depending on solar energy input, the depth of the water column, and mixing. Capturing this 3-D structure in habitat mapping efforts is essential for accurate predictions in delimiting thermal niches for fish species and requires good spatial and temporal datasets.

To quantify the effects of anthropogenic habitat loss on fish populations, the influence of natural changes in habitat through space and time should be gauged first. Both inter- and intra-annual natural changes, like macrophyte growth and senescence and temperature fluctuations, are important to capture. Of course, these factors can be modified by cultural processes, such as climate change. In lakes, most variation in these natural factors occurs in the nearshore zone. The nearshore, or littoral zone, needs to be characterised because it is important spawning and nursery habitat for many fishes.

If temperature is a factor in how fish distribute themselves then it is the area or volume of thermal habitat available at time scales relevant to fish that are important (Christie & Regier 1988) and can only be accurately estimated if the spatial variation in temperature is considered. Quantification of nearshore thermal habitat or its spatial variability has rarely been attempted in freshwater systems (Quinn and Kojis 1996,

Matuszek & Shuter 1996). In habitat studies, the horizontal variability in habitat has been largely ignored with ecologists opting for one-dimensional, mid-lake, temperature profiles to represent an entire lake (Casselman and Lewis 1996, Christie and Regier 1988, Rudstam and Magnuson 1985). To address the multivariate aspects defining habitat, spatial methods developed for determining thermal habitat need to be applied to other important habitat characteristics; such as water depth, substrate composition, vegetation, and protection from wind and wave processes.

Issues of resolution, relevance, and measurement must be addressed to characterise habitat. Assessment is also contingent on data availability. Dynamic habitat modelling is more difficult and adds complexity. Differing time scales for habitat change among variables also need to be reconciled at a scale relevant to fish-habitat interactions. Habitat models need process level descriptions of habitat quality, which can account for new conditions, unlike statistically based empirical relationships. Thus, the habitat features that are most important to productive capacity of the Great Lakes can be determined. When constructing habitat-based models, trade-offs between growth, survival, and behaviour must be reconciled. Initially, population models need to have some spatial resolution to test habitat-based hypotheses. Once general patterns are observed at a high spatial resolution then the spatial scale can be set for the appropriate population process that is limiting.

This dissertation examines the interaction between fish populations and fish habitat. In particular, physical habitat and the yellow perch population, *Perca flavescens* (Mitchill 1814), in Long Point Bay, Lake Erie was studied, with an emphasis on habitat constraints as a determinant of distributions and year class recruitment. Yellow perch, a commercially important fish species, has declined in abundance in recent years in many of the Great Lakes. However, since 1998, the Great Lakes' populations have recovered slightly, but the eastern basin abundance in Lake Erie remains low (Cook *et al.* 2001). There is some speculation that this decline was due to a global change in a habitat variable, such as temperature.

The Great Lakes Fishery Commission (GLFC) Habitat Task Group selected species from different thermal and reproductive guilds as candidates for modelling how habitat change affects population dynamics (Jones *et al.* 1998). Yellow perch was chosen as a test species for this study because it was complementary to the other fish species for which models were being developed by the GLFC, such as walleye, smallmouth bass and northern pike. Yellow perch is closely related to walleye, because it is a cool water species with spring spawning, typically in shallow areas with vegetation. Perch is also an important food source for the other fish species, is integral to the food web, and is of high commercial and sport fishing importance.

Long Point Bay, Lake Erie was chosen as the study area for characterising habitat features and testing hypotheses about yellow perch population dynamics. Long Point is a sand spit on the north shore of the eastern basin of Lake Erie. It is comprised of inner and outer bays, with the Inner Bay covering 7280 ha and the Outer Bay encompassing over 30,000 ha. The maximum depth of the entire bay is 60 m with the deepest point of Lake Erie just off the tip of the 32 km, Long Point sand spit. The area was designated, by the Convention on Wetlands in Ramsar, Iran, as an internationally important wetland site on May 24, 1982. Long Point Bay is considered an important spawning and nursery area for many fish species in the eastern basin (Ontario Ministry of Natural Resources 1998). Long Point Bay is an open system but there is genetic evidence of an Eastern Basin perch stock (samples were taken from Long Point Bay; Einhouse *et al.* 2000). It is also considered the main spawning and nursery habitat in the eastern basin (MacGregor & Witzel 1987).

The compilation of adequate habitat inventories for thermal and depth structure, macrophyte or wetland coverage, and bottom substrate was crucial. Several time-series or spatially extensive data sets have been collected in this region for physical and biological factors. An extensive compact airborne spectrographic imager (CASI) survey of macrophyte and substrate distribution in the nearshore zone was conducted using aerial remote sensing (Geomatics International Inc. 1997). A coarser scale substrate survey was conducted in the offshore waters of the eastern basin of Lake Erie in the 1970s (Rukavina 1976, Thomas *et al.* 1976). A detailed 1 m-contour, bathymetry map is available for Lake Erie (NOAA 1998). A combination of satellite imagery for sea surface temperature for the Great Lakes (Leshkevitch *et al.* 1993), point thermal profiles (Dahl *et al.* 1997, Graham *et al.* 1998), and time-series temperature data from other studies (Witzel, Unpublished data.) as well as this study, was collected. Once compiled, the inventories allowed examination of the spatial and temporal variability in habitat-supply features, a major objective of the study.

As habitat is inherently spatial, geographic information systems (GIS) and remote sensing of large areas are tools that can be used to determine wide-scale spatial patterns. The nearshore and offshore vegetation and substrate surveys, bathymetry, and temperature information were combined with fetch and wind data for Lake Erie as different layers in a geographical information system (GIS). The current use of grid-based models and bioenergetics modelling, as well as utilizing assessment tools like remote sensing and geographic information systems for habitat characterization, were expanded to determine the perch life stages affected by habitat factors. Combinations of the aforementioned variables were used to determine suitable fish habitat areas in Long Point. Data from a larval fish spatial survey, conducted in the Inner Bay of Long Point in 1998, were used to validate some of the initial habitat suitability results (Dimitru *et al.* Unpublished data.) Daily spatial and temporal

estimates of habitat suitability were then used in a spatially explicit model for yellow perch population dynamics in the first year of life to test hypotheses about spawning habitat selection and habitat interactions with perch eggs and larvae during early life history.

The following steps were taken to examine fish-habitat interactions and the ultimate development of a spatially explicit, habitat-based population model for yellow perch (Figure A).

- The selection of a study area and species for which habitat and fisheries data were available,
- The selection and compilation of spatially explicit, habitat information that is relevant to the life processes (vital rates) or preferences of the test species (Chapter 1),
- The incorporation of habitat information for the test species into a habitat assessment for the life stages of the test species in the study area. This involves the generation of suitability indices where no direct linkage between habitat and life processes has been established empirically (Chapter 2),
- Validation of habitat suitability assessments where adequate spatial distribution data exist (Chapter 3),
- The development of a spatially explicit, habitat-based population model, and the testing of alternate hypotheses using simulations, about how habitat affects early life history stages of perch (Chapter 4).

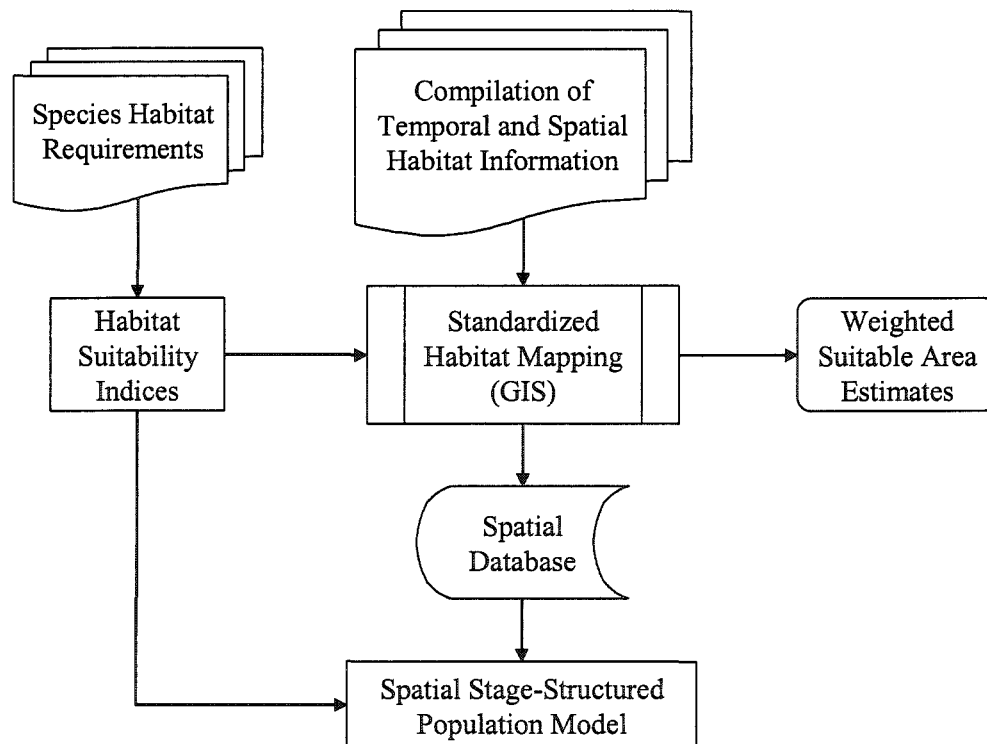


Figure A: Outline of steps used in the habitat assessment of the yellow perch population.

Chapter 1

Characterizing physical habitat from a fish's perspective.

Physical-biological interactions should be quantifiable in a hierarchical manner, if we approach the problems systematically.

– Roff & Taylor (2000)

1.0 INTRODUCTION

Chapter 1 focussed on collecting information on aspects of physical habitat, including bathymetric data, substrate type, vegetation, temperature and exposure to wind and wave processes. It begins with a brief introduction and description of these variables and their relative importance as fish community structuring factors, followed by a methodological description of how physical habitat in the Long Point Bay, Lake Erie ecosystem was mapped and modelled for different purposes in the thesis.

1.0.1 Spatial Issues and Fish Habitat

The scientific literature is replete with the habitat requirements of many species and the availability and presence of those habitats is usually linked, although heuristically, with population distributions, success and sometimes enhancement. With regard to distributions, Matthews (1998) wrote that nothing is more critical to zonation of fish in lakes than the existence of different kinds of littoral structure, substrate, or vegetation in shallow waters. Hayes (1999) stated that fish and other aquatic organisms need habitat to survive, and the productive capacity of the environment depends upon how well their needs are met. With regard to management of different species, Summerfelt (1999) suggested various habitat changes that would benefit different fish species. The enhancement of gravel shoals would improve walleye (*Sander vitreus*) and smallmouth bass (*Micropterus dolomieu*) habitat. The enhancement of shallow vegetated bays for yellow perch (*Perca flavescens*) and northern pike (*Esox lucius*) would be beneficial, as well as reducing the extent of fetch and windswept beaches for largemouth bass (*Micropterus salmoides*) and crappie (*Pomoxis nigromaculatus*) would improve recruitment in those species. Yet, the quantitative link between habitat and fish populations remains tenuous (Rose 2000), and therefore it is difficult to assess the long-term dynamics of these populations.

The *Fisheries Act of Canada* (R.S. 1985, c. F-14) implicitly states the importance of fish habitat for maintaining the productive capacity of aquatic systems. Surprisingly, there are few studies that address the process by which habitat affects populations other than through empirical connections between environmental variables and year class strength or experimental studies of habitat preferences. In the past, listed habitat requirements have historically concentrated on adult life stage requirements of commercially important species, while early life history requirements remain poorly understood. Notably, Lane *et al.* (1996a,b) have compiled early life stage, habitat associations for many species in Ontario. However, any population assessment would require the inclusion of all habitat requirements for the entire life cycle of a fish to be complete, such as in Minns *et al.* (1996) and Bartholow *et al.* (1993).

Jones *et al.* (1996) asked how productive capacity should be measured and how well we understand the relationship between

productive capacity and human-induced habitat change. To understand human-induced habitat change we must first understand natural habitat change and its relationship to productive capacity. Jones *et al.* (1996) also argued that defining meaningful, measurable metrics of habitat loss or gain is a need basic to all agencies whose mandate includes the conservation and restoration of aquatic habitats. Many investigations into the role of habitat and population dynamics have concentrated on empirically linking physical features to year class strength of different fish species or modelling microscale connections to a particular vital rate of a specific life stage or process. Both practices involve defining a habitat space or variable at some spatial and temporal scale. In the former case, habitat characteristics are often reduced to aggregate estimates across large spatial scales and over relatively longer periods where data is available. In the latter case, high spatial resolution of a small area over a short time window is often used. However, as Rose (2000) wrote, "...biological realism in modelling large-scale phenomena is often sacrificed" even though we recognize that habitat features vary significantly temporally and spatially. This study attempts to capture habitat variability on a time-scale that is meaningful to the early life stages of a fish at a higher spatial resolution than most large-scale studies.

Part of the output from habitat suitability models includes the relative weighting of habitat patches in space and their suitability, or potential contribution, to fish population dynamics. Some terrestrial conservation area definitions have been based on linking expert systems, simulation modelling, geographical information systems (GIS), and GAP analysis approaches (Conroy & Noon 1996), but rarely has this approach been taken in aquatic systems. GAP analysis is the overlaying of multiple layers of geographic information to find unique areas that may support higher production or species richness and diversity. In a similar fashion, habitat layers can be merged, manipulated, and modelled to obtain spatially explicit information (and temporally-explicit information, if time series data are available).

One of the main concerns of habitat mapping for use in population studies is that the variability of some environmental factors, which change significantly over time and three-dimensional (3-D) space, is not captured. Therefore, the traditional and static two-dimensional (2-D) approach to mapping suitable habitat areas does not necessarily work as it would for variables that do not change significantly over shorter periods, like bottom substrate. Most physical surveys of lakes are one-time only if spatially extensive, or cover a limited area or a limited number of points if temporally intensive. In many cases, nearshore and offshore surveys are often mutually exclusive and coastal areas may be ignored because of difficulty in sampling. Yet, it is widely recognized that the nearshore or littoral zone needs to be characterised because it is important spawning and nursery habitat for many fishes (Lane *et al.* 1996a, 1996b). This ecotone is the least likely to be mapped because of accessibility or

negotiability issues, as well as technical issues involved in obtaining data remotely.

The alternatives are to devote a lot of time and effort to collecting good spatial information at regular intervals or to use tools, such as GIS and physical modelling, to fill in gaps both spatially and temporally. Various sources of remotely sensed information have become available in the last decade but their utility in habitat mapping and population modelling has not been fully realized. Various geostatistical methods are available for manipulating data in geographic space that have been underutilized in biology to achieve a resolution in habitat information that is relevant to biological processes. In this thesis, these various interpolation and extrapolation methods, such as splines, distance weighting, triangulation, trend surface analysis, and kriging, were used in a GIS to map and model habitat characteristics from different sources into a standardized framework.

1.0.2 Physical Habitat Variables

Lacustrine habitat classification systems often include the following basic descriptors to varying degrees: water depth, substrate type, and a vegetation description. A Great Lakes habitat classification system reported in Sly & Busch (1992) identified two generic habitat types: lake or open-water habitat including circulatory basins or deepwater reefs; and nearshore habitat, which included open shoreline, bays or reefs. Wetland classification adopted a more detailed approach (Cowardin *et al.* 1979) with lacustrine (lake) and littoral (nearshore) habitat subsystems broken into further subclassifications. Lacustrine subsystems were defined as profundal and nonvegetated with bottom substrate classes of organic, rock, coarse, or fine sediments. Littoral subsystems were either classified as vegetated or nonvegetated with subclasses and types. Nonvegetated areas had different bottom types (organic, rock, coarse and fine subclasses), which were further categorized into a flat, a beach or bar, or a rocky shoreline. Vegetated areas were further classified into submergent (algal or vascular subclasses), floating-leafed, or emergent classes. Each of the vegetated types was further classified into orders of organic or mineral substrate content.

These generalised habitat classifications underlie the importance of vegetation, substrate, and bathymetry as important factors in defining habitat and offer a basic framework for classification from a fish's perspective. However, other physical factors are known to affect fish distributions and possibly population dynamics. Temperature, turbidity, and exposure are not only important as structuring influences of physical habitat, but they act on the distribution of fishes because of preferences, and have bioenergetics and survival implications for different life stages across the natural range of each variable. A brief description of each major habitat variable follows, as well as reasons why these habitat characteristics were dealt with or not in the remainder of this study.

Bathymetry

Bathymetry is the science of measuring sea floor depths in order to ascertain bottom topography. A common reference point is required because of changing water levels; therefore, the International Great Lakes Datum (1985) or IGLD85 is used as a frame of reference, which is 175.921 meters above sea level at Port Colbourne in Lake Erie. Any depth soundings for the eastern basin of this Great Lake are corrected to this low water level datum. Therefore, any data obtained on depths for Long Point Bay have been standardised to low water levels at this elevation.

Topography and water depth define the framework within which fishes live and structure hydrodynamic and thermal regimes to some extent due to circulation patterns and light penetration (Wetzel 1983). Water depth is often used in lake habitat classification, with the 5-m depth contour often delineating the nearshore and offshore zones of lakes. Many species have documented depth preferences, but preferences change due to ontogenetic shifts and may be affected by other factors, such as species interactions and seasonal temperatures. Minns *et al.* (1996) modelled different life stages of pike and habitat supply based on depth and hypsographic shape.

Substrate Type

Substrate type usually refers to a combination of surficial geology and sediments in aquatic areas. Substrate or sediment types are usually categorized by particle size or into geomorphologic types. A common classification would include clay, silt, sand, gravel, cobble, rubble, boulder, and bedrock (Sly & Busch 1992). Fishes have often been linked to preferred bottom substrate type, and are especially well documented for streams. Ultimately, the functional reasons for this type of association probably depend on the usefulness of that substrate to different life stages for fulfilling biological needs, such as feeding, spawning, and protection.

Vegetation

Aquatic vegetation usually refers to vascular plants, often categorized into emergent, submergent and floating-leaved types. Emergent plants extend above the surface of the water and are usually rigid. Submergent plants are entirely below the water surface and are not woody. Floating vegetation can be rooted or not, but most of the plant tissue is at the water surface. Wetlands and areas with submerged aquatic vegetation (SAV) have been identified as areas of higher productivity (Cyr & Downing 1988, Jeppesen *et al.* 1998, Søndergaard & Moss 1998) and are important in structuring littoral communities by providing cover and refugia (Killgore *et al.* 1989, Jacobsen *et al.* 1997, Crowder *et al.* 1998, Diehl & Kornijów 1998, Gasith & Hoyer 1998, Persson & Crowder 1998). Fish species richness for the lower Great Lakes was described by a nonlinear relationship with macrophyte density

by Randall *et al.* (1996). Even though percent cover or density of SAV and emergents is often used in fish suitability analysis instead of species-specific descriptions of plant distributions, some fishes do associate with certain plants or plant forms (Fischer & Eckmann 1997).

Most aquatic vegetation surveys occur during peak times in the percent cover and density of submergent and emergent plants. The intra-annual growth and senescence of vegetation and the interannual succession of different plant communities has largely been ignored in aquatic habitat surveys. The use of surveys from peak plant densities may not be adequate in habitat suitability assessments, especially when determining spring and fall spawning habitat availability when plants are at the beginning or end of their growing season.

Temperature

Water temperature varies over vertical and horizontal space and through time depending on solar energy input, the depth of the water column, and water flow and evaporation (Wetzel 1983). Capturing 3-D structure in habitat mapping efforts for different fish species is essential for accurate predictions of distributions and delimiting thermal niches. In habitat studies, the horizontal variability in temperature has been largely ignored, with ecologists opting for one-dimensional temperature profiles to represent an entire water body, assuming that water at the same depth, regardless of geographic position (nearshore or offshore), has the same temperature (Casselman & Lewis 1996, Christie & Regier 1988, Rudstam & Magnuson 1985). Existing habitat models have used surrogate measures for temperature, such as water depth, which likely relates to preferred water temperatures, but the relationship can be confounded. Also, they may have opted not to use spatially explicit representations of temperature because of the difficulty in obtaining data and modelling thermal dynamics (Christie & Regier 1988). However, Brandt *et al.* (1980) showed that different freshwater fish species segregate along temperature gradients with those patterns maintained despite rapid oscillations in thermocline location. Similarly, ocean currents and physical factors, in addition to vertical stability of the water column (thermocline stability), have been shown to predict suitable areas for anchovy (MacCall 1990).

In addition, many metabolic rates are affected by temperature and therefore population vital rates, at some level, must be affected. Most thermal habitat assessments refer to the work by Magnuson *et al.* (1979) that defined a fundamental thermal niche as 'a range of temperature around a species' final preferendum (preferred temperature) that defines the optimum conditions for activity and metabolism'. It is apparent that further investigation into the relative importance of thermal structure and habitat delineation is imperative if this factor might constrain a species at a particular life stage.

Yet, temperature does not act as the sole factor in defining habitat suitability and separating fundamental niche from realized niche can be

difficult. Fish were found in significantly lower temperatures in lakes than were selected in laboratory experiments (Ross and Siniff 1982) and fish have been documented as competing for favourable temperatures. Some conflicting reports of the effects of temperature on the life cycle and distribution of fish suggest that complex and multivariate interactions are at work, but this is consistent with the multidimensional definition of habitat.

The importance of temperature as a regulatory factor in population dynamics can be masked by other aspects of the environment. Negus *et al.* (1987) listed factors that modify fish behaviour in thermal gradients: acclimation temperature, food, light & dissolved oxygen, season, turbulence, photoperiod, and the distribution of competitors and predators. Not all these factors can be addressed at once in one modelling exercise, however, it does underlie the hyperdimensional nature, and hence difficulty, of defining niche and habitat space.

Fry (1947) described five major effects of temperature: controlling (setting the pace of development and metabolism), masking (affecting the expression of other environmental factors), limiting (influencing locomotory activity and hence distribution), directing (stimulating an orientation response), and finally as a lethal agent (chronic lethal minimum and maximum). More "cold" kills are reported than heat kills because, fish are able to increase their tolerance of high temperatures more quickly, fish lose heat tolerance slowly, and high temperatures induce frantic activity, which assists in fleeing whereas cold induces lethargy. Upper temperature tolerances are well above ambient temperatures in most natural habitats but not so for lower lethal temperatures (Beitinger *et al.* 2000).

Several temperature models exist for simulating lake temperature from very simple regression relationships that predict mean annual temperatures to complex 1D and 3D models that predict thermal profiles but require heat budgeting and meteorological inputs. A simple temperature model developed for Lake Opeongo, Ontario uses littoral depth, effective fetch, day of year and annual temperature as inputs to derive daily littoral temperatures (Matuszek & Shuter 1996). This model has been tested in the Long Point area (Chu *et al.* In press.), but does not capture the gradient of temperatures in some areas especially in areas of riverine input. Currently, 1D and 3D thermal models for Lakes Erie and Ontario exist (Schertzer *et al.* 1987; Y.P Chu, pers. com.) However, none of these methods or models was appropriate to use for predicting temperatures in Long Point Bay for one of the following reasons: inadequate temporal and spatial scale output, they required a lot of meteorological data, or the methodology was not yet fully developed.

Wind, Waves & Exposure

Aside from structuring the shoreline and vegetation, as well as affecting circulation patterns and thermal regimes, winds and waves affect

habitat selection at different life stages. Sheltered areas are preferred by most fish species because of high energetic costs of swimming and the difficulty in feeding in turbulent water (Clady & Hutchinson 1974; Craig & Kipling 1983; Lammens *et al.* 1990; Bergman 1991; Aalto & Newsome 1993; Bronte *et al.* 1993; Fisher *et al.* 1996; Lott *et al.* 1996; Mooij 1996; Xie & Eggleston 1999; Megrey & Hinckley 2001). Exposure or turbulence can be calculated using a range of physical models (Keddy 1984; Duarte & Kalff 1990; Wiesner 1991) but this variable has rarely been linked quantitatively to functional responses in fish but sometimes to other physical characteristics of habitat that may be related to wave energy, such as vegetation and substrate type.

Other Factors

Several other physical habitat factors could affect the distribution, habitat availability, and vital rates of fish populations. These include turbidity and light penetration, water levels, and dissolved oxygen levels, to name a few. Turbidity and light penetration would affect the ability of a visual predator to find and capture food (Loew & Wahl 1991; Loew *et al.* 1993), as well as the productivity of the system. Low dissolved oxygen conditions (Seifert & Spoor 1974, Lam *et al.* 1987) would affect the distribution and, ultimately, the mortality of fish depending on their tolerance limits. Water levels change the total amount of habitat available at different times of the year. Some habitats, such as wetlands, are disproportionately affected more than others.

The use of any of the factors listed in this introduction in a habitat-based assessment would depend entirely on the specific habitat requirements of a fish species. For example, light is not as important to yellow perch as it would be for walleye (*Sander vitreus*) to carry out its life cycle. Also, data needs to be available at a spatial and temporal resolution that is amenable to its application. Water level data for 1999 was collected for this study but the spatial resolution of elevation data used was not amenable to modelling water level fluctuations. Therefore, the shoreline and water depths were kept static to test other hypotheses about habitat and fish interactions. Also, information on dissolved oxygen was not available at a spatial and temporal scale that would be meaningful to this study.

1.1 METHODS & RESULTS

The following habitat features were chosen for use in subsequent habitat suitability and modelling efforts because of data availability and their significant links to yellow perch life stages: depth, temperature, macrophytes, substrate, and exposure (Table 1.1). Data were compiled from various sources for generating habitat map layers in a GIS. Sources included remote sensing information, field data, and existing digital maps. Sometimes several different sources of information were used to generate a particular habitat map or time-series.

1.1.1 Shoreline

A shoreline was needed to delimit water and land consistently between habitat layers. Several different sources of Lake Erie shorelines with differing resolutions were used and tested in this thesis. This standardization across habitat layers is important but usually involves a loss of information as data sources will have the “shoreline” set in different locations.

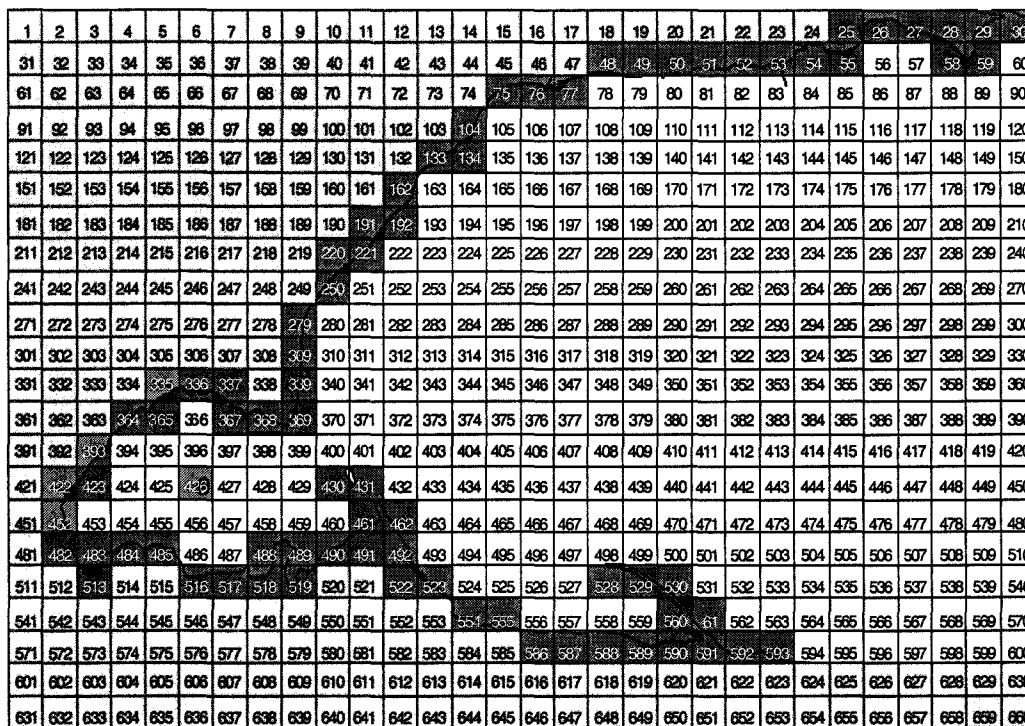
1. The 0-m polygon from the bathymetry coverage was used to define the shoreline in some habitat suitability analyses (Chapter 2). The 0-m contour in hydrographic mapping is corrected to the low water level datum (IGLD85). There is moderate shoreline detail but the nearshore is often inaccurate in shallow areas due to hydrographic survey limitations (P. Travaglini, DFO-CHS, Burlington, ON, pers.com.).
2. The “dry land” boundary from the Compact Airborne Spectrophotometric Imagery (CASI) survey was used as a shoreline in modelling efforts in combination with the bathymetry coverage (Chapter 4). If no water was present, the CASI survey assigned a dry land designation to the 3-m² pixel, which may have overlapped with wetland areas due to difficulty in determining water levels. Also, the shoreline was not corrected to the proper datum, and therefore represented the water level at the time of the survey.
3. Ontario Base Map (OBM) coverages of the Long Point area were obtained through an agreement between OMNR and McMaster Library (Kathy Moulder, pers. comm.). Twenty-two OBM sheets were appended (map-joined) to obtain a shoreline of Long Point. This shoreline was not as detailed as the CASI survey and was used in very early temperature work.
4. A low resolution Canadian shoreline from the Great Lakes Environmental Research Laboratory (GLERL) web site was created from an available vector file and compared with 0-m bathymetry contour. The GLERL shoreline was inaccurate and not used for any part of this study.
5. The lowest resolution shoreline was part of a graphic overlay used in positioning Advanced Very High Resolution Radiometry sea surface temperature (AVHRR SST) imagery. This shoreline was only used in processing remote sensing imagery and not used in any geographical analysis.
6. In general, a shoreline that was obtained from one of the habitat layers used in the analysis was more appropriate for consistency and standardisation to avoid slight differences in projections between data sources. There are two geographic data used to project spatial information in North America (North American Datum 1927 and NAD83), which are based on ground-truthing of set coordinates on the continent. Older spatial information was reprojected using NAD83 where necessary.

Table 1.1: A complete list of the data sources used for habitat map generation, statistics and modelling in different analyses for this study.

Variable	Source	Years	Reference
Bathymetry	<ul style="list-style-type: none"> National Oceanographic & Atmospheric Administration (NOAA) & the Canadian Hydrographic Service (CHS) 1-m contour bathymetry of Lake Erie 	1998	<ul style="list-style-type: none"> NOAA 1998, Minns <i>et al.</i> 1997
Substrate	<ul style="list-style-type: none"> Offshore survey, Lake Erie 	1976	<ul style="list-style-type: none"> Rukavina 1976, Thomas <i>et al.</i> 1976
	<ul style="list-style-type: none"> CASI survey, Long Point Bay 	July 1995	<ul style="list-style-type: none"> Geomatics Int'l Inc. 1997
Vegetation	<ul style="list-style-type: none"> CASI survey, Long Point Bay 	July 1995	<ul style="list-style-type: none"> Geomatics Int'l Inc. 1997
Wind	<ul style="list-style-type: none"> Environment Canada – Atmospheric & Environment Service wind direction and speed data from Long Point station (Stn. 6134F10) 	1999	<ul style="list-style-type: none"> W.M. Schertzer, pers.com.
Ice Cover	<ul style="list-style-type: none"> EC ice cover sheets, Lake Erie 	1993, 1994	<ul style="list-style-type: none"> Canadian Ice Service, unpublished data
	<ul style="list-style-type: none"> Lake Erie Biological Survey temperature profiles, DFO 	1993, 1994	<ul style="list-style-type: none"> Dahl <i>et al.</i> 1995, Graham <i>et al.</i> 1996
Temperature	<ul style="list-style-type: none"> NOAA CoastWatch AVHRR sea surface temperature imagery for the Great Lakes 	1993-1999	<ul style="list-style-type: none"> Schwab <i>et al.</i> 1992
	<ul style="list-style-type: none"> Ontario Ministry of Natural Resources long-term temperature monitoring, Inner Bay, Long Point Bay 	1993-2000	<ul style="list-style-type: none"> L.D. Witzel, pers.com.
	<ul style="list-style-type: none"> Port Dover Municipal Water Intake temperatures 	1999-2000	<ul style="list-style-type: none"> L.D. Witzel, pers.com.
	<ul style="list-style-type: none"> This study 	1999	<ul style="list-style-type: none"> Doka, in prep. (Chap. 1 & Appendix 1.3)

1.1.2 Spatial Resolution

The coarsest resolution for spatially explicit data in the data sources was the remotely sensed temperature imagery. The “base grid” of the SST imagery for Long Point was used to generate thermal layers, and in some cases to standardize the other spatial data to a common resolution. In early work, the grid cells that overlapped the shoreline were not included in analyses but in later modeling work, the overlap cells were treated differently and included. The approach that was used is outlined in each chapter’s methodology section but all methods are dealt with for each habitat variable in this chapter. The final version of the matrix is referred to as the “habitat grid” (Figure 1.01) and predominantly used in Chapter 4.



Land or N/A
 Water
 Overlap
 Reassigned

Figure 1.01: Grid matrix based on SST imagery resolution (1.4 km) used for standardizing habitat variables and in habitat-based modelling of the early life history stages of yellow perch.

In the Long Point SST imagery, the final 30 x 22 grid cells were assigned ID numbers from 1 to 660 beginning from the upper left corner, from left to right. This grid matrix resolution was used to standardise all other habitat layers (slightly different methodology was used in Chapter 2). The original grid was merged with the CASI shoreline to create a more detailed polygon coverage that incorporated shoreline features. Land polygons from the CASI survey, which included islands and nearshore

features such as marinas, were incorporated. Discrete land, water or overlap designations for each new polygon were appended to determine which of the original cells overlapped the new shoreline or were completely water. The area of water within each grid cell of the matrix was calculated by adding all the smaller polygon areas with water designations within each cell. In an effort to standardise the size of grid cells within the modelling environment a minimum water area per grid cell was calculated as a cut-off. Any cell (usually either a single water polygon or group of polygons) with less than the cut-off area was merged with the closest cell with similar habitat characteristics. Some grid cells were divided by land features (e.g. the small spit running northward from Long Point) and very small polygons were created along the shoreline in some cases. Grid cells that were divided by land features were reassigned to adjacent grid cell IDs (Figure 1.01).

The cut-off for merging adjacent cells was established by using a frequency plot of the area of water contained in each of the cells that overlapped the land-water interface and a rough calculation of the number of adult perch that this area could hold based on their home range size. The size distribution of overlap cells and their associated water areas was bimodal, with the lower mode having a mean around 100,000 m² and the higher mode around 429,526 m². The minimum home range calculations for an adult perch are $\log_e HR = -2.56 + 3.57 Y + 1.52 * (\log_e L)$ where $Y = 0$ in riverine environments and $Y = 1$ in lacustrine (HR = home range in m² and L = Length in mm; Minns 1995). The average size of adult perch is 20 cm. Therefore the home range of an average perch was calculated as 8634 m². The number of adult fish which could fit into the modal areas listed above would be 12 and 50 fish, respectively, based on the home range size. An area that supported less than a dozen fish was deemed to be too small of a cell area for modelling purposes. Therefore a cut-off of roughly 10 ha was chosen which resulted in 10 grid cell IDs being reassigned to neighbouring polygon groups. Leaving these cells separate may have introduced unpredictable effects on suitable area calculations in the model (Chapter 4).

Of the original 660 total cells in the grid matrix; 239 land cells, 86 overlap cells (which were further subdivided into land and water polygons) and 335 water cells were created. The 60 grid cells south of the Long Point spit were designated as not accessible and not used in any further analysis. After reassignment, there were 400 functional cells in total used in the modelling environment or base matrix. The cell numbering system, and the associated attributes, were linked to all the other habitat layers in the GIS by merging the matrix polygon coverage with other habitat coverages.

1.1.3 Bathymetry and Water Depth

Bathymetric soundings for all of Lake Erie were compiled by NOAA and the Canadian Hydrographic Service (CHS) using depth sounding surveys. One-metre depth contours were generated from the point data in

an ArcInfo coverage. A preliminary version of this coverage was supplied to the GIS lab at the Great Lakes Laboratory for Fisheries and Aquatic Sciences (GLLFAS) in Burlington (C.N. Bakelaar pers.com.). The original line coverage provided was corrected for node errors and was converted to a polygon coverage (Minns *et al.* 1999). The final, 1-m resolution bathymetric contour map for Lake Erie was used in this thesis (Figure 1.02; NOAA 1998).

The NOAA bathymetry polygon coverage for Lake Erie (Table 1.1) was converted to a NAD83 projection from NAD27 for consistency across habitat information layers. By merging the base grid from SST imagery and the contour polygon coverage for depth, a square polygon coverage was created. An average maximum depth was calculated for each grid cell using an area-weighted mean for all the original depth polygons (contours) within the cell's boundary. Maximum depths were also extracted for each cell. Depth calculations were rounded to the nearest metre for use in thermal layer generation.

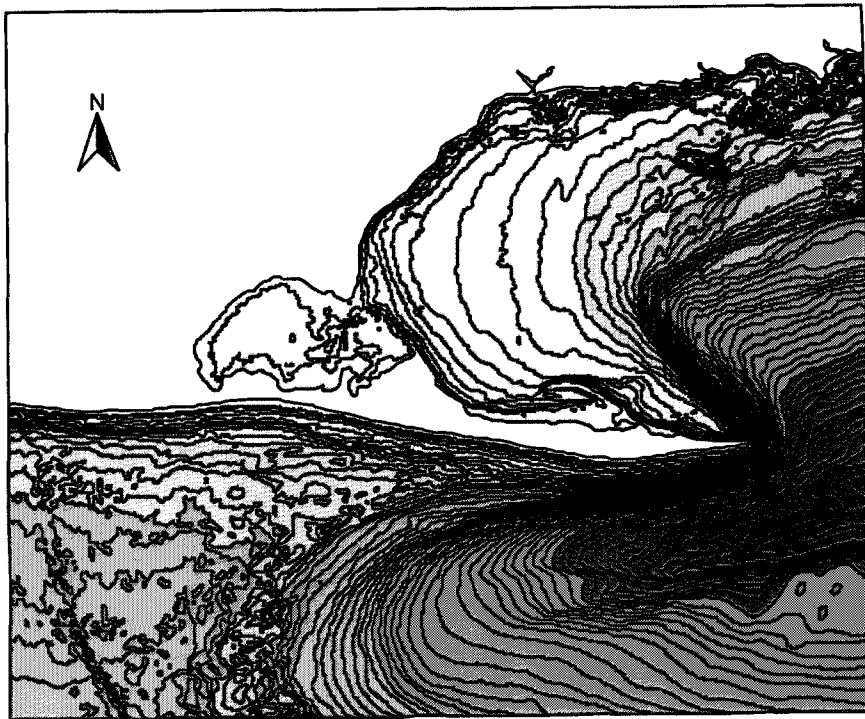


Figure 1.02: One-metre bathymetric contours of waters in Long Point Bay and Lake Erie south of Long Point spit. (Colours change at approximately 5-m intervals).

1.1.4 Substrate Type & Vegetation

Two sources of substrate & vegetation information were available for Long Point Bay, Lake Erie: a high-resolution, nearshore, remote sensing survey of Long Point and a field-based, point survey of offshore substrates in Lake Erie.

Compact Airborne Spectrophotometric Imagery (CASI) survey

A nearshore, CASI survey was conducted over Long Point Bay on July 27th of 1995 by various federal and provincial agencies. The remote-sensing survey covered areas up to 5-m depth. The spatial resolution of the CASI inventory was 3-m in a raster format. Geomatics International Inc. (1997) conducted a spectral analysis of the remote sensing information and converted the imagery to vegetation categories (densities and types; Figure 1.03) and substrate classifications (Figure 1.04). The original classifications can be found in Minns *et al.* (1999).

Offshore Substrate Surveys

Offshore substrate data was originally obtained from Thomas (1976) and Rukavina (1976) grab sample point surveys. The point samples were interpolated using Voronoi tessellation and substrate classification was similar to the CASI classifications used in the nearshore survey (Minns & Bakelaar 1999; Figure 1.05). Voronoi tessellation is derived from triangulated irregular network (TIN) methodology and is suitable for breaklines and abrupt changes. A triangulated irregular network, or TIN, is a vector coverage with fewer data points required than grid methods. TINs are not smooth surfaces and an even distribution of data is best. They are not suitable for extrapolation and the original data is kept in the final output.

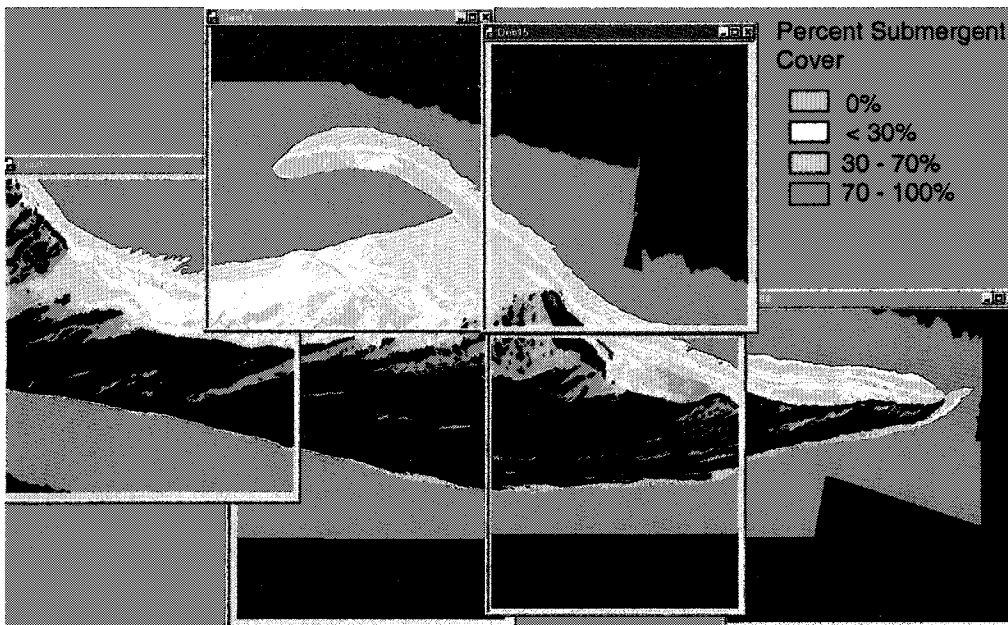


Figure 1.03: Several scenes of CASI survey information on submergent vegetation percent cover categories for the tip of Long Point sand bar. CASI survey raster information is very detailed at 3-m resolution.

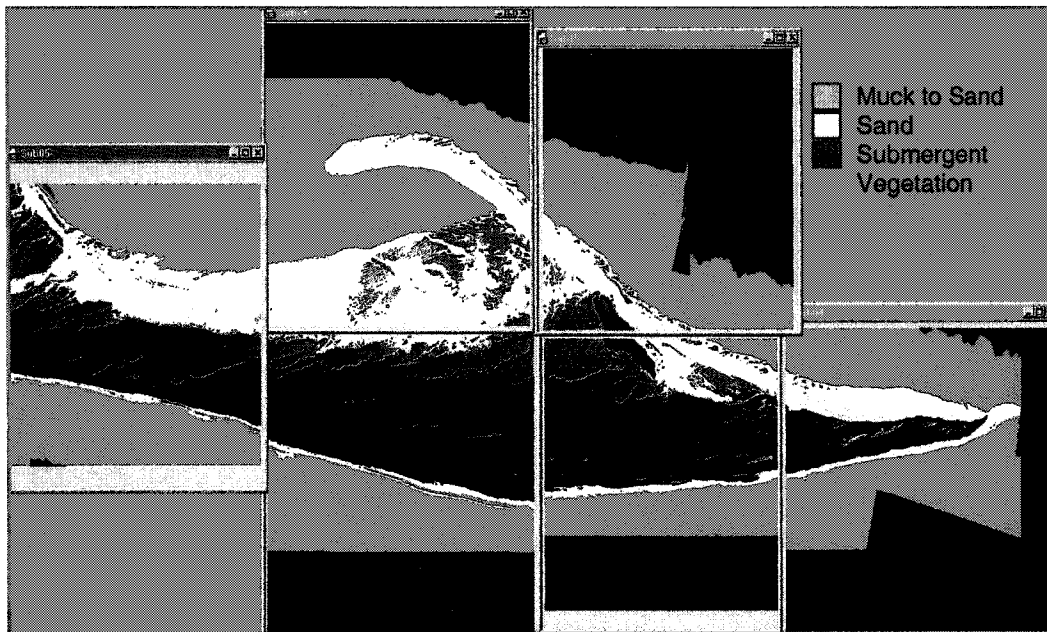


Figure 1.04: Several scenes of the CASI survey on substrate type for the tip of Long Point at 3-m resolution. Substrate type in dense submergent vegetation was assigned a combination of sand/muck/clay.

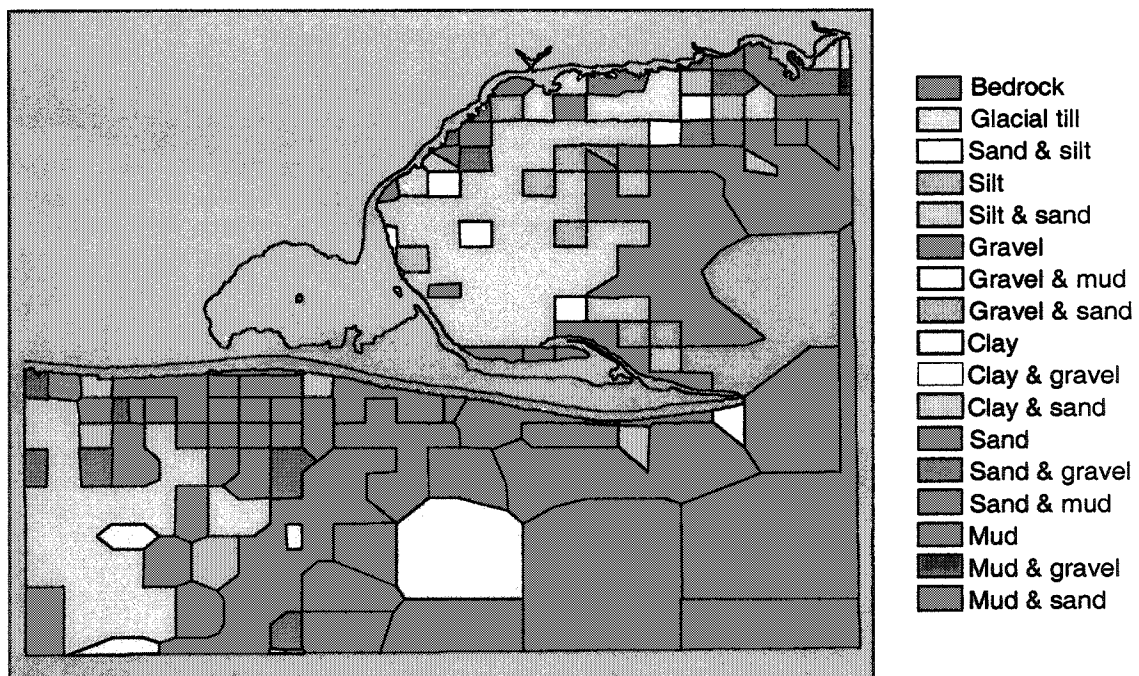


Figure 1.05: Voronoi polygons for substrate type interpolated from point survey data in Rukavina (1976) and Thomas *et al.* (1976) for an offshore survey of Lake Erie, including Long Point Bay (see Minns & Bakelaar 1999 and Minns *et al.* 1999 for a detailed methodology).

Substrate Type Standardization

Both nearshore and offshore substrate was classified into the categories that were used in the CASI (nearshore) survey of Long Point and merged into one coverage. Categories of substrate type included boulder, rubble, cobble, gravel, sand, silt, clay, bedrock and hardpan clay (Figure 1.06). Any empty polygons that were created between the nearshore and offshore coverages with missing data were assigned an average % composition of the surrounding polygons. Also, there was some misclassification error in determining substrate type from CASI data in certain areas due to the presence of vegetation. Therefore, assumptions were made about substrate composition in highly-vegetated areas that had missing data. These areas were assigned an equal combination of silt, sand and clay; consistent with inner bay soil types (MacGregor & Witzel 1987).

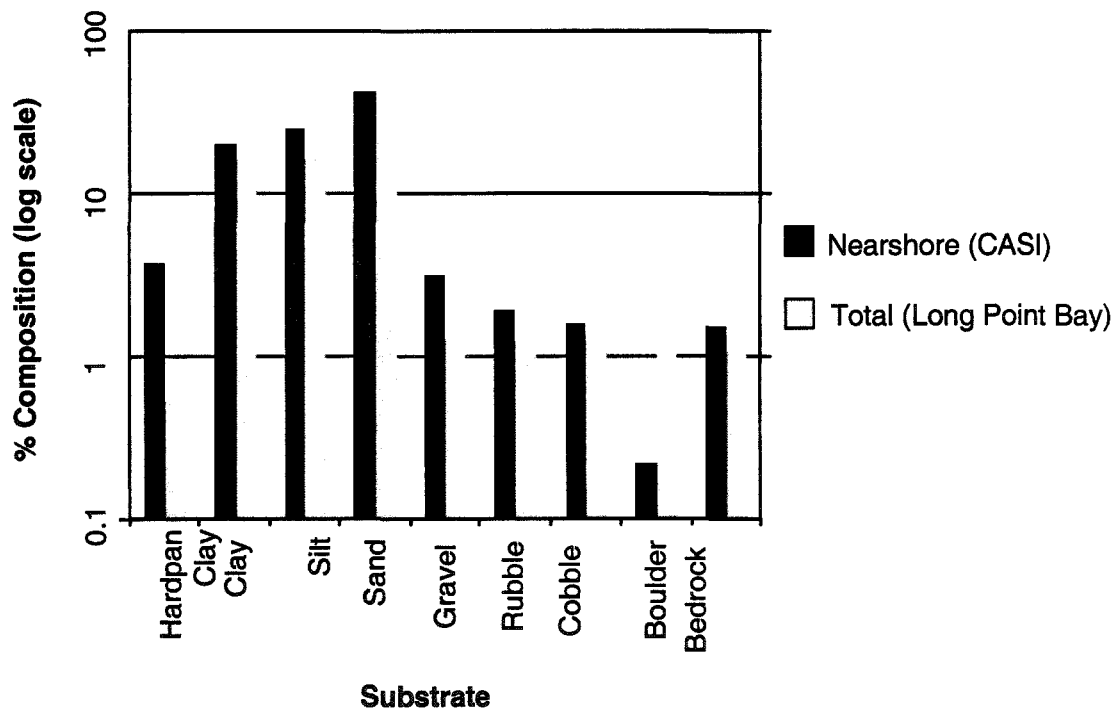


Figure 1.06: Comparison of the percent composition (log scale) of standardized substrate type classifications in the nearshore zone (CASI survey < 5 m) and in all of Long Point Bay, Lake Erie (offshore data from Rukavina 1976 and Thomas 1976).

The original 3-m resolution raster information was converted to a polygon coverage that merged cells of similar substrate composition from the CASI survey. Some of these polygons had percent composition values for mixed substrate types as attributes (e.g. 50% sand/silt combination; see original CASI categories in Minns *et al.* 1999). When the data was standardized to the habitat grid resolution, the grid polygon coverage was overlaid on the merged substrate polygon coverages and the grid cell IDs were appended to polygons that fell within each cell's

boundary. The dominant substrate type by grid cell is shown in Figure 1.07. The percent composition of each substrate type (from boulder to clay), based on a weighted average of the polygons contained within each cell, was calculated using Equation 1.01 and the water area within each cell of the habitat grid.

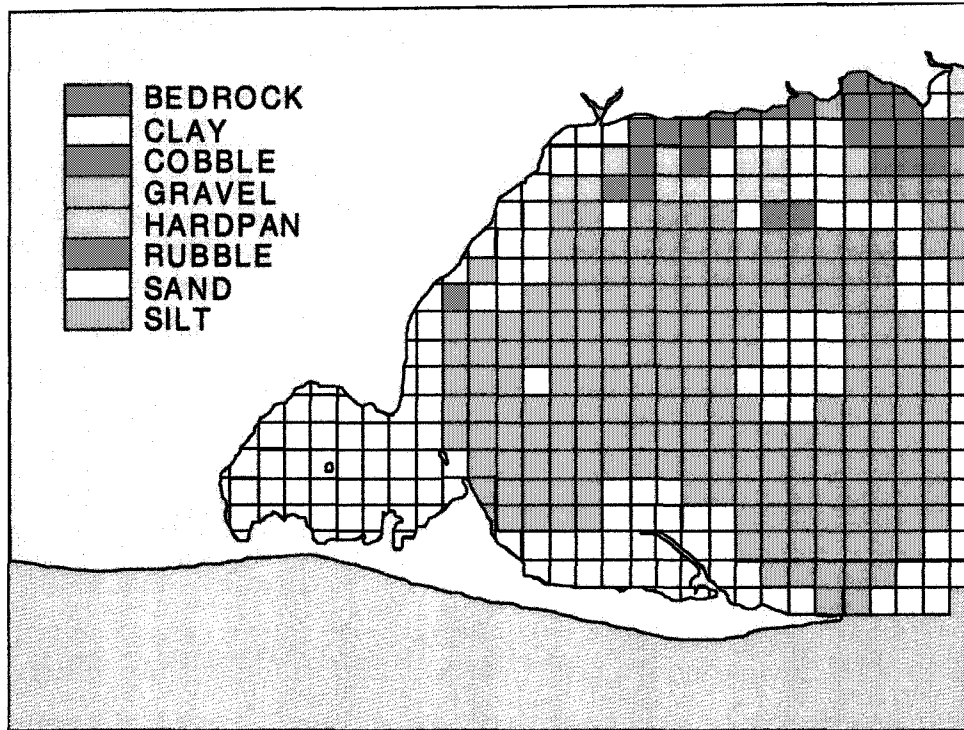


Figure 1.07: Dominant substrate type by cell in the habitat grid of Long Point Bay, Lake Erie.

Equation 1.01:
$$\%comp_a = \frac{\sum_{1 \rightarrow n} (\%comp_a \cdot area_1 \dots \%comp_a \cdot area_n)}{area_{H_2O}}$$
, where a =

substrate type and n = the number of polygons within the cell.

Vegetation Standardization & Time-series modelling

Emergent vegetation and submergent density polygon coverages were created from the high resolution CASI survey raster information and were standardized to the habitat grid resolution. In a similar fashion as the substrate reclassification, the percent area of emergent vegetation, no vegetation, and high (71-100% cover), medium (31-70% cover) and low (1-30% cover) submergent vegetation density categories was calculated for each grid cell. Any cells or polygons with missing values within the CASI nearshore boundary (up to a depth of 5 m), were assigned the characteristics of neighbouring cells using an 8-cell neighbourhood averaging. It was assumed that offshore areas were not vegetated beyond the CASI survey (> 5 m) and these cells were assigned to a 'no vegetation' category. There was some overlap between land polygons and

emergent vegetation coverages, because of the shoreline delineation. Therefore, only vegetation in water polygons were used in the calculations of percent cover. The dominant submergent vegetation in the habitat grid was mapped (Figure 1.08) and the percent composition of vegetation zones in the nearshore and all of Long Point Bay was summarized (Figure 1.09).

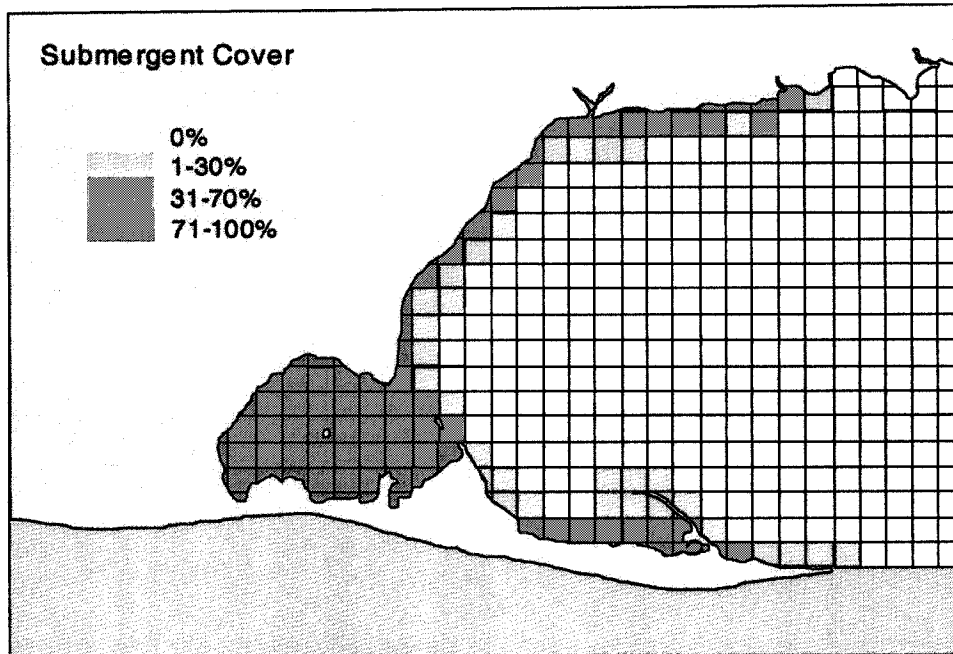


Figure 1.08: Dominant submergent vegetation category by cell, standardized to the habitat matrix resolution (Long Point Bay, Lake Erie).

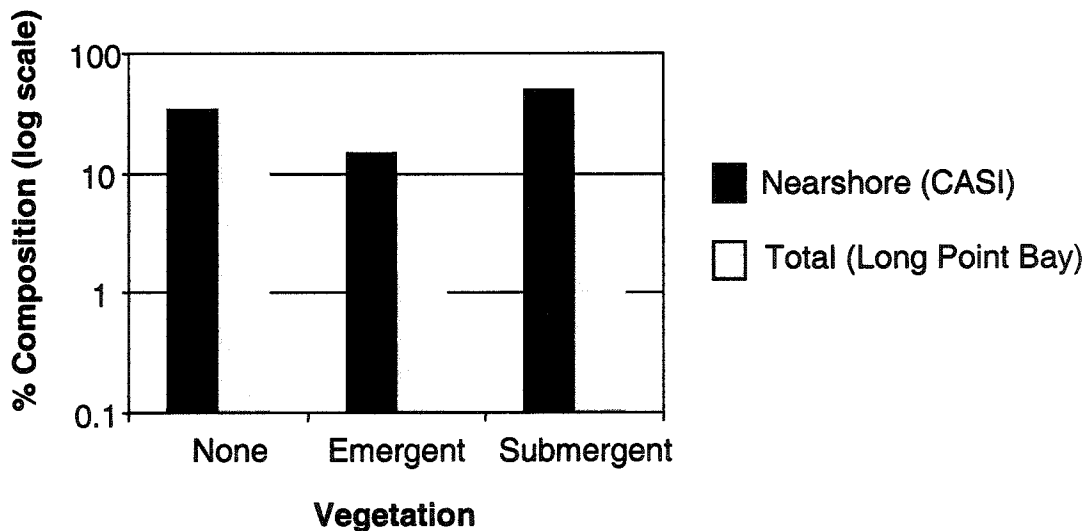


Figure 1.09: Percent composition of standardized vegetation categories in the nearshore zone compared to all of Long Point Bay, Lake Erie in July, 1995.

The July 1995 CASI survey findings were assumed to be representative of the maximum *annual* vegetation growth and areal extent during the 1990s. The following rules and algorithms were applied to the CASI vegetation values to mimic annual vegetation growth and senescence and to introduce daily temporal dynamics in vegetative cover. The temporal dynamics of vegetation has not commonly been used in habitat assessments because of labour-intensive field studies that would be required and also for lack of data on the patterns of vegetation growth and senescence. Habitat studies have been criticized for this oversight. Therefore, a model was developed that mimicked a generic growth/decay curve for vegetation on a daily basis.

1. An assumption was made that emergent vegetation roots and stalks remain intact in the water all year round even though above water the vegetation would grow and senesce. Therefore the extent and inferred density of emergent vegetation was set at CASI survey levels for the entire year.
2. Submergent vegetation spatial coverage follows a parabolic pattern of growth and decay (Wetzel 1983). The general equation for a parabolic curve is, $y=a(x-h)^2 + k$, where the maximum or critical point is (h, k). The dependent variable was set as percent cover of submergent vegetation and the independent variable as Julian day because of light. As the CASI survey was conducted on July 27th, $h =$ Julian day 212; the assumed date of maximum submergent vegetation density and areal coverage ($k =$ total CASI submergent % cover).
3. An arbitrary date of Dec 1st (Day 335) was chosen as the date when all submergent vegetation dies, therefore the upper x-intercept is (335,0). Substituting in the parabolic equation, the slope of the equation was solved as: $0 = a(335-212)^2 + k$ (where $k = 1$ or 100% cover as a proportion), therefore $a = -1/(123)^2$. This slope was used for all submergent vegetation cover in the final equation (Equation 1.02). This slope and equation were applied to all grid cells regardless of the total submergent vegetation cover to obtain the maximum % cover on each day of the year.

Equation 1.02: % total submergent = $-1/(123)^2 * (\text{Julian} - 212)^2 + \% \text{CASISubmergent}$

4. As submergent vegetation % cover is a combination of three different density categories (0-30%, 30-70% and 70-100% densities), the total submergent cover equation was used to calculate similar growth/decay curves for each category that would add to this total. The Julian days when 70% and 30% submergent cover occurred were determined from the total submergent vegetation growth/decay equation. 70% cover was reached at Day 279; 30% cover at Day 316. These dates (Julian days) were used as x-intercepts for other parabolic equations generated for each of the submergent vegetation density categories.

Slopes of the parabolic equations for those submergent categories were calculated in the same manner as outlined in step 3, the 70-100% submergent category had a slope of $-1/67^2$ and the 30-70% category's slope was $-1/104^2$. The final equations (1.03 and 1.04) were used to calculate the percent cover of each of these vegetation classes daily. (N.B. This approach assumed that density and areal coverage vary over time in the same manner.)

Equation 1.03: % 70-100 submergent = $-1/(67)^2 * (JD-212)^2 + \%CASI(70-100\%submergent)$, where JD = Julian Day

Equation 1.04: % 30-70 submergent = $-1/(104)^2 * (JD-212)^2 + \%30-70submergent$, where JD = Julian Day (Note that the term in the 30-70% equation is not the maximum 30-70% cover from the CASI survey, but incorporates the decrease in density of the 70-100% submergent category to the 30-70% category due to senescence. The contribution from the 70-100% category and the 30-70% maximum from the CASI survey was used as the critical point of the curve in this equation and is constantly changing over time.)

- The maximum percent cover of the 0-30% density submergent category was calculated by determining the remainder of the submergent area that was not used by other density categories (Equation 1.05).

Equation 1.05: %0-30 subm = % total subm – (%70-100 subm) – (%30-70 subm)

- Finally, the daily percent of the area with no vegetation was determined by subtracting the submergent and emergent areas from the total water area of each grid cell.

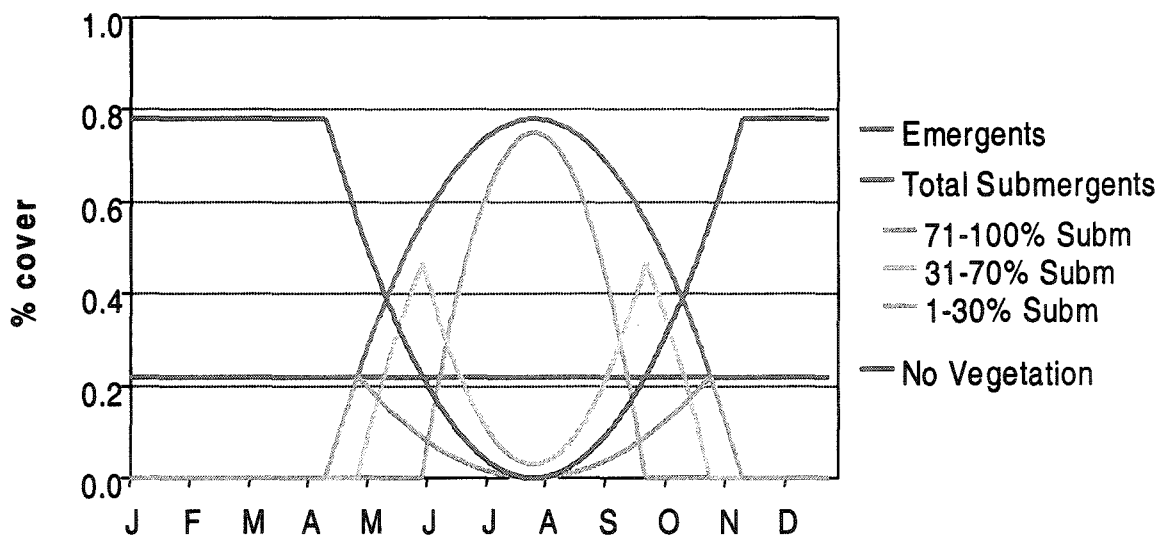


Figure 1.10: Example of the daily vegetation category changes due to modelled growth and senescence of macrophytes in a cell of the habitat grid with 21% emergent cover, 3% moderate density and 76% high density submergent coverage during peak times in Long Point Bay.

An example of the annual proportional changes in vegetation for one of the cells' in the habitat matrix is shown in Figure 1.10 with categories using the equations outlined above

1.1.5 Thermal Data

Three different sources of temperature information were used in this study at varying spatial and temporal scales: temperature profiles at a few stations collected at weekly to biweekly intervals in another study, Advanced Very High Resolution Radiometry (AVHRR) satellite images of sea surface temperature (SST) in the lower Great Lakes, and quarter-hour nearshore water temperatures collected as part of this study.

Lake Erie Biomonitoring Temperature Data

Temperature profiles were taken for the Lake Erie Biological (LEB) survey conducted by Fisheries & Oceans Canada (DFO) at 3 stations in the outer bay of Long Point every 2 weeks between April – October, 1993 and weekly between April – November, 1994 (Dahl *et al.* 1995, Graham *et al.* 1996). There were 3 LEB study sites at average depths of 6-, 9- and 38-m. A Hydrolab datalogger was used to take measurements every second while the Hydrolab was lowered on average $0.5 \text{ m}\cdot\text{s}^{-1}$. However, more readings were taken around the thermocline. Associated Loran-C positions were provided for each profile taken (Figure 1.11) and converted to latitude and longitude for use in a GIS.

The LEB profiles for each site and year were linearly interpolated and extrapolated through vertical space and time (using available ice cover charts) to produce daily profiles at 0.2-m depth intervals (for the 38-m site) and 0.1-m depth-intervals (6- & 9-m sites; Figures 1.12 & 1.13). [N.B. Interpolation was performed by W.S. Schertzer of Environment Canada (pers.com.).]

Even though LEB profiles were not taken at the exact same position each sampling date, the scatter of points covered an area roughly equivalent to the grid cell resolution of SST imagery. The error in spatial location was assumed to be negligible at this scale.

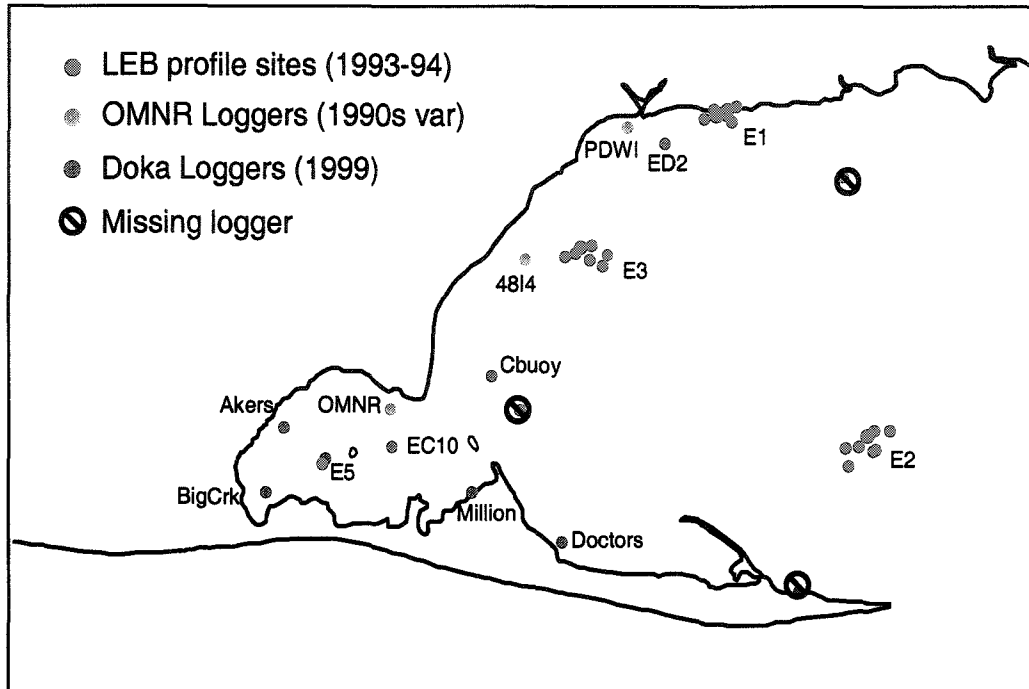


Figure 1.11: Lake Erie Biomonitoring sites for profile data (1993-1994), OMNR temperature logger locations (inner bay site is continuous through most of the 90s, other sites were 1999 only) including the Port Dover water intake, and nearshore temperature logger locations (1999) used in this thesis. (Please refer to Table 1.2 for an explanation of site codes and metadata.)

AVHRR imagery

Sea surface temperature information from satellite imagery is available for the Great Lakes from the National Oceanic and Atmospheric Administration (NOAA) CoastWatch program. NOAA supplies this information from satellites equipped with AVHRR; a radiation-detection instrument onboard several of NOAA's TIROS-N Polar Orbiting Environmental Satellites. The AVHRR remotely measures reflectance that is converted to sea surface temperature using algorithms for one or more wavelength bands (or channels) of electronic radiation (see AVHRR Pathfinder and NOAA's National Coastal Active Archive System (NCAAS) websites listed in references section). Reflectance values are averaged over the entire area of each pixel in the image. Sea surface temperature imagery estimates the temperature of the top 3 mm of a water body. The accuracy of the temperature data is reported as ± 1 °C (Vazquez *et al.* 1995, Leshkevitch *et al.* 1996).

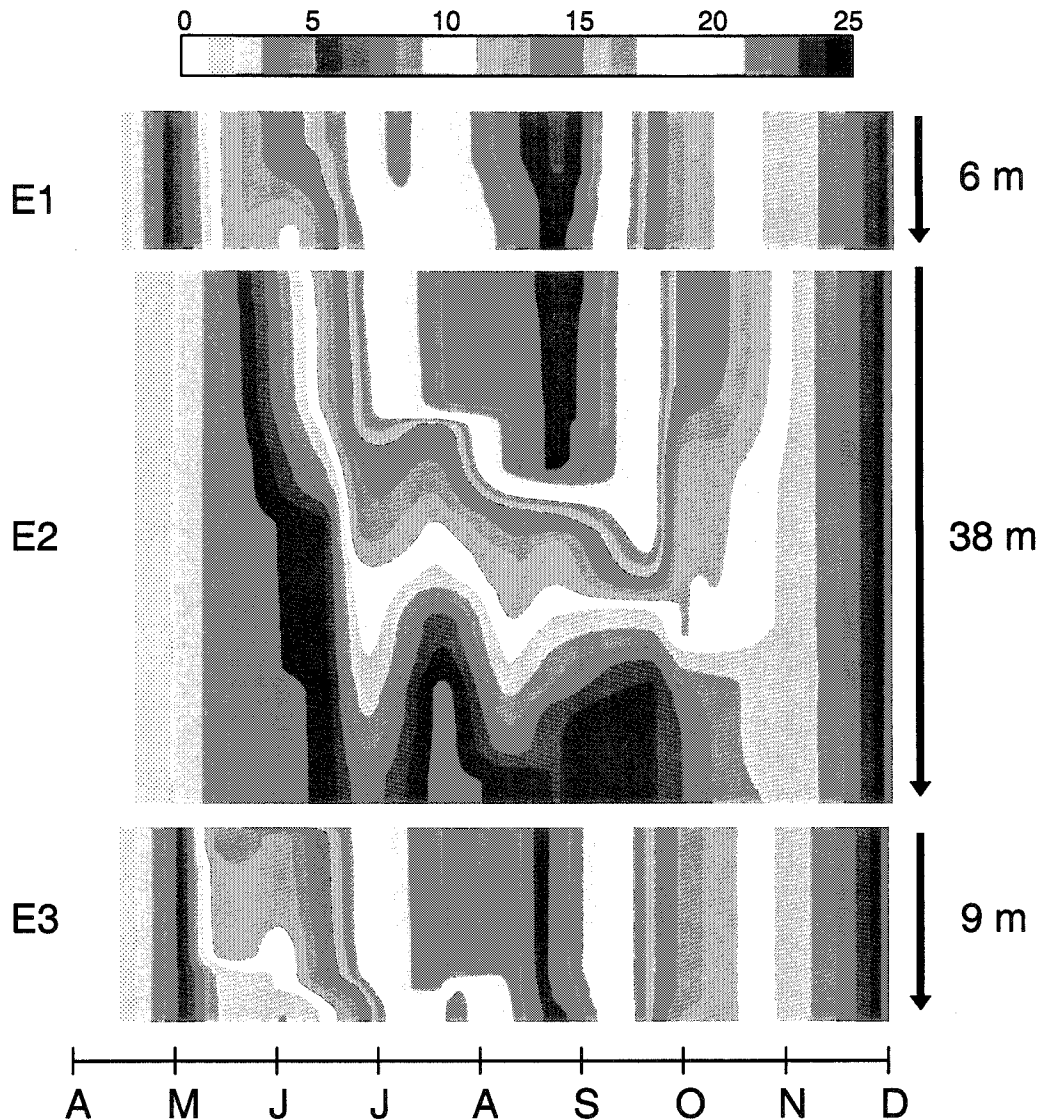


Figure 1.12: 1993 temperature profile time-series interpolated from biweekly profile samples taken at the outer bay LEB stations (E1, E2, E3) and extrapolated using available ice cover data for Long Point Bay, Lake Erie.

These data are assembled into discrete data sets and appended with Earth location and calibration information. Satellite passes occur over the Great Lakes four times daily (two day-time and two night-time passes). The image of the lower Great Lakes is a 512 x 512 pixel image of Lakes Huron, Erie and Ontario (Figure 1.14). The original extent of the CoastWatch scenes for the lower lakes is from latitude 40.765625 to 46.734375, and longitude -75.882812 to -84.156250. The raster imagery is available at a local area resolution of 1.1-km per pixel, although in practice it is 1.44-km resolution (see georeferencing section under thermal data). The NCAAS database is available for selecting specific scenes or

images from their website and then downloading the chosen files via file transfer protocol (FTP).

AVHRR imagery files are stored as binary data in compressed files. The original satellite data were converted using software provided by NOAA to generate colour images of sea surface temperature that are user-defined. DECCON v1.4 freeware (DECompression and CONversion software) is a US Army Corps of Engineers C program that decompresses CoastWatch imagery files. (See Appendix 1.1 for file nomenclature and format selections.)

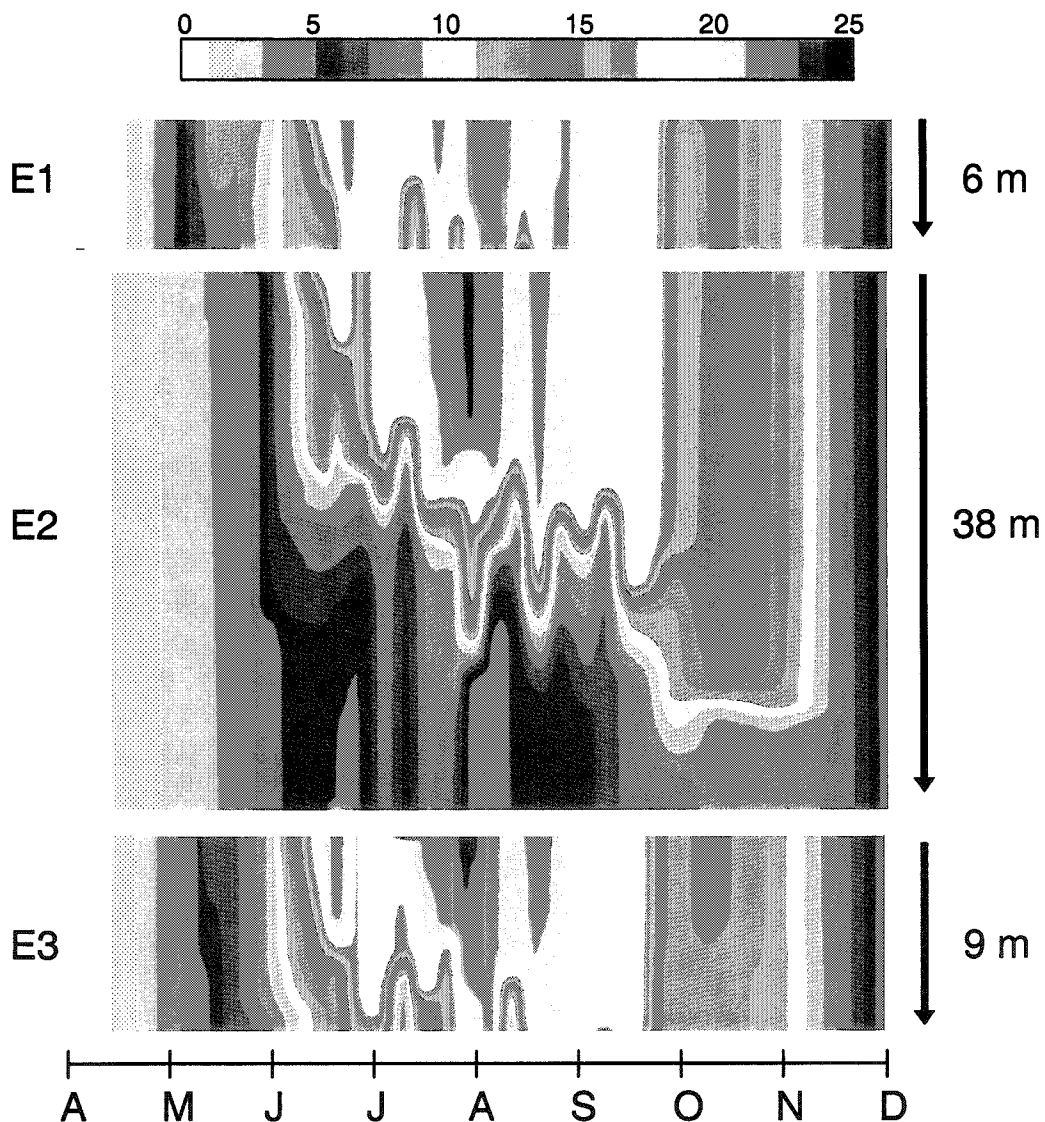


Figure 1.13: 1994 temperature profile time-series interpolated from weekly profile samples taken at the outer bay LEB stations and extrapolated using available ice cover data for Long Point Bay, Lake.

Centigrade temperature conversions are performed on the original 11-bit data that has been converted to a range of colour values (0-250) over a user-specified range of temperatures using DECCON. (For this study, the range of -5 to 35 °C was used.) All day-time and night-time passes or CoastWatch scenes for 1993, 1994 and 1999 were downloaded for conversion. The files are originally in IMGMAP format and can be converted to GIF, TIFF, SunRaster and plain raster image formats. Graphics overlays of the Great Lakes shoreline can be appended to images and associated metadata can also be extracted to ASCII format. Header information extracted for all compressed SST files provided information on the time of the pass and the satellite ID. These variables were used in a comparative study between satellite imagery derived temperatures and *in situ* temperatures collected from dataloggers. Appendix 1.3 outlines the results of this work.

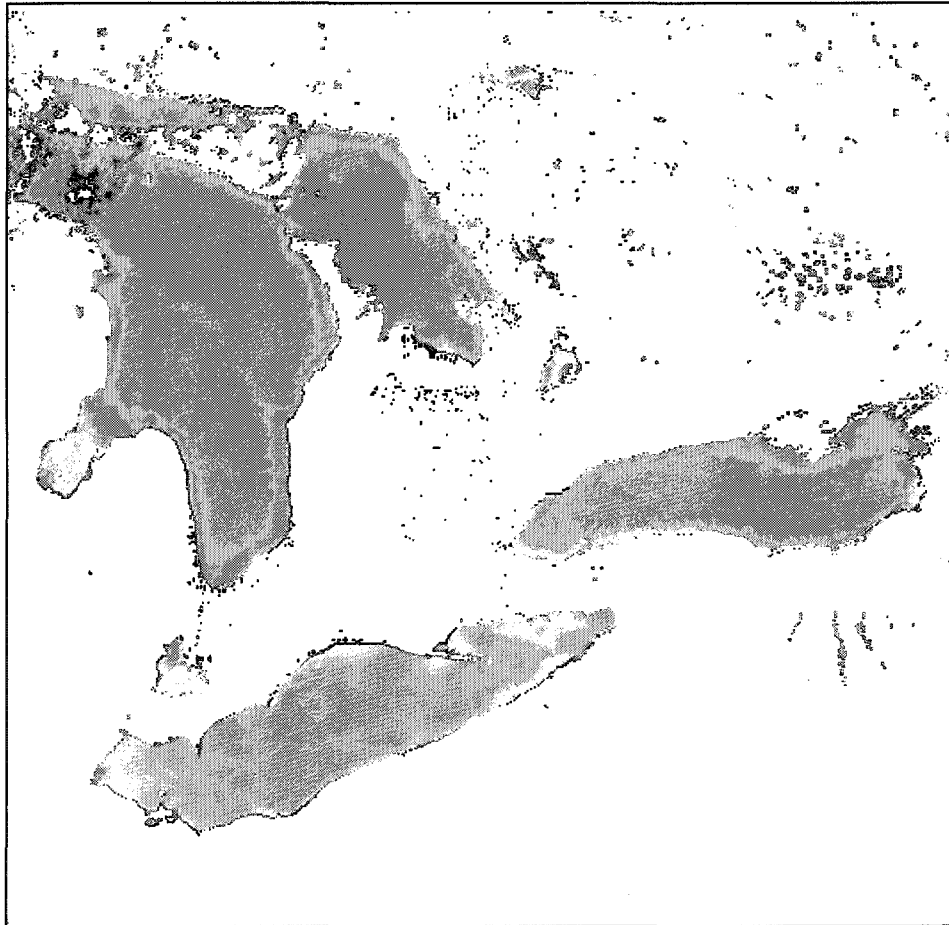


Figure 1.14: Example of the lower Great Lakes scene from AVHRR SST imagery, May 10, 1993 showing the high degree of spatial variability possible at different time of the year.

The images were checked visually to determine whether the Long Point area was cloud-free. Several scenes during the years were partially

or completely obscured by cloud cover. In 1999, 1460 images were processed by visual inspection. All bad passes and cloudy images of Long Point Bay were archived, leaving 326 that were considered usable images (180 daytime passes; 91 morning and 89 afternoon, and 146 night-time passes; 57 evening and 89 sunrise).

Due to the angle of incidence and swath path of the orbiting satellite the images required shifting to align them with the supplied graphic overlay of the Great Lakes shoreline. The shoreline graphic did not overlap very well in many cases with the thermal gradient between land and water, which is usually obvious in most images. Therefore, many images were visually corrected to be in the same geographic space before further processing by using the shoreline overlay to determine the number of vertical and horizontal pixels that the images required for alignment. Unfortunately the image shifts did not follow any consistent pattern and each required an individual, and therefore subjective, realignment. All the useable images were then reconverted without the overlay graphics embedded and with the proper shifts. Some images showed distinct seiche events occurring (i.e. distinct large temperatures drops from one cell or pixel to the next in offshore areas), therefore the correct geographic positioning of the image was very important.

The final cloudfree images were batch processed by using Arc Macro Language (AML) in ArcInfo v7.0.1 (Arc and Grid modules, ESRI®, Redlands, CA) for conversion of the image to a grid coverage, re-georegistration of the image into a Transverse Mercator projection (NAD 83), clipping of the image to the geographic area for analysis, and conversion of the pixel colour values to temperature values in the final grid coverages.

The original Mercator projection of the images was not standard, therefore reprojecting the raster images by rubber-sheeting or warping was necessary (Nelson May, Stennis Space Centre, pers. comm.) Due to the fact that the study area was quite small in comparison with the original image, and that the original image's georegistration and position was inaccurate, a more accurate, local georeferencing was accomplished by using known features and co-ordinates in the Long Point area. This clipped image was warped, using a rubber-sheeting method, to the correct Long Point Bay geographic space by using 10 UTM co-ordinates of prominent features in the area from a hard-copy map (Long Point 40-I/9 edition 7. 1994. EMR Can. 1000 UTM grid zone 17. NAD 83. Transverse Mercator projection) and linking them to grid cell co-ordinates.

During the rubber-sheeting or warp transformation of satellite imagery, there was transformation error when clipping to study area box coordinates. (Appendix 1.2; N.B. all satellite files that were converted to grids have the same error rates). The area of one pixel after transformation was $1.44 \text{ km} * 1.44 \text{ km} = 2.07 \text{ km}^2$ (cited as 1.1-km resolution by CoastWatch) but the discrepancy was not entirely related to image processing. The study area boundary was clipped to 533282.489 –

585429.565 m W and 4690775.557 – 4742922.634 m N in UTM coordinate space, Zone 17, which defined the Long Point study area.

The final, clipped grid (30 x 22 pixels) was converted to temperature values using Equation 1.07. The linear equation was determined from colour values, the independent variables, which ranged between 0-250, and a user-specified, temperature range of –5 to 35 °C, the dependent variable. Cloudy pixel values were very cold and were assigned a colour value of 0 automatically and therefore translate to temperature values of –5 °C, which could also indicate ice conditions. Any temperature below 0 °C was reassigned to null values. Any missing values in the water portion of the grid during ice-free conditions (i.e. clouds) were assigned new values by interpolation using a nearest neighbour (8-cell average) procedure in ArcInfo.

Equation 1.07: Temp (°C) = 0.16 * Colour – 5, where Temp = surface temperature

Nearshore temperature study

In situ temperature data were collected in order to validate nearshore satellite temperatures and to determine the temporal dynamics of thermal structure at a finer scale than satellite imagery provided. Ten, Onset StowAway Tidbit™ temperature dataloggers were deployed in the Long Point Bay area in 1999 (Figure 1.11; Table 1.2). Dataloggers were suspended in a white PVC tube that allowed water flow but shaded the logger from direct sunlight. PVC tubes were attached to anchors, wooden stakes or navigational buoys but all dataloggers were set at 0.5-1.5 m water depth. Two of the Long Point dataloggers were lost. The remaining dataloggers were deployed for various times between April and December. Dataloggers recorded temperatures every 15 minutes, however, due to technical difficulties some loggers had missing data in August and September, 1999.

An additional two dataloggers were deployed by the Ontario Ministry of Natural Resources (OMNR) in Port Dover, Ontario (Figure 1.11, Table 1.2). One OMNR logger was a long-term monitoring station for most of the 1990s where the logger was kept *in situ* year round. An additional source of temperature information was obtained from the Port Dover water treatment facility through the OMNR. All the data provided by the provincial agency was recorded at 2-hour intervals.

The temperatures from all 11 datalogger sites are shown in Figures 1.15 & 1.16. The range of temperatures recorded in the ice free season was 3 to 28 °C; overwinter water temperatures did not go below –1 °C . Inner bay dataloggers had similar thermal regimes in 1999 with subtle differences between sites and a transitional area in mid-bay that behaved like outer bay dataloggers, probably during inundations. Outer bay dataloggers were cooler and less variable, with the exception of the south shore, Doctors Inlet datalogger near the spit that was the most variable of all Long Point dataloggers

Table 1.2: List of datalogger site codes & descriptions, equipment, geographic locations, logger & site depths, deployment periods, recording intervals & deployment methods (CG = Coast Guard)

Site Name	Description	Logger Type	Latitude (Degrees)	Longitude (Degrees)	Logger Depth (m)	Site Depth (m)	Deployment Period	Record Interval	Installation Type
4814	Pembina gas well marker	Onset Hobo™	42.717	-80.273	5.0	7.0	07/19/99 - 12/31/99	2 hr	buoy
Akers	Wooden post (Aker's Marina)	Onset Tidbit™	42.637	-80.432	0.5	1.0	04/27/99 - 08/11/99 10/06/99 - 12/06/99	15 min	fixed post
BigCrk	Channel marker (Big Creek)	Onset Tidbit™	42.601	-80.443	0.5	0.5	06/06/99 - 08/11/99 10/06/99 - 12/06/99	15 min	bottom anchor
C-buoy	CG navigational buoy	Onset Tidbit™	42.653	-80.294	1.0	6.0	05/16/99 - 10/29/99	15 min	buoy
Doctors	Wooden post (Doctor's Inlet)	Onset Tidbit™	42.574	-80.25	0.5	1.0	04/27/99 - 08/11/99 10/06/99 - 12/06/99	15 min	fixed post
E5LEB	L. Erie Biomonitor site	Onset Tidbit™	42.612	-80.405	1.0	1.5	04/27/99 - 09/28/99	15 min	bottom
EC10	CG fixed light	Onset Tidbit™	42.619	-80.357	1.0	2.0	04/14/99 - 08/11/99 10/06/99 - 12/03/99	15 min	bottom
ED2	CG navigational buoy	Onset Tidbit™	42.765	-80.185	1.0	6.0	05/16/99 - 10/29/99	15 min	buoy
Million	Wooden post (Long Point Co.)	Onset Tidbit™	42.598	-80.313	0.5	1.0	04/27/99 - 08/11/99 10/10/99 - 12/06/99	15 min	fixed post
OMNR	OMNR logger	Onset Hobo™	42.638	-80.364	1.5	1.5	01/01/99 - 12/31/00	2 hr	bottom
PDWI	Port Dover Water Intake	Unknown	42.779	-80.215	1.5	3.0	05/13/99 - 12/31/99	2 hr	inline pipe

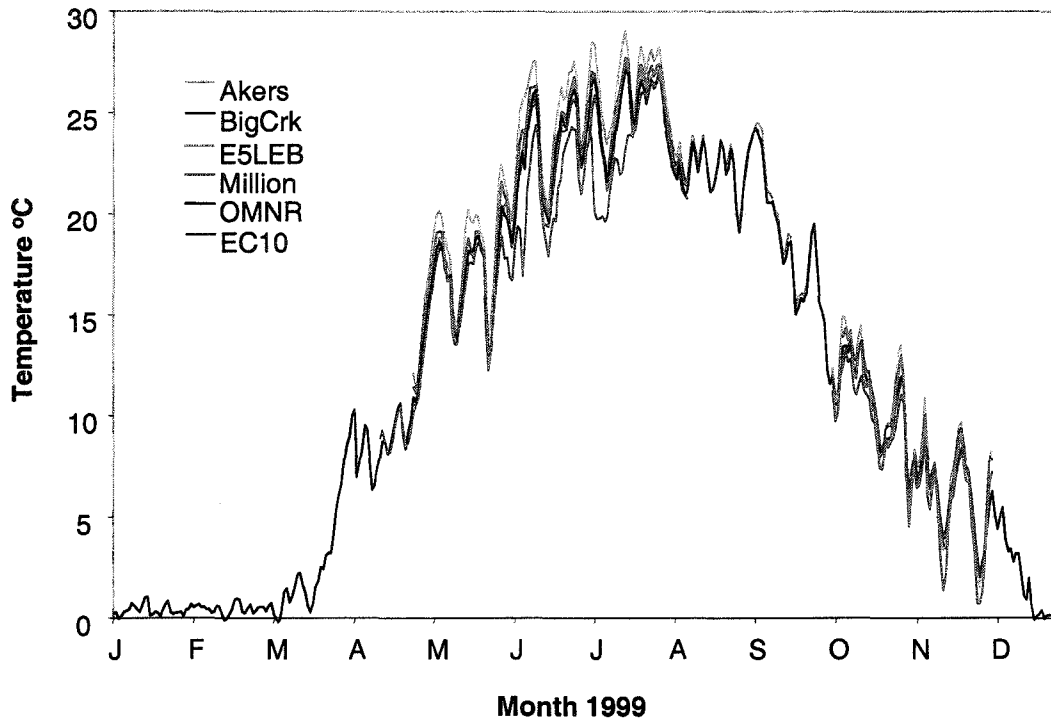


Figure 1.15: Daily temperature averages for the inner bay logger sites in 1999 (see Figure 1.10 for datalogger locations).

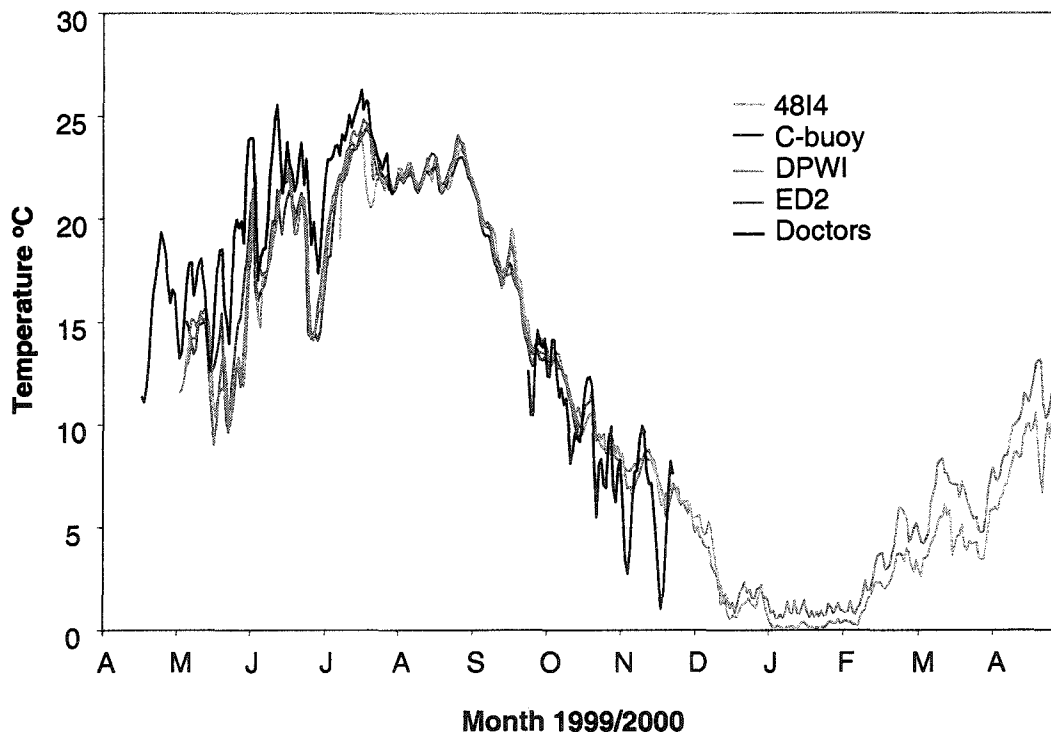


Figure 1.16: Daily temperature averages for the outer bay logger sites in 1999 & 2000 (see Figure 1.10 for datalogger locations).

1.1.6 Thermal Structure Recreation

1993/94 3D Thermal Structure

Originally, 3D thermal structure was recreated using a matrix interpolation method outlined in Appendix 1.3. A difference matrix was constructed by using 1 m, average temperature differences for the 6-, 9-, and 38-m LEB sites then linearly and diagonally interpolating between maximum depths to recreate temperatures profiles for all site depths in between. The 3D difference matrix or lookup table was used to create each 1-m depth layer below the satellite imagery surface temperature grid as a starting point. Using AML code in ArcInfo, temperatures in subsequent depth layers were reconstructed based on average temperature profile differences between 1-m intervals based on the date and the maximum depth of each cell. An example of the reconstructed depth layers is shown in Figure 1.17.

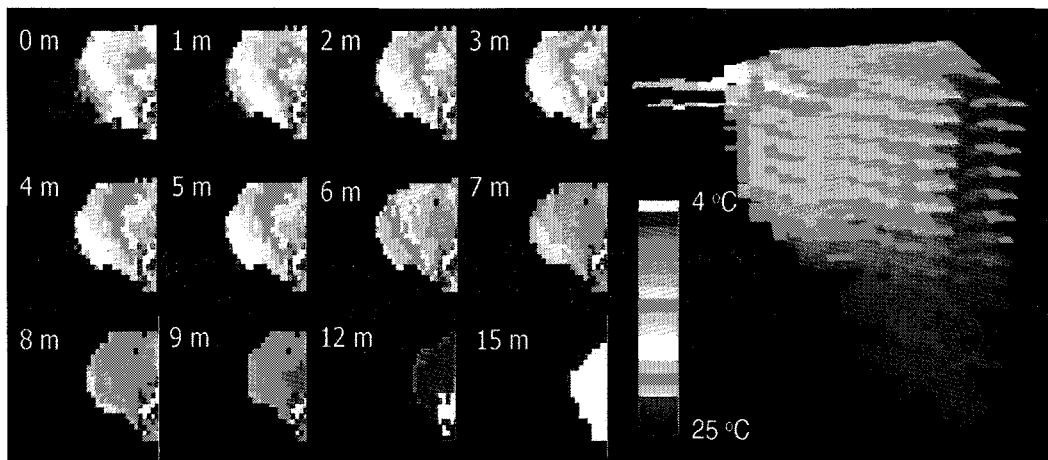


Figure 1.17: Thermal layers for May 10, 1993 in Long Point Bay based in interpolation and extrapolation of SST imagery and LEB profile data.

A TIN was created using the Long Point Bay bathymetry that allowed visualization of bottom temperatures that were extracted from the depth layers (Figure 1.18). A TIN is a vector coverage with fewer data points required than grid methods. TINs are not smooth surfaces and an even distribution of data is best. They are not suitable for extrapolation and the original data is kept. These temperature interpolations methods were only used in the initial work done to thermally characterize Long Point Bay for yellow perch thermal habitat (Chapter 2) where reconstruction of 4D thermal structure is an example of the type of methodology that could be used to calculate realistic thermal volumes but only works for years where profile data are available (i.e. 1993 & 1994 in Long Point Bay).

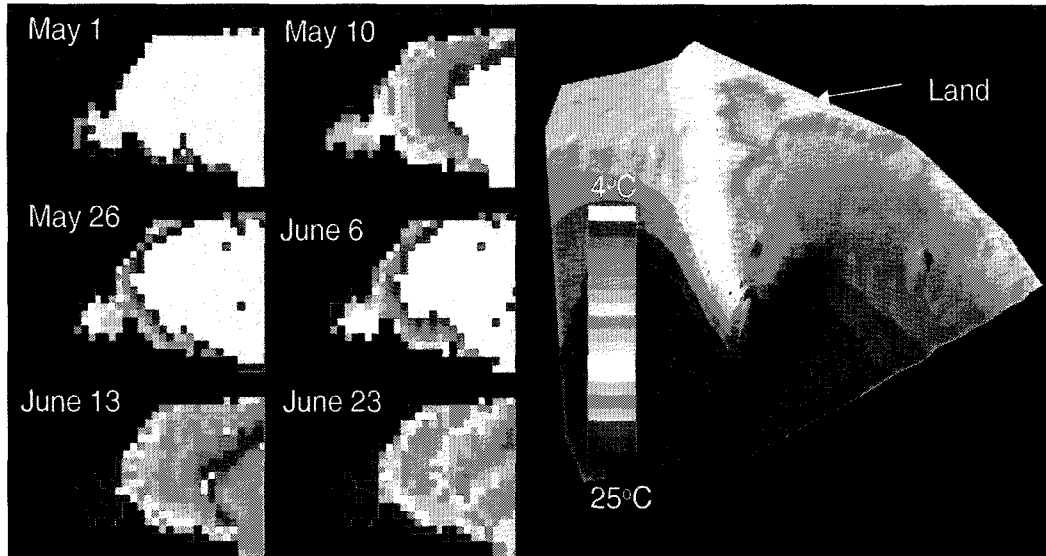


Figure 1.18: Long Point bottom 1-m temperatures extrapolated and interpolated from SST imagery and LEB profiles for different dates in 1993. May 10th temperatures were draped over a TIN of Long Point Bay derived from bathymetry values.

1999 3D Thermal Structure

Another method was employed to generate 4D thermal structure for 1999 using empirical patterns in thermocline depth, correlations during upwelling and downwelling events, and the rates of warming and cooling during different times of the year. This method was used to generate the daily temperature profiles in the habitat database for the modelling efforts in Chapter 4. Three sources of temperature data were used to recreate 1999 daily temperatures: surface temperatures derived from satellite information, LEB profile relationships, and nearshore temperatures from *in situ* dataloggers.

Grid-based SST images have high spatial resolution with some temporal resolution (up to four times daily, weather permitting), while point temperatures (both profiles and dataloggers) have some vertical and high temporal resolution, with a spatial component if more than one site was sampled. Remotely-sensed information can have high error rates for various reasons (see Appendix 1.3) whereas *in situ* temperatures are more accurate locally. To capitalize on the spatial and temporal resolutions of data from different sources while preserving accuracy, temperatures were used following these steps to obtain a 4D representation of thermal structure:

1. Remotely-sensed temperatures were corrected for systematic errors using *in situ* data to calibrate daily SST grids.
2. Time-series data was used to interpolate between corrected, average SST grids.
3. Daily profiles were estimated for each cell within the SST grid, based on general empirical models of Long Point thermal dynamics generated from historical data. Relationships between surface temperature, Julian date and different profile characteristics, such as

thermocline depth, were developed using the profile data from 1993 and 1994 and applied to 1999 daily surface temperatures to recreate 3D structure.

Correction of Nearshore SST Errors

The mismatch between logger and satellite temperatures was quite high at some times and in some locations, especially in the nearshore zone (Appendix 1.3). Various hypotheses about error rates were analysed using principal components and regression analysis, kriging, and temporal trend analysis to test spatial and temporal discrepancies between *in situ* and remotely-sensed data. Trend surface analysis emphasizes global versus local trends and uses least-squares linear, quadratic or cubic fit to interpolate point data. This is a smoothing and approximate method and the original data is not preserved and is highly affected by extreme and uneven data points, therefore extrapolation is not reliable. The purpose of kriging is to locally estimate the mean value of a *regionalised* variable by a weighted moving average. There is flexibility in the interpolation model used, therefore it is better than a simple distance-weighted average. Regionalised variables are neither random nor deterministic, therefore this method is better than inverse distance and triangulation because it takes the spatial process or variogram into account with error and uncertainty measurements. It also detects spatial dependence or autocorrelation but is not suitable for spikes, breaklines or abrupt changes in data. A global or local interpolator can be used and original data values are preserved. Semivariance is a measure of the degree of spatial correlation among sample data points as a function of the distance and direction between the points

Based on these results, various manipulations were performed to correct the erroneous temperatures in the grid matrix and maximise concordance with datalogger values. The results of satellite and *in situ* temperature comparisons revealed that nonlinear spatial relationships in error variance existed, but these were not consistent between dates. There were general trends in error rates between the inner and outer bays, between nearshore and offshore temperatures, and between satellite pass times. Therefore different correction methods were applied to selected zones in the Long Point grid matrix during different pass times, which included spatial interpolation techniques and statistically-determined correction factors.

These methods were applied in the following manner. Due to the differences observed in SST nearshore error rates and the different thermal regimes that were detected by dataloggers, the Long Point region was divided into three thermal zones (Figure 1.19). Water cells in the Long Point grid matrix were assigned to one of the following zones: an offshore region, a spit region and an inner bay region which resulted in 21 spit cells, 46 inner bay cells, and 344 outer bay cells. The surface temperature grids were corrected in the offshore zone with a different

correction factor depending on the time of the satellite pass. Correction factors were generated by using linear regression models (forced through the origin) that regressed daily temperature averages of all offshore loggers against corresponding grid cell temperatures from satellite imagery (Table 1.3).

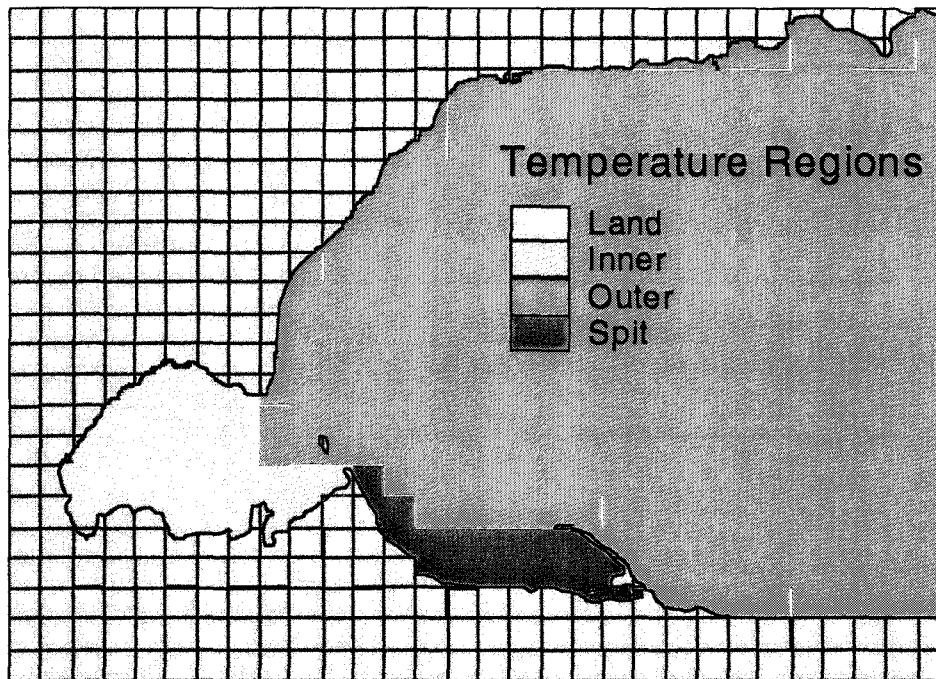


Figure 1.19: Thermal regions used in temperature modelling based on statistical analysis of satellite and dataloggers temperature data.

Table 1.3: Correction factors (linear regression coefficients for $y=mx$) for offshore grid cells determined from datalogger and satellite temperature comparisons at different pass times. The values were interpolated spatially for each pass time to obtain a grid of correction values to be applied to the appropriate satellite images.

Offshore Site Code	Satellite Pass Time			
	Sunrise	Morning	Afternoon	Evening
ED2	1.01	0.98	0.94	0.91
4814	1.03	0.98	0.97	0.94
C-buoy	1.01	0.97	0.94	0.91
OMNR	1.07	1.02	0.94	0.96
EC10	1.01	0.99	0.92	0.92
E5LEB	1.08	1.01	0.94	0.96

The correction factors for the datalogger sites were entered into their associated grid cells and were interpolated by splining in a GIS to

make a correction factor grid for the offshore zone. With the spline function, a smooth transition between points is created where the original data are preserved, it emphasizes trends, not anomalies, and is not good for patchy distributions. An offshore correction factor grid was created for sunrise, morning, afternoon and evening passes based on results from Appendix 1.3, which showed errors were not consistent across passes. All the SST temperature data in nearshore cells of the spit and inner bay regions were not used because the error rates were too high at the land-water interface, as well as at some additional cells in the inner bay that were not overlap cells. Selected offshore cells that corresponded to datalogger locations were used to predict the nearshore cell temperatures at other datalogger locations by using linear relationships with the highest regression coefficients between datalogger temperatures (Table 1.4; Figure 1.20). This step was taken to 'seed' the nearshore area with temperatures before extrapolating offshore temperatures into the nearshore zone, otherwise the spline function would not have extrapolated properly. The remainder of the missing cell values were generating by using a nonlinear spline function to extrapolate the existing temperatures into the warmer nearshore zone. Lastly, the temperature grids from the same day (up to 4 grids) were averaged to end up with 174 average temperature grids for 1999.

Table 1.4: Offshore cell IDs used to predict nearshore cell temperatures based on regression equations developed from 1999 datalogger temperatures.

Cell ID	Predicts (Cell ID)	Correction Equation
107	76	$T_{Near} = T_{Off}$
397	393	$T_{Near} = 1.07 * T_{Off}$
397	483	$T_{Near} = 0.93 * T_{Off}$
455	490	$T_{Near} = 1.01 * T_{Off}$
428	554	$T_{Near} = 0.99 * T_{Off}$
527	559	$T_{Near} = 1.02 * T_{Off}$

Surface Temperature Temporal Interpolation

1999 datalogger temperatures were used to temporally interpolate between existing grid cell temperatures to obtain daily surface temperatures for 191 days in 1999 that had missing SST imagery. The initial results showed that using daily temperature differences between logger data were better than linearly interpolating between grid temperatures when there were missing data, especially over longer periods of time (Appendix 1.3). Because different thermal regimes were exhibited by the *in situ* datalogger temperatures depending on their location, selected logger sites were chosen as representative of temporal

changes in each of the three thermal zones (inner, spit, and outer). If data was not available at the sentinel site then an alternate logger time series was chosen based on the best fit linear regression relationships between sentinel sites and adjacent logger sites. During winter months, only OMNR data was available. Spatial variability in surface temperature changes was assumed not to vary significantly during the winter months. The daily temperatures were calculated by using the previous day's temperature in that cell, whether interpolated or SST temperature, and adding the change in daily temperature for the appropriate logger site (ΔT_{logger}), either directly or by using the conversion algorithm in Table 1.5.

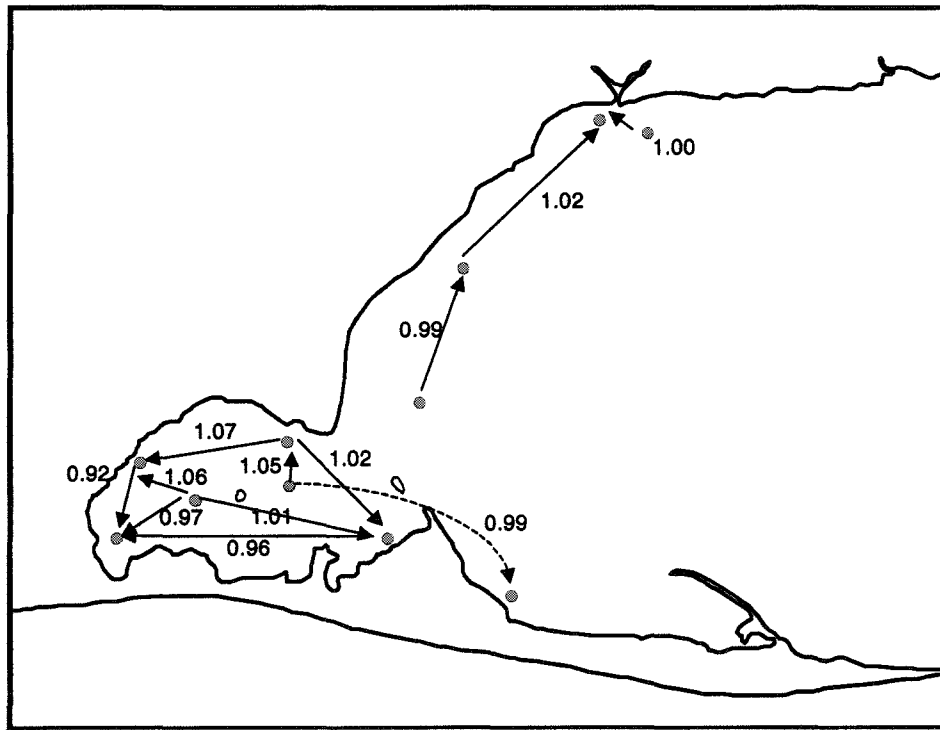


Figure 1.20: Map of significant regression coefficients ($p < 0.05$) calculated for converting temperatures at different datalogger locations in Long Point Bay. Arrows point to the independent variable in regression equations.

Table 1.5: Sentinel sites used for each region's temperature changes (temporal interpolation)

Thermal Region	Datalogger Locations
Inner Bay	ΔT_{OMNR}
Spit Area	$\Delta T_{\text{Doctors}}$ else ΔT_{OMNR} (Jan – Apr)
	else $\Delta T_{\text{C-buoy}}$ (Aug – Sep)
Outer Bay	ΔT_{DPWI}
	else ΔT_{OMNR} (Jan – Mar) else $\Delta T_{\text{DPWI}} = 0.6881 * \Delta T_{\text{OMNR}} + 1.6706$ ($r^2 = 0.9451$; Apr-May)

Temperature Profile Generation

A statistical analysis using 1993 and 1994 LEB profile data, produced empirical relationships and general models to calculate the depth of the thermocline, the thickness of the mesolimnion layer, and the rate of temperature decrease through the epi-, meso-, and hypolimnions. These relationships were generated because an accurate estimate of the changes in daily 3D thermal structure of Long Point Bay without actual profile data was necessary to calculate suitabilities and vital rates in yellow perch that are very sensitive to temperature.

Thermocline depth

The interpolated LEB data profiles were used to determine the depth of thermocline and thickness of the mesolimnion layer. The temperature difference between 0.5-m depth intervals was calculated for the daily LEB profiles (Figures 1.21, 1.22, & 1.23). For this analysis, the thermocline was defined as the depth at which the greatest temperature change per metre occurred, and which was greater than 1°C difference. Surface temperature changes, site depth and Julian day were significantly related to thermocline depth throughout the year.

In 1993 and 1994, the thermocline varied between 10 – 19 m in depth, on average, at the 38-m LEB site and increased in depth through the year from its establishment in the spring. The thermocline was not evident until the surface temperature in that location reached > 9 °C and was not usually at the 6-m site unless upwelling events were occurring.

The average depth and thickness of the mesolimnion for the 3 LEB sites were statistically linked to the depth of the site and day of year. The average depth of the thermocline (Z_T) was linearly related to the time of the year (Julian day) under normal and downwelling conditions (Equation 1.08);

Equation 1.08: $Z_T = JD * 0.144 - 14.98$, where JD = Julian day ($R^2 = 0.757$; SE = 3.813)

Under upwelling conditions when the thermocline depth was shallower than average the thermocline depth was also related to site depth (Equation 1.09):

Equation 1.09: $Z_T = Z_{MAX} * JD * 0.00379 - 0.516 * Z_{MAX} + 4.624$, where Z_{MAX} = Site depth (m); ($R^2 = 0.7$)

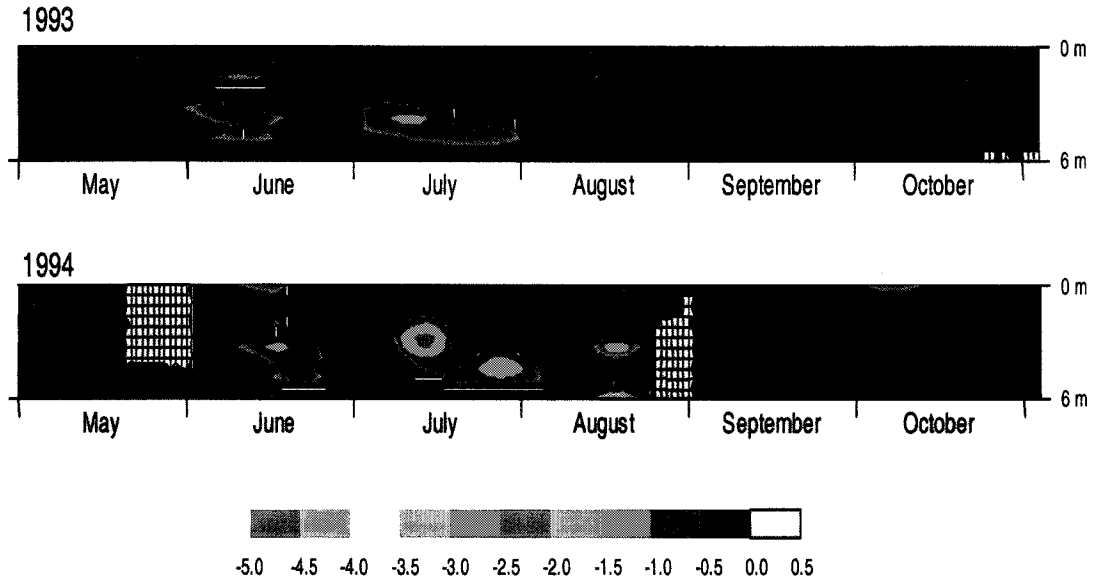


Figure 1.21: Temperature differences between 0.5-m intervals for temporally interpolated profiles at LEB Station E1 in 1993 & 1994.

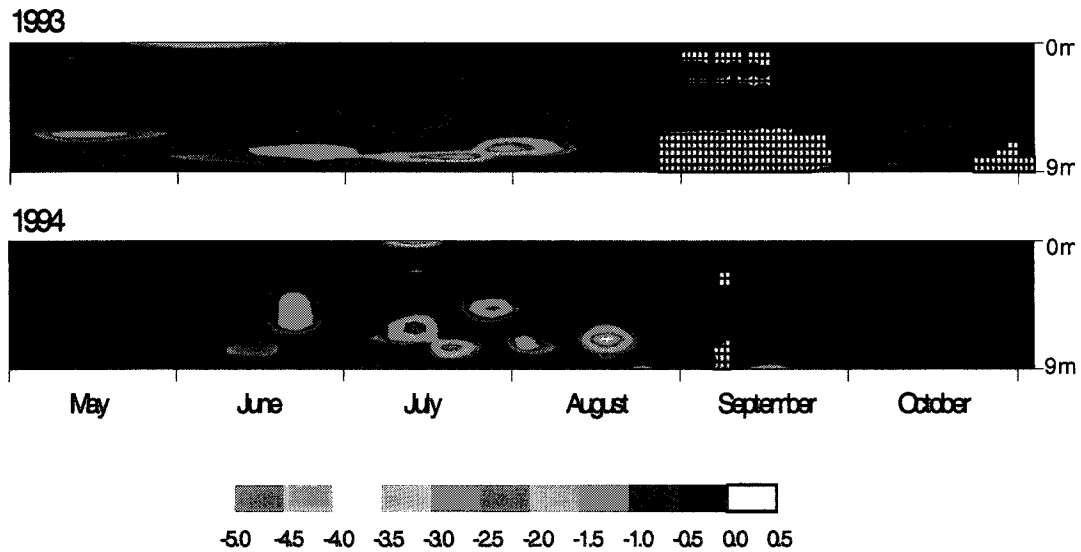


Figure 1.22: Temperature differences between 0.5-m intervals for temporally interpolated profiles at LEB Station E3 in 1993 & 1994.

Variation around the average thermocline depth at the 38-m site was assumed to be correlated with internal seiches. Upwelling and downwelling events have been related to surface temperature changes at nearshore sites (Bolgrien & Brooks 1992). This was tested in the outer bay where the surface temperature of the shallow LEB sites was compared to the variation of the thermocline. To cover the range of conditions possible under one model of thermocline depth, the slopes and intercepts of Equations 1.08 and 1.09 must be equal under certain conditions. A separate equation for the slope of the model was generated

to incorporate both functions. The slopes would be equal with the following scalar applied, $X/Z_{MAX} * Z_{MAX} * 0.00379 = 0.144$, where $X = 38$ under downwelling or normal conditions or Z_{MAX} under upwelling conditions.

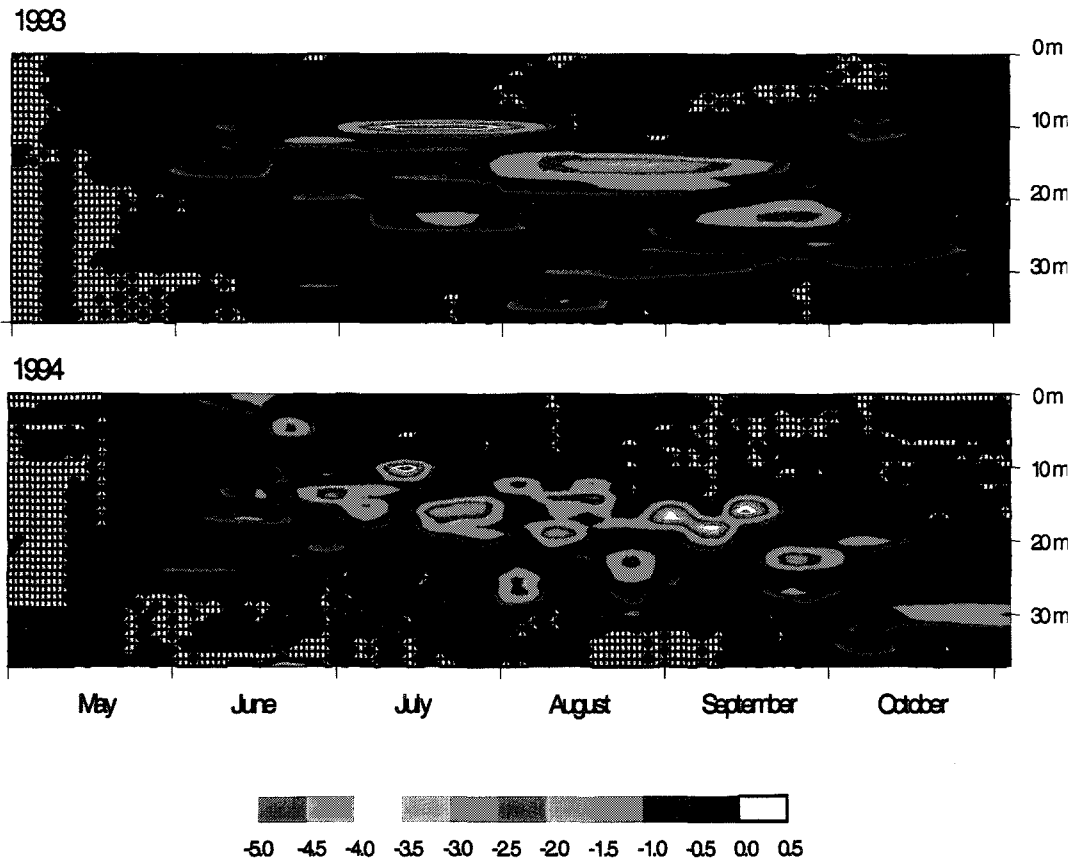


Figure 1.23: Temperature differences between 0.5-m intervals for temporally interpolated profiles at LEB Station E2 in 1993 & 1994.

Because nearshore sites (6- and 9-m LEB sites) act as ‘sentinel’ sites of upwelling and downwelling events, then the extremes of daily temperature changes were used to bound the scalar and create a new equation. Extremes in surface temperature changes at nearshore sites ranged from ± 7 °C. The relationship between daily temperature fluctuations at sentinel sites and the magnitude of the thermocline depth change due to wellings was assumed to be linear. Therefore, the slope of the relationship between the surface temperature difference (ΔT_0) and the T_z scalar (X) is $(38 - S_z)/14$. The x-intercept was solved for by substituting in the extreme condition values into the equations above, which yielded Equations 1.10 and 1.11.

Equation 1.10: $X = (38 - Z_{MAX})/14 * \Delta T_{0,W} + b$ (where $\Delta T_{0,W} = -7$ and $X = Z_{MAX}$ during upwellings)

Equation 1.11: $X = (38 - Z_{MAX})/14 * \Delta T_{0,W} + b$ (where $\Delta T_{0,W} = 7$ and $X = 38$ during downwellings)

Therefore $b = Z_{MAX}/2 + 19$ results. It follows that $X = (38 - Z_{MAX})/14 * \Delta T_0 + Z_{MAX}/2 + 19$, which can be reworked into Equation 1.12.

Equation 1.12: $X = (38 * (\Delta T_{0,W} + 7) - Z_{MAX} * (\Delta T_{0,W} - 7)) / 14$

Substituting into the original equation (Equation 1.09) with the equation for the scalar (X), the equation for thermocline depth now incorporated all the factors that affected thermocline depth throughout the year (Equation 1.13).

Equation 1.13: $Z_T = (50 * (\Delta T_{0,W} + 7) - S_z * (\Delta T_{0,W} - 7)) / 14 * JD * 0.00379 - 0.516 * S_z + 4.6247$ Where Z_T = thermocline depth, Z_{MAX} = site depth, and JD = Julian day and $\Delta T_{0,W}$ = surface temperature change in the welling zone. (NOTE: 38 has been changed to 50 in the final equation because this element of the model had more to do with the maximum depth of the site than the maximum depth of the thermocline and introduced some strange dynamics into profile predictions below this depth in its original form when tested and verified.)

The thermocline depth equation was applied to all the cells in the grid matrix each day and a “sentinel” site for indicating upwelling and downwelling events was used to calculate ΔT_0 . Cell 224 was the sentinel site and was close to LEB sites E1 and E3 as well as located in an area which is indicative of thermal fronts and upwellings in the eastern basin in SST imagery (Bolgrien & Brooks 1992, Ullman *et al.* 1998).

Logical tests were also used to correct thermocline depth predictions because the thermocline model only applied under certain conditions (i.e. during certain times of the year) and it also needed to be bounded for unrealistic output. For instance, the maximum depth of the thermocline was set at 32-m regardless of site depth or time of year. The logic statements outlined in Figure 1.24 were applied to prevent any errors due to extrapolation of the model beyond boundary conditions based on the empirical data.

Mesolimnion thickness

Mesolimnion thickness was defined as the sum of depth layers in metres that had greater than a $0.5 \text{ } ^\circ\text{C}\cdot\text{m}^{-1}$ change in temperature around the thermocline. The mesolimnion thickness of the LEB profiles was related to surface temperature throughout the year. A simple linear regression between surface temperature and mesolimnion thickness yielded Equation 1.14.

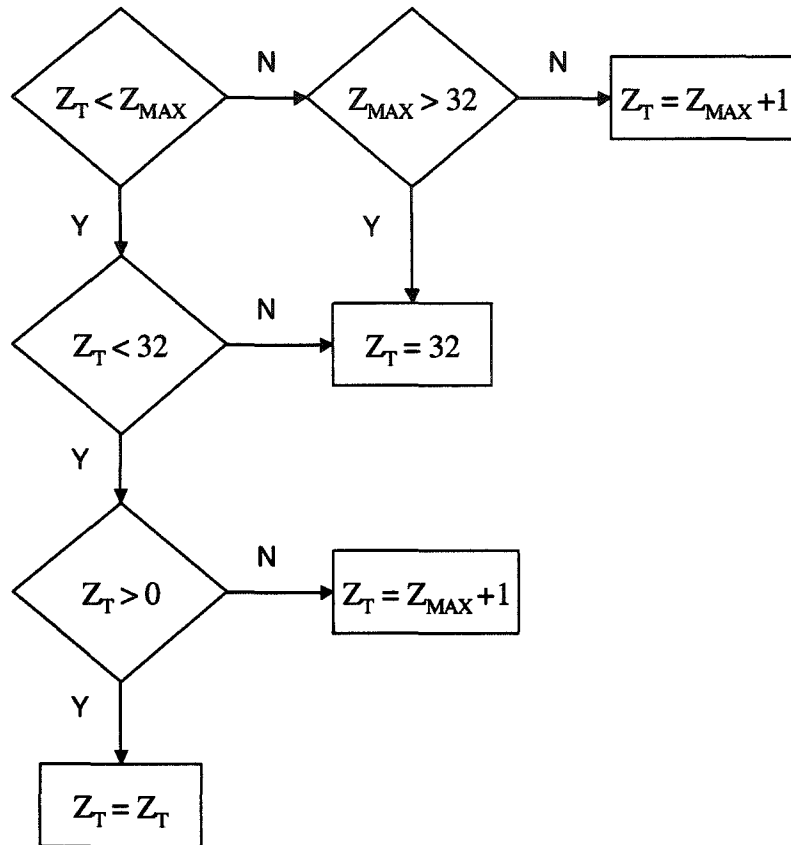


Figure 1.24: Logical statements to correct for predicted thermocline depths that are outside of boundary conditions. (Z_T = thermocline depth and Z_{MAX} = site depth)

(**Note:** The thermocline depth was set at $Z_{MAX} + 1$ if the surface temperature of that cell was below $10\text{ }^\circ\text{C}$, i.e. the entire profile was generated as epilimnion in this case. Final values were rounded to the nearest metre.)

Equation 1.14: $Meso = 0.49 * T_0 - 5.24$ ($R^2 = 0.713$, $SE = 1.074$), where Meso = mesolimnion thickness (m) and T_0 = surface temperature ($^\circ\text{C}$). [Note: Mesolimnion thickness was only calculated during thermocline set up and that only occurred once surface temperatures reached $10\text{ }^\circ\text{C}$.]

When upwelling occurred, the surface temperature decreased sharply and the thickness of the mesolimnion was compressed. During downwellings, the surface temperature rose and the thickness of the mesolimnion increased (Figure 1.22). Therefore variation around the linear equation above was a function of surface temperature change at that site. If surface temperature changes were minimal then the intercept of the equation was -5.24 , as above; the average condition. The largest surface temperature difference observed from one day to the next was $\pm 7\text{ }^\circ\text{C}$. Larger surface temperature changes corresponded to a change in the intercept to -3.24 during downwelling and -7.24 during upwellings but no change in slopes. Therefore, using these extremes, the intercept of the

original mesolimnion thickness relationship was modified using a linear relationship with a slope of $-2/7$ calculated by using the extreme endpoints of the function outlined above that defined the upper and lower boundaries of the mesolimnion thickness function by modifying the intercept. Therefore, the equation constant was modified by the ΔT_0 to obtain Equation (1.15).

$$\text{Equation 1.15: } \text{Meso} = 0.69 * T_0 - (\Delta T_0 * 0.286 + 5.24)$$

The thermocline usually occurred closer to the top of the mesolimnion layer. Therefore, the upper depth of the mesolimnion was arbitrarily set at $1/4$ of the mesolimnion thickness above the thermocline using Equation 1.16.

$$\text{Equation 1.16: } Z_{\text{TopMeso}} = Z_T - \text{Meso} / 4$$

Correspondingly, the depth of the bottom of the mesolimnion was calculated using Equation 1.17.

$$\text{Equation 1.17: } Z_{\text{BtmMeso}} = Z_T + \text{Meso} * 3 / 4 \text{ (or } Z_{\text{TopMeso}} + \text{Meso)}$$

If the thermocline depth (Z_T) was equal to the site depth (Z_{MAX}) + 1 (see previous section) then mesolimnion thickness (Meso) was set to 0 m to avoid assigning bottom depths in the profile to the mesolimnion layer erroneously. It was also mathematically possible for mesolimnion thickness to be negative, therefore, values for Meso were restricted to ≥ 0 m.

Mesolimnion Maximum and Total Profile Temperature Changes

The maximum temperature change over the entire mesolimnion (ΔT_{Meso}) in 1993 and 1994 at the 38-m site (the deepest site) was -17.5 and -12.6 °C respectively (N.B. Minimum ΔT_{Meso} could be as low as -0.5 °C at all sites). Average ΔT_{Meso} was related to the thickness of the mesolimnion layer (Meso) and was modified by site depth (Z_{MAX}) in a nonlinear fashion (Figure 1.25). However the data points were limited (N=3) so the following approach was taken. If $Z_{\text{MAX}} < 9$ m then Equation 1.18 applied, if Z_{MAX} is ≥ 9 m then Equation 1.19 was used.

$$\text{Equation 1.18: } \Delta T_{\text{Meso}} = \text{Meso} * (0.3197 - 0.3298 * Z_{\text{MAX}})$$

$$\text{Equation 1.19: } \Delta T_{\text{Meso}} = \text{Meso} * (0.0865 * Z_{\text{MAX}} - 3.2829 - 0.0008 * Z_{\text{MAX}}^2).$$

The maximum temperature changes at the thermocline (ΔT_T defined as the maximum difference per metre within the mesolimnion) at 6, 9 and 38 m LEB sites were -2.5 , -3.7 , and -6 °C, respectively. Maximum differences usually occurred during an upwelling (i.e. when the thermocline was compressed). During downwellings, the thermocline dropped in temperature between $0.5 - 3$ °C·m⁻¹ at the 38-m site. The minimum change in temperature per meter through the mesolimnion was

defined as $0.5\text{ }^{\circ}\text{C}$ at all sites. The change in temperature through the thermocline (ΔT_T) was correlated to the change in temperature through mesolimnion (ΔT_{Meso}) and varied due to up and downwellings; which are captured in surface temperature changes at the sentinel site ($\Delta T_{0,W}$; Equation 1.20). By definition the thermocline must have a minimum of $0.5\text{ }^{\circ}\text{C}\cdot\text{m}^{-1}$ temperature change, therefore, the maximum for ΔT_T was bounded at -0.5 .

Equation 1.20: $\Delta T_T = (0.18 - 0.026 * \Delta T_{0,W}) * \Delta T_{\text{Meso}} - 0.5$.

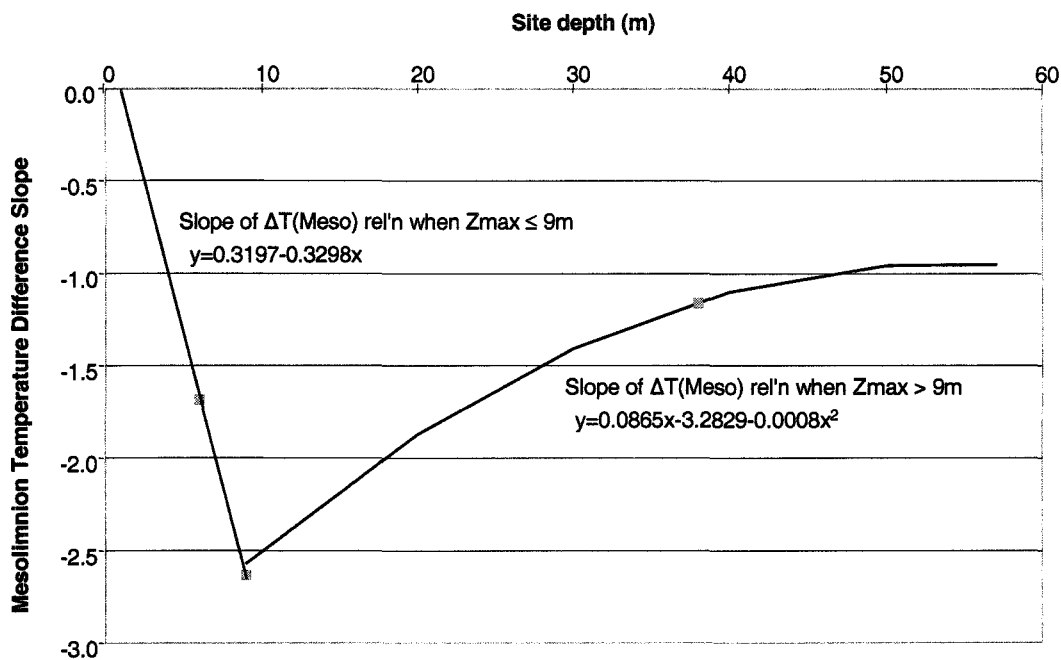


Figure 1.25: The slope of the equation for predicting the change in temperature over the mesolimnion from mesolimnion thickness was related to site depth by the relationships shown.

Limnion rates of temperature change

Average rates of cooling through the epilimnion, metalimnion and hypolimnion (and associated summary statistics) were calculated using the 1993 and 1994 LEB profile data and the following spatial and temporal thermal behaviour was gleaned from the LEB data. The average change in temperature throughout the entire epilimnion or hypolimnion ranged between $0 - 1\text{ }^{\circ}\text{C}$. In the hypolimnion, there was very little change below the 28-m depth, as well as very little change in temperature once $4\text{ }^{\circ}\text{C}$ was reached. Otherwise, the water in the hypolimnion cooled slightly if the temperature $> 4\text{ }^{\circ}\text{C}$. The warmest, hypolimnetic water recorded at the 38-m LEB site was $8-9\text{ }^{\circ}\text{C}$. During winter, the water is $0\text{ }^{\circ}\text{C}$ at the top and $2.5\text{ }^{\circ}\text{C}$ at bottom with the greatest difference in the top 1m. The lowest mesolimnion temperature, when the thermocline has been established, was $6\text{ }^{\circ}\text{C}$.

All water, no matter how deep, was the same temperature throughout the profile as the surface temperature between Dec 1 (Day 335) and Mar 31 (Day 90) until a 5 °C surface temperature threshold was exceeded. Water depths ≤ 3 m were assumed to be unithermal because the 6-m LEB site was isothermal except during upwellings, indicating the thermocline was deeper than 5-m depth, usually. If the surface temperature was < 4 °C, then an average rate of increase per meter was determined and used to generate profiles until 4 °C was reached and then temperatures were held constant.

There are 3 different equations that were applied to generate thermal profiles based on generalised rates of epilimnetic, mesolimnetic, and hypolimnetic temperature change. Winter warming rates were between 0.002 and 0.005 °C·m⁻¹ and all water was considered to be epilimnetic regardless of depth during that time. Once surface water temperatures reached 4 °C then cooling rates in the epilimnion were 0.005 °C·m⁻¹. Water in the mesolimnion was cooled based on the total and maximum temperature differences calculated earlier. Half of the total decrease in temperature through the mesolimnion, (not including the maximum difference that occurs at the thermocline), would occur above the thermocline and the remainder occurred below. The rates of temperature decrease per metre changed linearly both above and below the maximum temperature difference at the thermocline (see summary section for exact rates). If temperatures fell to 6 °C in the mesolimnion, then the rate of decrease was set at 0.1 °C·m⁻¹ for the remainder of the mesolimnion until temperatures reached a constant 5 °C. In hypolimnetic waters, the temperature was held constant once it reached 4 °C, otherwise the rate of decrease was 0.03 °C·m⁻¹ when temperatures were higher.

Summary of Profile Reconstruction

Using all the results from the analysis and modelling of the 1993-94 LEB data, the following final set of rules and equations were programmed to generate daily thermal profiles for each grid cell in the Long Point matrix.

1. Each day, the surface temperature and the site depth were extracted for each cell ID as well as the current and previous day's surface temperature for cell 224 (the sentinel site for up/downwellings).
2. A calculation of thermocline depth was determined using the following equation: $Z_T = (50 * (\Delta T_{0,W} + 7) - S_Z * (\Delta T_{0,W} - 7)) / 14 * JD * 0.00379 - 0.516 * Z_{MAX} + 4.6247$ where Z_T = thermocline depth, $\Delta T_{0,W}$ = surface temperature change between Day(JD-1) and Day(JD) at the welling site, (JD = Julian day).
3. Logic statements were used to determine whether Z_T should apply. For example, when the surface temperature was < 5 °C, Z_T was forced to equal $Z_{MAX} + 1$, or when Z_T exceeded the limit for thermocline depth, it was set at 32 m.

4. Mesolimnion thickness was calculated using the equation: $Meso = T_0 * 0.49 - (\Delta T_{0,W} * 0.286 + 5.24)$ where $\Delta T_{0,W}$ = surface temperature change at Cell 224 ($^{\circ}\text{C}\cdot\text{day}^{-1}$), and T_0 is the current cell's surface temperature. Meso is not calculated if $Z_T > Z_{MAX}$ or if $Z_T < 0$, which could happen mathematically.
5. Depths for the mesolimnion layer were calculated as follows: $Z_{TopMeso} = \frac{1}{4}$ of Meso above Z_T and $Z_{BtmMeso} = \frac{3}{4}$ of Meso below Z_T .
6. The change in temperature across the mesolimnion depended on the site depth (Z_{MAX}) and the mesolimnion thickness (Meso). If $Z_{MAX} < 9$ m then the linear function $\Delta T_{Meso} = Meso * 0.3197 - 0.3298 * Z_{MAX}$ was applied. If $Z_{MAX} \geq 9$ m then the quadratic function $\Delta T_{Meso} = Meso * (0.0865 * Z_{MAX} - 3.3829 - 0.0008 * Z_{MAX}^2)$ was applied.
7. The temperature difference at the thermocline was determined with the equation: $\Delta T_T = (0.18 - 0.026 * \Delta T_{0,W}) * \Delta T_{Meso} - 0.5$, but if $\Delta T_T < -0.5$ then ΔT_T was forced to equal -0.5 (the minimum requirement for mesolimnion waters).
8. Depending on the temperature at depth and the position within the profile the following rates of temperature change ($^{\circ}\text{C}\cdot\text{m}^{-1}$) were applied in generating the profile of any particular cell and depth layer (i):
 - a. Epilimnion
 - i) if $T_0 \leq 0.25$ $^{\circ}\text{C}$ then $\Delta T_i = 0.002$ $^{\circ}\text{C}\cdot\text{m}^{-1}$
 - ii) if $T_0 > 0.25$ $^{\circ}\text{C}$ and ≤ 4 then $\Delta T_i = 0.005$ $^{\circ}\text{C}\cdot\text{m}^{-1}$
 - iii) if $T_0 > 4$ $^{\circ}\text{C}$ then $\Delta T_i = -0.005$ $^{\circ}\text{C}\cdot\text{m}^{-1}$
 - b. Mesolimnion
 - i) If $Z_i < Z_T$ then $\Delta T_i = (\Delta T_{Meso} - \Delta T_T) / 2 / (Z_T - Z_{TopMeso})$
 - ii) If $Z_i = Z_T$ then $\Delta T_i = \Delta T_T$
 - iii) If $Z_i > Z_T$ then $\Delta T_i = (\Delta T_{Meso} - \Delta T_T) / 2 / (Z_{BtmMeso} - Z_T)$
 - iv) If $T_i < 6$ then $\Delta T_i = -0.1$ $^{\circ}\text{C}\cdot\text{m}^{-1}$
 - v) If $T_i < 5$ then $\Delta T_i = -0.002$ $^{\circ}\text{C}\cdot\text{m}^{-1}$
 - c. Hypolimnion
 - i) If $T_i < 4.2$ then $\Delta T_i = 0$
 - ii) Else $\Delta T_i = 0.03$ $^{\circ}\text{C}\cdot\text{m}^{-1}$

These rules were verified by plotting cross-sections and time-series at different times during the year for the Long Point Bay 3D model output to see if the model behaved within realistic boundaries. In particular capturing the spatial and temporal heterogeneity in thermal regimes between shallow and outer bay sections, as well as phenomena, such as the thermal bar event in spring was important. Figures 1.26 shows a latitudinal (east-west) cross-section of inner and outer bays showing distinct regions of warm and cold water, as well as a weak thermocline in spring between 7-9 m that is angled downwards because of slight downwelling. Figure 1.27 shows a time-series of profiles at a 40-m deep site from May through June of 1999 when the thermocline was developing.

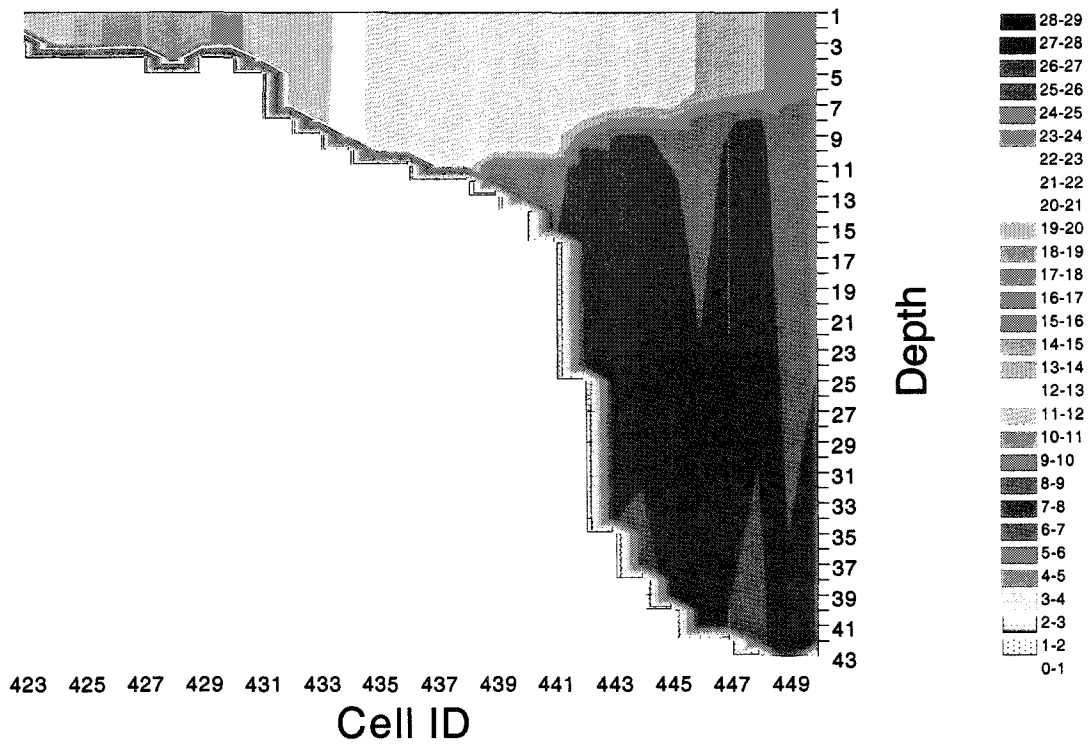


Figure 1.26: Latitudinal cross-section of profiles through inner and outer Long Point Bay in late spring, 1999 (See Figure 1.0 for Cell IDs). Surface temperatures ranged from 20 to 9 °C.

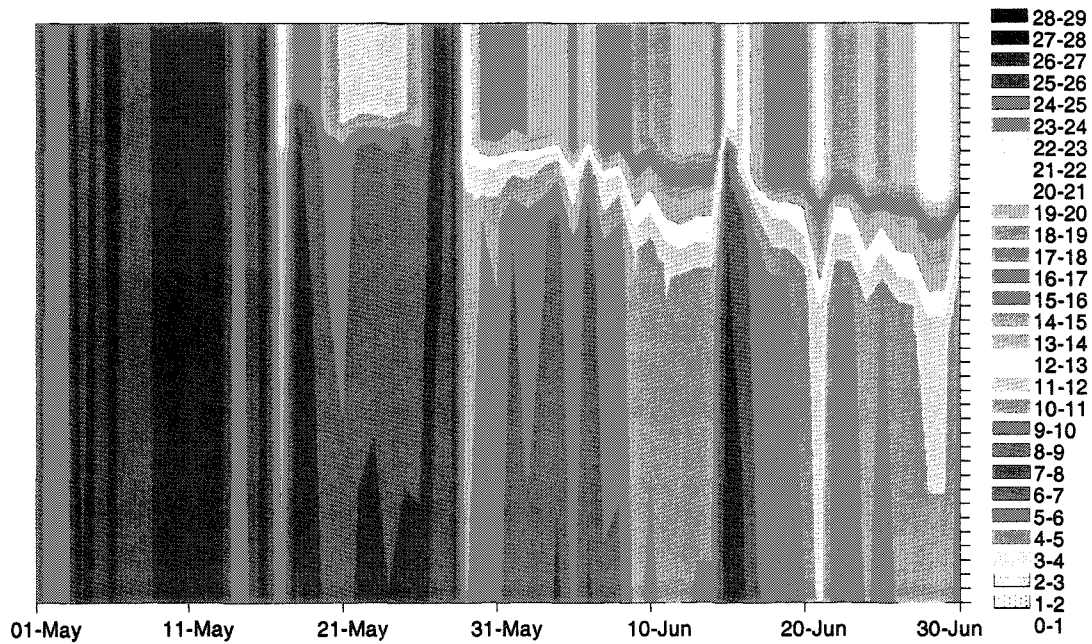


Figure 1.27: Time-series of profiles for a 40-m deep site in outer Long Point Bay in May and June, 1999 showing thermocline set-up, upwelling and downwelling events in mid-June.

1.1.6 Winds & Exposure

Environment Canada Meteorological Centre provided hourly wind measurements for a Long Point meteorological station for 1999 (Stn 6134F10, automatic, 1985/8/23 – present, synoptic hourly measurements, latitude 42° 34' and longitude 80° 3', elevation 175 feet). Data included wind speed ($\text{m}\cdot\text{s}^{-1}$) and direction rounded to the nearest 10° interval. Wind data and fetch can be used to calculate the relative exposure of a site. Fetch is the unobstructed distance across water between a point and the shoreline in a given direction. Direct fetch is the distance measured in one direction and effective fetch is the weighted average of fetches from several angles in the same general direction, where angles further from the main direction carry less weight. The latter method was used in the Long Point study using an equation from Scheffer *et al.* (1992; Equation 1.21).

Equation 1.21: $F = \Sigma(\cos(\angle) * L(a)) / \Sigma(\cos(\angle))$, where F= fetch (km), \angle = angle from primary direction (-45 through +45 degrees); L = Distance along angled direction

The centroid of the grid polygons were used to determine both direct and effective fetches at 10° angle intervals using an existing Arclnfo program that was modified for this input data (C.N. Bakelaar & P. Brunette pers.com.). Normally different angle intervals are used that correspond to standard directions (i.e. northeast), but data supplied from AES did not follow this format .

For each day in 1999, the hourly wind speeds were averaged for each of the 10° directions. A relative exposure for each point (centroid) was calculated based on an equation developed by Keddy (1984; Equation 1.22):

Equation 1.22 : $E = \sum_{\angle=1 \rightarrow 36} (W_{\angle} \cdot p \cdot F_{\angle})$, Where E = exposure ($\text{km}^2\cdot\text{hr}^{-1}$), $\angle = 10^\circ$ interval of wind direction, W = mean wind speed ($\text{km}\cdot\text{h}^{-1}$), p = the proportion of the day wind was from that direction (\angle), and F = the direct or effective fetch in that direction (km).

Effective fetches were used in the equation to calculate exposures. Missing wind data required that only days with more than 6 hourly wind measurements were used to calculate daily averages. September 16, 1999 was the only date that did not pass this criteria. Therefore, a daily exposure value was calculated by averaging September 15 and 17th exposures values. An example of a daily fetch map is shown in Figure 1.28.

While many references to sheltered or exposed fish habitat preferences exist (Aalto & Newsome 1993, Fischer & Eckmann 1997), the link to fish vital rates is largely not quantified. The calculation of exposure values, however, allowed for a relative exposure comparison between areas in Long Point Bay. The distribution of exposures for all grid cells under 1999 wind conditions is shown in Figure 1.29.

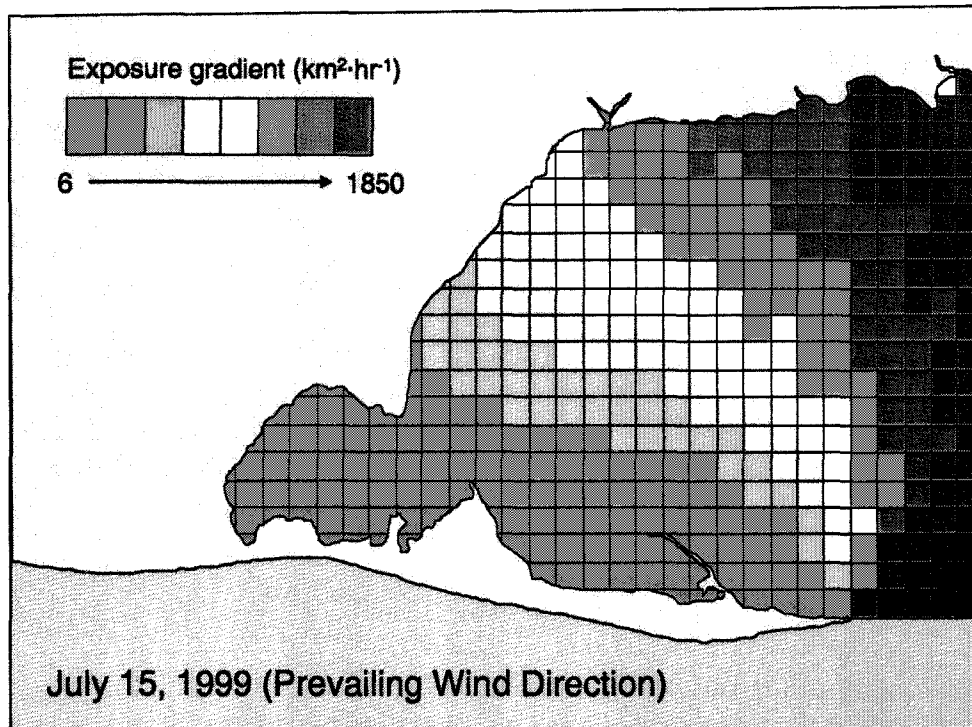


Figure 1.28: Example of an exposure map for Long Point Bay, Lake Erie based on July 15, 1999 wind conditions. Exposure values were calculated according to Keddy (1984).

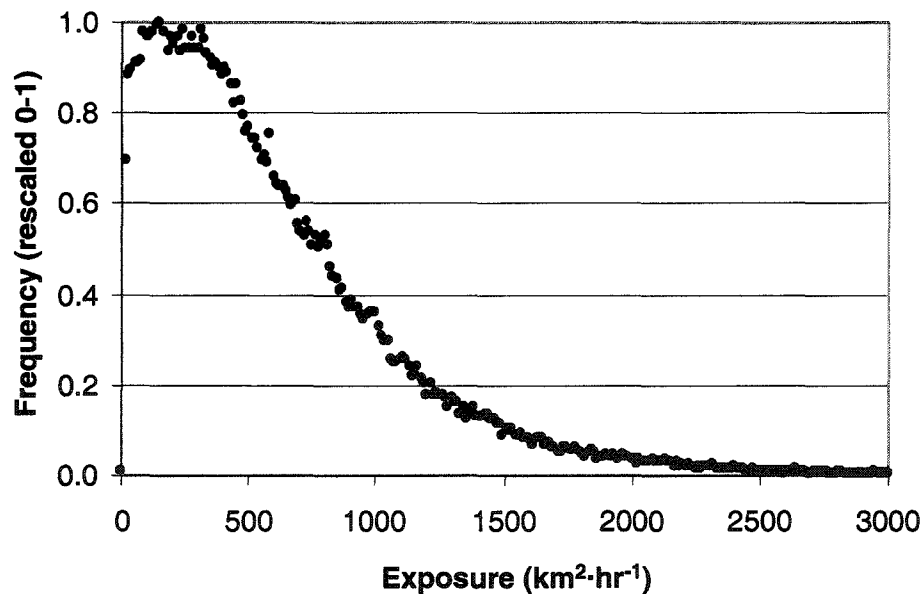


Figure 1.29: Frequency distribution of exposure values calculated for all grid cells and days in 1999 in Long Point Bay, Lake Erie.

1.2 DISCUSSION

Many larger scale studies of habitat-based effects on population dynamics of fish have ignored the spatial and temporal heterogeneity of

habitat. Various sources of information at differing resolutions were used in initial habitat analysis and then standardized for use in a habitat-based model (Table 1.6). Five elements of physical habitat in total were mapped or modelled because they are important to yellow perch: bathymetry, substrate type, vegetation, temperature and exposure. Not all the variables were used in every analysis but all the methodology was presented here for future reference. This chapter outlined the steps that were taken to ultimately capture this heterogeneity and variability at a moderate spatial resolution (1.4 km) and daily time step in Long Point Bay, Lake Erie.

In all subsequent analysis, bathymetry and substrate type were considered static throughout the analyses, even though different years in the 1990s were analysed in Chapters 2, 3 and 4 and the characteristics were surveyed at different times. A vegetation survey was modified through a generic model to obtain daily vegetation coverage changes over a year for the daily time-step employed in Chapter 4. In the initial habitat assessment work, vegetation was not modelled daily (Chapter 2 & 3). Temperature was interpolated and extrapolated both temporally and spatially. Initial habitat assessments used daytime, cloudfree, satellite imagery as the basis for 3D structure (Chapter 2), but was later modelled on a daily basis, using various data sources, and calibrated to the Long Point system (Chapter 4 & Appendix 1.3). Daily exposure values were calculated using shoreline, fetch, and wind information for the area (Chapter 4). All these steps provided a standardized basis for habitat suitability analysis and early life stage habitat-based modelling for yellow perch, *Perca flavescens*.

Table 1.6: A list of the habitat characteristics used in this study and the years they were surveyed, the spatial and temporal resolution used in each chapter's analyses for different years of thermal data.

Characteristic	Year(s) Surveyed	Spatial (Vertical) Resolution	Temporal Resolution	Chapter (Years Represented)
Bathymetry	Multiyear	• 1-m contours • 1.4-km	• Static • Static	• 2,3 (1993,1998) • 4 (1999)
Vegetation	1995	• 3-m • 1.4-km	• Static • Daily	• 2,3 (1993,1998) • 4 (1999)
Substrate	1995 & 1976	• 3-m, variable • 1.4-km	• Static • Static	• 2,3 (1993,1998) • 4 (1999)
Temperature	• 1993,1998 • 1999	• 1.4-km (1-m)	• Variable • Daily	• 2,3 (1993,1998) • 4 (1999)
Exposure	1999	• 1.4-km	• Daily	• 4 (1999)

The final database of habitat characteristics for each cell consisted of both static and temporally variable information:

- daily vegetation densities and classifications derived using a vegetation model based on CASI data maxima;
- daily, wind-speed and direction-based exposure measurements using effective fetch calculations;
- static, substrate percent composition from CASI and offshore point data,
- static, area-weighted, mean depth from bathymetry data and;
- daily temperatures by 1-m depth intervals using generalised profile relationships from LEB point data, and interpolating both spatially and temporally using satellite imagery and nearshore temperatures

Using the habitat tables and each cell ID and date combination for 1999 (the primary and secondary key fields in the database) the following information was extracted on a daily basis for use in the habitat model (Chapter 4): the temperature profile, a substrate array with the list of proportions for each substrate category, a macrophyte array with the list of percent areal coverage of the different macrophyte categories, an exposure value, and the average depth of the cell (Figure 1.30).

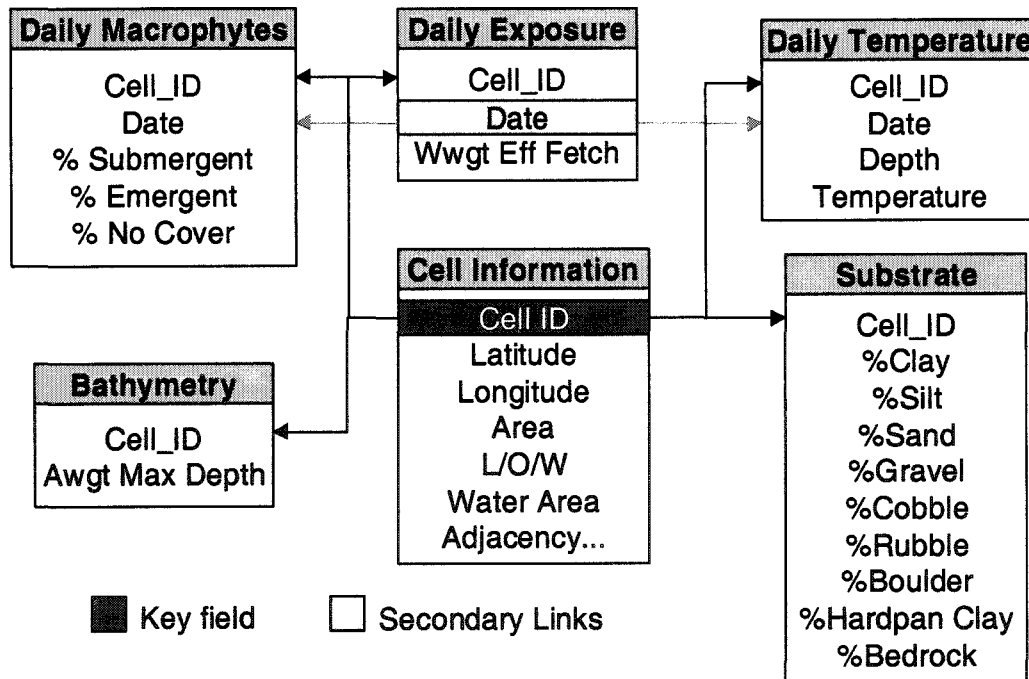


Figure 1.30: Structure of the habitat database used for modelling. Grid cell IDs linked the habitat attributes between tables, and date linked the daily habitat attributes. (Wwgt Eff Fetch = wind-weighted effective fetch, Awgt Max Depth = area-weighted maximum depth).

Chapter 2

Thermal and physical habitat assessment for yellow perch at different life stages.

*...changes in fish habitat can be integrated with changes in
fish growth, survival and reproduction... Hayes et al. (1996)*

2.0 INTRODUCTION

This chapter focuses on the connection between habitat and ontogenetic niche shifts in perch life history, with the aim of determining suitable habitat availability for the Long Point Bay perch population. To perform a habitat suitability assessment, the detailed habitat requirements and associations of yellow perch at different life stages were compiled (Appendix 2.1), along with details of perch life history and behaviour. It is difficult to distil the many, often conflicting, habitat associations of yellow perch reported in the literature into definitions of suitable habitat. Therefore, the habitat suitability indices and models used to map and identify the areas of suitable habitat for fish species are reviewed. Thermal habitat suitability indices were developed and applied to spatially explicit information for Long Point Bay, Lake Erie (Chapter 1). That habitat suitability analysis mainly focused on the location and variability of thermal habitat for different life stages. Here, thermal habitat is incorporated into a temporally-aggregated approach for determining annual physical habitat suitability and availability to further gauge which habitats may be limiting the perch population in the Long Point area.

2.0.1 Habitat suitability indices and habitat modelling

Habitat suitability assessments often exploit pattern-based relationships between species distributions and physical habitat characteristics (Hansen *et al.* 1999). Gap analysis is commonly used to map different characteristics of a landscape and overlay them to identify areas with a high degree of concordance with a species' habitat requirements (Conroy & Noon 1996). The use of a habitat suitability index (HSI) quantifies the relative importance of each characteristic on a relative scale. HSIs encapsulate complex sets of interactions between physical habitat and fish population dynamics by combining relative weightings of different variables into an index that ranges from 0 (unsuitable) to 1 (excellent). The suitability of one habitat variable, or a suite of variables, can be based on qualitative ranking or quantitative measurement of a species' preference for a particular habitat (pattern-based). Suitability can also be defined by how vital process rates of individuals (e.g. growth) or populations (e.g. dispersal) change in different habitats. Sometimes, the suitability of a location may be limited by ideal-free distribution rules or the habitat area required per individual. Suitability can be modified by carrying capacity or vital rate limitations due to density-dependent effects on the fish population's performance or production arising from space limitations. Often, subjective definitions of suitability are assigned using HSIs.

Regardless of the method used, the relative weightings incorporated into HSIs are based on suitabilities assigned to categorical or continuous habitat characteristics. Categorical habitat variables can be assigned suitabilities individually (i.e. substrate type can be high, medium

or low suitability) or in combinations of habitat characteristics (i.e. depth x substrate x vegetation categories). In either case, all categorical assignments are usually converted to numerical HSI scores when combined into an overall suitability for a habitat patch. Suitabilities can also be assigned by establishing a quantitative relationship between a continuous variable and some aspect of a life stage or population (i.e. preference gradients or growth potential).

Many habitat suitability index models have been developed for terrestrial and aquatic species, and used to define suitable habitat areas using several different approaches (e.g. moose – Hepinstall *et al.* 1996, fish & invertebrates -- Brown *et al.* 2000, birds – Delong & Lamberson 1999). [See National Wetlands Research Center (2003) for a list of HSI models for different fish and wildlife species.] Many HSI models are based on empirical relationships between species' distributions and habitat data.

Shirvell (1989) evaluated six salmonid habitat suitability models and their predicted population dynamics. He found they were not geographically transferable and needed recalibration for new areas. Because the models were empirical, they predicted well for the systems they were derived from (50-96%), but not for test datasets. Only 7 – 30% of the variation was explained in fish abundance or biomass in a new area. In addition, no variables, from a total of 33, were common among the six models that predicted fish abundance. He found that the optimum level of any one variable was relatively constant between geographic areas but the relative importance of a habitat variable was not. This can affect the methodology used to combine suitabilities within habitat patches in an area. Shirvell concluded that the appropriateness of the model should be determined in a specific area before its application. This implies that site-specific knowledge of limiting factors, or data, was needed to be available to test the appropriateness of each model. Shirvell's models were mainly based on pattern-based suitability assignments, which would need to be calibrated between systems, unless the entire geographic range of the species was considered. Hence, a generic approach to habitat suitability assignments based on the complete range of the species and the overall conditions that the species is found within should be used and not local distribution and habitat relationships. Local information cannot cover the entire range of possibilities within the species' fundamental niche. For this reason, an exhaustive literature review of *Perca flavescens*, and its habitat associations, was undertaken to assess habitat suitabilities over the range of the species with emphasis on process-based linkages (Appendices 2.1 & 2.2).

More examples of process-based approaches are increasing in the literature. For example, a simple model was constructed by Hughes (2000), which predicted the largest size of stream salmonid within 95% confidence intervals based on habitat selection theory and ranking habitat by potential growth rate. Brandt and others (Brandt & Hartman 1993,

Hondorp & Brandt 1996, Mason & Brant 1996b, 1999) have mapped the vertical and horizontal distribution of potential growth rates for several fish species in the Great Lakes using a bioenergetics approach with hydroacoustic surveys. Krieger *et al.* (1983) developed an HSI model using a quasi-process-based approach for the prediction of yellow perch abundance in whole ecosystems after conducting a literature review of habitat requirements in riverine and lacustrine systems.

The lacustrine HSI model (Krieger *et al.* 1983) for perch used littoral area and percent cover as surrogates for food and shelter (Figure 2.01). The former provided an indirect measure of the habitat available for insects and small forage fish. A water quality component of the HSI included temperature, dissolved oxygen (DO), and pH because these were commonly measured lake attributes and affected abundance, growth, or survival of perch. Reproduction was affected by percent cover in the littoral area because these areas are used for spawning. Temperature influenced spawning and development, while degree-days between 4 and 10 °C affected gamete viability. Trophic status was included in the HSI because it was related to yellow perch abundance in different water bodies. In their model, Krieger *et al.* (1983) assumed that the most limiting factor (V_1 - V_9) determined the carrying capacity of a water body. However, they did not take into the account the different habitat requirements of intermediate, early life history stages and the temporal and spatial variability of habitats within a ecosystem. Based on the review of habitat associations (Appendix 2.1), there are several characteristics which Krieger *et al.* may have overlooked that could affect suitable habitat supply estimates for yellow perch, such as substrate type and the degree of wind exposure.

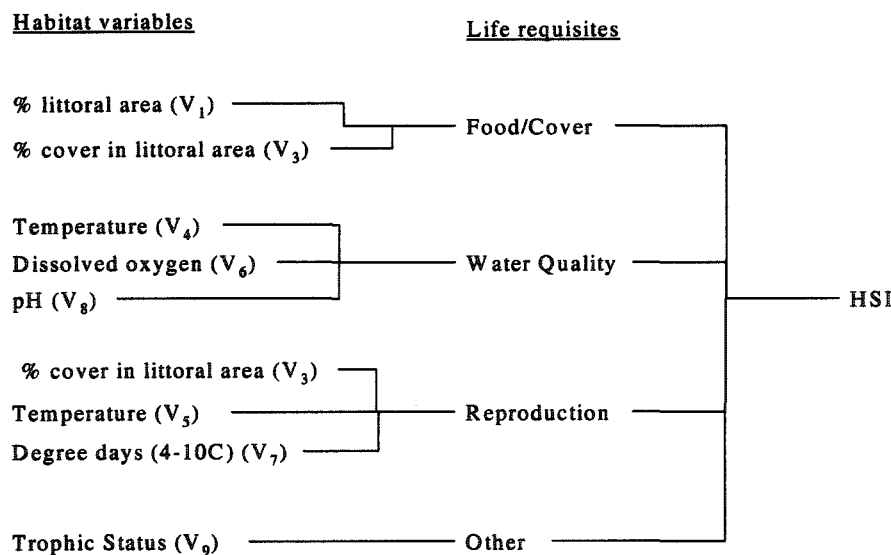


Figure 2.01: Habitat suitability model framework for yellow perch from Krieger *et al.* (1983).

The physical habitat simulation model (PHABSIM; Shuler & Nehring 1993) converted water depth, velocity, and substrate composition into fish habitat units in rivers and streams. Units were called weighted useable area (WUA) and calculated by using a composite suitability index obtained by multiplication of individual habitat suitabilities for cover, depth, and velocity criteria. Very low values (0 - 0.09) were considered unsuitable, while the remainder of the range (0.1 – 1) was liberally defined as suitable. This range was further subdivided into optimal (0.5-1.0) and acceptable (0.1-0.49) habitats. This is illustrative of the non-standard approach in habitat suitability assessment for determining meaningful thresholds for unsuitable, suitable, and optimal habitats. They did not find a linear relationship between stream fish densities and WUA predictions.

Minns *et al.* (1996) extended a similar approach to test the effect of habitat supply in an annual population model for pike, where the population was regulated by the weighted suitable area in a system that was specific to each life stage's habitat needs (WSA is equivalent to WUA). Proportions of WSA for spawning, fry, juveniles, and adults were calculated and based on a categorical assignment of suitability for depth, substrate, and vegetation combinations in Hamilton Harbour, Lake Ontario. The analysis was based on detailed maps to obtain annual estimates of habitat availability. Minns *et al.* (1996) found that early life stages of pike were limited by the lack of suitable habitat in Hamilton Harbour.

Here, a combination of different methodologies is used to address spatial and temporal habitat suitability and supply for yellow perch in Long Point Bay. Issues of scale and the method of habitat suitability calculation are addressed. The purpose of the analysis is to determine whether habitat is limiting for a particular life stage by using measures of suitable habitat supply, both thermal and physical.

2.0.2 Long Point Bay Yellow Perch Habitat Assessment

From the extensive literature review of yellow perch habitat associations, four variables were chosen for study. Those variables were temperature, depth, vegetative cover, and substrate type. These factors were chosen because they have often been used in habitat supply assessment, there was an *a priori* link to each life stage's habitat requirements, and there was adequate information both spatially and temporally to map each in Long Point Bay, Lake Erie. Dissolved oxygen, light and turbidity are not considered here because insufficient information was available. Information on water levels was available but adequate shoreline elevation information was not. Exposure, which includes wind & wave effects, is considered in the analysis in Chapter 4.

The life history of yellow perch was divided into five stages having different habitat requirements: spawning and egg, planktonic larvae, demersal young-of-the-year (YOYs), juveniles, and adults. Habitat areas

in Long Point were characterised for different life stages of perch using crudely weighted habitat suitability indices based on preferences. Where possible, habitat suitabilities were linked to vital rates. The HSIs were quantified, or ranked, according to thermal tolerances and preferences listed for each stage and the generic habitat preferences of the five perch life stages for the remaining variables.

The investigation focussed on the temporal and spatial variation in thermal structure and its effects on the location and area of suitable habitat availability for different life stages. The interaction between temperature and physical habitat and its effect on annual habitat availability estimates was also addressed. The implications of averaging spatially or temporally and ignoring habitat variability are discussed. The modifications necessary for using this type of analysis in habitat-based modelling of population dynamics is examined.

2.1 METHODS

Two types of habitat assessments were performed to identify suitable areas for yellow perch life stages: thermal only and all physical. The thermal habitat assessment was based on temperature relationships with vital rates (reproduction, growth, or mortality) in each successive life stage (Thorpe 1977, Hokanson 1977, Magnuson *et al.* 1979, and Casselman & Lewis 1996). For early reproductive stages, thermal mortality was chosen as the regulatory factor that determines suitable thermal habitat because early mortality affects recruitment. Although development and growth are also affected by temperature, survival is likely more critical; however, the two rates are related as optimal growth often occurs at optimal survival temperatures. For later life stages, thermal effects on growth were considered because older fish can self-regulate lethal effects by avoidance and movement to more suitable areas. Further, growth effects are considered most important after the first-year of life.

The overall habitat assessment combined a categorical suitability index approach based on work by Minns (1996), and Minns *et al.* (1999), with the thermal assessment work. The suitability categories were assigned to different vegetation densities, substrate types, and depth intervals based on preferences, or the likelihood of perch being associated with habitats. This analysis provides an initial assessment of habitat suitability and supply prior to incorporating habitat-based relationships into a population model for yellow perch in Chapter 4.

2.1.1 Suitable Thermal Habitat Assessment

The temperatures used to derive suitabilities for Long Point Bay were obtained using methods and data sources discussed in Chapter 1. The initial analysis of yellow perch habitat in Long Point Bay concentrated on temperature because it is linked to many processes throughout a fish's life history. The volume or area of thermal habitat is often ignored in habitat assessments, which mainly concentrate on static, physical habitat

assessments (Bakelaar *et al.* 2004). Here, thermal suitabilities were based on survival probabilities for early life stages (eggs and age-0) and as growth potential in older fish (juveniles and adults). Of the vital rates affected by temperature, these were considered the driving factors for habitat suitability and selection for the life stages. Also, many of the vital rates respond similarly to temperature. For example, thermal preferences for younger fish minimise mortality rates and maximise growth rates, whereas, growth rates in older fish link to fecundity and spawning rates.

Egg Development & Survival

A thermal survival curve for yellow perch eggs was determined from data in Thorpe (1977) over a range of temperatures (Figure 2.02). The best-fit equation was a third order polynomial where the proportion of survivors, relative to a maximum of 70% survivorship, was calculated to produce suitabilities between 0 and 1 (Equation 2.1). (NB. Maximum survivorship occurred over a 2-week period around 12 °C.)

The average monthly or daily bottom temperatures in 1993 between April and June, when eggs may be present, were converted into suitability maps based on the modified egg survival equation. The areal changes, and associated potential carrying capacity, were tracked to determine optimal times and locations for spawning. Optimal thermal habitat for eggs was defined using a suitability that is equivalent to a 50% egg survival rate.

Equation 2.1: $HSI_{T,egg} = 0.0003 * T_{btm}^3 - 0.0206 * T_{btm}^2 + 0.3664 * T_{btm} - 1.0339$ (N=9, $r^2=0.90$, if suitability < 0 then 0), where $HSI_{T,egg}$ = thermal suitability for eggs and T_{btm} = bottom temperature, °C

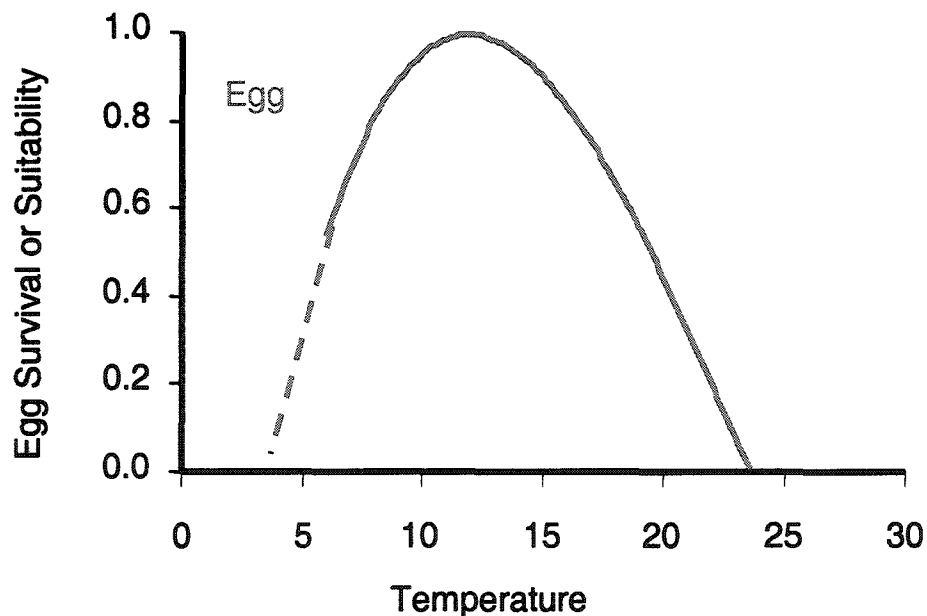


Figure 2.02: Habitat suitability of bottom temperatures (°C) for yellow perch eggs based on polynomial equation (2.1) derived from survival data from Thorpe (1977).

Age-0 Survival (Pelagic and Demersal Stages)

Larvae have a similar thermal response to eggs but at a higher temperature range. The curve for temperature and larval survival, which mimics thermal preference and growth potential curves, was based on data from Thorpe (1977; Figure 2.03). A third order polynomial fit the data for larval survival (Equation 2.2). Percent survival was rescaled between 0 and 1 based on the maximum survival rate.

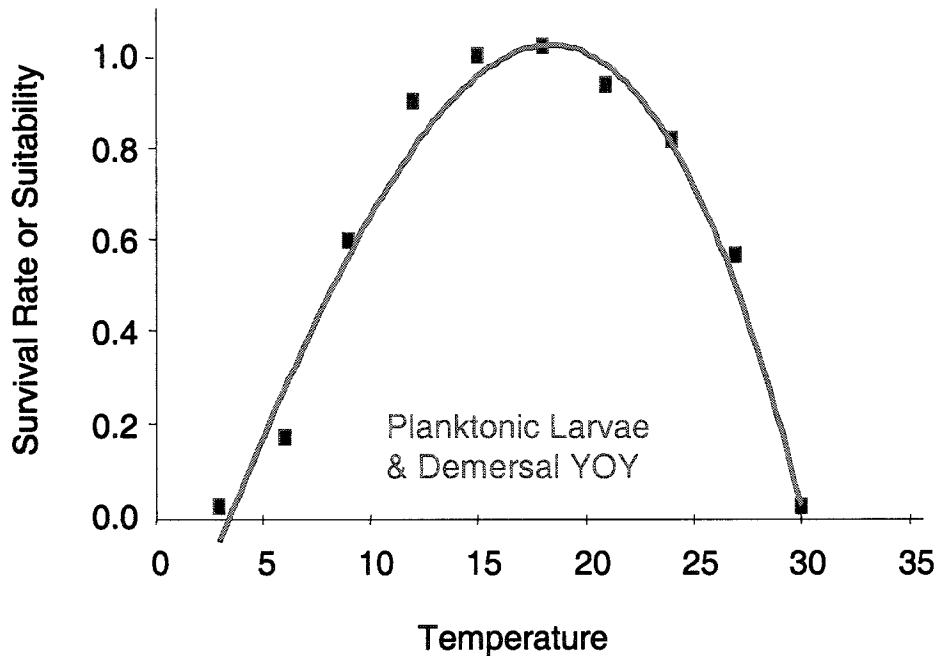


Figure 2.03: Thermal suitability curve for planktonic and demersal stages of age-0 yellow perch (Equation 2.2) based on larval survival data from (Thorpe 1977).

Equation 2.2: $HSI_{T,Larv} = -0.00001 * T^3 - 0.0003 * T^2 + 0.1201 * T - 0.5107$ ($N = 10$, $r^2 = 0.977$), where T = Water temperature, °C and $HSI_{T,Larv}$ = thermal HSI for larvae & YOYs.

The survival curve was used for both planktonic larvae and demersal YOY stages but different parts of the water column were used for calculating thermal habitat for each stage. Thermal suitability maps were constructed for pelagic larvae by averaging temperatures in the top 6 metres of the water column. Either specific dates or overall averages from the end of May to July were used in calculations. This 4-5 week period corresponds to the average time that planktonic larvae spend in this phase as cited in the literature (Appendix 2.1). Suitability maps for demersal larvae used bottom temperatures from July until September, which spans the period starting at the feeding shift from planktonic to benthic food sources to the end of the growing season, on average. July was used in both pelagic and demersal calculations and was considered an overlap period.

Juveniles & Adults

Thermal suitability curves for juveniles and adult fish were determined in a similar manner to earlier life stages (Thorpe 1977, Kitchell 1977, Koonce 1977). Growth potential and thermal relationships were used instead of survival curves because older fish are more mobile. The suitability equations were based on specific-growth equations from Hanson *et al.* (1997) and were fitted to fourth order polynomials. Curves were based on varying temperature only at maximum consumption rates for an average size fish at that life stage in Long Point Bay (Equations 2.3 & 2.4). Juvenile perch of age-1 and age-2 averaged 150 mm, while adult fish of age-3+ averaged 250 mm in the 1990s. The resulting growth potential curves are corroborated by field evidence for juveniles and adults, which have slightly different thermal preferences. On average, juveniles select and tolerate warmer temperatures than adults (Figure 2.04).

Equation 2.3: $HSI_{T,Juv} = 0.00009 * T^4 - 0.0025 * T^3 + 0.0311 * T^2 - 0.1493 * T + 0.3319$ ($r^2 = 0.996$)

Equation 2.4: $HSI_{T,Adlt} = -0.00001 * T^4 + 0.0006 * T^3 - 0.0069 * T^2 + 0.0691 * T + 0.0208$ ($r^2 = 0.990$)

Juvenile suitabilities were calculated in the following manner. Suitabilities were computed for the top 20 temperature layers (0-20 m) on specific dates, or averaged from April to September (the juvenile growing season). Adult suitabilities were calculated by using temperatures in the top 20 m of the temperature matrix between June and September (the adult growing season; Thorpe 1977). The growing season was longer for juveniles than for adults because adults do not feed during spawning.

Final thermal suitability maps were generated by extracting the maximum suitability in any depth layer for a particular grid cell, assuming that fish would select the depth that maximized growth potential (Brandt 1980). Monthly suitability maps were averaged over days where satellite imagery was available during the growing season.

Table 2.1: The depth strata averaged for each grid cell to obtain thermal HSI calculations for each life stage. Annual suitable areas were estimated by averaging over the period shown.

Life Stage	Depth Strata used in Thermal HSIs
Eggs	Bottom (April - May)
Planktonic Larva	Average Top 6 m (June - July)
Demersal YOY	Bottom (August – September)
Juvenile	Max in Top 20 m (May – September)
Adult	Max in Top 20 m (June - September)

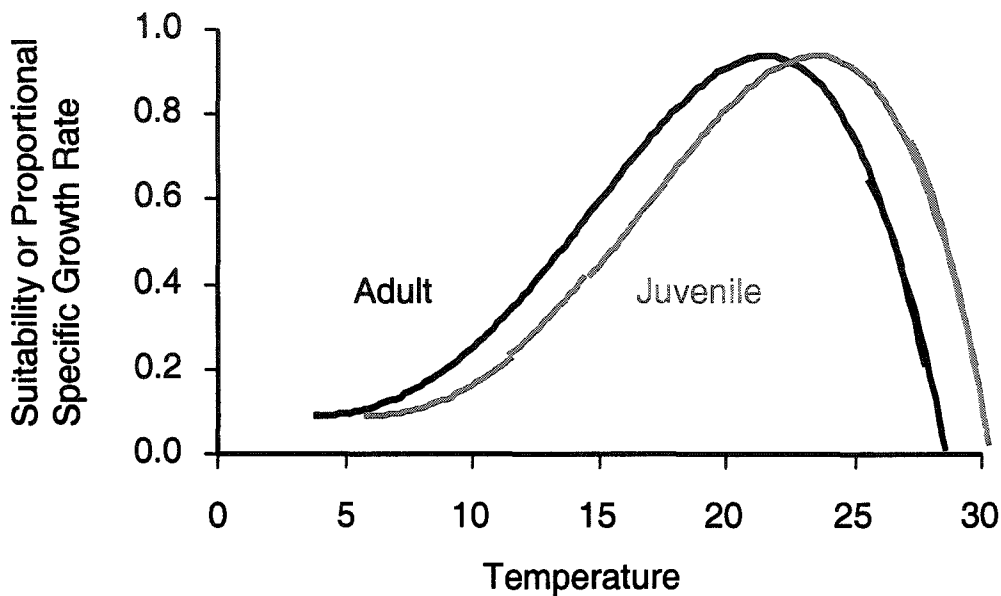


Figure 2.04: Thermal suitabilities for juvenile and adult yellow perch based on (Equations 2.3 and 2.4) and estimated from a bioenergetics model developed by Kitchell (1977) in Hanson *et al.* (1997).

The depth strata used and the period over which temperatures were averaged for seasonal comparisons are shown in Table 2.1 for all the life stages assessed. Suitable (acceptable) and optimal thermal habitat were defined as 0.5 and 0.8 suitability thresholds, respectively, depending on the life stage. These thresholds, unless otherwise stated, were used in calculating simple habitat supplies.

2.1.2 Overall Habitat Suitability Assessment

Categorical suitabilities were assigned to the habitat variables, other than temperature, used in this assessment. Relative probabilities of finding different life stages of perch, based on the literature review, were assigned as suitabilities to different depth categories based on Minns *et al.* (1995; Table 2.2). Substrate types associated with different life stages in the literature were assigned to very high, high, medium, low, and nil suitability categories (1.00, 0.75, 0.50, 0.25, and 0.00, respectively). Because substrates were often classified as combinations of substrate types in both CASI and offshore surveys (see Chapter 1), suitabilities were combined by weighted averaging across specific types based on the percent composition (Table 2.2; see Minns *et al.* 1999). Emergent and submergent vegetation densities were assigned suitabilities from the literature review based on the relative likelihood of finding different life stages in those habitats. Vegetation categories were combinations of densities and types (emergent or submergent) and assigned to either a high, medium, one of 2 low categories (depending on the probabilities), or a nil suitability category (1.00, 0.67, 0.33 or 0.25, 0.00). It should be noted that vegetation in this initial habitat suitability work did not vary daily. The

original static spatial map of summer vegetation coverage from the 1997 CASI survey was used in this analysis.

Habitat maps for all variables, including temperature, were merged into a unique polygon coverage in a GIS with different attributes for each polygon. In some cases, especially near the shoreline, the information on a specific habitat variable was missing because of non-overlapping spatial surveys. A unique polygon with a missing value was formed. These missing value polygons were not used in further habitat suitability analysis if they overlapped the shoreline. Any polygons in the offshore with missing values were assigned nearest neighbour values for the specific habitat characteristic lacking data. Once corrected, the individual habitat suitability assignments for each characteristic were arithmetically averaged within polygons, including thermal suitabilities, to obtain a final overall habitat suitability map for Long Point Bay.

Table 2.2: HSI values used for categorical variables: maximum site depth, substrate type, and vegetation density for different life stages of yellow perch (egg stage, pelagic larva, demersal larva and juveniles & adults). * Substrate classification used when vegetation classes 9-23 had unknown substrate

Habitat Characteristic	ID Code	Life Stage			
		Egg	PL	DL	Juv/Ad
DEPTH					
0-1 m	1	1.00	1.00	1.00	0.33
1-2 m	2	1.00	1.00	1.00	0.67
2-5 m	5	0.75	1.00	0.67	1.00
5-10 m	10	0.50	0.67	0.33	1.00
10-15 m	15	0.25	0.00	0.00	1.00
15-65 m	65	0.00	0.00	0.00	0.33
SUBSTRATE					
sand(34)/silt(33)/clay(33)*	1	0.36	0.89	0.89	0.69
sand(70)/silt(15)/clay(15)	2	0.43	0.95	0.95	0.72
sand(90)/silt(5)/clay(5)	3	0.50	1.00	1.00	0.75
cobble(33)/rubble(33)/gravel(34)	4	0.67	0.67	0.67	0.67
bedrock(40)/boulder(40)/hardpan(20)	5	0.20	0.00	0.00	0.28
sand(80)/silt(10)/clay(10)	6	0.46	0.97	0.97	0.73
VEGETATION					
Submergents					
No cover	8	0.25	0.33	0.25	0.33
15% submergent cover	9	0.67	1.00	1.00	0.67
50% submergent cover	10	1.00	0.67	1.00	0.67
85% submergent cover	11	0.67	0.67	0.75	0.00
100% submergent cover	12	0.00	0.00	0.00	0.33
Emergents					
45% submergent, 45% emergent	19	0.67	0.67	0.67	0.67
50% submergent, 40% emergent	20	0.67	0.67	0.67	0.67
90% emergents	21-22	0.25	0.25	0.25	0.25
100% emergents	23	0.00	0.25	0.25	0.25

This annual estimate of the most highly suitable areas for each life stage was calculated to determine a crude carrying capacity for the Long Point system. The life stage that may be limited by habitat constraints and that would warrant further investigation of habitat-related effects was estimated from this simple analysis. The degree of overlap between larval and YOY habitats with juvenile and adult habitat was crudely measured to assess the level of biotic interactions between the stages. This overlap was not relevant for the egg stage, as there is no threat of predation or changes to habitat suitability for eggs based on the presence of juvenile and adult fish.

2.2 SUITABLE THERMAL HABITAT RESULTS

2.2.1 Spawning & Egg Thermal Habitat

When mapped with a 3D depiction of seafloor elevation, the interaction between bottom temperature and water depth can be visualized (Figure 2.05) as it relates to egg suitabilities. On May 10, 1993, the shallow shelf area of the outer bay was good spawning and egg rearing habitat while temperature dropped steeply into the deep hole at the tip of the point where high mortality would occur at this time. At this time, when spawning may be taking place in Long Point Bay according to MacGregor & Witzel (1987), the temperatures of the inner bay have started to become slightly too warm for egg incubation.

When a time-series of spawning and egg thermal suitabilities were mapped, it became apparent that the thermal variability at the edge of the shelf in the outer bay, a typical upwelling area, and in the nearshore shallows was quite high (Figure 2.06).

The nearshore of the inner bay and north of the sand spit are the only areas that are suitable for spawning on April 6 through to May 1 in 1993. Between these dates, the suitable areas varied slightly. The inner bay (except for a portion of the northwest shore) and areas that are 10 m or shallower in the outer bay were thermally suitable for spawning and egg survival between May and June. Areas between 5 and 10 m were the most variable in temperature.

In June, the thermal tolerances of eggs were exceeded in the inner bay and warmer coastal areas where egg survival would have been 21% or lower ($HSI_{T,Egg} \leq 0.3$). This occurred because the thermal suitability curves for egg survival decay quickly over a short temperature range and the shallow waters of Long Point warm quickly. Interestingly, at this time, a large part of the outer bay, including very deep areas, could support egg incubation for periods long enough to ensure hatching. Two potential spawning zones occurred, with some overlap, where egg production might be supported at different times of the year. In 1993, the nearshore zone is viable in May and offshore areas would be viable in June.

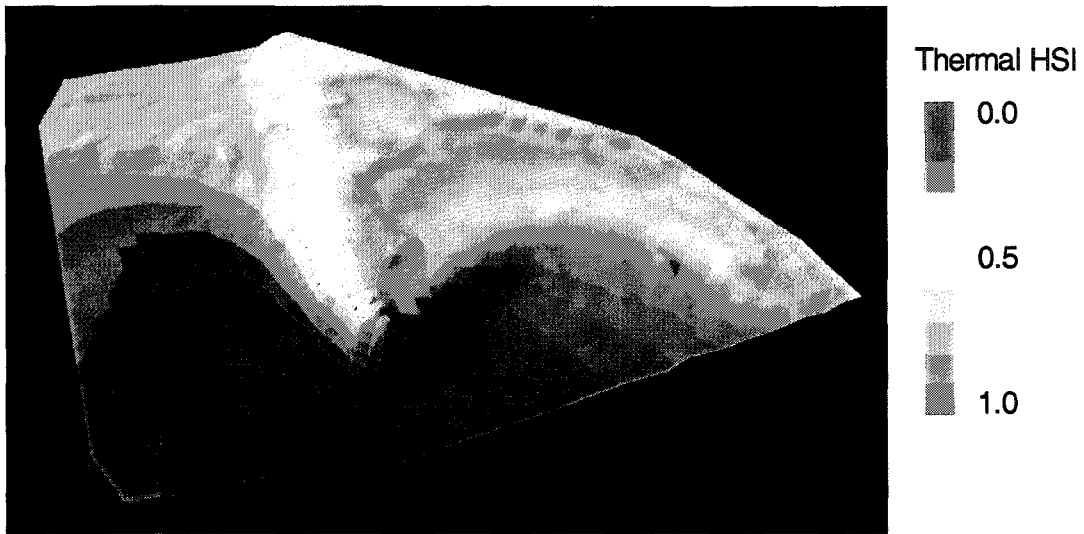


Figure 2.05: Perch egg thermal habitat suitabilities in May 1993 draped over a 3D-representation of bathymetry (elevation) in Long Point Bay, Lake Erie.

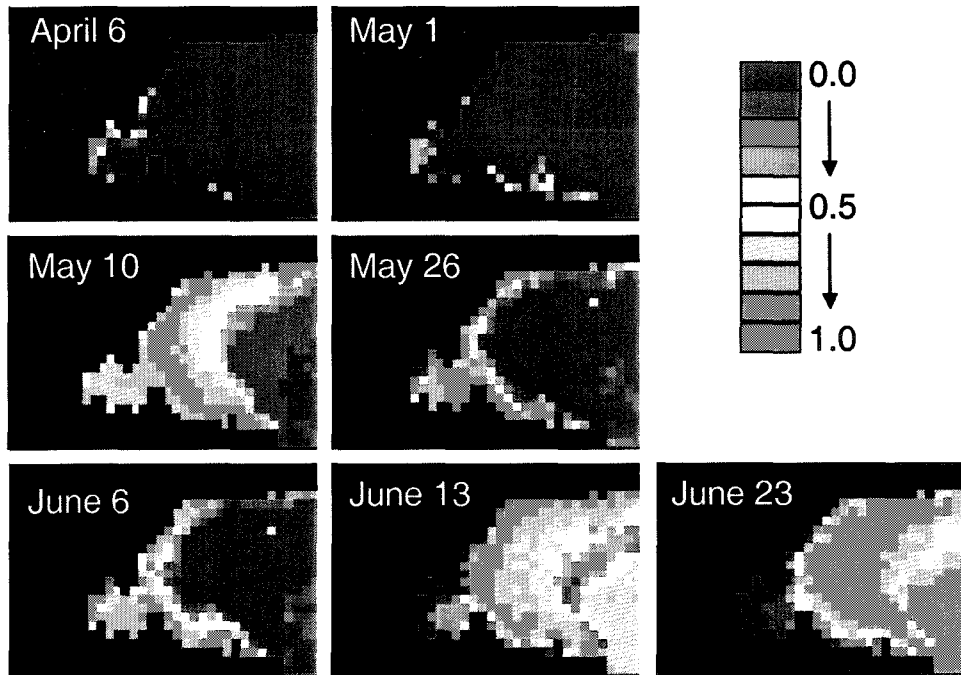


Figure 2.06: Bottom thermal suitabilities for perch eggs on selected dates between April 6 and June 23 1993, when AVHRR SST satellite imagery was available, in Long Point Bay, Lake Erie.

2.2.2 Pelagic Larva and Demersal YOY Thermal Habitat

A daily time-series of epilimnetic (top 6 m) thermal habitat for pelagic larval perch was mapped for July 1999 to show suitable area fluctuations over a shorter time frame (Figure 2.07). Daily 3D thermal structure was recreated for 1999 but not for 1993 because daily *in situ* temperatures were not available for the earlier time period for interpolating satellite imagery. By July, larvae have survived approximately 1-2 months from hatch. For the bulk of the month, temperatures were optimal throughout both bays, with the exception of warm periods in the north-western Inner Bay that make that area highly unsuitable for larvae. It is interesting to note that even during an upwelling in the outer bay, from July 6 to 11th, the temperatures remained only slightly sub-optimal in the upwelling zone. As the month progressed, the inner bay approached the 50% suitability range (indicating 50% of optimal survival) and the cooler offshore waters were more suitable with the 'upwelling' zone warming last. The upper epilimnetic waters become uniformly suboptimal by August, which may prompt behavioural thermoregulation and movement to lower depths.

The same generic pattern for pelagic larval thermal suitability emerged, on average in 1993. Nearshore suitabilities were much higher than offshore in June (Figure 2.08). The area of suitable thermal habitat was concentrated in the inner bay and protected coastal areas of the outer bay at this time. The upwelling zone in the offshore of the outer bay had the lowest suitability, between 0.5 and 0.6 maximum survival, averaged over June in the upper 6 m.

Demersal thermal habitat during 1993 between July and September averaged 50% of maximum survival or better throughout the whole bay. Even the deepest area reached temperatures that were only suboptimal, on average, during the warm summer months. The optimal thermal zone for YOY survival, with 10% or less thermal mortality, was consistently in demersal areas at mid-depths in the outer bay. The highest variability in suitable thermal habitat occurred in the deep-hole area and the inner bay's vegetated zone, a habitat that demersal larvae should prefer. The potential mismatch between demersal larvae habitat preferences and thermal preferences is discussed in the overall habitat assessment sections.

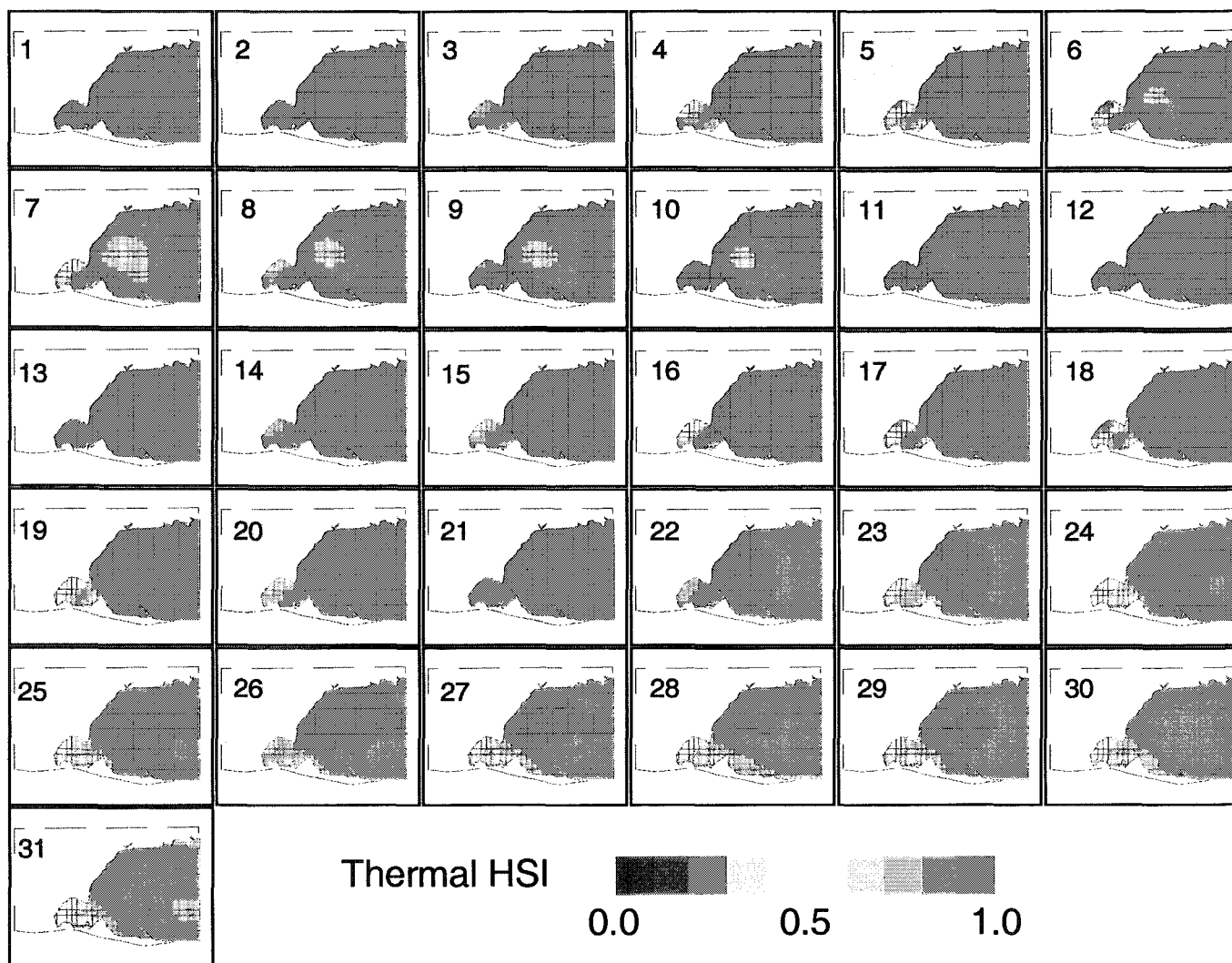


Figure 2.07: Daily time-series of epilimnetic thermal suitabilities for larval yellow perch based on the average temperature in the top 6 m of Long Point Bay from July 1 - 31, 1999.

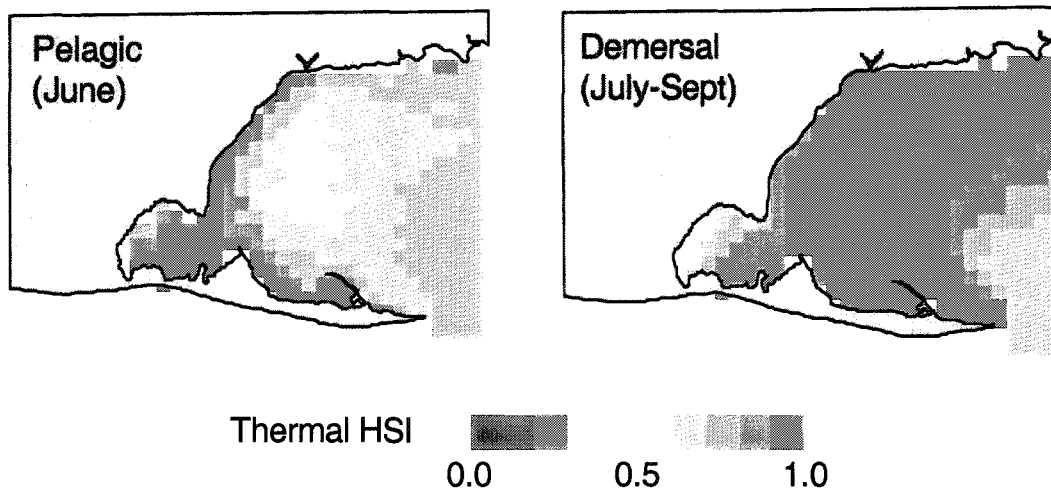


Figure 2.08: Average thermal suitabilities during the pelagic (June; 0-6m) and demersal (July – Sept; bottom) larval stages for 1993 in Long Point Bay, Lake Erie.

2.2.3 Juvenile & Adult Thermal Habitat

Juvenile growth potential was compared across depth layers on selected dates in the growing season of 1993 (Figure 2.09). At the end of May, suitable thermal habitat occurred in the inner bay and nearshore, protected areas of the outer bay, usually coastal areas. These areas overlapped with suitable spawning and larval habitat at that time. By the end of June, the bulk of Long Point Bay's volume was thermally suitable, except for warmer nearshore areas, and colder, north-shore deep waters. By the end of July, optimal temperatures for juvenile growth were concentrated around the thermocline. By the end of August on certain days, only water below the thermocline was thermally suitable for growth. The mid-growing season compression of the optimal thermal volume of juveniles has ramifications for biotic interactions and optimal foraging if thermal habitat does not overlap food resources. During turnover in autumn, the entire water column is moderately suitable for juveniles. The most suitable areas were located in the upper depths in offshore areas. By the end of November, the water had cooled to the point where only 30% of maximum growth potential could be achieved under maximum consumption rates, signalling the end of the growing season in 1993.

Thermal layers at 5-m intervals, as in Figure 2.09, can be misleading. Temperatures can change rapidly at the thermocline and close to the bottom, especially during upwellings from colder, deeper waters. When the maximum growth potentials for adults were extracted from the top 20 m in each spatial grid cell, thereby assuming perch move to the most suitable thermal layer, a different map of adult growth potential emerged because of thermal refuges within vertical profiles (Figure 2.10). Juveniles showed a similar pattern.

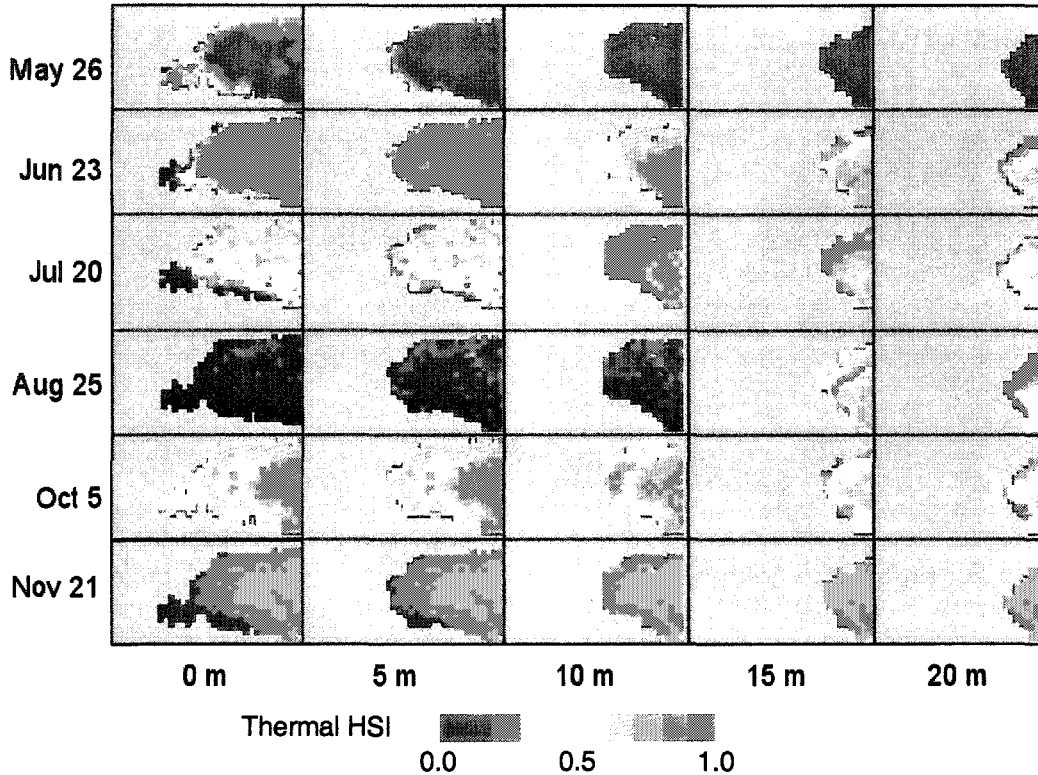


Figure 2.09: Juvenile thermal habitat suitabilities for growth at 5-m depth intervals on selected dates (May 26, June 23, July 20, August 25, October 5, and November 21) spanning the growing season in 1993.

This generalization holds most of the time. When the optimal thermal volume was compressed during epilimnetic warming in late summer, there were still areas of optimal growth throughout most of the bay in 1993. Therefore, the areal extent of suitable habitat was still large, but the volume decreased. In early June, the inner bay is optimal for adult growth, coinciding with the location where fish were most likely spawning. However, waters in these areas warm quickly, becoming suboptimal for adult growth. The bulk of the outer bay area in Long Point, albeit a thin depth layer at times, was optimally suitable for most of the growing period. When averaged across the season, the spatial pattern of optimal for both juvenile and adult growth was similar to demersal larvae survival patterns.

2.3 OVERALL HABITAT SUITABILITY RESULTS

Locations of suitable habitat based on depth, substrate, and vegetation suitabilities for the different perch life stages did not necessarily overlap with suitable thermal habitat. When all the habitat variables were assessed and combined into an overall suitability, suitable habitat areas were usually compressed because of mismatches and temporal averaging effects. For this analysis, optimal habitat was defined as a high suitability range between 0.76 and 1.00 for each habitat variable.

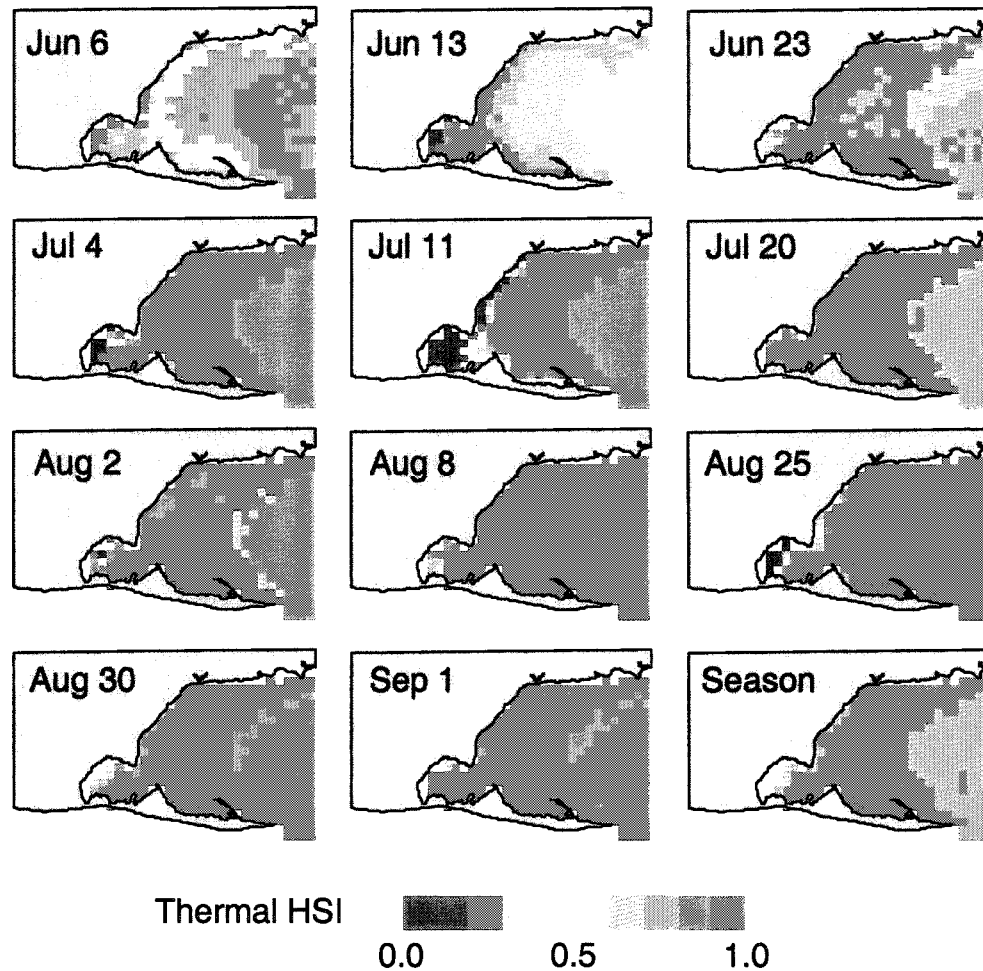


Figure 2.10: Adult thermal habitat suitabilities for growth within the top 20 m on selected dates in 1993 during the adult growing season in Long Point Bay, Lake Erie. The seasonal average for June to September is also shown.

Moderately suitable habitat was defined as a suitability range of 0.51-0.75, while low and very low suitability habitats were 0.26-0.50 and 0.10-0.25 respectively. If any habitat variable within a patch was designated as unsuitable then a suitability assignment of 0 was used, regardless of the other habitat factor scores.

2.3.1 Overall spawning & egg habitat suitability

The final suitability maps for spawning and egg incubation were based on preferences and survival rates, respectively. Optimal depths for spawning were found in the inner bay and south shore of the outer bay (Figure 2.11). Preferred spawning substrates were found along the north shore of the outer bay, while higher suitabilities for vegetation density were found in the inner bay and shallow areas of the outer bay south shore. The average bottom temperatures during the spawning months of April and May indicated low suitability, except for isolated warm areas

along the coasts. The average combination of all habitat factors indicated that the inner bay, and coastal areas of the outer bay with suitable substrate, was moderately suitable (between 0.50 - 0.75) for spawning and egg rearing. Very few areas had optimal spawning conditions for all physical habitat combinations.

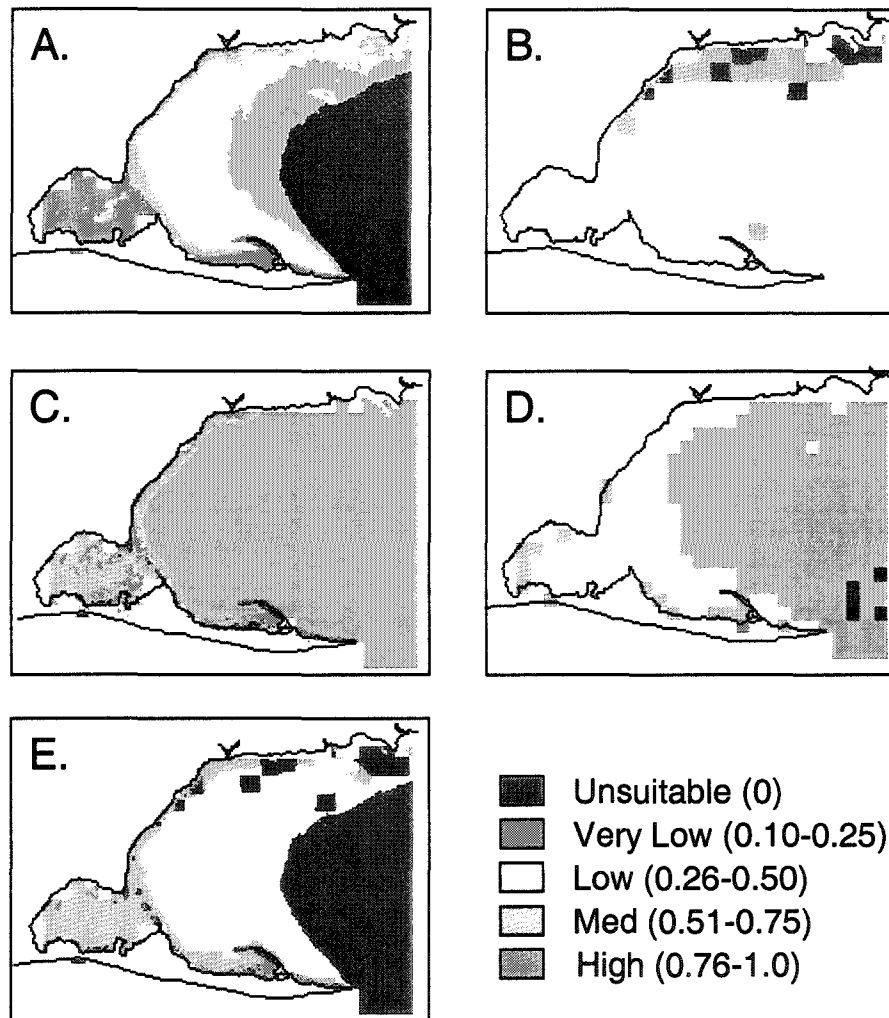


Figure 2.11: Spawning & egg suitabilities for the different habitat variables assessed in Long Point Bay, Lake Erie: A. maximum depth suitability for spawning, B. substrate suitability for spawning & egg development, C. vegetative suitability for spawning & egg development, D. average bottom thermal suitability for egg survival in April-May of 1993, E. overall habitat suitabilities for spawning and eggs.

2.3.2 Overall pelagic larvae habitat suitability

The average suitability maps were plotted for each habitat variable based on pelagic larvae preferences or survival suitabilities (Figure 2.12). Preferred site depths based on larval distributions were found in the inner bay and nearshore of the outer bay. Substrates over which larvae were

usually found were ubiquitous, with the exception of bedrock and hardpan clay areas along the north shore, which are not preferred.

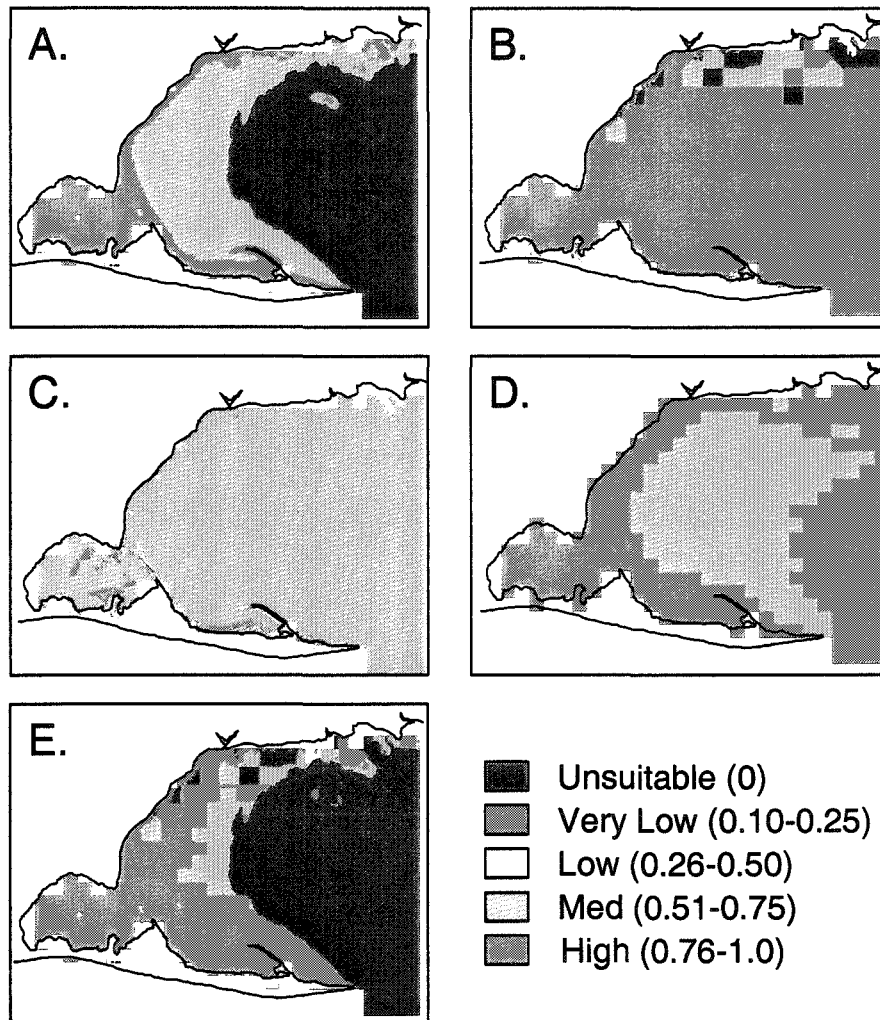


Figure 2.12: Pelagic larval (PL) suitabilities for the habitat variables in Long Point Bay, Lake Erie: A. depth suitability based on PL associations, B. substrate suitability based PL associations, C. vegetative suitability for PL, D. limnetic thermal suitability based on PL survival in June-July of 1993, E. average of all habitat suitabilities for pelagic larvae.

Suitable densities of submergent vegetation were found scattered in the inner bay but the bulk of the outer bay was moderately suitable for this larval stage because the literature information on vegetation preferences was variable. The average epilimnetic temperatures during June and July indicated a high suitability in most surface waters throughout the entire bay, except for slightly lower survival rates in the upwelling zone of the outer bay in 1993. The average combination of all habitat factors indicated that the inner bay and a large part of the outer bay, up to the 10 m contour, were highly suitable for pelagic larvae. There was a strong demarcation between optimal and unsuitable areas with little moderate and low suitability areas based on this classification scheme.

2.3.3 Overall demersal larvae habitat suitability

The final suitability maps for each habitat variable, based on demersal larvae preferences or survival suitabilities, are shown in Figure 2.13. Preferred maximum depths were found in the inner bay and coastal regions of the outer bay, similar to spawning areas. The map for substrate suitability is identical for pelagic and demersal larvae. No distinction was made in the literature between larval phases and distribution patterns over different substrates. Preferred densities of vegetation were also similar between larval stages, but not identical, and were found scattered throughout the inner bay. However, open areas without vegetation were also selected by demersal larvae in the literature. Therefore, the bulk of the outer bay was moderately suitable for all larval stages with or without vegetation according to this classification scheme.

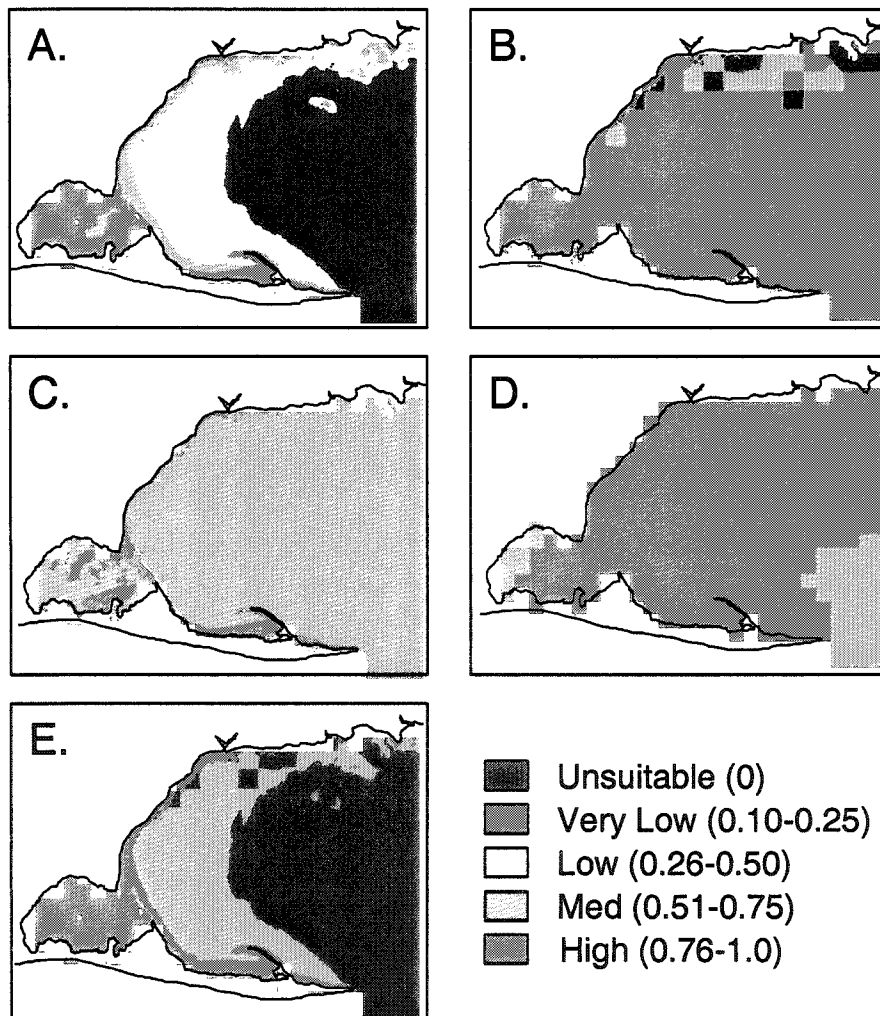


Figure 2.13: Demersal larval (DL) suitabilities for the different habitat variables assessed in Long Point Bay, Lake Erie. A. maximum depth suitability, B. substrate suitability, C. vegetative suitability, D. bottom thermal suitability in July-August of 1993, E. average of all habitat suitabilities for demersal larvae.

The average bottom temperatures during July and August of 1993 indicated high suitability areas for demersal larvae occurred throughout most benthic habitats on average. Only slightly lower survival rates were predicted over that period in the warmer waters of the inner bay and the colder, deep-hole area. The average combination of all habitat factors indicated that the inner bay and coastal areas of the outer bay were in the optimal range for demersal larvae, up to the 10 m contour, beyond which was unsuitable mainly due to depth constraints. Again, there seemed to be a strong demarcation between suitable and unsuitable areas with no low suitability areas (i.e. less than 50% suitable but greater than 0). The depth classification scheme was a major factor in this outcome for both larval stages.

2.3.4 Overall juvenile and adult habitat suitability

Juvenile and adult suitability assignments were very similar, except for thermal suitabilities; so overall habitat patterns do not differ much between the stages (Figures 2.14 and 2.15). Suitable depths for juveniles and adults were found mainly in the outer bay up to 15m. Substrate types, where juveniles and adults were likely found, also occurred in the outer bay intermixed with some low suitability habitats on the north shore. A preference for low-density submergents would restrict most of the inner bay at peak vegetation growth to these stages.

However, optimal thermal habitat for juveniles occurred at the boundary of the inner and outer bays in 1993 when averaged over the growing season (Figure 2.14D). Optimal thermal habitat for adults was uniformly distributed throughout the bay, with the exception of warm areas of the inner bay. This difference between juvenile and adult stages was probably due to the shorter adult growing season that coincided with warmer and more thermally suitable months. The overall average suitability of all factors combined overrode the thermal differences and juvenile and adult perch had very similar annual growing season suitability maps.

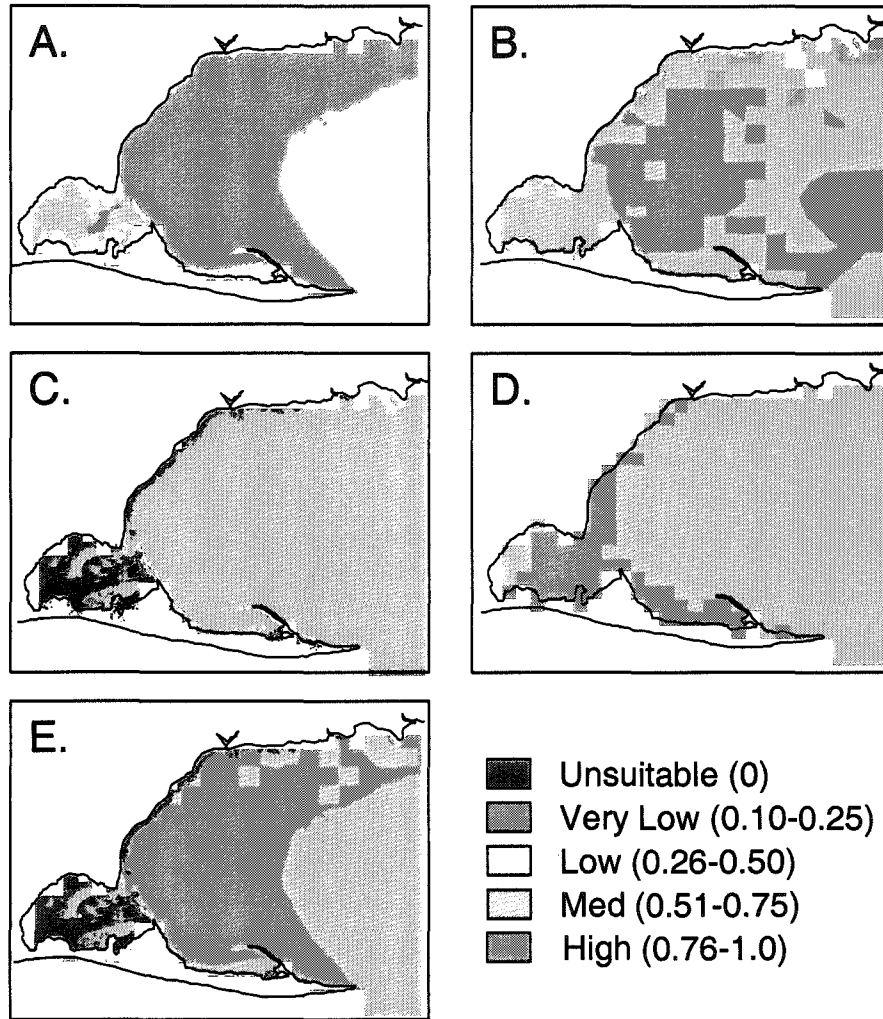


Figure 2.14: Juvenile perch suitabilities for the different habitat variables assessed in Long Point Bay, Lake Erie. A. maximum depth suitability, B. substrate suitability, C. vegetative suitability, D. average thermal suitability based on maximum potential growth in the water column from May-September of 1993, E. average of all habitat suitabilities for juveniles.

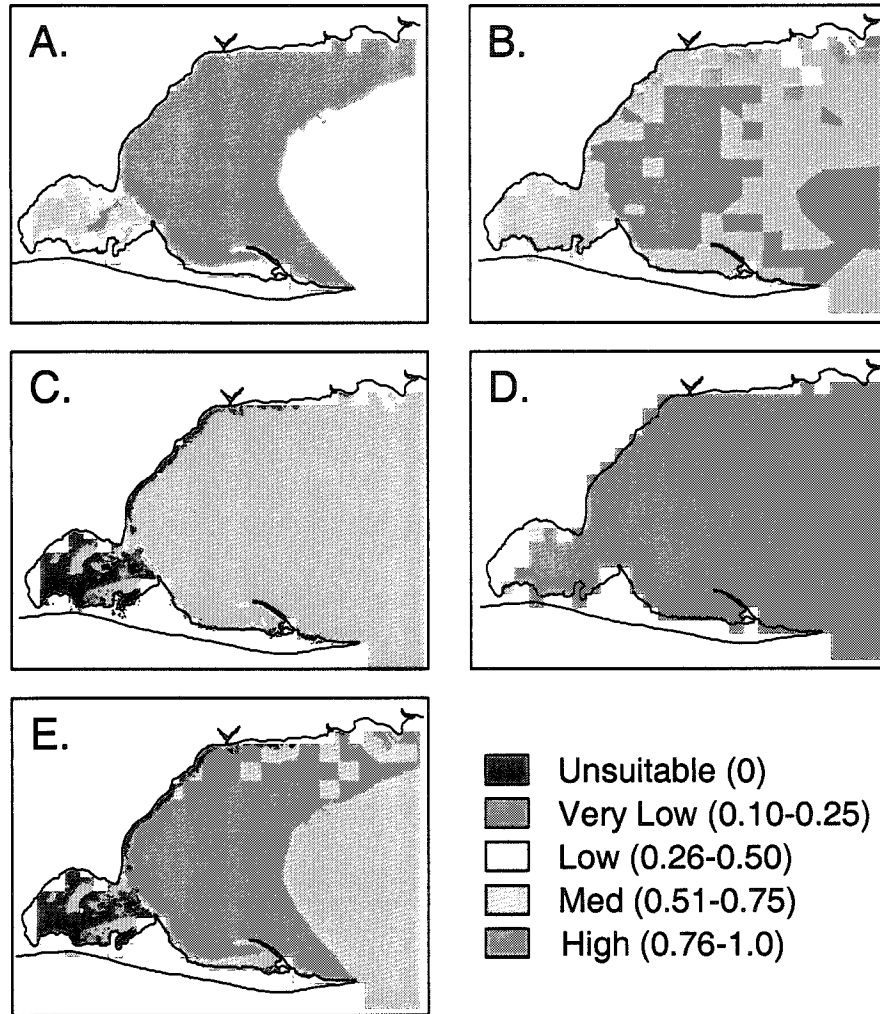


Figure 2.15: Adult perch suitabilities for the different habitat variables assessed in Long Point Bay, Lake Erie. A. maximum depth suitability based on habitat associations, B. substrate suitability based associations, C. vegetative suitability for adult associations, D. average thermal suitability based on maximum potential growth in the water column from June-September of 1993, E. average of all habitat suitabilities for adults.

2.4 CONCLUSIONS

2.4.1 Thermal Habitat

Temperature is more easily translated to vital rate relationships and suitabilities than other habitat characteristics because they have often been quantified in the laboratory and verified with field observations. By using a few simple temperature functions and mapping the 4D changes in thermal structure, one can predict most of the areas that fish inhabit during different phases of their life cycle while knowing little else about habitat preferences or behaviours. This finding is elaborated upon in the following sections.

Spawning & Egg Thermal Habitat

The thermally optimal areas for egg-rearing, defined as having a suitability of 0.7 or greater, varied widely from 12 to 30 km² in April, 30-400 km² in May, and 150-650 km² in June. Most reports for the Long Point Bay area indicated that spawning occurs in late April to early May but it is interesting to note that more thermally suitable habitat was actually available in later months. This indicates that other factors, not just egg survival, may be determining when spawning habitat selection takes place. It should be noted that there is evidence of two distinct spawning times in some lakes, because of different thermal regimes, producing different cohorts per annum (Sandstrom *et al.* 1997).

If spawning site fidelity occurs in yellow perch then nearshore areas in Long Point Bay should be selected based on previous records. These areas would correspond with predicted suitable thermal habitat in May. Unfortunately, only Goodyear (1982) has spawning records in the Long Point area to validate this prediction for optimal spawning habitat. There is a general paucity of data in the literature for spawning information and most evidence is anecdotal (i.e. accounts from fishermen who find eggs strands on trap nets in springtime). MacGregor and Witzel (1987) tried, but could not find, perch eggs in benthic sled surveys. Ripe females and larvae were collected at specific sampling locations and spawning sites were inferred.

Regardless, given an egg mass occupies roughly 0.25 m² and assuming that a site could only be used once per annum, then May suitable thermal areas would allow 120 million to 1.6 billion spawning events or egg masses to fill that space. The Great Lakes Fishery Commission (Kayle *et al.* 1998) estimated that 2.0-2.7 million perch (age-2+) existed in the eastern basin in 1993. Therefore, spawning sites do not appear to be limiting, even though suitabilities and areas appear lower and smaller for eggs than for other stages. If the average egg strand carries 10,000 eggs (the reproductive output from a 20 cm female), then conservatively, the highly suitable area for spawning during May would produce roughly 800 billion fry (at 95% fertilization success and 70% normal hatch rates).

The crude estimates of carrying capacity are probably based on over-estimates of suitable area because average annual suitabilities do not address thermal variability at specific locations. Areas of high temperature fluctuations are not viable for spawning and egg survival even though average suitability may be high. High spatial variation in temperatures already eliminated much of the outer bay from May to June. Temporal variation in water temperatures during the spring were quite high so eggs would be more susceptible to mortality events in shallow water than later life stages. This would affect spawning site selection, especially if there is a degree-day thermal cue. By averaging daily thermal suitabilities, the impacts on egg development of temperature fluctuations were not captured and the implications of reproductive timing

cannot be separated in this type of assessment. Several of these issues are addressed in Chapter 4.

Larval & YOY Thermal Habitat

Similar patterns in average thermal habitat for pelagic larval development were observed in two years, in 1993 and 1999. Generally, the mid-outer bay region or “upwelling” zone was less suitable on average due to large temperature fluctuations. The bulk of the bay is thermally optimal for larval survival for the duration of this life history phase. Early in ontogeny, larvae become pelagic and might passively disperse by currents. However, there is some evidence that they can regulate their vertical position in the water column to mitigate passive transport (Kennedy & Vinyard 1997, Watt-Pringle & Strydom 2003). Even so, the currents in Long Point Bay are such that the gyre would most likely keep larvae entrained within the bay (Boyce *et al.* 1989; Chen *et al.* 1997). This thermal analysis indicates that even though larvae may be passively distributed by currents at this time, survival would not be compromised by ambient temperatures. The suitable volume or area may be an over-estimate because short-term temperature fluctuations were not captured in the survival estimate. Mortality rates in areas with high variability should also account for acclimation effects, which were not addressed.

Suitable larval habitat in June (if 80% of maximum survival is used as a cut-off) overlaps with suitable egg thermal habitat distributions in late May. This indicates that upon hatch larvae would be in thermally suitable environments without much movement. The optimal larval area measured approximately 80 km². In the field, densities of larval perch have measured as high as 6850 ind·ha⁻¹ (Craig 1987). This translates to a carrying capacity of roughly 5.5 billion larvae. Once optimal thermal habitat for larvae extended to the outer bay’s epilimnetic waters in July, 600 km² of area is available. Therefore, limiting thermal habitat would occur early in the season and would be dependent on spawning and hatch times. The larval carrying capacity estimated at this time would be less than 1% of the maximum 800 billion fry estimated to hatch from available spawning habitat at carrying capacity. Later in summer, the upper 6m became less hospitable and the upwelling zone could create a thermal refuge with cooler, yet optimal, temperatures. This might extend the planktonic phase if directed larval movement were possible. This is unlikely for two reasons. One, temperature fluctuations are rapid in this zone and thermal mortality would be high outside of the optimal range. Two, strong currents can be associated with upwelling and downwelling events that cannot be avoided by larvae.

Pelagic and demersal larvae habitats differ vertically by definition. Horizontally, the predicted habitat areas were contiguous. Bottom temperatures at the transitional time between phases were highly suitable for YOYs feeding on benthos between July and September. Roughly, 650 km² of optimal habitat was estimated on average in the outer bay, that did not include the deep-hole area but included parts of the inner bay. This

area would support 44.5 billion larvae if the same maximum density limits apply as for planktonic larvae. This assumes there must be adequate food and shelter from other non-thermal sources of mortality (i.e. predators and exposure) in these areas. Different aspects of physical habitat mediate these effects depending on the vital rate involved. These are discussed in the overall habitat assessment section on demersal YOYs.

If larvae behaviourally thermoregulate and they orient to optimal temperatures then movements would bring them closer to the bottom around the time predicted for switching between food sources. This suggests that behavioural thermoregulation may prompt the switch to a benthic food source, which is more readily available, given that gape size is adequate. Alternatively, the switch may be prompted by declining food availability or increased predation pressure and may coincidentally also be thermally suitable. Because banding has developed at this stage, some authors suggest vegetated habitats are used as refugia (Eklov 1997). Thermally suitable areas may also be correlated with the presence of vegetation.

Juvenile & Adult Thermal Habitat

Three-dimensional mapping of juvenile growth potential showed that optimal (80% or greater) thermal volumes could be restrictive during the growing season. This would imply that averages are not necessarily good indicators of what actual growth potential over that period would be, or which areas are most suitable because the fish can move to optimize growth. This is evidence that the use of mid-basin average temperature profiles, that have been used in thermal habitat calculations historically, or the use of surface temperatures alone cannot suffice for predicting thermal habitat.

The compression of optimal thermal habitat through the year may explain why winter schools average 6.7 m vertically while summer schools average 2.5 m (Hergenrader & Hasler 1967) because vertical temperature variability is greater during the summer and more suitable temperatures were found in a narrow stratum. Also, if perch remain in an isocline of the most suitable thermal habitat (Brandt 1980) then suitable areas might be more appropriate to calculate than suitable volumes during the growing season. These times would also be the most limiting if food availability is mismatched or if density-dependent effects change distributions or vital rates because of crowding.

Overall, thermal growth potential for both juveniles and adults predicted that a large portion of the bay would be suitable for most of the growing season if fish can maintain their position in thermally suitable water, but if food is disconnected from the thermal habitat then it may be overestimated. It is especially likely during times when suitable temperatures were below the thermocline that more vertical movement or forays inshore from the ridge area of the outer bay would be necessary. This may explain observed behaviour of crepuscular, shoreward

movements increasing in distance as the thermocline deepens (Craig 1987); perhaps an optimization or trade-off between thermoregulatory behaviour and foraging behaviour might ensue because of the discrepancy until energetic costs of movement become too great.

Thermally suitable growing seasons and areas were not very different between juveniles and adults, even though spawning adults do not feed, and juveniles and adults have slightly different thermal optima. Thermal volumes may be separated vertically or horizontally, but at some point, will be compressed in both cases. It is interesting to note that optimal thermal areas also overlapped during spawning times. If distributions were layered, or if juveniles and adults do not exclude each other, then the suitable area was similar for both life stages, and the bulk of the optimal growing season occurred from July until September. In early summer, juveniles may be forced into suboptimal areas because of density-dependent or competitive interactions with adults. Thermally the most restricted period occurred in early June, after which optimal areas expanded to most of the bay. The greater the overlap, the more juveniles may be relegated to suboptimal habitat if densities are too high in optimal thermal habitat because of size-based competition (Eklov 1997).

Optimal thermal areas ranged from 80 to 780 km² during the growing season, which would support 1.7-17 million juvenile and adult perch at 2.2 ind·ha⁻¹, the upper average density recorded for Lake Erie. Half the number of age 1+ perch could be supported if 100 m home range size was used in calculations. Alternatively, 250 million to 2.4 billion fish at 312 ind·ha⁻¹, the highest density recorded for yellow perch, would define the carrying capacity that may apply to optimal areas. The number of adult & juvenile perch (age 2+ because age-1+ counts are not available) in 1992 and 1993 numbered between 2.0-2.7 million fish, closer to the lower carrying capacity estimates. In future, the limiting thermal habitat areas in different years for all stages might be calculated to compare to year-class strength.

The highest adult growth potential predicted by temperatures coincided with documented spawning areas in springtime. This raises the question as to whether reproduction occurs at this time because it is opportunistic, even though adults do not feed until spawning has ended, or whether these areas have been selected because the eggs are more likely to survive to the juvenile stage. This question is addressed in Chapter 4.

2.4.2 Overall habitat assessment

Most of the final habitat suitability maps were driven by depth associations and modified by the unsuitability of vegetation and substrate types for particular stages. In most cases, the inclusion of other habitat factors either homogenized the suitability of Long Point Bay (as was the case for spawning), or restricted the area of suitable thermal habitat predicted from the thermal habitat assessment. In some cases, suitable areas shifted altogether as in the case of demersal larvae. If the habitat factors affect the vital rates of any of these stages, perhaps through

density-dependent effects, then the carrying capacity of the bay would be diminished because of non-overlapping suitable areas. Biotic interactions within the fish community as a whole have not been considered directly, but the negative effects on the perch population exacerbated if the realised niche differs from optimal habitat.

Averaging of habitat suitabilities for spawning resulted in no optimal areas in April and May because preferred physical characteristics do not occur in the same place. The resulting suitabilities infer that suitable spawning habitat is relatively homogeneous but not optimal in Long Point Bay based on these criteria and method of calculation. The annual estimate of relatively high suitability spawning habitat would be 5 km², while 1500 km² would be moderately suitable. This area was significantly reduced from the thermal spawning habitat estimate. It is difficult to translate overall suitabilities into a predictive measure of carrying capacity because non-thermal sources of mortality on eggs have not been quantified, (i.e. the probability of smothering and desiccation). The low suitability and small area of suitable spawning habitat would indicate however, that spawning area might be limiting because it is the smallest available area of all the life stages. This contradicts the predictions from the thermal analysis. In addition, without quantitative evidence of the relationship between physical habitat characteristics and egg survival then the thermal areas should take precedence. In addition, vegetation grows and senesces, which could affect the overall suitability assignments at the time of spawning.

Fischer & Eckmann (1997) advocated that vertical and size segregation of fish within a site may be as important to habitat partitioning as horizontal distribution differences among sites. The temporal dimension should also be considered. Overall suitabilities predicted spawning and demersal habitat overlapped, but were separated temporally, unless there are two spawning periods. Juvenile and adult habitats also overlapped, but might be separated vertically or behaviourally. Moreover, suitable pelagic larval habitat was located between demersal and juvenile habitats. It is difficult to assess the level of interaction between life stages using an annual aggregate calculation of suitable habitat location and area availability. However, on average and using all physical criteria for evaluation, suitable habitat was predicted as spatially separate between life stages. When it occurs, the degree of overlap between larval and juvenile stages would probably be linked to the degree of cannibalism that occurs in different years. Therefore, in the future, a spatial assessment of the overlap of highly suitable habitat between stages should be undertaken in addition to the calculations of carrying capacity effects on an isolated life stage. Without a spatially explicit approach, weighted useable areas may overestimate the overlap between successive life stages or assume that biotic interactions were not important and areas were independent.

High-suitability, pelagic larval habitat overlapped, by roughly 50%, with juvenile and adult habitats. Potential cannibalism in overlap areas could dramatically reduce the suitable habitat area estimates for pelagic larvae, which would become more like optimal demersal areas if actively avoided (notwithstanding passive dispersal in exposed areas). Therefore, the inner bay may act as a refuge from cannibalism if juvenile and adult densities are too high. However, many other predators exist in the warmer, vegetated areas of the inner bay, such as pike. If high predation rates do occur in vegetated areas then small, relatively colourless larvae (pelagic phase) may fare better in open water environments until banding on larval fish becomes apparent. Demersal optimal habitat overlapped slightly with juvenile and adult habitat. However, the distributions predicted from the thermal analysis would separate life stages vertically, so the area-based overlap estimates are somewhat misleading if different depth strata were chosen. This provides a good reason to assess thermal structure in three dimensions.

From this assessment it is difficult to determine what the limiting life stage or limiting habitat might be. Many outcomes are contingent upon the timing of life stage events, particularly in the first year of life. It is apparent that spatial and temporal changes in thermal habitat can affect habitat suitability and its availability may be limiting. However, simulation of habitat-population interactions and testing of habitat weighting factors would be necessary before any conclusions are drawn about how habitat affects population dynamics. These methods are pursued in later analyses.

Chapter 3

Does suitable habitat predict fish distributions?

...the importance of the spatial arrangements of habitat types... suggest that nonrandom distribution at one scale may be due to processes occurring at different scales -
Essington and Kitchell (1999)

3.0 INTRODUCTION

Chapter 3 compares a known distribution of yellow perch YOY (larvae) with HSI predictions of habitat suitability as a validation exercise. There is a general lack of information, especially spatial data, available on the early life history stages of fish; even for fish as extensively studied as yellow perch in the Great Lakes. A one-time, spatial survey for YOY yellow perch was conducted in August, 1998 in the Inner Bay of Long Point. Abundance and size distributions from the survey were compared to thermal and HSI predictions of suitable habitat to test for correspondence. Also, the relative importance of different habitat factors used in HSIs was tested by comparing them individually to larval distributions. Assumptions about the relationship between food availability and habitat characteristics, especially vegetation, were tested, and the mechanistic link between the suitability of submerged aquatic vegetation (SAV) as a food source and as a refuge was explored.

According to a definition for the ideal free distribution (IFD), organisms will distribute themselves between areas so that the fitness of all individuals is equal to the mean fitness level of the population (Kennedy & Gray 1993). Habitat suitability index (HSI) models are predicated on IFD rules. The premise is that preferred habitats lend a fitness advantage and therefore are more suitable. It follows that fish distributions, and possibly sizes, should reflect habitat suitabilities. The habitat associations of young yellow perch gathered in Chapter 2 were used to generate habitat suitability indices based on preferences and fitness-based premises. These suitabilities in turn should predict young-of-the-year (YOY) fish distributions that have resulted from directed movement or differential mortality, and possibly growth differences between habitats.

It is important to test habitat suitability predictions against actual distributions, especially for early life stages that are more vulnerable to environmental change, but validation data is difficult to obtain. The spatial distribution of YOY perch from a survey conducted in the inner bay of the Long Point region was compared against habitat suitability predictions for the time of the survey. The main purpose of the analysis was to determine whether a simple HSI model can predict fish distributions, and sizes. Drel *et al.* (2000) found that two to three variables could be used to predict suitable habitat in most systems, while others suggest that significant variables should be retained from models across different systems to improve transferability (Leftwich *et al.* 1997). Therefore, the individual habitat characteristics used in habitat suitability indices for the Long Point system were compared to YOY distributions to assess their relative importance as contributing factors.

Several habitat model predictions have been compared with fish distributions to assess their predictability, with varying results. Shuler & Nehring (1993) compared empirical data of salmonid habitat use against

the suitability ratios of different riverine habitats. In their validation analysis, no statistically significant linear relationship between structural complexity and the population density of adult and juvenile brown and rainbow trout was found during low, medium, and high flows. One could argue that habitat suitability and fish distributions may not be linearly related; many population-environment relationships can be described by quadratic functions (i.e. temperature relationships with vital rates). Also, it is likely that some explanatory variables may be left out of suitability models reducing their predictive capability. Shirvell (1989) found that HSIs predicted well for systems where the models were developed between systems. However, those indices were empirically based models, whereas the approach used here is based on general rules and information across systems where yellow perch are found. Therefore, the models are not specifically calibrated to any particular system. Predictability may be low in either case, but whether distributions match predicted fitness-based distributions is also informative.

3.0.1 *P. flavescens* early life history and habitat associations

There are many contradictory accounts for first-year perch ontogeny. Perch typically spawn in April to June at depths between 0.5 and 8 m, on complex surfaces such as macrophytes, coarse woody debris, and coarser substrate types. The period of egg development usually lasts between 3 and 21 days and is mainly dependent on temperatures (Hokanson 1977, Kamler 2002). Larval swim-up occurs 1-2 days after hatching and fry are typically found in sheltered, inshore areas where they prefer open water close to moderate vegetation. Perch is considered a high-density species, tolerant of crowding and of other species. Fry may form shoals with other spring-spawning fish, therefore spatial distribution is clustered and not uniform.

Young perch are planktivorous initially, eventually switching to benthic food sources. However, feeding in perch may be more plastic than previously thought, as for many organisms (Takimoto 2003). Perch are generally considered opportunistic feeders, but selectivity does occur (MacDougall *et al.* 2001). There is evidence that YOYs selectively prefer zooplankton, with some seasonal variation in prey items. Some studies state that fry typically move to the littoral zone just after hatching in early June, become pelagic until October, and then move back to shallow waters where they switch to benthic macroinvertebrates (Thorpe 1977a). The maximum feeding rates occur mid-summer, with maintenance feeding in fall depending on food availability (Thorpe 1977b). Alternatively, size-based changes in feeding ecology and rates can occur. Other studies state that larval perch are pelagic until 2-cm long, at which time they move inshore to feed on benthic organisms (Craig 1987). Therefore, in August, when the survey in this analysis was conducted, they may have been eating both zooplankton and benthos (MacDougall *et al.* 2001).

Young perch feed continuously during daylight hours and require 20% of body weight per day for maintenance at 23 °C (Craig 1987), with

temperature being linked to many bioenergetic rates (Hanson *et al.* 1997). Also, there has been an inverse density-dependence of growth noted in some studies (Carlander 1997), and average larval size may be inversely related to larval density. In addition, Henderson & Nepszy (1989) showed no correlation between year-class strength and growth, implying that growth and survival are disconnected. Larvae are susceptible to high thermal mortality rates (<50% of maximum survival) at temperatures below 8 °C and above 27 °C. Therefore, larval size distributions were compared to larval density, temperatures, and habitat variables.

Various hypotheses have been postulated regarding habitat refugia from predation. Postlarval perch may move offshore to the epilimnion to avoid predation if predator density is high in vegetation. Conversely, demersal phase YOYs have been documented moving inshore to vegetated or structured areas to avoid predation once their characteristic banded colouration develops. Predators of perch include almost all warm to cold-water fish. Bird predators include mergansers, loons, cormorants, and herring gulls. The high fish and bird diversity in the Long Point area indicates that predation rates are probably high. Predation by larger perch and walleye occurs after YOY perch reach 18 mm or 0.08 g (Campbell 1998); at the time of the study perch were approximately 0.2 – 2.6 g. Adult perch do not inhabit vegetated areas except during spawning, so cannibalism should be minimized in vegetated areas.

3.0.2 Prey availability, habitat, and YOY distributions

High perch mortality rates can be caused by plankton shortages as well as predation, with 10.7% / day more larvae dying than through predation alone (Letcher *et al.* 1996). Vegetated areas are areas of high prey availability, both zooplankton and benthic invertebrates, but can also act as a refuge for prey (Cyr & Downing 1988; Jeppesen *et al.* 1998). Post (1990) found that juvenile growth rates were lower in open water than vegetated areas, resulting from a combination of thermal habitat and food availability. Therefore, if larval fish maximize potential growth rates they should be found in areas with a higher percent cover of vegetation or higher food concentrations. Several habitat-based hypotheses were tested based on the distribution of YOY predators and zooplankton prey.

Zooplankton was surveyed at the time of larval fish surveys in the inner bay of the Long Point area. Benthos was not surveyed. However, benthic invertebrate density may be related to bottom substrate type. The sediments of the inner bay range from highly organic muck to sand. It is hypothesized that in-benthos are positively correlated with vegetation cover and inversely related to low organic content substrates, such as sand. Depth distributions were also tested even though the inner bay is quite shallow; many citations refer to the depth preferences of fish and it is included in several habitat suitability models (Kreiger *et al.* 1983; Lane *et al.* 1996b).

3.1 METHODS

3.1.1 Fish & Zooplankton Data

Fisheries and Oceans Canada (DFO) and the Ontario Ministry of Natural Resources (OMNR) conducted a spatial survey of age-0 fish (YOYs) and zooplankton distributions on August 24-28, 1998 in the Inner Bay of Long Point (Dimitru *et al.* 1998, unpublished data). MacDougall *et al.* (2001) explains details of the juvenile fish sampling methodology. Trawls were towed for a standardized distance at set stations along four transects in the bay (N.B. 6.1-m modified Biloxi bottom trawl towed for 10 min at 1.6 knots). Stations were positioned 500 m apart in <1 m of water and 1000 m apart in >1 m water depth (Figure 3.01). For this analysis, the YOY samples were considered independent, not spatially correlated, from each other for two reasons (Hinch *et al.* 1994). One, adult home range is estimated at 100 m (Craig 1987), which is 1/5th the minimum distance between sample points, and is assumed to be larger than YOY home range size. Two, all the fish samples were collected over a brief, two-day period, therefore fish were unlikely to move between sites.

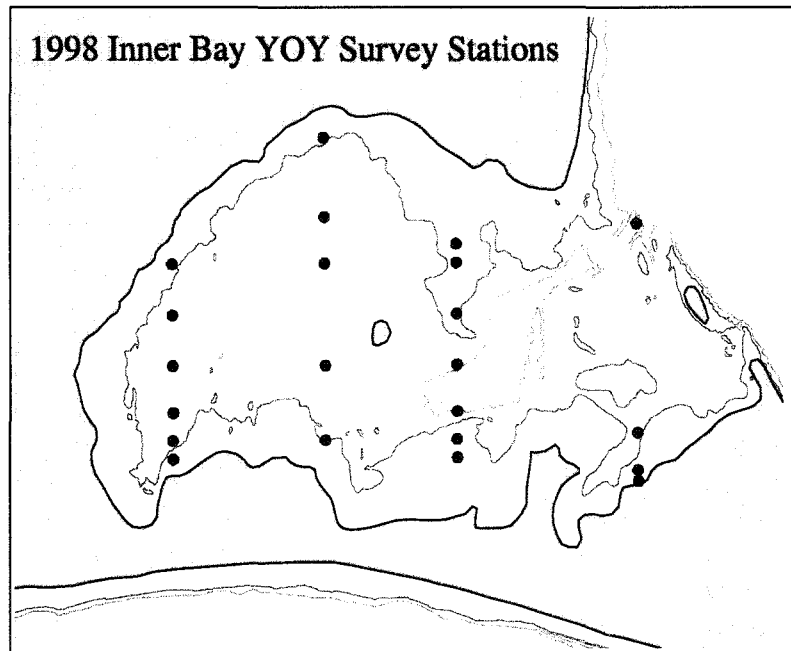


Figure 3.01: DFO and OMNR sampling locations on August 27-28, 1998 in the Inner Bay at Long Point, Lake Erie showing both planned and surveyed sampling locations for young-of-the-year fish and zooplankton samples (From Dimitru *et al.* 1998 unpublished data).

Zooplankton samples were taken with a 20L Schindler-Patalas trap at 3 points along the transect for each site. Samples were pooled and all zooplankton, including nauplii and copepodites were identified to species where possible, counted and weighed. Total abundance and wet-weight biomass estimates were determined for both fish and zooplankton

samples for each species separately. Data on yellow perch YOY catch per unit effort (CPUE; individuals per standard trawl), total biomass of YOY yellow perch, total zooplankton densities and biomass (not including copepod nauplii or eggs), was extracted from the data collected for each station. The average individual YOY weight was calculated by dividing total biomass by CPUE, because aggregate sample weights were recorded, not individual weights.

3.1.2 Habitat & Suitability Information

It was assumed that the recorded temperatures on the day of sampling would not be indicative of the thermal conditions to which the YOY perch and zooplankton would be responding. Therefore, AVHRR imagery for two weeks prior to, and including, the 1998 YOY and zooplankton sampling dates was used to determine average surface temperatures in the inner bay. AVHRR imagery was processed using the methodology outlined in Section 1.1.5, Chapter 1. These temperatures were then converted to thermal suitabilities based on the survival curve for larval yellow perch outlined in Equation 2.2, Chapter 2. (The suitability curve is shown in Figure 2.03.) The average August temperatures and thermal suitabilities for YOYs were mapped (Figure 3.02) for grid cells that were part of the initial SST grid.

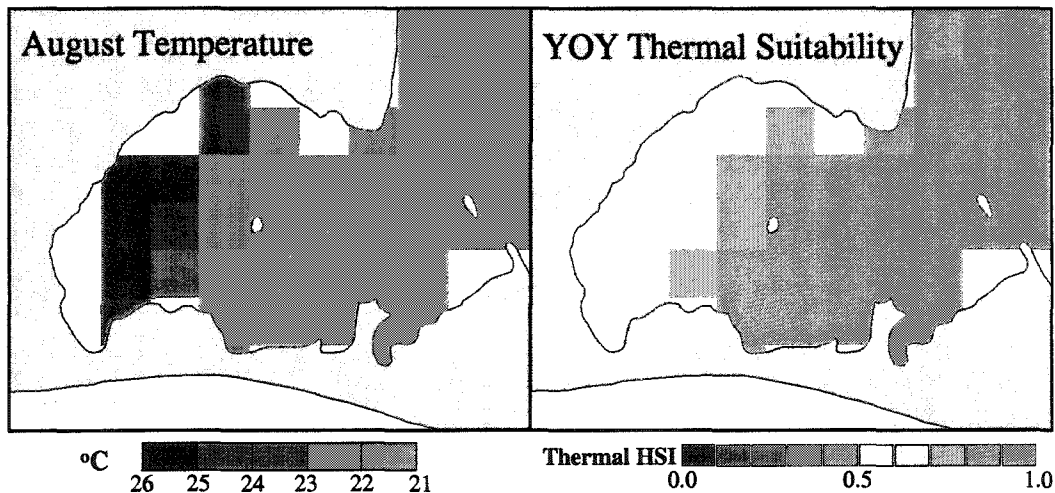


Figure 3.02: Average temperatures in August 1998 in the Inner Bay of Long Point Bay, Lake Erie converted to YOY thermal suitabilities based on survival probabilities. (See Figure 2.03 and Equation 2.2 in Chapter 2 for the thermal HSI curve and equation.)

Spatially explicit habitat information outlined in Chapter 1 was used to calculate habitat suitabilities for YOY perch in the inner bay and to extract relevant habitat data corresponding to each survey station. Detailed CASI survey maps for substrate type and vegetation percent cover, as well as a bathymetric contour map were overlain to create a polygon coverage of the inner bay (Figure 3.03). Each resultant polygon had a unique combination of the physical characteristics. The unique

combinations were assigned a final habitat suitability by arithmetically averaging the larval suitabilities for the individual characteristics (Table 2.5, Chapter 2).

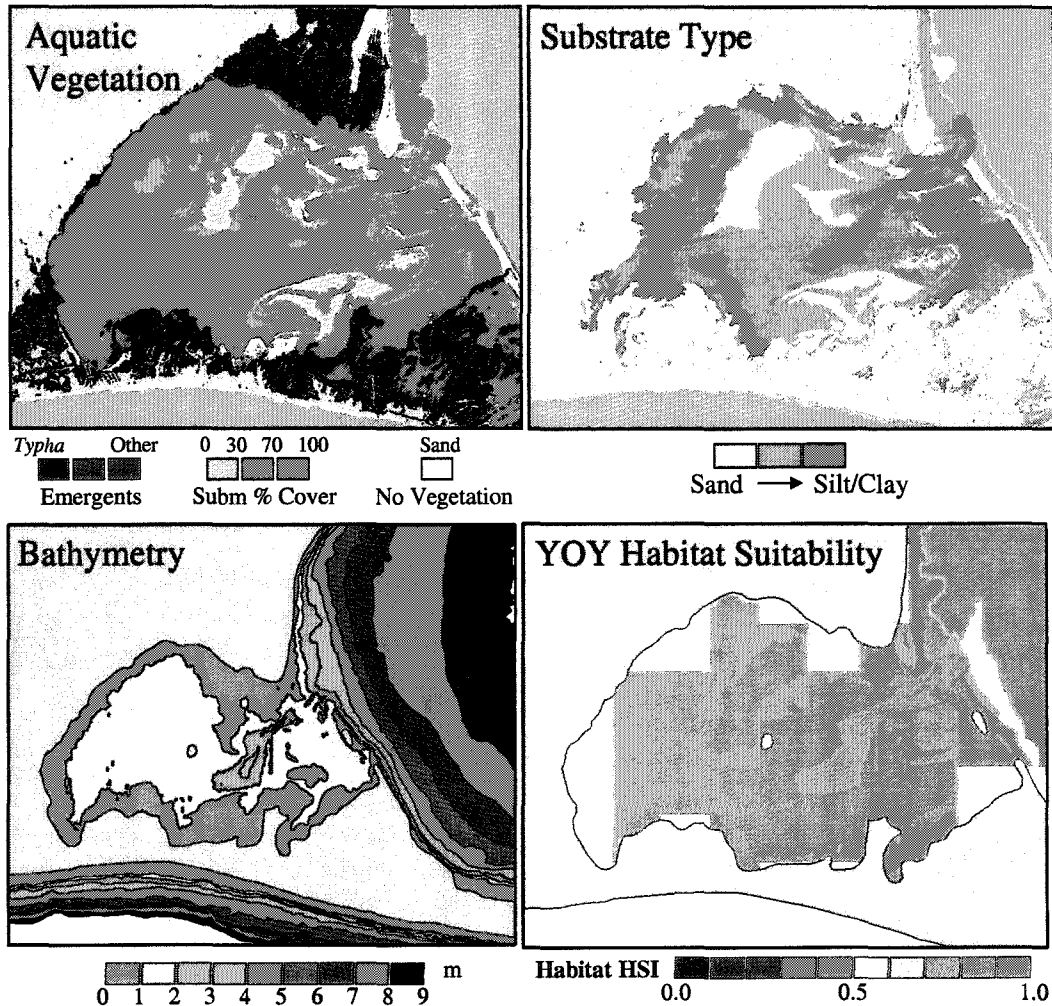


Figure 3.03: Physical habitat maps of the Inner Bay of Long Point, including aquatic vegetation (emergent and submergent vegetation categories), substrate type (sand, intermediate, and silt/clay categories), and bathymetry (water depths at 1-m contour intervals). Physical habitat features were converted to overall habitat suitability for YOY perch based on HSIs found in Table 2.5, Chapter 2.

The physical data and suitabilities that corresponded to the station locations were extracted from the maps for comparison with fish and zooplankton abundances and biomass estimates. Because the inner bay is mainly composed of sand, silt, and clay combinations of substrate type, the percent sand composition at each point was used as an indicator of substrate composition. In addition, surveys took place in varying densities of submergent vegetation; emergent vegetation areas were not included. Therefore, only percent submergent vegetation cover was used in the analysis.

3.1.3 Data Analysis

Independently, the abundance of perch and zooplankton was compared to individual or total biomass, respectively, using correlation analysis to determine if the two measures were autocorrelated (Systat® v10.2). To test if YOY size and spatial distributions corresponded with thermal and habitat suitability predictions, the abundance, and average individual weight of yellow perch YOYs was compared to the suitabilities at each station. YOY abundances and zooplankton densities were also compared to the individual physical characteristics at each site: depth, percent sand, and submergent vegetation cover. Least-squares regression analyses or simple ANOVAs were conducted to determine statistical significance at the $\alpha = 0.05$ level, if the data warranted. Variables were lumped for ANOVA calculations if necessary or log-transformed if there was unequal distribution of variance across data ranges.

3.2 RESULTS

3.2.1 YOY Perch Distributions

Yellow perch YOY distributions were clumped, but the average weight per individual at each site was relatively uniform, with a few exceptions (Figure 3.04). Higher abundances of YOYs were found in a southwesterly direction of the inner bay but CPUE varied highly between adjacent sites. Average YOY size ranged from 0.2 to 2.6 g between sites; the inner bay average across all sites was equal to 1.5 g.

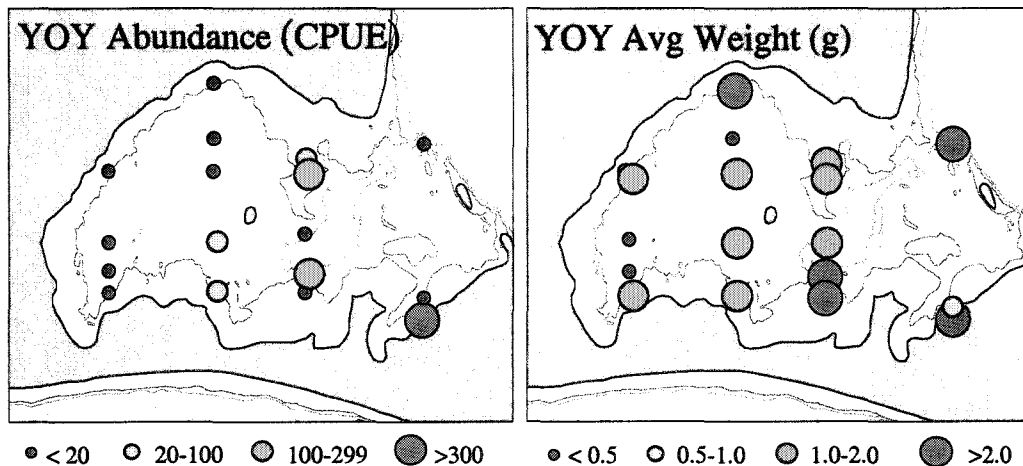


Figure 3.04: YOY abundance (# of individuals per 10-minute trawl) and average larval weight (mg) per trawl captured during an August, 1998 larval perch survey in the Inner Bay of Long Point Bay, Lake Erie (Dimitru *et al.* unpublished data; null values are not shown).

Young-of-the-year abundance data was skewed toward low catches therefore data was log-transformed for correlation analysis. Zero catches were not included in the analysis. The average individual size of

YOYs was slightly correlated with log-transformed CPUE data, but not significantly (N=17, R=0.41, p(2-tail)=0.102). The variance in average size was highest at low abundances, but the two variables were considered independent of each other in future analyses (Figure 3.05).

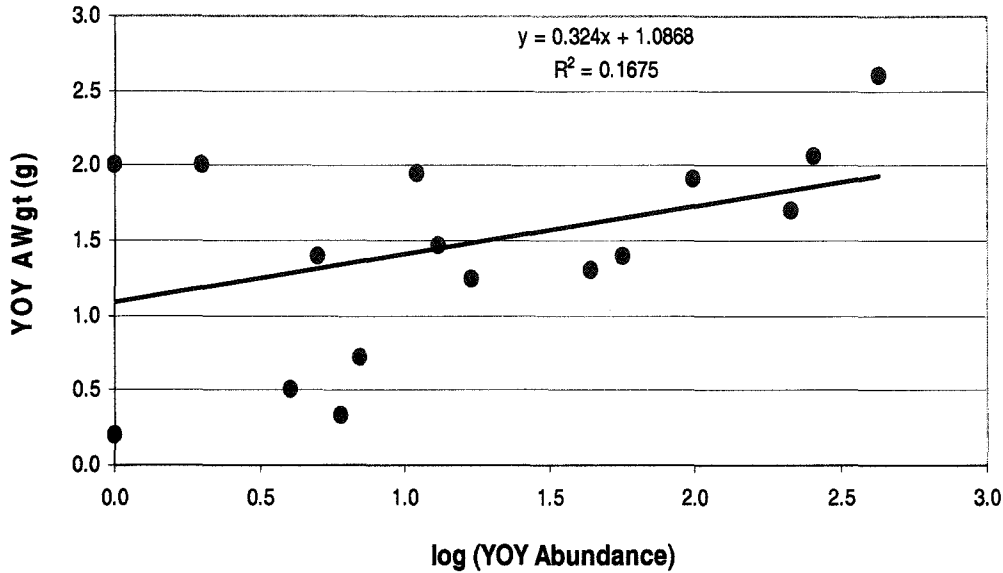


Figure 3.05: YOY abundance (CPUE = # of individuals per standard-length trawl) plotted against average individual YOY weight per trawl (g) from a larval spatial survey conducted in Long Point Bay (Dimitru *et al.* unpublished data).

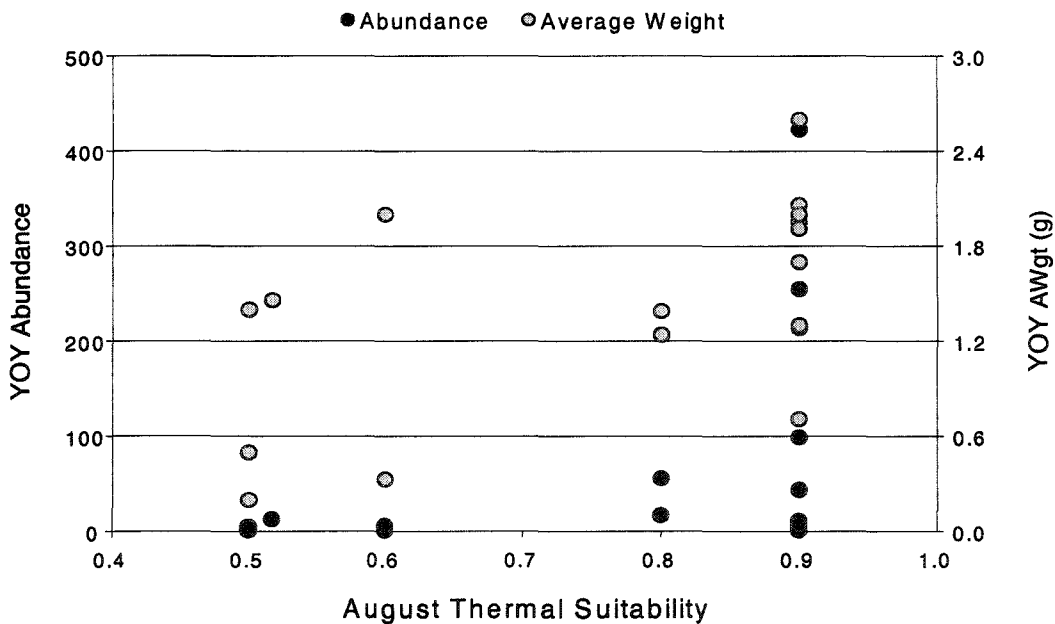


Figure 3.06: YOY abundance (# of individuals per trawl) and average YOY weight per trawl (mg) from a larval spatial survey conducted in Long Point Bay (Dimitru *et al.* unpublished data) plotted against the larval thermal suitability at each sampling point during August, 1998 based on average August temperatures.

Thermal suitabilities ranged between 0.5 and 0.9, with half of the bay having high thermal suitability according to temperature-survival curves. Temperatures to the northeast were above thermal optima at 26 °C, and ranged to 21 °C in the southwest (Figure 3.02). YOY abundance and average weight at each site was plotted against the thermal suitability at each site in August. There was a slight, positive trend between average size and thermal suitability, but the variance was high (Figure 3.06). All high-abundance catches (above 100 individuals / trawl) were found in high thermal suitability waters (HSI=0.9).

Physical habitat suitability was ranked highly and uniformly throughout the bay, ranging from 0.80-0.95 (Figure 3.03). YOY individual weight was only weakly related to habitat suitability, while abundances were unrelated to this aggregate measure (Figure 3.07). When physical habitat characteristics were analysed separately, the depth, and the percentage of sand in the substrate were unrelated to abundance and individual weight of YOYs caught (Figures 3.08 & 3.09). The maximum YOY average weight appeared to form a positive, linear relationship with percent submergent cover but the size distribution in high-percent cover submergents extended the full range of possible sizes (Figure 3.10).

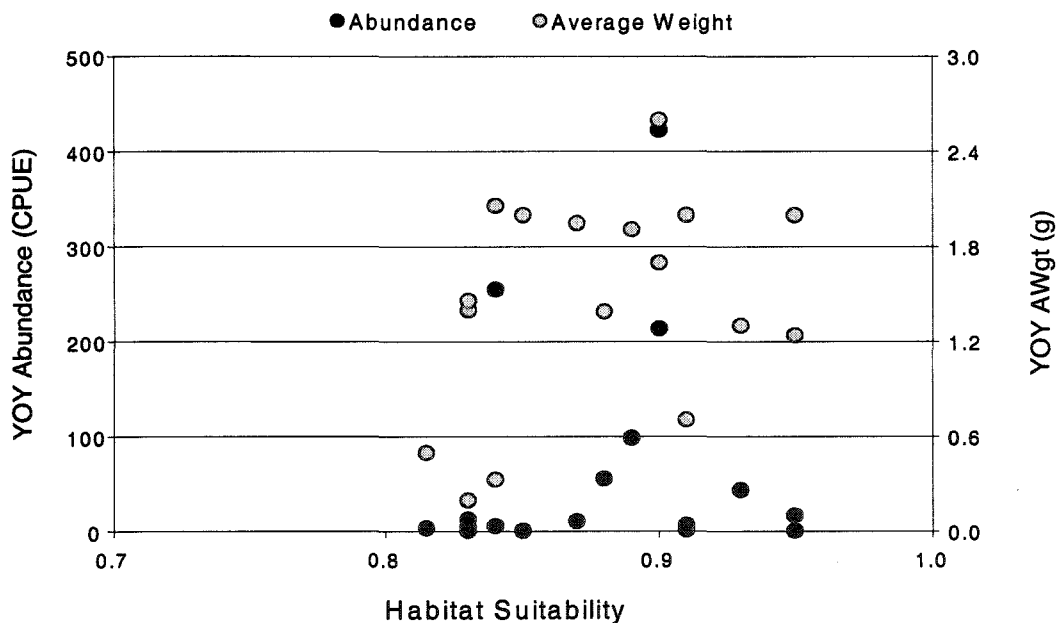


Figure 3.07: YOY abundance (# of individuals per standard trawl) and average YOY weight per trawl (mg) from a larval spatial survey conducted in Long Point Bay (Dimitru *et al.* unpublished data) plotted against the larval habitat suitability at each sampling point during August, 1998 based on depth, vegetation and substrate type associations.

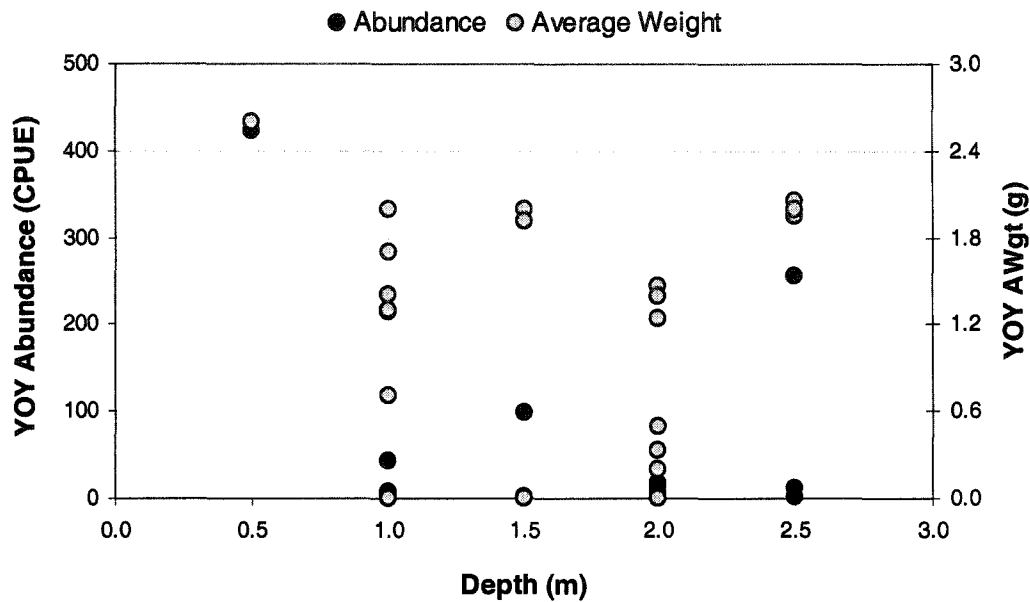


Figure 3.08: YOY abundance (# of individuals per standard trawl) and average YOY weight per trawl (g) from a larval spatial survey conducted in Long Point Bay during August, 1998 (Dimitru *et al.* unpublished data) plotted against the water depth (rounded to nearest 0.5 m) at each sampling point from bathymetry data.

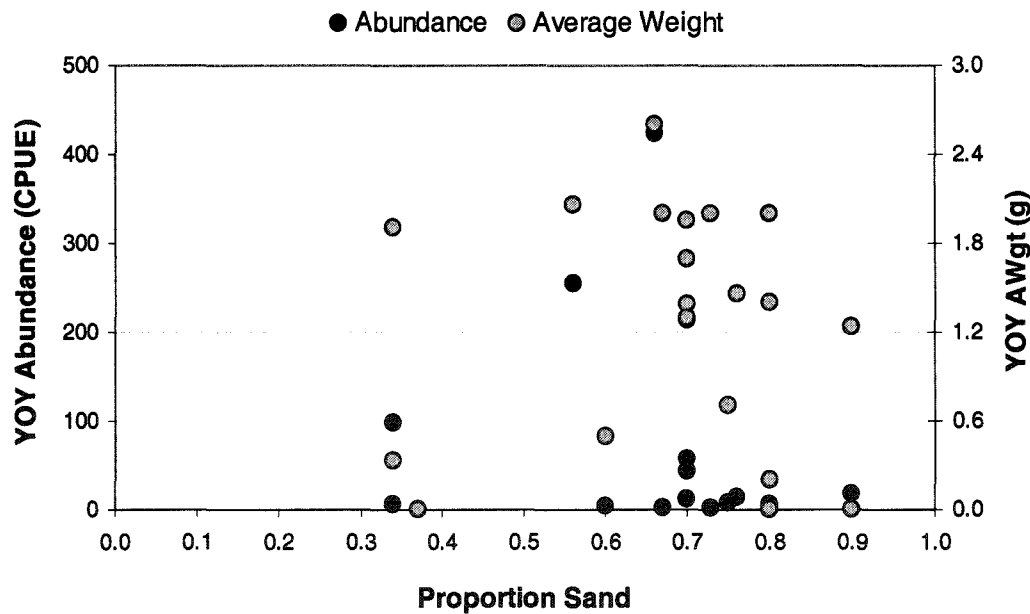


Figure 3.09: YOY abundance (# of individuals per standard trawl) and average YOY weight per trawl (g) from a larval spatial survey conducted in Long Point Bay (Dimitru *et al.* unpublished data) plotted against the proportion of sand in substrates at each sampling point during August, 1998.

In comparison, the high-abundance catches were only found in high percent cover (90% submergents), similar to the thermal suitability results (Figure 3.10). A significant linear regression resulted when (log+1)-

transformed YOY abundance data was regressed against an interaction term between percent submergents and thermal suitability. This equation obtained a higher adjusted R^2 value (Equation 3.1) than a step-wise multiple regression of the variables independently ($\text{adj-}R^2=0.39$). (N.B. Vegetation and temperature were not correlated and explained equal percentages of the variance in the step-wise model.)

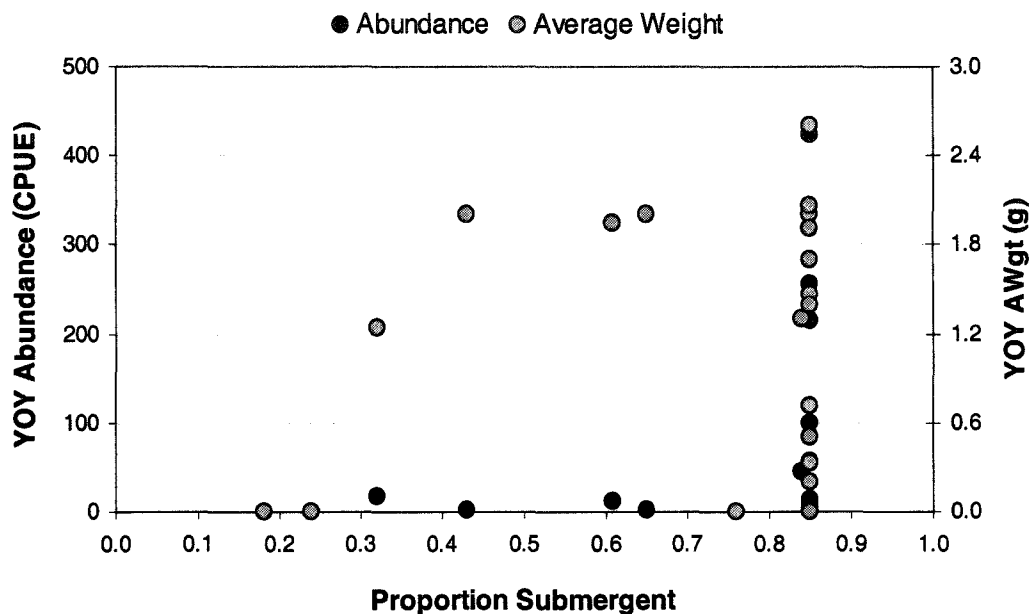


Figure 3.10: YOY abundance (# of individuals per standard trawl) and average YOY weight per trawl (g) from a larval spatial survey conducted in Long Point Bay (Dimitru *et al.* unpublished data) plotted against the proportion of submergent vegetation cover at each sampling point during August, 1998.

Equation 3.1: $\text{Log}(\text{YOY} + 1) = 3.02(\pm 0.73) * (\text{TempSuit} * \% \text{Subm}) - 0.65 (\pm 0.41)$; (N=22, $\text{Adj-}R^2=0.43$, $p=0.001$); where YOY = # / trawl (CPUE), TempSuit = Thermal Suitability, %Subm = percent submergent vegetation cover.

3.2.2 Crustacean Zooplankton Distributions

Only zooplankton adults were included in the following analysis, not eggs and nauplii. Zooplankton densities in the inner bay ranged from approximately 20,000 – 180,000 individuals per cubic metre in a total of 22 samples taken in the spatial survey of 1998. Total biomass at the sites ranged from 8.5 to 55 $\text{mg}\cdot\text{m}^{-3}$. Spatial statistics were not performed, but higher abundances and biomass estimates appeared to occur along a NW-SE transect within the bay (Figure 3.11). Zooplankton density ($\#\cdot\text{m}^{-3}$) and biomass ($\text{mg}\cdot\text{m}^{-3}$) were autocorrelated at each site (Figure 3.12; N=22, Pearson's $R=0.94$, $p<0.001$). Both variables were used in subsequent analysis, but either could be substituted in the equations developed. Zooplankton densities were mainly used.

Zooplankton density and biomass were unrelated to temperature, site depth, and the percentage of sand in the substrate, which ranged from 21 to 26 °C, 0.5 to 2.5 m, and 30-90% cover, respectively (Figures 3.13,

3.14 & 3.15). Zooplankton density was nonlinearly related to the proportion of submergent vegetation present at each site (Figure 3.16). The samples were biased towards high percent cover, so a categorical assignment of low (<33%, N=3), medium (34-66%, N=3) and high (>66%, N=16) vegetation was used in an ANOVA to test for significant differences in zooplankton density. Zooplankton densities in moderate cover were significantly lower than in low and high submergent cover (df=19, F=5.5, p=0.03), which were not significantly different from each other.

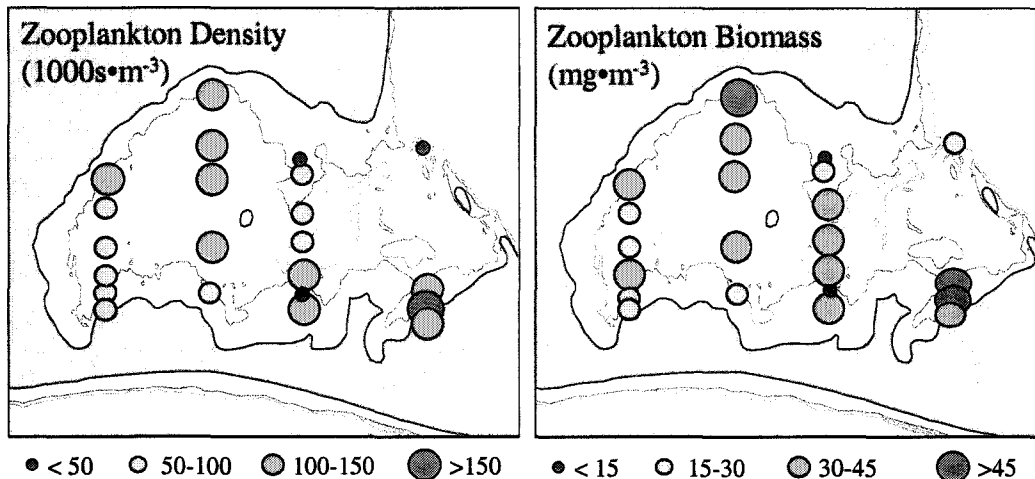


Figure 3.11: Zooplankton densities and total biomass (1000s of individuals or milligrams per cubic metre) collected during a spatial survey of the Inner Bay in Long Point Bay, Lake Erie during August 1998 (Dimitru *et al.* Unpublished data).

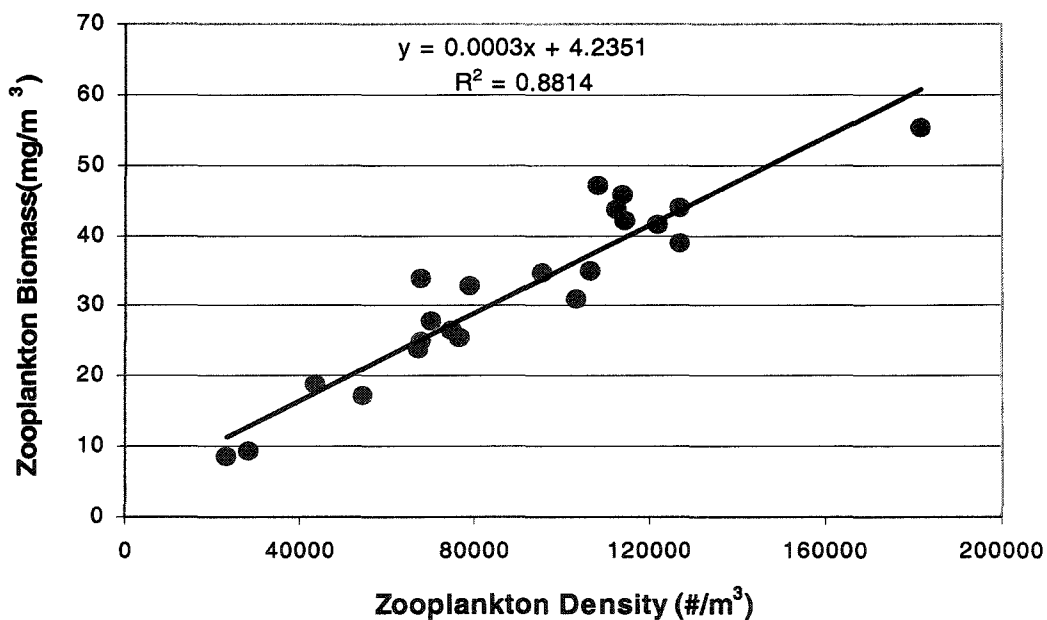


Figure 3.12: Zooplankton density (# of individuals·m³) plotted against total zooplankton biomass (mg·m³) from a spatial survey conducted in Long Point Bay (Dimitru *et al.* unpublished data; p<0.01).

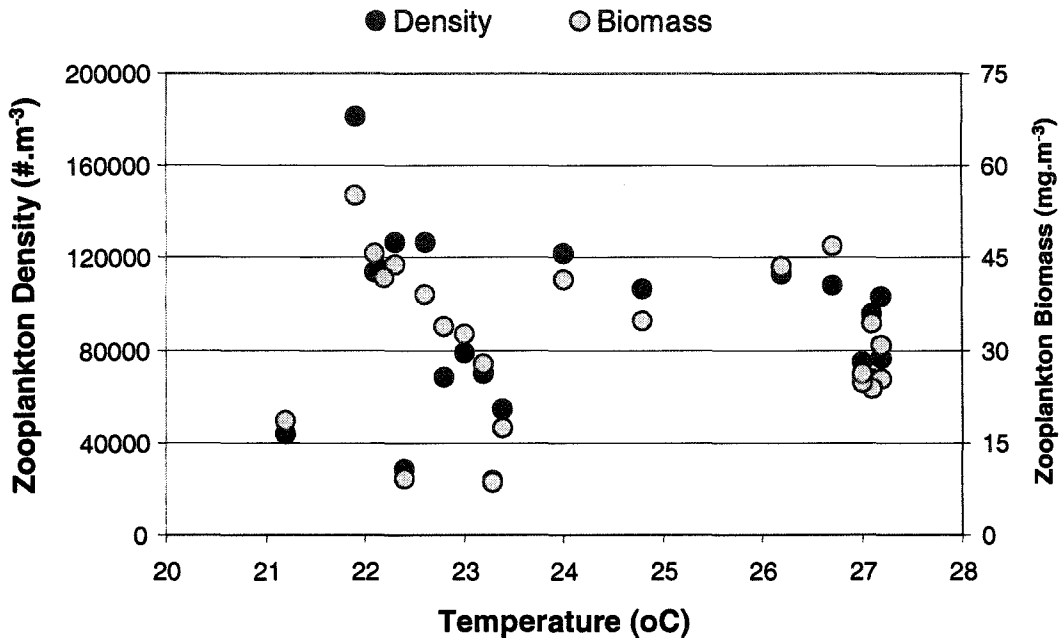


Figure 3.13: Zooplankton density (# per cubic metre) and biomass (mg per cubic metre) collected during a spatial survey on August 24-25, 1998 of the Inner Bay of Long Point Bay, Lake Erie (Dimitru *et al.* unpublished data) plotted against the average temperature of the site for the previous 2 weeks (derived from AVHRR sea surface temperature imagery) .

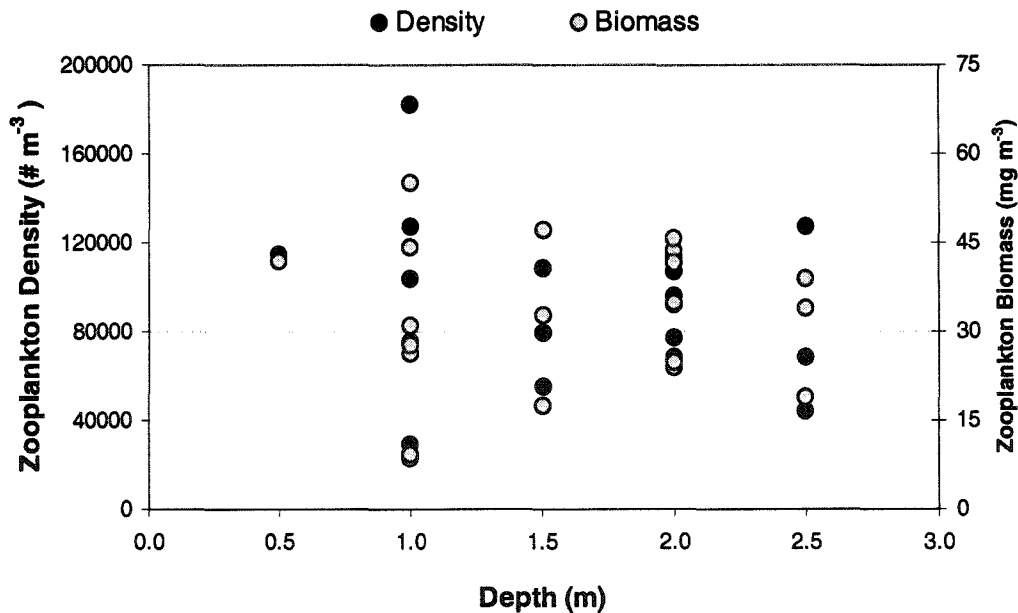


Figure 3.14: Zooplankton density (# per cubic metre) and biomass (mg per cubic metre) collected during a spatial survey of the Inner Bay of Long Point Bay, Lake Erie (Dimitru *et al.* unpublished data) plotted against the depth of the sampling point derived from bathymetric data.

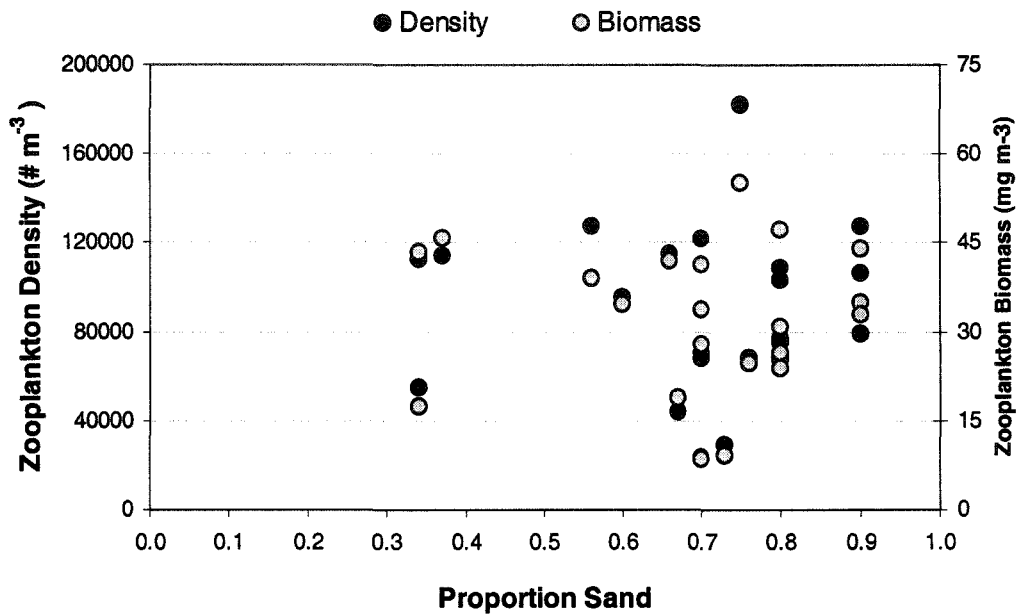


Figure 3.15: Zooplankton density (# per cubic metre) and biomass (mg per cubic metre) collected during a spatial survey of the Inner Bay of Long Point Bay, Lake Erie (Dimitru *et al.* unpublished data) plotted against the proportion of sandy substrate at the sampling point derived from a CASI survey.

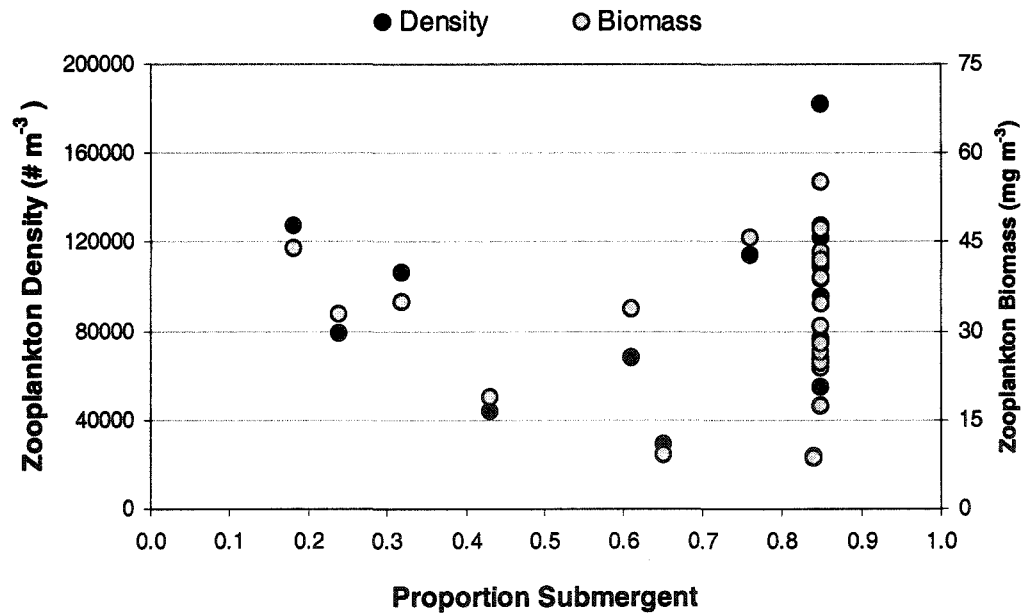


Figure 3.16: Zooplankton density (# per cubic metre) and biomass (mg per cubic metre) collected during a spatial survey of the Inner Bay of Long Point Bay, Lake Erie (Dimitru *et al.* unpublished data) plotted against the proportion of submergent vegetation cover at the sampling point derived from a CASI survey.

Individual YOY size was also compared to the zooplankton biomass collected at the same site. YOY size was unrelated to

zooplankton biomass (Figure 3.17). Lastly, the zooplankton distribution was compared with the yellow perch YOY distribution in the inner bay. A wedge-shaped distribution emerged where low YOY abundances were observed across the range of zooplankton densities, but the highest YOY abundances occurred at moderate zooplankton abundance (Figure 3.18).

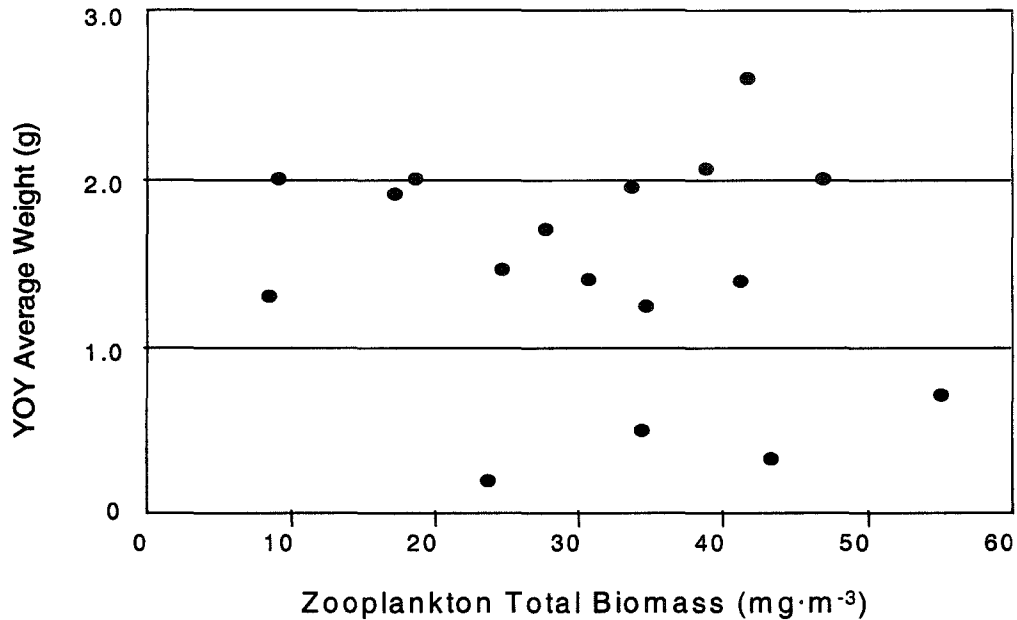


Figure 3.17: Zooplankton densities (# per cubic metre) versus YOY abundance (# per trawl) at each point in the spatial survey conducted in August 1998 in the Inner Bay of Long Point Bay, Lake Erie (Dimitru *et al.* unpublished data).

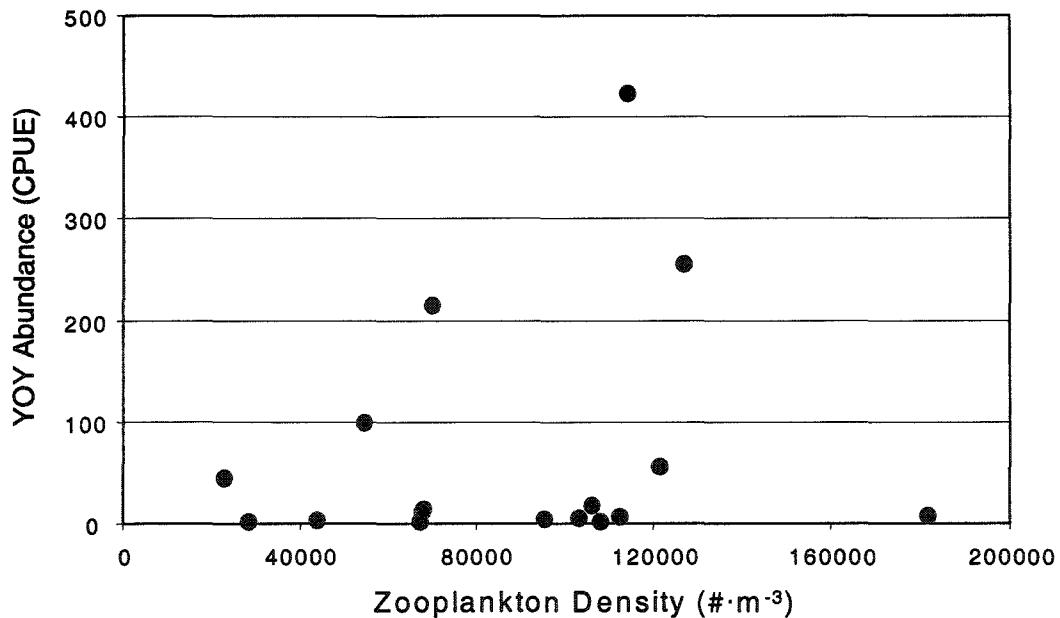


Figure 3.18: Zooplankton densities (# per cubic metre) versus YOY abundance (# per trawl) at each point in the spatial survey conducted in August 1998 in the Inner Bay of Long Point Bay, Lake Erie (Dimitru *et al.* unpublished data).

3.3 DISCUSSION

The grain size of habitat refers to how rapidly the environment changes relative to movements of the consumer (*sensu* Levins 1966). Fine-grained habitats are where distinct differences in patches and resource availability occur, while coarse-grained patches all look alike (Ranta *et al.* 2000). The Inner Bay is mainly composed of fine substrates and is therefore homogenous from a fish's perspective. If substrate type, in this analysis the percentage of sand, was at all linked to food abundance of benthic macroinvertebrates, the relationship was not significant. The depth range is also very limited and shallow. The individual HSI rankings indicated that the inner bay has highly preferred substrate types and depths throughout. Therefore, the Inner Bay is coarse-grained for both depth and substrate and no significant relationship within the restricted range of these variables and YOY size or abundance was obtained or should be expected.

The probability of finding a school of perch was much higher in very good thermal habitat than even moderately suitable thermal habitat. However, individuals were still found in areas with suitability ratings as low as 0.5, the lowest thermal suitability for the two weeks prior to the survey. Also, perch schools were only found in high-percent-cover submergents. The combination of highly suitable temperatures and dense macrophyte cover explained 43% of the variance in YOY abundance (CPUE) and the probability of finding a school of age-0 perch significantly increased in these areas. This implied that the definition of suitable habitat may be closer to a classical definition of optimal habitat. If so, the suitable area available to a life stage may be reduced from that predicted by the overall HSI model and weighted suitability areas may be overestimated.

The vegetation HSI, which was based on a compilation of habitat preferences from the literature, ranked low and moderate submergent cover as more suitable. The vegetation suitability predictions did not match the actual YOY distributions in this survey and contributed to the low predictability of the overall HSI. It may also indicate that under certain conditions there should be a hierarchical weighting of habitat characteristics where vegetation, when present, is a controlling factor. The mismatch between observed and predicted YOY perch distributions indicated the weight of some habitat variables may be underestimated in average HSI calculations, if distributions are indicative of higher fitness. Alternatively, predation pressure may be so high in the inner bay that YOY fish may be forced into less fit habitats, on average (Werner *et al.* 1983).

Both field and controlled enclosure experiments have documented increased use of vegetation by small fish under predation pressure, especially when an effective predator, like pike, is present (Diehl & Eklov 1995). Under these behaviourally modified distributions, growth was compromised by two mechanisms: the physical structure of vegetation interfered with feeding, and density-dependent food limitation occurred in small areas. This is why high-density submergents were ranked lower

than moderate cover in the original HSI for vegetation. However, survival is much lower in open habitat than vegetated habitat. Therefore, vegetated areas usually have higher densities and smaller fish (Randall *et al.* 1996), whereas exposed (open) areas were associated with larger fish. Therefore, certain habitats may maximize on survival but are less conducive to growth. Railsback (2003) also found that fish may be concentrated in areas that do not necessarily offer the highest overall fitness advantage. This is an argument for weighting the relative suitability of habitats differently for different process rates.

In the Long Point study, YOY abundance and YOY size were not related. The two most important factors were temperature and high percent cover vegetation for predicting the probability of high-density YOY areas. The probability of mortality due to thermal stress and predation is minimized in these locations and may not have an additional effect on growth because size differences were not significant. This would imply that food was not limiting and because YOY density was not related to YOY size, it also implies that densities were not limiting either. However, it is difficult to assess growth differences given the data available. The size of fish sampled would be dependent on when hatch occurred and on movement rates between habitats, in addition to possible habitat- or density-based effects on subsequent growth rates. Without this information, it is difficult to draw habitat-based conclusions. An experimental approach would be needed to test these hypotheses and to gather information on the age of YOY fish and movement rates.

Habitat occupancy and densities within habitats are also dependent on whether the system is at carrying capacity. Refining the HSI model, or using the lowest suitability to represent overall suitability, would improve the model's predictive capabilities for habitat occupancy, especially if temperatures were included. However, habitat suitability would not accurately predict densities at a particular location because of the variability within suitable habitats due to clumped distributions. Nevertheless, HSIs are not intended as predictive models of abundance at different scales, but for determining the location of suitable habitats and their relative availability. More suitable areas should have higher overall abundance within the entire habitat compared to others. It is unrealistic to think that high suitability habitat has high abundances at all sites, therefore suitability models should be probability based, especially if clumped distributions are involved. Even if distributions are clustered, the area per individual probably does not change, just the distribution of individuals within the suitable habitat. Therefore, strictly density-based statistical measures of habitat suitability can be misleading if collected at the wrong scale.

Zooplankton densities were nonlinearly related to vegetative cover and the probability of finding zooplankton in areas of low and high cover was greater. However, zooplankton density was highest at average YOY abundance levels. Predator density is not necessarily correlated with prey

density because local zooplankton abundance could be depleted due to grazing of the YOYs. Therefore, depending on the movement rates of YOYs, predation may or may not be responsible for local depletion of resources at high densities. Nevertheless, zooplankton densities were high in the vicinity of high-density YOY patches but not at the exact point. A spatial analysis might reveal that predator and prey distributions are contiguous but more samples would be required than in the current survey to assess significance at the level of patchiness observed.

In the study, zooplankton density and biomass were autocorrelated and zooplankton densities were high in both low and high-cover submergent areas. Therefore, open areas may offer a refuge from zooplanktivorous fish and could partly explain the observed distributions. However, the statistical relationship between vegetation and zooplankton in the study is somewhat tenuous because sample sizes were low in both low and medium cover. Calculating the probability of finding prey given habitat features is possible and therefore extrapolations about suitable growth habitat can be made. A conservative estimate of YOY consumption rates is 20% per day at 23 °C (Marmulla & Rosch 1990). Therefore, a 0.5-g fish would eat 0.1 g of zooplankton per day and a 2.5-g fish would eat 0.5 g of zooplankton per day. At these sizes and the highest zooplankton densities recorded in the survey, age-0 fish would require a minimum of 1.4 m³ and 7.1 m³ per individual per day, respectively.

The range of zooplankton densities varied widely in high cover because both larvae and zooplankton distributions were patchy. This indicated a clumped distribution similar to the clumped distribution of YOY fish in suitable habitat. Schooling, or clustered distributions of fish, may be a behavioural response to avoid predation pressure or to improve foraging efficiency. This behavioural response is probably occurring at both trophic levels because there is evidence that zooplankton modify spatial distributions in response to predation, especially in shallow habitats (Jacobsen *et al.* 1997).

A comparison of fish and zooplankton abundances resulted in a wedge-shaped relationship that indicates one of two possibilities. One, under-matching may be occurring and fish are not distributed ideally within the landscape (i.e. ideal free distribution is based on an entire knowledge of the system). Two, habitat selection in YOY fish is occurring for other reasons than zooplankton distributions. For example, young perch might be eating benthos or avoiding predation in low-density submergents. Fisher *et al.* (1999) found that larval abundance was related to biological variables, such as zooplankton abundance, and juvenile (YOY) abundance was related to substrate, water temperature, depth, and sometimes chironomid abundance. Perch during the time of the survey may be consuming both food sources. It would be difficult to test the substrate type-benthos hypothesis because no benthic samples were taken or gut content analysis performed.

In addition, other habitat factors may be important to YOY perch habitat selection. Many studies quote that sheltered areas are preferred by age-0 fish (Houde 1969, Thorpe 1977a, Goodyear 1982). Exposure to prevailing wind and waves is minimized on the south side of the bay. Unfortunately, no meteorological information was gathered during the time of the study, but the relationships between fish, zooplankton, and exposure, as well as the interactions with other habitat factors, require further investigation.

It is uncertain whether survey YOY distributions were a result of differential survival or movement. It would be difficult to distinguish unequal distributions that arose from directed movement from those that resulted for mechanistic reasons at a local scale, such as in high growth and high survival areas with little movement. Therefore, modelling and controlled experiments are needed to test some hypotheses about which rate, if any, is controlling distributions. Persson & Crowder (1998) recommended that habitat models and game theory be used to assess the effect of habitat shifts and its implications on population dynamics.

CHAPTER 4

**Can habitat be linked to fish population dynamics?
If so, how does habitat limit fish production?**

Natural and anthropogenic perturbations do not always equally affect all parts of an ecosystem, and all parts of an ecosystem do not equally contribute to maintain fish communities.

Boisclair (2001)

4.0 INTRODUCTION

This chapter focussed on the mechanistic links between habitat and yellow perch population dynamics rather than preference or distribution-based habitat suitability approaches (see Chapter 2). The model concentrated on the first year of life and the effect of consecutive constraints on early life stages with different habitat requirements. Early life stages included spawning, egg (survival and development), and planktonic larvae (growth and survival). Scenarios tested the ramifications of having no habitat preferences at spawning, thermal effects at different life stages, and finally, habitat-based effects. Habitat-based effects were applied where linkages between depth, temperature, vegetation, substrate type, or wave exposure could be established for growth and survival. The purpose of the model was to compare the potential growth and survival of consecutive life stages in a spatially explicit manner when different habitat-based rules are imposed.

There has been continued debate over whether habitat is an important factor in regulating population dynamics (Pulliam 1988, Ryder & Kerr 1989, Kelso & Wooley 1996, Minns 2001). Most ecologists would agree that physical habitat heterogeneity exists both spatially and temporally in lakes and rivers, that habitat preferences exist for certain species, and that some habitats (this includes thermal habitats) may be more advantageous than others for growth or survival. However, it is the link between population processes and habitat that remains tenuous (Rose 2000). In this chapter, habitat relationships and population dynamics are explored in the first year of life for yellow perch. The ramifications of imposing habitat-related behaviours, preferences and advantages are investigated in an iterative and step-wise manner to determine the potential importance of physical habitat and temperature as regulatory factors in fish population dynamics.

There are two main questions addressed by this study; by what mechanistic process can habitat be quantitatively linked to population dynamics, and, how can the interaction between habitat heterogeneity and population processes limit first-year fish production? Many approaches have been used to address the first question, most notably, population models that include environmental factors. Habitat-based models for fish species vary in complexity, spatial scale, and temporal scale, as well as the level of detail that is mapped or simulated (Great Lakes examples include Minns *et al.* 1996, Jones *et al.* 1998). Generally, the fish species of interest are divided into life stages that have different habitat requirements, and models can range from closed population models to life-stage specific. In this study, a habitat-based, spatially explicit matrix model was constructed based on current knowledge regarding interactions between lake habitat and yellow perch populations.

The second objective was addressed by testing different habitat-based rules at different life stages in the first year of life to compare their

relative effects on spawning success, survival and growth of eggs and fry, and ultimate first-year production. Chapter 4 begins with a discussion of habitat associations and fish population dynamics and a review of fish population models that are pertinent to fish habitat science. These approaches are compared to the one presented here for early life stages, referred to as the Long Point yellow perch habitat model or PercaSpace.

The core of this chapter addresses the spatial and temporal dynamics of fish populations in relation to their environment, or physical habitat, in the first year of life. The yellow perch population in Lake Erie, especially the eastern basin, has experienced dramatic fluctuations in recent years. There is speculation about whether some aspect of habitat, such as temperature, or a decline in suitable habitat, may be linked to the population fluctuations. PercaSpace concentrated on linking habitat to first year population dynamics in a quantitative way to elucidate those potential effects on year class strength.

4.0.1 Habitat associations with population dynamics

For habitat to affect fish production one of two conditions must be met, fish must have habitat preferences that affect density-dependent population rates, or different habitats must differentially affect individual vital rates directly, thereby affecting population dynamics. If a species has a preferred habitat, it could have resulted from an evolutionary selection for that habitat preference because of individual fitness differences between habitats that have defined the fundamental niche requirements (Grossman *et al.* 1995, Proulx 1999). However, it is difficult to establish habitat preferences if there is simply unequal distribution between habitat types (Railsback 2001), which may have resulted from competitive exclusion (i.e. the realised niche; *sensu* Hutchinson 1965).

Therefore, an extensive literature review of habitat preferences and associations in all types of systems with different fish communities should reveal what the hierarchy of habitat preferences are for perch in their fundamental niche (see Chapter 2 for habitat review). Even so, density-dependent processes would only become important once preferred habitats reached carrying capacity. If habitat influences vital rates directly, irrespective of density, then quantitative relationships need to be established between habitat factors and either reproductive, growth, or survival rates. The result of either of the conditions being true is that some physical habitats directly confer survival, reproductive, or growth advantages to individuals, or indirectly affect vital rates by creating clumped distributions and affecting density-dependent rates. This chapter explores the former hypothesis through quantifying how physical habitat, including temperature, modifies individual fish vital rates and thus population dynamics through spawning and early life stages.

Three factors directly affect potential growth rates in fish: water temperature, food consumption, and activity levels. These factors modify the maximum physiological growth capacity of perch, which is defined by individual metabolic rates (Kitchell 1977, Hanson *et al.* 1997), within limits

that are genetically determined. The amount of food ingested is a function of food availability and the catchability of prey items. Different systems have differing productivities that govern the maximum food availability but other biological and physical processes may restrict the abundance and availability of that food at a site-specific level. For example, prey availability can be affected by the density of predators, which affects the level of competition for food (Carpenter & Kitchell 1988). Habitat structure can affect food abundance because of varying primary production in certain areas, like wetlands (Cyr & Downing 1988, Diehl & Kornijow 1998, Sondergaard & Moss 1998), and varying catchability of prey items because of habitat complexity (Jacobsen *et al.* 1997, Carpenter *et al.* 1998, Jeppesen *et al.* 1998).

The same habitat features that produce differences in food availability may also differentially affect mortality rates. Factors that directly affect mortality rates are temperature and temperature fluctuations (Treasurer 1983, Sandstrom *et al.* 1997), starvation (Radke & Eckmann 1999), and high fish densities, which may increase the incidence of disease, competition, and predation, including cannibalism (Cushing 1974, Myers 1995). Predation rates may also vary depending on the fish species' behaviour and its trophic status, both of which could change depending on the habitat types available and the fish community composition of the system (Tonn & Pasckowski 1987, MacRae & Jackson 2001)

Similar outcomes in population dynamics can result if physical habitat differences create areas that are more suitable for growth, reproduction, or survival. This may result if fish select to maximise on these vital rates (optimal habitat selection), if fish have habitat preferences that affect densities (ideal free distribution in preferred habitat), or are relegated to areas by biotic interactions (small usable habitat) that in turn affect vital rates (See also Hayes 1999). Therefore, habitat selection by fish can be based solely on preferences or bioenergetic needs or both. Establishing these links quantitatively to vital rates is difficult but it is often assumed that by distributing themselves along preferential gradients or patches of preferred habitat; fish are changing their fitness levels (i.e. that habitat selection somehow affects reproductive output or growth potential). Growth potential has been investigated more than reproduction effects (Wilderhaber & Crowder 1990, Brandt & Kirsch 1993, Mason *et al.* 1995).

Alternately, fish may merely experience conditions in a particular area that are imposed, without selection, that alter reproduction and growth such that subsequent recruitment to the next year class is altered. For example, recruitment only varies if optimal thermal volumes throughout a system vary from year to year or if there is a mismatch between optima in two separate variables. In experiments conducted by Wildhaber & Crowder (1990) on juvenile bluegill, thermal preference overrode foraging, except when food was very low. This provides evidence for hierarchical habitat selection that can be used when

combining suitability assignments to habitat types.

If this spatial and temporal habitat space is not considered, as in static or aggregate approaches, then the variance around the mean condition, (i.e. mean size and mean reproductive output) is underestimated because of averaging or homogenization across relevant scales (see Chapter 2; Rose 2001). If indeed environmental conditions affect the growth and mortality of organisms, either directly or indirectly, then fisheries management models that are strictly based on intrinsic population factors, and which dismiss spatial and temporal variability in environmental factors as noise, may contribute to erroneous predictions in stock dynamics. For example, stock-recruitment relationships define the maximum reproductive output of a stock but could be limited by environmental factors that reduce predictability. Also, the search for an overarching regulator or a single controlling factor (i.e. rate limiting step, general law) may lead to an aggregate approach that ignores the spatial and temporal variability in the environment.

Physical habitat information at scales relevant to fish interactions has been difficult to obtain, and hypotheses about environmental regulation of vital rates difficult to test using traditional means. Remote sensing, geographic information systems, and computer simulation modelling are tools that can be used to address these issues of scale, habitat heterogeneity and hypothesis-testing in a virtual environment over time periods that are impossible to replicate in laboratory or field experiments. Their usefulness in this study and for habitat-based modelling is discussed in the following sections.

4.0.2 Computer Simulation Modelling

Models are useful tools for testing hypotheses about complex systems that may not be tested experimentally or empirically through trend analysis because of spatial or temporal constraints. Models may reveal complex interactions in system properties, and weaknesses or gaps in our knowledge and understanding, which can be used adaptively to revise research priorities. Model predictions can be compared with field observations for validation of the rules and assumptions that are inherent in all modelling exercises, as in most scientific studies.

Jorgensen (1988) outlined the main steps in model building (Figure 4.01). Initial steps involve defining the problem to be modelled, determining the model complexity and data requirements, and then building the equations that link different components of the system. Components of models include forcing functions and state variables. Forcing functions, or external variables, affect the simulated system in some way; while control functions are a subset of forcing functions that are manageable (i.e. regulated water levels or nutrient inputs, but not climate).

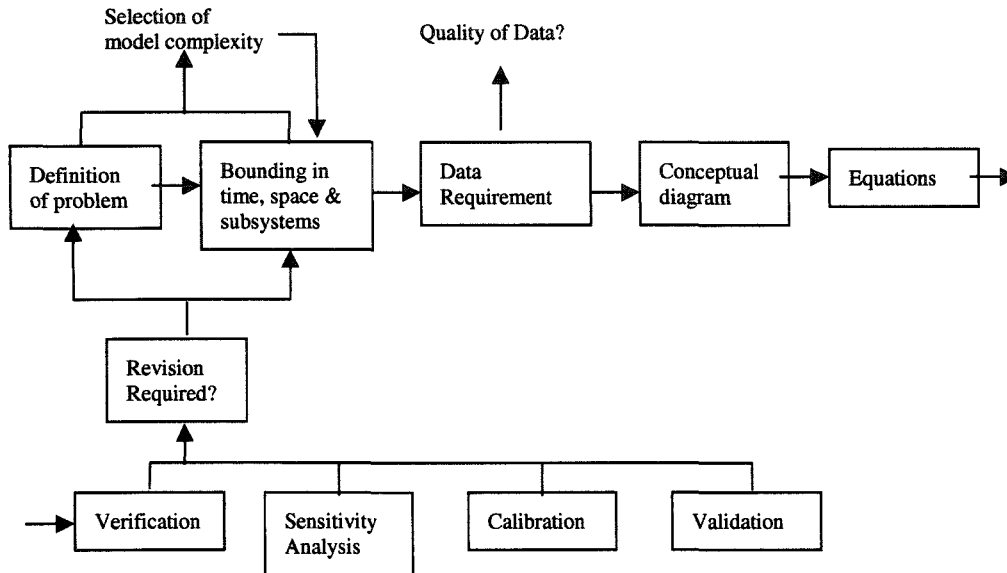


Figure 4.01: Flowchart of model building steps defined by Jorgensen (1988; Fig 2.2).

State variables are affected by forcing functions; mathematical equations that link the state and external variables (i.e. fish growth is a state variable affected by temperature, an external variable). Coefficients, or parameters, are modifiers of external variables that are included in mathematical representations (equations) of biological, chemical, or physical processes. Usually, a conceptual diagram is used to develop the relationships between forcing functions, state variables and processes. The final stages of model development involve verification and validation. Verification is the test of the internal logic of a model, which is largely subjective, and validation is an objective test of how well the output fit independent field data.

Classes of ecological models include several contrasting types: stochastic vs. deterministic, compartment vs. matrix, reductionistic vs. holistic, static vs. dynamic, distributed vs. lumped, linear vs. nonlinear, causal vs. blackbox, and autonomous vs. nonautonomous (Jorgensen 1988). The model presented here is a deterministic, dynamic, distributed, somewhere between reductionistic and holistic, nonlinear, causal, and nonautonomous matrix model.

Biological models can be classified into biodemographic, bioenergetic, or biogeochemical categories (Jorgensen 1988). The model presented in this chapter combined biodemographic and bioenergetic components, and used weight and abundance as the measurements. Biodemographic models conserve species or genetic information (i.e. the number of individuals), and are organised using life cycle patterns; the number of individuals or species is used as measurement. Bioenergetic models balance the conservation of energy or mass, their organisation is based on energy flow patterns and use energy or weight measurements.

4.0.3 Model Review

The following section reviews the different types of models that are relevant to this study, focusing on models of species interactions with their habitat space. The review covers population, metapopulation, and individual-based models, from general habitat suitability models to spatially explicit approaches. A table of comparisons for all the different models can be found in Appendix 4.1; contrasted with PercaSpace.

Population models with environmental relationships

A classical population modelling approach creates a static picture of changes in growth and mortality over time with concomitant changes in habitat variables and their distributions. These models are not usually spatially explicit, and involve no movement. Therefore, assumptions are made about the distribution of animals in different habitats and their suitabilities because individuals are not capable of moving and finding suitable habitat. Recent population models have included some spatially explicit descriptions of habitat and movement. (For a complete review of population models, read Levins 1966, Hastings 1990 and Kareiva 1990.)

One of the first habitat-based, full population models was developed by Minns *et al.* (1996) for northern pike. Depth, substrate type, and macrophyte coverage were used to calculate weighted usable areas (WUAs) by habitat suitability indices for three different life stages of pike in an annual, lumped population model. Population dynamics and carrying capacity was determined for the system based on the area required by individuals in each life stage (spawning, larval, and juvenile plus adult space requirements) to carry out life processes. The model results indicated that the availability of good nursery and juvenile-adult habitat were more important to population success than spawning habitat (Minns *et al.* 1996, Minns *et al.* 1999).

A juvenile walleye model developed for western Lake Erie (Jones *et al.* 1998) concentrated on the early life history of walleye from egg deposition to larval transport mortality, first feeding and growth until the first winter. Potential egg deposition was determined based on adult stock estimates, and available spawning habitat (categorised into good / average / poor habitat) was calculated based on substrate size and river velocity. An egg carrying capacity by habitat suitability was calculated and this determined the number of retained eggs per habitat type. Random vs. nonrandom selection of egg deposition by habitat types was tested. Egg survival, development, and hatching depended on habitat type and changing temperatures. The survival of emergent larvae transported to nursery habitat down-river was a function of river discharge and the transport time to nursery areas was a function of river velocity. The final product was an aggregate model of population level responses to habitat variation, similar to PercaSpace.

A salmonid population model (SALMOD; Bartholow *et al.* 1993) tested the hypothesis that mortality is directly related to spatially and temporally variable micro- and macrohabitat limitations of stream flow.

They defined microhabitat as a combination of physical variables that are used in small (metre-scale) localised areas, and macrohabitat as the abiotic complex of river segment influencing the distribution of organisms. Habitat capacity was defined as the level above which emigration occurs. The model resolution was defined on different scales: biological (the distance a given size fish can move), temporal (one time step) and spatial (the computational unit). This model used a weekly time step for one or more biological years (starting with the first week of spawning) and all rate parameters (growth and mortality were weekly) as well as physical state variables (streamflow and water temperature). Spatial scale was variable and defined by classification of unique mesohabitat types. Life history categorisation was related to fish size, behaviour, and reproductive state. Fish were tracked by cohorts within computational units. Adults and spawners were classified into sex-specific cohorts. Cohorts were initiated with a groups of eggs deposited in a single time step in a single computational unit by one or more spawners. Each cohort was classified by life stage (eggs, alevins, fry, presmolts, and immature smolts) and by length classes within life stages. Classes for the egg life stage were graded by percent development from deposition to emergence; classes were upgraded when they graduated to the next life stage. Growth and mortality were life stage- and class-specific. Part, or all, of a cohort was allowed to move into different computational units and was combined with a similar class when movement did occur. Habitat capacity was determined by hydraulic and thermal properties of mesohabitats. The model tracked spatially distinct cohorts that originated as eggs and grew as a function of water temperature. The main difference with PercaSpace and these types of models that that the latter concentrate on density dependent determinations of suitability and not direct linkages with vital rates.

Metapopulation models

Metapopulation models depict a population as spatially separate subpopulations with their own internal dynamics where individuals move between groups, they limit the spatial distribution of populations and individuals, have directional movement, and there is often different resource distribution among habitats. They address questions of population dynamics, interactions between subpopulations, and differential distributions of resources across habitats. (See Gilpin and Hanski 1991 for a review.)

Metapopulation models mainly deal with the mixing rates of different subpopulations and the stability of the overall population. High mixing rates mean that the subpopulations become one population. Intermediate rates allow different subpopulation rates, but are not completely isolated, whereas populations with low rates do not allow recolonisation. Hassell (1987) suggested that subpopulation density-dependence that occurred at different times (i.e. not all populations experience chaotic events at one time) would be obscured by overall

metapopulation dynamics. Mountford (1988) found the opposite, however they modelled competition for food differently because in the latter model, individuals have hierarchical access to food as opposed to equal in the former. (Note that the latter model did not have differing resources between habitats.) The distinction between the models depends on whether there is intraspecific competition that is modelled explicitly (i.e. resource availability was decoupled from population size where few individuals always had adequate resources and therefore population behaviour is less chaotic and increased stability). In PercaSpace, a comparison between unlimited resources with thermal variability in habitat was contrasted with habitat-related resource availability, although there were no density dependent effects on availability in either scenario.

The source-sink model of Pulliam and Danielson (1991) had different resource availability and sink habitats did not support subpopulations, but were supplied with reproductive individuals through immigration. Therefore, the metapopulation is heavily dependent on the source population and its ability to produce excess offspring. Pulliam and Danielson (1991) showed that selection of high reproductive-fitness habitat, and the number of patches sampled, significantly affected mixing between habitats and the size and persistence of metapopulations. The fewer patches that were sampled, the greater chance of sink habitat selection, and the population would be more susceptible to localised habitat loss. Therefore, time invested in reproductive site selection is important. For this reason, three scenarios regarding reproductive site selection and localised versus ideal free distribution of reproductive effort were tested in the Long Point perch habitat model (PercaSpace).

Reaction-diffusion models

Reaction-diffusion models incorporate spatial heterogeneity by assigning different diffusion parameters and growth dynamics to the population as a single entity that grows and spreads throughout a habitat by diffusion. Areas that have greater resources have faster population growth rates, greater capacity to support a population, and a lower rate of emigration than other areas. These models may not have explicit spatial habitat information incorporated but may use lumped estimates of spatial heterogeneity. Lotka-Volterra type population dynamics may be used and describe individual movement across habitat with non-biased, random diffusion terms (Tyler & Rose 1994). Reaction-diffusion methods are based on the probabilistic concept of random walks or quasi-random walks. Aggregate methods lead to deterministic population diffusion models similar to molecular diffusion. Parallel methods include habitat fragmentation effects by focusing on stochastic patch extinction, colonisation rates, and the frequency of patch occupancy rather than explicitly modelling dispersal.

Reaction-diffusion modelling typically involves continuous time and space partial differential equations to describe population change which is difficult in fragmented habitats. Discrete space differential equation

systems are better but complicated math prevents analysis beyond simple patches. Metapopulation models (colonisation/extinction) also require idealised structure. New methods use cellular automata models, percolation models, and demographic models coupled to a map lattice, which are based on cells rather than on patches. This allows the examination of within patch and between patch population dynamics with a single discrete-time, discrete-space, and reaction-diffusion model.

Habitat size, shape, and its arrangement were tested on populations using a discrete reaction-diffusion model (Bever and Flather 1999). Diffusion was modelled passively on a cellular grid of territories forming a coupled map lattice. Dispersal mortality was proportional to the amount of non-habitat and fully occupied habitat surrounding a given cell using a distance decay function. The model was verified for expected results for a single patch of uniform habitat, and then tested on heterogeneous and fragmented model landscapes. However, many reaction-diffusion models fail to recognise the autonomous behaviour of species (i.e. self-regulation, decision-making, and movement preferences) and do not explicitly derive from a realistic modelling space, as the Long Point PercaSpace model does.

Even so, the temporal changes in the environment are ignored in many models. Site selection based on behavioural thermoregulation was described by Neill (1974) and based on orientation by thermal preference. Hyman *et al.* (1991) integrated movements and a spatially explicit environment that included habitat types and food across multiple spatial scales. Adding a temporally changing environment to a spatially explicit, individual based model (SE-IBM) adjusts environmental characteristics that vary between patches during each time step; an aim of PercaSpace.

Individual-based models

The main differences between individual-based models (IBMs) and metapopulation models are the explicit consideration of individual movements, characterisation of habitat, dynamics of subpopulations within habitats, and intraspecific, individual behaviour. Movement in the Long Point landscape matrix was not addressed for the early life history stages modelled in PercaSpace. Movement would add a level of complexity that may have obscured patterns between reproductive habitat-based rules and first year production outcomes. Active and passive movements of larvae would need to be explicitly modelled and was beyond the scope of this thesis; however, larval movement should be addressed in future versions. The cell sizes are large enough so that there is justification for retaining larvae within one cell because larvae have been observed in proximity to spawning grounds in the field (Perrone *et al.* 1983) and that larvae can modify their vertical position to avoid being distributed by currents (Boehlert & Mundy 1988).

Individual-based models (IBMs) have used partial differential equations, Monte Carlo simulations or matrix approaches to track individuals within a population over time (Tyler & Rose 1994). Most IBMs

cover limited stages of a life cycle (i.e. first year of life) and focus on growth and foraging sometimes treating habitat as homogeneous. The models have small timesteps where the environment usually remains constant over space but not time and demographic characteristics of a population are derived by aggregation.

A bluegill model by Breck (1993) selected one of two foraging scenarios: an optimal diet model or a prey availability model as prey diminished then growth rate slowed. Bluegill density, temperature, and ingestion rate effects on growth controlled the number and size of bluegill at the end of summer, and not diet selection, (i.e. abiotic factors may be the limiting factors).

Smallmouth bass model simulations (DeAngelis *et al.* 1991) showed a density-dependent response of individual growth and population number. Hatching time differences had a pronounced effect on juvenile survivorship at large population sizes (different life stages were modelled separately), but had no effect at small population sizes (Note: Seasonal, average water temperature and number of daylight hours were used in the model with some daily variation in temperature).

The Rose and Cowan model (1993) for striped bass showed that larger females contribute disproportionately to the pool of surviving juveniles, and survivors were quick-growing at first feeding. There was an interaction between temperature, size of females and the level of food availability, which was not affected by the density of white perch larvae competing for the same food source. They concluded that larger females would lay more and larger eggs because they are in a favourable habitat.

Bioenergetic-based habitat models

One of the first bioenergetics-based models was developed for yellow perch (Kitchell 1977). It established a quantitative, mechanistic link between food availability, temperature, and individual growth rather than using an empirical, site-specific growth relationship developed from field measurements of size and cohort analysis. In bioenergetics models, there is a hierarchy of energy allocation to different body processes. Energy is apportioned to catabolic processes (maintenance & activity), waste losses (faeces, urine, specific dynamic action), and finally somatic storage (body growth) and gonad development. The premise is that evolution should select for mechanisms that reduce or minimize costs and maximise growth and reproduction. For example, herbivores will respire less, waste more, and grow less than carnivores (Kitchell 1977).

Van Winkle *et al.* (1997) found that small differences in the thermal parameter values in bioenergetics equations resulted in marked differences in individual fish growth and survival responses for rainbow trout to temperature changes. The differences between simulated fish would be similar to genotypic differences among fish in the field and therefore has ramifications on the source of growth variation, either environmental or genetic. In PercaSpace, a bioenergetic approach to evaluating growth potential in different habitats over time was undertaken.

Parameters have been calibrated for perch at different life stages quite extensively (Post 1990, Hanson *et al.* 1997). Perch were treated as distinct cohorts or super-individuals within each of the habitat cells of the model. It was assumed that fish within a habitat unit were influenced by environment alone and not density.

Habitat models

Habitat-based models can range from empirical or stage-structured population models to IBM-based modelling approaches. The level of spatial detail also varies significantly between models, as well as individual movement, which is dependent on spatial detail. Models include a consideration of habitat suitability and availability (either an aggregate or spatially explicit approach) usually based on a limited set of environmental parameters that define physical habitat. Density-dependent functions often link to population parameters or individual fitness by using carrying capacity or weighted suitable area estimates (WUAs), either at an annual, or finer, time scale.

Shuter *et al.* (1998) developed a lake trout life history model where habitat was aggregated and the time-step was annual. Lake area and total dissolved solids (TDS) were related to life history characteristics. For example, large lakes were related to greater maximum fish size, older fish, and greater age at first maturity, with lower natural mortality rates, and lower sustainable yields. High TDS lakes had higher growth rates in early life stages, lower age at maturity, larger size at maturity and higher natural mortality rates. Fishing mortality rate at maximum equilibrium yield was lower for small and low TDS lakes and therefore was more sensitive to overexploitation. Habitat quality parameters such as the rate of early survival and fecundity declined as the population approached carrying capacity. A scaling parameter for habitat available to the population was used, similar to a WUA approach outlined in Minns *et al.* (1996).

A habitat-based model was developed for stream salmonids by Bartholow *et al.* (1993). Physical state variables included stream flow, water temperature and habitat type, which was not defined explicitly. The habitat capacity for each life stage (size class) was a fixed number (or biomass) per unit of weighted usable area (WUA) parameterised by empirical relations. The model distributed fish throughout the stream in proportion to the availability of spawning habitat. Spawning was delayed until temperature was adequate, and adults with *in vivo* eggs were subject to increased mortality if spawning was delayed. Excess spawners, (i.e. over the redd capacity) spawned in unsuitable habitat or did not spawn and lost eggs. Temperature was a direct source of mortality, independent of food supply, predation, and density. If habitat carrying capacity was exceeded then partial cohorts above capacity for their life stage were moved sequentially from one unit to the next. Residents had precedent over transients. The authors note that they considered this approach better than previous attempts at testing habitat-based hypotheses because it combined an aggregated, classical population model that

tracks super-individual growth and mortality at high spatial resolution. This was also the aim of the Long Point PercaSpace.

Spatially explicit models

Tyler & Rose (1994) reviewed population models with spatial heterogeneity or individual variability, individual movement in heterogeneous environments, and spatially explicit, individual-based models (SE-IBMs) of fish populations. IBMs with spatial detail break up a well-mixed compartment (homogeneous habitat) into smaller, discrete, but contiguous units. Models that describe the spatial heterogeneity of the habitat usually answer questions about the spatial distribution of a fish population rather than questions related to the numbers and characteristics of surviving individuals. By combining aspects of spatially explicit models, bioenergetics models and population modelling, the Long Point perch habitat model attempts to address the impact of spawning distributions, as well as the numbers and characteristics of first-year life stages that result.

Usually only selected spatial characteristics about an area are used in the models. Many of these models are constructed to address questions about an individual's knowledge of its surrounding habitat, like whether individuals have memory? How do individuals measure habitat quality? Does the presence of competitors affect habitat quality (i.e. is quality density-dependent)? Many theories about habitat selection and movement centre on fitness-related rules. Individuals leave patches to maximise fitness or leave when their current fitness is low. However, fitness can be measured in different 'currencies' that determine individual habitat use because individuals could be maximising survivorship, growth, or reproduction. The latter is often neglected and I would argue that the hierarchy of which rate is maximised is not necessarily fixed in space and time, as is the variability of spatial environment within which the fish function. The Long Point perch habitat model addresses these types of questions.

Individual behaviour in models is either based on pattern-matching rules, which in turn are based on observed distributions of fish, or process-based rules related to the response of individuals to environmental conditions. The approach taken depends on the availability of data on populations and their environment as well as the spatial resolution of the model. Pattern-matching is useful where individuals do not affect their own movements. If their spatial location is related to behaviour then relationships with the known environment are needed (i.e. there are mechanistic reasons why certain habitat is selected) and pattern-matching rules cannot explore the consequences of habitat changes for which data do not exist. Process-based rules can address population responses to unobserved conditions because the environment affects movement or behaviour. This approach is useful for modelling infrequent events, like hurricanes, floods, or drought, and large-scale changes, such as global warming, or anthropogenic disturbances, like dredging, infilling, and

pollution (Ludlow & Hardy 1996, Rose 2001)

Process-based movement should relate individual movement to fitness but has its pitfalls, (i.e. what currency to use for different life stages?). Not many quantitative relationships exist between environmental factors and their impact on fitness. Tyler and Rose (1994) caution that if using an individual-based approach then avoid the pitfall of developing rules for population fitness as opposed to individual movement decisions, and the movement set of rules that individuals use must satisfy conditions of an evolutionarily stable strategy (ESS). Because of potential trade-offs between different currencies this would be really difficult to determine *a priori* to model testing, so perhaps can be tackled systematically as in PercaSpace simulations, where movement-based rules are implied in spawning site selection.

There are several examples of spatial models that use mechanistic and pattern-based approaches. Bartsch *et al.* (1989) followed the spatial distribution of herring larvae, by using a combination of hydrodynamic and IBM modelling. Individual larvae were tracked from spawning. Their location and habitat characteristics were updated every 40 minutes! They used vertically-distinct, advection fields based on depth strata in hydrodynamic modelling. Jager *et al.* (1993) constructed the instream flow incremental methodology (IFIM), where an IBM was fused with a habitat model of patches or cells, which followed fish through the first year and updated habitat and individuals at a daily time step. They replaced the weighted usable area index (an index that is a measure of habitat suitability and availability in many habitat-based models) with a mechanistic description of individual movement. PercaSpace replaced WUA with mechanistic linkages between habitat and development, growth and survival rates.

The marginal value theorem (MVT) by Charnov (1976) espoused that a forager departs a patch when its instantaneous rate of food intake drops to the average intake rate for the entire habitat. The theory of ideal free distribution (IFD) uses energy intake as the fitness currency and has accurately predicted equilibrium distributions of fish among patches with different levels of resources in laboratory and natural habitats (Kennedy & Gray 1993). Net energy gain can be used as currency instead of intake and it should be noted that predators can change the energetic costs of patch selections. Avoiding predation in itself may be important to habitat selection, therefore individuals may act to minimise the ratio of mortality risk to growth rate (i.e. being dead is far worse than being hungry). Also, if growth is proportional to foraging rate then the ratio of foraging to mortality risk can be substituted for growth (Bernstein *et al.* 1999). It should be noted that selection changes throughout complex life history strategies, and with seasonal components to reproduction, therefore it is not adequate to just model growth, when survival to reproduction may be favoured. PercaSpace used different habitat suitabilities for different life stages based on their mechanistic relations to growth and mortality

separately. It addressed the seasonality of reproduction and spawning habitat selection, and its subsequent effect on larval growth and survival when site fidelity is maintained in a variable environment.

SE-IBMs may address the spatial location of individuals due to interspecific behaviours (i.e. due to aggression, territoriality and interference competition), individual differences in size, energy reserves, and reproductive status that may affect movement ability, (i.e. YOYs composed mainly of large initial size or fast-growing individuals), as well as habitat selection strategies and patterns. The size of a 'patch' or the scale used should depend on the movement abilities of fish being modelled and the timestep of the model (i.e. the time step for movement should match the coarsest spatial scale of the model). When movement is not explicitly addressed, as with PercaSpace, the time step should match the smallest life stage requirement (daily in this case because of spawning and egg development), the hypothesis being tested, as well as the spatial limitations imposed by data constraints (smaller time steps would not be feasible to model).

Habitat models cannot address all aspects of a habitat. Pearson *et al.* (1999) created a SE terrestrial model for a species with usable habitat preferences. The habitat changes were modelled using real data from LANDSAT and cadastre information, similar to PercaSpace. They concluded that landscape change and habitat availability were not directly linked because other factors that define habitat suitability were not addressed. Walters *et al.* (1992) concluded that the mismatch between model and real life fish distributions meant that an important element had been left out, i.e. food was not the only driving factor for describing fish distributions. Therefore validation of habitat rankings with field data is important before testing assumptions (Chapter 3), but there are many data gaps that warrant further study.

The survival of juvenile yellow perch (actually YOYs at 20 mm initial length) in Oneida Lake was modelled daily over a growing season in a spatially explicit environment with a foraging model subcomponent (Tyler & Rose 1997). The environment was 10x10 grid cells (or habitats of 10,000 m³) varying in food density and predator abundance but with a constant abiotic condition of 20 °C and 12h daylight. Simulations ended when fish had either died from predation or were 70 mm (a size at which they are substantially less susceptible to predation) or when the simulation reached 150 days (any fish at this point < 70 mm was considered dead because of overwinter survival rates). Rules were similar to those used in the Long Point perch habitat model. One main difference is that zooplankton were modelled as separate populations in each cell and not as characteristics of habitat. Each cell had two subhabitats (open water and refuge). YOYs could not feed in refuge habitats but were not predated. Consumption was a Poisson process where mean consumption rate was a product of zooplankton density and the volume searched.

Bioenergetic rates were determined by larval size and the time

spent feeding, and therefore predator encounters, were a function of actual consumption compared to maximum consumption. Individual fitness at the end of the day was compared to an estimate of environment-wide fitness (Tyler & Rose 1997). Four movement scenarios or departure rules (random, maximum growth, minimum mortality or minimum ratio of mortality to growth) were tested. Three predator distributions were also used: uncorrelated, correlated with zooplankton, and correlated with juveniles. And three hypotheses were postulated and tested, the relationship between cell departure rule and initial cohort abundance, which departure rule was an evolutionary stable strategy, and whether predictions differed between spatially explicit and homogeneous environments. A similar rule-based approach was taken with PercaSpace as well as experimental testing in a modelling environment. An exception was that habitat varied in space and time and was not theoretical, but simulated natural conditions based on data.

Other Yellow Perch Models

Other models have been constructed that are relevant to yellow perch studies. A probabilistic model was developed by Koonce *et al.* (1977) that had stock specific optimal spawning temperatures of 5 °C. The time of spawning was estimated from temperature records for specific lakes. The time required to complete the egg phase and egg survival were functions of incubation temperature. Similar equations were applied to the probability of surviving the swim-up phase, which only required one day, and to the probability of surviving the pelagic larval phase, which was based on weight per individual, a temperature-dependent fraction of maximum growth rate. Therefore, survival of the larval phase was dependent on the time required to complete the phase and a temperature-dependent mortality rate. PercaSpace used similar egg stage equations, however, differed in the representation of space and survival calculations for larval perch.

4.1 METHODS

The yellow perch model presented here used a realistic, temporally-varying and spatially explicit representation of an embayment in Lake Erie as the modelled habitat, instead of a theoretical (completely simulated) set of habitat patches of varying quality used in many models described. A matrix approach was used but cells were not linked objects therefore movement of individuals between cells within the matrix was not modelled, however vertical movement within a cell was allowed. Instead the relative importance of a temporally varying, spatially heterogeneous habitat and the possible connections between habitat and life stage processes were concentrated upon, especially the ramifications on first year production, without complicating or obscuring patterns by allowing movement. A daily time-step was chosen because of the concentration on early life history. This timestep was needed for first year production

estimates and the coarsest spatial scale of the habitat data collected matched this timestep (temperature data). An assumption, as with many spatially explicit models, was that the environment within a cell of the habitat grid or matrix was homogeneous.

The model focused on general process-based habitat associations that were sometimes linked to pattern-based rules but were not specific to the geographic area of study to avoid problems with circularity in the model. The model was similar to Tyler and Rose's modelling approach (1997) where experiments were conducted about different habitat-based rules, except that the habitat space was always heterogeneous (spatially explicit). The implications of having no habitat preferences were compared with having different habitat requirements in a realistic space; a subtle yet important divergence from Tyler and Rose's approach, which tested predictions within a heterogeneous and homogeneous environment.

Jorgensen's (1988) steps in model development were used to conceptualise the habitat-based matrix model presented here. The initial steps involved defining the problem, which included bounding in space, time and subsystems, as well as defining the model complexity as described previously. Then a listing of data requirements for the model was determined and quality checks were performed. A conceptual diagram of the model was constructed and the equations to link each step were compiled and coded. The final stages of model development deal with verification, calibration, validation, and sensitivity analysis. The necessary adjustments or revisions were made at each testing phase, but sensitivity analysis was not performed. Scenario-testing, or experiments, were conducted to test hypotheses about population responses (output changes) due to habitat-driven forcing functions.

4.1.1 Bounding in time, space and subsystems

Long Point Bay of Lake Erie has been studied extensively. Spatial habitat information, as well as fisheries data, were used in equation development and model testing (see Chapter 1). The extent of the study area was defined as the deep water area just east of the tip of Long Point to the shallow, Inner Bay, not including the main basins of Lake Erie proper (see Figure 1.1). The model focused on the daily temporal changes (where applicable) through 1999 of five habitat features: bathymetry, substrate type, vegetation coverage, wind exposure and temperature. Habitat data was compiled for the 1990s. The final model focused on the spawning, egg, larval and juvenile stages (the first year of life) of yellow perch and used the same spatiotemporal scale and resolution for each life stage to minimise model complexity and computational problems with changing spatial scales.

4.1.2 Definition of model complexity

A spatially explicit, matrix approach was adopted because habitat varies through space and time. The intent was to move away from

aggregate methods and address the actual environmental variability that egg and young fish would encounter on a daily basis. The spatial resolution of the modelling grid was defined using the coarsest resolution of habitat information available; the temperature data. The use of a base grid (from SST imagery) automatically made the model a matrix-type of approach. A larger cell size (SST grid cell size = 1.4 km) made it easier to handle computations until the model dynamics were fine-tuned. (A grid-based approach also made it easier to deal with spatial scale standardisation and will make it easier to deal with neighbourhoods and movement in future development.)

The resolution of the AVHRR satellite imagery was used to standardise the habitat layers to the same geographic extent, and to establish a grid-based approach to habitat characterisation for modelling efforts. The geographic extent was originally defined by the CASI survey of the Long Point area and the early thermal work in Chapter 1. The CASI survey was used to delimit the shoreline in the grid-based approach.

The yellow perch population was subdivided into life stages with different habitat requirements. The model was not a full population model but concentrated on the early life history stages of spawning adults, eggs, and planktonic larvae and juveniles. Habitat suitability indices were used for environmental characteristics that have been connected to preferences or to vital rates (either growth or survival) of the life stages but for which a quantitative causal link had not been established (See Chapters 2, 3). A relative comparison of spatial and temporal dynamics in the first year was conducted to tease apart the effect of habitat and its possible constraints on population dynamics (e.g. spawning site selection and timing).

A spatially explicit, bioenergetics and ESS approach to habitat selection and effects was used. An iterative process was adopted to sequentially compare the population dynamics at different life stages when there are no habitat preferences to when there is a complete interaction between habitat and vital rates at different stages. This is different from testing whether habitat is homogeneous because we already know that the environment is variable. The fish's perception of habitat and its relative effects after spawning site selection were tested instead. Biotic interactions were implied through habitat suitability weightings on vital rates based on qualitative evidence or linked directly through empirical relationships, as in the case of temperature and growth and mortality rates.

4.1.3 Data requirements

The model design incorporated species interactions with their habitat space. Therefore detailed data on the habitat of Long Point Bay was required for habitat characterisation as well as data on vital rate relationships between temperature and other physical habitat. Physical variables were used that have been linked to yellow perch reproduction, including egg development, larval growth or mortality. The input included bathymetry, thermal regime, substrate type, vegetation and wind

exposure. (See Chapter 1 for a full explanation of data sources and habitat matrix development.) Information on perch size at hatch and zooplankton distribution by habitat type was also required to parameterize the model.

4.1.4 Conceptual diagrams

A conceptual diagram of how habitat was related to different stages in the first year of life for yellow perch is outlined in Figure 4.02. Three separate life stages were considered: spawning, egg stage (which included hatching and swim-up substages with separate mortality components), and the planktonic larvae stage. How this schema was applied to the habitat matrix and incorporated into the modelling logic is shown in Section 4.1.8.

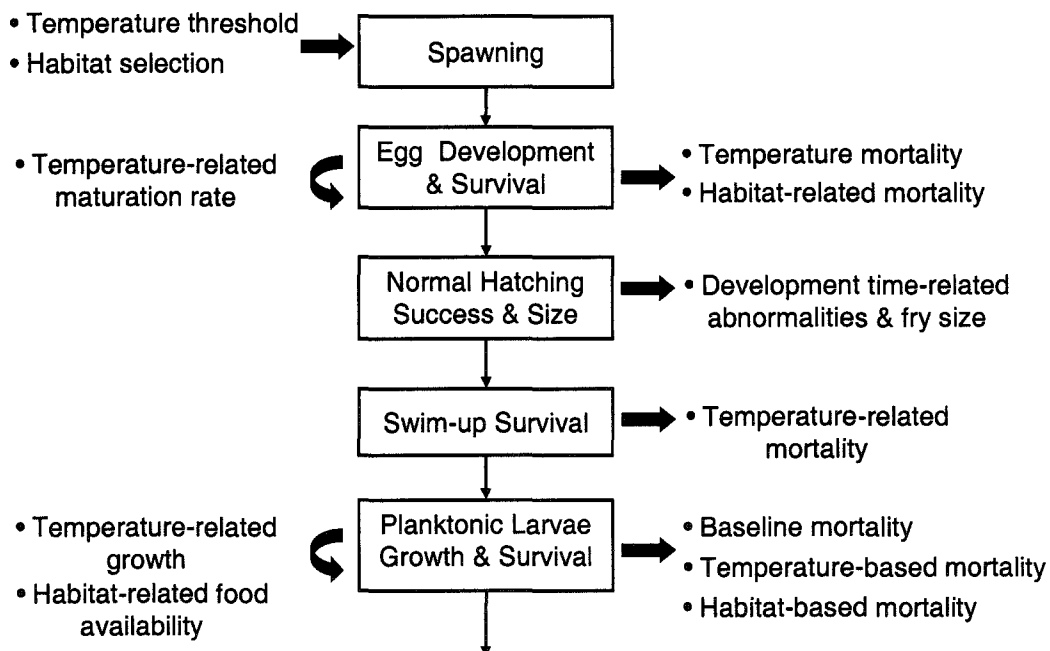


Figure 4.02: Conceptual diagram of how habitat relates to the first-year life stages of yellow perch. Arrows on the left signify reproduction and growth rates, whereas arrows on the right signify mortality rates.

4.1.5 Equations

A detailed description of the equations used in the model follows but this section concentrates on the logic used in constructing or modifying the equations. The study relatively compared perch distributions and the timing of different early life stage events. Comparisons were based on changing the levels of interaction between vital rates and the physical environment. If equations were not already available that linked habitat variables directly to population rate processes then suitability curves for the variable and spawning, egg development and survival, or larval growth and mortality were developed. Habitat relationships for all life stages was collected in Chapter 2, but concentrated on early life stages for this

analysis. Information on spawning, embryonic development, larval fish, and young-of-the-year (YOY) were collected that included habitat preferences, distribution patterns, and direct links between environmental variables and vital rates.

Temperature and habitat-based resources defined growth potential and mortality. Physical habitat relationships with zooplankton availability were gathered as well as relative predation rates. HSIs for growth and mortality were calculated separately because different aspects of habitat affect food availability and predation pressure. Habitat suitability index (HSI) relationships for different combinations of exposure, bathymetry, substrate type, macrophyte associations and temperature (only if the effect was separate from direct bioenergetic effects), were developed where relative differences could not be quantified. This use of HSIs differed from earlier work (Chapters 2 & 3) and concentrated on growth (food) and mortality (predation) differences within the environment rather than just preferences for particular habitats. [Note: For a short period of time during pre-feeding growth, yolk-sac fry were allowed to grow and die until swim-up due to temperature changes only]. Maximum consumption and average mortality rates were used in scenarios where habitat (other than temperature) was not a regulatory factor. There were no density-dependent effects imposed on the yellow perch egg and larval vital rates.

The behaviour or location of different life stages was modelled explicitly by only using the habitat information where those stages would occur (i.e. only bottom temperatures were used for egg development). The passive and active movement of larval fish is acknowledged but no movement between cells was modelled during the swim-up and larval phases to simplify basic rule-based comparisons (model experiments) and to avoid obscuring patterns in space and time. However, it should be noted that vertical movement within a cell was allowed. Larvae selected a depth stratum within the water column after they hatched and reached the swim-up stage. Depths were chosen based on minimising mortality due to temperature and then larvae either fed on food available at that depth or they fed at maximum consumption rates depending on the scenario. The hierarchy of habitat selection was based on the results of thermal regulation and optimal foraging experiments conducted by Wildhaber and Crowder (1990).

Depending on the scenario, either uniform or habitat-based differences in food availability were used. In the former scenario, food availability varied in different habitats, mainly including vegetation categories, which modified larval growth rates along with the temperature experienced that day. Yellow perch bioenergetic equations were modified to define this growth potential in different habitats. The HSIs for larval growth modified the scalar in the growth equation for maximum consumption rates in bioenergetics equations (Boisclair 2001). Weight was used instead of energy equivalents in the bioenergetics equations because no specific prey items were modelled, a generalised density of

zooplankton food source was used instead. Food availability was calibrated to Long Point Bay zooplankton densities.

The sources of mortality at this age were a combination of natural (temperature-related plus a base natural mortality due to other factors, such as disease), and predation, up to a maximum of 30% per day observed in some embayments (Mason & Brandt 1996). Larvae died based on a relative predation pressure associated with habitat type.

4.1.6 Yellow Perch Model Description

A daily time step was used for the model. The model was programmed in Microsoft Visual Basic® using a Microsoft Access® database to provide input variable data to the model and to store output. The following sections outline the equations and logic employed in different subcomponents of the model

Spawning and Habitat

Spawning is potentially cued by the time of year (day length after winter) or temperature, or both because they are related. Some references cite that spawning peaks at 6-12 °C (Thorpe 1977) while others restrict it to between 7-11 °C (Craig 1987). Because perch put all reproductive effort in one spawning site it is likely that some effort would be made in scouting spawning locations and the timing of egg release would be critical. Therefore, spawning site selection may be chosen based on temperature stability over time and the physical characteristics of a site. In the model, three options, or spawning scenarios, were used to test this assumption: no habitat or thermal effects (S1; the null case), habitat selectivity (S2 or S2*) based on HSIs for spawning but does not include temperature (see also Chapter 2), and habitat selectivity with a degree day threshold as a spawning cue (S3 or S3*) based on relative suitabilities.

In the final scenario, the initiation of spawning was cued by 5 consecutive days between 6 and 12 °C, inclusively. This temperature range encompasses slightly suboptimal temperatures for egg development. Bottom temperatures were used for cumulative degree day calculations for spawning initiation. In this case, a binary variable modified the overall HSI value for the cell. HSIs for spawning were calculated in the following manner. For variables other than temperature, categorical or continuous variables were converted to relative suitabilities based on spawning preferences for that category (a constant) or by using an equation. Then variable-specific HSIs were combined into an overall HSI for spawning using geometric means.

There were two types of egg allocation used in the spawning scenarios. An equal distribution of 1000 eggs per cell (S1) was used, which under habitat-based scenarios was modified by daily, site-specific characteristics (S2 or S3). Alternatively, an ideal free distribution of a maximum of 400,000 eggs throughout the entire matrix was employed (S2* or S3*). In habitat-based scenarios, the overall spawning HSI

modified the number of eggs laid in the cell under each type of egg allocation.

Substrate & Vegetation Spawning HSI ($HSI_{Spn,Sub}$ & $HSI_{Spn,Veg}$)

The relative weightings of vegetation suitabilities were based on an extensive literature survey that suggested low to moderate submergent vegetation densities were preferred by perch as spawning substrate (Thorpe 1977, Collette 1977, Goodyear 1982, Krieger 1983, Craig 1987, Lane *et al.* 1996). Unvegetated areas were used by perch; however, these areas usually had some structure (i.e. boulders or woody debris). Therefore the spawning HSIs for substrate type were assigned by a relative weighting for rugosity; from boulders to clay, with smooth surfaces like bedrock ranked higher than fine sediments because of the potential for egg smothering in the latter (Fisher *et al.* 1996, Robillard & Marsden 2001). Substrate type was only considered in areas where there was no or little vegetation. (i.e. If $HSI_{Spn,Veg} \leq 0.5$ then $HSI_{Spn,Sub}$ was calculated, otherwise $HSI_{Spn,Sub} = HSI_{Spn,Veg}$). Table 4.1 shows the HSI values assigned to each category, which differed slightly from Chapter 2.

Depth Spawning HSI ($HSI_{Spn,Z}$)

Perch generally choose nearshore areas for spawning (less than 10m); however, spawning has been documented at 35 m depths (Thorpe 1977, Goodyear 1982, Lane *et al.* 1996). Therefore any depth < 10 m was considered highly suitable ($HSI_{Spn,Z} = 1$). A linear function of HSIs between 10 m and 35 m was used, which ranged from an HSI of 1 at 10 m to an HSI of 0 at 35 m and below (considered unsuitable for spawning). Table 4.1 shows the equations used to assign HSI values to each grid cell based on area-weighted maximum depths.

Exposure Spawning HSI ($HSI_{Spn,Exp}$)

The calculation of wind-weighted effective fetch values, or exposures, is explained in Chapter 1. Perch spawning distributions have been correlated with sheltered areas; however, no quantitative links have been established. The assumption was that perch in Long Point would be acclimated to the average exposure conditions but not to extreme events, (i.e. stagnant or highly turbulent waters would not be selected for spawning). The distribution of exposures for the entire year of 1999 peaked at $400 \text{ km}^2 \cdot \text{hr}^{-1}$ above which it was assumed that egg strands would be at higher risk of stranding or it would be more difficult to spawn and fertilise eggs (Figure 4.03). The distribution was highly skewed to the right (Weibull-like distribution) and was described as two separate curves, a cubic function above the mode and a constant or linear function was chosen to represent the distribution below the mode. HSI values for exposure were rescaled by 1000 (the frequency of the mode) to obtain HSI values between 0 and 1. Table 4.1 outlines the equations used to assign HSI values based on exposures. A logic statement was used to bound the $HSI_{Spn,Exp}$ values between 0 and 1, because of intermediate levels between 200 and $400 \text{ km}^2 \cdot \text{hr}^{-1}$ was capped at 100% suitability.

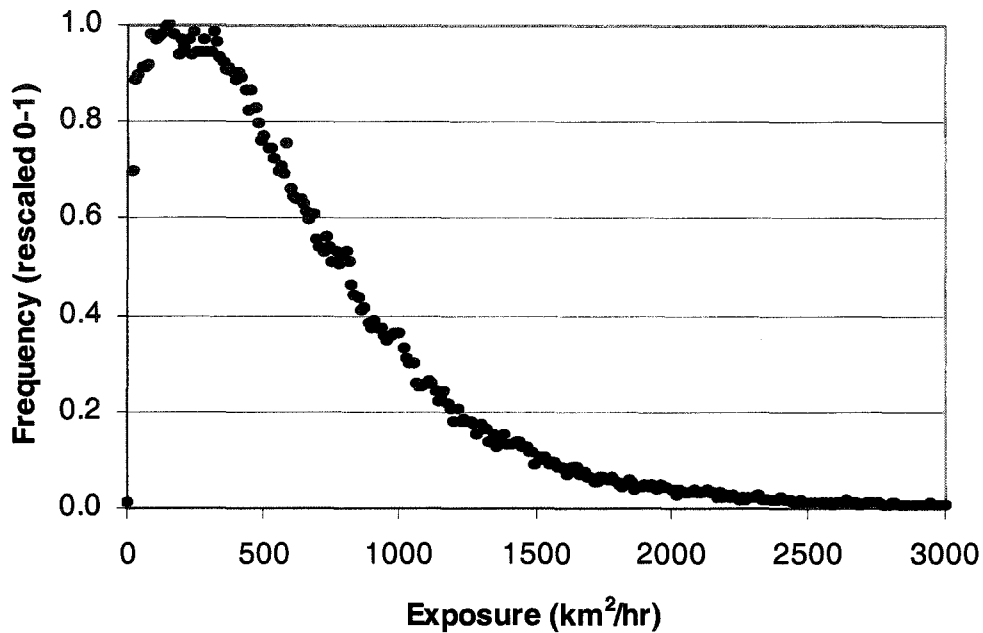


Figure 4.03: The frequency distribution of exposure values for all cells in the habitat matrix during 1999. Frequency counts have been rescaled between 0 and 1 so that exposure HSI equations could be developed (Frequency at the mode was 1000).

Overall Spawning HSI

The HSIs for categorical habitat variables, such as vegetation and substrate, were calculated by weighting with the proportional areas of each subcategory within a cell and then summing to determine the HSI for that variable. All the HSIs were combined into an overall HSI for spawning by using a geometric mean, which gave an overall HSI of 0 if any of the habitat variables had an $HSI_{Spn,X} = 0$, where $X = \{Z, Veg, Sub, Exp\}$. This may be a more realistic approach to habitat suitability assessment from a fish's perspective than arithmetic averaging of HSI values (Chapter 2), because if an area is not suitable for any one particular reason then the fish would most likely not utilise it, regardless of its other characteristics.

Egg Survival and Development

This model component determined the relative survival and time to hatch for eggs in different cells of the matrix once deposited. Data from Thorpe (1977) for time to hatch at different temperatures was reworked into an equation for daily egg development (Figure 4.04; Equation 4.01). The proportion of development undergone in one day was calculated by the inverse of days to hatch, $1/t(\text{hatch})$. The maximum number of days that eggs could develop was set as 30 days, after which time normal hatching success was virtually nil in laboratory experiments (Hokanson 1974).

Table 4.1: Physical habitat variables and subcategories that were assigned different habitat suitabilities based on spawning preferences that have been documented for yellow perch.

Variable	Condition	HSI
Bathymetry	≤ 10 m	1.0
	>10 and < 35 m	$-0.04 * (Z_{MAX}) + 1.4$
	≥ 35 m	0
Vegetation	Emergent Vegetation	0.25
	71-100% Submergent Cover	0.75
	31 -70% Submergent Cover	1.0
	≤ 30% Submergent Cover	1.0
	No Vegetation	0.5
Substrate	Boulder	0.8
	Cobble	0.7
	Rubble	0.6
	Gravel	0.5
	Bedrock	0.4
	Hardpan Clay	0.3
	Sand	0.2
	Silt	0.1
	Clay	0.0
Exposure	< 400 km ² ·hr ⁻¹ where Z _{MAX} ≤ 5m	$3.1915 * E / 1000, HSI \neq >1$
	≥ 400 km ² ·hr ⁻¹ where Z _{MAX} ≤ 5m	$(-10^{-7} * E^3 + 9 * 10^{-4} * E^2 - 2.0935 * E + 1721.7) / 1000, HSI \neq < 0 \text{ or } >1$

Equation 4.01: $t(\text{hatch, days}) = 2467.7(T)^{-2.0606}$ (N = 14, $r^2=0.9479$), where T = temperature, °C

The calculation of daily egg development rates and mortality rates for each cell was based on temperature alone under the default scenario. (Note: A causal link between other habitat variables and egg development could not be established.) Daily egg mortality rates over different temperature ranges are listed in Table 4.2. These equations were reworked into daily rates from data in Hokanson (1974) and Koonce *et al.* (1977), and bounded between 0 and 1 where necessary.

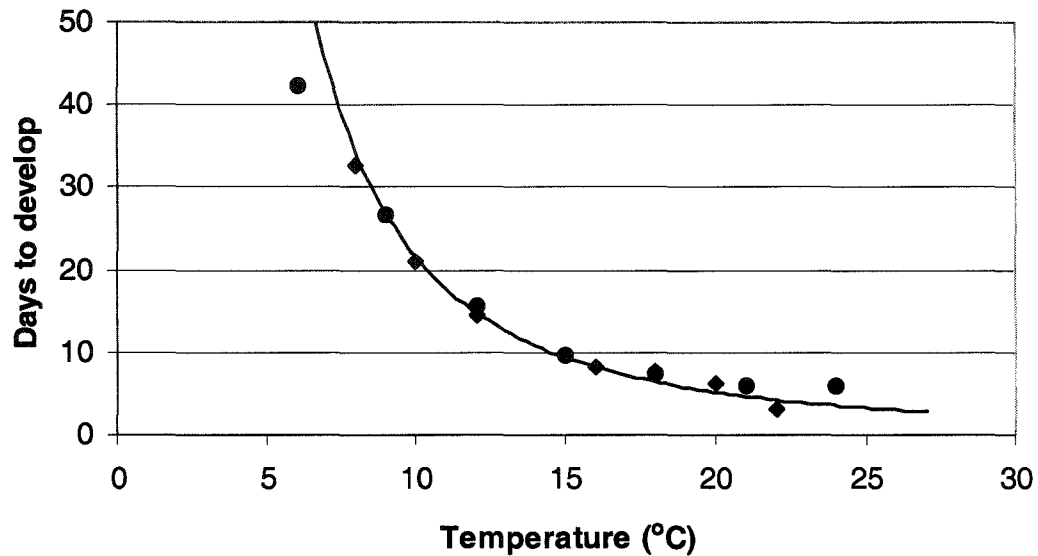


Figure 4.04: The relationship between temperature and the time to develop in days for yellow perch eggs (Data from Hokanson 1974, Koonce *et al.* 1977)

Habitat effects on egg mortality were incorporated into modelling scenarios. Egg strands are fairly durable and are not usually predated upon because of a gelatinous sheath that covers the eggs (Thorpe 1977). However, windrows of eggs have been documented under high wave conditions (Clady & Hutchinson 1974) that lead to death due to physical disturbance or desiccation. Therefore, the upper and lower five percent of the exposure distribution for Long Point was used as an arbitrary cut-off point for extreme weather events: either a potential high risk of stranding or lack of oxygenation due to stagnant waters. If the $HSI_{Spn,Exp}$ was within that extreme range (≤ 0.05) then Equation 4.02 was used to modify daily egg mortality in addition to mortality due to temperature effects by a minimum of 50%.

Table 4.2: Daily mortality rates of yellow perch eggs in different temperature ranges. (Based on data in Hokanson 1974 and Koonce *et al.* 1997.)

Temperature range	Daily mortality equation	r^2
0-18	$M_{Egg} = 0.002T^2 - 0.0345T + 0.1403$	0.972
>18-23	$M_{Egg} = 0.14T - 2.32$	0.973
>23	$M_{Egg} = 1.0$	

Equation 4.02: $M_{Egg} = 1 - 10^* HSI_{Spn,Exp}$

It was assumed that eggs deposited below 5 m would not be susceptible to wave action. (Note: Therefore only cells with 5 m or less maximum depth were included in these exposure HSI calculations.) Also, the presence of moderately dense or higher vegetation negated the stranding risks due to exposure because egg strands would not be as vulnerable (i.e. rule was only applied when vegetation cover $\leq 30\%$).

Swim-up Phase

Upon hatching, the percentage of eggs that were normal was calculated based on data from Thorpe (1977). This accounted for abnormal fry that died within 24 hours after hatching. The length of the fry at hatch was also calculated. Both functions were dependent on temperatures experienced during development and immediately after hatching (Figure 4.05 and 4.06). The percentage of hatched eggs that were normal was defined by Equation 4.03, and developed from data in Thorpe (1977). Hatch length was related to temperature by Equation 4.04.

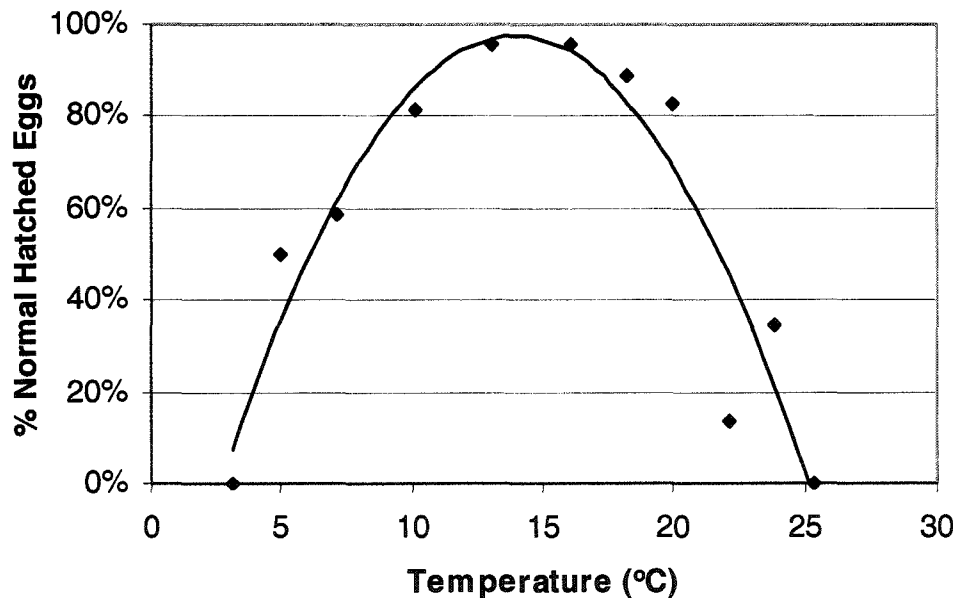


Figure 4.05: The relationship between temperature during development and the percentage of hatched eggs that are normal for yellow perch. (Data from Thorpe 1977).

Equation 4.03: $\%NormHatch = -0.0077 * T^2 + 0.2138 * T - 0.5127$ ($r^2 = 0.877$)

Where %NormHatch = the percentage of eggs that are hatched normally and T = average temperature experienced during development.

Equation 4.04: $L \text{ (mm)} = -0.015 * T^2 + 0.3951 * T + 3.7278$ ($r^2=0.879$).

Where L = length in mm and T = average temperature experienced during development.

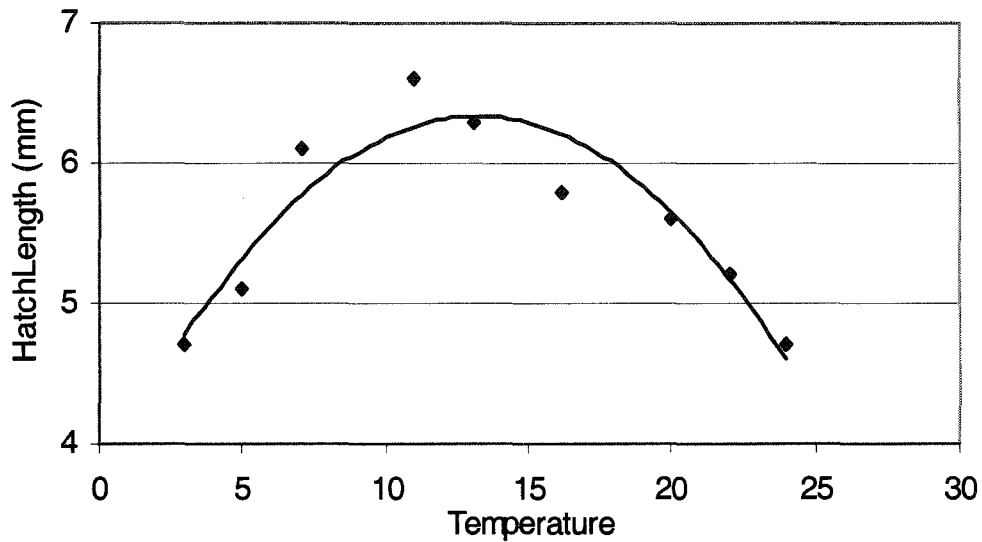


Figure 4.06: The relationship between temperature experienced during egg development and the hatch length of yellow perch yolk-sac fry. (Data from Hokanson & Kleiner 1974.)

The equation for determining size at hatch was based on temperature relationships derived from Hokanson & Kleiner (1974), who used average temperature experienced by larvae during development. For both these equations bottom temperatures were used, including calculations for the growth and mortality of larvae after hatch until the swim-up stage. Swim-up occurs, on average, one day after hatching at temperatures $> 13^{\circ}\text{C}$ and 2 days at lower temperatures. Therefore hatched fry were kept at the bottom until 1 or 2 days had elapsed depending on the bottom temperature at hatch. Percent survival was calculated at the end of this period based on temperature and survival data from normal hatch to swim-up using Equation 4.05 (Figure 4.07), derived from data in Thorpe (1977).

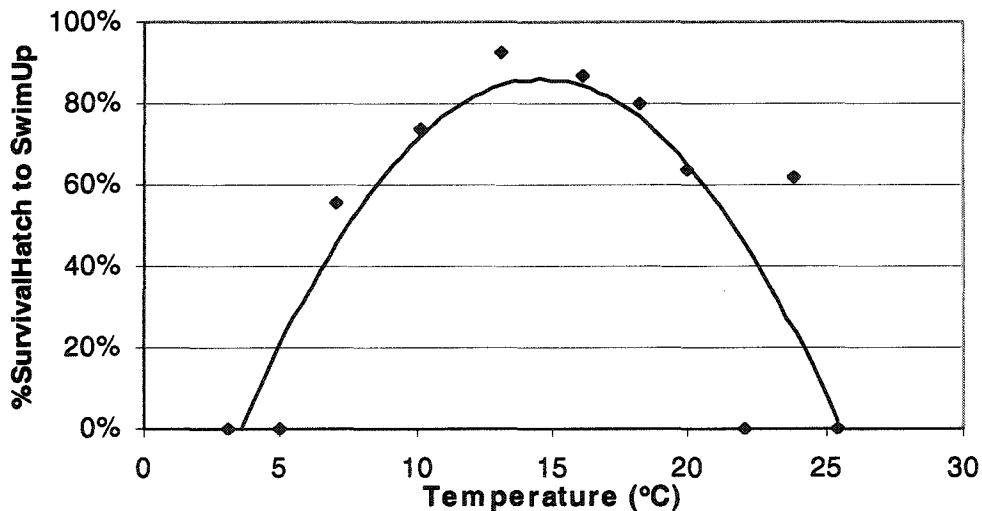


Figure 4.07: The relationship between temperature and the percent survival of yellow perch yolk-sac fry to the swim-up stage after hatch (Data from Thorpe 1977).

Equation 4.05: $\%SurvSwimup = -0.0071 * T^2 + 0.2077 * T - 0.6529$ ($r^2=0.7254$) where $\%SurvSwimup$ = percentage of larvae surviving from hatch to swim-up stage and T = average temperature during pre-swim-up phase.

YOY Stage Growth (Pelagic Phase)

The literature states that exogenous feeding occurs at 3-5 days post-hatch (Craig 1987). In the model, larvae fed the day after they reached swim-up stage (Day 2 or 3). Fry were assumed to be positively phototactic and to thermoregulate immediately. Initial fish lengths predicted from the size at hatch equation were converted to weights for use in bioenergetics equations. The length to weight relationship was based on data from several sources (Equation 4.06; Post *et al.* 1997, McGregor & Witzel 1987, Romare 2000),

Equation 4.06: $W = 10^{-5.263} * L^{3.188}$, W = weight (g) and L = length (mm).

Growth of larvae at the most suitable thermal depths was determined by the standard bioenergetics equations used for yellow perch with slight modifications to incorporate habitat effects (Wisconsin bioenergetics model - Kitchell 1977, Hanson *et al.* 1997). Larvae were not allowed to move between cells but remained in the cell where the eggs were deposited; however, the depth stratum they occupied was varied. To determine larval position in the water column, temperature profiles for each cell were used and the optimal temperature, and therefore depth, for larval survival (i.e. to minimise mortality) was determined. The assumption was that fry move to thermally suitable habitat first and then eat what is available (Wildhaber & Crowder 1990). The most suitable depth was based on a larval thermal-survival HSI equation rescaled from actual mortality rates in laboratory experiments (Equation 4.07, Hokanson 1977; also see Chapter 2).

Equation 4.07: $HSI_{Temp,Larv} = -0.0001 * T^3 - 0.0003 * T^2 + 0.1201 * T - 0.4107$

Depending on the scenario conducted, either maximum feeding rates were used in the consumption equation or maximum rates were modified by the relative food availability (based on the habitat characteristics associated with that cell and water depth). The temperature at that depth was used directly in bioenergetics equations. Other habitat characteristics, such as depth, were related to food separately from temperature effects by using an HSI for growth that reflects the relative ability to obtain food and the relative availability of food in that particular environment. Bioenergetics equations were used and modified in the following manner. The general form of the consumption equation (4.08):

Equation 4.08: $C = (R+A+S) + (F+U) + (\Delta B + G)$

[where R = respiration, A = active metabolism, S = specific dynamic action, F = egestion, U = excretion, ΔB = somatic growth, G = gonad production]

Solving for larval production (ΔB , when $G=0$), the remainder of the variables were calculated using modifications of Kitchell's yellow perch bioenergetics model (1977). However, the consumption equation calibrated for warm-water species was used that is based on temperature-dependence (Equation 4.09; Post 1990).

Equation 4.09: $C = C_{\max} * p * f(T)$,

[where p , or the proportion of maximum consumption, was modified by the HSI for growth and $f(T)$ changed daily based on the temperature at the depth location of the larvae.]

The maximum consumption (C_{\max} ; Equation 4.10) and temperature-modifier equations ($f(T)$; Equation 4.11) were calculated daily based on the weight of individual larvae in each cell and the preferred temperatures available.

Equation 4.10: $C_{\max} = CA * W^{CB}$ and

Equation 4.11: $f(T) = V^X * e^{(X-(1-V))}$, where $V = (CTM-T) / (CTM-CTO)$ and $X = (Z^2 * (1 + 40 / Y)^{0.5})^2 / 400$, where $Z = \ln(CQ) * (CTM-CTO)$, and $Y = \ln(CQ) * (CTM - CTO + 2)$

The definition of variables and parameter estimates and units for the equations above are listed in Appendices 4.2 and 4.3. The HSIs calculated for larval growth modified maximum food availability (P), which was calculated using the following equation (4.12) developed by Post *et al.* (1997).

Equation 4.12: $P = 0.679 * Zoop / 1000^{0.278}$ where $Zoop = zooplankton\ density\ mg \cdot L^{-1}$.

A time-series curve (parabolic equation) for zooplankton density was developed based on time-series, macrozooplankton data from Lake Erie Biomonitoring (LEB) sites. (See Figure 1.1 for LEB site locations.)

Table 4.3: Average macrozooplankton concentrations for 1993/1994 LEB sites. Whole season zooplankton averages for Outer Bay LEB sites (May-Oct.) Macrozooplankton estimates, $\mu g \cdot L^{-1}$ (no zebra mussel veligers; Dahl *et al.* 1995, Graham *et al.* 1996).

Year	Site	1993	1994	1998
Cladocerans	E1	3175	968	--
Total(#·m ⁻³)	E1	17919	9790	--
Cladocerans	E1	1.89	0.96	1.37
Total ($\mu g \cdot L^{-1}$)	E1	20.18	12.33	13.83
Cladocerans	E2	5130	2778	--
Total(#·m ⁻³)	E2	12448	10603	--
Cladocerans	E2	4.94	6.76	5.27
Total ($\mu g \cdot L^{-1}$)	E2	20.38	18.54	18.13
Cladocerans	E3	1541	1553	--
Total(#·m ⁻³)	E3	16352	8307	--
Cladocerans	E3	1.03	1.37	2.15
Total ($\mu g \cdot L^{-1}$)	E3	19.53	9.07	24.88

NB: 1994 – peak in fall cladocerans with lower summer values

Annual averages for the outer bay sites in different years are shown in Table 4.3 to illustrate year to year variability. In the ice-free season, total zooplankton samples for sites E1 (a 6m nearshore site in the outer bay), E2 (an offshore site in the outer bay) and E3 (a 9m nearshore site in the outer bay) had a mean biomass of 15.44 ± 4.17 , 19.01 ± 1.20 , 17.86 ± 7.99 ($\text{mg}\cdot\text{m}^{-3}$, including standard deviations), respectively across all years sampled. The mean densities and production indicated that the eastern basin was oligotrophic (Dahl *et al.* 1995, Graham *et al.* 1996). Based on a spatial survey of the inner bay in 1998 (Dimitru *et al.* pers. comm.), the average seasonal concentration in July to October of cladocerans alone was $10.60 \text{ mg}\cdot\text{m}^{-3}$ with the maximum at $19.26 \text{ mg}\cdot\text{m}^{-3}$. The variability in August of zooplankton densities in the inner bay was high, from $8.58 \text{ mg}\cdot\text{m}^{-3}$ to $85.73 \text{ mg}\cdot\text{m}^{-3}$. The density of zooplankton at the outer bay sites also usually peaked in August. Based on the maximum zooplankton density, the date of the maximum (summer) and minimum zooplankton concentrations (fall), a generic parabolic curve of zooplankton biomass (Equation 4.13) with a maximum of $50 \text{ mg}\cdot\text{m}^{-3}$ at Day 212 (July 31) over time was generated. A minimum of $10 \text{ mg}\cdot\text{m}^{-3}$ was set as an overwinter food level (Figure 4.08; Graham *et al.* 1996). This equation was modified depending on the vegetation present and depth of larvae.

Equation 4.13: $B_{\text{zoop}} = (-1/12^2 * J - 212)^2 + 50$ where B_{zoop} = biomass of zooplankton in $\text{mg}\cdot\text{m}^{-3}$ and $\geq 10 \text{ mg}\cdot\text{m}^{-3}$.

It was assumed that no food was available below 10 m, the usual depth of light penetration for the Long Point area, above this point the zooplankton were assumed to be well mixed even though it is recognised that zooplankton can exhibit diel vertical migration (Masson & Pinel-Alloul 1998, Steinhart & Wurtsbaugh 1999). It was assumed because the time step was daily that zooplankton would be in the epilimnion for most of the day. The food availability by depth location and Julian day was given in mg of zooplankton per m^3 . Conversion of zooplankton biomass in $\text{mg}\cdot\text{L}^{-1}$ to P values, the feeding rate modifier used in consumption equations, was performed. (N.B. It was necessary to convert the zooplankton biomass equation from $\text{mg}\cdot\text{m}^{-3}$.)

P was then scaled by the HSIs for larval growth, which used only exposure and vegetation habitat characteristics. Because food availability has already been modified in P by varying the densities by habitat, the HSI modified for relative prey catchability so that overall proportions of maximum consumption (P) would reflect both qualities of the environment. Vegetation influenced growth by affecting the relative availability (a combination of zooplankton abundance and relative catchability) of zooplankton: no and low submergent vegetation ($\text{HSI}_{\text{Veg,FryGrw}} = 1.0$), moderate vegetation ($\text{HSI}_{\text{Veg,FryGrw}} = 0.5$), high-density submergent vegetation ($\text{HSI}_{\text{Veg,FryGrw}} = 0.25$), and emergent vegetation ($\text{HSI}_{\text{Veg,FryGrw}} =$

0.1). Most evidence supports a higher relative abundance of zooplankton and benthic invertebrates in vegetated and wetland areas, however there is debate over the accessibility of those prey items in densely vegetated areas (Persson & Greenberg 1990, Kornijow 1997).

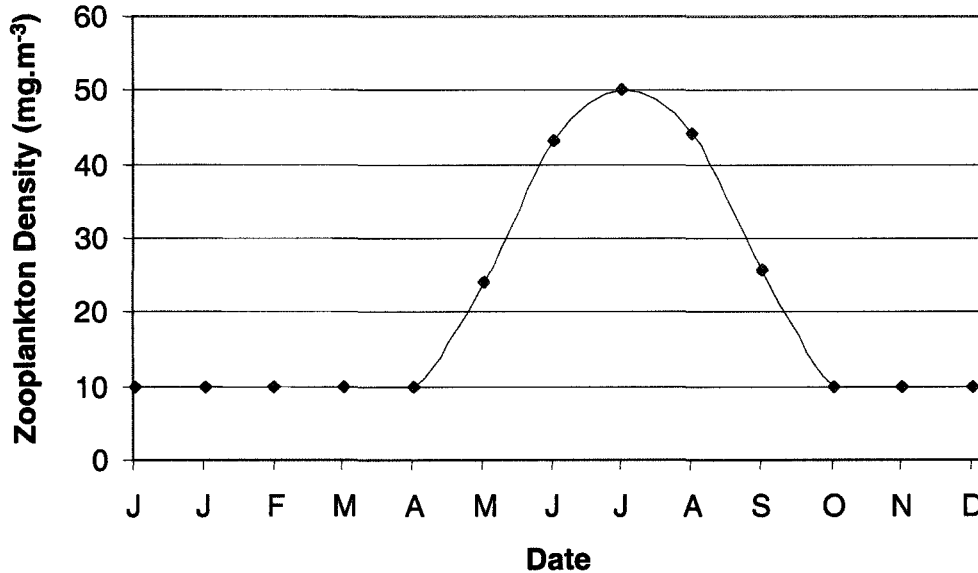


Figure 4.08: Generalised annual, maximum zooplankton density in the Long Point Bay region. (Converted to mg·L⁻¹ for use in bioenergetics P equation.)

Exposure HSI for larval growth were calculated in a similar fashion to egg suitabilities and were based on the frequency distribution of exposures in 1999. It was assumed that 1999 was an average year and that fish were acclimated to average exposure conditions in Long Point Bay, which may signify an exposure preference for the average condition, or increasing difficulty in obtaining food at the extremes of the distribution (Tyler & Clapp 1995, Xie & Eggleston 1999). The exposure HSI for YOY growth was applied in the top 5 m of the water column, at deeper depths the HSI for exposure was considered a nonfactor (i.e. $HSI_{Exp,FryGrw} = 1$; Equation 4.14). Note that substrate was not included in HSI calculations for planktonic larval growth. Depth and temperature were indirectly included in the bioenergetics component of the model. The abundance of prey items varied by depth and time of year, which are also related to light and temperature regimes. The final value for P, the consumption rate modifier, was determined by a geometric mean of the following terms (Equation 4.15).

Equation 4.14: $HSI_{Exp,FryGrw} = 1.742 * e^{(E * -0.0019)}$, if below 5m depth then $HSI_{Exp,FryGrw} = 1$. (Note: this was a slightly different equation than used for egg survival because no adverse effect occurs at low values of exposure (E, km²). Values were capped at 1 below

Equation 4.15: $P = ((0.679 * B_{zoo} / 1000)^{0.278} * HSI_{Exp,FryGrw} * HSI_{Veg,FryGrw})^{0.333}$.

The bioenergetics equations for respiration were updated with daily temperatures and the activity modifier in the equation was not affected by habitat characteristics but remained constant at 4.4 (Hanson *et al.* 1997). Early in model development, the activity modifier was varied by habitat type based on temperature and relative energy expended foraging and avoiding predation. The output was extremely sensitive and needs to be calibrated properly for yellow perch. Activity rates were varied by the HSI for growth and HSI mortality (i.e. maximising growth and minimising mortality) and scaled to range between 1-11 (the range of activity levels for all larval fishes listed in Hanson *et al.* 1997). This was compared to using the generic activity level of 4.4 given for perch fry in the Wisconsin model but introduced so much variability into the system that without calibration or validation data it was necessary to hold constant at the recommended levels.

Equation 2 for respiration from Hanson *et al.* (1997) was used with coefficients for fry (Equation 4.16, Appendices 4.4 & 4.5), as well as the equation for specific dynamic action, $S = SDA * (C-F)$, Boisclair & Leggett 1989, Boisclair & Sirois 1993, Madon & Culver 1993).

Equation 4.16: $R = RA * W^{RB} * [f(T) * ACT]$ where $f(T) = V^x * e^{(X*(1-V))} * ACT$ where $V = (RTM-T) / (RTM-RTO)$ and $X = (Z^2 * (1 + 40 / Y)^{0.5})^2 / 400$, where $Z = \ln(RQ) * (RTM - RTO)$, and $Y = \ln(RQ) * (RTM - RTO + 2)$

The equations for egestion and excretion were also the same as in Hanson *et al.* (1997), $F = FA * C$ and $U = UA * (C-F)$. For fry, $FA = 0.15$ was used (as the proportion of consumption allocated to faecal production) and $UA = 0.15$ (as the proportion of assimilated energy). It was assumed that there was no environmental (habitat-based) regulation of waste production other than through consumption.

Fry grew until Oct 31st and then were held at a constant weight until the end of the model run. This was chosen as an arbitrary date when planktonic YOYs may switch to benthos, perhaps because zooplankton prey are no longer abundant. The larval size was considered the size reached before over-wintering. If the larval weight of survivors on October 31st was less than 1 g then all larvae perished in that cell.

YOY Stage Survival (Pelagic Phase)

Daily larval mortality was calculated in the following manner. HSIs for fry mortality incorporated how habitat might affect natural mortality and predation pressure. A $HSI_{FrySurv}$ equal to 1 indicated high survival. Substrate type and depth location were assumed not to affect mortality because larvae should be feeding on plankton and are removed from sediments and predators should be efficient enough to find larvae in the entire water column. The HSIs for mortality and exposure effects were considered to be the same as growth HSI effects ($HSI_{ExpFryGrw} = HSI_{ExpFrySurv}$), where low to moderate levels of disturbance are preferred because of avoidance behaviour associated with high exposure levels,

possibly linked to high mortality rates. A walleye model for western Lake Erie used river discharge to model larval survival in a similar manner (Jones *et al.* 1998).

The equation relating larval survival and temperature from Chapter 2 was used to calculate a depth preference (see YOY growth section) and this preferred temperature was used to modify the daily mortality rate ($HSI_{Temp,Larv}$). If the position of fry in the water column determined by thermal preference was not within 1 m of the bottom then they were assumed to be in “open water” and the $HSI_{VegFrySurv} = 1$; indicating a low mortality rate set at a minimum level. Otherwise, low and moderate vegetation densities have much higher and successful predatory events (Rossier *et al.* 1996, Micheli & Peterson 1999), especially for ambush predators like pike, which are abundant in Long Point. Therefore $HSI_{VegFrySurv}$ was assigned these values if larvae were within 1 m of the bottom; no vegetation = 1, low-density submergents = 0.25, moderate submergent density = 0, high-density submergent vegetation = 0.75 and emergent vegetation = 1 (a nonlinear relationship between vegetation density because of a combination of reactive distance of the larvae and negotiability for the predator). The overall HSI for larval survival, $HSI_{FrySurv}$, was equal to the geometric mean of HSIs for exposure, vegetation, and temperature (Equation 4.16). The HSI was then used in a modified daily mortality equation for the population of larvae within a cell (Equation 4.17). An assumption of the model was that larvae (YOYs) were distributed equally throughout each cell in the matrix.

Equation 4.16: $HSI_{FrySurv} = (HSI_{ExpFrySurv} * HSI_{Temp,Larv} * HSI_{VegFrySurv})^{0.33}$

Equation 4.17: $N_t = N_{t-1} \cdot e^{-(M_{YOY})}$ where $M_{YOY} = (1 - HSI_{FrySurv}) * 0.3$, $t = \text{day}$.

Mortality rates ranged from 0 to 30%, which was the highest observed, daily predation and natural mortality rate documented for yellow perch in an embayment of Lake Ontario and Long Point was assumed to have a similar predation pressure (Mason & Brandt 1996). When temperature was the only source of mortality then $HSI_{FrySurv} = HSI_{Temp,Larv}$.

4.1.7 Model Output Variables

The output from the model included HSIs for spawning, egg development, larval growth and mortality, as well as the temperature at larval location (depth). The number of eggs and larvae in each cell, as well as their hatch and overwintering size sorted by spawning and hatch dates in 1999 were included in output tables for each of the scenarios outlined in the following section. The model logic and flow are shown in Figure 4.09.

The output of the model included the eggs hatched on different days of the year in different cells as well as larval size and abundance on each day after hatching until Oct 31st, arbitrarily set as a cut-off date after which the larvae were assumed to become demersal and overwinter.

Initially, the model was run iteratively for each life stage to test for realistic output under the simplest conditions. HSIs and calculated habitat characteristics were quality checked for obvious errors and outliers. Calibration and validation are discussed in the conclusions by comparing the results to available data on size and the sparse spatial distribution information on perch available for early life stages; specific information from the eastern basin of Lake Erie or Long Point Bay was used where possible in the 1990s.

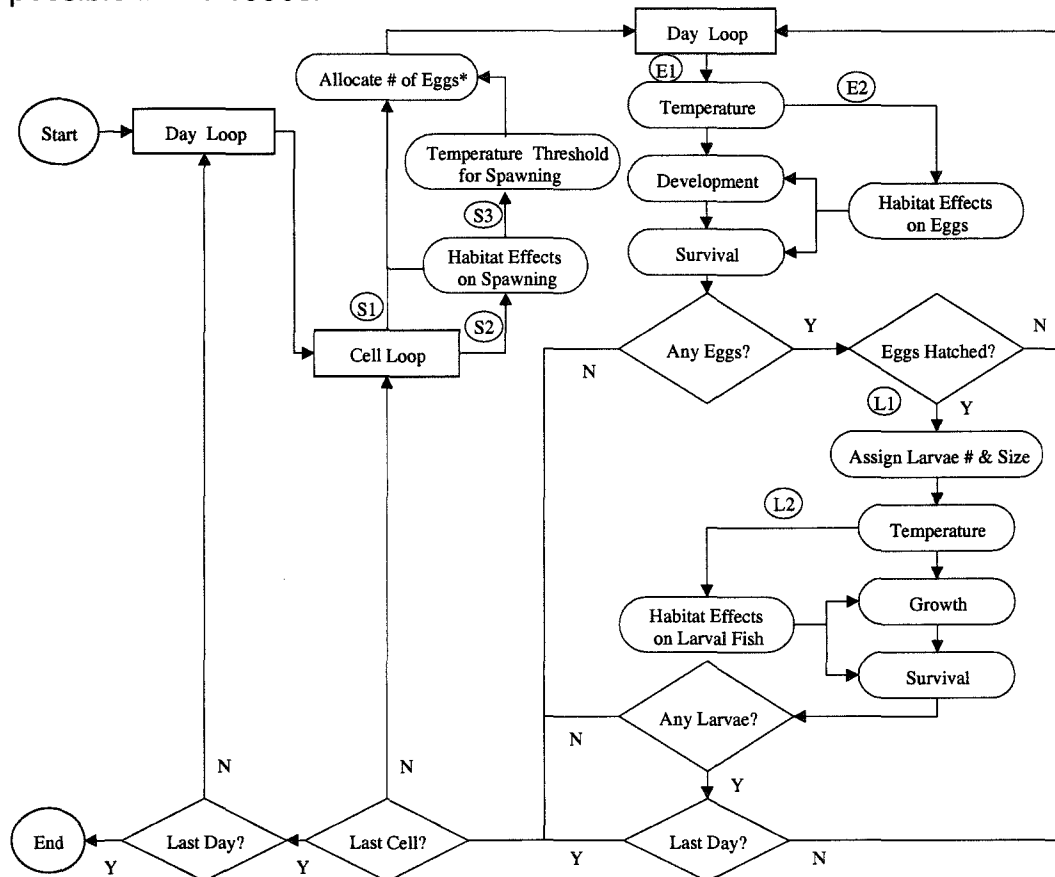


Figure 4.09: Schematic diagram of the order of operations in the model logic. The numbers indicate the different pathways that were used to test the different habitat-based scenarios. (* indicates the allocation of eggs to each grid cell was performed in two different ways: modification of spawning effort by site-specific habitat suitability or ideal free redistribution of spawning effort.)

4.1.8 Testing Habitat Limitations Using Scenarios

Scenario testing concentrated on the comparisons of habitat, temperature only effects and physical habitat effects on early population dynamics of yellow perch, as well as the effects of spawning time. Different scenarios were investigated to tease apart the relative effects of consecutive, or concurrent, habitat interactions on the population dynamics of yellow perch. Combinations of the following scenarios for each life stage were used: three different scenarios for spawning (plus an additional 2 modifications that involved reallocation of eggs based on an

ideal free distribution strategy), two scenarios for egg development, and two scenarios for larval development. These experiments evaluated the relative importance of habitat constraints at different life stages. All combinations of these life-stage specific scenarios were tested (Figure 4.10). Most contrasts between scenarios involved a comparison between temperature-effects-only versus temperature-and-habitat-effects scenarios. Each combination is outlined in Table 4.4 showing how the stage-based scenarios were numbered and combined.

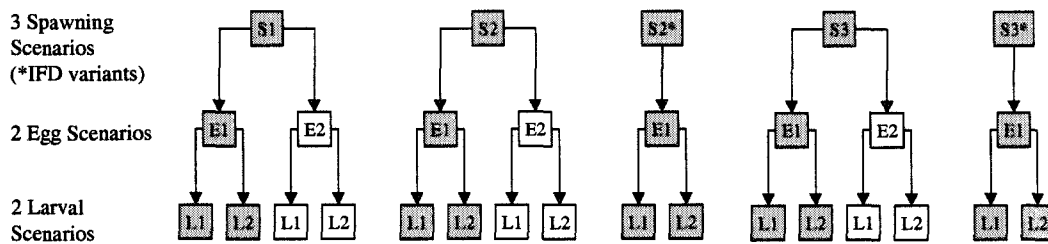


Figure 4.10: Flow diagram outlining how the lifestage specific scenarios were combined and tested concomitantly. (Shading indicates the scenarios that are presented in Section 4.2)

Table 4.4: The model scenarios were implemented and assessed in a stepwise procedure using 16 different combinations of the life stage scenarios outlined above. (Shading corresponds to Figure 4.10. H = Habitat, T=Temperature)

Scenario Code	Spawning Scenario (#)	Egg Scenario (#)	Larval Scenario (#)
S1E1L1	No Effects (S1)	T Only (E1)	T Only (L1)
S1E1L2	No Effects (S1)	T Only (E1)	H & T (L2)
S1E2L1	No Effects (S1)	H & T (E2)	T Only (L1)
S1E2L2	No Effects (S1)	H & T (E2)	H & T (L2)
S2E1L1	H Selection (S2)	T Only (E1)	T Only (L1)
S2E1L2	H Selection (S2)	T Only (E1)	H & T (L2)
S2E2L1	H Selection (S2)	H & T (E2)	T Only (L1)
S2E2L2	H Selection (S2)	H & T (E2)	H & T (L2)
S2*E1L1	H Selection (S2*)	T Only (E1)	T Only (L1)
S2*E1L2	H Selection (S2*)	T Only (E1)	H & T (L2)
S3E1L1	H & T (S3)	T Only (E1)	T Only (L1)
S3E1L2	H & T (S3)	T Only (E1)	H & T (L2)
S3E2L1	H & T (S3)	H & T (E2)	T Only (L1)
S3E2L2	H & T (S3)	H & T (E2)	H & T (L2)
S3*E1L1	H & T (S3*)	T Only (E1)	T Only (L1)
S3*E1L2	H & T (S3*)	T Only (E1)	H & T (L2)

Spawning

Spawning Scenario 1 (S1): To investigate the timing of life stage events and their interactions with a changing environment, 1000 eggs were placed in each cell on each day from January 1 to October 31. (An arbitrary termination date for spawning was chosen because no larvae that hatched after this spawning date could possibly survive the winter because of their small size.) There was no habitat preference for spawning sites or temperature thresholds to initiate spawning under this scenario. This was the reference condition for spawning, as if all areas and spawning times were equal.

Spawning Scenario 2 (S2): Each day, 1000 eggs were scaled by the overall HSI_{spawn} for that cell. This scenario reflected a local relative weighting of spawning effort based on the spawning preferences of perch and the habitat conditions on that day.

Spawning Scenario 3 (S3): The initial number of eggs (1000) was scaled by the HSI_{spawn} , but spawning could only be initiated if a degree day threshold was reached, otherwise $HSI_{\text{spawn}} = 0$. The threshold was surpassed if water temperatures within that cell were between 6-12 °C for 5 consecutive days. This threshold favoured areas and times with slightly suboptimal temperatures for egg development and relatively low temperature variability.

Additional scenarios were added that modified the daily egg allocation to an ideal free distribution of spawning effort for the entire system instead of a relative weighting based on local habitat suitability.

Spawning Scenario 2* (S2*): The total number of eggs in the matrix (1000 eggs·cell⁻¹ x 400 cells = 400,000 eggs) were allocated based on the distribution of HSIs for spawning in the matrix on that day. (Allocations were based on Equation 4.17 and habitat selection of spawning sites outlined in Spawning Scenario S2 above.)

Equation 4.18:
$$EggsSpawned(Date, Cell) = \frac{HSI_{\text{spawn}}(Date, Cell)}{\sum_{Cell=1}^{400} HSI_{\text{spawn}}(Date, Cell)} \cdot 400000$$

Spawning Scenario 3* (S3*): Equation 4.18 was used to modify the number of eggs of the maximum (400,000) allocated each day to each cell, however the scenario was based on the HSI assignments for Spawning Scenario S3 outlined above; a combination of habitat selection and temperature threshold.

Spawning Output: Each spawning date in 1999, the number of eggs spawned per cell was recorded for each scenario.

Egg Development & Survival

Egg Scenario 1 (E1): Under this 'default' scenario, the eggs in each cell were only affected by the temperatures that they encountered after deposition. Temperatures affected survival rates and development times

directly.

Egg Scenario 2 (E2): The $HSI_{Spn,Exp}$ was used to modify the daily survival of eggs. Aside from temperature, exposure was the only habitat variable considered to affect egg survival (i.e. risk of destruction or stranding of eggs) because no empirical evidence linked any of the other habitat factors to survival rates. Exposure, modified by water depth and vegetation, was used to vary mortality above the natural mortality experienced at different temperatures. Only the top 5th percentile of exposures experienced in Long Point Bay in 1999, in other words, extreme events, were chosen as a potential risk (Note: this is different than in spawning calculations). Up to 50% additional egg mortality was applied in these extreme cases. Egg stranding does occur under extreme wind events (Clady & Hutchinson 1974) but there is very little data to validate this value.

Development times were not linked to any habitat factors except temperature. Therefore, development in all scenarios was modelled as in Scenario E1 and separate HSIs were not necessary for development and survival rates as temperature was used directly.

Egg Output: The number of eggs hatched and their hatch dates were recorded for the eggs spawned on a certain date. For all scenarios, the percentage of normally hatched eggs was calculated based on the temperature at hatch. The size at hatch was calculated based on the average temperature during development. Hatched fry were raised to the swim-up stage before the larval scenarios were applied. Growth did not occur during this time, just yolk-sac absorption and mortality rates were based on the egg scenario being tested. The number of swim-up larvae surviving at the end of this brief period was recorded.

Larval Growth and Survival

Larval Scenario 1 (L1): Daily larval growth rates were applied that were dependent on the optimal survival temperatures within the current cell's thermal profile. Under this default scenario, standard P and ACT values were used in bioenergetics equations (i.e. there were no habitat effects and larvae fed at C_{max} levels). Mortality rates were based on the temperatures encountered and were not habitat-based.

Larval Scenario 2 (L2): Daily larval growth and mortality rates were applied based on the optimal survival temperature, and its associated depth, within the profile of that cell. Maximum ration (the P value) was weighted based on the HSI for larval growth and default ACT values were used in bioenergetics equations (i.e. habitat affected food availability but not activity level). Base mortality rates were varied by HSIs for larval mortality (i.e. by habitat type) and were a relative weighting of physical disturbance and susceptibility to predation.

Larval Output: The size and number of larvae that survived to October 31st (an arbitrary date chosen for the end of the planktonic larval stage before overwintering begins) for each spawning date was recorded.

4.2 RESULTS

Each scenario's output was compared, both temporally and spatially in an iterative fashion, to test assumptions pertaining to life history strategies, and habitat interactions with population dynamics. A series of graphs depicting the daily distribution of life stage abundances, larval sizes, and larval production estimates are shown for each scenario that exhibited noticeable differences in spatial or temporal patterns. The graphs depict distributions by spawning date, and sometimes hatch date, from March until December (January and February rarely had data to plot), of the number of eggs spawned, the number of eggs hatched, the number of over-wintering larvae, or the average larval gain in biomass for each cell in the model grid. Each cell's value is plotted for each day and colour-coded by the number of datapoints at that value, so the changes in frequency distribution for that attribute can be visualized throughout the year. An effort was made to standardise the axis scales for comparison between scenarios. (Scale exceptions are noted in figure captions.) Daily totals for abundances or biomass were also plotted on each graph. A comparison of plots for consecutive life stages show how initial conditions and subsequent events, like the timing of spawning, the relative distribution of reproductive effort, and habitat influences at key points in early life history, can consecutively affect the overall first-year production in the system. (Comparative statistics can be found in Appendix 4.6.)

A series of maps for each scenario were also generated depicting total eggs spawned, eggs hatched, and larval abundance (i.e. comparative survival at each stage) by spawning month. The average larval size (comparative growth), or total larval production by grid cell in Long Point was also mapped by spawning month for standardization. (Comparative statistics can also be found in the Appendix 4.7). From this comparative analysis, the optimal spawning dates, hatch dates, and areas for egg development and nursery habitat were determined under 1999 thermal conditions. Optimal times and areas were based on the relative abundances (i.e. higher survival rates) and growth rates of larvae that were produced from each of the grid cells that represent the system. The cumulative effects on overall production are predicated on the level of interaction between each life stage and their physical habitat, which has not been considered in many other modelling approaches.

4.2.1 Uniform Spawning Scenario Combinations

Spawning Scenario S1 (Baseline Scenario): The baseline scenario for spawning had no habitat selectivity or thermal thresholds, i.e. all habitat was the same all the time. The maximum number of eggs (1000) was spawned in each cell on each day for the simulation, therefore no graphs or maps for spawning are shown because each month 28,000+ eggs were spawned uniformly in each cell and 400,000 eggs in total were spawned each day in the system. This was the scenario against which all spawning scenarios were compared.

Eggs developed and survived based on temperatures, or the level of habitat-based disturbance they encountered, depending on the scenario. The graphs shown in this section plot the number of surviving *swim-up larvae* against both spawning and hatch dates separately. Comparison of these two graphs gives an indirect measure of development rates at different times of the year. The maps depict the total number of *hatched eggs* by cell based on the month in which they were spawned. The difference between plotting swim-up larvae in graphs and hatched eggs is that swim-up larvae have accounted for high mortality in abnormally hatched eggs and also the temperature-based survival of yolk-sac fry that are unable to swim from the lake bottom for 1 or 2 days before swim-up can occur. (Comparative statistics between all life stages are shown in Appendix 4.6.)

Egg Scenario S1E1: The pattern of eggs that survived to *hatch* in Scenario S1E1 matched the pattern observed for eggs *spawned* under thermal and habitat constraints (S2, with the exception of the summer hatch), even though the maximum number of eggs were spawned each day in the former scenario. Most of the surviving swim-up larvae shown in Figures 4.13 and 4.14 were spawned at the end of March to October (Note: November would have a successful egg hatch if the model did not contain an arbitrary cut-off date for egg development of October 31). The daily number of surviving swim-up larvae increased in variability when hatch dates were plotted instead of spawning dates.

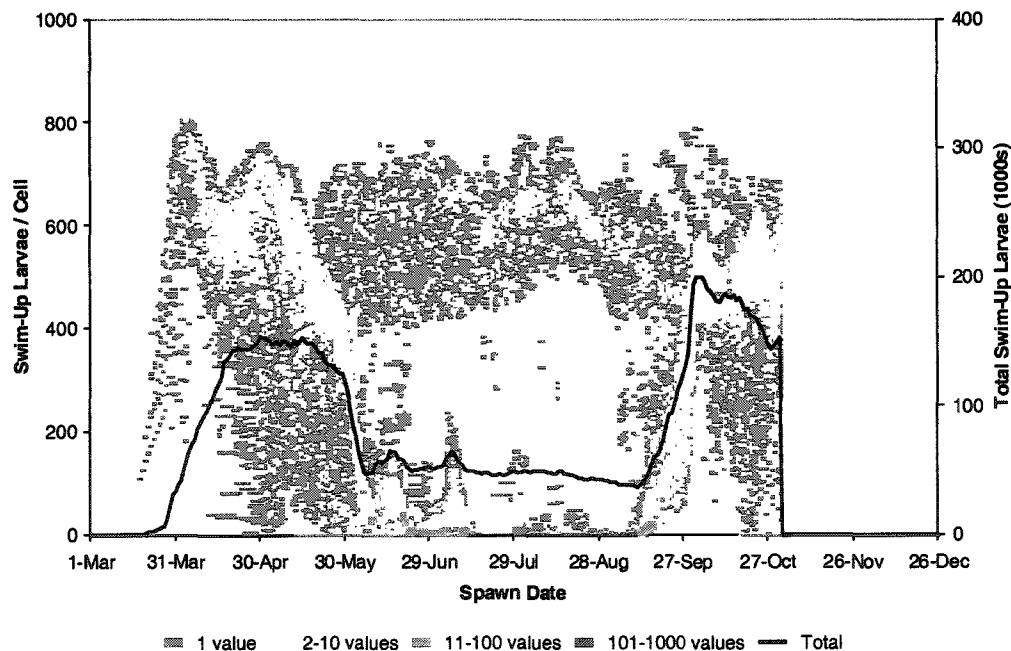


Figure 4.13: Frequency distribution of virtual eggs hatched per cell (# of values per point is colour-coded) and total number of eggs hatched in Long Point Bay by spawning date in 1999 under Scenario S1E1 conditions; temperature effects after spawning.

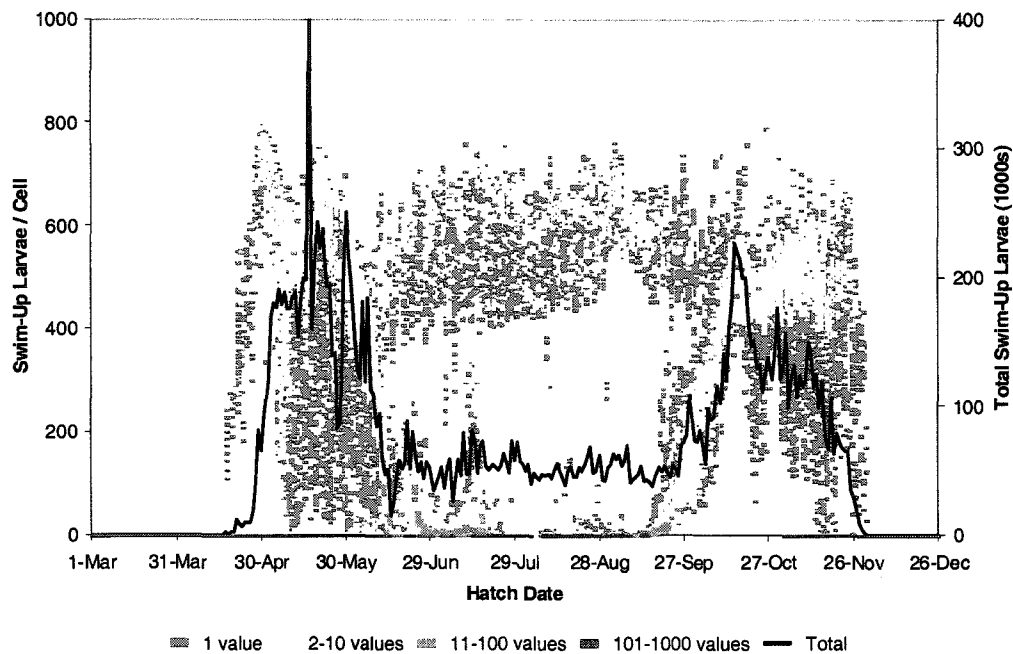


Figure 4.14: Frequency distribution of virtual eggs hatched per cell (# of values per point is colour-coded) and the total number of eggs hatched in Long Point Bay by **hatch date** in 1999 under Scenario S1E1 conditions; temperature effects after spawning.

There was more variability in the number of eggs hatched between successive hatch dates than between spawning dates because of the spatial and temporal variability of temperature in the system. Increasing temperatures tended to compress an extended spring spawning period into a narrow hatch period due to faster egg development rates because of the thermal regime. The opposite was true in the fall when the hatch period extended due to different egg development rates in different parts of the system. This spawn to hatch pattern was repeated throughout the scenarios.

During peak survival periods, roughly 50% of eggs survived to the swim-up larval stage and different regions of the bay contributed towards the larval pool at different times (Figure 4.15). The highest survival rate from spawn to hatch per cell was 80% between March and October. An interesting and unexpected result of the uniform spawning scenario was the high survival of eggs based on temperatures in the 'deep hole' area throughout the summer.

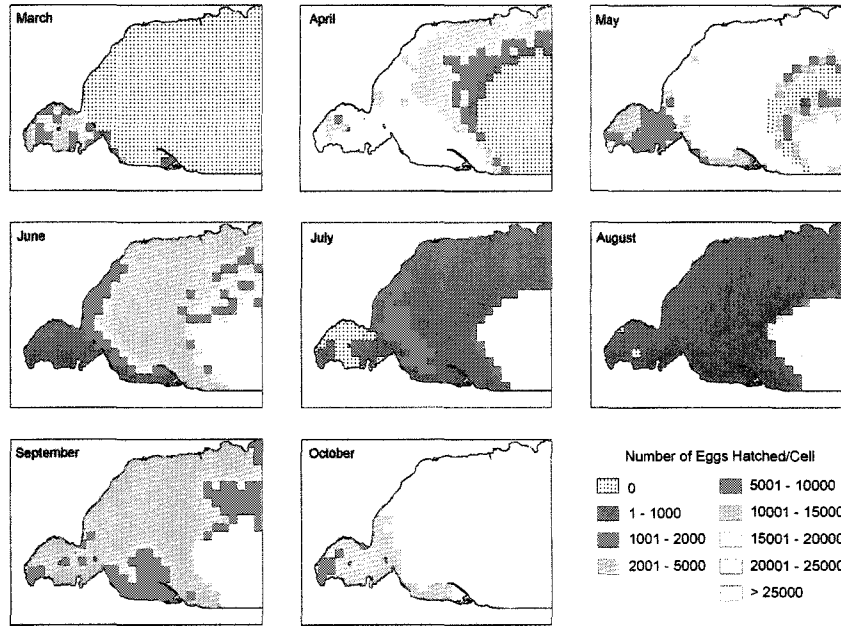


Figure 4.15: Monthly maps of the total number of virtual eggs hatched in each cell in Long Point Bay by spawning month, March until October, 1999 under Scenario S1E1 conditions.

Graphs for Egg Scenario E2 combinations are not shown in the results because physical habitat influences were negligible on egg and fry survival. Only subtle spatial differences between E1 and E2 output materialized, where a few cells along the shoreline of the outer bay in April and May were affected by extreme wind events (Figures 4.16, 4.32 & 4.63).

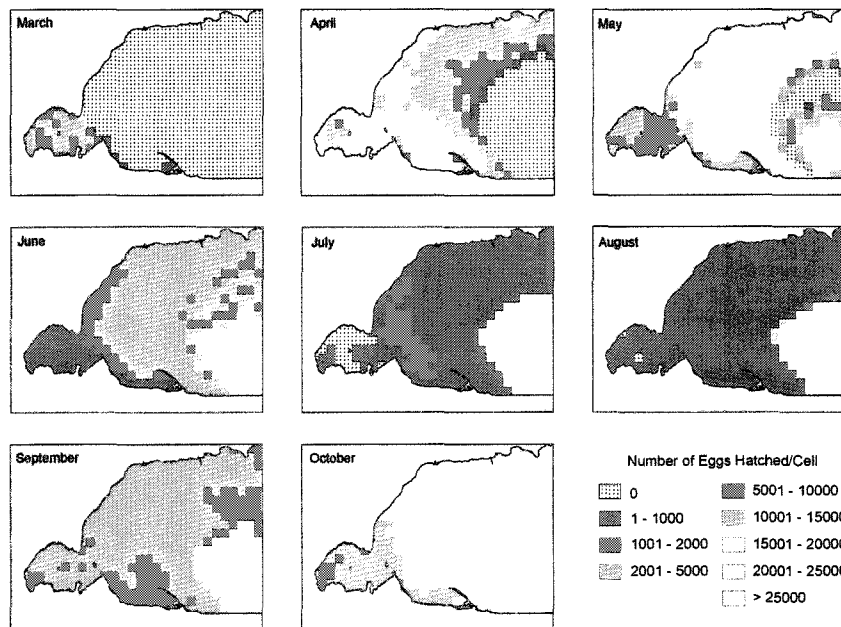


Figure 4.16: Monthly maps of the total number of virtual eggs hatched in each cell in Long Point Bay by spawning month, March until October, 1999 under Scenario S1E2 conditions.

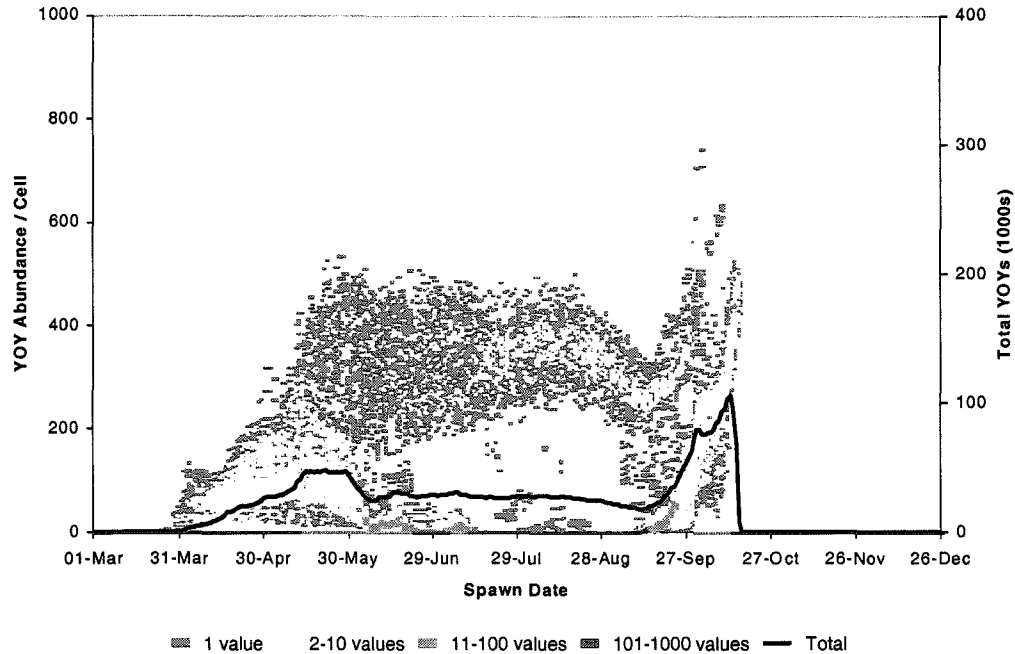


Figure 4.17: Frequency distribution by spawning date of virtual YOYs per cell (# of values per point is colour-coded) and the total number of YOYs that survived to October 31, 1999 in Long Point Bay under Scenario S1E1L1 conditions; spawning with temperature effects on eggs & larvae.

These relative abundance maps are the only results shown for Egg Scenario E2 (i.e. the only ones that use habitat and temperature effects on the egg stage) because there were no significant effects on overall production. Maps for these scenarios are shown together with their corresponding E1 Egg Scenarios to facilitate comparisons between similar spawning scenarios (S1-S3). [Note: E2 scenarios were not conducted for S2* and S3* because of the insignificant differences observed in other comparisons. See Appendix 4.6.]

Larval Scenario S1E1L1: Larvae under this scenario experienced a daily mortality rate modified by the best available temperature in the profile of the cell they occupied. The original bimodal distribution, with constant summer recruitment, to the swim-up stage became flattened when larval abundance was assessed at the end of the year (Figure 4.17). Only an early fall peak of YOY recruitment remained from fall spawning otherwise a relatively consistent recruitment rate was produced for the remainder of the year. YOYs that were spawned early in the year were susceptible to different sources of mortality for a longer period before overwintering. Larvae that were spawned in the Inner Bay of Long Point during spring would have higher thermal mortality rates than in other areas or unless spawning occurred later in the year (Figure 4.18).

The graph of the temporal growth distribution for yellow perch outlined two trajectories for exponential growth defined by nearshore and

offshore thermal regimes (Figure 4.19). Nearshore variability in growth was significantly greater than offshore; especially the older the larvae became (Figure 4.20). The larval increase in size in both regions ranged from 10 g to just above 14 g by November. The greatest growth rates, (at maximum consumption in this scenario), based on temperatures in the Inner Bay and along the south shore of the outer bay, occurred for larvae that had been spawned between March and June. Individual biomass increased a maximum of 15 g throughout this time.

The bulk of larvae were produced during two spawning weeks in May and numbers declined as cells became unsuitable in summer with a smaller, potential peak in production again in fall under these scenario conditions (Figure 4.19). Contribution to overall production included both growth and survival in cells until the end of October, so even though growth rates were highest in certain areas the greatest production occurred in the Inner Bay for a brief time early in the year (Figure 4.21). The thermal regime in the nearshore outer bay, and deep hole area was conducive to larval production throughout the summer given maximum consumption rates. A uniform, spatial distribution of production throughout all of Long Point Bay was predicted in fall under these conditions.

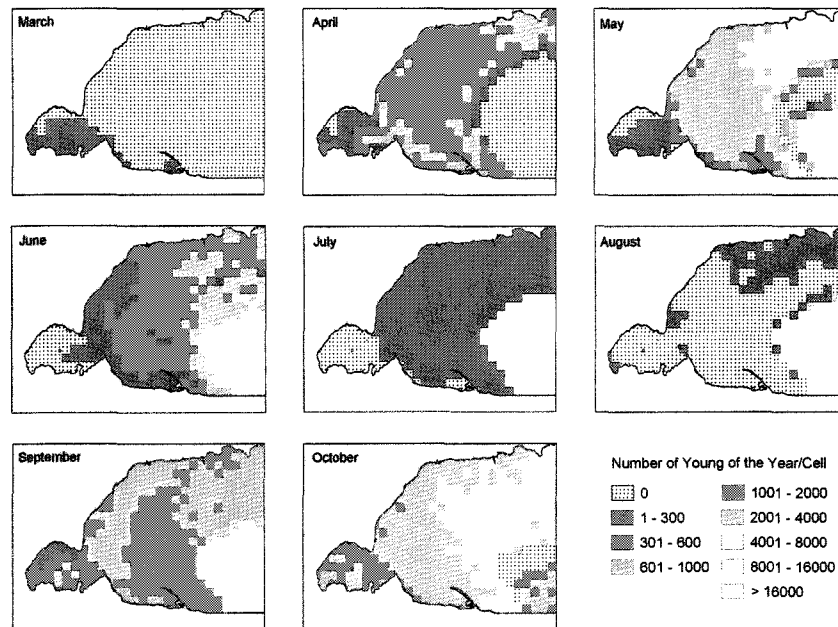


Figure 4.18: Monthly maps of the total number of virtual YOYs that survive until October 31st in each cell in Long Point Bay by spawning month, March until October, 1999 under Scenario S1E1L1 conditions.

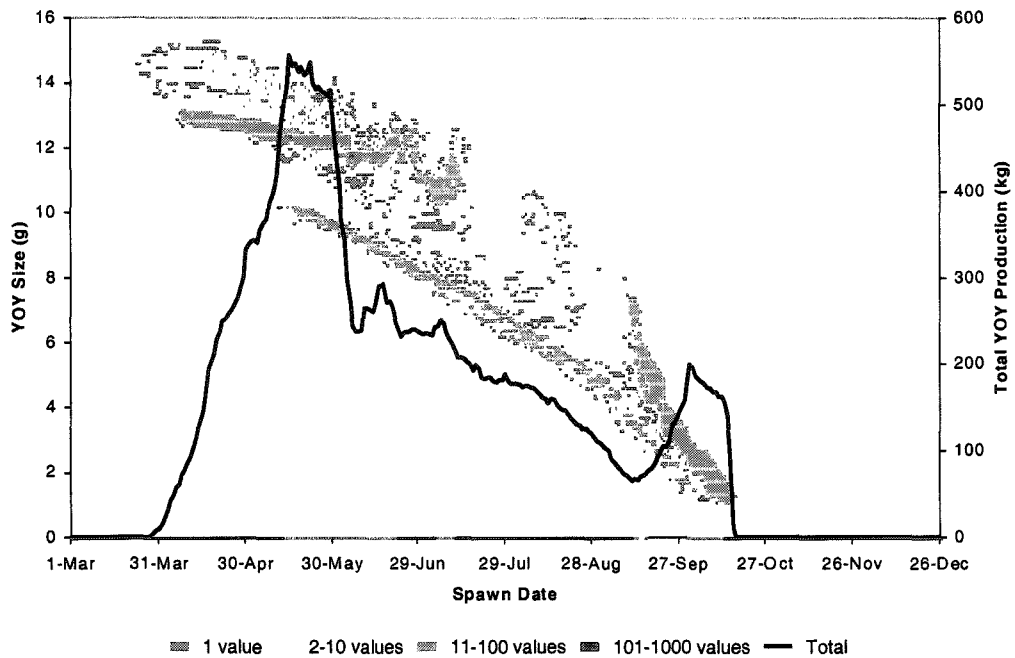


Figure 4.19: Frequency distribution by spawning date of YOY average size (g) per cell (# of values is colour-coded) and the total production of YOYs (kg) that survived to October 31, 1999 in Long Point Bay under Scenario S1E1L1 conditions; uniform spawning, temperature effects on eggs and larvae.

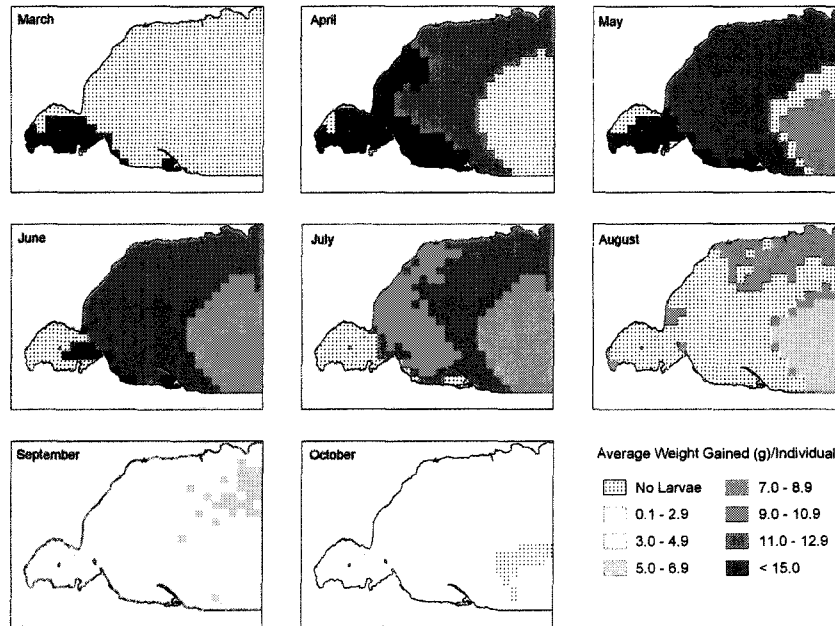


Figure 4.20: Monthly maps of the average weight gain (g) of virtual YOYs that survive until October 31st in each cell in Long Point Bay by spawning month, March until October, 1999 under Scenario S1E1L1 conditions.

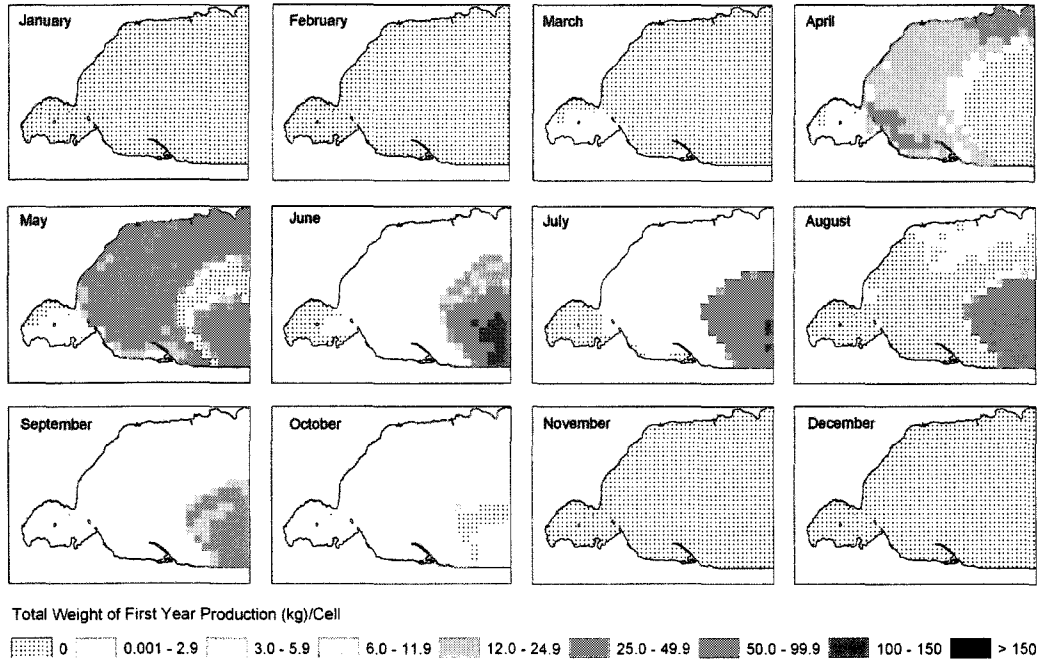


Figure 4.21: Monthly maps of the total production (kg) of virtual YOYs that survived until October 31st in each cell in Long Point Bay from the month of spawning in 1999 under Scenario S1E1L1 conditions.

Larval Scenario S1E1L2: After ubiquitous spawning, eggs were subjected to local temperature effects only, then free-swimming larvae were allowed to select preferred depths based on temperatures (similar to Scenario L1). However, subsequent feeding and mortality rates were determined by local habitat conditions and not just temperatures. The resulting YOY distribution indicated that larvae that remained in cells that were optimal for spring spawning and egg development were not as abundant by the overwintering stage as previous scenarios (Figure 4.22). Any eggs that were spawned in summer (possible under S1 scenarios) did not survive to overwinter in deeper waters.

Spatially, the Inner Bay was not suitable larval habitat under these conditions and the whole system was not conducive to YOY survival in summer. A mismatch between food and thermal preferences in the system may have occurred creating a more “patchy” environment (Figure 4.23). Shallow nearshore areas contributed less to surviving YOYs and the spatial distribution of YOYs became more variable under this scenario, except during October. Larvae in the southern portion of the outer bay had a greater chance of success than along the north shore.

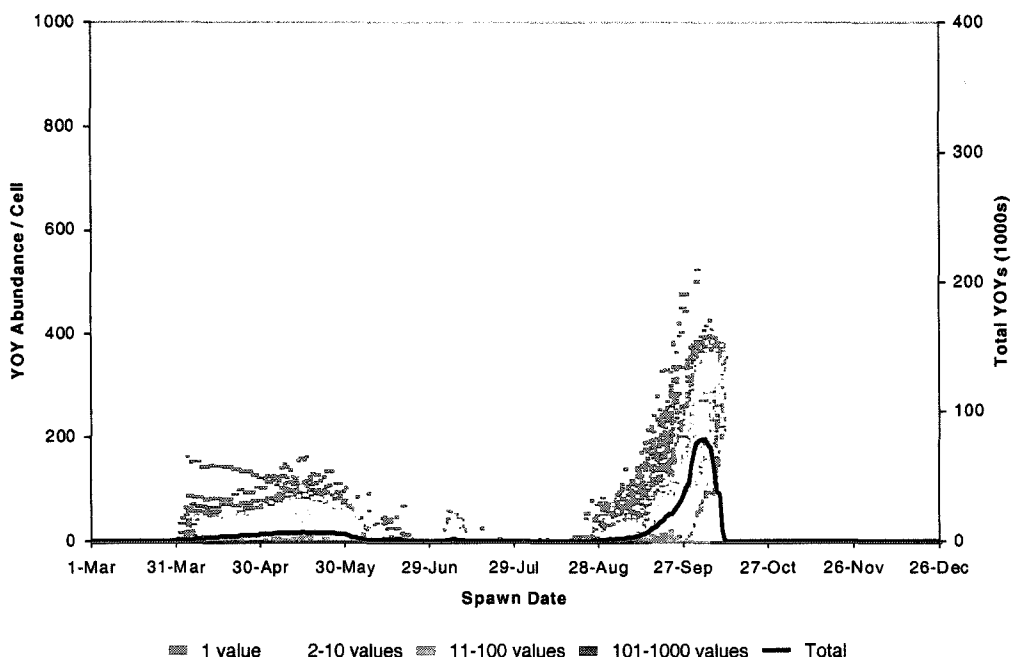


Figure 4.22: Frequency distribution by spawning date of virtual YOYs per cell (# of values per point is colour-coded) and the total YOYs that survived to October 31, 1999 in Long Point Bay (Scenario S1E1L2; spawning with temperature effects on eggs, temperature and habitat effects on larvae).

The size distribution of larvae at the end of October was bimodal for larvae spawned in the spring and summer (Figure 4.24). The relative size range and variability did not change significantly over successful spawning times (i.e. larvae were the same size at the end of October no matter when they were spawned). The smaller-sized cohort ranged from 2 – 4 g while the larger ranged from 7 – 9 g. The two cohort sizes converged for fall spawners around mid-October and ranged from 1 – 4 g by the beginning of November. Spatially, a few isolated pockets of high growth occurred in 1999 along the south shore of the outer bay (Figure 4.25). Most of the high-growth cohort originated between April and July in nearshore areas above thermocline depth. The low-growth cohort originated from the volume of water offshore, including the deep hole area from early spawning. The potential biomass accumulated by larvae from fall spawning was homogenous across the entire bay (i.e. not much spatial variability in growth).

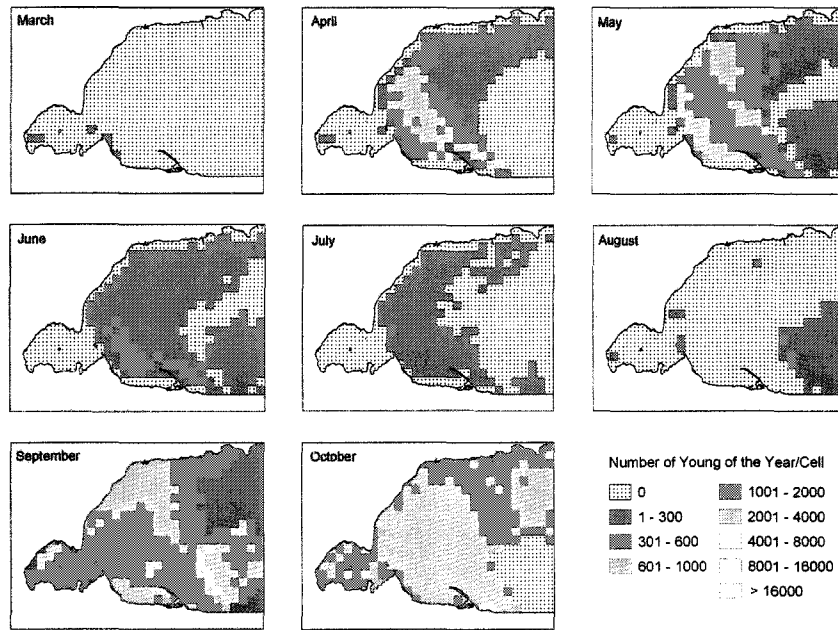


Figure 4.23: Monthly maps of the total number of virtual YOYs that survive until October 31st in each cell in Long Point Bay by spawning month, March until October, 1999 under Scenario S1E1L2 conditions.

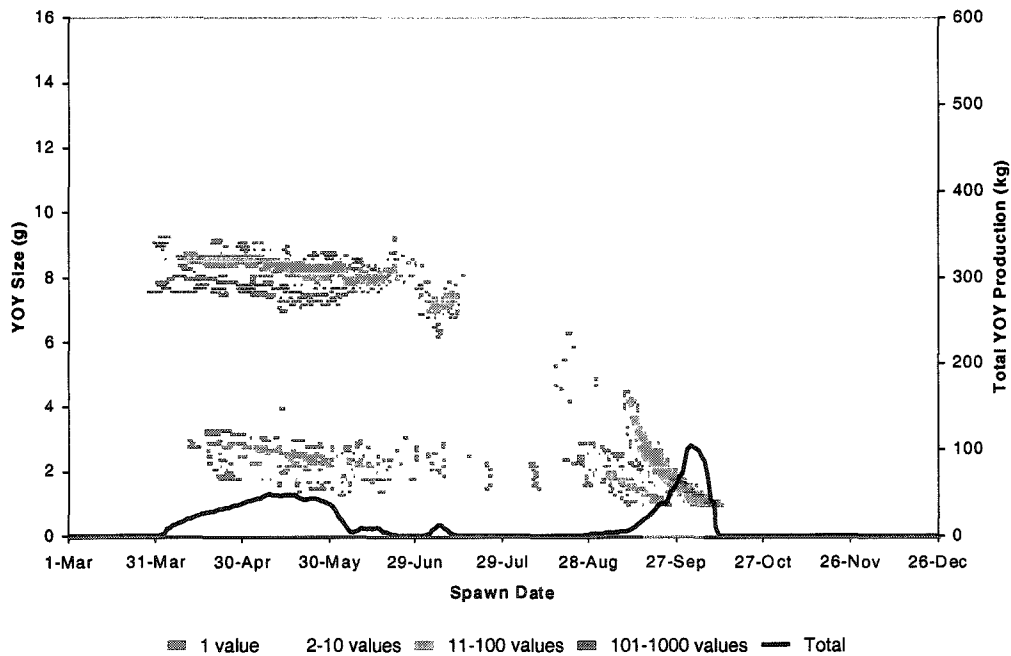


Figure 4.24: Frequency distribution by spawning date of YOY average size (g) per cell (# of values per point is colour-coded) and the total production of YOYs (kg) that survived to October 31, 1999 in Long Point Bay under Scenario S1E1L2 conditions; spawning with temperature effects on eggs and temperature & habitat effects on larvae.

The predicted yearly production of larvae, spawned in the summer, dropped with habitat restrictions at the larval stage (Figure 4.24). Spatially, system-wide production was much reduced in this scenario, when most of outer bay became unsuitable and contributed less than 3 kg

of YOY production per cell compared to 150 kg in some scenarios (Figure 4.26). Also, under this scenario, the Inner Bay only contributed to production during autumn. Outer bay nearshore areas, especially to the south, had the greatest contribution to production during April and May spawning months.

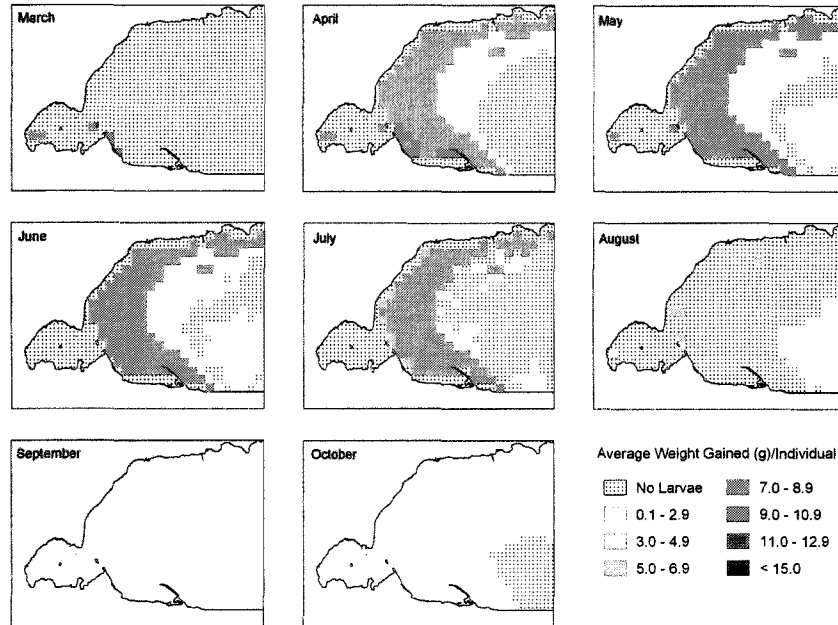


Figure 4.25: Monthly maps of the average weight gain (g) of virtual YOYs that survive until October 31st in each cell in Long Point Bay by spawning month, March until October, 1999 under Scenario S1E1L2 conditions.

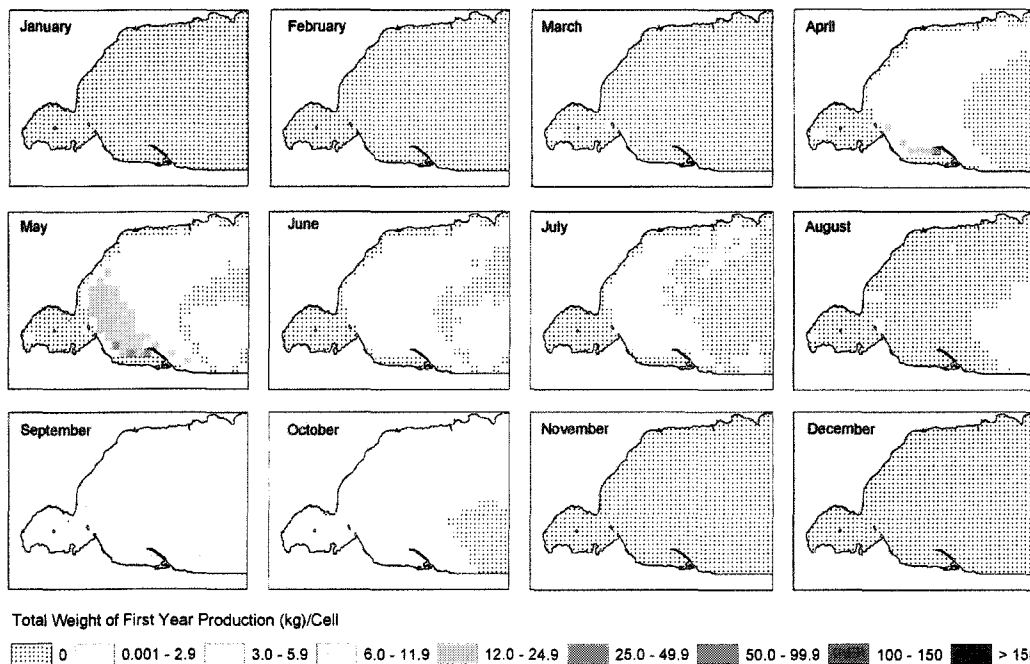


Figure 4.26: Monthly maps of the total production (kg) of virtual YOYs that survived until October 31st in each cell in Long Point Bay from the month of spawning in 1999 under Scenario S1E1L2 conditions.

4.2.2 Habitat-Effects Spawning, Scenario Combinations

Two different types of distributions were tested under habitat-effects only scenarios for spawning: equal (homogeneous) egg distribution with local habitat weighting and ideal-free egg distribution based on system-wide habitat weighting.

Equal Initial Egg Distribution

Spawning Scenario S2: When reproductive allocation was weighted by the local habitat suitability for spawning (based on characteristics other than temperature) then the resulting number of eggs allocated per cell was a function of the HSI distributions (Figures 4.27 & 4.28). The variability in HSIs for spawning was dictated by vegetation and exposure changes, as substrate type and site depth remain unchanged. (Note: not one cell at any time was allocated the maximum number of 1000 eggs in this scenario, indicating that 'perfect' conditions for spawning rarely occurred.)

The number of cells allocated greater than 75% of the maximum potential number of eggs increased in the summer months but the overall daily reproductive allocation to the whole system did not vary much over the year; from approximately 150,000 eggs / day in the spring and fall months up to 190,000 eggs / day in the summer months. Two types of cells emerged: a group that followed the parabolic pattern of vegetation development that achieve a maximum density and suitability in July, and a group of cells with constant HSIs that were only affected by exposures on a sporadic basis.

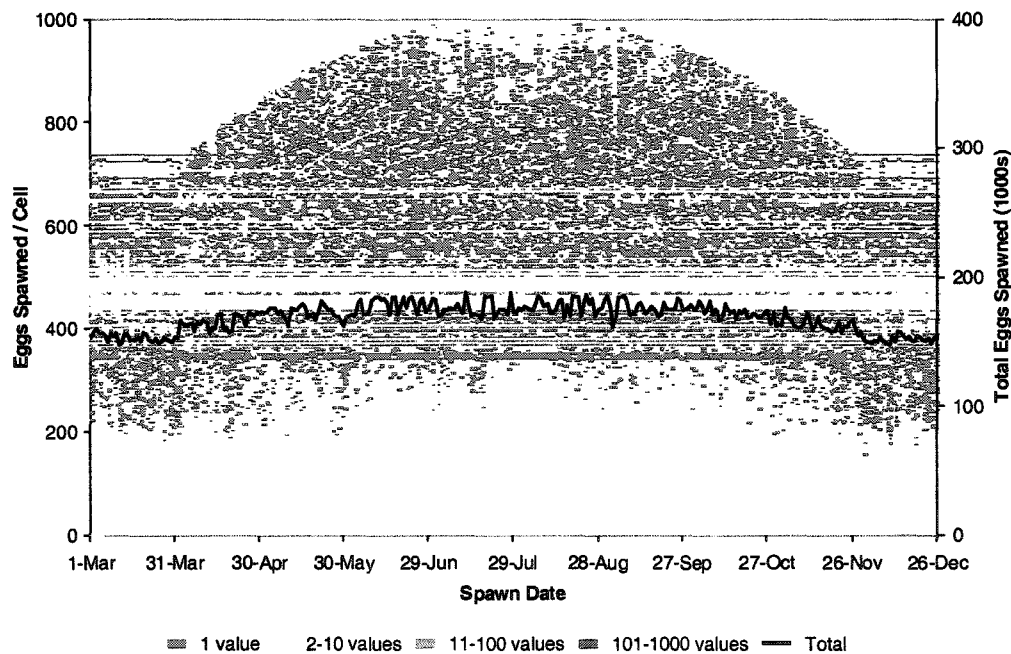


Figure 4.27: Frequency distribution of virtual eggs spawned per cell (# of values per point is colour-coded) and total number of eggs spawned in Long Point Bay by date in 1999 under Scenario S2 conditions; habitat selection.

The change was largely due to vegetation growth along the shoreline and Inner Bay areas that resulted in increased habitat suitability for spawning. The daily egg deposition dropped by a minimum of 50% compared to the baseline scenario, mainly due to the exclusion of deepwater areas beyond 30m depth as nonspawning habitat..

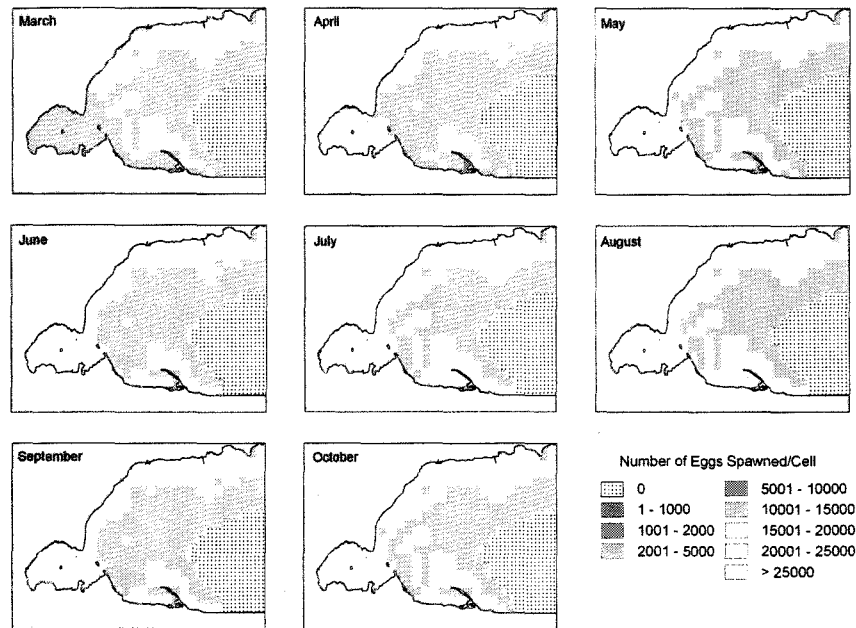


Figure 4.28: Monthly maps of the total number of virtual eggs spawned in each cell in Long Point Bay from March until October, 1999 under Scenario S2 conditions.

Egg Scenario S2E1: Successful completion of the swim-up stage (with initial habitat constraints for spawning and then temperature-related development and survival for eggs and yolk-sac fry) resulted in a bimodal distribution of spawning dates in April and May, and again in October (Figure 4.29). The results were similar to Scenario S1E1 but with a reduced number of hatched eggs, however still proportional to the number spawned. Hatch dates for spring spawn occurred during May and early June, with a compression of the hatch period relative to spawning period as noted previously (Figure 4.30). There was very little summer hatch under Scenario S2E1 conditions because 80 cells located in deeper water were no longer available for spawning because of spawning habitat constraints (Figure 4.31). The spatial results for Scenario S2E2 were similar to S2E1, with the exception of certain nearshore sites usually in open embayments where the fetch could be high from certain directions (Figure 4.32). Areas affected included bays near Peacock Point (north shore of outer bay), Big Rice Bay (south shore Inner Bay) and Big Bluff Bay (south shore outer bay) in April.

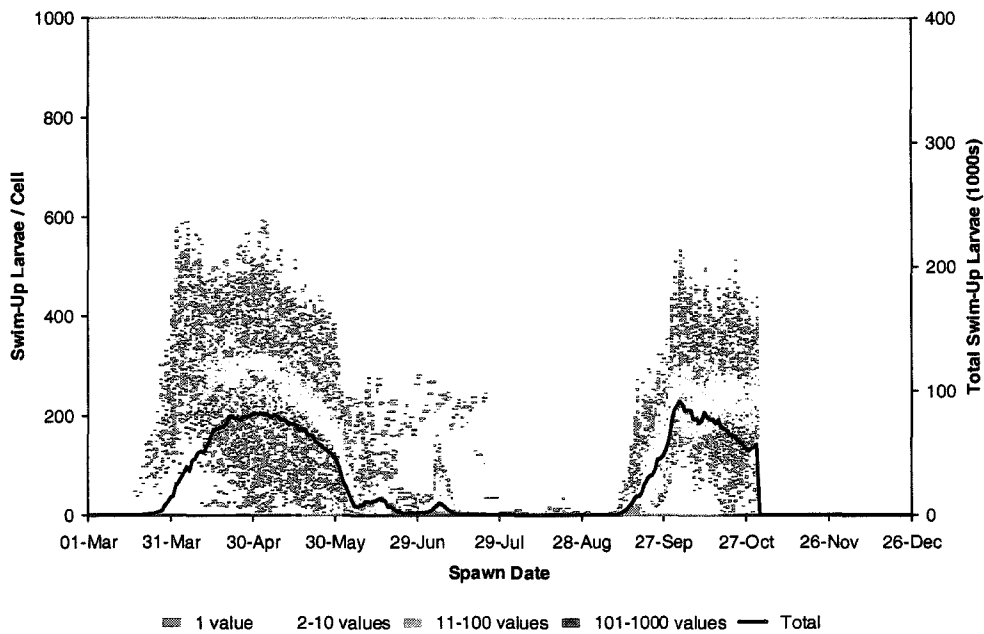


Figure 4.29: Frequency distribution of virtual eggs hatched per cell (# of values per point is colour-coded) and the total number of eggs hatched in Long Point Bay by spawning date in 1999 under Scenario S2E1 conditions; spawning site selection and temperature effects on eggs.

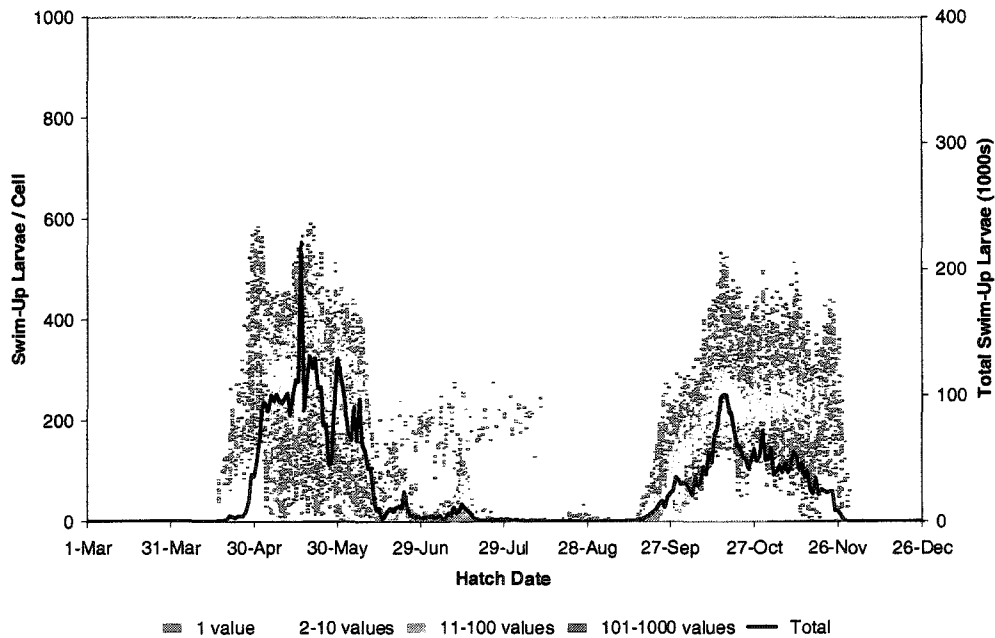


Figure 4.30: Frequency distribution of virtual eggs hatched per cell (# of values per point is colour-coded) and the total number of eggs hatched in Long Point Bay by hatch date in 1999 under Scenario S2E1 conditions; spawning site selection and temperature effects on eggs.

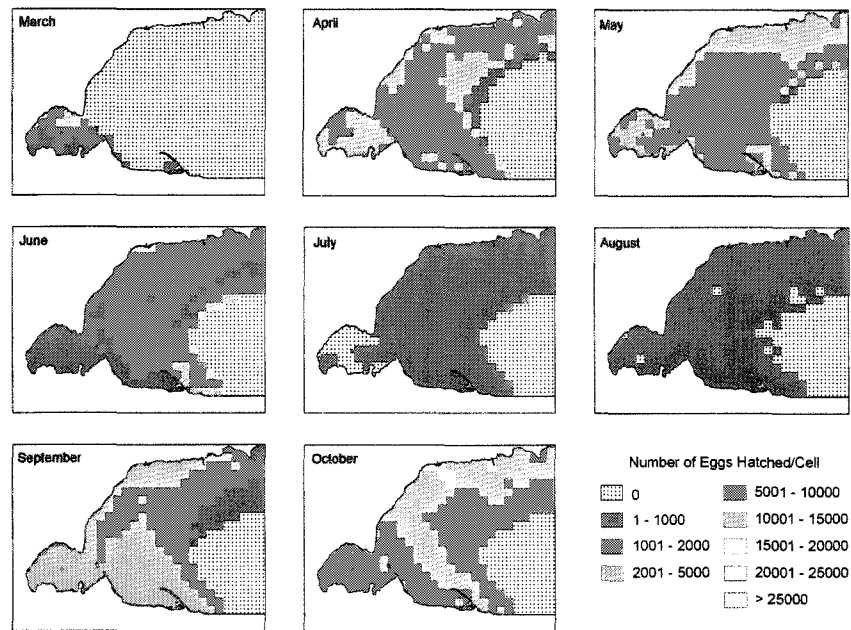


Figure 4.31: Monthly maps of the total number of virtual eggs hatched in each cell in Long Point Bay by spawning month, March until October, 1999 under Scenario S2E1 conditions.

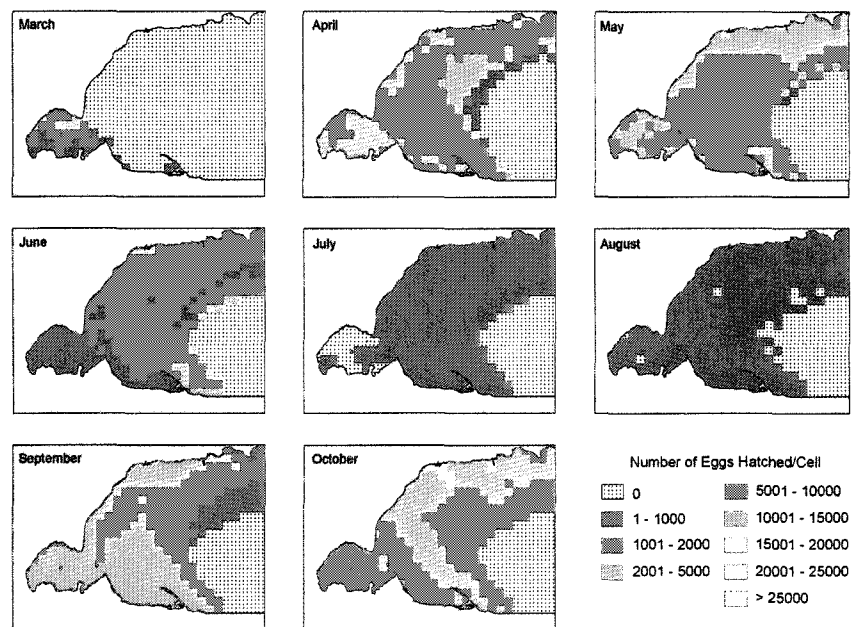


Figure 4.32: Monthly maps of the total number of virtual eggs hatched in each cell in Long Point Bay by spawning month, March until October, 1999 under Scenario S2E2 conditions.

Larval Scenario S2E1L1: Compared to the distribution of swim-up larvae (or hatched eggs) for this scenario (where there was relatively equal survivorship from both spring and fall spawning), the YOYs surviving to overwinter were reduced proportionately more in the springtime spawning group than the fall spawn in S2E1L1, probably due to reasons

discussed in S1E1L1 results (Figure 4.33). The greatest YOY survival occurred in the outer bay during April, May and October (Figure 4.34), but in different areas each month. From April spawning, a north and south shore high survival zone existed. Central and western outer bay areas were more successful areas for larvae resulting from May spawning. Inner Bay areas contributed more to yields in fall spawning months, especially in October, when most of the habitat and temperatures were suitable but larvae were also recently hatched, so thermal effects on YOY survival had not been observed yet. Time-series patterns for total production were similar to the results obtained with uniform spawning and larval habitat restriction scenarios. However, the spring cohort did not contribute as much to overall production when the larvae were limited by habitat.

Under reproductive habitat restrictions the small individuals contributed from the deep hole were eliminated and therefore summer production was reduced (Figures 4.35 & 4.36). The remaining production from the spring and fall was also reduced from the base scenario (S1E1L1). This reduction also applied to the spatial and temporal heterogeneity of larval production where less distinct zones of higher production were predicted, especially from May spawning (Figure 4.37).

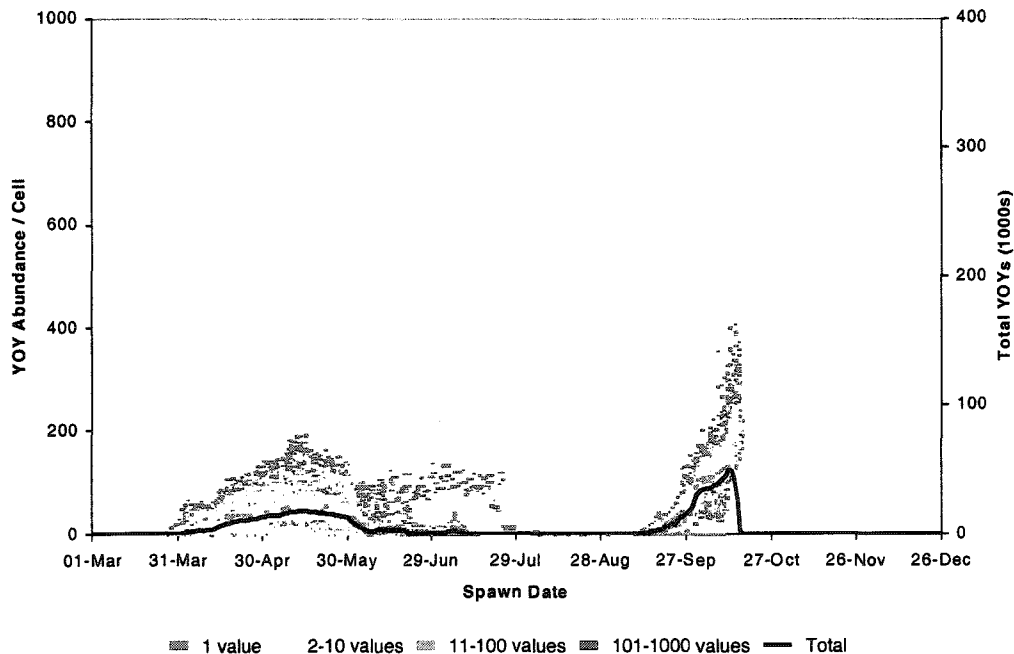


Figure 4.33: Frequency distribution by spawning date of virtual YOYs per cell (# of values is colour-coded) and the total number of YOYs that survived to October 31, 1999 in Long Point Bay under Scenario S2E1L1 conditions; spawning site selection with temperature effects on eggs & larvae.

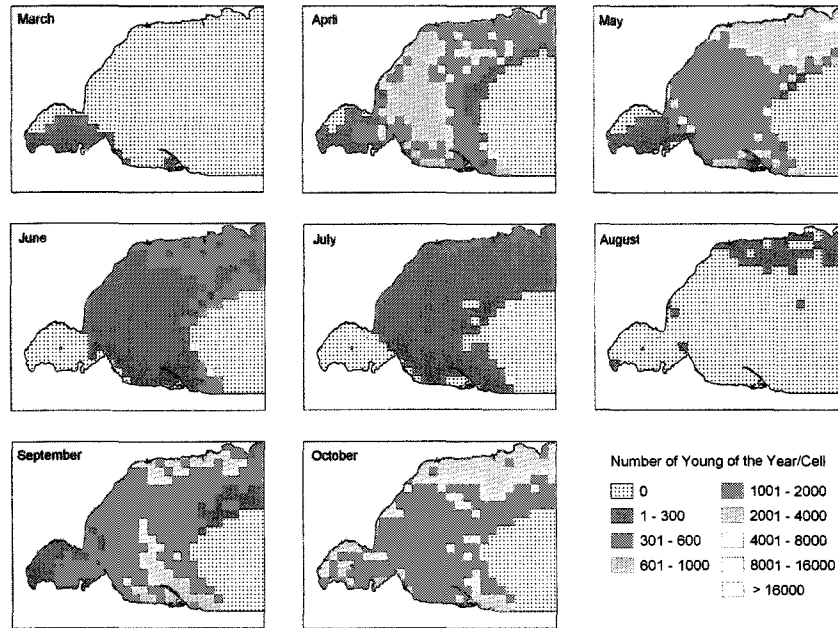


Figure 4.34: Monthly maps of the total number of virtual YOYs that survive until October 31st in each cell in Long Point Bay by spawning month, March until October, 1999 under Scenario S2E1L1 conditions.

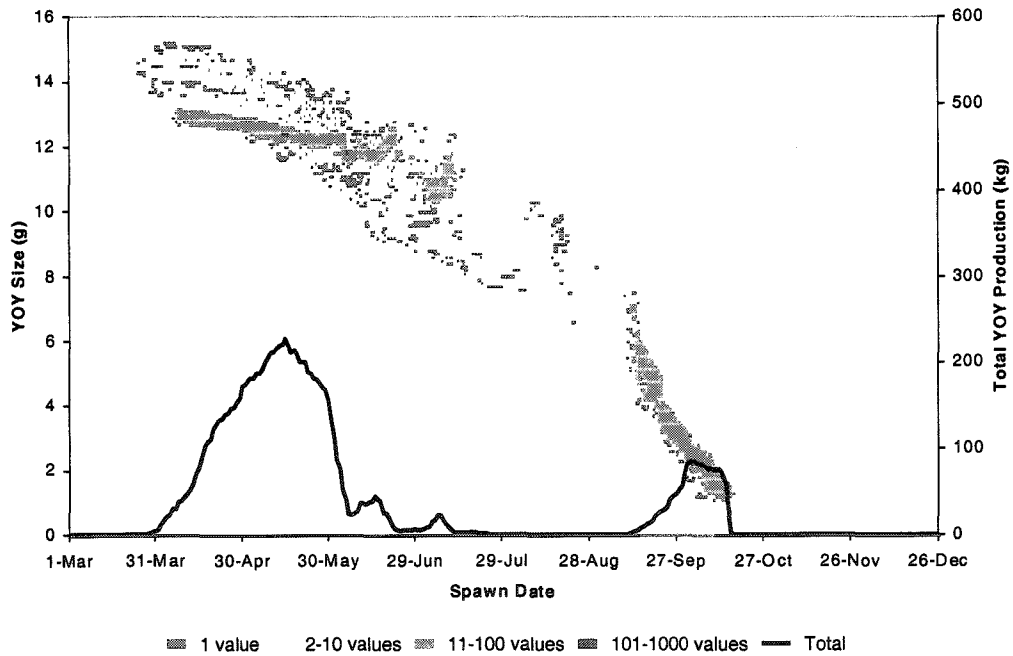


Figure 4.35: Frequency distribution by spawning date of YOY average size (g) per cell (# of values per point is colour-coded) and the total production of YOYs (kg) that survived to October 31, 1999 in Long Point Bay under Scenario S2E1L1 conditions; spawning site selection with temperature effects on eggs and larvae.

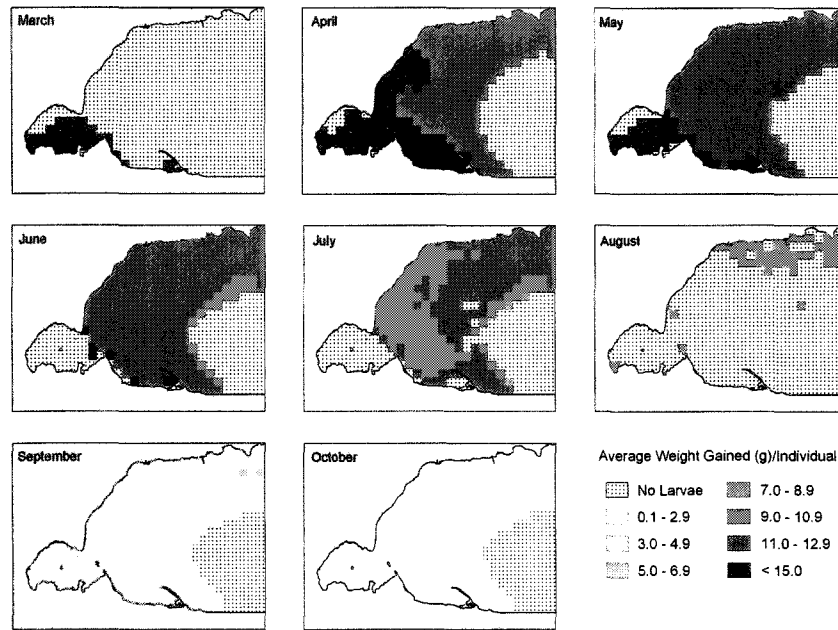


Figure 4.36: Monthly maps of the average weight gain (g) of virtual YOYs that survive until October 31st in each cell in Long Point Bay by spawning month, March until October, 1999 under Scenario S2E1L1 conditions.

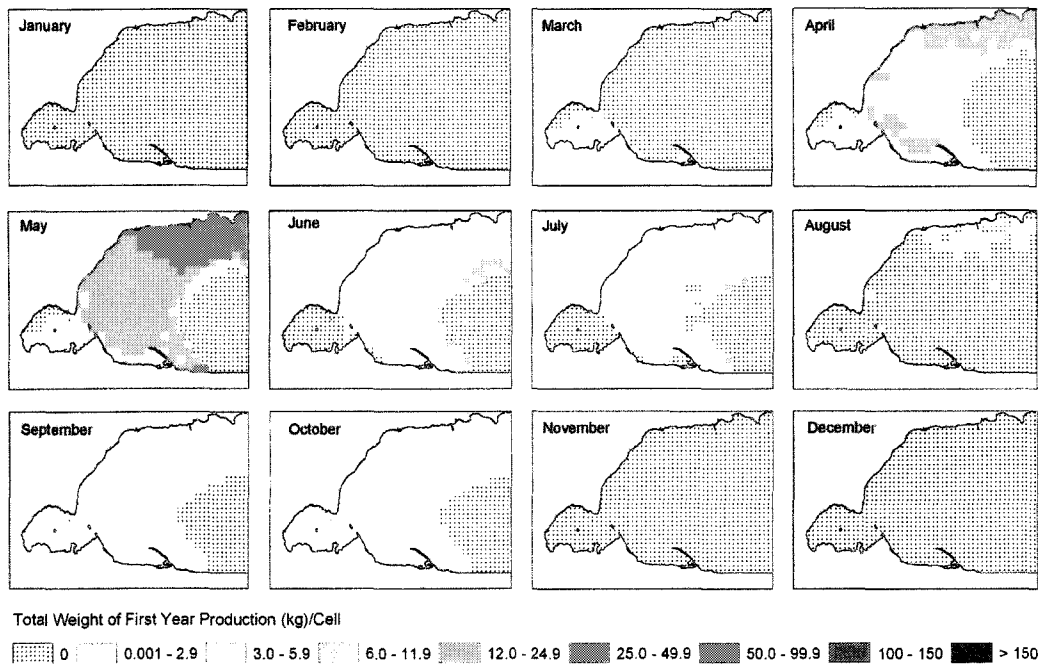


Figure 4.37: Monthly maps of the total production (kg) of virtual YOYs that survived until October 31st in each cell in Long Point Bay from the month of spawning in 1999 under Scenario S2E1L1 conditions.

Larval Scenario S2E1L2: When initial spawning was modified by local habitat suitability, instead of uniformly allocated, the same temporal pattern of surviving YOYs was produced as in Scenario S1E1L2 but with

lower overall abundances (Figure 4.38). Successful spring spawning windows lasted from April until June and were not further reduced at the egg and larval stages. Although daily survivorship to overwintering YOYs was reduced throughout the spawning year compared to YOY survivorship in scenarios without spawning habitat effects. The window for successful fall spawning to overwintering YOY narrowed to a short period in late September early October, but daily survivorship from the swim-up stage was relatively higher than for spring spawn, probably due to a longer exposure of spring larvae to different sources of mortality before overwintering; already observed in many scenarios.

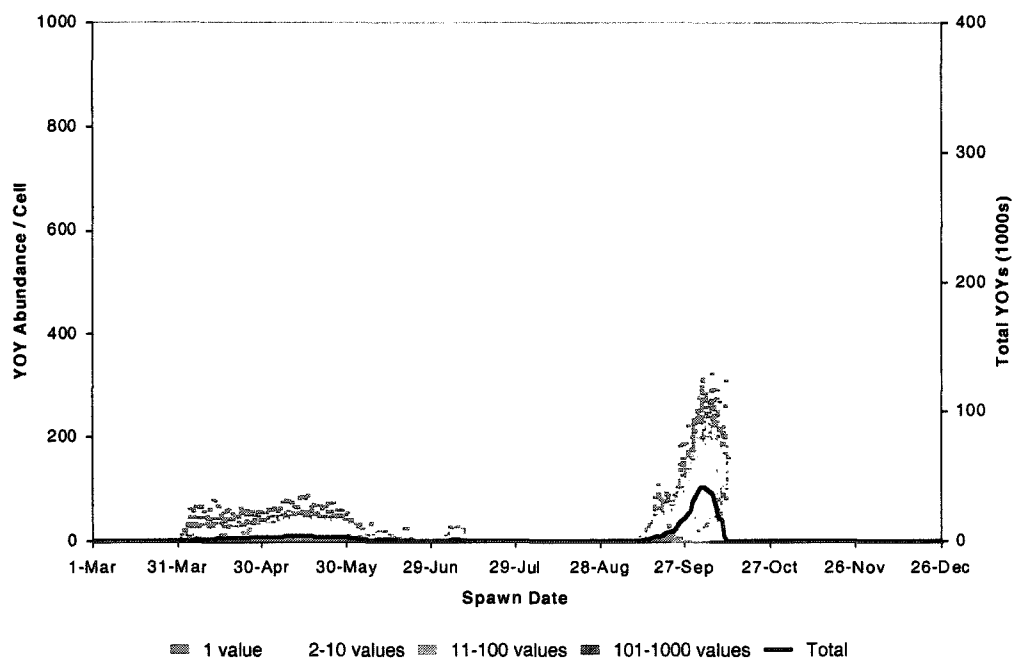


Figure 4.38: Frequency distribution by spawning date of virtual YOYs per cell (# of values per point is colour-coded) and the total YOY survival to October 31, 1999 in Long Point Bay under S2E1L2 conditions; spawning selection with thermal effects on eggs, thermal and habitat effects on larvae.

Low nearshore YOY survival was evident during the spring spawning months (Figure 4.39). In most spawning months, the south shore and sheltered areas contributed a greater proportion of YOYs to the system, with the exception of October. The growth distribution and production predicted under these scenario conditions (Figure 4.40) were very similar to S1E1L2 output. However, the smaller-sized larvae in the fall cohort disappeared, mainly because the deep hole area was no longer available for spawning due to habitat restrictions (Figure 4.41). Most larvae were produced in the Inner Bay in the fall but low individual growth was possible throughout most of the system. The highest potential growth, although reduced from maximum feeding conditions, was concentrated around nearshore, shallow areas (but not coastal) of the

outer bay. Overall YOY production was halved when habitat restrictions were placed on larvae (Figure 4.40). However, theoretical fall spawning still had higher peak larval production compared to spring spawning. Spatial patterns of production were similar to the previous larval scenario (S2E1L1) and areas of slightly higher productivity were evident in the southern half of the outer bay (Figure 4.42).

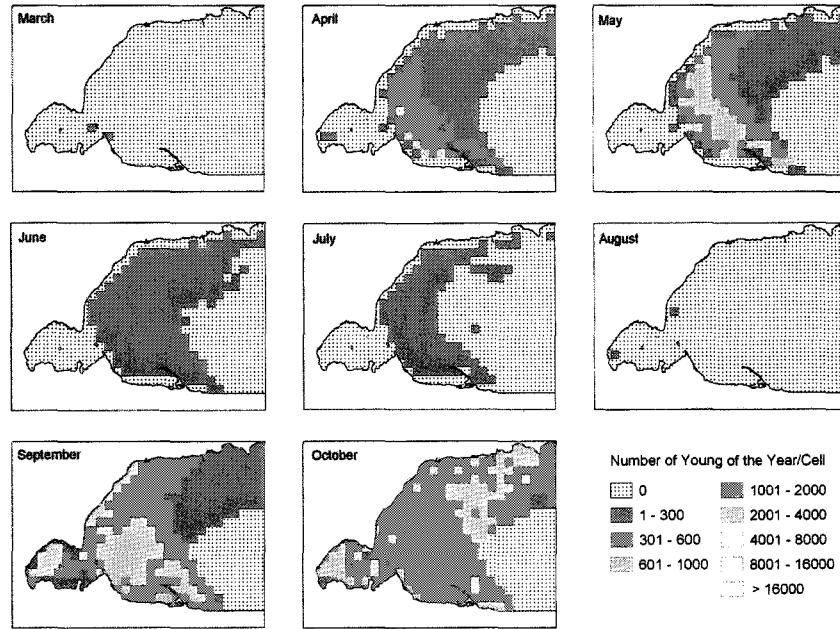


Figure 4.39: Monthly maps of the total number of virtual YOYs that survive until October 31st in each cell in Long Point Bay by spawning month, March until October, 1999 under Scenario S2E1L2 conditions.

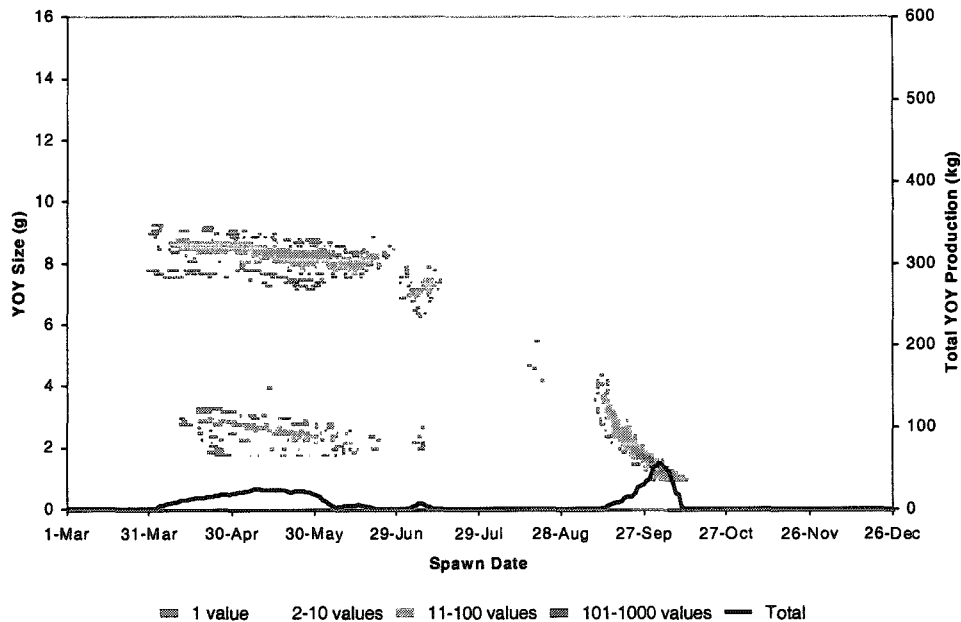


Figure 4.40: Frequency distribution by spawning date of YOY average size (g) per cell and the total production of surviving YOYs (kg) on October 31, 1999 in Long Point Bay (Scenario S2E1L2; habitat-based spawning with temperature & habitat effects on larvae.)

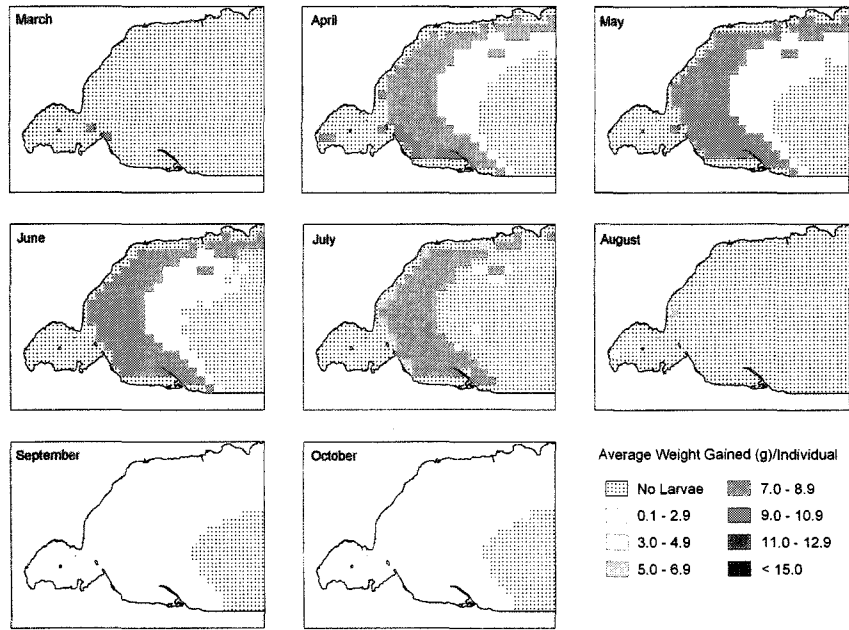


Figure 4.41: Monthly maps of the average weight gain (g) of virtual YOYs that survive until October 31st in each cell in Long Point Bay by spawning month, March until October, 1999 under Scenario S2E1L2 conditions.

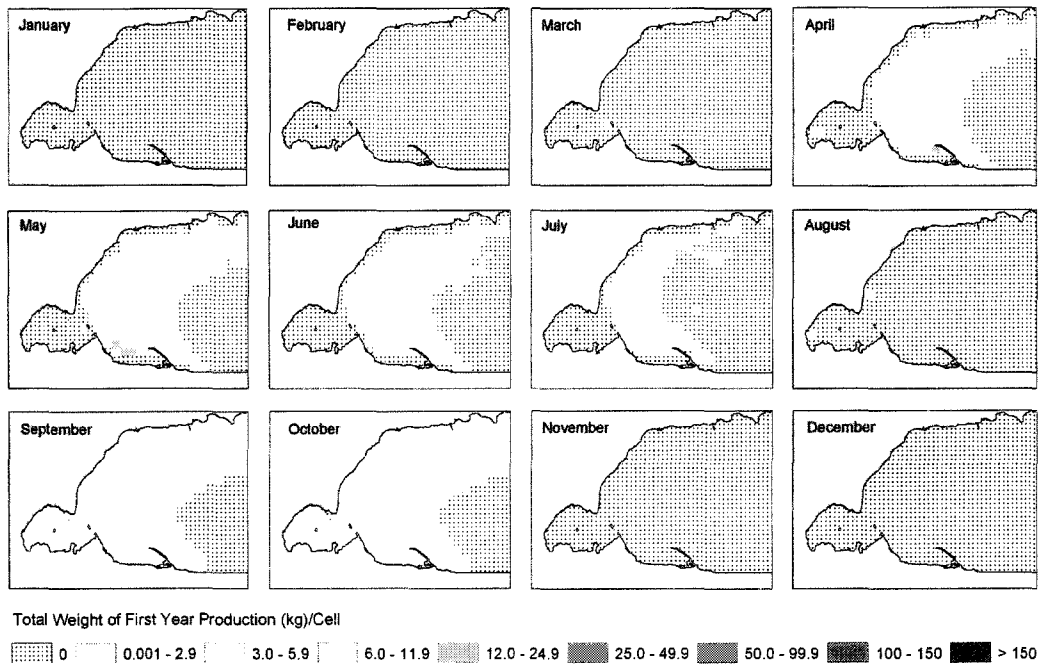


Figure 4.42: Monthly maps of the total production (kg) of virtual YOYs that survived until October 31st in each cell in Long Point Bay from the month of spawning in 1999 under Scenario S2E1L2 conditions.

Ideal-Free Initial Egg Distribution

Both Spawning Scenarios S2* and S3* dealt with an allocation of the initial reproductive effort in the whole system rather than in a particular cell depending on local conditions. These scenarios mimicked an ideal free distribution of reproductive output and also implied that spawners had knowledge of the whole system. The baseline scenario was still Scenario S1 where all habitats were treated equally. However, under ideal-free conditions, the maximum number of eggs that could be allocated to any one cell was potentially greater than 1000; up an absolute maximum of 400,000 eggs if only one cell in the system were suitable on that day.

*Spawning Scenario S2**: Only the physical characteristics, not temperature, of a site were considered in this scenario which allocated eggs based on the relative habitat suitability distribution for that day (Figure 4.43 & 4.44). The maximum number of eggs in the system was spawned each day but individual cell densities ranged from 500 to 2300 eggs /cell. The spatial distribution of reproductive effort followed the same pattern as Scenario S2 however the relative abundance of eggs spawned was much higher because the reproductive effort was not scaled by the HSI at the site-level but rather reallocated to the best available sites by a regional scale weighting.

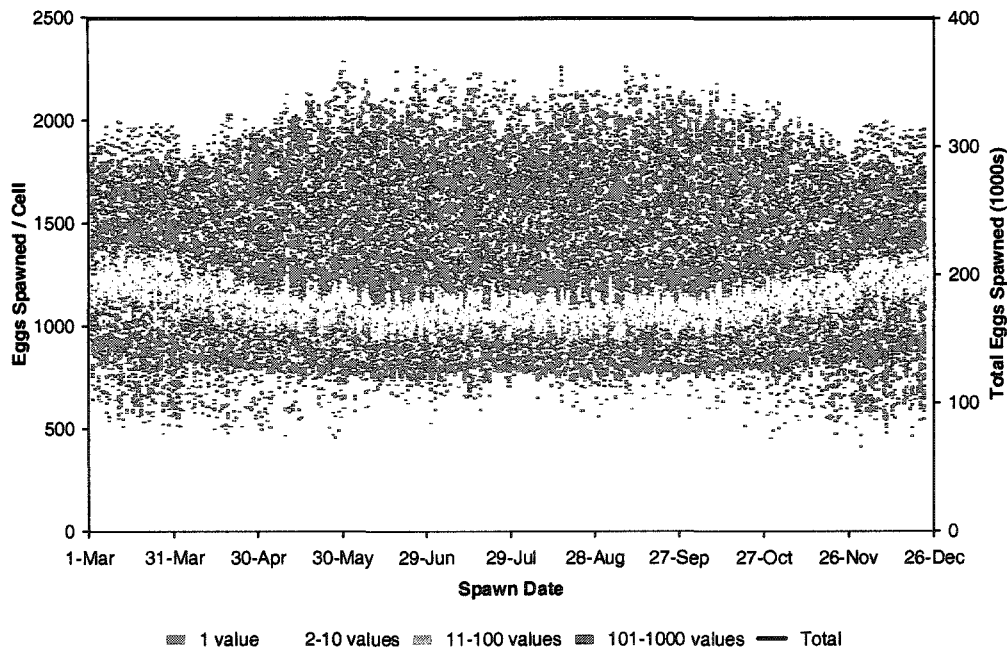


Figure 4.43: Frequency distribution of virtual eggs spawned per cell (# of values per point is colour-coded) and the total number of eggs spawned in Long Point Bay by date in 1999 under Scenario S2* conditions; habitat selection with IFD. [Note: the total is always 400,000 eggs/day.]

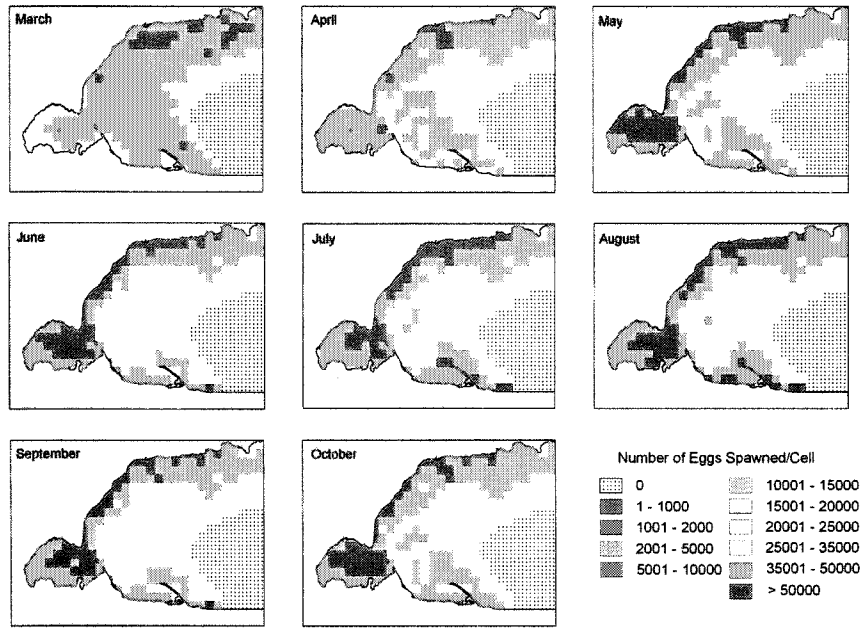


Figure 4.44: Monthly maps of the total number of virtual eggs spawned in each cell in Long Point Bay from March until October, 1999 under Scenario S2* conditions.

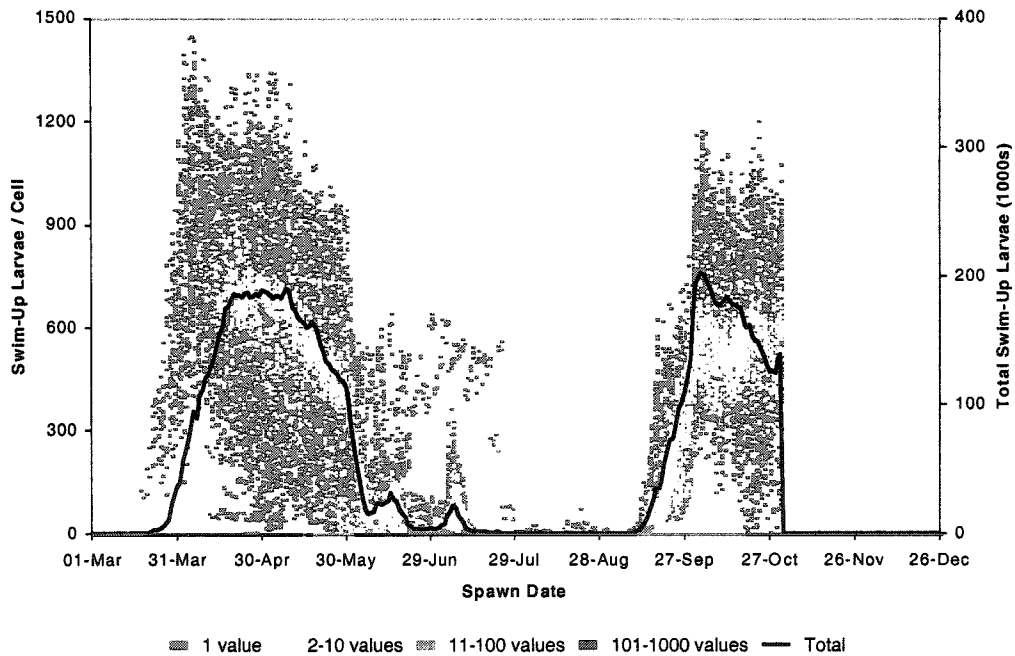


Figure 4.45: Frequency distribution of virtual eggs hatched per cell (# of values is colour-coded) and the total eggs hatched in Long Point Bay by spawning date in 1999 under Scenario S2*E1 conditions; IFD spawning and temperature effects on eggs. [Note: the X1- axis max has changed.]

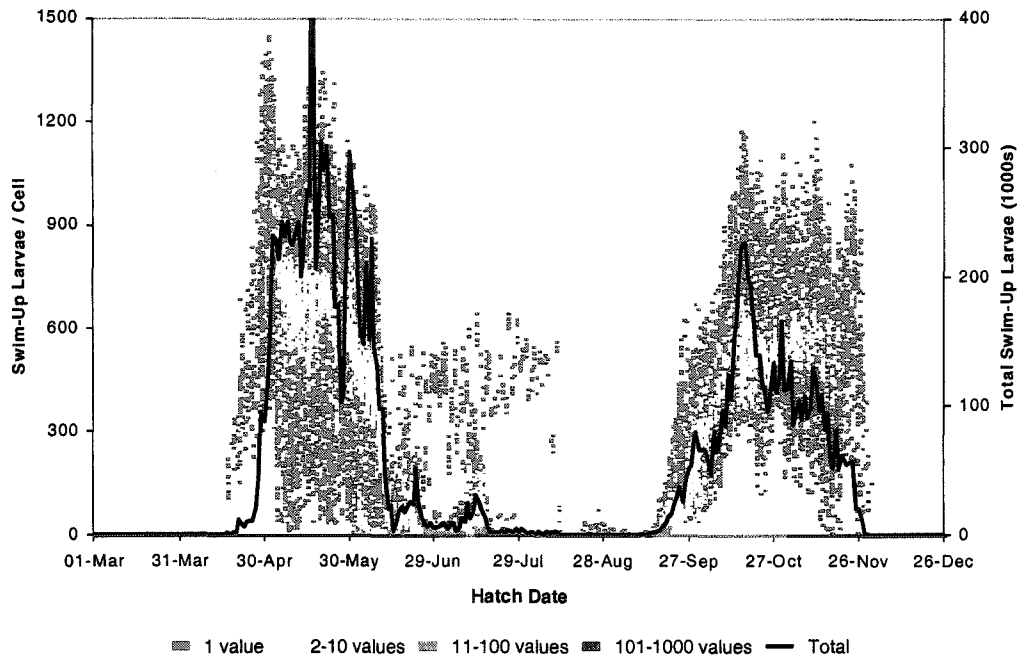


Figure 4.46: Frequency distribution of virtual eggs hatched per cell (# of values per point is colour-coded) and the total number of eggs hatched in Long Point Bay by hatch date in 1999 under Scenario S2*E1 conditions; IFD spawning site selection and temperature effects on eggs.

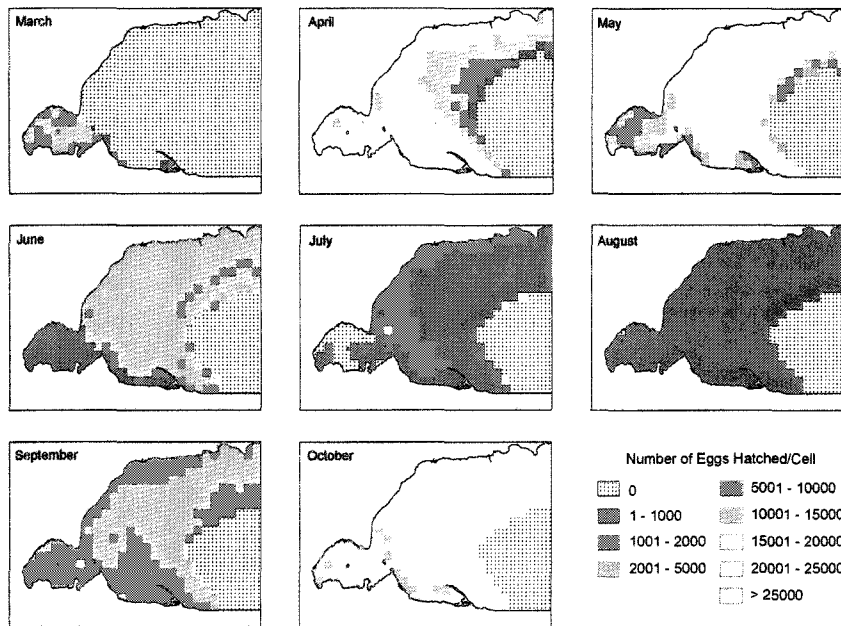


Figure 4.47: Monthly maps of the total number of virtual eggs hatched in each cell in Long Point Bay by spawning month, March until October, 1999 under Scenario S2*E1 conditions.

*Egg Scenario S2*E1:* The same temporal pattern for swim-up larvae emerged under ideal free spawning distributions as under local

modification of reproductive effort based on habitat conditions (Scenario S2E1; Figure 4.45). However, during peak survival periods, the number of surviving swim-up larvae was tripled under IFD conditions, but the temporal pattern of hatched eggs remained the same although much more variable daily (Figure 4.46). The total number of virtual eggs hatched based on their spawning month was higher and more variable but also followed the same spatial pattern as scenario S2E1 (Figure 4.47).

*Larval Scenario S2*E1L1:* With an IFD of spawning effort based on physical habitat preferences, the same patterns in larval attributes as without IFD were repeated both temporally and spatially (Figures 4.48 & 4.49). However, survivorship to YOY overwintering was doubled, mainly because the eggs allocated to each cell were doubled under this scenario. It is interesting to note that survival to hatch was tripled compared to the non-IFD scenario but subsequent survival to the YOY stage reduced the relative initial advantage of this spawning scenario. High egg abundance areas were not the same as higher YOY abundance areas.

The same range of larval size distribution emerged as under non-IFD scenario S2E1L1, with the exception that more individuals survived and therefore the distribution was more kurtotic (Figure 4.50). The larvae that gained the most weight, between 13 and 15 g under maximum consumption rates, were spawned between March and June in the Inner Bay and southwestern part of the outer bay of Long Point (Figure 4.51). Between April and June, in a large part of the outer bay (excluding the deep hole area) larvae could gain 9-13 g before winter under those thermal conditions. From July until October, if eggs were spawned, then the maximum growth possible by winter declined exponentially. Compared to other months, August had the fewest number of cells that sustained survival and growth from spawning until overwintering.

Because of higher abundances, the overall larval production was doubled compared to the non-IFD scenario (Figure 4.50). However, the spring peak was higher compared to S2E1L1, with additional small peaks in production until early July. The fall peak in production persisted in this scenario but was less than half of the production from spring spawning. When spatial patterns in growth were combined with spatial differences in survivorship of larvae to overwintering then the relative spatial contributions to production were different than potential growth patterns (Figure 4.52). The highest biomass was produced in the outer bay during April and May, especially the north shore of the outer bay, where production was mainly driven by a higher survival rate from spawning to overwintering.

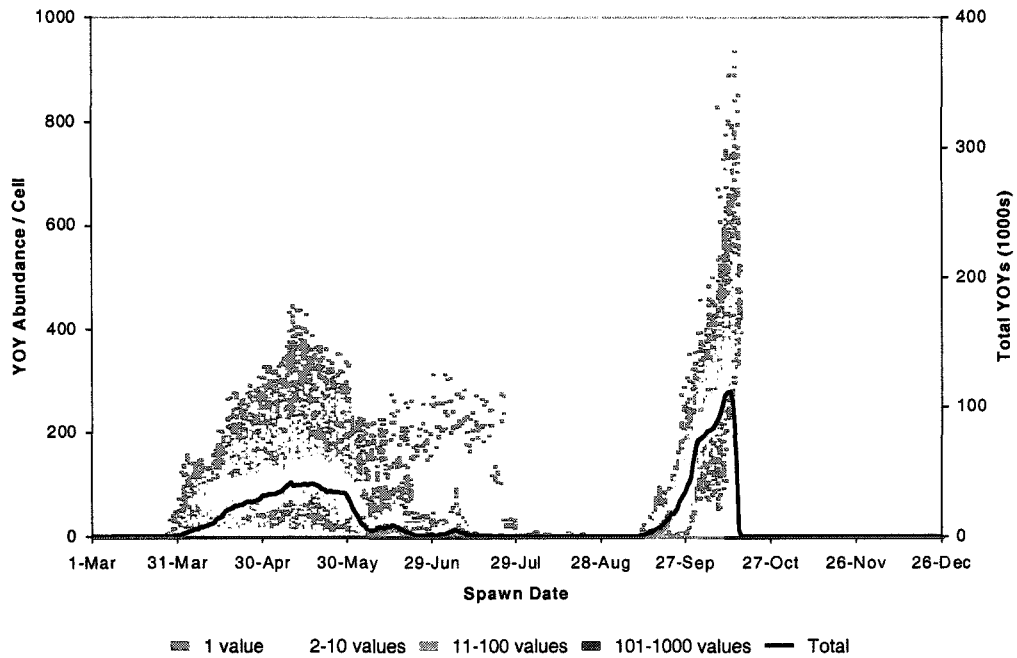


Figure 4.48: Frequency distribution by spawning date of virtual YOYs per cell (# of values per point is colour-coded) and the total YOYs that survived to October 31, 1999 in Long Point Bay under Scenario S2*E1L1 conditions; IFD spawning site selection with temperature effects on eggs & larvae.

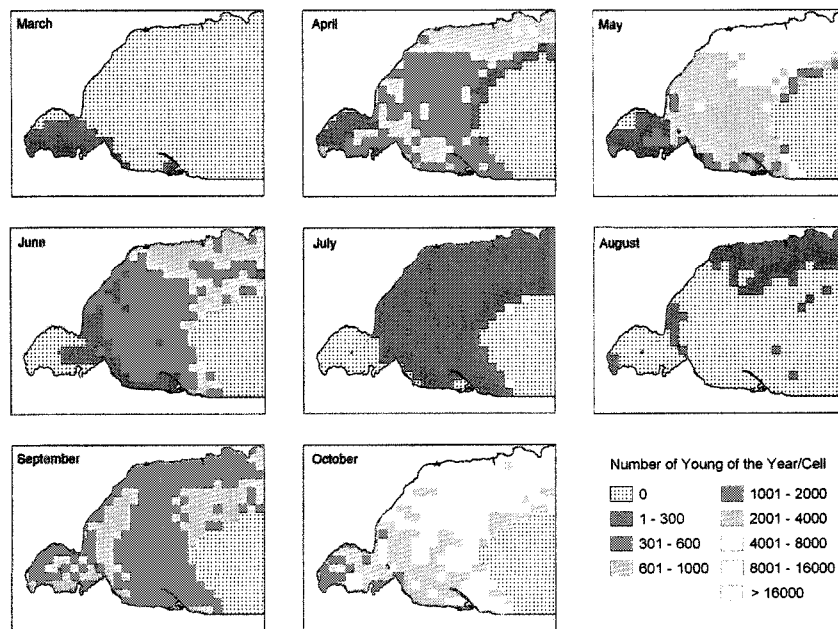


Figure 4.49: Monthly maps of the total number of virtual YOYs that survive until October 31st in each cell in Long Point Bay by spawning month, March until October, 1999 under Scenario S2*E1L1 conditions.

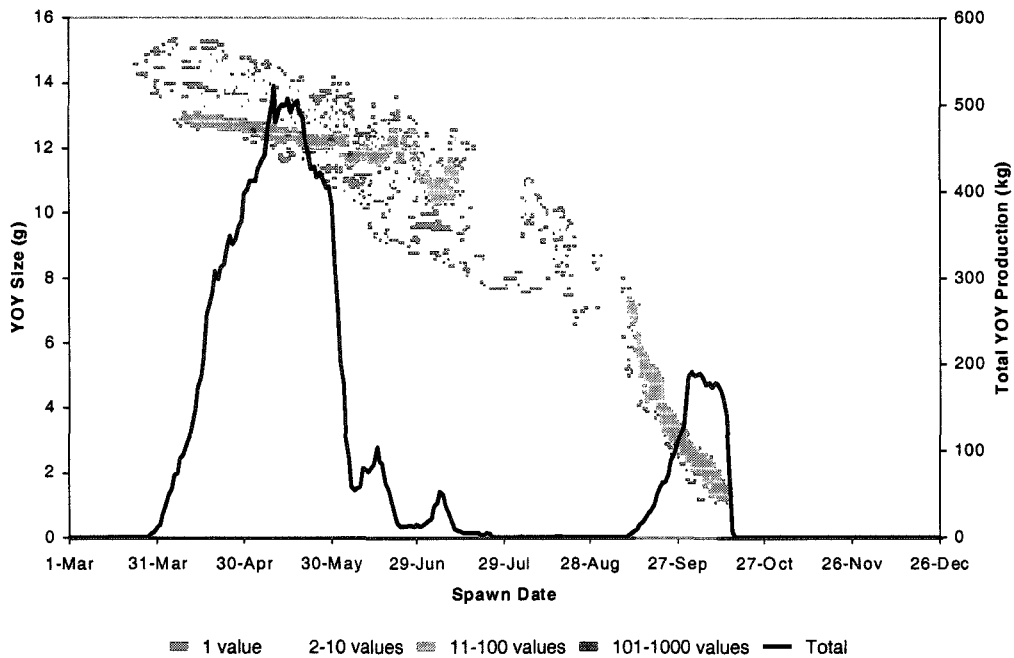


Figure 4.50: Frequency distribution by spawning date of YOY average size (g) per cell (# of values per point is colour-coded) and the total production of YOYs (kg) by October 31, 1999 in Long Point Bay (Scenario S2*E1L1 conditions; IFD spawning with temperature effects on eggs and larvae).

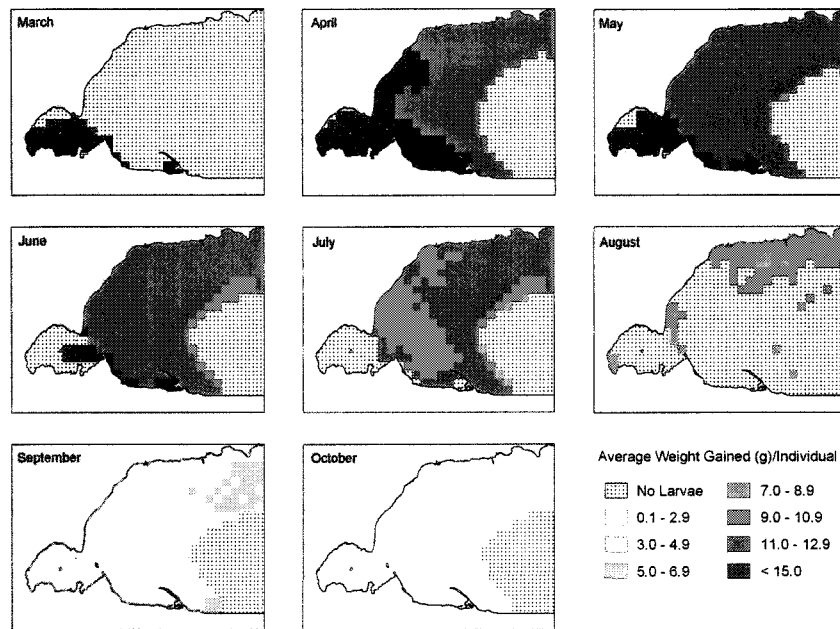


Figure 4.51: Monthly maps of the average weight gain (g) of virtual YOYs that survive until October 31st in each cell in Long Point Bay by spawning month, 1999 under Scenario S2*E1L1 conditions.

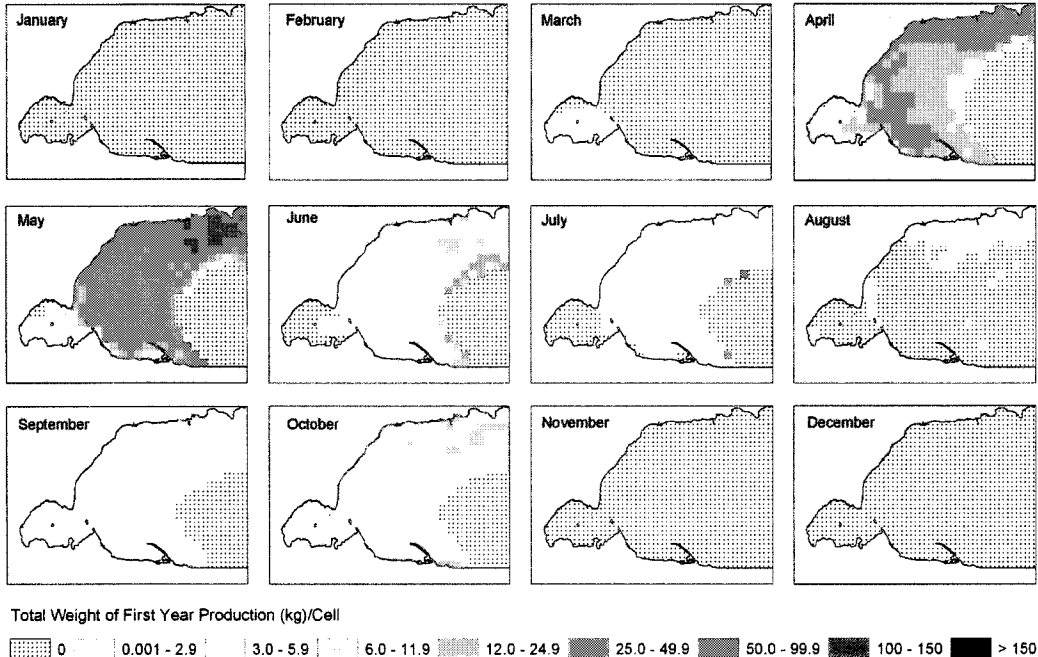


Figure 4.52: Monthly maps of the total production (kg) of virtual YOYs that survived until October 31st in each cell in Long Point Bay from the month of spawning in 1999 under Scenario S2*E1L1 conditions.

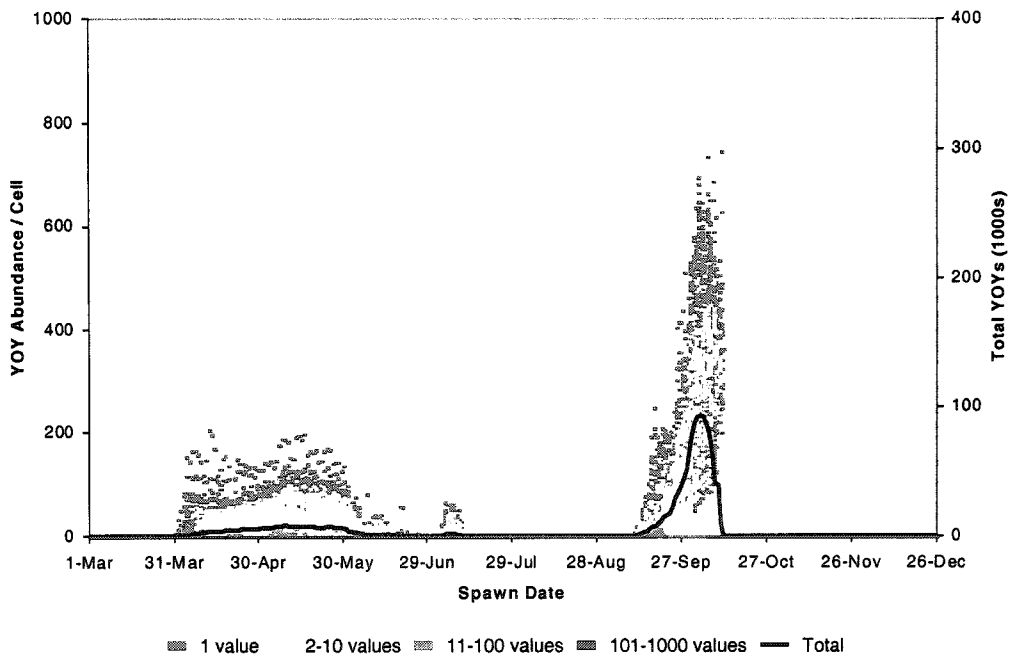


Figure 4.53: Frequency distribution of virtual YOYs per cell (# of values is colour-coded) and the total number of surviving YOYs on October 31, 1999 by spawning date in Long Point Bay. (Scenario S2*E1L2; IFD habitat-based spawning, temperature & habitat effects on larvae.)

Larval Scenario S2*E1L2: As with many previous contrasts between the different larval scenarios, disparate habitat effects on mortality and growth decreased the overall larvae abundance by the end of the year, especially those resulting from spring spawning (Figure 4.53). IFD spawning did not improve final abundances dramatically because habitat suitability was not that different. The areas of greatest survival (from spawning to over-wintering) were located slightly off the south shore of the outer bay in the springtime. In the fall, the inner and outer bays, with the exception of the deep hole, were highly productive, but only during a short period between mid-September and mid-October (Figure 4.54).

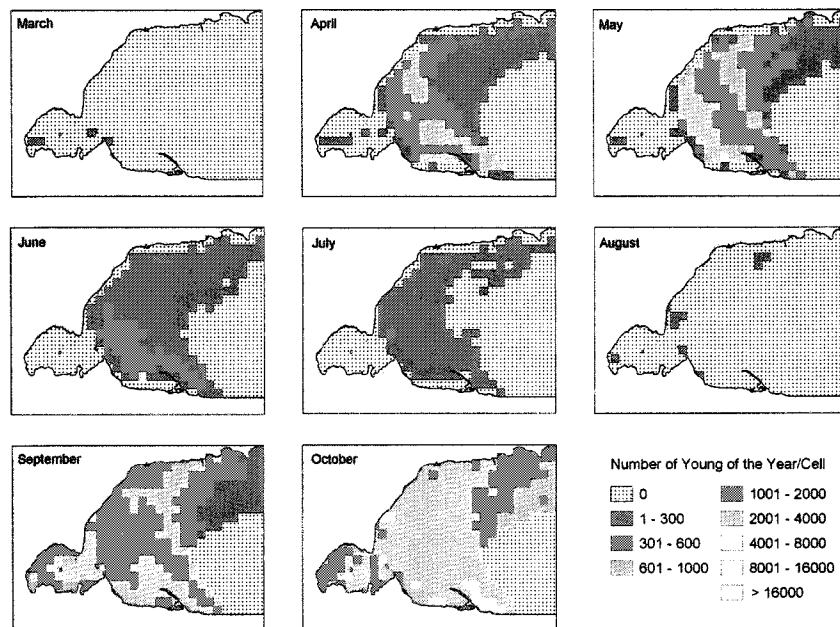


Figure 4.54: Monthly maps of the total number of virtual YOYs that survive until October 31st in each cell in Long Point Bay by spawning month, March until October, 1999 under Scenario S2*E1L2 conditions.

The final larval size distributions did not differ significantly from previous scenarios without IFD (Figure 4.55). A few more cells had surviving larvae, probably a result of a larger number of eggs being deposited. However, the same spatial distribution of relative weight gain during the same time of year was predicted. The few cells with more eggs meant that some survived until overwintering just by sheer volume (Figure 4.56).

The greater number of eggs allocated to the system resulted in double the potential larval production compared to scenario S2E1L2 but significantly reduced spring production compared to S2*E1L1 (Figure 4.55). Spatially, there was a slight expansion of high production zones compared to S2E1L1; mainly concentrated in the nearshore, but not coastal areas (which are too shallow) of the outer bay (Figure 4.57). The Inner Bay was only viable for sporadic spring but mainly fall spawning and

subsequent life stage survival.

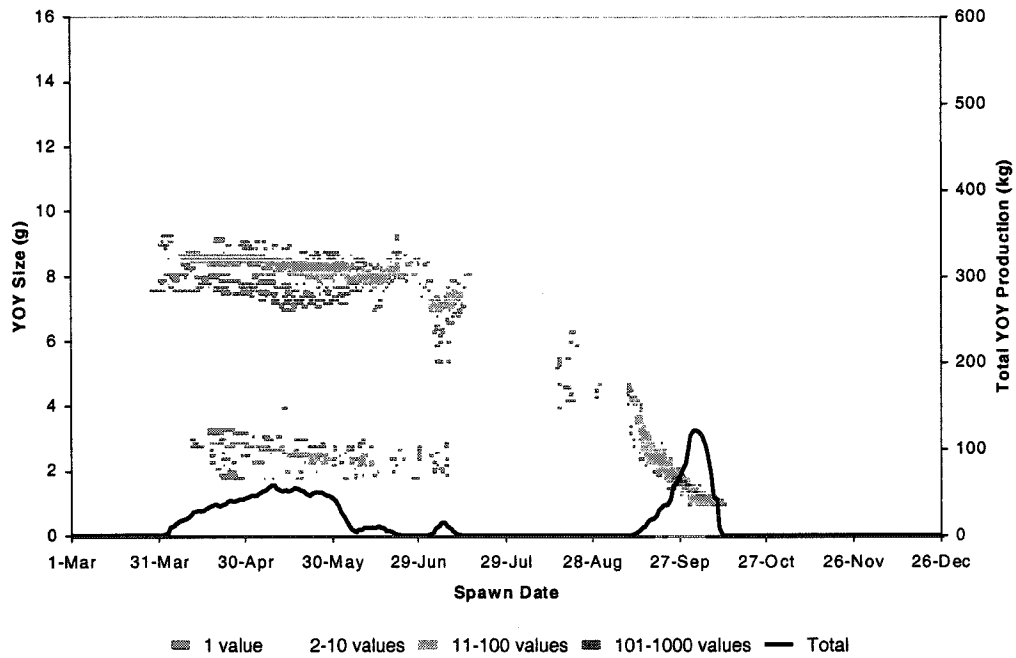


Figure 4.55: Frequency distribution by spawning date of YOY average size (g) per cell (# of values per point is colour-coded) and the total production of YOYs (kg) that survived to October 31, 1999 in Long Point Bay under Scenario S2*E1L2 conditions; IFD spawning site selection with temperature effects on eggs and temperature & habitat effects on larvae.

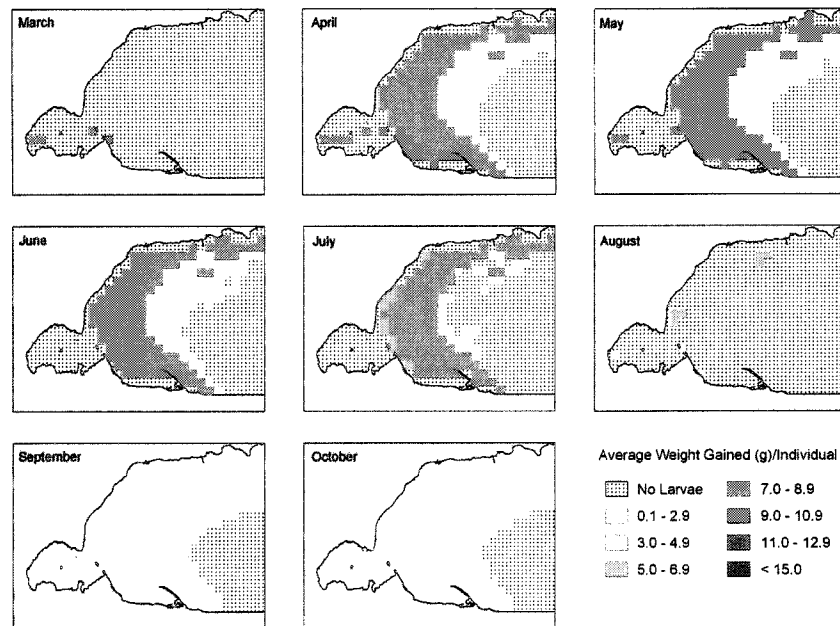


Figure 4.56: Monthly maps of the average weight gain (g) of virtual YOYs that survive until October 31st in each cell in Long Point Bay by spawning month, March until October, 1999 under Scenario S2*E1L2 conditions.

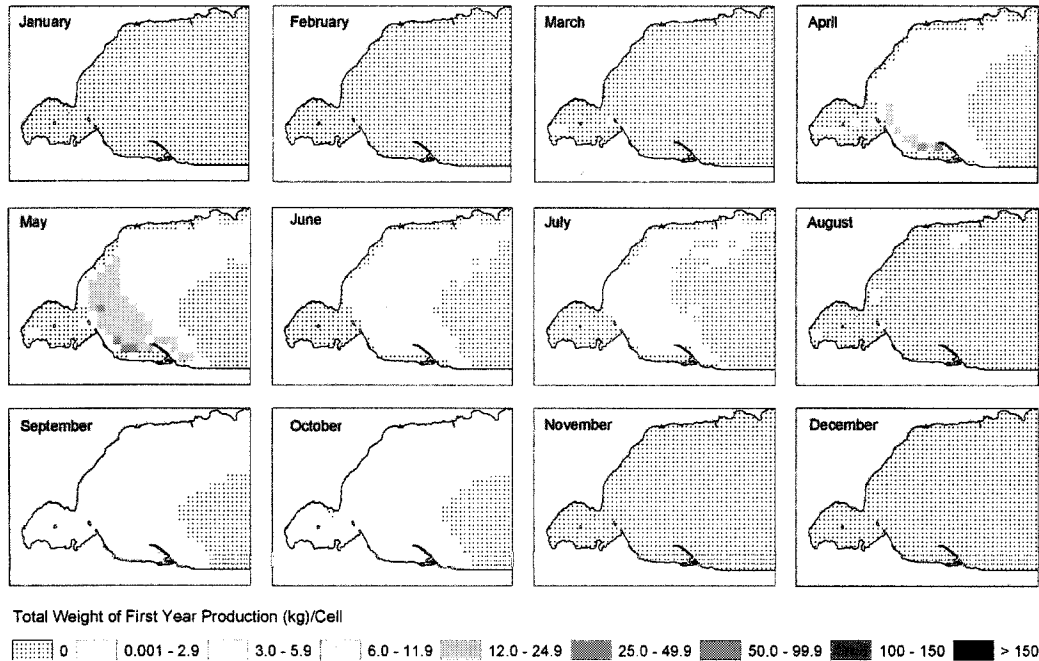


Figure 4.57: Monthly maps of the total production (kg) of virtual YOYs that survived until October 31st in each cell in Long Point Bay from the month of spawning in 1999 under Scenario S2*E1L2 conditions.

4.2.3 Thermal & Habitat-Effects Spawning, Scenario Combinations

The two types of egg distributions, equal with local habitat weighting and ideal-free with system-wide weighting, as outlined in Section 4.2.2, were tested when both thermal and habitat-effects were applied to all life stages.

Equal Initial Egg Distribution

Spawning Scenario S3: When a temperature threshold for spawning was imposed in addition to the overall physical habitat suitability of the sites, then the period for spawning, the spawning areas, and the daily reproductive allocation to the system were dramatically reduced (Figures 4.58 & 4.59). The temperature criteria for spawning depended on the thermal stability in an area for optimal egg development (5 days at 6-12 °C). Two periods in 1999 met those thermal criteria; April to May and the end of October to early December. (Keep in mind that the thermal threshold was based on absolute temperatures and not warming or cooling trends.) Egg allocation to the system was more variable under this scenario than previously. The maximum number of eggs were spawned on May 15th (90,000) and on November 10th (162,000), which is beyond the overwinter survival cutoff.

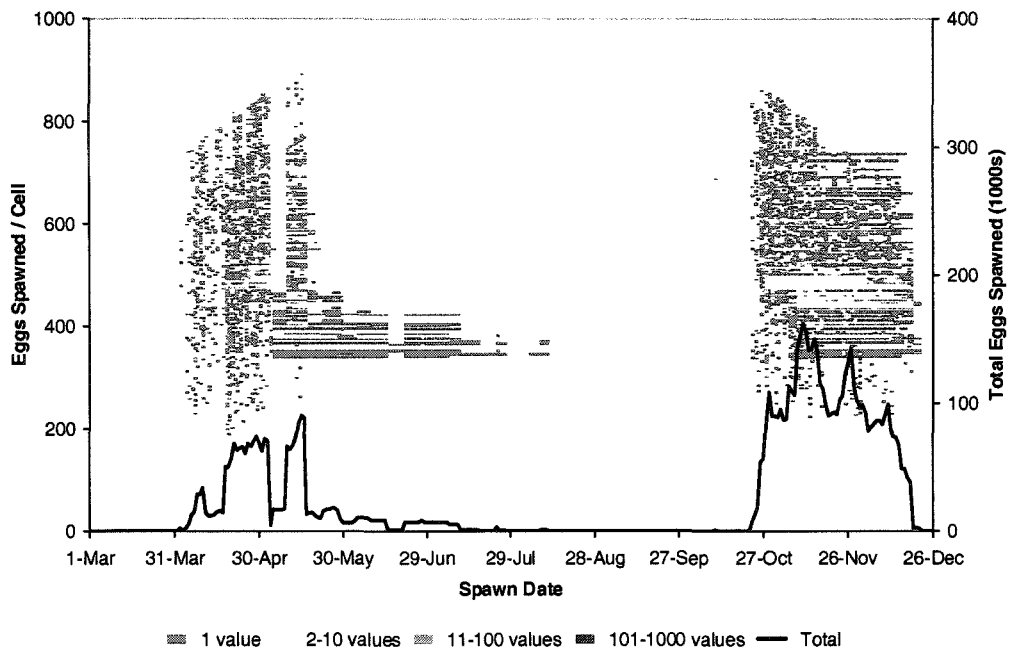


Figure 4.58: Frequency distribution of virtual eggs spawned per cell (# of values per point is colour-coded) and the total number of eggs spawned in Long Point Bay by date in 1999 under Scenario S3 conditions; habitat selection with thermal threshold.

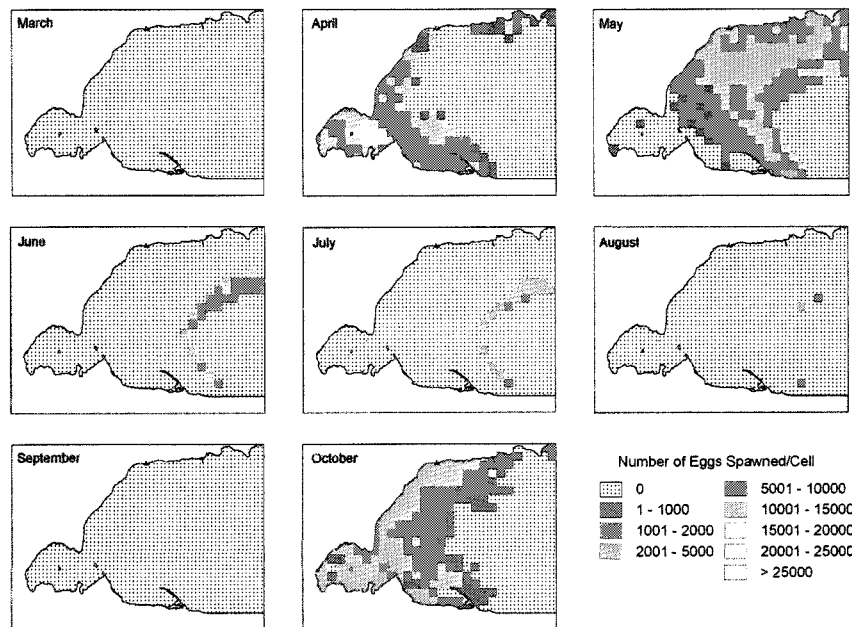


Figure 4.59: Monthly maps of the total number of virtual eggs spawned in each cell in Long Point Bay from March until October, 1999 under Scenario S3 conditions.

The Inner Bay of Long Point had the most favourable conditions for spawning in April, however became too warm by May when the offshore, but shallower areas, of the outer bay were more favourable. In June, only a narrow band of offshore substrate was thermally suitable for spawning. Nearshore areas would become thermally favourable for spawning again in October through early December.

Egg Scenario S3E1: The total number of surviving swim-up larvae in the system was dramatically reduced due to the initial number of eggs in the system constrained by thermal thresholds. Hatch abundance declined proportionately to the original number of eggs in the system, as with other scenarios (Figure 4.60). The surviving number of swim-up larvae produced in the fall was reduced due to the size criteria imposed by the model and the small number of eggs hatched before November 31st (Figure 4.61). The surviving swim-up larvae occupy the same relative spatial distribution that was defined under the spawning criteria for this scenario (Figure 4.62).

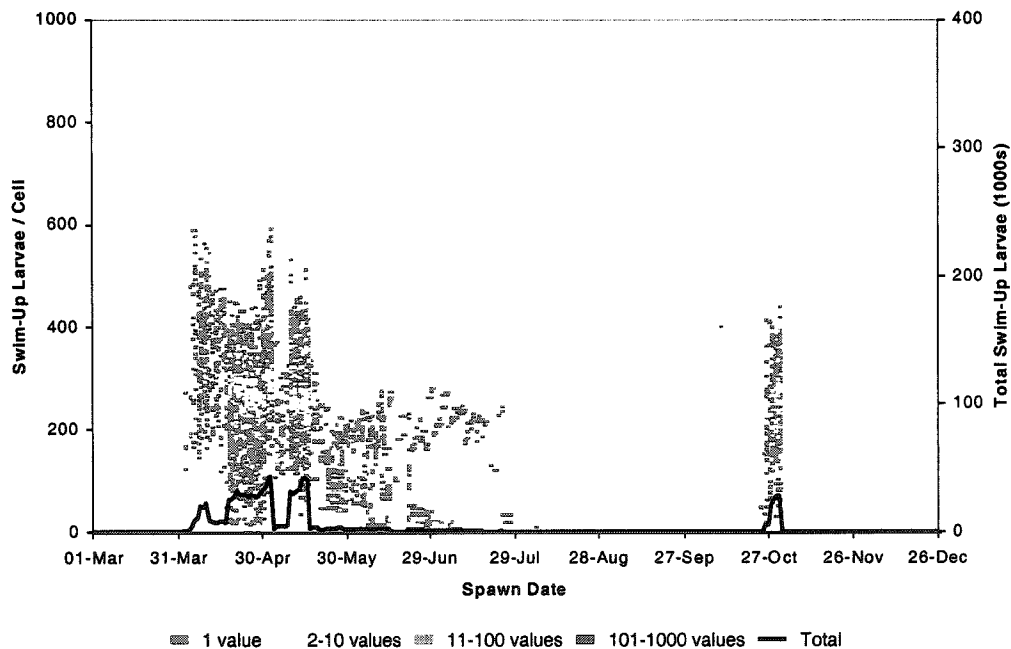


Figure 4.60: Frequency distribution of virtual eggs hatched per cell (# of values per point is colour-coded) and the total eggs hatched in Long Point Bay by spawning date in 1999 under Scenario S3E1 conditions; spawning site selection with temperature cue and temperature effects on eggs.

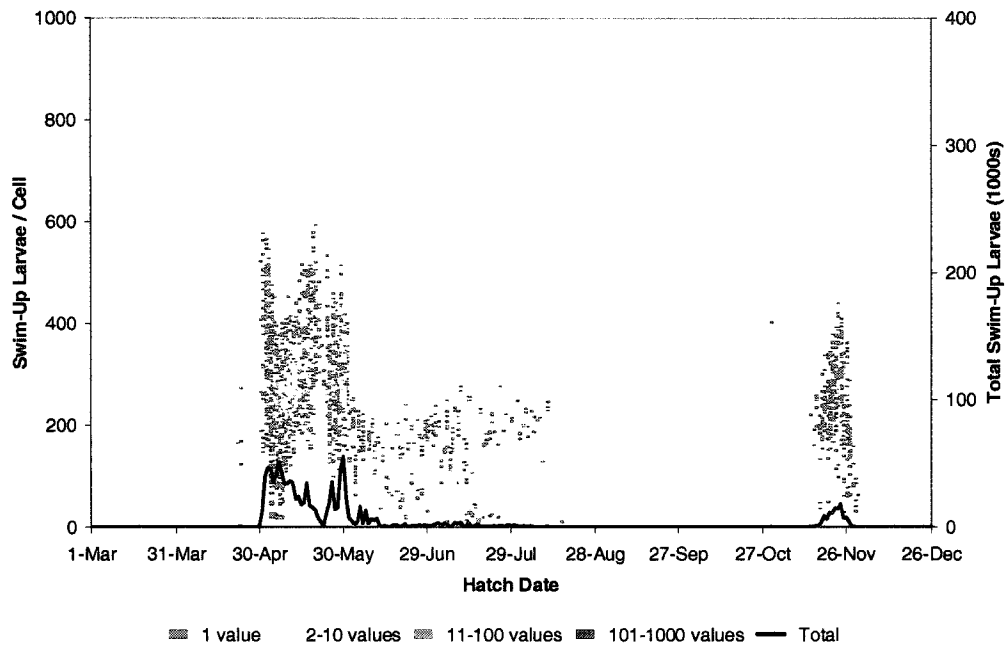


Figure 4.61: Frequency distribution of virtual eggs hatched per cell (# of values per point is colour-coded) and the total number of eggs hatched in Long Point Bay by hatch date in 1999 under Scenario S3E1 conditions; spawning site selection with temperature cue and temperature effects on eggs.

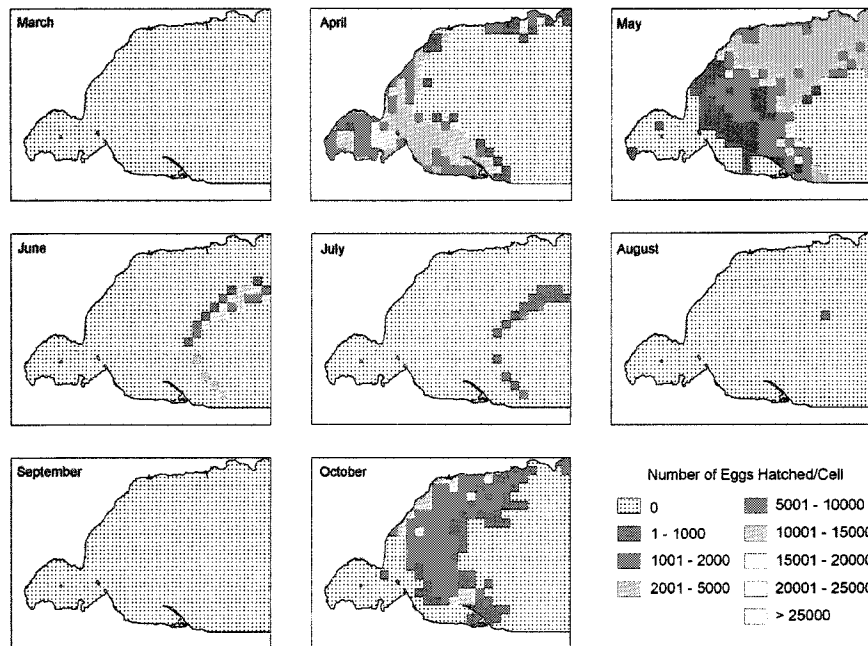


Figure 4.62: Monthly maps of the total number of virtual eggs hatched in each cell in Long Point Bay by spawning month, March until October, 1999 under Scenario S3E1 conditions.

Again, only subtle differences between scenario E1 and E2 overall swim-up survival, especially in April, were observed under 1999 habitat and thermal conditions (Figure 4.63). Proportionately, these small egg survival differences increase in significance with more habitat restrictions at the spawning stage.

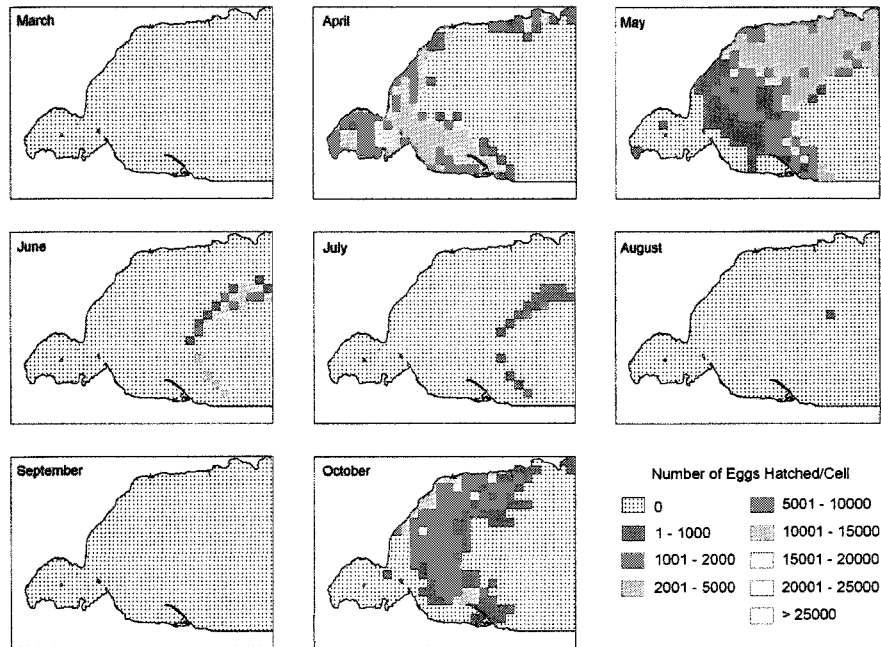


Figure 4.63: Monthly maps of the total number of virtual eggs hatched in each cell in Long Point Bay by spawning month, March until October, 1999 under Scenario S3E2 conditions.

Larval Scenario S3E1L1: After larval survival based on temperature alone was imposed, the only surviving virtual larvae at the overwintering stage were spawned between April and July, but predominantly in May (Figure 4.64). The total abundance of individuals was dramatically reduced compared to other scenarios. Successful spawning and rearing areas move progressively from the Inner Bay to deeper waters through the spring months. Fall spawning and larval survival was not sustainable under these conditions (Figure 4.65).

The final size distribution of YOYs at the end of October ranged from 7.5 to 15 g with the average larvae weighing 12 g (Figure 4.66). A near linear distribution of final sizes with reduced daily variability throughout the spawning time was produced with the addition of the thermal threshold.

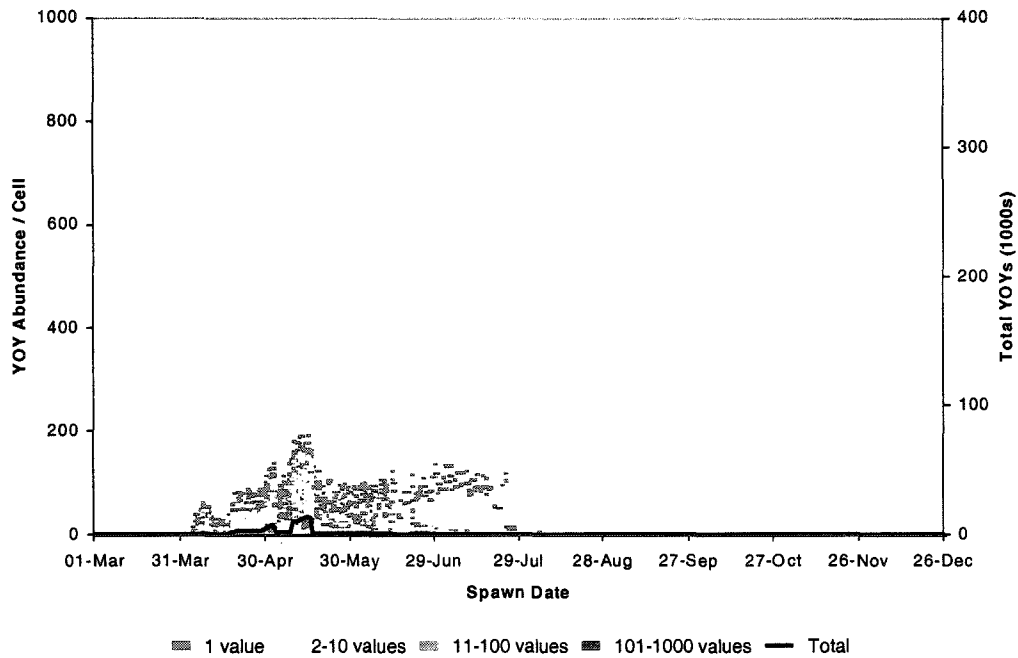


Figure 4.64: Frequency distribution by spawning date of virtual YOYs per cell (# of values per point is colour-coded) and the total number of YOYs that survived to October 31, 1999 in Long Point Bay under Scenario S3E1L1 conditions; spawning site selection with thermal cue and temperature effects on eggs & larvae.

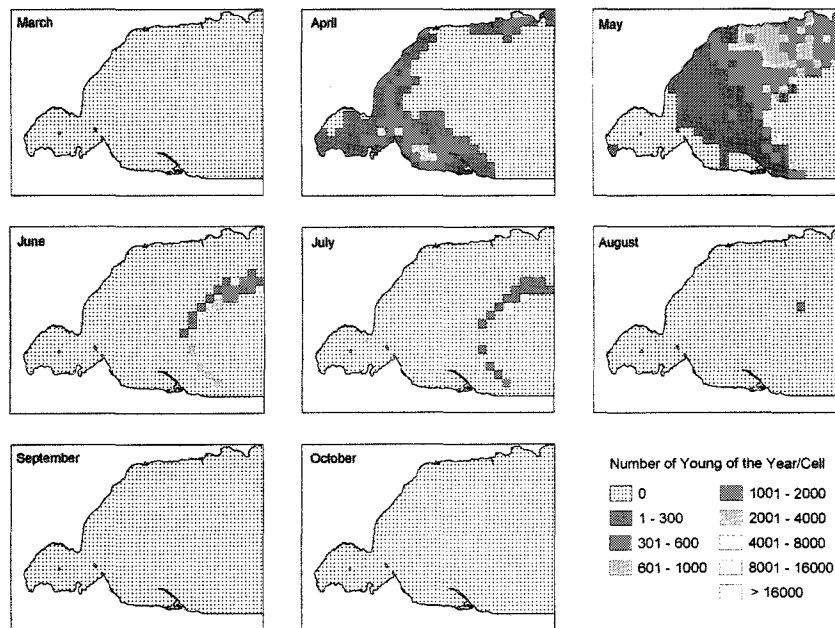


Figure 4.65: Monthly maps of the total number of virtual YOYs that survive until October 31st in each cell in Long Point Bay by spawning month, March until October, 1999 under Scenario S3E1L1 conditions.

The highest weight gain was experienced by early-spawned fish in the Inner Bay and nearshore, outer bay areas (Figure 4.67). A larger, highly suitable area became available in the outer bay in May than in April, which had localised pockets of higher growth but less distinct zones. Larvae from spring spawning were relegated to a thin band of midwater maximum depths in the outer bay in order to successfully complete all first-year life stages.

Several peaks in larval production (different from previous patterns) were produced from spring spawning, but the strongest contribution came from an early May cohort (Figure 4.66). Thermal thresholds on spawning reduced overall productivity dramatically because of low suitability weighting for local conditions. Relatively, the south shore in April and the north shore in May were relatively the most productive areas. However, overall spawning was dramatically reduced from the base scenario because of thresholds and initial spawning restrictions (i.e. local versus system-wide allocation of reproductive effort; Figure 4.68).

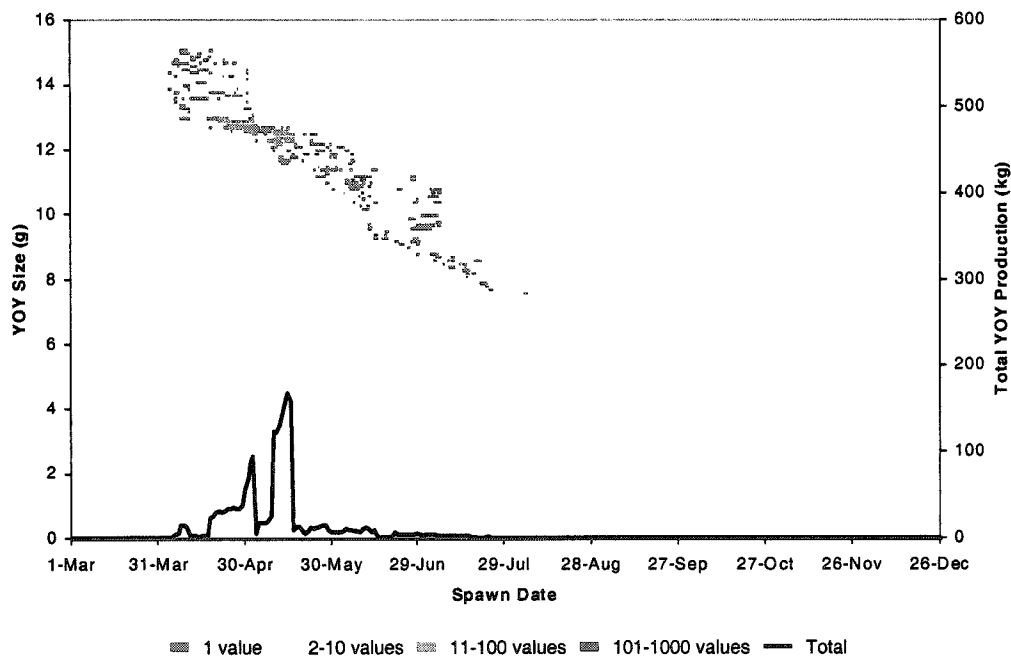


Figure 4.66: Frequency distribution by spawning date of YOY average size (g) per cell (# of values per point is colour-coded) and the total production of YOYs (kg) that survived to October 31, 1999 in Long Point Bay under Scenario S3E1L1 conditions; spawning site selection with temperature cue and temperature effects on eggs and larvae.

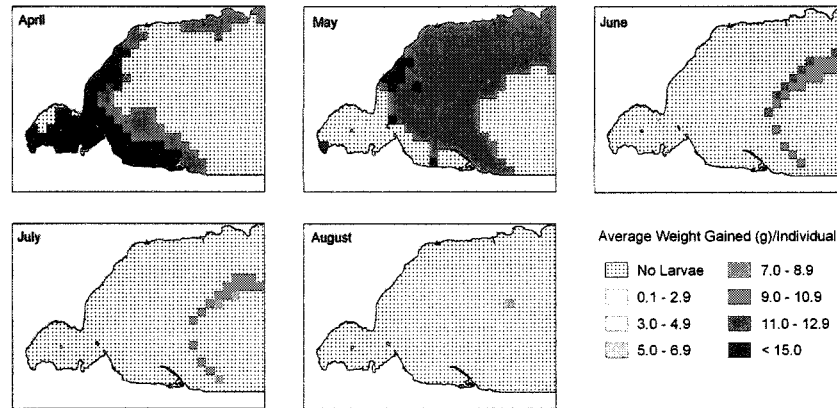


Figure 4.67: Monthly maps of the average weight gain (g) of virtual YOYs that survive until October 31st in each cell in Long Point Bay by spawning month, April until August, 1999 under Scenario S3E1L1 conditions.

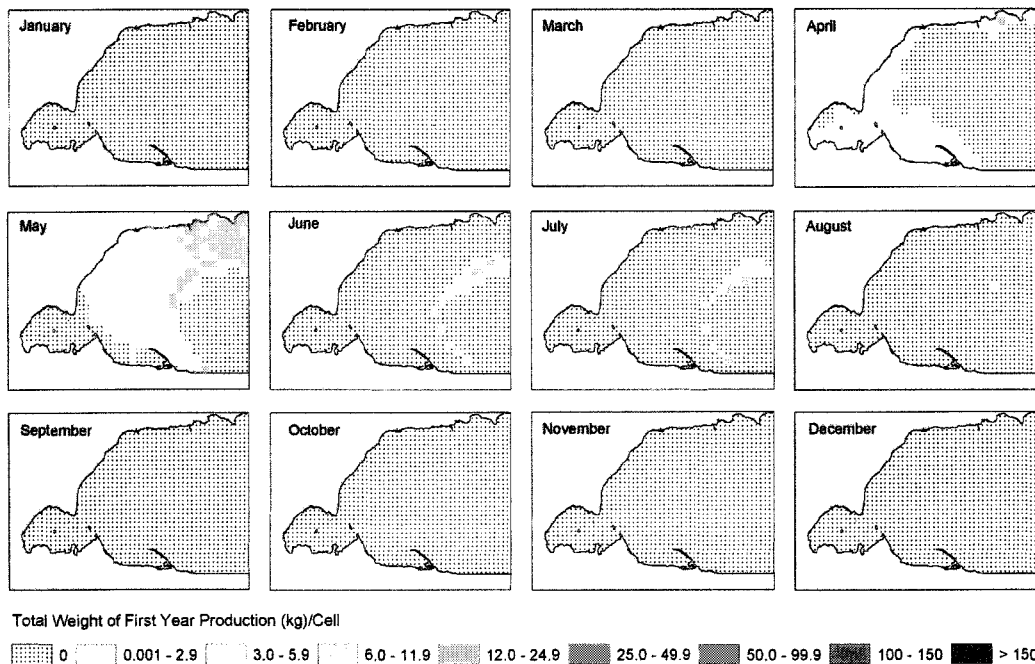


Figure 4.68: Monthly maps of the total production (kg) of virtual YOYs that survived until October 31st in each cell in Long Point Bay from the month of spawning in 1999 under Scenario S3E1L1 conditions.

Larval Scenario S3E1L2: Under full habitat and thermal restrictions, the number of surviving YOYs and the period during which spawning to overwintering was successful was greatly reduced (Figure 4.69). Spawning in April on the south shore of the outer bay was the most productive area for both spawning and nursery habitat combined (Figure 4.70), although less than 100 individuals / cell or 10% of spawned eggs survived. Under this scenario, the fall spawning cohort would not survive the larval stage because of a mismatch between thermal preferences and habitat-based food availability in the outer bay region.

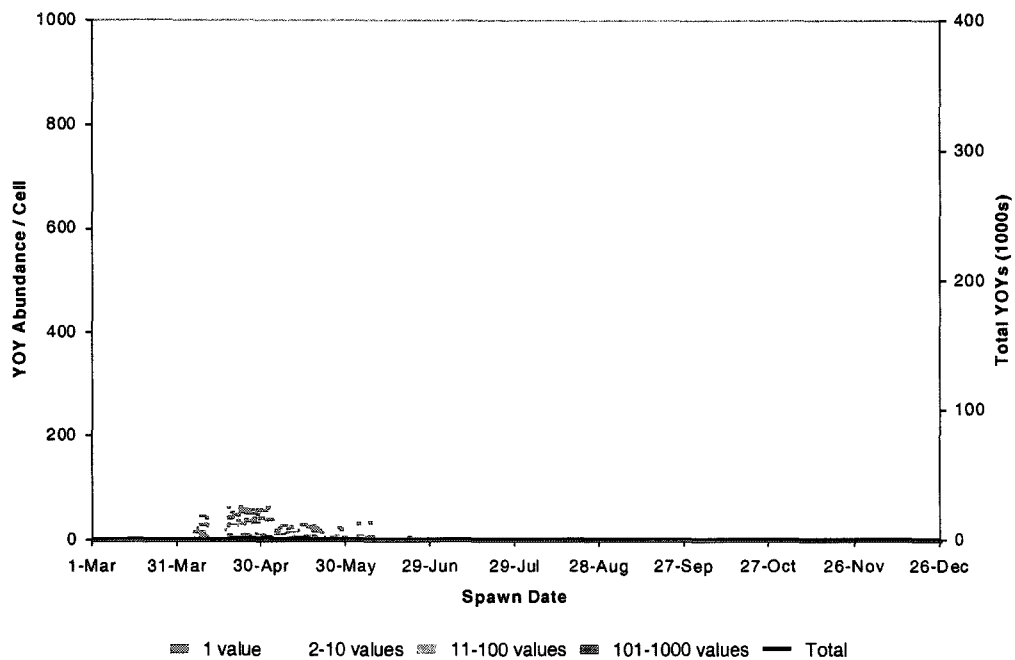


Figure 4.69: Frequency distribution by spawning date of virtual YOYs per cell (# of values per point is colour-coded) and the total number of YOYs that survived to October 31, 1999 in Long Point Bay under Scenario S3E1L2 conditions; spawning site selection with temperature cue, temperature effects on eggs, and temperature & habitat effects on larvae.

Under thermal spawning restrictions, the duration of successful spawning was limited from April to June, when two distinctly-sized cohorts survived until the end of October because of larval habitat restrictions (Figure 4.71). A faster-growing cohort ranged in size from 8 – 9.5 g and a slower-growing cohort maintained sizes of 2 - 4 g through the year. Larvae that were spawned in April had the best growth in selected areas: the outer bay along the spit up to the 5 m depth contour, at the mouth of Big Creek, and along the north shore closer to Nanticoke (Figure 4.72). Two size cohorts developed from May spawning, one nearshore and one midwater group.

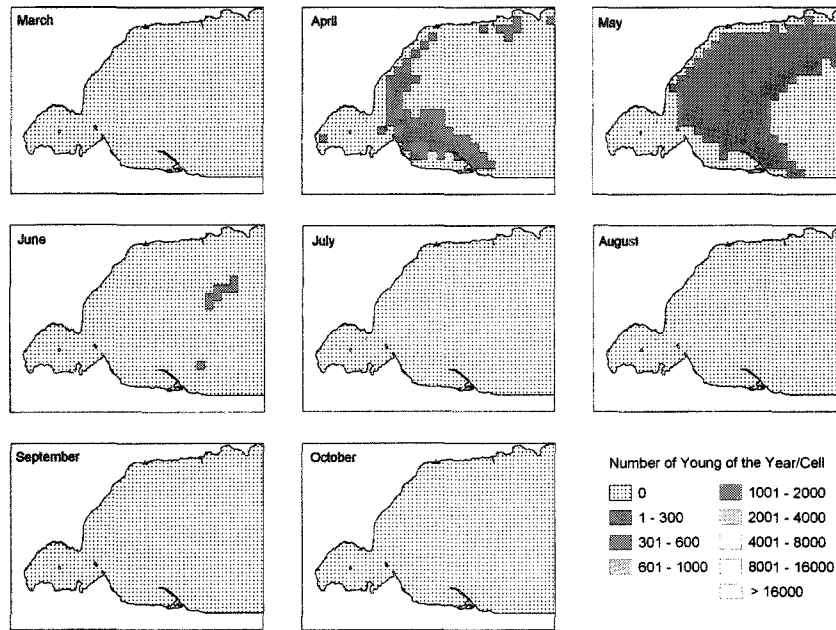


Figure 4.70: Monthly maps of the total number of virtual YOYs that survive until October 31st in each cell in Long Point Bay by spawning month, March until October, 1999 under Scenario S3E1L2 conditions.

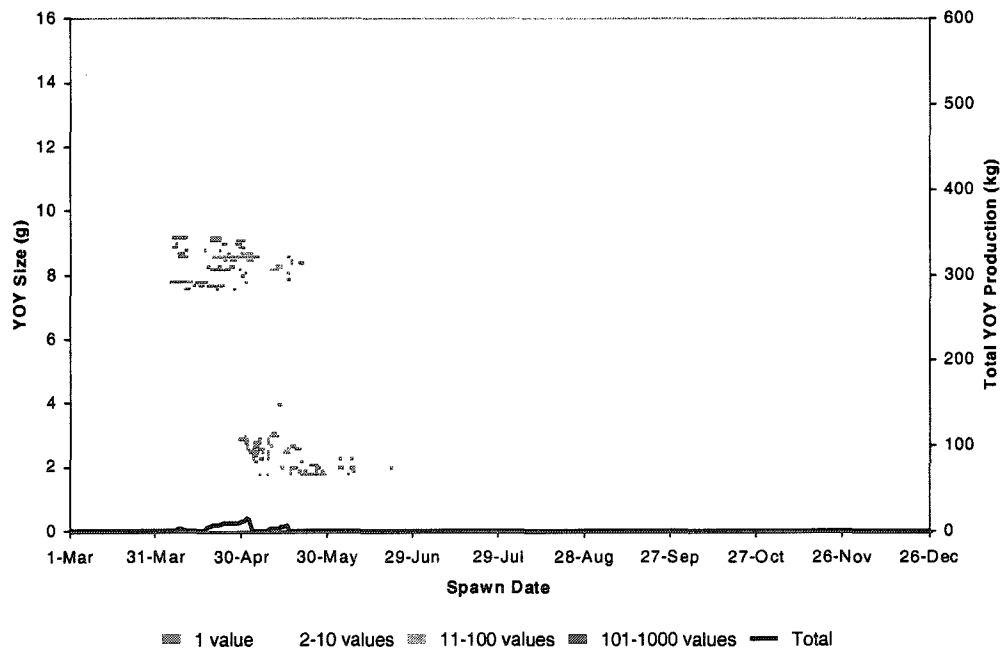


Figure 4.71: Frequency distribution by spawning date of YOY average size (g) per cell (# of values per point is colour-coded) and the total production of YOYs (kg) that survived to October 31, 1999 in Long Point Bay under Scenario S3E1L2 conditions; spawning site selection with temperature cue, temperature effects on eggs and temperature & habitat effects on larvae.

This scenario had the lowest larval production. Production peaked at the end of April under full habitat constraints (Figure 4.71). The best time for spawning to occur and ensure survival to the YOY overwinter stage was in April to May. Spatially, the south shore of the outer bay emerged as the best area for survival of consecutive stages and for overall production under these conditions (Figure 4.73).

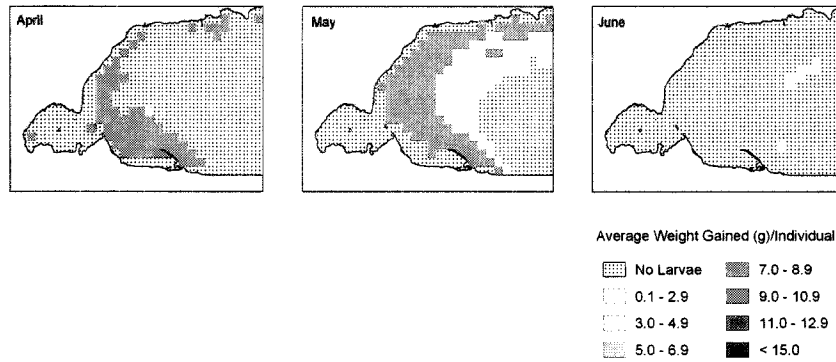


Figure 4.72: Monthly maps of the average weight gain (g) of virtual YOYs that survive until October 31st in each cell in Long Point Bay by spawning month, April until June, 1999 under Scenario S3E1L2 conditions.

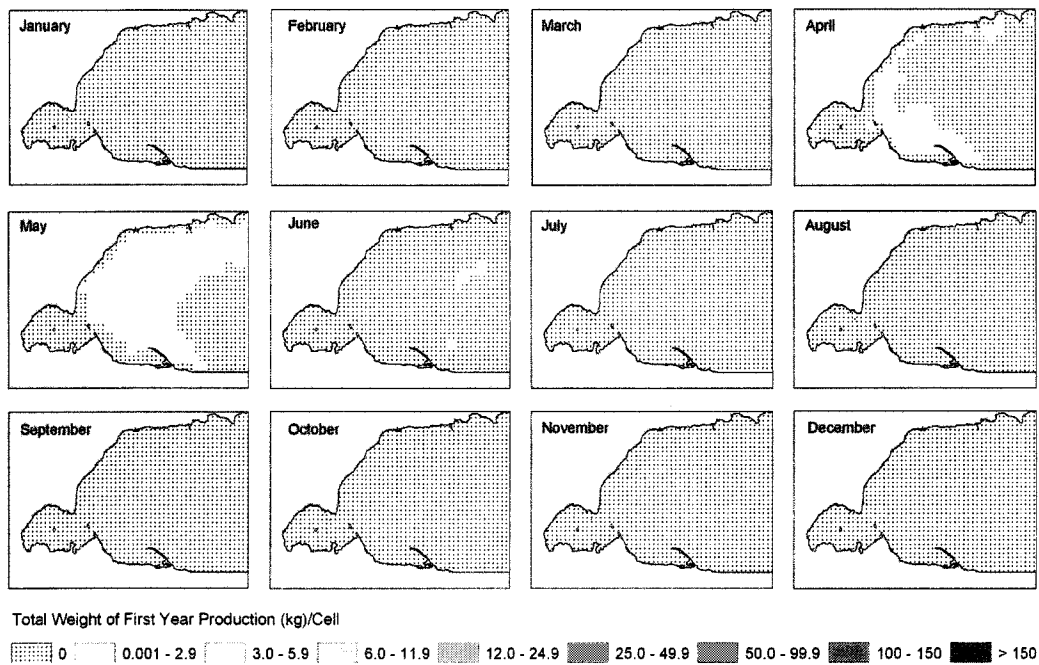


Figure 4.73: Monthly maps of the total production (kg) of virtual YOYs that survived until October 31st in each cell in Long Point Bay from the month of spawning in 1999 under Scenario S3E1L2 conditions.

Ideal-Free Initial Egg Distribution

Spawning Scenario S3*: Under thermal threshold scenarios, the number of cells available for reproduction decreased substantially for most of the year (Figure 4.74). However, ideal free distribution of reproductive effort required that only one cell was available on any given day. These conditions were met inclusively between April and July, and late October to December when the maximum number of eggs was allotted per day during that time. A combination of habitat conditions and bottom temperatures during the winter months (Jan-Mar) and part of the summer (Aug-Sep) render the entire bay completely unsuitable for spawning (Figure 4.75).

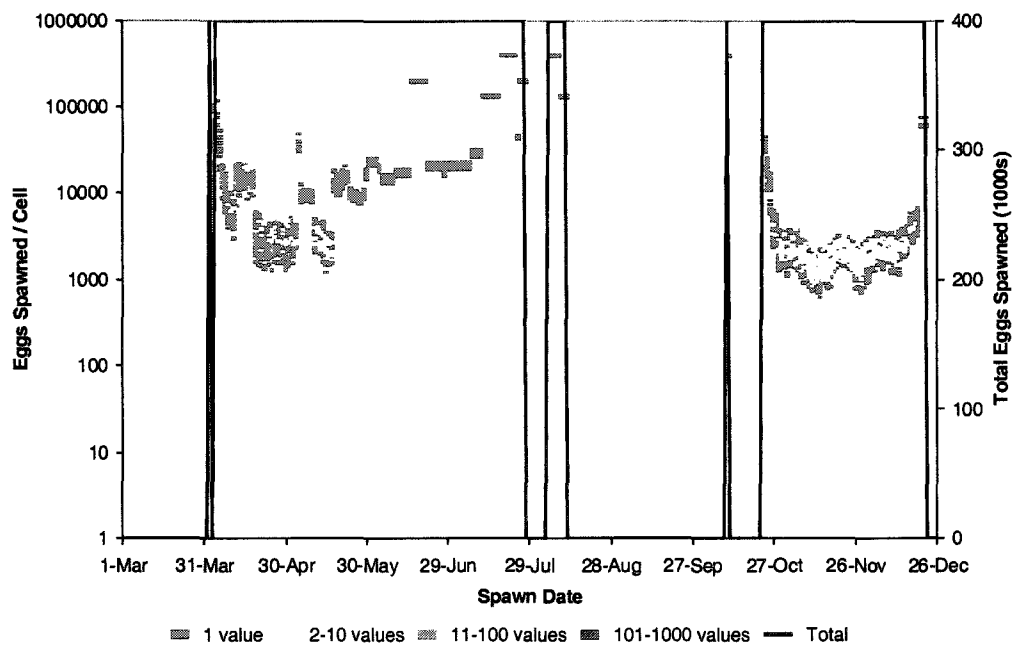


Figure 4.74: Frequency distribution of virtual eggs spawned per cell (# of values per point is colour-coded) and the total number of eggs spawned in Long Point Bay by date in 1999 under Scenario S3* conditions; habitat selection with thermal threshold and IFD. [Note: the X1- axis is logarithmic therefore zeros do not appear.]

Spatially, the Inner Bay and the south shore of the outer bay were most suitable in April for spawning. The north shore and moderately deep parts of the outer bay became suitable in May. A narrow band of deeper areas became suitable throughout June and July at the maximum edge of suitable spawning depths. The Inner Bay became thermally suitable in October again with high potential egg abundance. Moderate suitability and abundances occurred in the nearshore, outer bay areas.

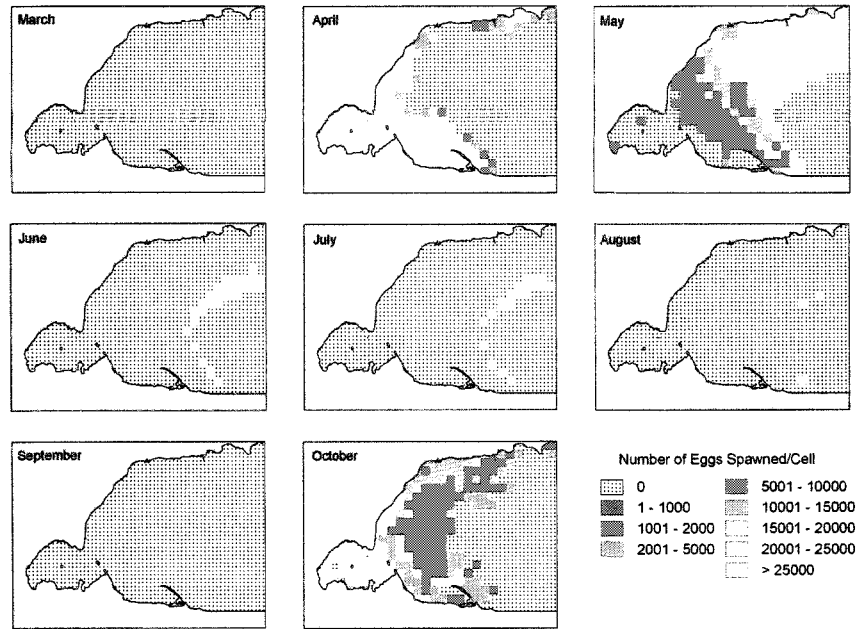


Figure 4.75: Monthly maps of the total number of virtual eggs spawned in each cell in Long Point Bay from March until October, 1999 under Scenario S3* conditions.

*Egg Scenario S3*E1:* As in Scenario S2*E1, more eggs survived under IFD conditions because more eggs were spawned in total due to system-wide redistribution and not local weighting. The spatial pattern of hatched eggs remained the same under both IFD and local-HSI spawning scenarios with thermal thresholds (Figure 4.76). However, the temporal pattern of surviving swim-up larvae was quite different under IFD rules than in previous scenarios. The period of potential spawning success extended from April until late July but daily survival of swim-up larvae was highly variable. The highest daily fry yields occurred when most of the eggs were spawned in a limited number of cells, but this trend was not consistent. Lower, yet more consistent, overall swimup survival was observed when a greater number of cells met spawning conditions. Spawn from April hatched en masse at the beginning of May, after which an extended emergence of fry that was highly variable lasted until mid August (Figures 4.77 & 4.78).

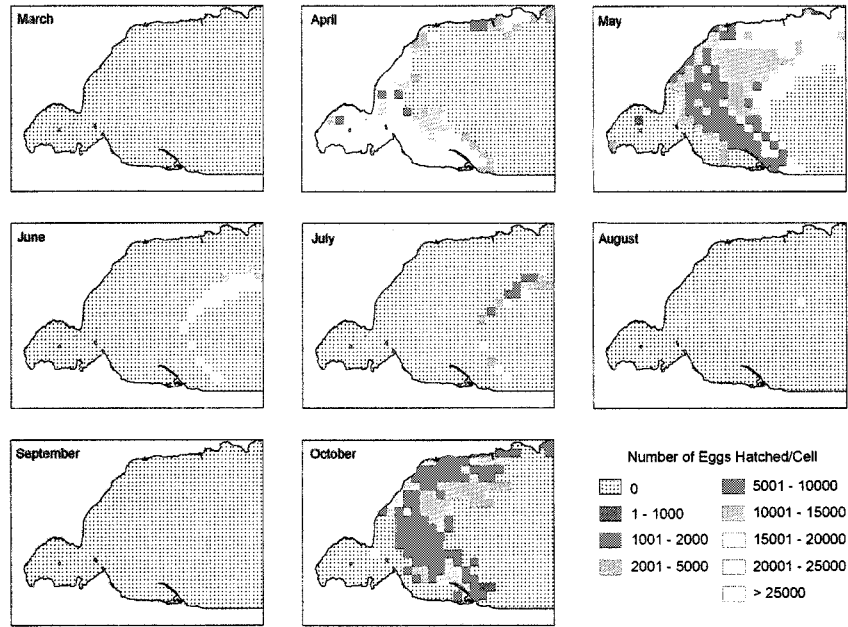


Figure 4.76: Monthly maps of the total number of virtual eggs hatched in each cell in Long Point Bay by spawning month, March until October, 1999 under Scenario S3*E1 conditions.

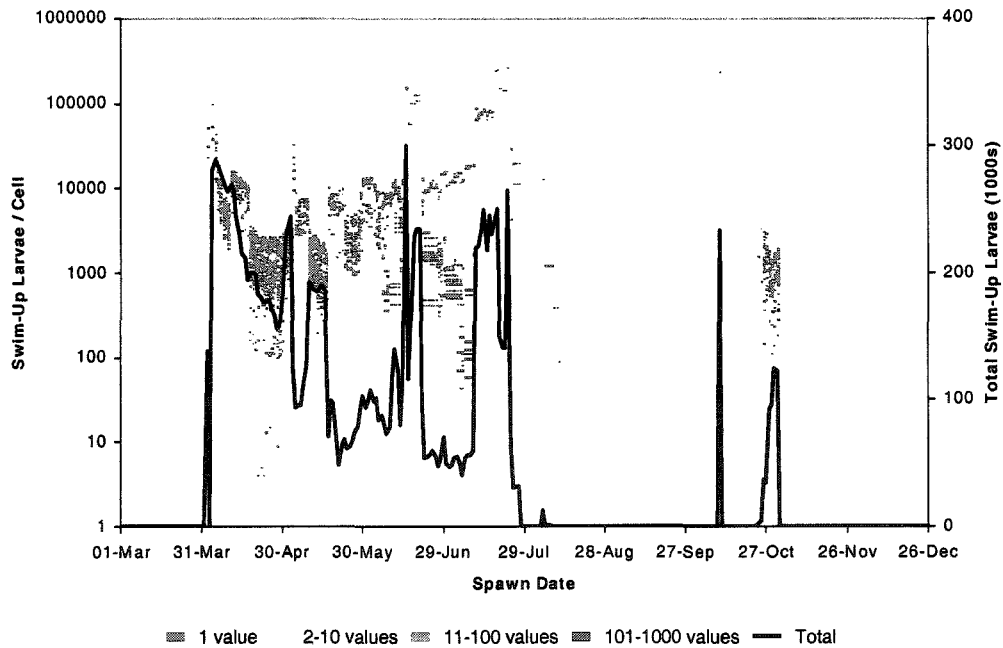


Figure 4.77: Frequency distribution of virtual eggs hatched per cell (# of values per point is colour-coded) and the total eggs hatched per spawning date in 1999 (Scenario S3*E1 ; IFD spawning site selection with thermal cue and thermal effects on eggs. [Note: the X1-axis is logarithmic.]

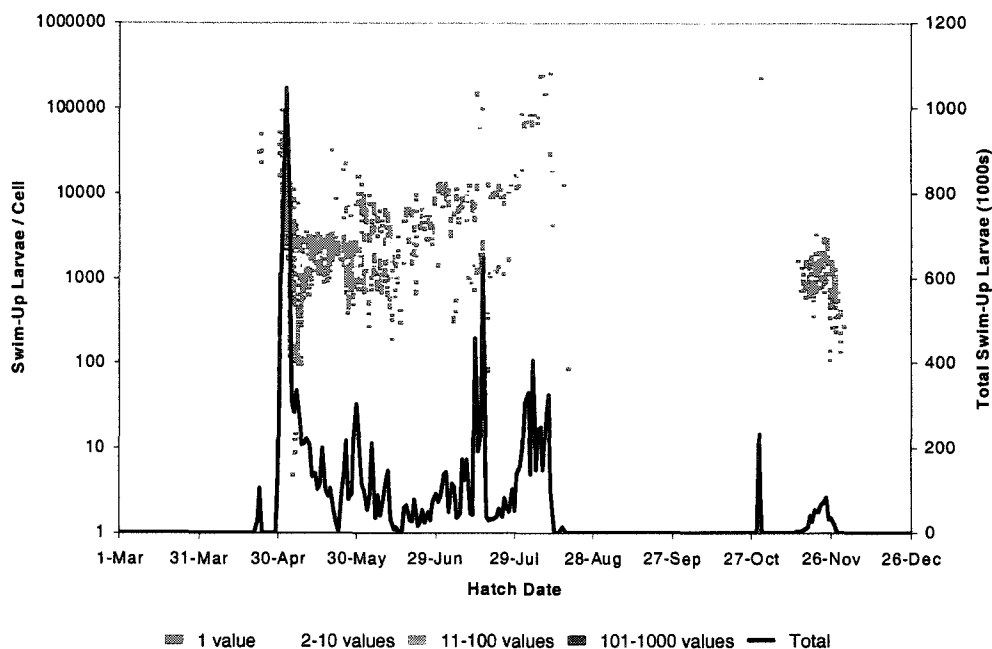


Figure 4.78: Frequency distribution of virtual eggs hatched per cell (# of values is colour-coded) and the total eggs hatched in Long Point Bay by hatch date in 1999 (Scenario S3*E1; IFD spawning site selection with temperature cue and temperature effects on eggs. [Note: the X1- axis is logarithmic.]

*Larval Scenario S3*E1L1:* The extension of the successful spawning window (April – July), under IFD thermal threshold criteria, persisted past the egg stage to the overwintering larval stage (Figure 4.79). Multiple peaks of larvae were produced but did not necessarily correspond to peaks in spawning. For example, the early high survival peak of swim-up larvae in April did not persist to the YOY stage. Conversely, a mid-July peak from a few cells contributed about 25% of the total potential larval abundance. [Note: a quadratic relationship existed between the number of daily spawning cells available and overall larval survival.]

The model predicted that many of the predemersal larvae that were spawned in June and July would successfully inhabit a narrow band of mid-depth waters in the outer bay (Figure 4.80). Under S3*E1L1 scenario conditions, the final size distribution of larvae was a negative linear function over time from April to July inclusively (Figure 4.81). Individual larval biomass theoretically ranged from 8 to 16 g at maximum consumption rates. Greater variability was observed in potential growth from April spawning in the Inner Bay thermal regime than at other areas and times (Figure 4.82).

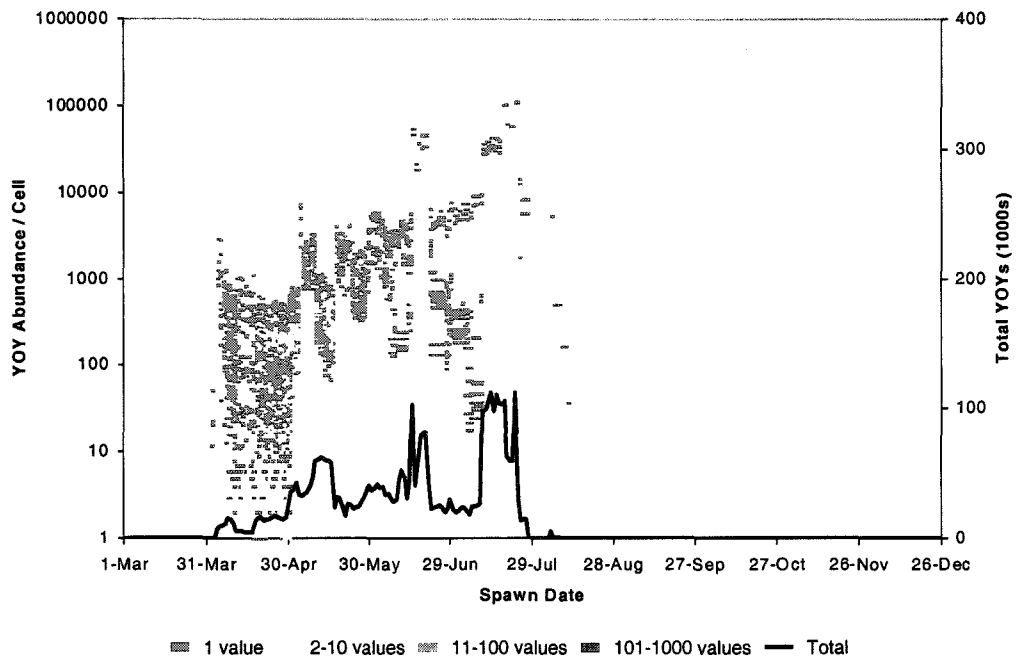


Figure 4.79: Frequency distribution by spawning date of virtual YOYs per cell (# of values per point is colour-coded) and the total number of YOYs that survived to October 31, 1999 in Long Point Bay under Scenario S3*E1L1 conditions; IFD spawning site selection with temperature cue, temperature effects on eggs & larvae. [Note: the X1- axis is logarithmic.]

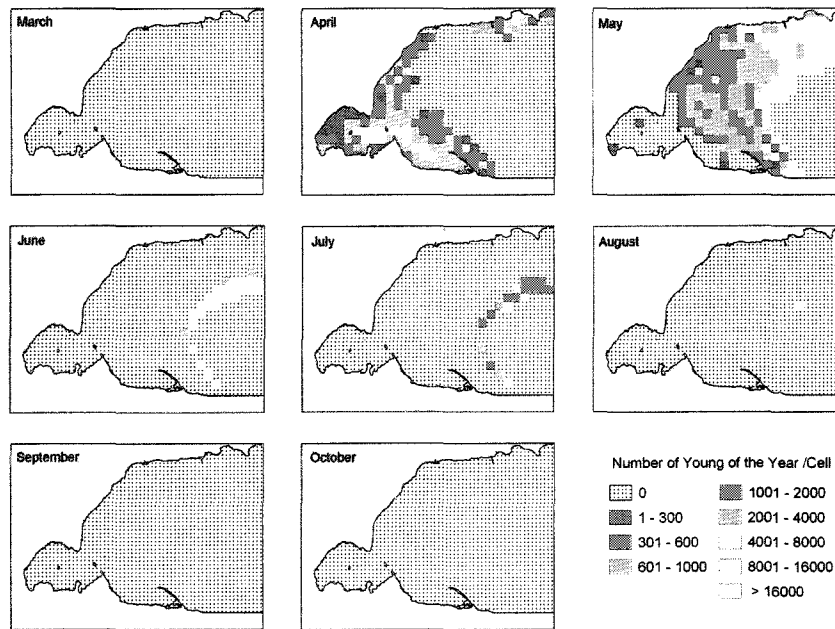


Figure 4.80: Monthly maps of the total number of virtual YOYs that survive until October 31st in each cell in Long Point Bay by spawning month, March until October, 1999 under Scenario S3*E1L1 conditions.

Although the greatest weight gains were probable in both the Inner Bay and the south shore of the outer bay in April. The maximum potential weight gain progressively moved to deeper waters for May-spawned larvae and finally to a small section of mid-depth water just at the edge of the deep hole area for successful June to July spawning. If spawning occurred at these times then growth in those cells would be maximized due to local temperatures and would produce larvae from 8 to 11 g by the end of fall given maximum food availability.

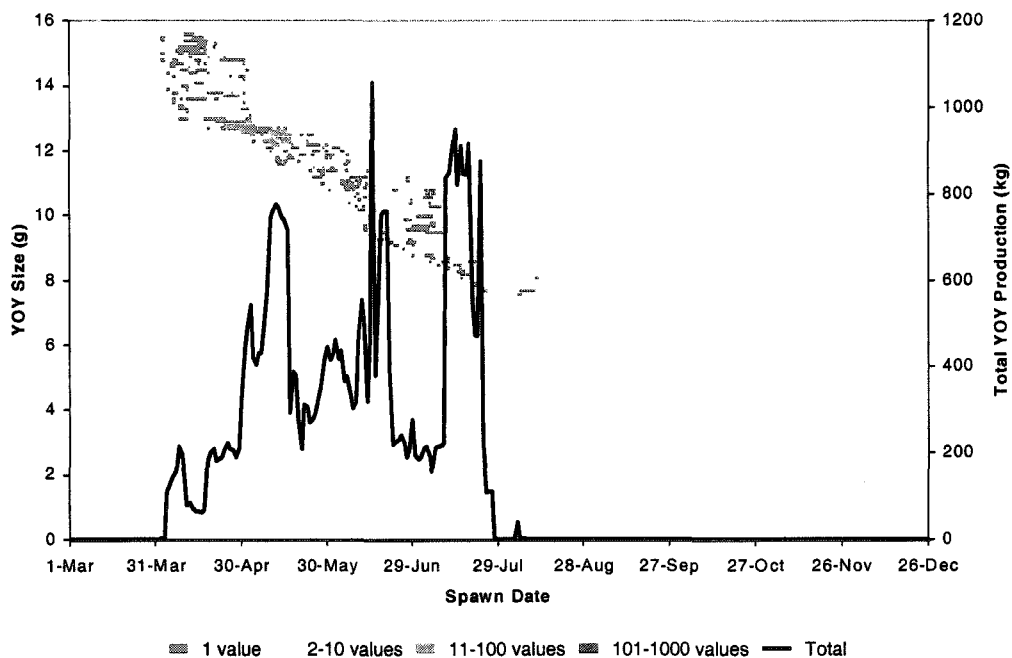


Figure 4.81: Frequency distribution by spawning date of YOY average size (g) per cell (# of values per point is colour-coded) and the total production of YOYs (kg) that survived to October 31, 1999 in Long Point Bay under Scenario S3*E1L1 conditions; IFD spawning site selection with temperature cue and temperature effects on eggs and larvae.

Larval production under thermal spawning thresholds and IFD distribution of spawning was the highest and most variable of any of the scenarios (Figure 4.81). The spatial extent of larval production was the same as scenario S3E1L1, but with more pronounced high-production areas (Figure 4.83). The Inner Bay was only suitable for all life stages if eggs were spawned in April. There was high spatial variability in production with the most suitable zones at the mouth of Big Creek and the estuary between inner and outer bays. High production results from both high initial reproductive allocation to the site and high survival and growth rates afterwards. Suitable areas for first year production moved northwards to Nanticoke and to the mixing zone where water depths reach thermocline depth. Production dropped in August when only one cell supported all life stages successfully and much of Long Point did not meet thermal threshold spawning requirements.

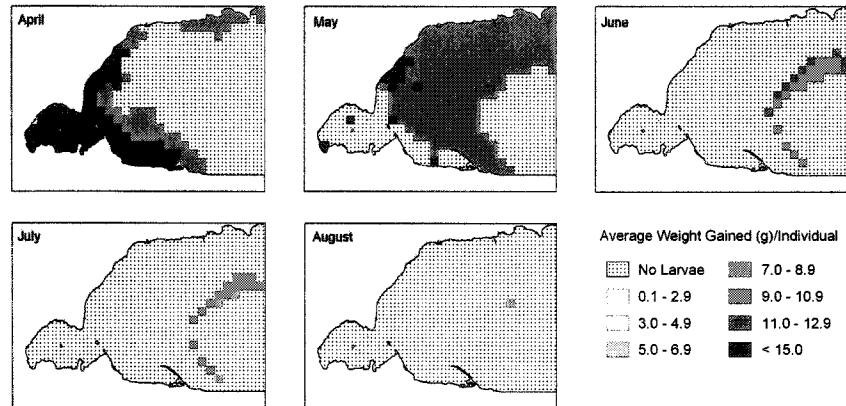


Figure 4.82: Monthly maps of the average weight gain (g) of virtual YOYs that survive until October 31st in each cell in Long Point Bay by spawning month, April until August, 1999 under Scenario S3*E1L1 conditions.

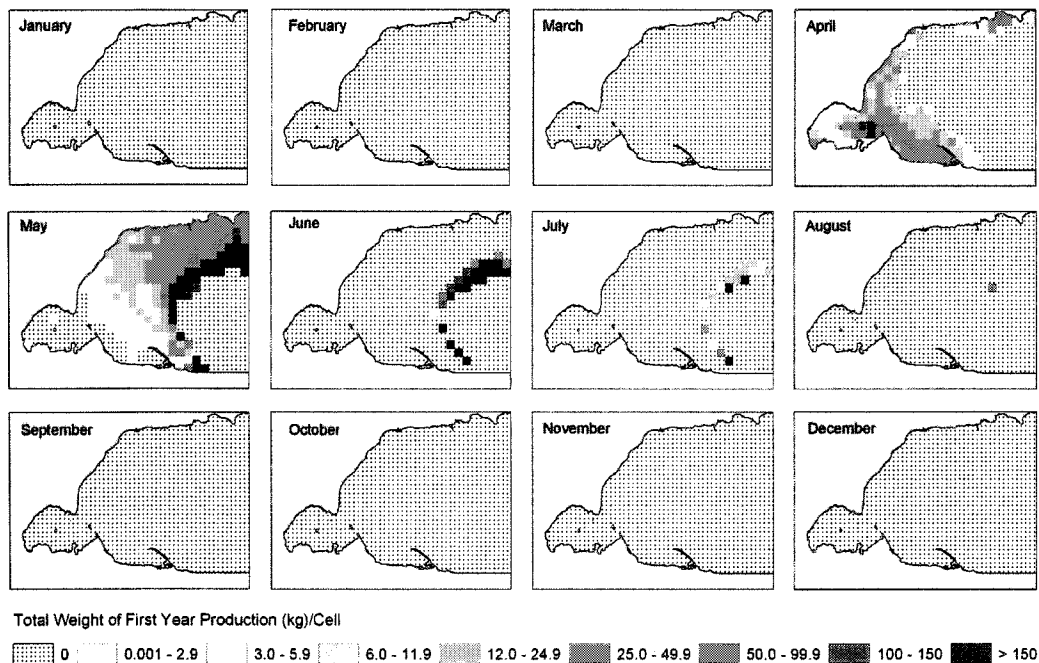


Figure 4.83: Monthly maps of the total production (kg) of virtual YOYs that survived until October 31st in each cell in Long Point Bay from the month of spawning in 1999 under Scenario S3*E1L1 conditions.

*Larval Scenario S3*E1L2:* The total number of surviving planktonic larvae in the system, under full habitat and thermal restrictions with ideal free distribution of spawning, was only slightly higher than non-IFD conditions (Figure 4.84). The spawning period for successful completion of the initial life phases was narrowed to April and May, not including June and July as in the complementary L1 scenario. The areas for survival from spawning to overwintering were also limited under these scenario conditions (Figure 4.85). A relatively narrow band of shallow water along

the south shore of the outer bay, with patchy areas of the Inner Bay and outer north shore provided the best habitat and thermal regimes in April. In May, much of the outer bay, with the exception of the south shore and deep hole, is suitable for survival from spawning to YOY, and was concentrated in a narrow band in deeper waters.

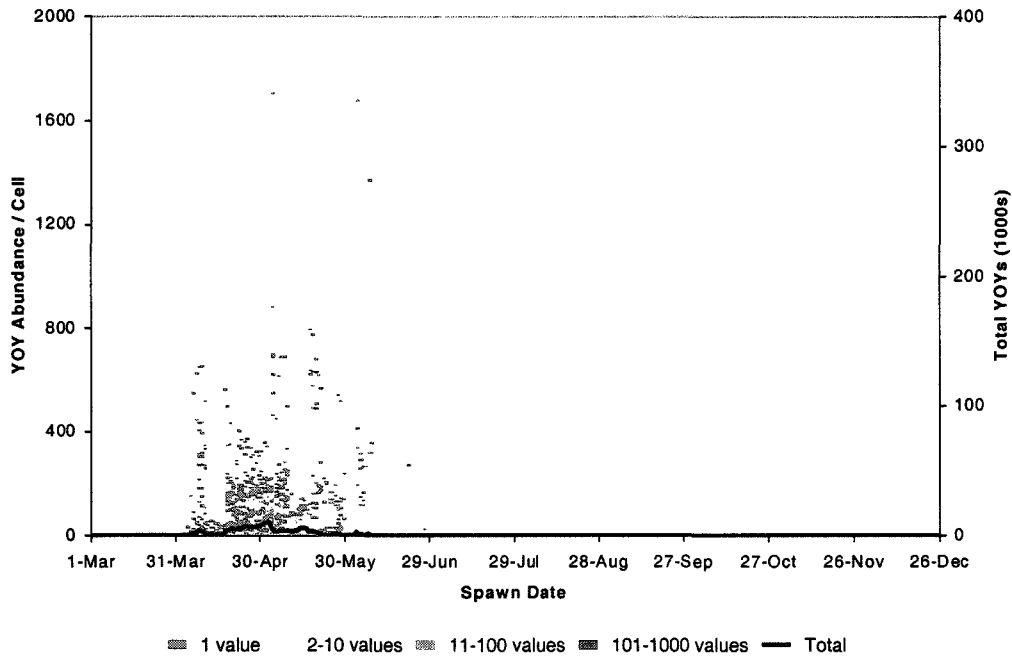


Figure 4.84: Frequency distribution by spawning date of virtual YOYs per cell (# of values is colour-coded) and the total number of YOYs that survived to October 31, 1999 in Long Point Bay under Scenario S3*E1L2 conditions; IFD spawning site selection with temperature cue, temperature effects on eggs, and temperature & habitat effects on larvae. [Note: the X1- axis maximum has changed.]

Two spring-spawned cohorts survived until fall, which were similar in size to scenario S3E1L2 virtual larvae (Figure 4.86). However, the current IFD scenario predicted more variability in the size range within each cohort and more cells contained larvae. This scenario restricted the time frame and areal extent for spawning and successful completion of the life cycle with a much reduced overall production compared to scenarios with no habitat effects (Figure 4.87). As with previous IFD scenarios, the larval production at the end of the year was greater than scenarios with local, habitat-weighted spawning because of no local carrying capacity.

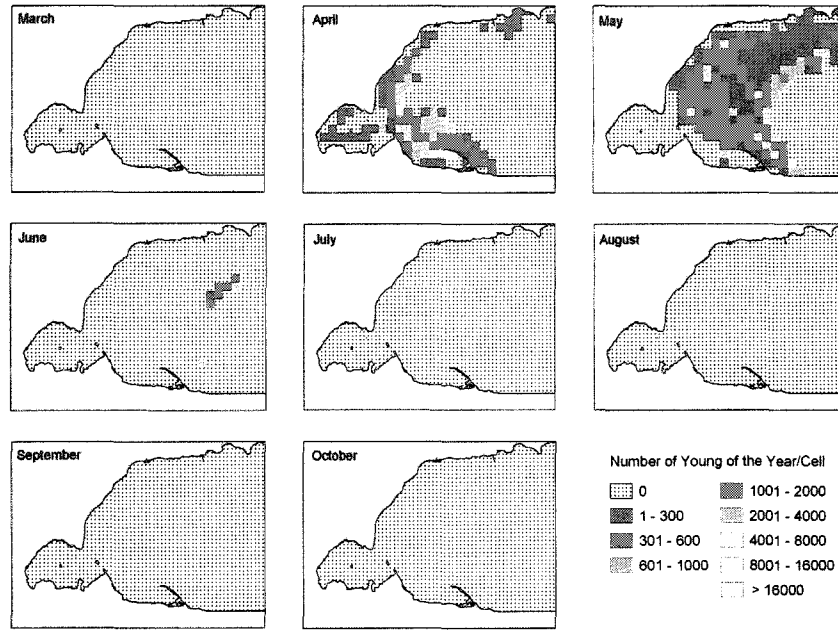


Figure 4.85: Monthly maps of the total number of virtual YOYs that survive until October 31st in each cell in Long Point Bay by spawning month, March until October, 1999 under Scenario S3*E1L2 conditions.

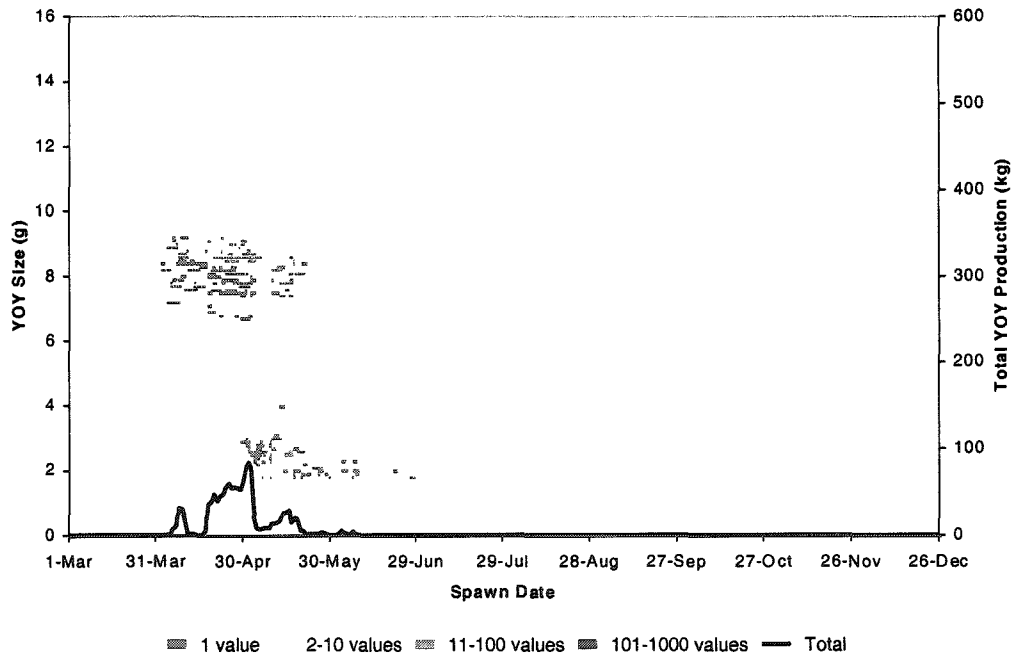


Figure 4.86: Frequency distribution by spawning date of YOY average size (g) per cell (# of values per point is colour-coded) and the total production of YOYs (kg) that survived to October 31, 1999 in Long Point Bay under Scenario S3*E1L2 conditions; IFD spawning site selection with temperature cue and temperature effects on eggs, temperature & habitat effects on larvae.

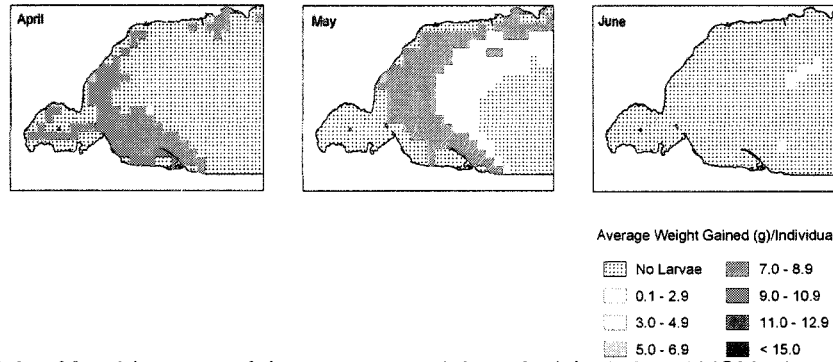


Figure 4.87: Monthly maps of the average weight gain (g) of virtual YOYs that survive until October 31st in each cell in Long Point Bay by spawning month, April until June, 1999 under Scenario S3*E1L2 conditions.

With the incorporation of larval habitat effects, however, the expansion in time and space of successful completion of the first year of life under IFD reproduction rules was lost as the high production window created under S3*E1L1 conditions was restricted to three production pulses resulting from spawning in April to June inclusively (Figure 4.86). The very high production observed in the upwelling zone under strictly thermal effects on larvae was no longer present under full habitat restrictions, indicating a potential mismatch between thermal and feeding habitat suitability (Figure 4.88). The Inner Bay and coastal zone contributed less towards overall production than in previous scenarios and a relatively higher contribution was predicted from the south shore of the outer bay; a more sheltered area.

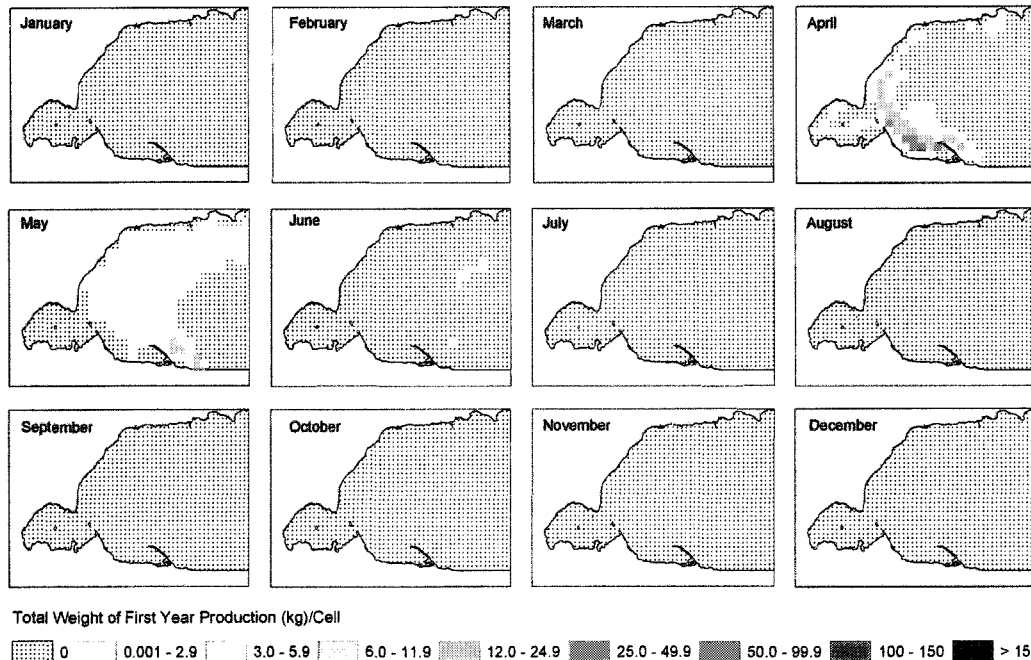


Figure 4.88: Monthly maps of the total production (kg) of virtual YOYs that survived until October 31st in each cell in Long Point Bay from the month of spawning in 1999 under Scenario S3*E1L2 conditions.

4.2.5 Final Scenario Comparisons

The more rules or constraints that were placed on each life stage, the lower the potential production, but to varying degrees. With temperature thresholds imposed on spawning the production potential became more variable. All scenarios, with the exception of S3*E1L1, followed the same general pattern of production (Figure 4.89). IFD distributions for habitat alone (i.e. not including a temperature cue) were very similar to local-weighting scenarios. The major difference between the base scenario and subsequent scenarios with spawning habitat preferences was that summer spawning and successful larval production were predicted in the former. Although IFD of reproductive effort based on temperature thresholds extended the window for production potential and daily variability, it would only make a difference in systems where thermal structure was the driving force behind growth and mortality and there were no habitat differences, (i.e. food was not limiting in different areas and matched ideal temperature distributions).

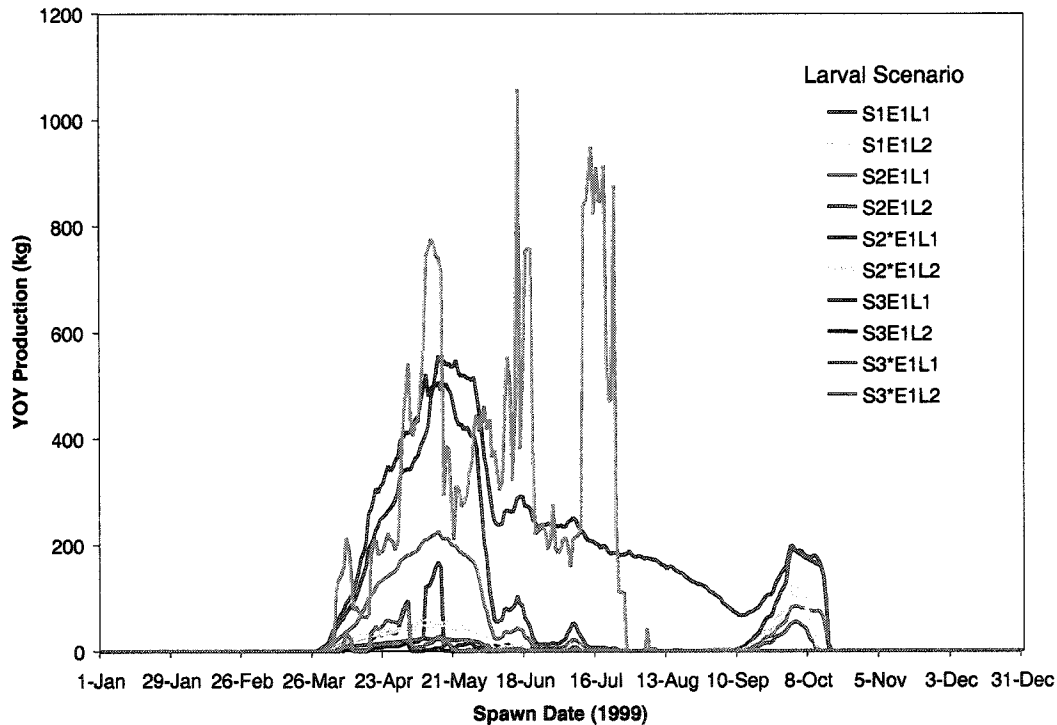


Figure 4.89: Scenario comparisons of the potential YOY production (kg) by October 31, 1999 in Long Point Bay plotted by spawning date. See Table 4.4 for a description of scenarios.

See Appendix 4.6 for annual statistics on eggs, swimup, and YOYs for each scenario, as well as the number of days per year with potential survival from eggs to overwintering. Appendix 4.7 contains statistics for the most abundant (successful) spawning days in spring and fall for each successive life stage, as well as the number of remaining cells contributing to the abundances from those spawning dates.

4.3 DISCUSSION & CONCLUSIONS

The answers to the central questions of this chapter hinge on the links between habitat and early fish production. Those questions included: a) whether habitat can limit fish production?, b) if so, what are the habitat constraints on carrying capacity and stock dynamics?, and c) do these constraints create a productivity bottleneck at a particular life stage? The growth, survival and production rates resulting from different model experiments were compared to assess the relative importance of thermal and physical habitat and to examine how different life stages are affected. Habitat selection is an emergent property of the combined action of differential fitness, habitat availability, population abundance and size structure, and competition (Railsback & Harvey 2002). Two of those factors were examined here; fitness at each life stage, as well as habitat availability and carrying capacity, at different scales on initial spawning conditions.

The scenario results of PercaSpace, show how spatial and temporal heterogeneity may affect population dynamics. Parsing the underlying drivers and compressing the vast amounts of simulated results into accessible summaries is difficult in spatially explicit models. I compared the detailed scenario results by compressing the output data into population metrics to illustrate several emergent features. Simple metrics included the space (number of cells) and time (days) that were required for successful completion of different life stages in the first year of life. The temporal and spatial interactions between habitat and production efficiency were examined with more complex metrics: a) the proportion of production that was lost to overwinter mortality due to larval size constraints; b) larval production efficiency for different spawning rules, and; c) the percent difference in selected population statistics between thermal and habitat-based effects at the larval stage, given different spawning strategies. Given these findings, critical habitat requirements, limiting habitat, and productive capacity are discussed with reference to spawning strategy and the influence of environmental variability in yellow perch.

4.3.1 Life History Stages

Shuter & Regier (1989) stated that habitat is the amount of living space that is environmentally suitable. As shown in the methodology, different suitabilities were defined for different life stages (i.e. spawning, egg, YOY), and for different vital rates within each stage. Several alternate hypotheses arise because of the dynamic definition of habitat suitability within and between each stage. For example, good spawning habitat may encapsulate all the needs of the first year of life or may mostly benefit the egg stage because this stage cannot move. Good egg habitat could be defined as areas with faster development rates or areas that have improved survival to hatch. Good fry habitat could encompass good growth or high survival rates or both. These alternative definitions for

suitable habitat at each life stage are discussed relative to the scenario outcomes.

Spawning

The S1 scenario combinations showed which habitat is best if a spawner were non-selective for both temperature and habitat effects. The second scenario (S2) showed outcomes if specific habitats were selected at the spawning stage and the third scenario (S3) showed what happens if temperature is also considered as a spawning cue. The more restrictive the spawning requirements, the lower the reproductive investment and hence, potential first-year production, if severe local carrying capacities were applied. Not one cell at any time was allocated the maximum number of 1000 eggs in local habitat-weighted scenarios (S2), indicating that 'perfect' physical habitat conditions for spawning never occurred. This is assuming that hierarchical, geometric combinations of individual habitat variables capture how the fish perceives its habitat. The driving variable was depth selection and excluded very deep areas in the bay where egg survival was predicted to be high at certain times because of stable thermal regimes, as seen in S1 combinations. This indicated that egg survival and development was not the limiting factor for spawning site selection and timing, but subsequent larval growth and survival. Successful spawning encompasses a selection of habitats for the completion of all life stages, especially if larvae remain locally, because for a site to be successful reproduction must be successful in progeny. Therefore, a strategy that minimizes losses across multiple stages, given unpredictable environments, is preferable.

The match between the known life history in Long Point and the initial conditions predicted by the spawning scenarios indicates emergent habitat selection. The location and timing of spawning predicted by the S3 spawning scenario (thermal threshold with habitat selection) concurred with documented spawning areas and times of yellow perch in Long Point Bay (Goodyear 1982; Figure 4.90). Spawning scenarios showed that thermal requirements for good spawning habitat should be incorporated into habitat assessments because it is the only criteria that limited their spawning to times when perch actually do spawn, although it is acknowledged that daylength may have a role in addition to a thermal cue (Thorpe 1977). If the presence of moderately-dense vegetation were the key to spawning success then spawning would most likely occur during peak development times for aquatic vegetation in July and August. This indicates that some habitat variables need not be included, or a relative weighting should be applied, in habitat suitability calculations, as all variables may not be equal. Vegetation may be correlated with other variables that immediately benefit the eggs, like low turbulence. However, if spawning does occur in areas that maximise larval growth or survival, then peak vegetative cover corresponds well with this strategy.

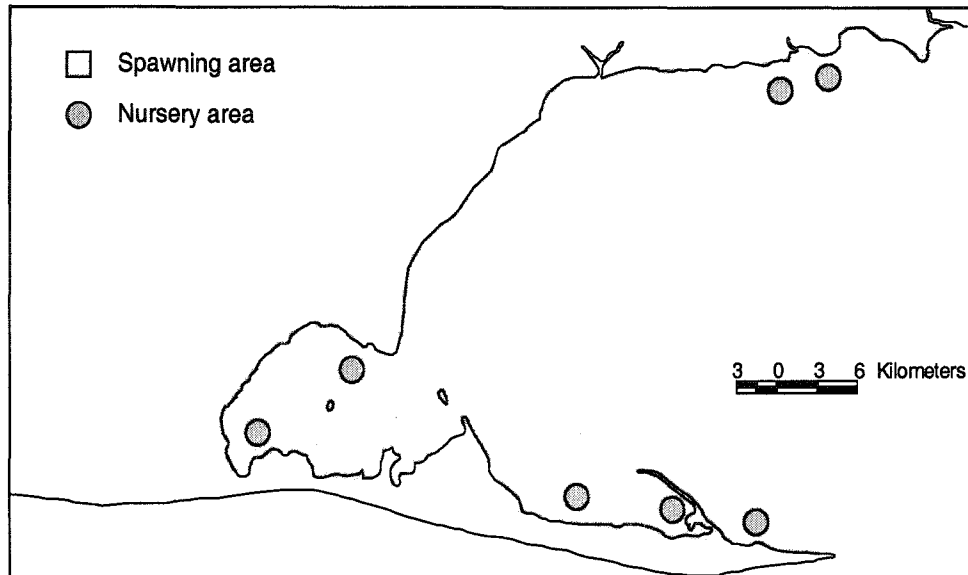


Figure 4.90: Historical spawning and nursery areas for yellow perch in the Long Point Bay Region. Modified from Goodyear (1982).

Egg Stage

The more specific and localized the habitat requirements the more susceptible and critical is the life stage to population dynamics (Langton 1996). In the PercaSpace model, eggs mainly require good thermal habitat and on rare occasions exposure can have a detrimental effect (at least in 1999). Habitat selection by perch during spawning did make subtle differences on overall egg dynamics, even though direct habitat effects on egg survival were negligible. If initial conditions were restricted by thermal cues at spawning then exposed habitat became more relevant to egg survival. The relative drop in egg production between E1 to E2 scenarios increased due to spawning habitat restrictions, from S1 at 0.125%, to S2 at 0.127% and S3 at 0.34% reduction in successful egg hatch. Although the reductions are small, they imply that the spatial and temporal occurrence of good thermal habitat overlaps with exposed areas and that egg production may be more susceptible to random catastrophic events because of the compressed time period.

YOY Stage

Results at the YOY stage are due to cumulative effects at preceding life stages. The implications of habitat choice from an evolutionary or behavioural standpoint are important to consider. Only two stages involve habitat choice; spawning and larval stages. In this model, only the spawning stage incorporated selectivity and larvae were retained in the initial spawning site area (1.4 km²). However, if fish select spawning habitat because of a bioenergetic advantage to subsequent life stages, the spawning behaviour is an evolutionarily stable strategy (ESS). Faster development times and higher growth rates, with lower energy expenditure searching for good larval habitat, would result given good local environmental conditions. Also, certain habitats may provide refugia

to both eggs and larvae, and if spawning fish select habitat because of a survival advantage then high egg and larval survival may result. High production can result if both areas overlap.

Individual Growth vs. Larval Production

The larval scenarios were contrasted to compare potential areas of high growth to areas of high survival and production from both a thermal and habitat-based perspective. Daily growth rates were affected by spatial differences in habitat suitabilities that often produced similar results regardless of the initial conditions. For example, two size cohorts were produced if habitat-based prey was disconnected from thermal preferences at the larval stage (L2 scenarios), which often occurred in the offshore zone. As thermal regulation superseded foraging in the model, there were two months of low-prey conditions for outer bay larvae because of a mismatch between preferred temperatures and food availability. Post *et al.* (1997) determined that age-0 cohort splitting occurred due to density-dependent and competitive effects but PercaSpace showed that the same outcome arises from habitat-based differences and behaviours that are independent of density.

The small cohort in some scenarios resulted because optimal temperatures were below the thermocline based on behavioural thermoregulation (Crowder & Magnuson 1983). To optimally forage, larvae would need to make forays for food into upper layers and tolerate hotter temperatures, or move laterally much greater distances to more suitable areas. Neither of these behaviours was modelled explicitly but a simple test of the former option was conducted. If foraging supersedes behavioural thermoregulation then larvae need to always be in the top 10 m, and hence subject to exposure and sub-optimal temperatures. The larval growth achievable under these conditions in the outer bay was recalculated for cell 384 specifically; a cell at the shelf edge which is 32 m deep. If spring-spawned larvae optimally foraged in the top 10 m in this cell then they would have obtained a weight of 8.0 g by the end of October instead of 2.5 g under S1L2 rules. If larvae had adequate food at optimal thermal conditions (S1L1) they achieved 9.6 g by November. In this example, the thermal mortality component was not calculated in the upper layers so there is no guarantee that larvae would have survived to the size quoted. However, these growth differences would have implications on age-at-maturity (Railsback 2001), and longevity and cannibalism rates (Claessen *et al.* 2000; Also see Chapter 2) as faster-growing fish can mature sooner, die younger, and may cannibalize smaller fish.

Spatially, the results indicated that to maximize on growth did not necessarily maximise on larval production because of differences in survival rates. Production patterns were often different from potential growth patterns, which have ramifications on only using growth potential exclusively for defining optimal habitat (Brandt & Hartman 1993). Railsback (2003) also found that preferred habitat (based on density relationships) was not necessarily the fittest choice.

The spatial patterns of growth and production were compared across the scenarios for fish spawned between April and June only (Table 4.5). In most cases, L1 scenarios had noncontiguous regions of high production and high growth. High growth areas consistently occurred in the inner bay and interestingly, in slightly different regions of the outer bay depending on the spawning scenario. High production areas occurred in the outer bay in the northeast, with some additional areas depending on the spawning scenario (i.e. in the deep hole in S1 conditions, and the connecting channel under S3 conditions). The mismatch arose from a difference in the thermal mortality rates and the timing of potential spawning in the inner and outer bay areas. Interestingly, the distance between outer bay, high-growth and high-production areas was minimised under S3* spawning conditions.

In the long term, a few large individuals in some areas may contribute disproportionately to future production even though higher abundances of smaller individuals exist in other places. Because of a size-selective advantage early in life, those individuals may add an unequal reproductive contribution of larger females to the spawning stock (Scott *et al.* 1999). Therefore, a trade-off between individual growth and mortality may result that has a large effect on populations at low abundance levels.

Table 4.5: Comparison of the location of high larval growth and high larval production nuclei across the spawning and larval scenarios.

Scenario (E1 variant implied)	Location of high growth area	Location of high production area
S1L1	Inner Bay, channel	NE nearshore outer, deep hole
S2L1 & S2*L1	Inner Bay, S shore outer	NE nearshore outer
S3L1	Inner, W & S nearshore outer	NE nearshore outer, channel
S3*L1	Inner, NW nearshore outer	NE nearshore outer, channel
S1L2	S shore outer bay	S shore outer bay
S2L2 & S2*L2	S shore outer bay	S shore outer bay
S3L2	Weak S shore outer	Weak S shore outer
S3*L2	SW outer bay	SW outer bay

Taylor (1987) found in a reaction diffusion model with spatial heterogeneity, that multiple population nuclei were created by resource selection. In PercaSpace, two nuclei were created under some scenarios along the north or south shore of the outer bay because of spatial heterogeneity in habitat that had differing abundance and size structure of larvae. This may create metapopulations under certain conditions due to just the random movement of spawners and selection of high suitability areas.

In L2 scenarios, high growth & production regions overlapped in Long Point creating one central nucleus that varied in intensity and subtly by location in spawning scenarios. Because of differential habitat-based growth and mortality, the south shore of the outer bay is favoured for both

individual growth and total larval production. The inner bay because of habitat-based mortality was no longer the nucleus for high growth because no larvae survived until October. The nucleus shifted slightly to the southwest under S3* spawning.

4.3.2 Limiting life stage

Individual female perch lay all their reproductive effort for one year at once; therefore, spawning site selection must play an important role. Selection's impact on production can be gauged by how much it is reduced at each stage. An evolutionary stable strategy (ESS) would minimize losses across all stages or concentrate loss reduction at a limiting stage. The maximum daily abundance at the peak of each stage during the first year varies between the scenarios (Figure 4.91). The maximum abundance of eggs spawned was limited more by habitat availability than by thermal conditions. Only the S3* scenarios (system-wide IFD of reproductive effort for thermal cues) would be limited at the larval stage. In all other scenarios, egg mortality limited the success of first year peak abundance, with the greatest loss occurring after both uniform spawning (S1) and IFD-habitat-selection spawning (S2*) as initial conditions.

Habitat differences in larval survival (L1 versus L2) did not affect maximum daily larval abundance between similar scenarios significantly unless a thermal cue under IFD spawning conditions (S3*) was imposed. When the larval stage became limiting during these scenarios, egg survival benefits did not make a difference to final peak abundance. S3*L1 peak larval abundances converged with those of S2*L1; indicating the distribution of spawning effort into either good physical habitat or good thermal habitat would favour egg or larval survival but not both, with the same overall outcome. The S3*L2 scenario converged with S3L1; indicating that the system carrying capacity might be locally limited if habitat-based differences in survival occur at the larval stage.

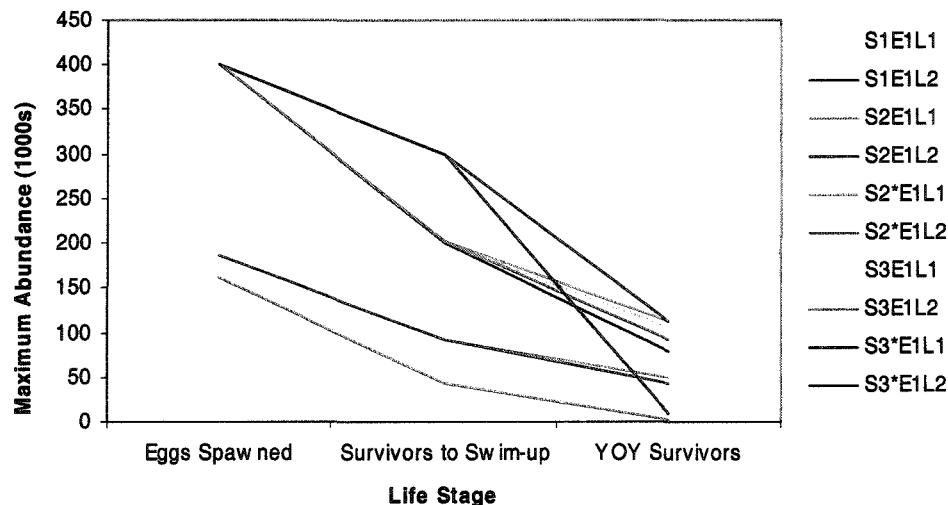


Figure 4.91: The potential daily maximum abundance of successive life stages of yellow perch in the Long Point system under different scenario conditions.

When daily abundances were integrated across all spawning dates, the total potential annual abundance predicted by each scenario followed a logarithmic relationship with different initial abundances across life stages (Figure 4.92). A straight line on the logarithmic y-axis indicated that mortality across life stages did not diverge from a logarithmic decay function. This was the case in all L1 scenarios where greater losses in total potential production always occurred at the egg stage regardless of the spawning scenario.

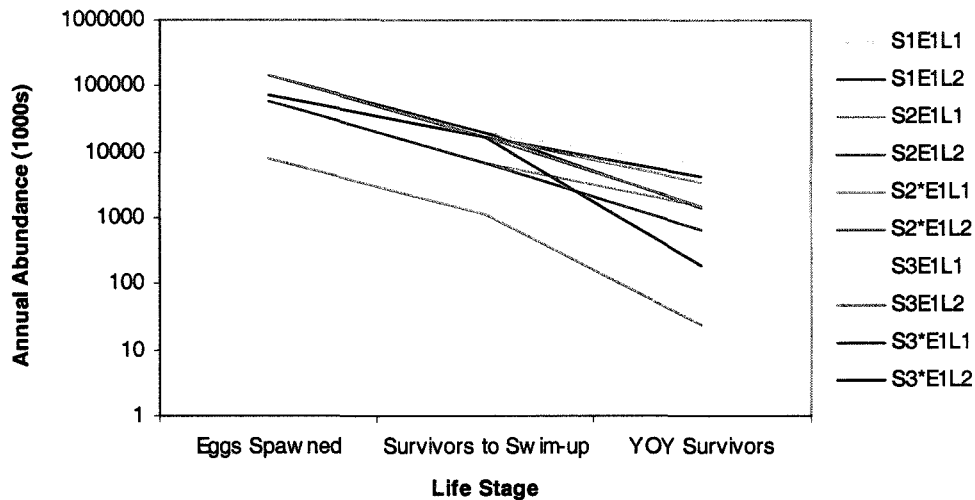


Figure 4.92: The potential annual abundance of successive life stages of yellow perch in the Long Point system under different scenario conditions.

The loss pattern diverged under IFD thermal and habitat selection at spawning ($S3^*$) where egg loss was minimized, subsequent larval losses deviated from the curve. Scenarios converged at the integrated total egg and larval abundances but were slightly different than in maximum daily abundance predictions. For example, system-wide redistribution ($S2^*$ & $S3^*$) and uniform spawning scenarios ($S1$) converged at the same potential annual egg abundance even though different areas were used in Long Point. $S1L2$ and $S2^*L2$ scenarios converged with $S2L1$ scenarios indicating that local habitat constraints at the larval stage overrode the initial starting conditions. The smallest reductions occurred in locally-weighted spawning scenarios but the overall production was dramatically reduced in the whole system due to starting conditions. If larvae were able to move outside of the area in which eggs were deposited then larval mortality may be mitigated to achieve higher overall abundance.

Larval Scenario $S2E1L2$ produced the same final pattern as $S1E1L2$ which implies that habitat selectivity during spawning may be a result of habitat restrictions at the egg or larval stage. The underlying relationship between successive habitat “choices” or selection pressures and habitat variability is important and may be an emergent property. How consistently does the same habitat occur at the same location,

between years, and how consistent are the choices for habitat use? Because habitat is variable and outcomes are a result of constant selection pressures, production would depend on the level of variability and the rate of adaptation or plasticity. Perhaps the real limits to production occur when there is a mismatch between historically successful strategies and current environmental conditions.

Similar to PercaSpace results, Tyler & Rose (1997) showed that predation distribution, the number of juveniles, the zooplankton density, and the larval behaviour rule affected cohort survivorship using an experimental approach in a SE-IBM. They indicated that no rule is an ESS constantly and ESS-like rules (overall fitness) are better than using rules with the highest survivorship in the first year, and also that density effects on survivorship were much greater in SE-IBMs with fitness-based rules than in homogeneous environments.

4.3.3 Space & Time Limitations

Restrictions to potential production in the system occur both spatially and temporally; the latter is often not considered. When and not where may be more important to variability in production. For example, the optimal spawning dates for peak production at each successive life stage changed in different scenarios (Appendix 4.7). Also, the number of spawning days during the year that resulted in successful completion of each phase varied considerably (Figure 4.93). A thermal cue at spawning is the most restrictive to the window of opportunity for successful spawning. Habitat was not restrictive at this stage year-round (i.e. there was always habitat available that met some spawning criteria). The successful time window to YOY survival was only subtly different between IFD and local strategies, especially under thermal cue conditions, indicating that timing was not affected by the relative allocation of reproductive effort (i.e. bad cells were bad cells regardless of the number of eggs allocated).

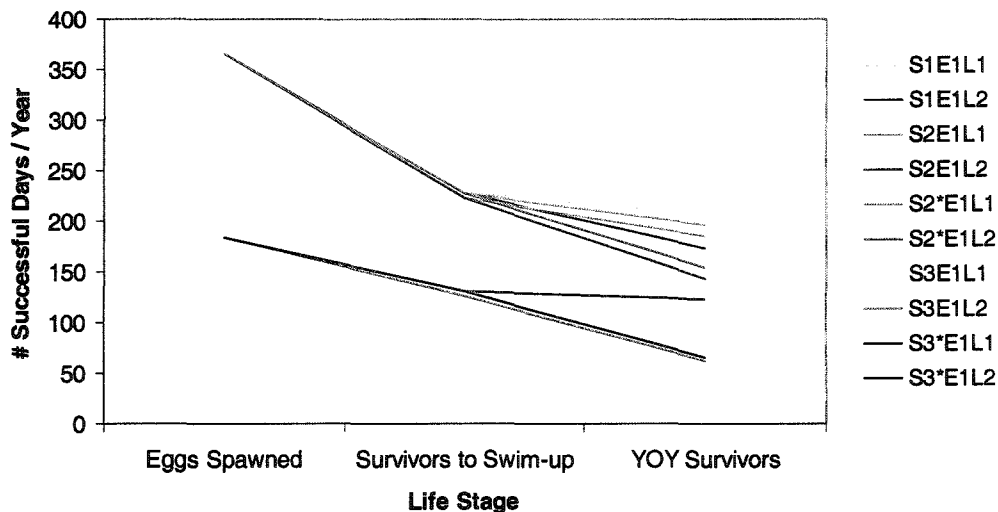


Figure 4.93: The number of days of the year in 1999 that would have suitable habitat in the Long Point system for successive life stages under different scenario conditions.

Habitat-based mortality at the larval stage (L2 scenarios) limited the successful spawning time window the most, regardless of the initial spawning tactics. Only the S3L1 and S3*L1 strategies did not narrow the time window significantly after the successful completion of the swim-up stage. In most scenarios, the dates that successfully produced overwintering larvae comprised 40 to 62% of the initial spawning dates; the proportion of which changed subtly due to habitat constraints at the larval stage. The model should be tested using different years to determine how much difference a thermal cue could make to successful time windows because the outcome can be very restrictive to overall production within a system. However, initial results showed that walleye spawning lasted for four weeks, but a window of 4-7 days produced the best survival (Jones *et al.* 1998), so a few days may be all that is required to meet carrying capacity within a system.

In the S3* scenario combinations, very high egg and larval abundances resulted from the use of very little space at times (Figure 4.94). Even though the highest abundances resulted from a few cells, the potential variability was greater because the lowest larval abundances also resulted from the use of small spawning areas. A wedge-shaped distribution of data points indicated a potential trade-off between slightly lower overall abundances and larger minimum area requirements that were more stable in egg production output. Lower, yet more consistent, overall swim-up survival was observed when a greater number of cells met thermal spawning conditions.

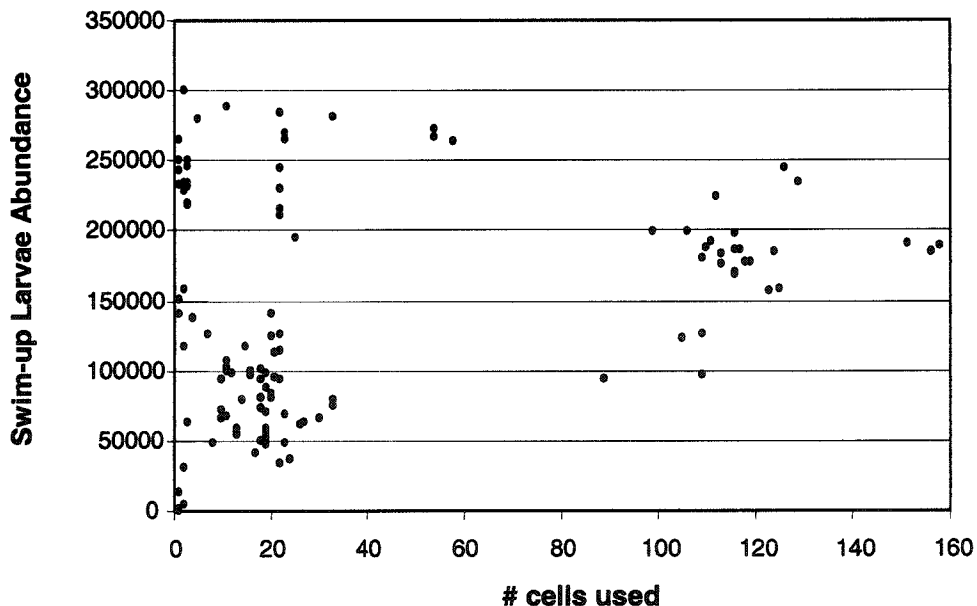


Figure 4.95: The number of cells used each day for spawning under S3* conditions in 1999 compared to the abundance of swim-up larvae surviving from that day's spawn under E1 conditions.

This has implications for bet-hedging spawning strategies due to the probabilities of egg survival. The variability inversely decreased in overall survival to swim-up, with the number of daily spawning cells available under IFD thermal conditions. In 1999, the small suitable areas corresponded to the edges of the spawning window, which has implications for early and late spawners. If thermal conditions are good for egg development this period can contribute a significant amount of production to the system, especially at the tail of the optimal window, but is much riskier.

A plot of the number of successful spawning days that produced larvae versus the annual larval production formed an exponential curve, with the exception of the S3*E1L1 scenario (Figure 4.96). More successful spawning days were completed under unrestricted spawning scenarios (S1 compared to S3), as well as with temperature-effects-only versus habitat-effects on larvae (L1 compared to L2). Rose (2000) stated that a minor change in complex habitat can produce dis-proportionate population responses. This is one of the main conclusions of the analysis, especially when the minor change in habitat created a match between good thermal habitat and food with no additional habitat-based mortality.

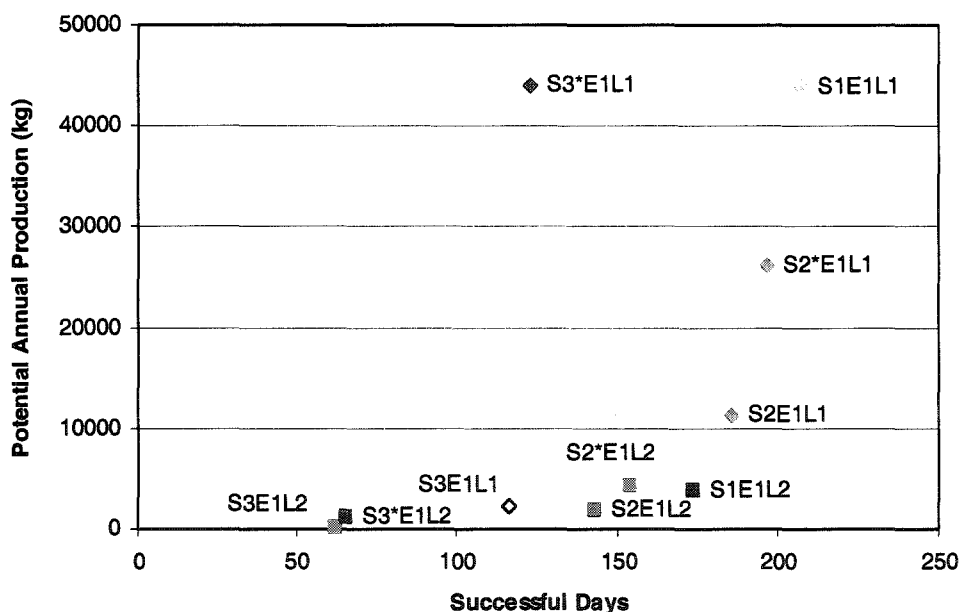


Figure 4.96: The number of spawning days in 1999 that successfully produced larvae by October 31st plotted against the potential annual production of larvae under different scenario conditions.

The proportion of original spawning dates to dates that successfully produce larvae (a measure of timing efficiency) was compared to the production efficiency of reproductive energy allocation (Figure 4.97). The relationship depended on whether habitat-based differences in larval mortality existed and the spawning strategy employed. If larvae were only

affected by thermal habitat availability (L1) then ideal free distributions in physical and thermal habitat selection at spawning (S3*) would be highly efficient in timing and energy allocation. However, the same spawning strategy would be one of the least exact for timing, and slightly reduced in production efficiency, if larvae were affected by habitat-related risks.

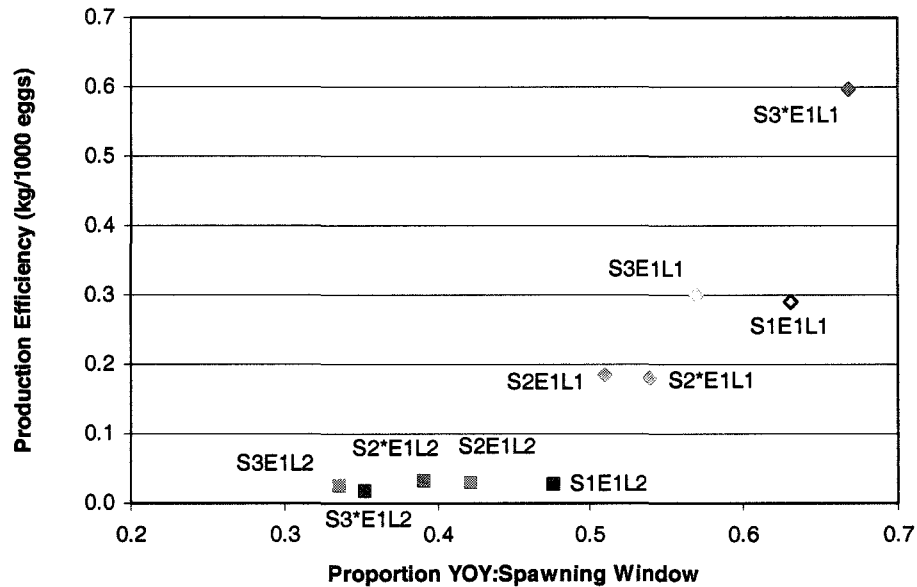


Figure 4.97: The ratio of successful spawning days in 1999 compared to the production efficiency (kg of larvae produced per 1000 eggs laid) of each scenario in Long Point Bay.

The number of cells that were successful from spawning to YOY stage was limited more by temperature and less by physical habitat in the Long Point system (Figure 4.98). Under L2 scenarios fewer cells are successful, especially under S3 variations with very little difference in overall production efficiency. In L1 scenarios, S2 spawning has more successful spawning area but S3* spawning made more efficient use of space, due to high potential production in a few cells later in the spawning window (Figure 4.99). There was an inverse relationship between the proportion of area successfully used and overall production in L1 scenarios. More habitat cells have larvae but thermal survival is lower at high temperatures even though growth may be improved.

A lower proportion of cells were successful than successful days given the initial conditions for each scenario. In heterogeneous, single patch systems, critical patch size populations approached Gaussian spatial distributions with the total population constrained by the capacity of the most limiting cell (Bever and Flather 1999). Therefore the number of cells has a big effect but could be constrained by selection of marginal cells and days under certain conditions.

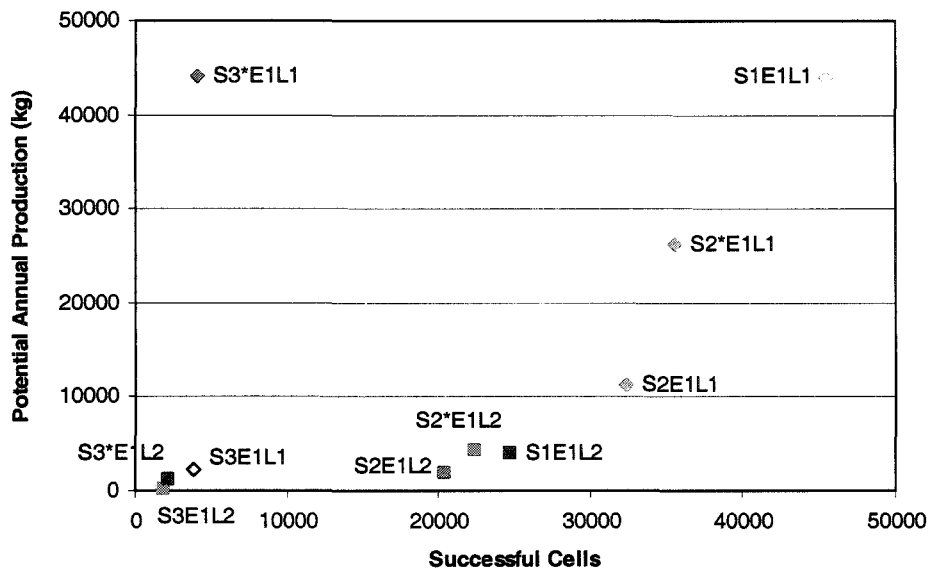


Figure 4.98: The number of grid cells in the Long Point grid that produced larvae in 1999 versus the potential annual production under different scenario conditions (The maximum number of successful cells possible is 304 days x 400 cells = 121,600.)

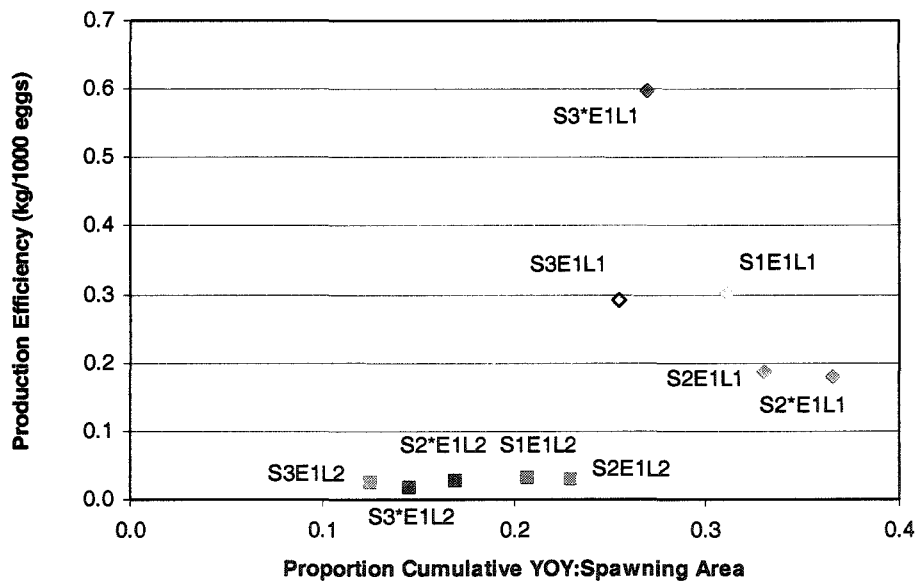


Figure 4.99: The ratio of total annual YOY area (Σ of successful cells over successful days) to cumulative spawning area compared to production efficiency for each scenario (kg of larvae produced per 1000 eggs laid).

Limiting habitat implies density-dependent mechanisms, but PercaSpace tested habitat-based interactions and no density-effect was imposed, (i.e. density of larvae or eggs or spawners did not affect the suitability of sites). The limits to production (temporal, spatial, and stage) showed that under local spawning scenarios, (as if the system is saturated), production is limited by space. Under IFD-allocation scenarios

it is implied that the system is not saturated (no cell is at carrying capacity) and there is room for redistribution according to system-wide habitat suitabilities. Thus, if the expected growth response of fish in an altered thermal habitat is not manifested (i.e. L1 versus L2 scenarios) it may be due to limitations in food abundance (Hayes *et al.* 1996). But habitat is also important if linked to mortality differences due to predation pressure. A temperature match with habitat-related rates seemed to emerge as the driving factor behind potential differences in production. Therefore, changes in habitat quality and quantity are an important measure beyond static measures of standing crop (Hayes *et al.* 1996) because it may allow for surplus production.

4.3.4 Overwinter Survival

In some scenarios, a large number of small larvae contributed to overall production by hatching later in the year, because the cumulative mortality threat for these cohorts was less when the population census was taken in October. Because all fish were included in production estimates, a significant overwinter survival component was not addressed that would contribute to the following years production and age-0 success rates, especially for virtual, fall-spawned fish.

Young-of-the-year model simulations (Post 1990) demonstrated that consumption and growth of larval and juvenile fish were more sensitive to variation in temperature and prey availability than those of adults. Up to 46% mortality occurred in young-of-the-year yellow perch over-winter. When starved, smaller individuals were most likely to die. Winter duration is an important determinant of total and size-selective mortality. Results from a stochastic simulation model, incorporating observed variability in both first year growth and winter duration, suggested that overwinter starvation mortality caused substantial variability in year-class strength that is independent of adult stock size (Post and Evans 1989).

Overwinter survival is a composite of low growth, and thermal and starvation mortality. In yellow perch experiments conducted by Post and Evans (1989), fish were susceptible to overwinter mortality depending on larval size in October and winter duration (measured in days below 6 °C). Conservatively, any fish < 70 mm had a 50% overwinter survival rate but 100% mortality was assumed in the following analyses. Final larval weights were converted to lengths using a length: weight relationship specific to Long Point, to determine which fish from the scenario results would overwinter. A 70-mm yellow perch would weigh 4.25 g.

Four different outcomes in larval size distribution were possible once overwinter survival sizes were accounted for; 70-105 mm (S1, S2, S2* & L1 combinations), 85-105 mm (S3, S3* & L1 combinations), 80-90 mm (S1, S2, S2*, S3* & L2 combinations), and 85-90 mm (S3L2 scenario). The widest size distributions arose from scenarios where the larvae could overwinter from late September spawning, where the inner and outer bays contributed larvae, and when there were no thermal cues

for spawning. Most of the fall production would not be successful post-equinox in 1999 in any scenario due to time constraints on growth rates. When thermal cues were imposed on spawning site selection, the potential spawning window in spring became truncated and limited the summer-spawned, smaller larval sizes that could be achieved in other scenarios. No overwinter mortality occurred in these circumstances. Size distributions did not change under S3*L1 conditions but the viable spawning window was extended, with a high potential contribution to production from summer spawning.

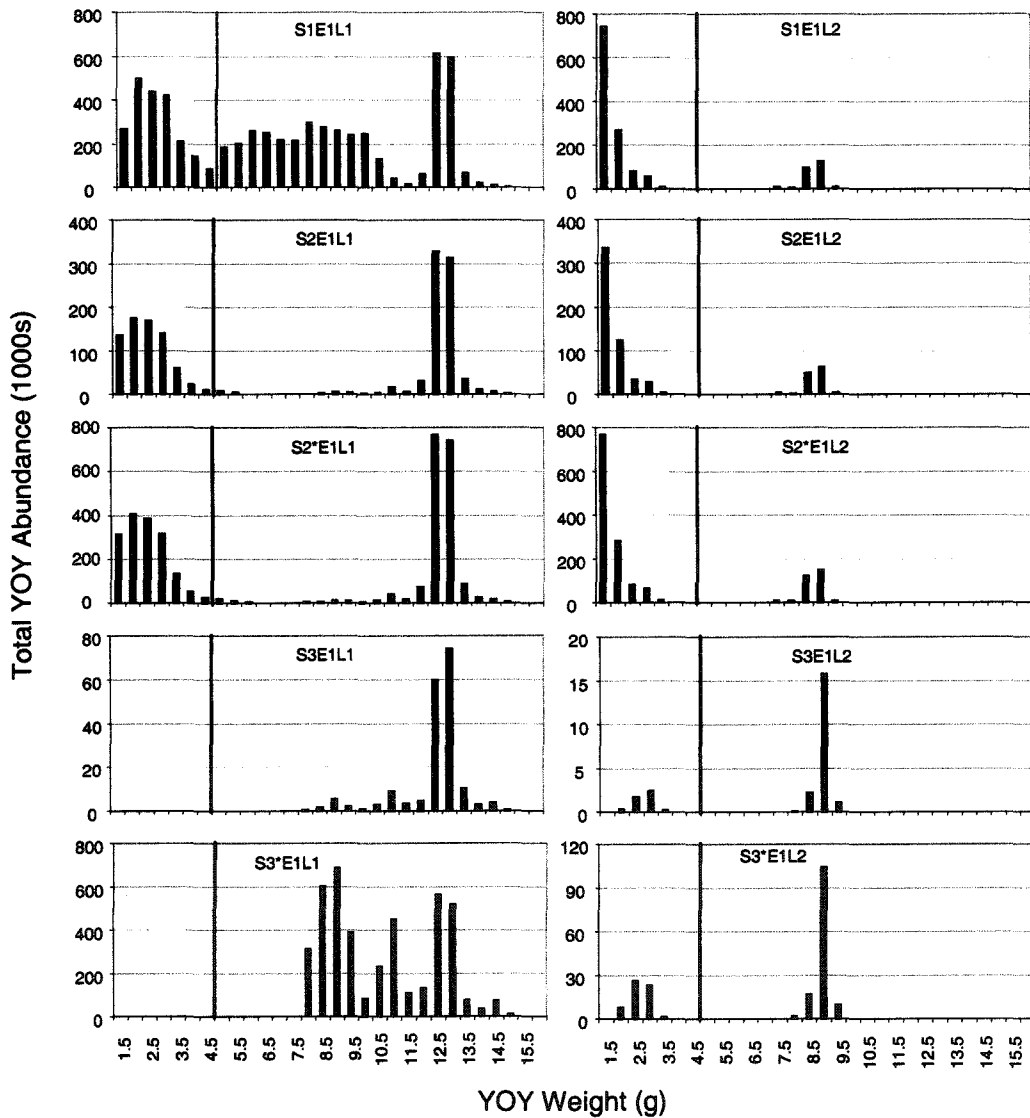


Figure 4.100: Frequency histograms of virtual size categories (weight; grams) based on annual totals (1000s of individuals) for each of the scenario results. The vertical line indicates the size restriction (4.25g) for overwinter survival. (Note the y-axes ranges vary between scenarios.)

The largest YOYs, at 105 mm, were only possible with no habitat-related food restrictions (L1). In all L2 scenarios, the early-spawned, outer bay cohort (2.5 g spring cohort larvae) never exceeded overwinter size thresholds because of habitat mismatches, as well as any fall spawn because of time constraints. Generally, the best thermal habitat for growth (L1) differed from the best food availability (L2) and produced differing spatial patterns in maximum size distributions of larvae. The thermal-cue spawning scenario, without ideal free distribution (S3) resulted in the narrowest larval size range at the end of October because larvae from the outer bay did not contribute. This was not the case for the S3* scenario.

The final larval size differences were not great. The spatial and temporal variation throughout the bay could produce larvae that differed by 3 g at the end of the year that were spawned on the same day. Temporal variation in spawning from the beginning of April to the end of May could produce larvae that were on average 1g different. These temporal differences may also be negated by additional habitat effects because early-hatched larval growth was slower initially. This may indicate that spatial variation in thermal regimes is more important for introducing size variability into the population than timing within the spawning period.

The percent decrease from L1 to L2 scenarios were calculated for fall and overwinter larval abundances and production, as well as individual growth differences, for each spawning scenario combination (Table 4.6). This was a measure of the relative effects that habitat-based growth and survival would have at the larval stage given different starting conditions. Habitat-based differences in fall larval abundance ranged from 56-96%; with the S3* scenario, (spawning site selection based on thermal cues and habitat, with no local carrying capacity) having the greatest difference between L1 and L2 variations. However, subsequent overwinter loss in abundance due to larval growth differences between scenarios were highest in habitat-based spawning (S2 & S2*).

Growth differences were the greatest in scenarios that resulted in two cohorts (S1, S2 & S2*). Loss in production due to larval habitat restrictions was high across all spawning scenarios (83-97%), but lowest for habitat selection at spawning (S2 & S2*). This would indicate that either growth or abundance is limiting but the overall loss in production due to habitat limitations at the larval stage is a trade-off. When overwinter survival is taken into consideration, production differences between L1 and L2 variations were equal across spawning scenarios. S3* scenario combinations produce very different outcomes in all population metrics, perhaps the most important of which was over winter survival and habitat-based mortality and growth differences.

Table 4.6: Comparisons of the percent decreases from L1 (thermal effects on larval maximum feeding and mortality) to L2 scenarios (thermal & habitat-based effects on larval food availability and mortality). (T = temperature and + = habitat-based spawning)
Note: all results use E1 egg scenarios.

Spawning Scenario*	Percent Decreases from L1 to L2 Scenarios				
	Reduction in Fall Abundance	Overwinter Abundance Loss	Loss in Individual Growth	Loss in Annual Production	Overwinter Production Loss
S1 (Uniform)	77%	17%	60%	91%	4%
S2 (Local +)	56%	28%	61%	83%	6%
S2* (System +)	57%	27%	62%	83%	6%
S3 (Local T +)	86%	3%	39%	92%	0%
S3* (System T +)	96%	1%	34%	97%	0%

Production efficiency (a measure of larval biomass per egg production in kg/1000 eggs) was compared across all scenarios to the proportion of production lost due to overwinter mortality (Figure 4.100). Production efficiency was used as a measure of reproductive energy loss and may indicate the most stable strategies given the assumptions of each scenario. Any subsequent overwinter loss would further decrease the efficacy of the strategies. Uniform and habitat-weighted spawning strategies, especially with habitat-based growth differences at the larval stage made significant differences to production efficiency and overwinter survival. Fall larval survival was further reduced by 40-50% by overwinter mortality. In general, thermal selection at spawning fared better than other scenarios.

The scenarios showed evidence supporting the match / mismatch hypothesis (Fortier & Gagne 1990) when all L2 scenarios result in the same production efficiency and size of larvae. This indicates that habitat-based limitations, if larvae remain near spawning grounds, would act as an equalizing agent regardless of the habitat effects and survival efficiency of previous stages and indicate that habitat differences may be limiting larvae.

The high egg production predictions for the deep hole were unexpected because perch are not supposed to spawn beyond 35m. The results may be indicative of fall spawning success rates in general than for perch specifically. Fall larval production in unrestricted spawning scenarios was contributed from the entire bay homogeneously, especially during turnover times. It illustrates that temperatures at these depths and times are not limiting for spawning and egg development, but may be for larvae, depending on habitat restrictions and overwinter survival mechanisms. This implies that spawning times and different life history strategies, i.e. fall vs. spring spawners could be favoured as long as eggs

or larvae had overwinter survival mechanisms which could improve first year production overall. YOY survival, especially overwinter success, had a relatively large influence on spawning location and timing, even though the egg stage showed the greatest declines comparatively. Strand *et al.* (2002) also found that spawning pattern, longevity, and energy allocation were the most sensitive to stochastic juvenile survival. This speaks to comparative life history strategies (e.g. large egg sizes could capitalize on high fall production because of higher overwinter survival).

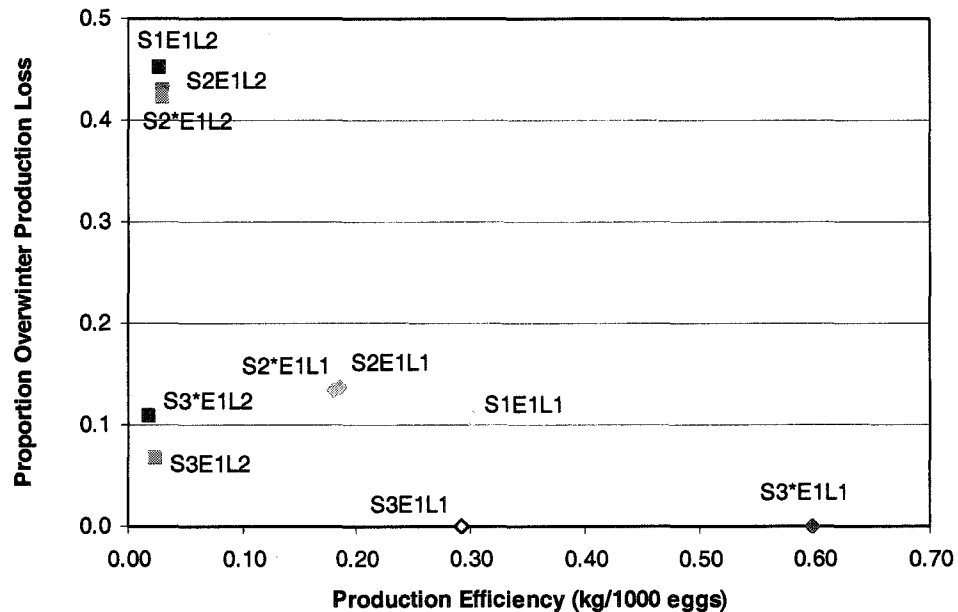


Figure 4.100: The production efficiency (kg of larvae produced per 1000 eggs laid) compared to the predicted overwinter mortality production loss for each scenario based on a size criteria for overwintering (Post & Evans 1989; 70 mm = 4.25 g for yellow perch).

4.3.5 General Conclusions

The results of L2 scenarios indicated a mismatch between habitat-related food, predation pressure, and thermal preferences in the system that may create a more “patchy” environment (see Figure 4.23). The patchiness can be greater than would appear by overlaying habitat features because habitat relates differently to the various vital rates. Even so, predation pressure and food vary differently with the environment but they may be negatively correlated with each other. The Inner Bay only contributed to larval production during autumn in some cases even though egg production could be quite high in spring. This indicates that larvae cannot remain in high egg production zones and are forced to move to improve survival. Good growth temperatures tended to have low thermal mortality, but the additional mortality imposed by habitat-related differences created this pattern. This is further evidence that larval movement should be modelled in the future.

In the end, the total number of surviving planktonic larvae in the system, under full habitat and thermal restrictions with ideal free

distribution of spawning ($S3^*$), was only slightly higher than non-IFD conditions (see Figure 4.84 in results). This implies that if there is a habitat and temperature mismatch at the larval stage then IFD spawning does not offer an advantage if larvae remain in the same site. It may offer improved efficiency until the egg stage, however, only if there is no local carrying capacity. When food availability and temperature were matched with no predation differences between habitats (L1 scenarios), then the system can oscillate between a productive and limited state (Figure 4.98). Hobbs & Hanley (1990) found that wildlife habitat management was only important in a stable system, when habitat becomes limiting at carry capacity. In the same way, variable environmental processes can combine to increase suitable habitat availability.

McCann & Shuter (1996) classified yellow perch as a periodic strategist that inhabits predictable seasonal environments. Periodic spawners are larger, long-lived, have high fecundity with one spawning event and no parental care, have later maturation, and were classed as a modified r-strategist. Parental care reflects the indirect allocation of energy by an adult to offspring in terms of activities designed to enhance offspring survival. Enhancement of juvenile survivorship is not strictly dependent on direct parental care, as seen in the PercaSpace results, but could involve habitat selection strategies. Parental care may involve the production of the egg sheath for protection and the selection of where to allocate the entire annual reproductive reserve, which would be easier in a predictable environment. Therefore, perch spawning, or periodic spawners in general, may be specifically geared towards predicting a stable environment that would maximise future fitness.

McCann & Shuter (1996) concluded that an egg biomass (e_{crit}) per spawning event needed to be exceeded for the recruitment biomass from spawning biomass proportion to be functional, similar to the YOY biomass per egg production efficiency used in this chapter. A periodic strategy would trade juvenile growth for juvenile survivorship and therefore should select for good growth conditions in the first year. Therefore, the scenario results indicate the inner bay should be selected providing extremely high predation rates in vegetated areas do not occur. Periodic spawners also trade fecundity for adult survivorship. With high year-to-year variability in habitat, a strategy for allocating reproduction over several years in a short spawning window would improve the probabilities of producing a large year class when temperature and habitat match as shown in $S3^*$ scenarios. Perhaps the habitat conditions that create strong year-classes should be considered critical habitat.

[Southwood (1988)] stated that interactions of processes along the spatial and temporal axis may complicate ecological response patterns, which may be non-linear.

Statzner et al. 2001

GENERAL CONCLUSIONS

Many studies of fish population dynamics have ignored the spatial heterogeneity and temporal variability of habitat. Here, various sources of information at different resolutions were used to characterize habitat for yellow perch in Long Point Bay. The results showed that it was possible to integrate field and remotely sensed data into a realistic representation of 4D (space-time_ thermal structure for a water body. A realistic representation of physical habitat was created so that subsequent analyses primarily reflected the habitat suitability assignments and modelled fish responses. All the habitat variables were standardized to a common spatial scale, that of the temperature data, for use in a habitat-based, early life stage model. The modelling required a trade-off between assessing habitat at the scale relevant to fish and the level of complexity in the analysis. Analysis in Chapter 2 indicated some variables were functionally coarser-grained than others from a fish's perspective, and at times was greater than the resolution used in the final analysis. The modelling of early life history dynamics of a fish population subject to this variability demonstrated the importance of fish-habitat interactions without becoming computationally too complex.

The study focused on the interaction between temperature and other physical habitat features as determinants of perch distribution and dynamics. Using a few simple temperature functions and mapping the 4D changes in thermal structure, the areas that fish inhabit during different phases of their life cycle were predicted without reference to other habitat preferences or behaviours. For example, documented spawning areas corresponded with predicted suitable thermal habitat for perch eggs in May. However, the habitat suitability (Chapter 2) and modelling analysis (Chapter 4) also both predicted that a greater area of thermally suitable spawning and egg-rearing habitat was available in later months and in different areas than spawning reports indicated for Long Point Bay. These emergent discrepancies between predicted and actual habitat usage illustrate two points. One, knowledge of fish distributions and mechanistic links between vital rates and habitat factors for different life stages is valuable information. Two, given acceptable confidence in the former information, this type of analysis helps identify the limiting behaviour, rate, stage, or habitat that regulates a population within an area.

For example, cues for spawning in perch made a large difference in first year production estimates in PercaSpace. Spawning was only

induced by thermal cues in the model but may also be triggered by photoperiod (Kolkovski & Dabrowski 1998), which would likely further restrict outcomes if included. Even so, spawning sites were not limiting though suitabilities were lower and areas were smaller for eggs than for other stages. Crude estimates of carrying capacity indicated that 800 billion fry could hatch from optimal thermal areas, while 5.5 billion larvae could be supported during thermally restricted times at high densities; allowing a possible 99.9% mortality rate between stages. Given minimum space requirements of juveniles and adults, 2 million to 2.4 billion juvenile and adult perch could be supported in thermally suitable habitat; allowing a range of 50 - 99.9% mortality. Actual adult perch abundance in the Eastern Basin is estimated at 2-2.7 million during the year that was analysed, at the lower end of the predicted range of carrying capacity.

Habitat suitability assessment indicated that most of the bay area was thermally optimal for larval survival over the duration of this life history phase. Generally, the thermal regime in the mid-outer bay region, or upwelling zone, was less suitable. Suitable larval habitat in June overlapped with suitable egg thermal habitat distributions in late May, indicating that eggs hatched into thermally suitable environments. Thermal habitat analysis also showed that behavioural thermoregulation in late summer may prompt the switch to benthic food sources in young of the year fish. For older age classes, 3D mapping of juvenile growth potential showed that optimal ($HSI \geq 0.8$) thermal volumes could be restrictive during the growing season. However, overall thermal growth potential for both juveniles and adults covered a large area of the bay for most of the growing season, if fish maintained their position in thermally suitable layers. If food is disconnected from the thermal habitat then suitable areas may be overestimated. Thermally suitable growing seasons and areas were not very different between juveniles and adults, so if suitable space is restricted due to size-based interactions juveniles may be affected by density-dependence.

High-suitability, pelagic larval habitat overlapped, by roughly 50%, with juvenile and adult habitats. Potential cannibalism in overlap areas could dramatically reduce the suitable habitat area estimates for pelagic larvae, which would become more like optimal demersal areas if actively avoided (notwithstanding passive dispersal in exposed areas). Therefore, the inner bay may act as a refuge from cannibalism if juvenile and adult densities are too high. Demersal optimal habitat overlapped slightly with juvenile and adult habitat. However, the distributions predicted from the thermal analysis would separate life stages vertically, so the area-based overlap estimates are somewhat misleading if different depth strata are chosen.

In most cases, the inclusion of other habitat factors either homogenized the suitability of Long Point Bay (as was the case for spawning), or restricted the area of suitable thermal habitat predicted from the thermal habitat assessment. In some cases, suitable areas shifted

altogether as in the case of demersal larvae. If the habitat factors affect the vital rates of any of these stages, perhaps through density-dependent effects, then the carrying capacity of the bay would be diminished because of non-overlapping suitable areas. A spatial assessment of the overlap of highly suitable habitat between stages should be undertaken in addition to the calculations of carrying capacity effects on an isolated life stage. Without a spatially explicit approach, aggregate weighted useable areas may overestimate the overlap between successive life stages or assume that biotic interactions were not important and the areas independent.

Larval perch habitat suitabilities were validated in Chapter 3. A combination of highly suitable temperatures and dense macrophyte cover explained 43% of the variance in YOY abundance (CPUE) and the probability of finding a school of age-0 perch significantly increased in these areas. This implied that the definition of suitable habitat may be closer to a classical definition of optimal habitat. If the inner bay larval abundance is at carrying capacity, the suitable area available to a life stage may be reduced from that predicted by the overall HSI model and weighted suitability areas may be overestimated in models that use this measurement of habitat availability.

Under certain conditions hierarchical weighting of habitat characteristics should be used. Vegetation, when present, could be a controlling factor in the inner bay because other physical attributes were not predictive of larval distributions. The mismatch between observed and predicted YOY perch distributions indicated the weight of some habitat variables may be underestimated in average HSI calculations, if distributions are indicative of higher fitness. Refining the HSI model, or using the lowest suitability to represent overall suitability, would improve the model's predictive capabilities for habitat occupancy, especially if temperatures were included. In addition, suitability models should be probability based, especially if clumped distributions are involved. However, even if distributions are clustered, the area per individual probably does not change, just the distribution of individuals within the suitable habitat. Therefore, strictly density-based statistical measures of habitat suitability can be misleading if collected at the wrong scale due to clustered distributions of organisms within suitable habitat.

Alternatively, predation pressure may be so high in the inner bay that YOY fish may be forced into less fit habitats. The probability of mortality due to thermal stress and predation is minimized in these inner bay locations but may not have an additional effect on growth because size differences were not significant across habitats. Therefore, certain habitats may maximize survival rates while less conducive to growth. Railsback (2003) also found that fish may be concentrated in areas that do not necessarily offer the highest overall fitness advantage. This is an argument for weighting the relative suitability of habitats differently for different vital process rates, as in Chapter 4.

Zooplankton densities were nonlinearly related to vegetative cover, (resembling a negative quadratic relationship but was non-significant, and the probability of finding zooplankton in areas of low and high cover was greater than in moderate densities. Zooplankton densities were high in both low and high-cover submergent areas. Therefore, open areas may offer a refuge from zooplanktivorous fish and could partly explain the observed distributions. Age-0 fish would require a minimum of 1.4 m³ and 7.1 m³ per individual per day, respectively, based on documented consumption rates and the availability of zooplankton in these areas. The range of zooplankton densities varied widely in high cover because both larvae and zooplankton distributions were patchy. This behavioural response is probably occurring at both trophic levels because there is evidence that zooplankton modify spatial distributions in response to predation, especially in shallow habitats (Jacobsen *et al.* 1997). It would be difficult to distinguish unequal distributions that arose from directed movement from those that resulted for mechanistic reasons at a local scale, such as in high growth and high survival areas with little movement. Therefore, a combination of modelling and controlled experiments were needed to test hypotheses about which vital rate, if any, is controlling distribution.

Two vital rate characteristics were examined in Chapter 4; fitness at each life stage, as well as initial spawning rates in response to habitat availability and carrying capacity at different scales. No cell was at any time allocated the maximum number of eggs in local habitat-weighted scenarios, indicating the absence of 'perfect' physical habitat conditions for spawning. This is similar to results obtained in the simple habitat assessment in Chapter 2, even though the methodology was different. Additionally, Chapter 4 results indicated that egg survival and development was not the limiting factor for spawning site selection and timing, but subsequent larval growth and survival.

Spawning should encompass a selection of habitats or a strategy that increases the likelihood of completion of all life stages, especially if larvae remain locally. The location and timing of spawning predicted by the thermal threshold with locally-weighted habitat selection at spawning scenario concurred with documented spawning areas and times of yellow perch in Long Point Bay. This may indicate that the system is at carrying capacity. The analysis showed that eggs may be more susceptible to random catastrophic events under this reproductive strategy, but the probability of a storm event occurring is lower because of the compressed time period.

Daily growth rates were affected by spatial differences in habitat suitabilities that often produced similar results regardless of the initial conditions. For example, two size cohorts were produced if habitat-based prey was disconnected from thermal preferences at the larval stage, which mainly occurred in the offshore zone. Age-0 cohort splitting has occurred due to density-dependent and competitive effects (Post *et al.* 1997) but

PercaSpace showed that the same outcome can arise from habitat-based differences and behaviours that are independent of density. However, if spring-spawned larvae optimally foraged in the top 10 m instead of behaviourally thermoregulating, then larger sizes could be achieved by fall in the smaller cohort. However, growth would not be as high as under conditions with adequate food at more suitable temperatures. This may indicate that offshore larvae may have to trade-off between starvation and other habitat-related mortality risks.

Thermally, the results indicated that a strategy to maximize growth did not necessarily maximise larval production because of differences in survival rates. Production patterns were often different from potential growth patterns. This has ramifications on using growth potential exclusively for defining optimal habitat. When food availability and predation was uniform, non-contiguous regions of high production and high growth resulted. High growth areas consistently occurred in the inner bay and in slightly different regions of the outer bay depending on the spawning scenario. High production areas occurred in the outer bay to the northeast. The mismatch arose from a difference in the thermal mortality rates and the timing of spawning in the inner and outer bay areas. The distance between high-growth and high-production areas in the outer bay was minimised under thermal-cue spawning conditions. When habitat-based food availability and mortality were imposed, however, high growth & production regions overlapped in Long Point creating one central nucleus that varied in intensity, and subtly by location, in different spawning scenarios.

An evolutionary stable strategy (ESS) would minimize losses across all stages or concentrate loss reduction at a limiting stage. This was the case in all L1 scenarios where greater losses in total potential production always occurred at the egg stage regardless of the spawning scenario, which may indicate that thermal habitat is not limiting larvae. Under IFD thermal and habitat selection at spawning (S3*) egg loss was minimized, but subsequent larval losses were higher and deviated from the exponential decay curve. Only the S3* scenarios would be limited at the larval stage. All of these assume that larvae remain within 1.4 km² of their hatch space.

When the larval stage became limiting during these scenarios, egg survival benefits did not make a difference to final peak abundance. The results indicated that the distribution of spawning effort into either good physical habitat or good thermal habitat would favour egg or larval survival, but not both, with the same overall outcome. Also, the system carrying capacity might be locally limited if habitat-based differences in survival occur at the larval stage. Local habitat constraints at the larval stage overrode the initial starting conditions. The smallest production losses occurred in locally-weighted spawning scenarios but the overall production was dramatically reduced in the whole system due to starting conditions. If larvae were able to move outside of the area in which eggs

were deposited then larval mortality may be mitigated to achieve higher overall abundance. Similar to PercaSpace results, Tyler & Rose (1997) showed that predation distribution, the number of juveniles, the zooplankton density, and the larval behaviour rule affected cohort survivorship using an experimental approach in a SE-IBM.

Only the thermal cue scenarios did not narrow the successful time window significantly between the egg and the swim-up stage. Further, in most scenarios, the dates that successfully produced overwintering larvae comprised 40 to 62% of the initial spawning dates; the proportion of which changed subtly due to habitat constraints at the larval stage. In the S3* scenario combinations, very high egg and larval abundances resulted from the use of very little space at times. Lower, but more consistent, overall swim-up survival was observed when a greater number of cells met thermal spawning conditions. In 1999, the small suitable areas corresponded to the edges of the spawning window, which has implications for early and late spawners. If thermal conditions are good for egg development this period can contribute a significant amount of production to the system, especially at the tail of the optimal window, but is a much riskier allocation of reproductive resources.

Rose (2000) stated that a minor change in complex habitat can produce disproportionate population responses. PercaSpace analysis concurs, especially when the minor change in habitat created a match between good thermal habitat and food with no additional habitat-based mortality. If larvae were only affected by thermal habitat availability (L1 scenarios), then ideal free distributions in physical and thermal habitat selection at spawning (S3*) would be highly efficient in timing and energy allocation. However, the same spawning strategy would be one of the least exact for timing, and slightly reduced in production efficiency, if larvae were affected by habitat-related risks. Therefore it is difficult to determine if the space is limited by habitat constraints at the larval stage or by spawning site selection. Is there an implicit trade-off between larval and egg survival?

A lower proportion of habitat cells were successful than successful days given the initial conditions for each scenario. Therefore the number of cells has a big effect but could be constrained by the selection of marginal cells and days under certain conditions. Therefore, spatial heterogeneity may be more important than temporal variability. The limits to production (temporal, spatial, and stage) showed that under local spawning scenarios, (as if the system is saturated), production is limited by space. Thus, if the expected growth response of fish in an altered thermal habitat is not manifested (i.e. L1 versus L2 scenarios) it may be due to limitations in food abundance. But habitat is also important if linked to mortality differences due to predation pressure. A temperature match with habitat-related rates seemed to emerge as the driving factor behind potential differences in production. Therefore, changes in habitat quality and quantity are an important measure beyond static measures of

reproductive individuals used for management purposes (Hayes et al 1996) because it may allow for surplus production. In the future, temperature-habitat quality synchrony may be disrupted or enhanced by climate change and could adversely or positively affect population dynamics (Magnuson *et al.* 1990). Testing these scenarios would be a valuable application of PercaSpace.

A question that arises is how consistently does the same habitat occur at the same location between years and are choices for habitat use also consistent? Annual production would depend on the level of variability and the rate of adaptation or plasticity in the population. Perhaps the real limits to production occur when there is a mismatch between historically successful strategies and unusual environmental conditions. Examples of unpredictable conditions would include extremely warm or cold years (Casselman 2002) or coincidental storm events that cause windrows for perch eggs (Clady & Hutchinson 1974).

The widest size distributions arose from scenarios where the larvae could overwinter from late September spawning, where the inner and outer bays contributed larvae, and when there were no thermal cues for spawning. When thermal cues were imposed on spawning site selection, the potential spawning window in spring became truncated and limited the summer-spawned, smaller larval sizes that could be achieved in other scenarios. No overwinter mortality occurred in these circumstances. Size distributions did not change under S3*L1 conditions but the viable spawning window was extended, with a high potential contribution to production from summer spawning.

In all L2 scenarios, the early-spawned, outer bay cohort (2.5 g spring cohort larvae) never exceeded overwinter size thresholds because of habitat mismatches, as well as any fall spawn because of time constraints. Food and not temperature was limiting under these conditions. Generally, the best thermal habitat for growth (L1) differed from the best food availability (L2) and produced differing spatial patterns in maximum size distributions of larvae. The spatial and temporal variation throughout the bay could produce larvae that differed by 3 g at the end of the year that were spawned on the same day. Temporal variation in spawning from the beginning of April to the end of May could produce larvae that were on average 1g different. This may indicate that spatial variation in thermal regimes is more important for introducing size variability into the population than timing within the spawning period.

Growth differences between L1 and L2 scenarios were the greatest in those with two cohorts (S1, S2 & S2*). Loss in production due to larval habitat restrictions was high across all spawning scenarios (83-97%), but lowest for habitat selection at spawning (S2 & S2*). This would indicate that either growth or abundance is limiting but the overall loss in production due to habitat limitations at the larval stage is a trade-off. When overwinter survival is taken into consideration, production differences between L1 and L2 variations were equalized across spawning

scenarios. Improved fall larval survival in habitat-based spawning was reduced by 40-50% due to overwinter mortality. In general, thermal selection at spawning fared better than other scenarios. S3* scenario combinations produced very different outcomes in all population metrics, a result of overwinter survival and habitat-based mortality and growth differences.

The scenarios showed evidence supporting the match / mismatch hypothesis (Fortier & Gagne 1990) when all L2 scenarios result in the same production efficiency and size of larvae. This indicates that habitat-based limitations, if larvae remain near spawning grounds, would act as an equalizing agent regardless of the habitat effects and survival efficiency of previous stages and also indicates that habitat differences may be limiting larvae.

High potential fall egg production illustrates that temperatures at these depths and times are not limiting for spawning and egg development, but may be for larvae because of overwinter survival mechanisms. This implies different life history strategies, (i.e. fall vs. spring spawners), would be favoured depending on overwinter survival mechanisms. YOY survival, especially overwinter success, had a relatively large influence on spawning location and timing, even though the egg stage showed the greatest declines comparatively. Strand *et al.* (2002) also found that spawning pattern, longevity, and energy allocation were the most sensitive to stochastic juvenile survival.

The results of L2 scenarios indicated a mismatch between habitat-related food, predation pressure, and thermal preferences in the system that may create a "patchy" environment. The granularity of the habitat can be greater than the patchiness of habitat features because of the underlying functional relationships between habitat and the various vital rates. Good growth temperatures tended to have low thermal mortality, but the additional mortality imposed by habitat-related differences created this pattern. This implies that if there is a habitat and temperature mismatch at the larval stage then IFD spawning does not offer an advantage if larvae remain in the same site. This spawning strategy may offer improved efficiency until the egg stage, however, only if there is no local carrying capacity. Therefore, larvae cannot remain in high egg production zones and would be forced to move to improve survival.

When food availability and temperature were matched with no predation differences between habitats (L1 scenarios), then the system can oscillate between a productive and limited state but only if there is no local carrying capacity. Therefore, perch spawning, or periodic spawners in general, may be specifically geared towards predicting a stable environment that would maximise future fitness. A periodic strategy would trade juvenile growth for juvenile survivorship and therefore should select for good growth conditions in the first year. The scenario results indicated the inner bay should be selected for maximising growth, provided there

are not high predation rates in vegetated areas as indicated by the brief larval survey of the inner bay in 1998 (Chapter 3).

Perhaps the habitat conditions that create strong year-classes should be considered critical habitat. The modelling analysis in Chapter 4 emphasized the importance of spawning behaviour knowledge, the quantification of habitat-life stage interactions, and habitat heterogeneity because very different spatial, temporal, and overall production outcomes can result. From a management perspective, this type of analysis can target important areas at important times of a fish's life cycle for protection. Even if the critical habitat cannot be protected or enhanced (i.e. thermal habitat), the analysis can predict which areas and times would most likely affect populations and can be used for assessment and quota management purposes.

UNCERTAINTY IN THE ANALYSES

During habitat characterization, there was significant error between field and remotely sensed data on certain days from different sources. Inaccuracy could result for positional errors when matching field surface temperatures with specific pixels, a particular problem in nearshore areas. Once improved accuracy in georegistration is possible and corrected then any additional variance in error rates was linked to presence of aquatic vegetation in coastal areas. The use of field data between cloudfree satellite passes was important to adequately capture the temporal dynamics of the system because interpolation error was as high as 5 °C and satellite estimates may be up to 9°C discrepant before correction.

Other possible sources of error include mapping error and suitability assignment error. Although only one year of temperature data was used as a test, it also was convenient to use as a baseline to test changes in habitat-based rules in PercaSpace before introducing interannual variability, a further layer of computational complexity. An effort to preserve the original resolution of the data was made at amalgamating at the grid cell level would tend to homogenize small scale differences in habitat. Standardizing the matrix allows for simplification of the output data; even under the current resolution 146,000 cell-days were modelled in each run.

There are several sources of uncertainty in the habitat suitability assessment. Temporal changes in habitat characteristics were not considered, except for temperature. This is a source of intra- and interannual error, especially for characteristics that change over shorter periods like vegetation rather than substrate. Although catastrophic storm events can dramatically alter soft substrate distributions and water depths. Water level fluctuations will also influence water depths, which were not considered in the assessment. However, the coarseness of variable classifications and suitability assignments, especially because the resolution of the temperature grid is 1.4 km, means that minor water level fluctuations will not change suitable habitat area estimates significantly.

The resolution of the habitat maps does introduce another set of errors that are probably the most critical, especially if it is mismatched from the scale at which fish interact with their environment. This would vary by life stage.

The overall habitat assessments should likely not be equally weighting all the habitat characteristics to define suitable habitat in each life stages. For example, bathymetry or water depth is not important for egg development or survival because once the eggs are laid no direct benefits or disadvantages are incurred by water depth, other than perhaps protecting the eggs from UV degradation or from drying in extremely shallow situations. Similarly, substrate should not be a consideration for the pelagic larval phase, as they do not encounter bottom substrate by definition, unless situated in shallow water of 6m or less. Nevertheless, substrate does not infer any direct benefits as a source of food at this stage but may as potential shelter. It may also indirectly indicate large-scale water movements and turbulence patterns responsible for the establishment of erosional and depositional zones. In either case, it is difficult to quantify the effect without more experimentation.

It was probably an error to include substrate into calculations when vegetation was present because structure is the overriding preference. By averaging the habitat suitabilities, any dominance of a particular habitat variable may be dampened if there is a hierarchy of selection. This is one of the major drawbacks of simple HSI models. It is difficult to establish a statistically based relative weighting because of the lack of empirical relationships or data to establish the hierarchical relationship between variables. Autocorrelation between some variables should also be taken into consideration, like depth and temperature effects. Depth relationships may be significant because other factors, such as light and temperature, are autocorrelated with depth at certain times. This might explain the wide range of depth preferences reported for perch within different ecosystems and at different times of the year (Appendix 2.1) because it is not the true habitat feature influencing distributions.

The method of calculating final suitabilities also introduces error. Different methods for averaging individual habitat characteristics and their relative suitabilities have been used (i.e. geometric versus arithmetic means; Brown *et al.* 2000). Some assessments use the lowest value for any particular characteristic as the suitability for the patch as that is most likely the limiting factor (Krieger *et al.* 1983). The method of assigning suitabilities by combinations of attributes (Minns *et al.* 1996) and not averaging across individual variables, as shown here, may be more practical. However, the former method also has inherent problems when there are nonlinear relationships and different factors become limiting or unsuitable closer to the extremes of their range. Functional suitabilities become difficult to assign in either case.

Leaving some characteristics, like light, out of the assessment may have introduced some error but it is unrealistic to think that all

characteristics of the environment can be assessed or are equally important. Some habitat characteristics will not vary significantly, especially within a limited geographic area such as Long Point Bay. Probably for these reasons, Leftwich *et al.* (1997) and Freeman (1999) found a high level of discordance between HSI models for fish. Variables used in determining suitability were not consistent and the predictability of HSI models in new areas was poor, especially when highly calibrated to distributions within a specific system. Any HSI model should be validated with actual distribution data. For some life stages, this is more difficult because of the paucity of data for early life stages. A survey in the inner bay of Long Point was conducted in 1998 and predicted larval distributions based on habitat suitability analysis are compared in Chapter 3.

Leftwich *et al.* (1997) advocated a hierarchical approach to habitat modelling where variable retention across models may improve transferability between systems, but Duel *et al.* (2000) performed sensitivity analysis that indicated most habitat suitability can be predicted by two to three factors with an uncertainty of 0.1 or 10%. Determining these factors is important, but they most likely vary across life stages. Ryder & Kerr (1989) suggested that environmental assessments should focus on dissolved oxygen (DO), temperature, light and nutrients, which they considered to be limiting environmental factors. However, substrate and vegetation add an additional component because of structural complexity. Further work on teasing apart these individual effects and defining suitable habitat is needed because currently egg allocation in PercaSpace depends on HSI assignments which can be subjectively weighted.

Quantitatively, it is difficult to define 'perfect' spawning habitat but the analyses have proven that definition should include temperature. The S2 scenario results implied that all habitats becomes homogeneous for suitability and does not vary significantly, aside from thermally, across Long Point Bay. Perhaps certain characteristics or groupings should be assigned higher suitabilities in the model if this is not the case, as indicated in Chapter 3, or spawning should be a binary value where suitability is not a gradient but either suitable or unsuitable. The question is whether spawning requirements are truly not very specific and mainly geared towards egg survival. The answer has many implications on the carry capacity of the system because of the inferred suitability values. Although, Craig & Kipling (1983) stated that temperature effects on fry survival, through its effect on food, was the limiting factor, with reproductive biomass always enough to sustain the system even at low population sizes.

Density-dependent processes may be important because they limit food and change mortality rates, and therefore could change habitat suitabilities at high enough densities (Hayes *et al.* 1996). However, this was not tested under the current scenarios. Carrying capacity was imposed indirectly at the spawning stage and the results highlight areas

that might be able to support higher densities or times when density-dependence would matter. For example, IFD spawning conditions that are spatially restricted may result in density-dependent effects after hatch. Hayes et al. (1996) stated that physical habitat functions in a density-independent manner, as was modelled in PercaSpace. However, vital rates are a combination of both density and suitability at a site because successful survival to second year (or to reproduction, for that matter) selects for areas and life strategies that work. Therefore, density-dependent post-hatch functions were implied by the different reproductive allocation strategies employed in PercaSpace.

Local habitat-weighted spawning scenarios implied a local carrying capacity which created a cumulative system-wide carrying capacity. IFD scenarios assumed that a system-wide carrying capacity existed but that no local carrying capacity existed. In Chapter 2, 120 million possible spawning events were predicted from the adult population of perch in the eastern basin based on Lake Erie Management Unit data (Einhouse et al. 2000). One cell, 1.4 km², would be able to hold 7.84 million egg strands if 0.25 m² each were needed for space requirements. Therefore, roughly 15.3 cells could accommodate all spawning events in one day. And theoretically, one cell would be able to accommodate 400,000 strands (not eggs) deposited each day for 19.6 days before reaching capacity; roughly the length of the spawning season. This implies that the egg production in the system could be higher than the scenario defaults and that a potential trade-off between spatial and temporal spawning strategies could develop (i.e. selecting the most efficient time to spawn versus selecting the most efficient place to spawn).

The model predicted that many of the pre-demersal larvae spawned in June and July under IFD conditions successfully inhabit a narrow band of mid-depth waters in the outer bay (Figure 4.80). These transitional zones could be areas of high potential productivity but are unpredictable environments. It is uncertain whether this is a true result or an artefact of modelling without spawning or larval validation data for the outer bay. Also, ambient temperatures were used as indicators of suitability and not the variability in temperatures, which would make a difference in this steep, upwelling zone. However, this pattern was repeated in several different years (see Chap. 2) and may be the key to high production because it creates a temporal refuge if late spawning occurs and temperature is the driving factor.

Rose (2000) commented on the difficulties of linking quantitative relationships between the environment and fish populations. Detectability in patterns can be masked by interannual variation and interaction among climatic variables that affect population dynamics and that make isolating effects of individual stressors difficult. PercaSpace tested systematically the interaction between temperature and physical habitat but a complete sensitivity analysis of HSI variables will be necessary.

These results were obtained without sacrificing biological realism in modelling large-scale phenomena. The cumulative effects of environmental variables on successive life stages were studied with PercaSpace. This model substituted variability in individuals with variability in the environment of spatially-distributed cohorts. One of the benefits of modelling in a realistic environment is the ability to validate with field data, which was shown to a limited extent by corroborating spawning and larval locations, however more time series data is needed at proper spatial scales and from different life stages to validate the model.

Potential errors included landscape measurement error, misclassification of habitat suitability, and incorrect habitat-related growth and mortality relationships, which could contribute to increasing output error, respectively. The latter is probably the most important to parameterize. Ruckelshaus et al. (1997) determined error rate propagation in spatially explicit population models (SE-PMs) but many of the uncertainty calculations dealt with migration rates. In PercaSpace, error in the model is mainly be due to uncalibrated suitability assignments and links to vital rates, and not necessarily error in habitat mapping (Minns et al. 1999). Ruckelshaus et al. (1999) reaffirmed that accurate data and rate predictions are still necessary to have models with good predictive power and use in conservation but the aim of PercaSpace was a comparative study between habitat effects at different stages so predictive power is less important and the scenarios were meant to realistically capture the extremes. PercaSpace and similar models can provide constructive guidance for future field work and experimental studies of fish-habitat linkages to address these issues.

In a habitat-based approach linking habit with population and individual rates is important, which may be intensive, especially when modelling or interpolating physical processes and habitat. Empirical and observational approaches (correlation and regression with actual data) are less intensive, but they do not usually show what controls population dynamics and vital rates. A process-based approach allowed exploration of direct questions that link mechanistically to population dynamics and does not infer cause-and-effect between pattern-based relationships (Shuter & Regier 1989). There is a trade-off between the process-driven mechanistic approach to modelling (IBM and spatially explicit approaches) and aggregated, holistic approaches (MEI-yield and THV-yield). However, the two extremes should inform one another. (i.e. the outcomes should allow connection between inferred mechanisms and observed aggregate patterns). We can identify large-scale aggregated phenomena when we seek to understand them at the level of detail at which the mechanisms operate.

FUTURE ANALYSES

Linking suitabilities to the probabilities of finding certain life stages or species because of distributions may incorrectly infer that those habitat

characteristics actually provide a growth or survival advantage. For example, it is unclear how water depth *directly* affects spawning or egg success, other than through the possible effects of atmospheric pressure. However, the availability of preferred depths in a system could limit egg carrying capacity indirectly, as depth is correlated with temperature, vegetation, and to some extent substrate type through wave exposure.

In future, sensitivity analyses could be performed to determine the changes in final suitable area predictions based on error estimates at each step. For example, thermal tolerances do not change immediately between life stages. Individual variation exists within life stages and gradual changes in physiological optima probably take place. It would also be important to take acclimation temperature into consideration in future assessments.

HSIs are often a qualitative and relative assignment of a numeric suitability that actually represents a range of probabilities or suitabilities. For example, something that is moderately suitable at 0.5 may represent a range of suitabilities from 0.25-0.75. Therefore, it would be prudent to perform a sensitivity analysis or an error analysis on the categorical suitability assignments to determine what the temporal and spatial error estimates of suitable times and areas are for different life stages and the potential ramifications on population dynamics. Future experiments should be conducted to verify any emergent properties that arise from habitat suitability model predictions (Railsback *et al.* 2003), such as the importance and location of thermal habitat and variability. Every effort should be made to quantify the relationships between habitat and individual vital rates because the link remains tenuous.

Eggs mainly require good thermal habitat and on rare occasions exposure would have a detrimental effect based on the PercaSpace scheme. It would be prudent to compare other years to assess the relative impact of overlap between temperature and exposure on population dynamics through egg survival, which may impose further habitat restrictions on production potential or increase year-to-year variability. However, if temperature relationships are the most quantified and we are overlooking other potential sources of environmental regulation for development and survival at this stage. For example, vegetation is often reported as the preferred spawning habitat in most accounts. Perhaps vegetation and other associated variables have been spuriously related to egg success because vegetation occurs in good thermal, sheltered habitat. Alternatively, there are other aspects of vegetation, such as dissolved oxygen levels, shading, and siltation-prevention that are important to egg survival, which are not accounted for in PercaSpace. In future scenarios, PercaSpace should compare temperature selection only during spawning and then compare outcomes to the existing scenarios to determine if other habitat features add significantly to habitat restrictions.

The spatial patterns in food availability used in scenarios may result from differential grazing, differential primary production, or probably both (Hayes et al. 1996). Feedback due to grazing was not considered in the model because controlled numbers of larvae were used in the scenarios. The zooplankton data used to generate time series was not detailed enough to reconstruct a realistic estimate of spatial distributions. Therefore, relative growth rates were used in different areas based on generalized differences in prey abundance. Also, a smaller time step would be required to model forays from optimal thermal habitat into optimal foraging habitat. Energetic trade-offs in a realistic system should be tested in a future version of PercaSpace.

Community interactions within habitats were not addressed directly in the model but implied through growth and mortality differences. Competition or density-dependent effects were not included as they would be difficult to parameterize. Sublethal effects on population dynamics were also not incorporated, such as environmental effects on size and age-at-maturity which will be addressed with completion of a full population model and incorporation of larval & older age-class movement. Using nearest neighbour analysis, a cell adjacency table was constructed by determining the cell IDs of water polygons that were adjacent to each other (i.e. their borders were shared and no land features blocked accessibility or "movement" from one cell to the next). This connectivity table will be used in the future assessment of movement to address differences in scenario outcomes. If larvae were allowed to move, either passively or actively, would the same patterns emerge between spawning strategies or local versus system-wide scenarios?

There is a need to add additional thermal components into the model and to test year-to-year variability in the environment. Also, daily temperature differences should be incorporated into habitat suitabilities in addition to the absolute temperatures that are currently modelled. The acclimation temperature and rapid temperature fluctuations can both ameliorate thermal mortality and exacerbate it, respectively. Also, the vegetation extents and wind conditions in 1999 should be compared in the model to test their relative contribution to annual variability in year class strength that can be compared with longer term yellow perch dynamics in Long Point.

Yellow perch probably 'switch' to benthos earlier in the first year then is currently modeled in PercaSpace in the Long Point region (MacDougall *et al.* 2001). The planktonic stage is thought to last for 4-5 weeks but the length is more likely dependent on food availability and accessibility. Additional scenarios should include diet shifts that are regulated by growth to a certain size or age, or a switch dependent on food availability, which would be habitat-based or temporally-based. However, if feeding is more opportunistic as several authors suggest (Hayes & Taylor 1990, Takimoto 2003), niches and feeding shifts are more plastic. Differences across L1 and L2 scenarios might be minimized

if larvae could forage for many prey items and offshore larvae could reach maximum intake if they switch to benthos earlier. This requires further evolution of decision rules.

Once all these issues are addressed then the impact of habitat alterations and fishing mortality can be tested. Crowder *et al.* (1998) suggested that spatial interactions and fishing mortality were more important than egg survival to population dynamics. Habitat complexity could offer refugia from this additional source of mortality and larval dynamics should be taken into account. If large fluctuations in year class strength do occur because of habitat carrying capacity changes, then fishing mortality may be mitigated. Large-scale habitat management experiments (Jones 2003) indicate that habitat enhancement may be less beneficial than previously thought, but success depends on lag times for prey items and fish to acclimate to changes. PercaSpace cannot account for prey density lags but the spawning strategy employed, knowledge of the system, and dispersal into new habitats can be tested. Habitat alterations in Long Point, especially in vegetation or deposition of finer substrates, are realistic. Changes could create greater physical habitat heterogeneity, especially if good thermal habitat separates further from other preferred habitats. It would be useful to determine the relative impact of these factors on perch dynamics. the potential contribution of habitat to fish population dynamics has been demonstrated. Knowledge of habitat variability (both spatially and temporally), carrying capacity, and reproductive allocation behaviours are the key to determining limits to production.

BIBLIOGRAPHY (including Appendices)

- Aalto, S. K., and G. E. Newsome. 1993. Winds and the demic structure of a population of yellow perch (*Perca flavescens*). *Canadian Journal of Fisheries and Aquatic Sciences* 50:496-501.
- Ansari, R. H., and S. U. Qadri. 1989. Individual variation in the foraging strategies of young yellow perch (*Perca flavescens*) from the Ottawa River. *Hydrobiologia* 174:207-212.
- Bakelaar, C. N., P. Brunette, P. M. Cooley, S. E. Doka, E. S. Millard, C. K. Minns, and H. A. Morrison. 2004. Geographic Information Systems Applications in Lake Fisheries. Pages 113-152 in W. L. Fisher and F. J. Rahel, editors. *Geographic information Systems in Fisheries*. American Fisheries Society, Bethesda, Maryland.
- Baker, E. A., S. A. Tolentino, and T. S. McComish. 1992. Evidence for yellow perch predation on *Bythotrephes cederstroemi* in southern Lake Michigan. *Journal of Great Lakes Research* 18:190-193.
- Balon, E. K. 1975. Reproductive guilds of fishes: A proposal and definition. *Journal of the Fisheries Research Board of Canada* 32:822-964.
- Bartholow, J. M., J. L. Laake, C. B. Stalnaker, and S. C. Williamson. 1993. A salmonid population model with emphasis on habitat limitations. *Rivers* 4:265-279.
- Bartsch, J., K. Brander, M. Heath, P. Munk, K. Richardson, and E. Svendsen. 1989. Modelling the advection of herring larvae in the North Sea. *Nature* 340:632-636.
- Beitinger, T. L., and W. A. Bennett. 2000. Quantification of the role of acclimation temperature in temperature tolerance of fishes. *Environmental Biology of Fishes* 58:277-288.
- Beitinger, T. L., W. A. Bennett, and R. W. McCauley. 2000. Temperature tolerances of North American freshwater fishes exposed to dynamic changes in temperature. *Environmental Biology of Fishes* 58:237-275.
- Bergman, E. 1991. Changes in abundance of two percids, *Perca fluviatilis*, and *Gymnocephalus cernuus*, along a productivity gradient: relations to feeding strategies and competitive abilities. *Canadian Journal of Fisheries and Aquatic Sciences* 48:536-545.
- Bernstein, C., P. Auger, and J. C. Poggiale. 1999. Predator migration decisions, the ideal free distribution, and predator-prey dynamics. *The American Naturalist* 153:267-281.
- Bevers, M., and C. H. Flather. 1999. Numerically exploring habitat fragmentation effects on populations using cell-based coupled map lattices. *Theoretical Population Biology* 55:61-76.
- Boehlert, G. W., and B. C. Mundy. 1988. Roles of behavioural and physical factors in larval and juvenile fish recruitment to estuarine nursery areas. Pages 51-67 in M. P. Weinstein, editor. *Larval fish and shellfish transport through inlets*. AFS, Ocean Springs, MS.

- Boisclair, D. 2001. Fish habitat modeling: from conceptual framework to functional tools. *Canadian Journal of Fisheries and Aquatic Sciences* 58:1-9.
- Boisclair, D., and W. C. Leggett. 1989. The importance of activity in bioenergetics models applied to actively foraging fishes. *Canadian Journal of Fisheries and Aquatic Sciences* 46:1859-1867.
- Boisclair, D., and P. Sirois. 1993. Testing assumptions of fish bioenergetics models by direct estimation of growth, consumption, and activity rates. *Transactions of the American Fisheries Society* 122:784-796.
- Boyce, F. M., M. A. Donelan, P. F. Hamblin, C. R. Murthy, and S. T.J. 1989. Thermal structure and circulation in the Great Lakes. *Atmosphere-Ocean* 27:607-642.
- Brandt, S. B., and K. J. Hartman. 1993. Innovative approaches with bioenergetics models: future applications to fish ecology and management. *Transactions of the American Fisheries Society* 122:731-735.
- Brandt, S. B., and J. Kirsch. 1993. Spatially explicit models of striped bass growth potential in Chesapeake Bay. *Transactions of the American Fisheries Society* 122:845-869.
- Brandt, S. B., J. J. Magnuson, and L. B. Crowder. 1980. Thermal habitat partitioning by fishes in Lake Michigan. *Canadian Journal of Fisheries and Aquatic Sciences* 37:1557-1564.
- Breck, J. E. 1993. Foraging theory and piscivorous fish: are forage fish just big zooplankton? *Transactions of the American Fisheries Society* 122:902-911.
- Bronte, C. R., J. H. Selgeby, and D. V. Swedberg. 1993. Dynamics of a yellow perch population in western Lake Superior. *North American Journal of Fisheries Management* 13:511-523.
- Brown, S. K., K. R. Buja, S. H. Jury, M. E. Monaco, and A. Banner. 2000. Habitat suitability index models for eight fish and invertebrate species in Casco and Sheepscot Bays, Maine. *North American Journal of Fisheries Management* 20:408-435.
- Bystrom, P., L. Persson, and E. Wahlstrom. 1998. Competing predators and prey: juvenile bottlenecks in whole-lake experiments. *Ecology* 79:2153-2167.
- Carlander, K. D. 1997. Yellow Perch, *Perca flavescens* (Mitchill). Pages 125-179 in *Handbook for Freshwater Fishery Biology: Life History Data on Ichthyopercid and Percid Fishes of the United States and Canada*. Iowa State University Press, Ames, Iowa.
- Carpenter, S. R., and J. F. Kitchell. 1992. Trophic cascade and biomanipulation: interface of research and management - a reply to the comment by DeMelo et al. *Limnology Oceanography* 37:208-213.
- Carpenter, S. R., M. Olson, P. Cunningham, S. Gafny, N. Nibbelink, T. Pellett, C. Storlie, A. Trebitz, and K. Wilson. 1998. Macrophyte structure and growth of bluegill (*Lepomis macrochirus*): design of a multilake experiment. Pages 217-226 in E. Jeppesen, M. Søndergaard, M. Søndergaard, and K. Christoffersen, editors. *The Structuring Role of Submerged Macrophytes in Lakes*. Springer-Verlag Inc., New York.

- Casselman, J. M. 2002. Effects of temperature, global extremes, and climate change on year-class production of warmwater, coolwater, and coldwater fishes in the Great Lakes basin. Pages 39-60 *in* American Fisheries Society Symposium 32. American Fisheries Society. Bethesda, MD.
- Casselman, J. M., and C. A. Lewis. 1996. Habitat requirements of northern pike (*Esox lucius*). Canadian Journal of Fisheries and Aquatic Sciences 53:161-174.
- Charnov, E. L. 1976. Optimal foraging, the marginal value theorem. Theoretical Population Biology 9:129-136.
- Christie, G. C., and H. A. Regier. 1988. Measures of optimal thermal habitat and their relationship to yields for four commercial fish species. Canadian Journal of Fisheries and Aquatic Sciences 45:301-314.
- Chu, C., N. C. Collins, N. P. Lester, and B. J. Shuter. 2001 (Unpublished report). Predicting littoral temperatures. University of Toronto. Mississauga, ON. 13 pp.
- Clady, M., and B. Hutchinson. 1974. Effect of high winds on eggs of yellow perch, *Perca flavescens*, in Oneida Lake, New York. American Midland Naturalist 91:453-459.
- Claessen, D., A. M. de Roos, and L. Persson. 2000. Dwarfs and giants: cannibalism and competition in size-structured populations. American Naturalist 155:219-237.
- Conroy, M. J., and B. R. Noon. 1996. Mapping of species richness for conservation of biological diversity: conceptual and methodological issues. Ecological Applications 6:763-773.
- Cook, A., M. Thomas, D. Einhouse, K. Kayle, R. Kenyon, C. Knight, P. Ryan, S. Sandstrom, B. Sutherland, and B. Morrison. 2001. Report of the Lake Erie Yellow Perch Task Group. Lake Erie Committee of the Great Lakes Fishery Commission.
- Craig, J. F. 1987. The Biology of Perch and Related Fish. Timber Press, Portland, Oregon.
- Craig, J. F., and C. Kipling. 1983. Reproduction effort versus the environment; case histories of Windermere perch, *Perca fluviatilis* L., and pike, *Esox lucius* L. Journal of Fish Biology 22:713-727.
- Crowder, L. B., and J. J. Magnuson. 1982. Cost-benefit analysis of temperature and food resource use: a synthesis with examples from the fishes. Pages 189-221 *in* W. P. Aspey and S. I. Lustick, editors. Behavioural Bioenergetics: The Cost of Survival in Vertebrates. Ohio State University Press, Columbus, OH.
- Crowder, L. B., E. W. McCollum, and T. H. Martin. 1998. Changing perspectives on food web interactions in lake littoral zones. Pages 240-249 *in* E. Jeppesen, M. Søndergaard, M. Søndergaard, and K. Christoffersen, editors. The Structuring Role of Submerged Macrophytes in Lakes. Springer-Verlag Inc., New York.
- Cushing, D. H. 1974. The possible density-dependence of larval mortality and adult mortality in fishes. Pages 103-111 *in* J. H. S. Blaxter, editor. The early life history of fish. Springer-Verlag, New York.
- Cyr, H., and J. A. Downing. 1988. The abundance of phytophilous invertebrates on different species of submerged macrophytes. Freshwater Biology 20:365-374.

- Dahl, J. A., D. M. Graham, R. Dermott, O. E. Johannsson, E. S. Millard, and D. D. Myles. 1995. Lake Erie 1993, western, west central and eastern basins: change in trophic status, and assessment of the abundance, biomass and production of the lower trophic levels. Canadian Technical Report of Fisheries and Aquatic Sciences 2070, Burlington, Ontario.
- Danehy, R. J., N. H. Ringler, and J. E. Gannon. 1991. Influence of nearshore structure on growth and diets of yellow perch (*Perca flavescens*) and white perch (*Morone americana*) in Mexico Bay, Lake Ontario. *Journal of Great Lakes Research* 17:183-193.
- Danzmann, R. G., D. S. MacLennan, D. G. Hector, P. D. N. Hebert, and J. Kolasa. 1991. Acute and final temperature preference as predictors of Lake St. Clair fish catchability. *Canadian Journal of Fisheries and Aquatic Sciences* 48:1408-1418.
- DeAngelis, D. L., B. J. Shuter, M. S. Ridgway, and M. Scheffer. 1993. Modeling growth and survival in an age-0 fish cohort. *Transactions of the American Fisheries Society* 122:927-941.
- DeAngelis, D. L., L. Godbout, and B. J. Shuter. 1991. An individual-based approach to predicting density-dependent dynamics in smallmouth bass populations. *Ecological Modelling* 57:91-115.
- Delong, A. K., and R. H. Lamberson. 1999. A habitat based model for the distribution of forest interior nesting birds in a fragmented landscape. *Natural Resource Modeling* 12:129-146.
- Diehl, S., and P. Eklöv. 1995. Effects of piscivore-mediated habitat use on resources, diet, and growth of perch. *Ecology* 76:1712-1726.
- Diehl, S., and R. Kornijów. 1998. Influence of submerged macrophytes on trophic interactions among fish and macroinvertebrates. Pages 24-90 *in* E. Jeppesen, M. Søndergaard, M. Søndergaard, and K. Christoffersen, editors. *The Structuring Role of Submerged Macrophytes in Lakes*. Springer-Verlag Inc., New York.
- Dimitru, C., O. E. Johannsson*, T. MacDougall, and C. Giroux. Unpublished Data. * Corresponding author. Fisheries & Oceans Canada. Great Lakes Laboratory for Fisheries and Aquatic Sciences. 867 Lakeshore Rd. Burlington, ON. L7R 4A6.
- Dörner, H., A. Wagner, and J. Benndorf. 1999. Predation by piscivorous fish on age-0 fish: spatial and temporal variability in a biomanipulated lake (Bautzen Reservoir, Germany). *Hydrobiologia* 408/409:39-46.
- Duel, H., S. Groot, G. Van der Lee, and D. T. Van der Molen. 2000. Uncertainty analysis of habitat evaluation methods. Pages 1-13 *in* L. Majone and M. Majone, editors. *New Trends in Water and Environmental Engineering for Safety and Life*. Balkema, Rotterdam.
- Einhouse, D., K. Kayle, R. Kenyon, C. Knight, P. Ryan, S. Sandstrom, B. Sutherland, and M. Thomas. 2000. Report of the Lake Erie Yellow Perch Task Group. Standing Technical Committee, Lake Erie Committee, Great Lakes Fishery Commission. 19+ pp.
- Eklöv, P. 1997. Effects of habitat complexity and prey abundance on the spatial and temporal distributions of perch (*Perca fluviatilis*) and pike (*Esox lucius*). *Canadian Journal of Fisheries and Aquatic Sciences* 54:1520-1531.

- Essington, T. E., and J. F. Kitchell. 1999. New perspectives in the analysis of fish distributions: a case study on the spatial distribution of largemouth bass (*Micropterus salmoides*). *Canadian Journal of Fisheries and Aquatic Sciences* 56:52-60.
- Falk, M. R. 1971. Food habits, gastric digestion and food consumption rates of yellow perch, *Perca fluviatilis flavescens* (Mitchill), in West Blue Lake, Manitoba. M.Sc. University of Manitoba, Winnipeg, Manitoba.
- Ferguson, R. G. 1958. The preferred temperature of fish and their midsummer distribution in temperate lakes and streams. *Journal of the Fisheries Research Board of Canada* 15:607-624.
- Fischer, P., and R. Eckmann. 1997. Spatial distribution of littoral fish species in a large European lake, Lake Constance, Germany. *Archives of Hydrobiology* 140:91-116.
- Fisher, S. J., and D. W. Willis. 1997. Early life history of yellow perch in two South Dakota glacial lakes. *Journal of Freshwater Ecology* 12:421-429.
- Fisher, S. J., C. R. Pyle, and D. W. Willis. 1999. Habitat use by age-0 yellow perch in two South Dakota glacial lakes. *Ecology of Freshwater Fish* 8:85-93.
- Fisher, S.J., K.L. Pope, L.J. Templeton, and D.W. Willis. 1996. Yellow perch spawning habitats in Pickerel Lake, S. Dakota. *The Prairie Naturalist* 28:65-75
- Fortier, L., and J. A. Gagne. 1990. Larval herring (*Clupea harengus*) dispersion, growth, and survival in the St. Lawrence estuary: match/mismatch or membership/vagrancy? *Canadian Journal of Fisheries and Aquatic Sciences* 47:1898-1912.
- Freeman, M. C. 1999. Comment: transferability of habitat suitability criteria. *North American Journal of Fisheries Management* 19:623-625.
- Fry, F. E. J. 1947. Effects of the environment on animal activity. *Biological Series* 55, University of Toronto Studies.
- Garner, P., S. Clough, S. W. Griffiths, D. Deans, and A. Ibbotson. 1998. Use of shallow marginal habitat by *Phoxinus phoxinus*: a trade-off between temperature and food? *Journal Of Fish Biology* 52:600-609.
- Gasith, A., and M. V. Hoyer. 1998. Structuring role of macrophytes in lakes: changing influence along lake size and depth gradients. Pages 381-392 in E. Jeppesen, M. Søndergaard, M. Søndergaard, and K. Christoffersen, editors. *The Structuring Role of Submerged Macrophytes in Lakes*. Springer-Verlag Inc., NY.
- Gaudreau, N., and D. Boisclair. 1998. The influence of spatial heterogeneity on the study of fish horizontal daily migration. *Fisheries Research* 35:65-73.
- Geomatics International Inc. 1997. Discrimination of substrate, submerged vegetation density and species assemblages, and wetland species assemblages using airborne remotely sensed imagery, Long Point, Lake Erie, Ontario. Unpublished Report. Burlington, Canada.
- Giannico, G. R., and M. C. Healey. 1999. Ideal free distribution theory as a tool to examine juvenile coho salmon (*Oncorhynchus kisutch*) habitat choice under different conditions of food abundance and cover. *Canadian Journal of Fisheries and Aquatic Sciences* 56:2362-2373.

- Gilpin, M., and I. Hanski. 1991. Metapopulation dynamics: empirical and theoretical investigations. Academic Press, London.
- Goodyear, C.S., T.A Edsall, D.M. Ormsby, G.D. Moss, and P.E. Polanski. 1982a. Atlas of the Spawning and Nursery Areas of Great Lakes Fishes. Volume I – Summary by Geographic Area. FWS/OBS-82/52, U.S. Dept of Interior, Fish and Wildlife Service and U.S. Dept of the Army, Corp. of Engineers. Washington, D.C.
- Goodyear, C.S., T.A Edsall, D.M. Ormsby, G.D. Moss, and P.E. Polanski. 1982b. Atlas of the Spawning and Nursery Areas of Great Lakes Fishes. Volume IX – Lake Erie. FWS/OBS-82/52, U.S. Dept of Interior, Fish and Wildlife Service and U.S. Dept of the Army, Corp of Engineers. Washington, D.C.
- Goodyear, C.S., T.A Edsall, D.M. Ormsby, G.D. Moss, and P.E. Polanski. 1982c. Atlas of the Spawning and Nursery Areas of Great Lakes Fishes. Volume XIII – Species Reproduction Characteristics. FWS/OBS-82/52, U.S. Dept of Interior, Fish and Wildlife Service and U.S. Dept of the Army, Corp of Engineers. Washington, D.C.
- Graham, D. M., J. A. Dahl, E. S. Millard, O. E. Johannsson, and L. L. White. 1996. Assessment of abundance, biomass and production of the lower trophic levels in the eastern basin of Lake Erie, 1994. Canadian Technical Report of Fisheries and Aquatic Sciences 2110, Fisheries and Oceans Canada, Burlington, Ontario.
- Hansen, A. J., J. J. Rotella, M. P. V. Kraska, and D. Brown. 1999. Dynamic habitat and population analysis: an approach to resolve the biodiversity manager's dilemma. *Ecological Applications* 9:1459-1476.
- Hanson, P. C., T. B. Johnson, D. E. Schindler, and J. F. Kitchell. 1997. Fish Bioenergetics 3.0 for Windows. University of Wisconsin Center for Limnology, Madison, Wisconsin.
- Hasler, A. D., and J. E. Bardach. 1949. Daily migrations of perch in Lake Mendota, Wisconsin. *Journal Wildlife Management* 13:40-51.
- Hassell, M. P. 1987. Detecting regulation in patchily distributed animal population. *Journal of Animal Ecology* 54:323-334.
- Hastings, A. 1990. Spatial heterogeneity and ecological models. *Ecology* 71:426-428.
- Havens, K. E., A. D. Steinman, and B. Fry. 2001. Spatial variation in food web structure and function in a large, shallow subtropical lake (Lake Okeechobee, Florida, USA). *Verh. Internat. Verein. Limnol.* 27:3470-3475.
- Hayes, D. 1999. Issues affecting fish habitat in the Great Lakes basin. Pages 209-238 in W. W. Taylor and C. P. Ferreri, editors. *Great Lakes Fisheries Policy and Management: a Binational Perspective*. Michigan State University Press, East Lansing.
- Hayes, D. B., and W. W. Taylor. 1990. Reproductive strategy in yellow perch (*Perca flavescens*): effects of diet ontogeny, mortality, and survival costs. *Canadian Journal of Fisheries and Aquatic Sciences* 1990:921-927.
- Hayes, D. B., W. W. Taylor, and J. C. Schneider. 1992. Response of yellow perch and the benthic invertebrate community to a reduction in the abundance of white suckers. *Transactions of the American Fisheries Society* 121:36-53.

- Hayes, D. M., C. P. Ferreri, and W. W. Taylor. 1996. Linking fish habitat to their population dynamics. *Canadian Journal of Fisheries and Aquatic Sciences* 53:383-390.
- Hayward, R. S., and F. J. Margraf. 1987. Eutrophication effects on prey size and food available to yellow perch in Lake Erie. *Transactions of the American Fisheries Society* 116:210-223.
- Henderson, B. A. 1985. Factors affecting growth and recruitment of yellow perch, *Perca flavescens* Mitchill, in South Bay, Lake Huron. *Journal of Fish Biology* 26:449-458.
- Henderson, B. A., and S. J. Nepszy. 1989. Yellow perch (*Perca flavescens*) growth and mortality rates in Lake St. Clair and the three basins of Lake Erie, 1963-86. *Journal of Great Lakes Research* 15:317-326.
- Hepinstall, J. A., L. P. Queen, and P. A. Jordan. 1996. Application of a modified habitat suitability index model for moose. *Photogrammetric Engineering and Remote Sensing* 62:1281-1286.
- Hinch, S. G., K. M. Somers, and N. C. Collins. 1994. Spatial autocorrelation and assessment of habitat-abundance relationships in littoral zone fish. *Canadian Journal of Fisheries and Aquatic Sciences* 51:701-712.
- Hobbs, N. T., and T. A. Hanley. 1990. Habitat evaluation: do use and availability data reflect carrying capacity? *Journal of Wildlife Management* 54:515-522.
- Hokanson, K. E. F. 1977. Temperature requirements of some percids and adaptations to the seasonal temperature cycle. *Journal of the Fisheries Research Board of Canada* 34:1524-1550.
- Hokanson, K. E. F., and C. F. Kleiner. 1974. Effects of constant and rising temperatures on survival and developmental rates of embryonic and larval yellow perch, *Perca flavescens* (Mitchill). Pages 437-448 in J. H. S. Blaxter, editor. *The Early Life History of Fish*. Springer-Verlag, New York.
- Hondorp, D. W., and S. B. Brandt. 1996. Spatially-explicit models of fish growth rate: tools for assessing habitat quality. *Great Lakes Research Review* 2:11-19.
- Houde, E. D. 1969. Sustained swimming ability of larvae of walleye (*Stizostedion vitreum vitreum*) and yellow perch (*Perca flavescens*). *Journal of the Fisheries Research Board of Canada* 26:1647-1659.
- Hughes, N. F. 2000. Testing the ability of habitat selection theory to predict interannual movement patterns of a drift-feeding salmonid. *Ecology of Freshwater Fish* 9:4-8.
- Hutchinson, G. E. 1965. The niche: an abstractly inhabited hypervolume. Pages 26-78 in *The Ecological Theatre and the Evolutionary Play*. Yale University Press, New Haven, Conn.
- Hyman, J. B., J. B. McAninch, and D. L. DeAngelis. 1991. An individual-based simulation model of herbivory in a heterogeneous landscape. Pages 443-475 in M. G. Turner and R. H. Gardner, editors. *Quantitative Methods in Landscape Ecology*. Springer-Verlag, Heidelberg.

- Jacobsen, L., M. R. Perrow, F. Landkildehus, M. Hjerne, T. L. Lauridsen, and S. Berg. 1997. Interactions between piscivores, zooplanktivores and zooplankton in submerged macrophytes: preliminary observations from enclosure and pond experiments. *Hydrobiologia* 342/343:197-205.
- Jager, H. I., D. L. DeAngelis, M. Sabo, M. Sale, and D. Orth. 1993. An individual-based model of smallmouth bass populations in streams. *Rivers* 4:91-113.
- Jansen, W. A., and W. C. Mackay. 1992. Foraging in yellow perch, *Perca flavescens*: biological and physical factors affecting diel periodicity in feeding, consumption, and movement. *Environmental Biology of Fishes* 34:287-303.
- Jeppesen, E., T. L. Lauridsen, T. Kairesalo, and M. R. Perrow. 1998. Impact of submerged macrophytes on fish-zooplankton interactions in lakes. Pages 91-114 in E. Jeppesen, M. Søndergaard, M. Søndergaard, and K. Christoffersen, editors. *The Structuring Role of Submerged Macrophytes in Lakes*. Springer-Verlag Inc., New York.
- Johnson, T. B., and D. O. Evans. 1991. Behaviour, energetics, and associated mortality of young-of-the-year white perch (*Morone americana*) and yellow perch (*Perca flavescens*) under simulated winter conditions. *Canadian Journal of Fisheries and Aquatic Sciences* 48:672-680.
- Jones, M. L., N. P. Lester, D. B. Hayes, J. Stockwell, and C. Chu. 1998 (Unpublished report). Linking habitat supply to fish community objectives using a population dynamics approach. Annual Progress Report to Great Lakes Fishery Commission. Michigan State University & University of Toronto.
- Jones, M.L., R.G. Randall, D. Hayes, W. Dunlop, J. Imhof, G. Lacroix, and N.J.R. Ward. 1996. Assessing the ecological effects of habitat change: moving beyond productive capacity. *Canadian J. of Fisheries and Aquatic Sciences* 53:446-457.
- Jorgensen, S. E. 1988. *Fundamentals of Ecological Modelling*, 1 edition. Elsevier. Amsterdam.
- Kamler, E. 2002. Ontogeny of yolk-feeding fish: an ecological perspective. *Reviews in Fish Biology and Fisheries* 12:79-103.
- Kareiva, P. M. 1990. Population dynamics in spatially complex environment: theory and data. *Philosophical Transactions of the Royal Society*. 330B:175-190.
- Kayle, K., R. Kenyon, C. Knight, J. Paine, P. Ryan, B. Sutherland, and M. Thomas. 1998. Report of the Lake Erie yellow perch task group. Informal Report. Great Lakes Fishery Commission. Lake Erie Committee. Grand Island, NY.
- Keddy, P. A. 1984. Quantifying a within-lake gradient of wave energy in Gillfillan Lake, Nova Scotia. *Canadian Journal of Botany* 62:301-309.
- Kelso, J. R. M. 1976. Movement of yellow perch (*Perca flavescens*) and white sucker (*Catostomus commersoni*) in a nearshore Great Lakes habitat subject to a thermal discharge. *Journal of the Fisheries Research Board of Canada* 33:42-53.
- Kelso, J. R. M., and K. Wooley. 1996. Introduction to the International Workshop on the Science and Management for Habitat Conservation and Restoration Strategies (HabCARES). *Canadian Journal of Fisheries and Aquatic Sciences* 53:1-2.

- Kennedy, M., and R. D. Gray. 1993. Can ecological theory predict the distribution of foraging animals? A critical analysis of experiments on the Ideal Free Distribution. *Oikos* 68:158-166.
- Killgore, K. J., R. P. I. Morgan, and N. B. Rybicki. 1989. Distribution and abundance of fishes associated with submersed aquatic plants in the Potomac River. *North American Journal of Fisheries Management* 9:101-111.
- Kitchell, J. F., D. J. Stewart, and D. Weininger. 1977. Applications of a bioenergetics model to yellow perch (*Perca flavescens*) and walleye (*Stizostedion vitreum vitreum*). *Journal of the Fisheries Research Board of Canada* 34:1922-1935.
- Koonce, J. F., T. B. Bagenal, R. F. Carline, K. E. F. Hokanson, and M. Nagiég. 1977. Factors influencing year-class strength of percids: a summary and a model of temperature effects. *Journal of the Fisheries Research Board of Canada* 34:1900-1909.
- Kornijow, R. 1997. The impact of predation by perch on the size-structure of *Chironomus* larvae -- the role of vertical distribution of the prey in the bottom sediments, and habitat complexity. *Hydrobiologia* 342/343:207-213.
- Krieger, D. A., J. W. Terrell, and P. C. Nelson. 1983. Habitat suitability information: yellow perch. *Fish and Wildlife Report FWS/OBS-82/10.55*, US Dept. of the Interior, Washington, D.C.
- Kubecka, J., and M. Wittingerova. 1998. Horizontal beaming as a crucial component of acoustic fish stock assessment in freshwater reservoirs. *Fisheries Research* 35:99-106.
- Lam, D. C. L., W. M. Schertzer, and A. S. Fraser. 1987. Oxygen depletion in Lake Erie: modeling the physical, chemical, and biological interactions, 1972 and 1979. *Journal of Great Lakes Research* 13:770-781.
- Lammens, E. H. R. R., W. L. T. Van Densen, and R. Knijn. 1990. The fish community structure in Tjeukemeer in relation to fishery and habitat utilization. *Journal of Fish Biology* 36:933-945.
- Lane, J. A., C. B. Portt, and C. K. Minns. 1996a. Adult habitat characteristics of Great Lakes Fishes. *Canadian Manuscript Report of Fisheries and Aquatic Sciences* 2358, DFO.
- Lane, J. A., C. B. Portt, and C. K. Minns. 1996b. Nursery habitat characteristics of Great Lakes fishes. *Canadian Manuscript Report of Fisheries and Aquatic Sciences* 2338, DFO.
- Lane, J. A., C. B. Portt, and C. K. Minns. 1996c. Spawning habitat characteristics of Great Lakes Fishes. *Canadian Manuscript Report of Fisheries and Aquatic Sciences* 2368, DFO.
- Langton, R. W., R. S. Steneck, V. Gotceitas, F. Juanes, and P. Lawton. 1996. The interface between fisheries research and habitat management. *North American Journal of Fisheries Management* 16:1-7.
- Leach, J. H., M. G. Johnson, J. R. M. Kelso, J. Hartmann, W. Numann, and B. Entz. 1977. Responses of percid fishes and their habitats to eutrophication. *Journal of the Fisheries Research Board of Canada* 34:1964-1971.

- Leftwich, K. L., P. L. Angermeier, and C. A. Dolloff. 1997. Factors influencing behavior and transferability of habitat models for a benthic stream fish. *Transactions of the American Fisheries Society* 126:725-734.
- Leshkevich, G. A., D. J. Schwab, and G. C. Muhr. 1996. Satellite environmental monitoring of the Great Lakes: Great Lakes CoastWatch Program update. *Marine Technology Society* 30:28-35.
- Letcher, B. H., J. A. Rice, L. B. Crowder, and F. P. Binkowski. 1996. Size-dependent effects of continuous and intermittent feeding on starvation time and mass loss in starving yellow perch larvae and juveniles. *Transactions of the American Fisheries Society* 125:14-26.
- Levins, R. 1966. The strategy of model building in population biology. *American Scientist* 54:421-431.
- Loew, E. R., and C. M. Wahl. 1991. A short-wavelength sensitive cone mechanism in juvenile yellow perch, *Perca flavescens*. *Vision Research* 31:353-360.
- Loew, E. R., W. N. McFarland, E. L. Mills, and D. Hunter. 1993. A chromatic action spectrum for planktonic predation by juvenile yellow perch, *Perca flavescens*. *Can J. Zool* 71:384-386.
- Lott, J. P., D. W. Willis, and D. O. Lucchesi. 1996. Relationship of food habits to yellow perch growth and population structure in South Dakota lakes. *Journal of Freshwater Ecology* 11:27-37.
- MacCall, A. D. 1990. *Dynamic geography of marine fish populations*. University of Washington Press. Seattle WA. 153 pp.
- MacDougall, T. M., H. P. Benoit, R. Dermott, O. E. Johannsson, T. B. Johnson, E. S. Millard, and M. Munawar. 2001. Lake Erie 1998: Assessment of abundance, biomass, and production of the lower trophic levels, diets of juvenile yellow perch and trends in the fishery. Canadian Technical Report of Fisheries and Aquatic Sciences 2376, GLLFAS, Burlington, Ontario.
- MacGregor, R. B., and L. D. Witzel. 1987. A twelve year study of the fish community in the Nanticoke Region of Long Point Bay, Lake Erie: 1971-1983 summary report. Lake Erie Fisheries Assessment Unit Report 1987-3, OMNR, Port Dover.
- MacRae, P. S. D., and D. A. Jackson. 2001. The influence of smallmouth bass (*Micropterus dolomieu*) predation and habitat complexity of the structure of littoral zone fish assemblages. *Canadian Journal of Fisheries and Aquatic Sciences* 58:342-351.
- Madon, S. P., and D. A. Culver. 1993. Bioenergetics model for larval and juvenile walleyes: an *in situ* approach with experimental ponds. *Transactions of the American Fisheries Society* 122:797-813.
- Magnuson, J. J., L. B. Crowder, and P. A. Medvick. 1979. Temperature as an ecological resource. *American Zoologist*. 19:331-343.
- Magnuson, J. J., J. D. Meisner, and D. K. Hill. 1990. Potential changes in the thermal habitat of Great Lakes fish after global climate warming. *Transactions of the American Fisheries Society* 119:254-264.
- Marmulla, G., and R. Rosch. 1990. Maximum daily ration of juvenile fish fed on living natural zooplankton. *Journal of Fish Biology* 36:789-801.

- Mason, D. M., A. Goyke, and S. B. Brandt. 1995. A spatially explicit bioenergetics measure of habitat quality for adult salmonines: comparison between Lakes Michigan and Ontario. *Canadian Journal of Fisheries and Aquatic Sciences* 52:1572-1583.
- Mason, D. M., and S. B. Brandt. 1996a. Effect of alewife predation on survival of larval yellow perch in an embayment of Lake Ontario. *Canadian Journal of Fisheries and Aquatic Sciences* 53:1609-1617.
- Mason, D. M., and S. B. Brandt. 1996b. Effects of spatial scale and foraging efficiency on the predictions made by spatially-explicit models of fish growth rate potential. *Environmental Biology of Fishes* 45:283-298.
- Mason, D. M., and S. B. Brandt. 1999. Space, time, and scale: new perspectives in fish ecology and management. *Canadian Journal of Fisheries and Aquatic Sciences* 56:1-3.
- Masson, S., and B. Pinel-Alloul. 1998. Spatial distribution of zooplankton biomass size fractions in a bog lake: abiotic and (or) biotic regulation? *Canadian Journal of Zoology* 76:805-823.
- Matthews, W. J. 1998. *Patterns in Freshwater Fish Ecology*, 1 edition. Chapman & Hall, New York.
- Mattila, J. 1992. The effect of habitat complexity on predation efficiency of perch *Perca fluviatilis* L. and ruffe *Gymnocephalus cernuus* (L.). *Journal of Experimental Marine Biology and Ecology*. 157:55-67.
- Matuszek, J. E., and B. J. Shuter. 1996. An empirical method for the prediction of daily water temperatures in the littoral zone of temperate lakes. *Transactions of the American Fisheries Society* 125:622-627.
- McCann, K., and B. Shuter. 1997. Bioenergetics of life history strategies and the comparative allometry of reproduction. *Canadian Journal of Fisheries and Aquatic Sciences* 54:1289-1298.
- Megrey, B. A., and S. Hinckley. 2001. Effect of turbulence on feeding of larval fishes: a sensitivity analysis using an individual-based model. *ICES Journal of Marine Science* 58:1015-1029.
- Mélard, C., E. Baras, L. Mary, and P. Kestemont. 1996. Relationships between stocking density, growth, cannibalism and survival rate in intensively cultured larvae and juveniles of perch (*Perca fluviatilis*). *Ann. Zool. Fennici* 33:643-651.
- Messier, F., J. A. Virgl, and L. Marinelli. 1990. Density-dependent habitat selection in muskrats: a test of the ideal free distribution model. *Oecologia* 84:380-385.
- Micheli, F., and C. H. Peterson. 1999. Estuarine vegetated habitats as corridors for predator movements. *Conservation Biology* 13:869-881.
- Mills, E. L., R. Sherman, and D. S. Robson. 1989. Effect of zooplankton abundance and body size on growth of age-0 yellow perch (*Perca flavescens*) in Oneida Lake, New York, 1975-86. *Canadian Journal of Fisheries and Aquatic Sciences* 46:880-886.
- Minns, C. K. 2001. Science for freshwater fish habitat management in Canada: current status and future prospects. *Journal of the Aquatic Ecosystem Health and Management Society* 4:251-261.

- Minns, C. K., and C. N. Bakelaar. 1999. A method for quantifying the supply of suitable habitat for fish stocks in Lake Erie. Pages 481-496 in M. Munawar, T. Edsall, and I. F. Munawar, editors. State of Lake Erie (SOLE) - Past, Present and Future. Backhuys Publishers, Leiden, The Netherlands.
- Minns, C. K., and J. E. Moore. 1995. Factors limiting the distributions of Ontario's freshwater fishes: the role of climate and other variables, and the potential impacts of climate change. Canadian Special Publication of Fisheries and Aquatic Sciences 121:137-160.
- Minns, C. K., J. D. Meisner, J. E. Moore, L. A. Grieg, and R. G. Randall. 1995. Defensible methods for pre-and post-development assessment of fish habitat in the Great Lakes. I. A prototype methodology for headlands and offshore structures. Canadian Manuscript Report of Fisheries and Aquatic Sciences 2328, Fisheries and Oceans Canada, Burlington, Ontario.
- Minns, C. K., R. G. Randall, J. E. Moore, and V. W. Cairns. 1996. A model simulating the impact of habitat supply limits on northern pike, *Esox lucius*, in Hamilton Harbour, Lake Ontario. Canadian Journal of Fisheries and Aquatic Sciences 53:20-34.
- Minns, C. K., S. E. Doka, C. N. Bakelaar, P. C. Brunette, and W. M. Schertzer. 1999. Identifying habitats essential for pike *Esox lucius* L. in the Long Point region of Lake Erie: a suitable supply approach. Pages 363-382 in L. R. Benaka, editor. Fish Habitat: Essential Fish Habitat and Rehabilitation. American Fisheries Society, Bethesda, Maryland.
- Mooij, W. M. 1996. Variation in abundance and survival of fish larvae in shallow eutrophic lake Tjeukemeer. Environmental Biology of Fishes 46:265-279.
- Morrison, T. W., W. E. Lynch Jr., and K. Dabrowski. 1997. Predation on zebra mussels by freshwater drum and yellow perch in western Lake Erie. Journal of Great Lakes Research 23:177-189.
- Mountford, M. D. 1988. Population regulation: density dependence, and heterogeneity. Journal of Animal Ecology. 57:845-858.
- Myers, R. A. 1995. Recruitment of marine fish: the relative roles of density-dependent and density-independent mortality in the egg, larval, and juvenile stages. Marine Ecology Progress Series 128:308-309.
- Negus, M. T., J. M. Aho, and C. S. Anderson. 1987. Influences of acclimation temperature and development stage on behavioural responses of lake chubsuckers to temperature gradients. American Fisheries Society Symposium 2:157-163.
- Neill, W. H. 1979. Mechanisms of fish distribution in heterothermal environments. American Zoologist. 19:305-317.
- Neill, W. H., and J. J. Magnuson. 1974. Distributional ecology and behavioural thermoregulation of fishes in relation to heated effluent from a power plant at Lake Monona, Wisconsin. Transactions of the American Fisheries Society 103:663-710.
- Odum, E. P. 1971. Fundamentals of Ecology, 3rd edition. W.B. Saunders Company, Philadelphia, PA.

- Ontario Ministry of Natural Resources -- Fish and Wildlife Branch. 1998. Lake Erie Fisheries Report 1997. Lake Erie Committee Meeting OMNR, Wheatley, Ontario.
- Ontario Ministry of Natural Resources - Fish and Wildlife Branch. 2000. Lake Erie Fisheries Report 1999. Lake Erie Committee, Great Lakes Fishery Commission. 68pp.
- Parrish, D. L., and F. J. Margraf. 1993. Growth responses of age-0 white perch and yellow perch from field-enclosure experiments. *Hydrobiologia* 254:119-123.
- Pearson, S. M., M. G. Turner, and J. B. Drake. 1999. Landscape change and habitat availability in the southern Appalachian Highlands and Olympic Peninsula. *Ecological Applications* 9:1288-1304.
- Perrone Jr., M., P. J. Schneeberger, and D. J. Jude. 1983. Distribution of larval yellow perch (*Perca flavescens*) in nearshore waters of southeastern Lake Michigan. *J. Great Lakes Research* 9:517-522.
- Perrow, M. R., A. J. D. Jowitt, J. H. Stansfield, and G. L. Phillips. 1999. The practical importance of the interactions between fish, zooplankton and macrophytes in shallow lake restoration. *Hydrobiologia* 395/396:199-210.
- Persson, L., and L. A. Greenberg. 1990. Optimal foraging and habitat shift in perch (*Perca fluviatilis*) in a resource gradient. *Ecology* 71:12699-11713.
- Persson, L., and L. B. Crowder. 1998. Fish-habitat interactions mediated via ontogenetic niche shifts. Pages 3-23 in E. Jeppesen, M. Søndergaard, M. Søndergaard, and K. Christoffersen, editors. *The Structuring Role of Submerged Macrophytes in Lakes*. Springer-Verlag Inc., New York.
- Petit, G. D. 1973. Effects of dissolved oxygen on survival and behavior of selected fishes of western Lake Erie. *Bulletin of the Ohio Biological Survey* 4:73pp.
- Post, J. R. 1990. Metabolic allometry of larval and juvenile yellow perch (*Perca flavescens*): *in situ* estimates and bioenergetic models. *Canadian Journal of Fisheries and Aquatic Sciences* 47:554-560.
- Post, J. R., and D. J. McQueen. 1994. Variability in first-year growth of yellow perch (*Perca flavescens*): predictions from a simple model, observations, and an experiment. *Canadian Journal of Fisheries and Aquatic Sciences* 51:2501-2512.
- Post, J. R., and D. O. Evans. 1989. Size-dependent overwinter mortality of young-of-the-year yellow perch (*Perca flavescens*): laboratory, *in situ* enclosure, and field experiments. *Canadian Journal of Fisheries and Aquatic Sciences* 46:1958-1968.
- Post, J. R., M. R. S. Johannes, and D. J. McQueen. 1997. Evidence of density-dependent cohort splitting in age-0 yellow perch (*Perca flavescens*): potential behavioural mechanisms and population-level consequences. *Canadian Journal of Fisheries and Aquatic Sciences* 54:867-875.
- Pothoven, S. A., T. F. Nalepa, and S. B. Brandt. 2000. Age-0 and age-1 yellow perch diet in southeastern Lake Michigan. *Journal of Great Lakes Research* 26:235-239.
- Powles, P. M., and S. M. Warlen. 1988. Estimation of hatch periods for yellow perch, based on otolith readings from juveniles (Age-0). Pages 1-6 in R. D. Hoyt,

- editor. 11th Annual Larval Fish Conference. American Fisheries Society, Houghton, MI.
- Prout, M. W., E. L. Mills, and J. L. Forney. 1990. Diet, growth, and potential competitive interactions between age-0 white perch and yellow perch in Oneida Lake, New York. *Transactions of the American Fisheries Society* 119:966-975.
- Pulliam, H. R. 1988. Sources, sinks and population regulation. *The American Naturalist* 132:652-661.
- Pulliam, H. R., and B. J. Danielson. 1991. Sources, sinks, and habitat selection: a landscape perspective on population dynamics. *American Naturalist* 137:S50-S66.
- Quinn, N., and B. L. Kojis. 1996. Monitoring sea water temperatures adjacent to shallow benthic communities in the Caribbean Sea: a comparison of AVHRR satellite records and *in situ* subsurface observations. *Marine Technology Society Journal* 28:10-18.
- Radke, R. J., and R. Eckmann. 1999. First-year overwinter mortality in Eurasian perch (*Perca fluviatilis* L.): results from a field study and a simulation experiment. *Ecology of Freshwater Fish* 8:94-101.
- Railsback, S. F. 2001. Concepts from complex adaptive systems as a framework for individual-based modelling. *Ecological Modelling* 139:47-62.
- Railsback, S. F., H. B. Stauffer, and B. C. Harvey. 2003. What can habitat preference models tell us? Tests using a virtual trout population. *Ecological Applications* 13:1580-1594.
- Randall, R. G., C. K. Minns, V. W. Cairns, and J. E. Moore. 1996. The relationship between an index of fish production and submerged macrophytes and other habitat features at three littoral areas in the Great Lakes. *Canadian Journal of Fisheries and Aquatic Sciences* 53:35-44.
- Ranta, E., P. Lundberg, and V. Kaitala. 2000. Size of environmental grain and resource matching. *Oikos* 89:573-576.
- Robillard, S. R., and J. E. Marsden. 2001. Spawning substrate preferences of yellow perch along a sand-cobble shoreline in southwestern Lake Michigan. *North American Journal of Fisheries Management* 21:208-215.
- Roff, J. C., and M. F. Taylor. 2000. National frameworks for marine conservation - a hierarchical geophysical approach. *Aquatic Conservation: Marine and Freshwater Ecosystems* 10:209-223.
- Romare, P. 2000. Growth of larval and juvenile perch: the importance of diet and fish density. *Journal of Fish Biology* 56:876-889.
- Rose, K. A. 2000. Why are quantitative relationships between environmental quality and fish populations so elusive? *Ecological Applications* 10:367-385.
- Ross, J., P. M. Powles, and M. Berrill. 1977. Thermal selection and related behavior in larval yellow perch (*Perca flavescens*). *Canadian Field-Naturalist* 91:406-410.
- Ross, M. J., and D. B. Siniff. 1982. Temperatures selected in a power plant thermal effluent by adult yellow perch (*Perca flavescens*) in winter. *Canadian Journal of Fisheries and Aquatic Sciences* 39:346-349.

- Rossier, O., E. Castella, and J.-B. Lachavanne. 1996. Influence of submerged aquatic vegetation on size class distribution of perch (*Perca fluviatilis*) and roach (*Rutilus rutilus*) in the littoral zone of Lake Geneva (Switzerland). *Aquatic Sciences* 58: 1-14.
- Ruckelshaus, M., C. Hartway, and P. Kareiva. 1997. Assessing the data requirements of spatially explicit dispersal models. *Conservation Biology* 11:1298-1306.
- Rudstam, L. G., and J. J. Magnuson. 1985. Predicting the vertical distribution of fish populations: analysis of cisco, *Coregonus artedii*, and yellow perch, *Perca flavescens*. *Canadian Journal of Fisheries and Aquatic Sciences* 42:1178-1188.
- Rukavina, N. A. 1976. Nearshore sediments of Lakes Ontario and Erie. *Geoscience Canada* 3:185-190.
- Ryder, R. A., and S. R. Kerr. 1989. Environmental priorities: placing habitat in hierarchic perspective. Pages 2-12 in C. D. Levings, L. B. Holtby, and H. M.A., editors. *Proceedings of the National Workshop on Effects of Habitat Alteration on Salmonid Stocks*.
- Sandstrom, O., I. Abrahamsson, J. Andersson, and M. Vetemaa. 1997. Temperature effects on spawning and egg development in Eurasian perch. *Journal of Fish Biology* 51:1015-1024.
- Schertzer, W.M., J.H. Saylor, F.M. Boyce, D.G. Robertson, and F. Rosa. 1987. Seasonal thermal cycle of Lake Erie. *J. of Great Lakes Research* 13:468-486.
- Schertzer, W.M. Environment Canada. 867 Lakeshore Rd. Burlington ON Canada. L7R 4A6
- Scott, W. B., and E. J. Crossman. 1998. Yellow Perch (*Perca flavescens*). Pages 755-761 in *Freshwater Fishes of Canada*. Galt House Publications Ltd., Oakville.
- Shirvell, C. S. 1989. Habitat models and their predictive capability to infer habitat effects on stock size. *Canadian Special Publication of Fisheries and Aquatic Sciences* 105.
- Shuler, S. W., and R. B. Nehring. 1993. Using the physical habitat simulation model to evaluate a stream habitat enhancement project. *Rivers* 4:175-193.
- Shuter, B. J., and H. A. Regier. 1989. The ecology of fish and populations: dealing with interactions between levels. Pages 33-49 in C. D. Levings, L. B. Hiltby, and M. Henderson, editors. *Proceedings of the National Workshop on Effects of Habitat Alteration on Salmonid Stocks*.
- Shuter, B. J., and J. R. Post. 1990. Climate, population viability, and the zoogeography of temperate fishes. *Transactions of the American Fisheries Society* 119:314-336.
- Shuter, B. J., M. L. Jones, R. M. Korver, and N. P. Lester. 1998. A general, life history based model for regional management of fish stocks: the inland lake trout (*Salvelinus namaycush*) fisheries of Ontario. *Canadian Journal of Fisheries and Aquatic Sciences* 55:2161-2177.

- Siefert, R. E., and W. A. Spoor. 1974. Effects of reduced oxygen on embryos and larvae of the white sucker, coho salmon, brook trout, and walleye. Pages 487-495 in J. H. S. Blaxter, editor. *The Early Life History of Fish*. Springer-Verlag, NY.
- Sly, P. G., and W.-D. N. Busch. 1992. Introduction to the process, procedure, and concepts used in the development of an aquatic habitat classification system for lakes. Pages 1-13 in W.-D. N. B. a. P. G. Sly, editor. *The Development of an Aquatic Habitat Classification System for Lakes*. CRC Press, Boca Raton, FL.
- Søndergaard, M., and B. Moss. 1998. Impact of submerged macrophytes on phytoplankton in shallow freshwater lakes. Pages 115-132 in E. Jeppesen, M. Søndergaard, M. Søndergaard, and K. Christoffersen, editors. *The Structuring Role of Submerged Macrophytes in Lakes*. Springer-Verlag Inc., New York.
- Sousa, W. P. 1984. The role of disturbance in natural communities. *Annual Review of Ecology and Systematics* 15:353-391.
- Steinhart, G. B., and W. A. Wurtsbaugh. 1999. Under-ice diel vertical migrations of *Oncorhynchus nerka* and their zooplankton prey. *Canadian Journal of Fisheries and Aquatic Sciences* 56:152-161.
- Strand, E., G. Huse, and J. Giske. 2002. Artificial evolution of life history and behavior. *The American Naturalist* 159:624-644.
- Summerfelt, R. C. 1999. Lake and Reservoir Habitat Management. Pages 285-320 in C. C. Kohler and W. A. Hubert, editors. *Inland Fisheries Management in North America*. American Fisheries Society, Bethesda, Maryland.
- Takimoto, G. 2003. Adaptive plasticity in ontogenetic niche shifts stabilizes consumer-resource dynamics. *The American Naturalist* 162:93-109.
- Taylor, R. J. 1987. The geometry of colonization: 1. Islands. *Oikos* 48:225-231.
- Thomas, C. D. 1994. Extinction, colonization, and metapopulations environmental tracking by rare species. *Canadian Journal of Fisheries and Aquatic Sciences* 53:20-34.
- Thomas, R. L., J.-M. Jaquet, A. L. W. Kemp, and C. F. M. Lewis. 1976. Surficial sediments of Lake Erie. *Journal of the Fisheries Research Board of Canada* 33:385-403.
- Thorpe, J. 1977a. Synopsis of biological data on the perch *Perca fluviatilis* Linnaeus, 1758 and *Perca flavescens* Mitchill, 1814. FAO Fisheries Synopsis 113, FAO, Rome.
- Thorpe, J. E. 1977b. Morphology, physiology, behavior, and ecology of *Perca fluviatilis* L. and *P. flavescens* Mitchill. *Journal of the Fisheries Research Board of Canada* 34:1504-1514.
- Tonn, W. M., and C. A. Pasckowski. 1987. Habitat use of the central mudminnow (*Umbra limi*) and yellow perch (*Perca flavescens*) in Umbra-Perca assemblages: the roles of competition, predation, and the abiotic environment. *Canadian Journal of Zoology* 65:862-870.
- Treasurer, J. W. 1983. Estimates of egg and viable embryo production in a lacustrine perch, *Perca fluviatilis*. *Environmental Biology Fish* 8:3-16.

- Tyler, J. A., and D. P. Clapp. 1995. Perceptual constraints on stream fish habitat selection: effects of food availability and water velocity. *Ecology of Freshwater Fish* 4:9-16.
- Tyler, J. A., and K. A. Rose. 1994. Individual variability and spatial heterogeneity in fish population models. *Reviews in Fish Biology and Fisheries* 4:91-123.
- Tyler, J. A., and K. A. Rose. 1997. Effects of individual habitat selection in a heterogeneous environment on fish cohort survivorship: a modelling analysis. *Journal of Animal Ecology* 66:122-136.
- Van Winkle, W., K. A. Rose, B. J. Shuter, H. I. Jager, and B. D. Holcomb. 1997. Effects of climatic temperature change on growth, survival, and reproduction of rainbow trout: predictions from a simulation model. *Canadian Journal of Fisheries and Aquatic Sciences* 54:2526-2542.
- Vazquez, J., A. Van Tran, R. Sumagaysay, E. Smith, and M. Hamilton. 1995. NOAA/NASA AVHRR Ocean Pathfinder Sea Surface Temperature Data Set User's Guide Version 1.2. Jet Propulsion Laboratory, California Institute of Technology. 39 pp.
- Viljanen, M., and I. J. Holopainen. 1982. Population density of perch (*Perca fluviatilis* L.) at egg, larval and adult stages in the dys-oligotrophic Lake Suomunjarvi, Finland. *Annales Zoologici Fennici* 19:39-46.
- Wahl, C. M., E. L. Mills, W. N. McFarland, and J. S. DeGisi. 1993. Ontogenetic changes in prey selection and visual acuity of the yellow perch, *Perca flavescens*. *Canadian Journal of Fisheries and Aquatic Sciences* 50:743-749.
- Walters, C. J., C. G. Hannah, and K. Thompson. 1992. A microcomputer program for simulating effects of physical transport process on fish larvae. *Fish. Oceanography*. 1:11-19.
- Wells, L. 1977. Changes in yellow perch (*Perca flavescens*) populations of Lake Michigan, 1954-75. *Journal of the Fisheries Research Board of Canada* 34:1821-1829.
- Wetzel, R. G. 1983. *Limnology*, Second Edition. Saunders College Publishing.
- Witzel, L.D. Lake Erie Management Unit. Ministry of Natural Resources. P.O. Box 429. Port Dover, ON. N0A 1N0.
- Wiegand, T., K. A. Moloney, J. Naves, and F. Knauer. 1999. Finding the missing link between landscape structure and population dynamics: a spatially explicit perspective. *American Naturalist* 154:605-627.
- Wildhaber, M. L., and L. B. Crowder. 1990. Testing a bioenergetics-based habitat choice model: bluegill (*Lepomis macrochirus*) responses to food availability and temperature. *Canadian Journal of Fisheries and Aquatic Sciences* 47:1664-1671.
- Winemiller, K. O., and K. A. Rose. 1992. Patterns of life-history diversification in North American fishes: implications for population regulation. *Canadian Journal of Fisheries and Aquatic Sciences* 49:2196-2218.
- Wu, L., and D. A. Culver. 1992. Ontogenetic diet shift in Lake Erie age-0 yellow perch (*Perca flavescens*): a size-related response to zooplankton density. *Canadian Journal of Fisheries and Aquatic Sciences* 49:1932-1937.

Xie, L., and D. B. Eggleston. 1999. Computer simulations of wind-induced estuarine circulation patterns and estuary-shelf exchange processes: the potential role of wind forcing on larval transport. *Estuarine, Coastal and Shelf Science* 49:221-234.

APPENDICES

Appendix 1.1: Background information for (A.) CoastWatch satellite images (or scenes) file nomenclature convention and (B.) Format options selected for this study during image file generation in the DECCON software program

A. NCAAS File naming convention: RYYDDH.STT where, R = Region Code, YY = Year, DDD = Julian Day (1 – 365), HH = Hour (0 – 23), S = Subregion Code, TT = Product Code

e.g. g9313020.ed1 where Region Code = g (Great Lakes), Year = 1993, Julian Day = 130, Hour = 20:00, Subregion Code = e (Lakes Erie, Ontario & Huron), Product Code = D1 (MCSST Daytime Split-Window)

B. Selected DECCON format options:

File Format: TIFF

Colormap: Spectrum

Conversion Type: Surface Temperature

Low Temperature: -5

High Temperature: 35

Vertical Adjustment: variable*

Horizontal Adjustment: variable*

* N.B. The following were optional and used to determine individual image adjustments, but not included in final image):

Graphics Overlay Planes(1-4)?: No, Yes, No, No

Graphics: Embedded (Overlay Colour: 0, Background Colour: 255)

Header Information in Separate File?: Y

Parameter Information in Separate File?: Y

Appendix 1.2: The following map coordinates (1:50,000 UTM grid zone 17 © 1994 Long Point 40-I/9 ed'n 7 EMR Can, NAD 83) for prominent features in Long Point Bay were used to georegister the satellite imagery to a Universal Transverse Mercator projection.

Map Coordinates		UTM Coordinates (Zone 17)	
X-coordinate	Y-coordinate	Northing	Easting
255.0	148.0	578500	4711200
249.0	150.0	571000	4713400
242.0	150.0	562000	4713000
239.5	152.5	558500	4717800
230.0	152.0	546000	4715000
223.0	155.0	545300	4719000
234.0	158.0	549600	4723400
237.0	156.5	554000	4722000
237.5	159.5	555200	4727000
241.5	164.5	560000	4733000

coeff #	Forward transformation coefficients		Backward transformation coefficients	
	Coeff X	Coeff Y	Coeff X	Coeff Y
0	3311505.562	4490464.782	-790.862	-3173.67
1	1091.152	60.208	0.001	0.000
2	-220.680	1388.322	0.000	0.001
RMS Error	2089.857	526.911	1.851	0.384
Chi-square	43675043.458	2776351.828	34.263	1.472

Appendix 1.3: Manuscript submitted to Photogrammetric Engineering and Remote Sensing journal documenting the validation analysis and matrix method of interpolation used in the thermal habitat assessment

Reconstructing thermal structure in the nearshore zone of lakes using satellite imagery, *in situ* data and GIS: methodology and error analysis

AUTHORS: SUSAN E. DOKA ^{1,2}

AFFILIATION: ¹ MCMASTER UNIVERSITY, DEPT. OF BIOLOGY, 1280 MAIN ST. W., HAMILTON, ONTARIO L8S 4L8

² CURRENT ADDRESS: GREAT LAKES LABORATORY FOR FISHERIES AND AQUATIC SCIENCES, FISHERIES AND OCEANS CANADA, 867 LAKESHORE RD., BOX 5050, BURLINGTON, ONTARIO L7R 4A6

SHORT TITLE: 4D Thermal Structure Reconstruction in Lakes

SHORT DESCRIPTION:

KEYWORDS: nearshore, temperature, AVHRR, temporal pattern, spatial pattern, 4D

ABSTRACT

Satellite imagery, field temperature profiles, and bathymetric data were integrated to provide both spatially and temporally explicit representations of the thermal regime in Long Point Bay, Lake Erie. Several assumptions had to be tested, and an empirical model developed, to merge the different data sources. The assumptions tested the accuracy of nearshore sea surface temperature (SST) measured by remote sensing versus *in situ* data, the links between physical habitat variables and satellite error rates, and whether a statistical or spatial model can be developed to correct satellite-derived SSTs for the nearshore zone. Results showed that the type of pass, time of day, and correct positioning of the image were important in minimising error rates. Nearshore vegetated sites may have additional error to correct. Linear interpolation between cloudfree satellite passes did not capture temporal dynamics in daily temperatures and actual data should be used. A methodology for linear interpolation of limited profile data is presented for recreating 3D thermal structure, which is superior to using one profile for an entire basin or embayment.

INTRODUCTION

Temperature affects gonadal development (Tanasichuk and Mackay 1989), egg development rate and mortality (Sandstrom et al. 1997), spawning site selection (Williamson et al. 1997), and growth rates for all life stages of fish (Wismer and Christie 1987; Mooij 1996). In many cases the optimal temperature for growth or egg development is a few degrees removed from the harmful effects threshold (Thorpe 1977; Casselman and Lewis 1996). Therefore, capturing 4D thermal structure is essential for understanding the spatial and temporal effects on distribution and vital rates (reproduction, mortality and growth) of fish populations. Four-dimensional, lake thermal structure was reconstructed in a GIS for developing thermal habitat supply models for fish.

Data from different sources, such as satellite imagery, field temperature profiles, and bathymetry were integrated to provide both spatial and temporal thermal data. To construct 3D matrices of thermal structure over time, several hypotheses were tested, and an empirical model developed. The accuracy of sea surface temperature (SST) measurements by remote sensing was compared to *in situ* temperature data, especially in nearshore areas. If a mismatch occurred between remotely sensed and actual temperatures, then certain physical or measurement variables may relate to error in remotely sensed values. In the nearshore zone, potentially confounding factors were investigated, like the presence of aquatic vegetation, overlap of imagery pixels with land, and the exposure of the site (a measure of wave potential). If a statistical link existed between the variables and error rates, a predictive model was developed to correct satellite-derived SST estimates for the nearshore area.

AVHRR SST imagery provides good spatial coverage of surface temperatures. Once the nearshore SST temperatures were validated then a 4D picture of thermal dynamics was obtained using temperature profiles and time series data. The use of time series data to interpolate between cloud-free SST images was compared with using simple linear interpolation between pixel values in satellite imagery. This comparison determined whether time series data was required for capturing nearshore temperature fluctuations when satellite imagery is not available on cloudy days. A methodology was also developed for using a limited number of temperature profiles to recreate 3D structure by interpolation and extrapolation from a corrected surface temperature image. In previous assessments, optimal thermal habitat for fish was calculated by using one temperature profile to represent an entire lake or basin (Christie and Regier 1988; Magnuson *et al.* 1990). This does not account for spatial variability in temperature. Alternatively, the use of complex simulation models for predicting thermal structure, or the deployment of a large number of temperature logger arrays, is necessary to capture 3D dynamics at a high spatial resolution. The methodology presented here is a compromise between the two approaches that maintains spatial patterns while simplifying the amount of data required.

Site Description

Long Point Bay, Lake Erie was chosen as a test area for combining GIS work, *in situ* temperature logger data, and satellite imagery into a time series of 3D thermal structure. The bay is a well-established nursery for fishes (MacGregor and Witzel 1987; Witzel 1989). The physical habitat is heterogeneous and variable in time and space. As well, there are historical records of fish and habitat data available (Minns *et al.* 1999). Long Point Bay is

situated in the eastern basin of Lake Erie and is comprised of an inner and outer bay area with the Inner Bay covering 7280 ha (Figure A1.3.1). The outer bay reaches 60m depth, with the deepest point of Lake Erie just off the tip of the 32-km Long Point sand spit. The Convention on Wetlands in Ramsar, Iran designated the area an internationally significant wetland on May 24, 1982, due to its importance as fish and wildlife habitat for the eastern basin of Lake Erie. Long Point Bay supports a highly diverse fish community, which in turn supports commercial and sport fisheries for centrarchids and percids, especially smallmouth bass and yellow perch. These fisheries are highly managed, therefore an understanding of the interaction of interannual and spatial variability in temperature with the life cycle and habitat requirements of these fish will be very useful.

MATERIALS

Several data sources were used to obtain the most accurate representation of thermal structure through time and space. The data sources include:

- point samples of actual water temperatures at a fine temporal scale (15 min intervals),
- coarse spatial estimates of surface temperature remote sensing at longer time intervals (hours to days),
- point samples of temperature profiles at a coarse temporal scale (weeks).

To reconstruct 4D thermal structure, two additional pieces of information were acquired:

- a Long Point shoreline coverage to delimit the land-water interface of the system,
- a bathymetric map of the area to delimit the depth of the system.

Bathymetry

A detailed bathymetric map of 1-m contour intervals was obtained in a GIS format jointly from the Canadian Hydrographic Service (CHS) and NOAA (NESDIS 1997). The original line coverage provided was corrected for node errors and was converted to a polygon coverage (Minns *et al.* 1999).

In situ Temperature

Eight water temperature loggers (Onset Stowaway TidbiT™) were set at various nearshore and offshore locations in Long Point Bay between April and December of 1999 to calibrate remote sensing temperatures in the nearshore zone (Figure A1.3.1). The Ontario Ministry of Natural Resources (OMNR Port Dover) also deployed two in situ loggers in 1999. In addition, temperatures from the Port Dover municipal water intake (DPWI) were obtained. Temperature dataloggers were situated to maximise the spatial coverage throughout Long Point Bay (Table A1.3.1), especially in the nearshore zone where satellite information may be erroneous. Figure A1.3.2 shows the time series data collected at three of the sites and exemplifies the temperature variability within and between sites.

The study loggers recorded temperatures at 15-minute intervals, with the exception of OMNR loggers and DPWI, which recorded at 2-hour intervals. Geographic coordinates for the logger locations were recorded using corrected GPS readings; with the exception of the location of DPWI where coordinates

were estimated from a chart of Long Point Bay (Long Point 40-1/9 edition 7. 1994. EMR Can. NAD 83.)

Temperature profiles were collected during the Lake Erie Biomonitoring (LEB) survey conducted in 1993 and 1994 and were used in the matrix model. LEB thermal profiles were measured with a Hydrolab datalogger during weekly sampling between May and October (Dahl *et al.* 1995; Graham, Dahl *et al.* 1996). Temperature measurements were recorded at 0.2-m intervals within the thermocline and 0.5 m intervals otherwise. Loran-C positions were provided for the location of each weekly profile. There were 3 LEB sampling locations in the outer bay at maximum depths of 6, 9 and 38 m. The profiles for each site were linearly interpolated and extrapolated through time (using available ice cover charts). The output included temperatures at 0.2 m depth-intervals (for 38 m site) and 0.1 m depth-intervals (6 & 9 m sites) for all of 1993 and 1994 (Figure A1.3.3, similar to Lam and Schertzer 1987; Schertzer 1987).

Remote Sensing

Sea surface temperature (SST) images for the Great Lakes are available through Advanced Very High Resolution Radiometer (AVHRR) satellite imagery provided by the National Oceanic and Atmospheric Administration (NOAA) of the U.S. government. AVHRR is an infrared radiation-detection instrument onboard several of NOAA's Polar Orbiting Environmental Satellites (POES). The NOAA CoastWatch Active Access System (NCAAS) database is available for selecting specific scenes or images that have already been processed and compressed. The imagery for the lower Great Lakes (Lakes Huron, Erie and Ontario) is available at a 1.44 km resolution. The accuracy of the temperature data is reported as ± 1 °C (McMillin and Crosby 1984).

The original satellite information provided through NCAAS was post-processed into SST images using software provided by NOAA to generate colour images of sea surface temperature that were user-defined. DECCON v1.4 freeware (DECompression and CONVersion) is a C program that decompresses National Environmental Satellite, Data and Information Service (NESDIS) CoastWatch imagery files. The data are originally in IMGMAP format and can be decompressed and converted into albedoes or surface temperature in several different image formats. Associated metadata for each satellite pass can be extracted from header information and a graphic overlay of the Great Lakes shoreline can be appended to the SST imagery. The latter is important for geographically registering the imagery and DECCON allows the user to shift the initial image by a set number of vertical and horizontal pixels to match the overlay graphics. The resultant image is a 512 x 512 raster file for Lake Huron, Ontario and Erie. Centigrade temperature conversions were performed on the final, full spectrum colour images (range of pixel values are 0-250, not 256) that represent a user-defined range of temperature values. In this case, the temperature conversion range of -5 to 35 °C was used for every image to maintain consistency in the colour value output.

Methods

To obtain as accurate as possible representation of thermal structure there are several hypotheses about errors that need to be tested at each step of data integration between all the different sources (Figure A1.3.4). These hypotheses outline the sequence of the data analysis in the subsequent section.

Initially, satellite temperatures were validated with actual temperatures. The nearshore one was of particular interest. If accurate measurements of the nearshore zone were not possible within appropriate limits, then error rates were compared with physical attributes of the logger sites to see if a pattern emerged. The comparison between satellite attributes and nearshore temperature error rates took up the bulk of the analysis. Next, a test of whether linear interpolation between cloudfree days was adequate enough to capture real time variability was undertaken. And finally a methodology for obtaining an accurate 4D picture of thermal dynamics in an embayment is presented; a significant deviation from 1D representation of thermal structure through time.

Satellite image processing and GIS coverage generation

All daytime (ED1) and night-time (ES7) Great Lakes CoastWatch scenes for 1999 were downloaded for conversion. However, only cloudfree images were kept. Due to the angle of incidence and swath path of the orbiting satellite the initial images required shifting to align them with the graphics overlay of the Great Lakes shoreline. The overlay was used to determine the shift in vertical and horizontal pixels that the images required for alignment. Even though this is a rather subjective alignment of the shoreline, the images can be several kilometres off the georegistration coordinates given for the corners of the satellite imagery. Contrary to previous reports, there was not a consistent offset for the images depending on the particular satellite and pass type (Schwab *et al.* 1992). The implications of potential positional error were examined in the analysis of variables contributing to temperature estimate errors.

Cloudfree images were batch processed using Arc Macro Language (AML) in ARC/INFO v7.0.1 (Arc and Grid modules, ESRI®, Redlands, CA) for converting images to grid coverages. This step involved georegistration of the TIFF image into a Transverse Mercator projection (NAD 83) by warping, clipping the geographic area for analysis from the larger scene, and converting pixel colour values to temperature values. Although Great Lakes CoastWatch scenes are already projected in a Mercator projection, the clipped study area is quite small in comparison with the original image. A more accurate local georeferencing was accomplished by using the relative location of known features in the shifted TIF files and their corresponding coordinates in the analysis area. This was accomplished by warping, or by rubber sheeting, the Long Point Bay area using 10 UTM coordinates of prominent features matched to particular pixels after shifting the images (Long Point 40-I/9 edition 7. 1994. EMR Can. 1000 UTM grid zone 17. NAD 83. Transverse Mercator projection). The final, clipped grid (38 x 38 pixels) was converted to temperature values using the following linear equation, $\text{Temp } (^{\circ}\text{C}) = 0.16 * \text{ColourValue} - 5$, where colour values can range between 0-250 (i.e. not 256) and the user-specified, temperature range was -5 to 35 °C.

Using the 0-m contour from the bathymetry coverage, the grid cells from the temperature coverage were assigned to land, overlap and water designations (Figure A1.3.5). The overlap cells are pixels that cover the land-water interface and the temperature values can be biased because each temperature value is an average over the 2 km^2 area of the cell. In addition, the bathymetry coverage was used to assign the average depth to each grid cell in the SST coverage

(rounded to the nearest meter). The depth of each grid cell was used in the generation of 1m thermal layers in the development of the 3D matrix model.

Statistical analysis and modelling

A database of temperature values from the different sources was constructed so that SST values for particular grid cells (pixels from the original satellite imagery) were matched with the appropriate datalogger (N.B. satellite pass times were rounded to the nearest 15 minute interval to match temperature loggers). The statistical analysis and modelling that was undertaken for reconstructing 3D thermal structure was divided into three sections. First, correlation analysis of satellite and logger temperatures, analysis of variance (ANOVA), linear regression and principal components analysis (PCA) of the variables that could potentially be contributing to errors in satellite-derived temperatures were employed. Second, spatial analysis and interpolation by kriging (SYSTAT v9.0) were used to develop a model to calibrate SST images and a matrix model was developed for converting, corrected SST images to temperature grids at set depth intervals or to bottom temperatures. Third, a Variables of interest in the analyses included remote sensing variables (satellite ID and image positioning), temporal variables (time of day, time of year), physical variables (water depth, wind exposure) and spatial variables (geographic position, shore and bay location, logger depth). The intensive comparison of satellite and in-situ temperatures was a critical first step for generating an accurate first layer (0-1 m temperatures) for the matrix modelling component.

Matrix model

Initially a grid coverage was created using the bathymetry contour map and based on the grid structure of the satellite images. In this way, a maximum depth was defined for each water pixel in the Long Point region. Using the interpolated profile data from the LEB study sites in 1993, different matrices were generated for each cloudfree satellite pass (only afternoon passes were used). Since there are only 3 sites in the outer bay, spatial interpolation was not an option to populate the grid cells in each coverage with temperatures based on actual values. Instead the thermal profiles were used to generate vectors of temperature differences from one meter to the next for 6, 9 and 38m deep sites respectively. Since the deepest profile site was 38 m, a 38x38 matrix was constructed with the columns the matrix representing the maximum depth of each pixel (up to 38m) and the rows representing the depth position of the profile. The temperature differences between each 1m interval for the three profiles were used as data in the matrix. The remaining values were filled by linear interpolation, both diagonally and horizontally, to obtain a full matrix. Pixels that had a maximum depth of less than 6m were assumed to be unithermal. Figure A1.3.6 is graphic representation of an example difference matrix. The large peaks represent the thermocline.

The processed satellite images were used as starting grids of surface temperatures (representing 0-m). Depending on the maximum depth of each pixel, the difference from the current pixel temperature to the next 1m-interval was subtracted and the grid for the next depth layer was created. If the depth layer being generated exceeded the maximum depth of the pixel then a null value was assigned. [Note: The maximum depth of a pixel within the Long Point

grid coverage was 60m. Any pixel with greater than 38m maximum depth was assumed to be unithermal after the 38th depth layer.]

RESULTS

Comparison of satellite and logger data

The relationship between all the estimated satellite temperatures and the actual measured datalogger temperatures was statistically a 1:1 linear relationship ($R^2=0.781$, $p<0.001$, $n=1533$), however the standard error in the estimates was quite high at 3.27 °C. Individual data point errors were up to ± 10 °C at particular times (Figure A1.3.7 & A1.3.8). Even when the type of satellite pass (daytime or night-time) and the orbiting satellite (NOAA 14 or 15) were taken into consideration in regression analyses, the average error in the estimate still ranged from 2.07 to 3.78 °C. (Table A1.3.2). Therefore subsequent analyses investigated whether other factors account for the error in temperature estimates or if the location of sites and their associated physical attributes contributed to this error.

Temperature errors and physical or measurement attribute comparisons

For the remainder of the analyses, the difference between the recorded datalogger temperatures and the satellite temperature estimates was used as the dependent variable. Temperature error was tested against other physical and geographic attributes of the Long Point system or against attributes linked to the type of satellite pass or with data collection.

Using ANOVA, the categorical variables, like satellite ID and pass type, closest shore, water zone, sub-bay, hour and time of day of the satellite pass were statistically compared with the temperature error between satellite and logger values (Table A1.3.3). All of these attributes had significant differences between the factor means for temperature error. The categorical variables that explained most of the variance were the time of day of the pass and the pass type, which accounted for approximately 40% of the variance in temperature error. Daytime temperatures were approximately 1.0 °C cooler than satellite estimates and night-time temperatures were on average 1.5 °C warmer, however the range in errors exceeded ± 10 °C. There was also a significant difference between the timing of the pass, (which was not related to satellite ID), and error rates where twilight passes were on average 2.0 °C cooler across sites and afternoon passes were 1.8 °C warmer than actual temperatures. (Figure A1.3.9).

There was a significant effect of site on temperature measurement error (the eastern shore, vegetated areas had the highest error rates). When these highly variable sites were dropped from the time of day analysis, a slightly different pattern emerged where morning, afternoon and evening temperature differences were between -0.5 and -1.0 °C (logger-satellite) and only twilight satellite values were, on average, a half a degree warmer than actual ones. This is consistent with the reported error rates of ± 1 °C, however the maximum error was still as high as ± 9 °C. Most of the categorical variables tested were heavily influenced by the highly vegetated nearshore sites in the inner bay, but it has yet to be determined whether positional error of the image or habitat variables are the key to correcting for this error. Since other, moderately vegetated sites in the

inner bay had relatively good concordance, then the latter source of error may be more likely.

PCA analysis results indicated that the temperature difference between satellite measurements and logger values was associated with three components. The bulk of the temperature error variance was negatively associated with the time of the pass (hour) and positively associated with the number of pixels the satellite image was vertically shifted to line up with the Great Lakes shoreline. There was a slight correlation between wind direction (measured in degrees), horizontal shift and temperature error in this component. Mismatches or errors between satellite and actual temperatures were also a minor part of two other components in the analysis. One component was dominated by the geographic coordinates and depth of the site, as well as with exposure of the site (a measure of fetch and daily wind values). Temperature error was positively related to these factors. Two variables, wind direction and exposure of the site, dominated the other component. Twenty percent of temperature error variability related positively to wind direction, and negatively to site exposure. However, satellite measurement and image processing variables dominated the principal component. This indicated that the time of day of the satellite pass and positional error were major sources in temperature measurement error and should be corrected before any subsequent analysis of habitat effects are considered.

Positional Error

A discriminant analysis of the time of the satellite pass (twilight, morning, afternoon or evening) and the shifts (measured in number of pixels) required to georegister the images, showed that the two variables were linked (Figure A1.3.10). There was considerable overlap between the pass types, however the afternoon passes were generally shifted to the northwest, evening passes were shifted along an east-west axis, and morning and twilight passes were generally shifted to the northeast for alignment and georegistration. Because the error rates were related to either horizontal or vertical shifts in the images, an analysis of reshifting the images was undertaken (Figure A1.3.11).

Only images from daytime passes were analysed. The reduction in error between the satellite and actual temperatures was measured if the image were shifted to one of the eight surrounding pixels. If the error rates were still the lowest in the original position then an assignment of (0,0) was given. The number of images that benefited from reshifting was determined and the results showed that most images would benefit from a shift to the west. There were slight differences in between the two different satellites (NOAA 14 or 15). This would indicate the final image may not have been in the proper geographic space.

An analysis of the spatial relationship of temperature errors in the Long Point region was undertaken. The inner and outer bay areas were divided into two separate sections for the initial spatial analysis of temperature error because the initial ANOVA results indicated there was a difference between inner and outer bay sites. Three-dimensional polynomial equations were fit to temperature errors at the inner bay sites and the data was separated into monthly and 'time of pass' groupings. Preliminary data analysis had indicated the time of day was a significant factor and that the time of year (month) may also be associated with error rates. The month did not affect the general pattern of error observed

between the different passes, but it did affect the range of errors observed (i.e. satellite errors showed the same shape of curve when compared between pass times in different months but there was an increasingly positive trend in the position of the curve as the year progressed where the intercept increased). Figure A1.3.12 shows the polynomial surfaces generated for the month of June. Similar patterns were observed in May and July. It must be noted however that twilight passes in June were the only data with a significant polynomial fit (adjusted $r^2=0.71$, $p<0.001$). The same patterns were repeated between months, although not significantly, where the morning and evening passes indicate consistent error over the whole of Long Point inner bay, while the afternoon passes were too variable to establish a definite trend.

Kriging analysis for all of the Long Point sites (not separated into inner and outer bays) showed a general pattern of spatial variability in temperature errors similar to the polynomial equations. Figure A1.3.13 is an example of the general pattern observed where there was an east to west gradient in temperature error, which was nonlinear. Error rates showed a southeast to northwest trend with higher error rates closer to shore, especially in the inner bay region. However the pattern was not repeatable from one day to the next within similar pass types.

Interpolation Errors

As illustrated by Figure A1.3.14, the period between cloudfree images varies and sometimes extends over a week. The logger site at Long Point Co. was located in the nearshore area, however the error rate between logger and satellite temperatures was one of the lowest for all sites, including offshore ones. Even with corrected satellite temperature estimates, if the temperature in any one pixel was linearly interpolated between pass dates to obtain daily temperatures for that pixel (especially during longer, cloudy periods), the error rate for the predictions was greater than the average error between remotely sensed and actual temperatures. For example, between May 20 and May 27 at the LPC site, the average error between interpolated temperatures and actual values is approximately 2 °C (ranges between 0 and 5 °C). The variability in temperature during cloudy periods, especially along nearshore areas where the temperatures were most variable, was lost if linear interpolation was used. When the weather is most unpredictable, (i.e. during turnover events), capturing this variability in thermal structure over time in habitat assessments is important for spring and fall spawning fish. The use of linear interpolation without correcting for actual fluctuations would lead to erroneous results.

Matrix or grid model results

The final grids produced by employing the matrix approach are shown in Figure A1.3.15. Spatial variability in water temperatures can be quite high in a diverse system like Long Point, especially in spring, where temperatures ranged from 4 °C in offshore areas to 25 °C in shallow vegetated areas. If the offshore profile temperature were used as a basis for the entire nearshore area then this spatial variability would be lost. Also, nearshore areas can vary considerably over a short time span in a particular location. For example, on the north shore of the inner bay region, the bottom temperature (a composite of the maximum depth layer temperatures for each pixel) rose from 5 °C to 18 °C at the beginning of May and then back to 14 °C by the end of May (Figure A1.3.16). This does

not take into consideration any diurnal fluctuations that would normally be observed, which would increase the variability. Conversely, the temperature variability of the upper thermal layers offshore did not vary that much and if used as a surrogate temperature measurement for nearshore areas would underestimate the warmth and variability of the nearshore zone, especially in the inner bay region.

DISCUSSION

The results showed that it was possible to integrate field and remotely sensed data into a realistic representation of 4-D thermal structure for a water body, with a few caveats. The errors involved in the process need to be corrected and consideration should be given to the application of the final product and what level of error in temperature estimates is acceptable.

The thermal structure in Long Point can be quite changeable. That variability is probably more important to the relative suitability of a particular area than the temperature at any one point in time (Ross et al. 1977; Brandt, Magnuson et al. 1980; Magnuson et al. 1990; Shuter and Post 1990). Highly variable sites will be less suitable but it also depends on the range of temperature covered during the fluctuations in temperature. Large fluctuations in the extremes of the temperature suitability curves for a fish species would be more detrimental than in the midrange.

There was significant error between field and remotely sensed data on certain days that were accounted for by the following errors. There may be error in using the surface temperature values in wetland areas due to the presence of emergent macrophytes. However, this is confounded with the fact that the time of day has an effect on the error rates between actual temperatures and satellite estimates. In addition, the geographic positioning of the images were difficult and was complicated by the shifting of images covarying with the time of the satellite pass (see Schwab et al. 1992, (Budd *et al.* 1998) for additional evidence). The possibility of inaccurate georegistration of the small portion of the original satellite image due to the difficulty associated with coarse resolution and the shifting of images to match shoreline overlays, which is somewhat arbitrary. Therefore the inaccuracy could result from positional errors when matching field surface temperatures with specific pixels, ending up with values that are overlapping with land areas, and not a complication of vegetation in the nearshore area. Once absolute accuracy in georegistration is possible and can be corrected for, then any additional variance in the error rates was linked to the presence of aquatic vegetation in coastal areas.

Another source of error in the analysis is the interpolation between sampling dates for the satellite imagery. As shown with the analysis of linear interpolation between satellite temperatures versus finer scale field temperature measurements, the use of real data between cloudfree satellite passes is important to adequately capture the temporal dynamics of the system. Interpolation values could be up to 5 °C off from actual values, compounded with the fact that satellite estimates could be up to 9 °C off (even in the offshore), then any subsequent measure of thermal suitability would be very biased.

Based on the findings, a proper methodology to follow for reconstructing 4D thermal structure in an area was outlined. Initially proper georegistration is imperative. Even so, this may pose a problem in highly vegetated areas, where temperatures can be corrected based on the time of day of the satellite pass and

a sine function similar to that outlined in Figure A1.3.9. Nonvegetated nearshore areas were not as susceptible to errors in satellite measurements of temperature, even though the pixels were fairly close to land features. Once corrected satellite temperature maps are obtained than using actual temperature data to interpolate between cloudfree dates was important in minimising errors due to interpolation. And lastly, the use of the matrix method and a few temperature profiles for obtaining 3D thermal structure was superior to using offshore profiles only to represent the entire area. The use of predictive equations as outline in Bolgrien and Brooks (1992) would be useful for predicting temperature profiles during different years.

In conclusion, merging *in situ* temperatures with satellite information provides the best representation of thermal structure that either one alone can provide. Once corrections can be based on empirical relationships and geographic positioning of the images is improved, this method should provide a better and systematic approach than extremely complex modelling approaches or overly simplistic surrogate measures that lose spatial and temporal variability.

Appendix A1.3: Glossary of acronyms

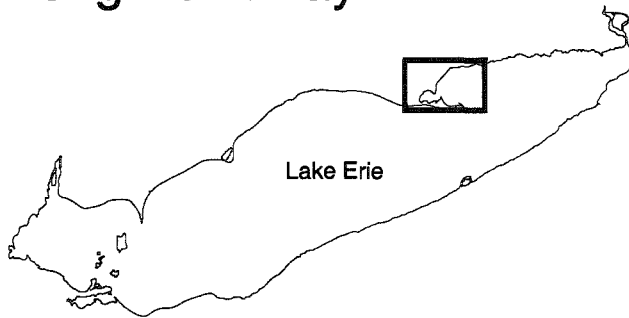
ED1	Lower Great Lakes daytime split window satellite pass
ES7	Lower Great Lakes night-time triple window satellite pass
SST	Sea Surface Temperature
AVHRR	Advanced Very High Resolution Radiometer
POES	Polar Orbiting Environmental Satellite
NOAA	National Oceanic And Atmospheric Administration
UTM	Universal Transverse Mercator
NCAAS	National CoastWatch Active Archive System
DECCON	Decompression and Conversion software
NESDIS	National Environmental Satellite Data Information System
AML	Arc Marco Language
NAD	North American Datum
OMNR	Ontario Ministry of Natural Resources
CHS	Canadian Hydrographic Service
CCG	Canadian Coast Guard

REFERENCES

- Bolgrien, D. W. and A. S. Brooks 1992). Analysis of thermal features of Lake Michigan from AVHRR satellite images. *Journal of Great Lakes Research* **18**(2): 259-266.
- Brandt, S. B., J. J. Magnuson, et al. 1980). Thermal habitat partitioning by fishes in Lake Michigan. *CJFAS* **37**: 1557-1564.
- Budd, J. W., W. C. Kerfoot, et al. 1998. Documenting complex surface temperature patterns from advanced very high resolution radiometer (AVHRR) imagery of Saginaw Bay, Lake Huron. *Journal of Great Lakes Research* **24**(3): 582-594.
- Casselmann, J. M. and C. A. Lewis 1996). Habitat requirements of northern pike *Esox lucius*. *CJFAS* **53**suppl 1): 161-174.
- Christie, G. C. and H. A. Regier 1988. Measures of optimal thermal habitat and their relationship to yields for four commercial fish species. *CJFAS* **452**: 301-314.
- Dahl, J. A., D. M. Graham, et al. 1995. Lake Erie 1993, western, west central and eastern basins: change in trophic status, and assessment of the abundance, biomass and production of the lower trophic levels. Burlington, Ontario, Great Lakes Laboratory for Fisheries and Aquatic Sciences.

- Graham, D. M., J. A. Dahl, et al. 1996. Assessment of abundance, biomass and production of the lower trophic levels in the eastern basin of Lake Erie, 1994. Burlington, Ontario, Fisheries and Oceans Canada.
- Lam, D. C. L. and W. M. Schertzer 1987. Lake Erie thermocline model results: comparison with 1967 - 1982 data and relation to anoxic occurrences. *J. Great Lakes Res* **13**(4): 757-769.
- MacGregor, R. B. and L. D. Witzel 1987. A twelve year study of the fish community in the Nanticoke Region of Long Point Bay, Lake Erie: 1971-1983 summary report. Port Dover, OMNR: 616.
- Magnuson, J. J., J. D. Meisner, et al. 1990. Potential changes in the thermal habitat of Great Lakes fish after global climate warming. *Trans Am Fish Soc* **119**: 254-264.
- McMillin, L. M. and D. S. Crosby 1984. Theory and validation of the multiple window sea surface temperature technique. *Journal of Geophysical Research* **89**(c3): 3655-3661.
- Minns, C. K., S. E. Doka, et al. 1999. Identifying habitats essential for pike *Esox lucius* L. in the Long Point region of Lake Erie: a suitable supply approach. *Fish Habitat: Essential Fish Habitat and Rehabilitation*. L. R. Benaka. Bethesda, Maryland, American Fisheries Society. **22**: 363-382.
- Mooij, W. M. 1996. Variation in abundance and survival of fish larvae in shallow eutrophic lake Tjeukemeer. *Environmental Biology of Fishes* **46**: 265-279.
- Ross, J., P. M. Powles, et al. 1977. Thermal selection and reared behavior in larval yellow perch *Perca flavescens*. *Canadian Field-Naturalist* **91**: 406-410.
- Sandstrom, O., I. Abrahamsson, et al. 1997. Temperature effects on spawning and egg development in Eurasian perch. *J Fish Biol* **51**: 1015-1024.
- Schertzer, W. M. 1987. Heat balance and heat storage estimates for Lake Erie, 1967 to 1982. *J. Great Lakes Res.* **13**: 454-467.
- Schwab, D. J., G. A. Leshkevich, et al. 1992. Satellite measurements of surface water temperature in the Great Lakes: Great Lakes CoastWatch. *Journal of Great Lakes Research* **18**: 247-258.
- Shuter, B. J. and J. R. Post 1990. Climate, population viability, and the zoogeography of temperate fishes. *Trans Am Fish Soc* **119**: 314-336.
- Tanasichuk, R. W. and W. C. Mackay 1989. Quantitative and qualitative characteristics of somatic and gonadal growth of yellow perch *Perca flavescens* from Lac Ste. Anne, Alberta. *CJFAS* **46**: 989-994.
- Thorpe, J. 1977. Synopsis of biological data on the perch *Perca fluviatilis* Linnaeus, 1758 and *Perca flavescens* Mitchill, 1814. Rome, FAO: 138.
- Williamson, C. E., S. L. Metzgar, et al. 1997. Solar ultraviolet radiation and the spawning habitat of yellow perch, *Perca flavescens*. *Ecological Applications* **7**: 1017-1023.
- Wisner, D. A. and A. E. Christie 1987. Temperature relationships of Great Lakes Fishes: a data compilation. Ann Arbor, Michigan, Great Lakes Fishery Commission: 198.
- Witzel, L. D. 1989. A description and ecological perspective of smallmouth bass spawning areas in Long Point Bay, Lake Erie, with emphasis on sanctuary boundaries in inner bay. pp. 51.

Long Point Bay



- 1. 4814
- 2. Akers
- 3. Big Creek
- 4. C buoy
- 5. Doctors
- 6. DPWI
- 7. LEB Sites
 - A. E1 C. E3
 - B. E2 D. E5
- 8. EC10
- 9. ED2
- 10. Million
- 11. OMNR

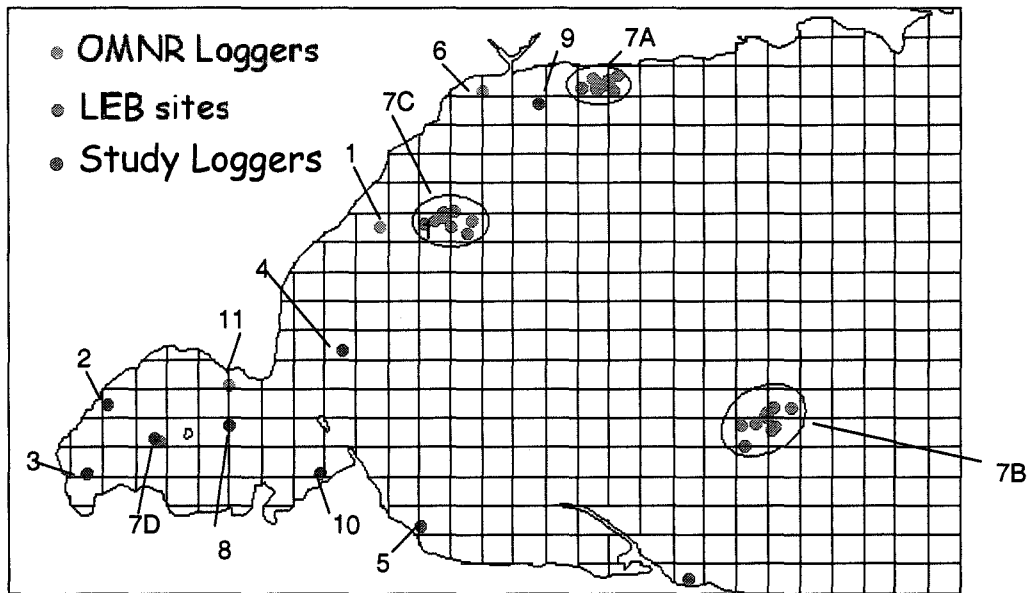


Figure A1.3.1: Long Point Bay, Lake Erie showing the location of the study loggers, OMNR loggers and Lake Erie Biomonitoring sites within the grid matrix for SST imagery. Long Point Bay is comprised of an inner bay sites 2,3,7D,8,10,11 and outer bay sites 1,4,5,6,7ABC,9 area.

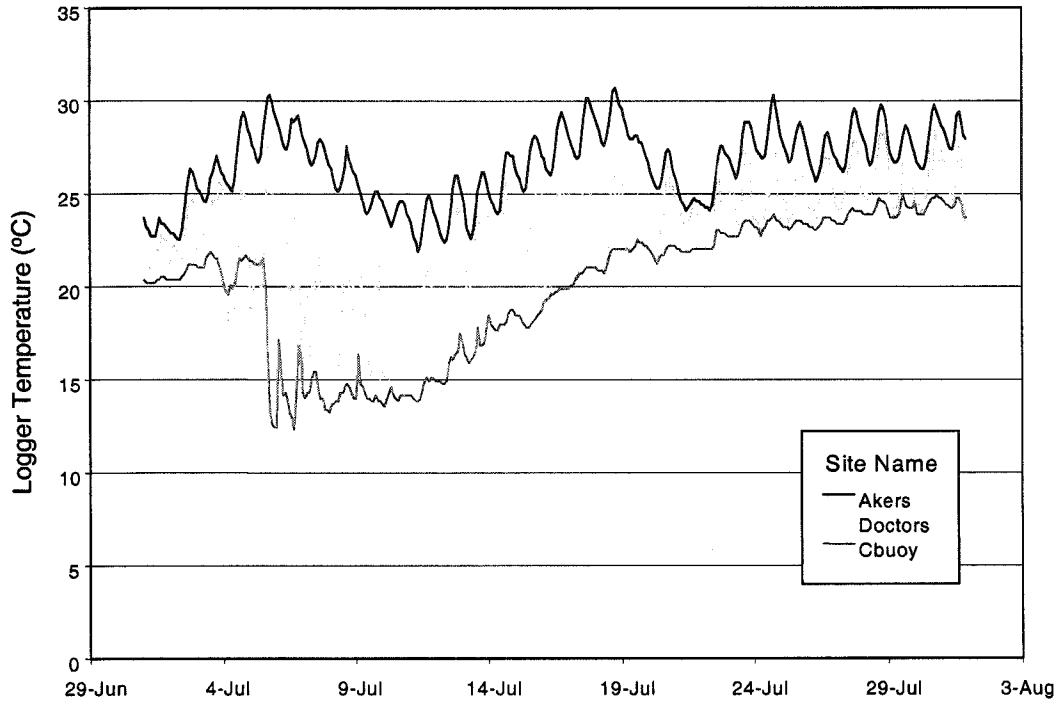


Figure A1.3.2: Time series of datalogger temperature values recorded at 3 different sites in Long Point Bay, July 1999, to illustrate the potential spatial and temporal variability in observed thermal structure. Akers is a nearshore site situated in the inner bay, Doctors is a nearshore site on the outer bay, and C buoy is located offshore just outside of the inner bay.

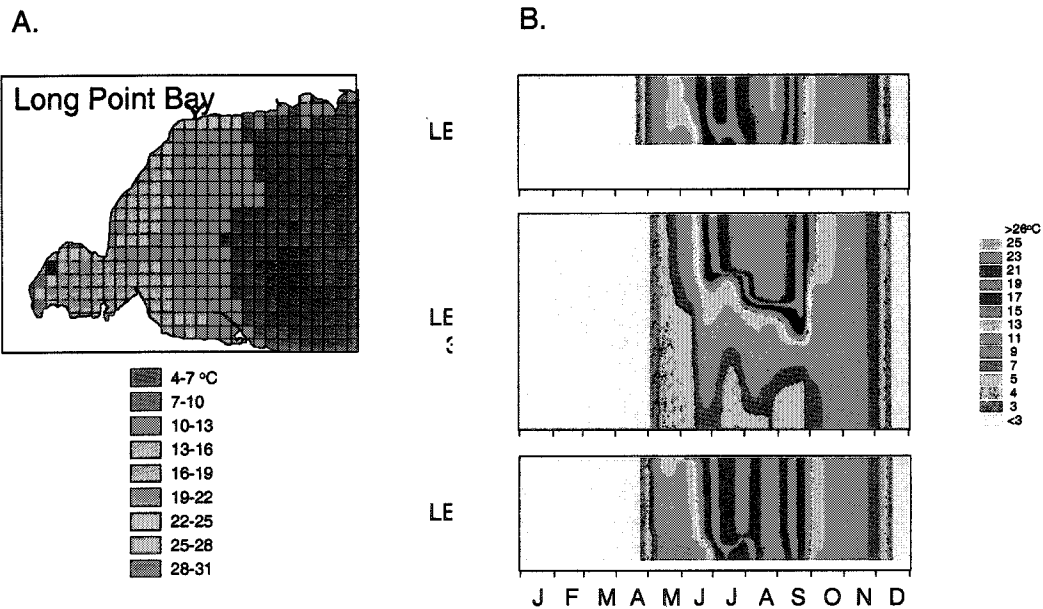


Figure A1.3.3: A. Satellite image NOAA-14 AVHRR, May 1, 1999 17:15 showing spatial variability in surface temperature in Long Point Bay, Lake Erie and B. Representation of the daily vertical profiles for the three Long Point Bay, Lake Erie Biomonitoring stations in1993.

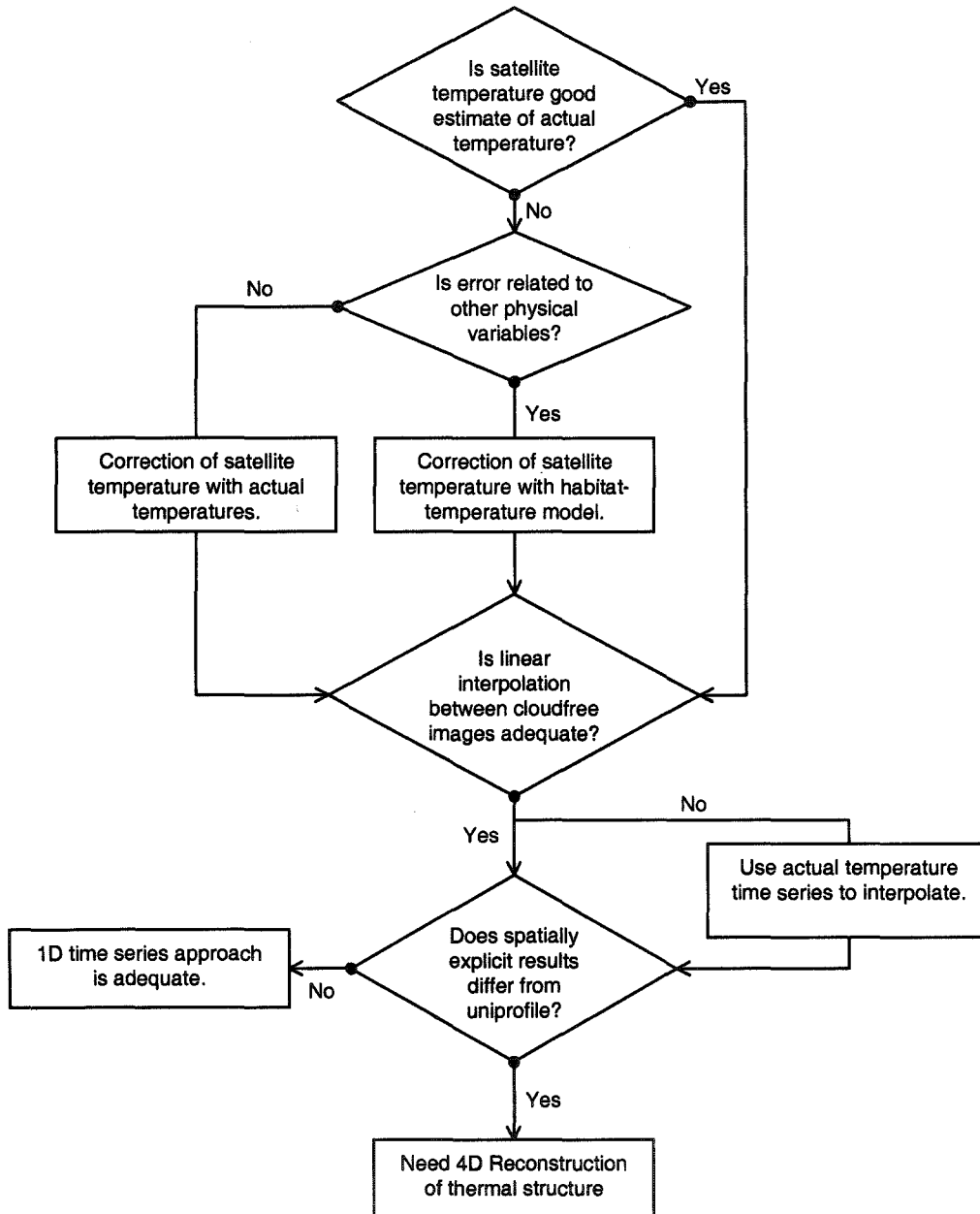


Figure A1.3.4: Decision tree outlining the hypotheses that were tested when different temperature data sources were combined to obtain a 4D representation of thermal structure for fish habitat modelling purposes.

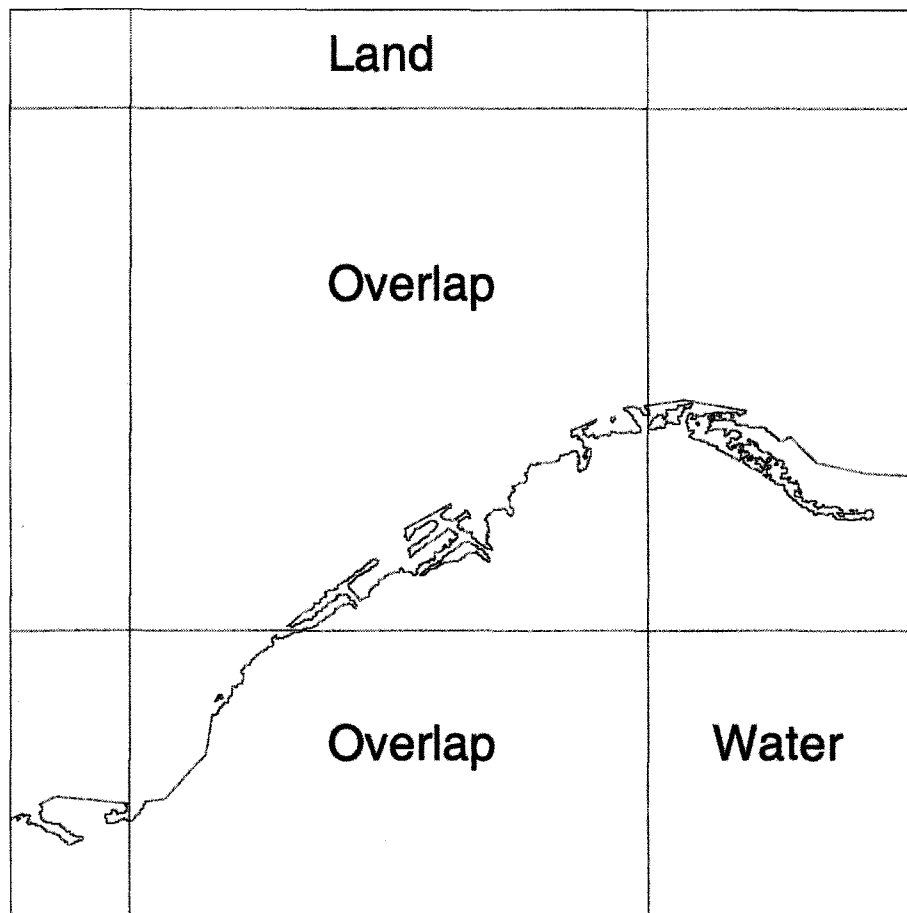


Figure A1.3.5: Close-up of Long Point shoreline showing the level of pixel overlap in AVHRR satellite imagery at the land-water interface.

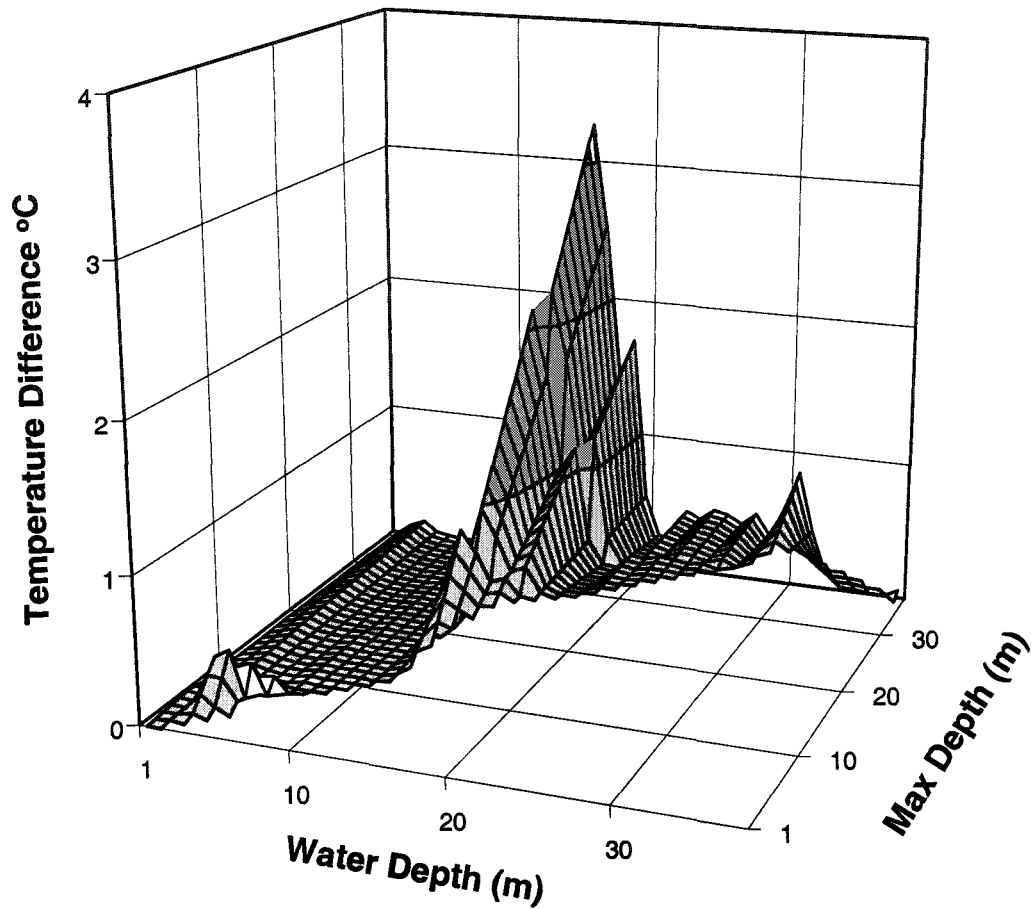


Figure A1.3.6: An example of a temperature difference matrix that was generated for the grid model for August 25, 1993. The graph shows the temperature that was subtracted from each temperature layer to create the subsequent one, until the maximum number of layers was reached for that pixel defined by the maximum depth of the pixel or grid cell. The white bars represent actual field profiles and the grey areas are linearly interpolated horizontally and diagonally.

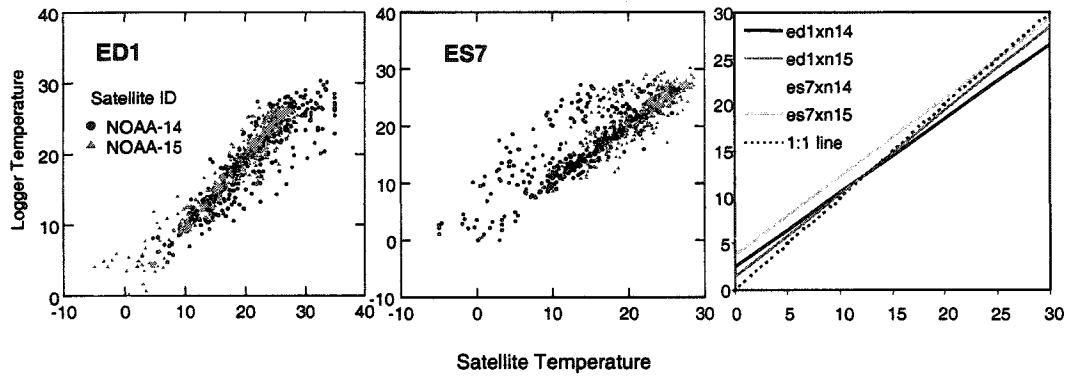


Figure A1.3.7: Correlation between satellite temperatures and logger temperatures for daytime ED1 and night-time ES7 passes of NOAA-14 and NOAA-15. Includes nearshore and offshore sites. Linear regression results for different satellite passes ed1xNOAA-14=afternoon, ed1xNOAA-15=morning, es7xNOAA-14=twilight, es7xNOAA-15=evening. The dashed line is a 1:1 fit between measurements for comparison.

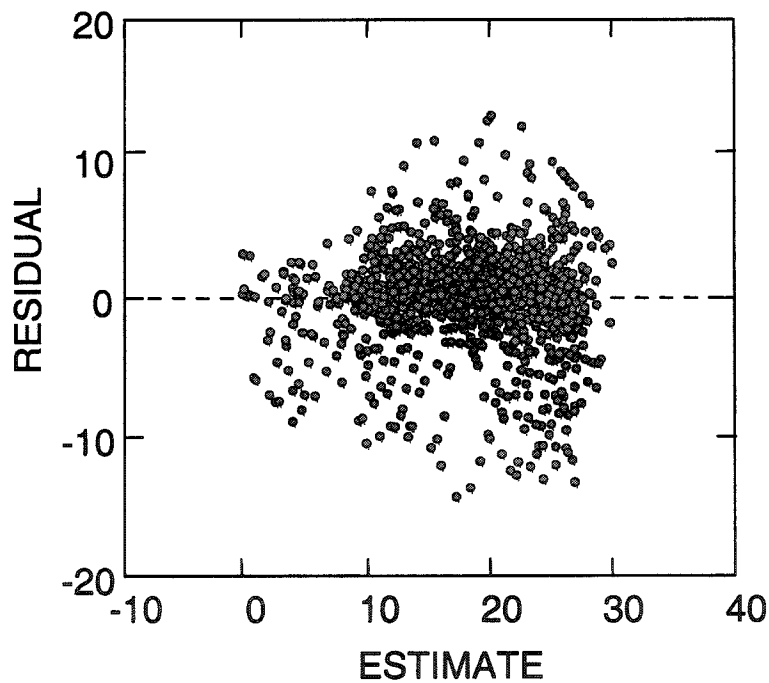


Figure A1.3.8: Residual plot of the linear regression analysis of all satellite versus datalogger temperatures in Long Point Bay 11 sites, N=1533.

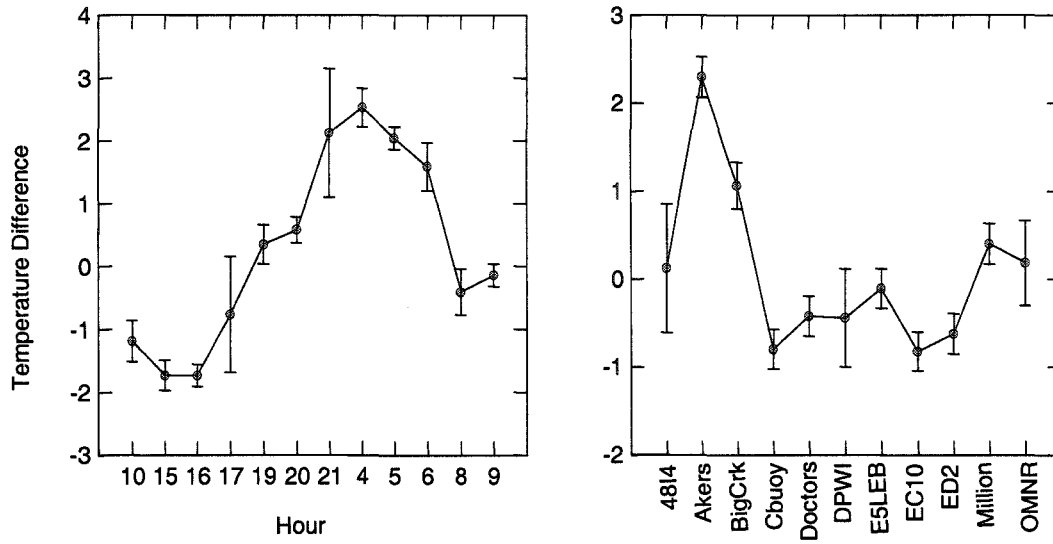


Figure A1.3.9: Least square means plot error bars = standard error of datalogger and satellite temperature differences against two categorical variables hour and site.

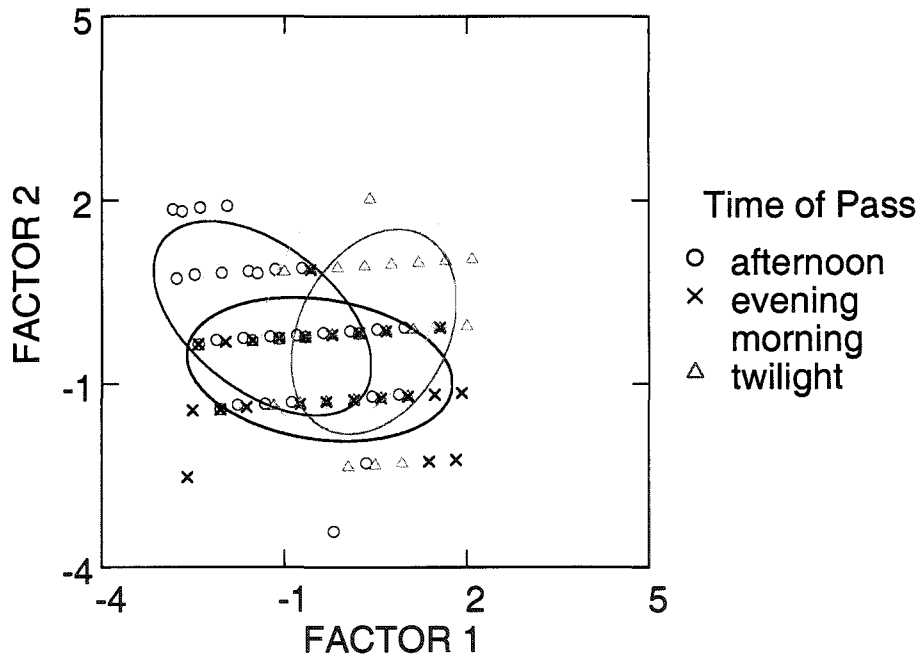


Figure A1.3.10: Results of discriminant analysis for the time of pass (afternoon & twilight = NOAA 14; morning & evening = NOAA 15). Factors are combinations of the vertical and horizontal shifts (Factor 1 is predominantly a vertical shift while Factor 2 is mainly horizontal) that were applied to each image to align it with the shoreline and correct the geographic positioning.

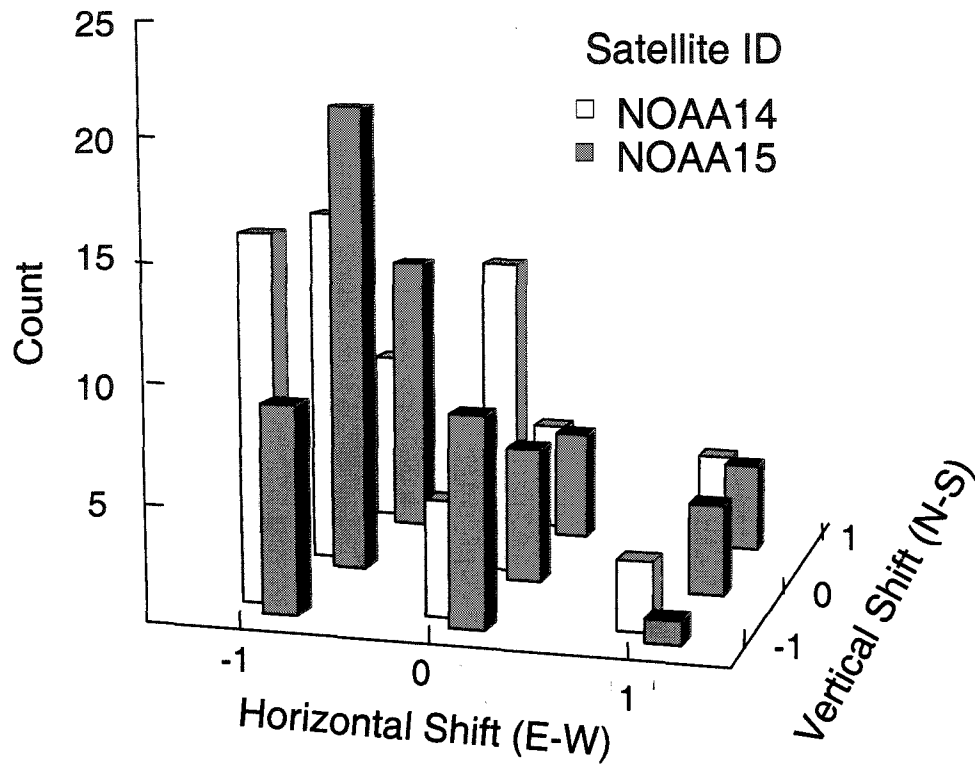


Figure A1.3.11: The number of satellite images where reshifting after the initial geographic registration by one adjacent cell including corners showed that an improvement in temperature estimates would result if the images were shifted to the east NOAA 15 or south-easterly direction NOAA 14 in most cases. A higher percentage of NOAA 14 passes than NOAA 15 did not improve with shifting 0,0, even though the variability in NOAA 14 temperature error was higher (see Figure A1.3.10).

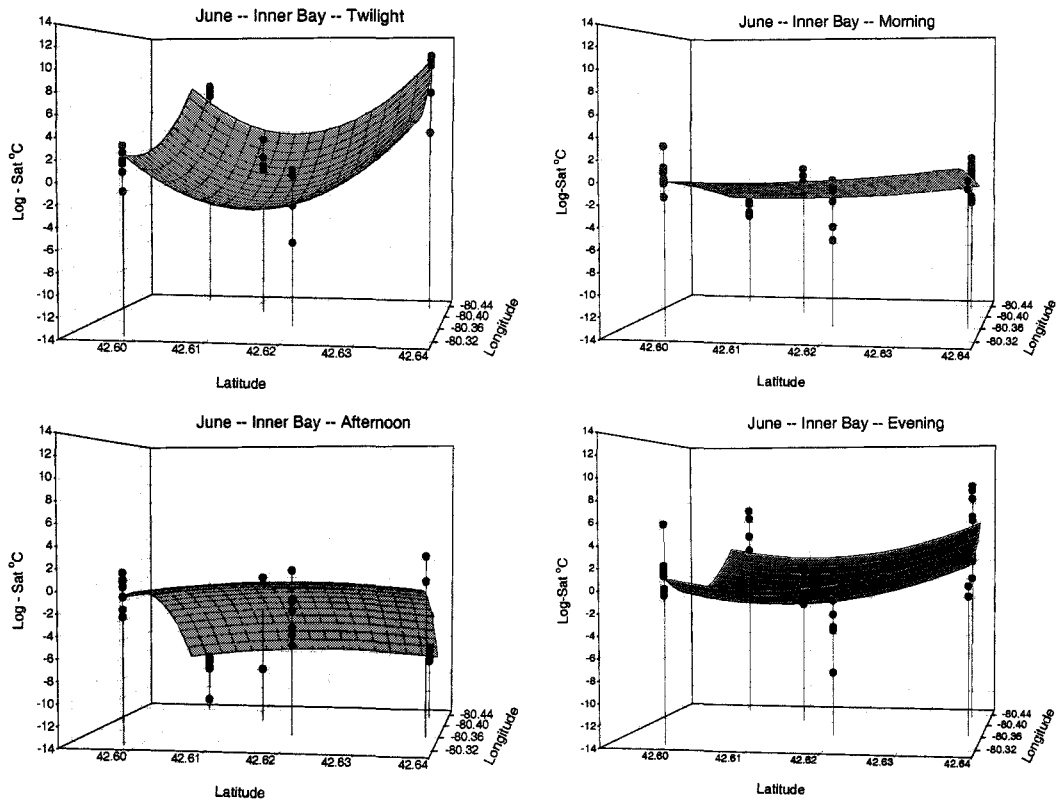


Figure A1.3.12: 3D polynomial plots of temperature error datalogger – satellite at five sites in the Inner Bay of Long Point Bay left to right: Million, BigCrk, E5LEB, EC10, Akers during four different satellite pass times in June, 1999. All points are shown that were used in surface generation and represents each cloudfree satellite temperature and matching datalogger temperature difference.

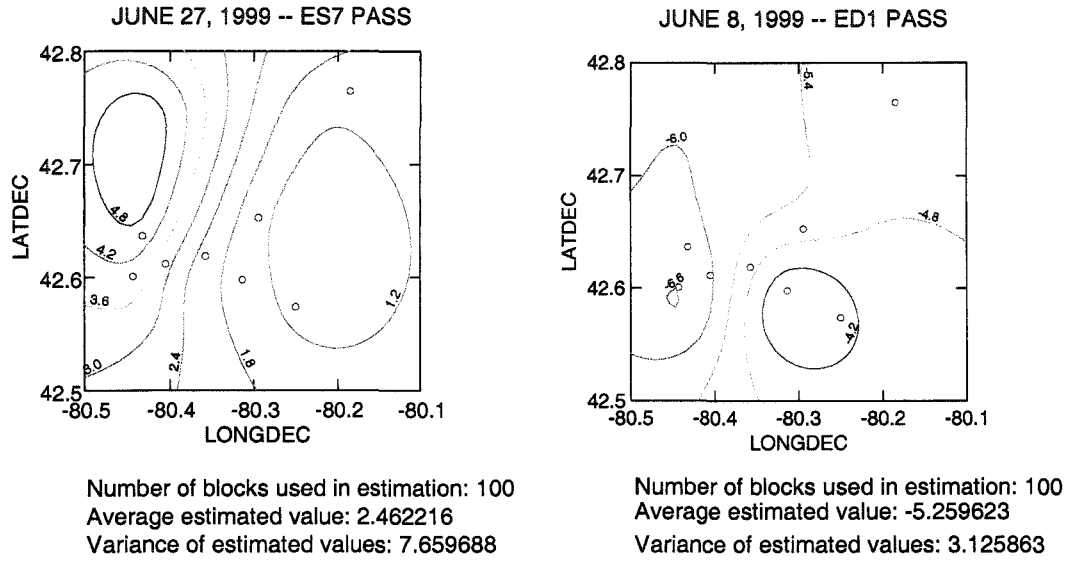


Figure A1.3.13: Contour maps of nonlinear kriging analysis results for temperature errors between dataloggers and satellite estimates points = logger locations on two dates in 1999. The average error and the variance are shown for each day.

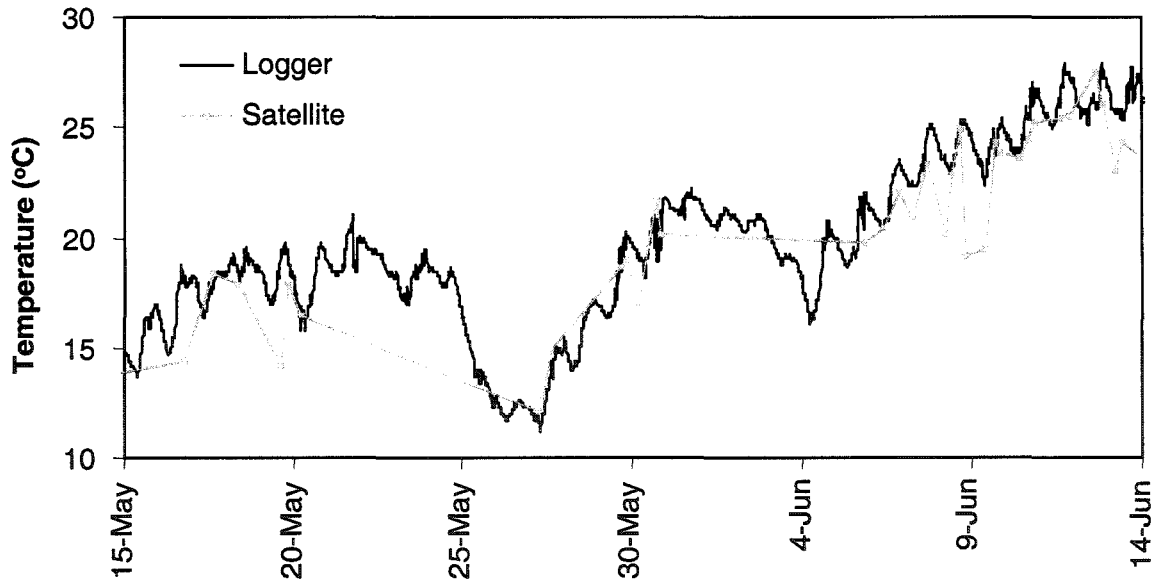


Figure A1.3.14: Datalogger temperatures at 15-min intervals at the Long Point Co. site compared to linear interpolation between remotely sensed temperatures during cloudfree passes between May 15 and June 14, 1999.

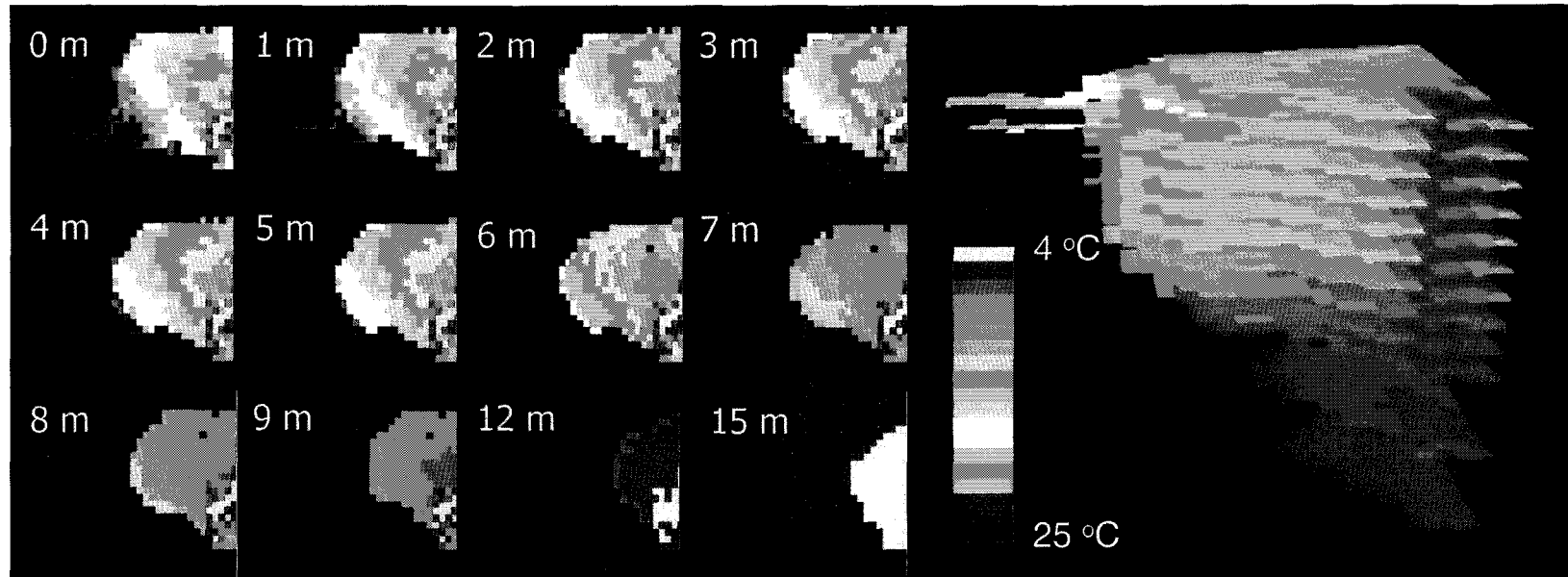


Figure A1.3.15: Temperature layers at different depths on May 30, 1993 generated using the matrix or grid model. The layers for May 21, 1993 is shown 'stacked' on show how volumes of different temperatures can be visualized. Each pixel or grid cell is 1.44 km. Note: overlap pixels were not used in 3D layer generation

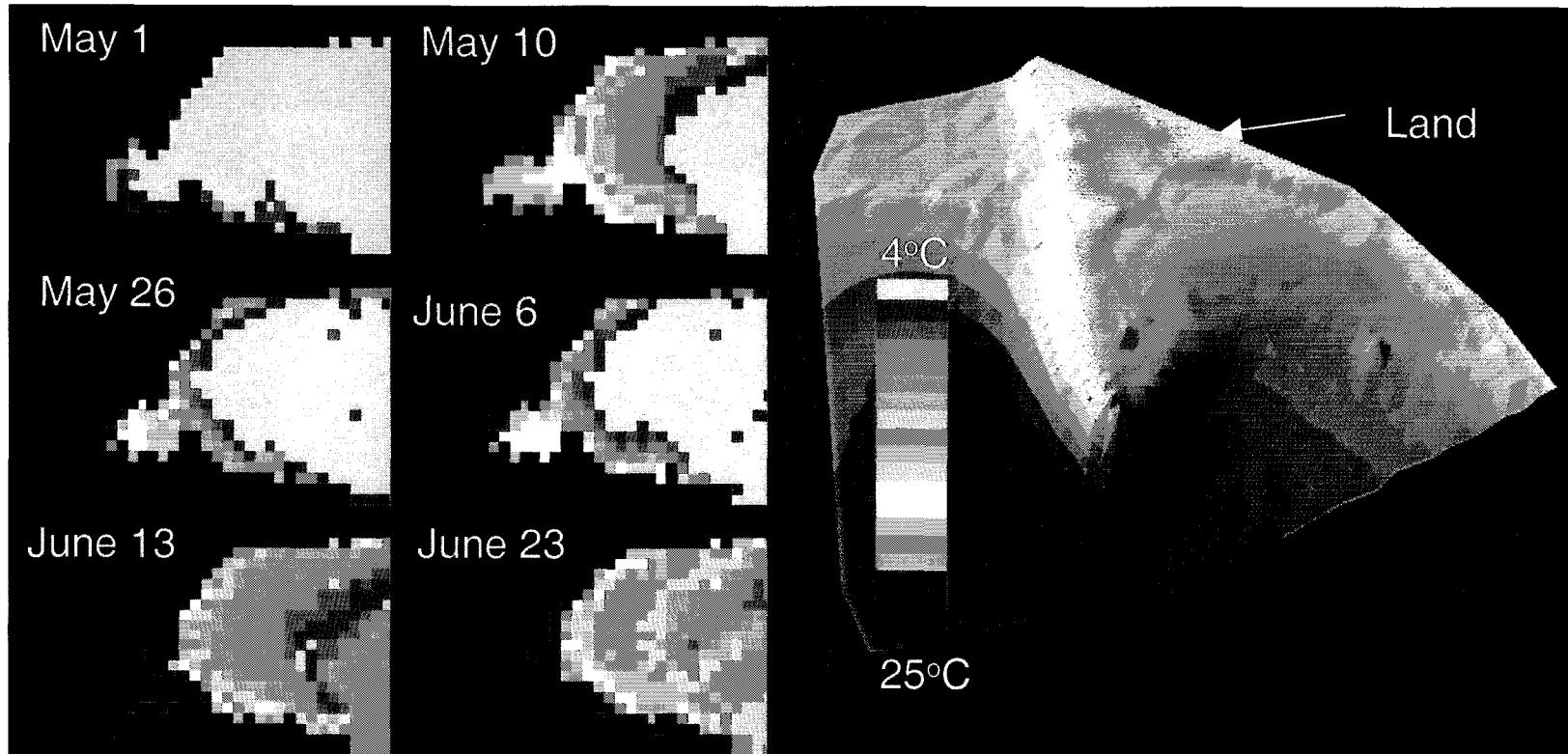


Figure A1.3.16: Time series of bottom temperatures in Long Point Bay through May and June of 1993 showing how variable temperature is spatially and within a relatively short time span. The May 10th temperature grid is draped over a TIN coverage of bathymetry to show how temperature changes with depth. [Note: Overlap pixels were not used in bottom layer generation.]

Table A1.3.1: Metadata for *in situ* temperature loggers in Long Point Bay thermal study.

Site Name	Bay	On/Off Shore	N/S Shore	Latitude Degrees	Longitude Degrees	Logger Depth m	Maximum Depth	Deployment Method	Deployment Period	Description
4814	outer	off	north	42.717	-80.273	5.0	7.0	buoy	07/19/99 - 12/31/99	Talisman gas well marker
Akers	inner	on	north	42.637	-80.432	0.5	1.0	fixed post	04/27/99 - 08/11/99 10/06/99 - 12/06/99	Wooden post Aker's Marina
BigCrk	inner	on	south	42.601	-80.443	0.5	0.5	bottom	06/06/99 - 08/11/99 10/06/99 - 12/06/99	Marina channel marker
Cbuoy	outer	off	mid	42.653	-80.294	1.0	6.0	buoy	05/16/99 - 10/29/99	Coast Guard navigational buoy
Doctors	outer	on	south	42.574	-80.25	0.5	1.0	fixed post	04/27/99 - 08/11/99 10/06/99 - 12/06/99	Wooden post Doctor's Inlet
DPWI	outer	on	north	42.779	-80.215	5.0	3.0	fixed pipe	05/13/99 - 12/31/99	Port Dover Municipal Intake
E5LEB	inner	off	mid	42.612	-80.405	1.0	1.5	bottom	04/27/99 - 09/28/99	Lake Erie Biomonitoring site
EC10	inner	off	mid	42.619	-80.357	1.0	2.0	bottom	04/14/99 - 08/11/99 10/06/99 - 12/03/99	Coast Guard fixed light
ED2	outer	off	north	42.765	-80.185	1.0	6.0	buoy	05/16/99 - 10/29/99	Coast Guard navigational buoy
Million	inner	on	south	42.598	-80.313	0.5	1.0	fixed post	04/27/99 - 08/11/99 10/10/99 - 12/06/99	Wooden post Long Point Co.
OMNR	inner	off	north	42.638	-80.364	1.5	1.5	bottom	01/01/99 - 12/31/99	OMNR permanent logger

Table A1.3.2: Regression analysis was performed on satellite versus datalogger temperature values. The number of observations, regression equation slopes and constants, adjusted multiple R^2 values, and standard errors of the regression estimates are shown for all data, satellite ID groups, and pass types. * indicates that the constants in the regression equations were slightly non-significant at the $p = 0.05$ level

Group	N	Slope SE	Constant SE	Adj multiple R^2	$SE_{estimate}$
All data	1533	0.998 0.014	0	0.781	3.27
ED1	839	1.048 0.014	0	0.863	2.55
ES7	694	0.948 0.021	0	0.745	3.46
NOAA-14	835	1.029 0.021	-0.694 0.41*	0.740	3.78
NOAA-15	698	0.956 0.016	0.831 0.32	0.844	2.49
ED1 x N14	429	1.026 0.023	1.195 0.47	0.822	2.80
ED1 x N15	410	1.047 0.016	-0.501 0.31*	0.911	2.07
ES7 x N14	406	0.927 0.029	-0.855 0.53*	0.722	3.67
ES7 x N15	288	0.813 0.033	3.478 0.726	0.685	2.77

Table A1.3.3: Separate simple ANOVA results of different geographic (closest shore, site, bay, physical shore zone, logger depth), and measurement attributes (hour and time of pass, satellite ID, datalogger deployment method), for comparison of error rates between datalogger and satellite temperatures. The least square means for each category are also shown. Negative numbers indicate that satellite values are higher than in situ temperatures. * See Figure A1.3.9 for site and hour means.

Variable	# Factors	Multiple R	F ratio	P value	Factor Means
Satellite ID	2 (NOAA 14,15)	0.264	62.911	0.001	-1.7, -0.3
Closest Shore	3 (N, S, mid-bay)	0.161	20.296	0.001	0.7, 0.3, -0.6
Shore Zone	2 (near, offshore)	0.207	68.983	0.001	0.8, -0.5
Site	10 *	0.315	16.891	0.001	* see Fig A1.3.9
Logger Depth	4 0.5, 1, 1.5, 5 m	0.217	25.392	0.001	0.9, -0.6, 0.3, 0.0
Deployment	3 (btm, buoy, fixed)	0.172	23.555	0.001	0.0, -0.7, 0.8
Sub-Bay	2 (inner, outer)	0.163	41.450	0.001	0.5, -0.6
Hour	12 *				* see Fig A1.3.9
Time of Day	4 (twilight, morning, afternoon, evening)	0.443	123.917	0.001	2.0, -0.4, -1.8, 0.5
Pass Type	2 (ED1, ES7)	0.388	273.379	0.001	-1.0, 1.5

Appendix 2.1: Literature Review of Yellow Perch (*Perca flavescens*) Habitat Requirements

A2.1.1 *P. flavescens* Life History & Habitat Requirements

In this section, yellow perch biology and life history is compiled across different life stages. (A synopsis of all the habitat associations by life stage is presented in a table in Appendix 2.1.) The distribution of yellow perch in North America ranges from Florida, north along the east coast to Nova Scotia (but not Cape Breton), and westward to the Midwestern states and Alberta. The natural range of yellow perch overlaps that of walleye; a closely related species (Scott & Crossman 1998). Perch growth rates are intermediate compared to other freshwater fish species and limited to the post-spawning period in spring through to early fall (Craig & Kipling 1983, Winemiller & Rose 1992). Age of maturity, longevity, and the number of age classes are also intermediate for percids when compared to other fish species. However, *Perca* spp. population biomass and resiliency (probably referring to the variation in abundance between years) is highest among the percids (Hokanson 1977).

Perca fluviatilis (Eurasian perch) and *Perca flavescens* (North American or yellow perch) are biologically very similar with only certain morphological differences (the position of the predorsal bone) that maintain them as separate species (Thorpe 1977). This review has used some information on *P. fluviatilis* from European literature as a surrogate for *P. flavescens* if information was not available for the Great Lakes or North America.

Hokanson (1977) extensively studied the environmental conditions, especially thermal conditions, under which yellow perch were found. Studies indicated that under average thermal conditions, like those in the Great Lakes, perch populations have a variable rate of recruitment depending on the rate of temperature increase throughout the spawning season and food availability for larvae. Because thermal habitat is often ignored in habitat suitability and supply assessments, it is the focus of separate and joint measures of temporal and spatial variability in habitat availability for different life stages of yellow perch. There are several other factors that could potentially limit a perch population, however, and these are reviewed here in detail for all the life history stages with different ontogenetic niche requirements, with a particular focus on temperature as part of that physical habitat.

A2.1.2 Reproduction and Habitat Requirements

Perch generally spawn after walleye (*Stizostedion vitreum*), which coincides with white sucker (*Catostomus commersoni*) spawning in the spring. However, suckers do not appear to be competitors for spawning areas with yellow perch because the habitats used are slightly different (Scott & Crossman 1998). Tagging experiments indicated that perch may return to the same spawning areas year after year (Craig 1987).

Spawning migration usually begins in late March to early May. The spawning period lasts for 1 – 4 weeks between April to August depending on the location, but usually occurs between April and June throughout most of their range. Mating females shed their entire store of eggs at once in a strand with a gelatinous sheath while several males fertilise the eggs. Fertilisation rates are high with a 78-95% success rate. And mortality due to predation is negligible, except perhaps by swans, because of the inedible sheath.

Fecundity relationships can be used to determine the number of eggs produced based on female size using either weight or length as the independent variable. A fecundity relationship (power function) was developed for Long Point Bay based on several years of egg biomass data (MacGregor & Witzel 1987), where the intercept and the slope were inversely related and were also functions of fish size. They found no relationship between the size of females and egg size, yolk size, fry length or hatching success. Lake Erie estimates of fecundity from the western basin for 18 – 33 cm fish are 8,618 – 78,742 eggs per female, respectively. Fecundity decreases after age 8.

Hatch times have been recorded at 8 - 10 days in the Great Lakes. Larval swim-up occurs 1-2 days after hatching and multiple emergences of larvae can occur in one year indicating either disparate spawning or development times (Thorpe 1977). Density estimates for perch eggs in the Long Point Bay area are not available. Egg surveys have been conducted but no eggs were found, just locations of adult perch exhibiting spawning behaviour (MacGregor & Witzel 1987). In Europe, the mean density of *P. fluviatilis* eggs was documented as 320,000 eggs/ha at 0-3 m depth with little variation between years (Viljanen & Holopainen 1982). Unfortunately, no additional environmental information was given for the same time frame so temperatures and other habitat characteristics could not be related to densities.

The influence of different environmental factors on the gonadal development, fecundity, spawning behaviour, egg development and egg survival are reviewed in the following sections. Quantitative relationships were sought but mainly qualitative descriptions were found.

Bathymetry & Reproduction

A variety of depths have been reported for yellow perch spawning. In general, perch spawning is thought to occur at 0.5 – 3 m depths in slow-moving or static water. In southeastern Lake Michigan, yellow perch males arrive at spawning grounds first and stage at 6 –12 m water depth, while females are in deeper water (>18 m) until migration to spawning grounds. . Egg masses were found at 8-12 m in Nova Scotia lakes (Scott & Crossman 1998). Eggs in Lake Erie were found to a depth of 20 m with the highest densities at < 9 m (Goodyear 1982a,b). Littoral and pelagic sampling of Eurasian perch eggs and larvae (0-10 m) indicated that the 0-3 m zone had the highest densities of eggs (28·m⁻²) and larvae (10-25

individuals $\cdot 100 \text{ m}^{-3}$), while adult perch were found in the 0-4 m zone and rarely > 6 m depth (Eklov 1997). The spawning depth difference between *P. flavescens* and *P. fluviatilis* may be due to habitat differences between European and North American lakes and the range of depths available (i.e. not many European lakes are as deep as the Great Lakes) rather than differences in preferences between the two species.

Vegetation, Cover & Reproduction

Yellow perch are characterised as non-obligatory plant spawners (phyto-lithophils) and have been documented as spawning in both rivers and lakes (Balon 1975). Vegetation and woody debris are selected for spawning site locations (Craig 1987) however the absence of these habitat types does not prevent spawning from actually occurring. Thorpe (1977) listed perch as spawning at depths of 0.5 – 8 m on weeds and logs where the currents were low over sand and gravel substrates. However, perch spawned in both vegetated and non-vegetated basins of an embayment in Lake Ontario with an average water depth of 5-7 m (Mason & Brandt 1996). In South Dakota, spawning occurred in shallow water where eggs were attached to submerged plants and trees (Fisher *et al.* 1996, Fisher & Willis 1997). Perch generally require submerged objects (coarse woody debris) or vegetation for egg strand deposition and it is thought that this prevents siltation of the egg strands by suspending them above the substrate (Craig 1987). Therefore, perch eggs may be less susceptible than other fish eggs to deoxygenation because strands are deposited on vegetation. Although diurnal dissolved oxygen levels in heavily vegetated areas can vary significantly (Wetzel 1983).

Stocking rates of 73,500 *Perca fluviatilis* eggs per acre were adequate to saturate ponds with cattails but over 100,000 were needed to saturate plankton-rich ponds without vegetation (Mélard *et al.* 1996). It is unclear what the authors refer to as saturation but the implication is that the carrying capacity of eggs differs between habitat types.

Substrate & Reproduction

Perch appear to use any substrate on which the eggs strands can be suspended above the sediment. Craig (1987) stated that spawning occurred in several systems over boulders, gravel, aquatic macrophytes, roots of trees, dead branches and other materials in 0.5 – 8.0 m of water. Thorpe (1977) stated that random deposition of eggs occurs on submerged objects, including vegetation, rocks, brush, debris and almost any bottom type in up to 22 m, but usually less than 9 m. Most studies indicate a preference for coarser substrate types.

Exposure, Wind and Waves & Reproduction

Sheltered littoral areas in lakes and tributaries are favoured for spawning, usually near vegetation along shorelines, and in harbours, bays, and creek mouths. Higher fecundity has been observed in exposed areas rather than sheltered areas but it is unclear what the mechanism for

this response would be (Tsai and Gibson 1971 in Craig 1987) because egg loss does occur due to storm events, which would be more destructive in exposed areas. High winds have created windrows of perch eggs in Lake Oneida (Mills *et al.* 1989) in some years. Therefore spawning in highly exposed areas would not be an evolutionarily stable strategy to undertake for yellow perch, although areas of moderate exposure would be less likely to become deoxygenated and stagnant, so there may be a trade-off for egg survival at moderate exposure levels.

Temperature & Reproduction

Temperature is a major factor affecting gonad maturation, spawning, egg survival and development. Thorpe (1977), in a synopsis of perch information, indicates that migration to spawning grounds occurs after ice break up (at 2.2-6.8 °C), and that peak spawning occurs between 6-12 °C, in 1-3 m of water over a sand or gravel substrate in vegetated areas. Gamete viability was highest between 8-11 °C and preferred temperatures of adult yellow perch seem to correspond to requirements for gametogenesis and spawning success (Ross and Siniff 1982) while spring temperature may have an important role in the fertilization and hatch success of yellow perch (Eschenroder 1977). Spawning may be induced by a temperature threshold for a certain number of days (i.e. degree days). Spawning temperature cues may be related to gonad maturation temperatures with a spawning peak at 6-12 °C. However, spawning has been documented over a wide range of temperatures from 3-23 °C (Hokanson 1977).

The spawning period usually lasts for 2-14 days but the duration may depend on temperature fluctuations and water levels during staging. Perch held at 10 °C spawned at the same time as fish held at 2-3 °C, which suggested that photoperiod may be important. Both temperature and perhaps day length may trigger spawning as it occurs at lower temperatures and later dates as latitude increases (Thorpe 1977b). Historical Great Lakes records in Craig (1987) documented spawning in Lake Ontario between May and June in the Bay of Quinte area and at the end of April and May in Collins Bay, both at temperatures of 10 °C. In Lake Huron, spawning was documented between mid-April and May and in Lake Michigan in April to May at 7.2 °C.

Hatching can occur anywhere from 5 - 30 days after spawning but is dependent on incubation temperatures. The highest percentage hatch was at incubation temperatures of 9-16 °C, and thermal tolerances of eggs ranged from 4 to 21 °C in early stages and from 7-23 °C in later developmental stages until hatching (Hokanson 1977). Egg survival was optimal with a temperature increase of 0.5-1.0 °C per day that improved survival, as well as decreasing hatch times and abnormalities, over egg incubation at constant temperatures (Hokanson & Kleiner 1974). The highest egg viability was achieved with adults acclimated to 6 - 9 °C. The time to develop decreased with increasing incubation temperatures,

although egg survival was also nonlinearly related to temperature. In some studies, there appeared to be a heat requirement in degree days for successful incubation that was similar to percent survival differences (Craig 1987).

Egg strands are resistant to minor temperature fluctuations but empirical relationships between egg development, egg survival and temperature have been well established (Hokanson 1977). Infertility, mortality and deformity rates can also vary with temperature, air exposure, and pH (Craig 1987). Egg survival rates until the 8-mm fry stage varied from 1.6 – 18.4%, which was positively correlated with temperature and with wind velocity in Oneida Lake. Wind-driven events may cause internal seiches in deeper lakes which cause thermal shocking of egg masses for yellow perch (Aalto and Newsome 1993). At very high temperatures during egg development, European perch egg sheaths degraded and eggs were more susceptible to infection (Sandstrom *et al.* 1997).

Other Physicochemical Variables & Reproduction

Spring water levels and the area of terrestrial vegetation inundated were linked to spawning success for perch in South Dakota lakes (Fisher *et al.* 1996). This indicates that the area of vegetation available may be limiting. Treasurer (1983) linked egg mortality to air exposure (desiccation), increases or decreases in temperature (a nonlinear relationship), and decreases in pH. However, eggs are protected from desiccation if they become exposed to air for short periods of time. Henderson (1985) found that yellow perch recruitment was a function of water levels in South Bay, Lake Huron (predicted from age-1 abundance) and neither water temperature during spawning and hatching, nor temperatures encountered during the first year, were explanatory. He suggested that these results could be confounded by predation effects, but this is unlikely because there are few natural egg predators (with the exception of some water birds) as egg strands are considered to be unpalatable by most taxa; especially by fish (Thorpe 1977, Craig 1987).

A2.1.3 Larval & Age-0 Stages and Habitat Requirements

Yellow perch early ontogeny after hatch undergoes several prolarval stages; swim-up larvae (yolk-sac fry), yolk-sac absorption, and first feeding. After which point, postlarvae feed until the end of the first growing season, and are commonly referred to as young-of-the-year (YOY) or age-0 perch. Thorpe (1977) referenced three forms of YOY fish with different growth rates: a planktivorous surface-feeding form, a phytophilic benthic form, and a piscivorous deep-water form. This mirrors the postlarval temporal patterns in feeding from pelagic planktivore, littoral benthivore, to piscivore. Switching between forms is thought to be size and food related, but discrepancies are the rule. Fish size and zooplankton density determined the shift from a pelagic to benthic food source (Wu & Culver 1992). The pelagic period lasted from lengths of 9 to

19 mm, a duration of 14-31 days, in Lake Erie in the 1960s (Carlander 1997) but this is variable.

Size or age chronology is difficult to determine for stages as not all are evident in all lakes and perch are generally considered opportunistic feeders (MacDougall *et al.* 2001). The types of food consumed through the ontogeny of yellow perch are rotifers, crustacean zooplankton, benthic insect larvae, larger crustaceans, molluscs, leeches, and fish (rapid growth occurs if fish and crayfish are available; Thorpe 1977). Combinations of the above food items usually occurs at any one time, but the size of prey is gape-limited. Cannibalistic behaviour has been observed in postlarval stages (between 2.1-2.5 cm, but this behaviour is probably not restricted to this range). The level of cannibalism in juvenile yellow perch depended on the availability of other food sources (Mélard *et al.* 1996) which may be habitat-dependent.

The duration and success of each stage can be affected by many intrinsic (population) and extrinsic (environmental) factors that affect vital rates, such as food availability and growth rates, natural mortality and predation, competition and density-dependence. Passive versus active movements can affect the influence of environment or habitat which also interact with the biotic influences on population and individual rates. A review of these different vital rates and the influence of different habitat factors follows.

Age-0 Food and Growth

Habitat restrictions may increase resource limitation (perhaps in refuge habitats) and limit consumption. Larval perch fed continuously during daylight hours and required 2% of body weight/day for maintenance at 23 °C. The annual variation in first year growth of perch in Lake Oneida was a function of *Daphnia* density and when larval perch switch to a benthic food sources, growth decreased (Prout *et al.* 1990). Therefore, energy densities of benthic food sources may be lower because consumption rates remain the same, assuming that foraging activity did not increase. Therefore, it would be advantageous to extend the pelagic phase given adequate food supply.

Age-0 Mortality and Predation

As well as food availability, the distribution of predators (including older perch) is critical to survival in early life stages. Predation by larger perch and walleye (and presumably other fish) is size dependent (when YOY reach 18 mm). Age-0+ walleye feed primarily on age-0+ yellow perch (Dorner *et al.* 1999). The percentage of age-0 yellow perch cannibalism and predation changed seasonally, from 0% of diets in April and May (during spawning), to 100% of all perch diets and 80% of other predator diets by August. There was a strong indication that smaller size classes were consumed preferentially, but the difference was not that significant.

Dorner *et al.* (1999) stated that daily predation rates differed in the littoral and pelagic zones between May to mid-August. A maximum of $0.06 \text{ fish}\cdot\text{m}^{-3}\cdot\text{day}^{-1}$ were predated in the littoral zone (the minimum was 0.01, with an average of 0.03) and maximum of $0.14 \text{ fish}\cdot\text{m}^{-3}\cdot\text{day}^{-1}$ were eaten in the pelagic zone (minimum of 0.03, average of 0.05). However, it was unclear how the researchers accounted for movement between habitat types or if these values were corrected for densities in each zone. The general consensus in the literature is that postlarval perch may move offshore to the epilimnion to avoid predation, so the higher predation rates in this area may reflect higher densities.

Predation risk affects zooplanktivorous fish distributions which affects zooplankton distributions (i.e. trophic cascade, Carpenter & Kitchell 1992). High mortality rates can be caused by plankton shortages as well as predation and cannibalism. Approximately 10.7% / day more perch were dying above the predation rate (~25% eaten by adult perch) due to starvation. In controlled experiments, the mortality of larval perch, starved for 7 days after hatch then fed for 20 days, was 94% in aquaria and 66% in ponds. All larvae starved for 9 days died (Letcher *et al.* 1996). Therefore the proximity of nursery and spawning habitats as well as the timing of hatch to swim-up and first feeding can be critical.

Although spottail shiner and YOY alewife occupy the same thermal habitat in Lake Michigan, they did not compete for food with yellow perch. However, alewife consumed larval perch in late April and early May in embayments of Lake Ontario three weeks after hatch (Mason & Brandt 1996). Therefore fish assemblages and habitat overlap between species may affect distributions or mortality rates directly. Instantaneous daily mortality rates with predation were as high as 80% per day. The decline in larval perch was greatest within the first 10 days, up to 99% mortality. Therefore, if refuges are available mortality rates by habitat types would differ.

Age-0 Competition & Density-Dependence

Perch are thought to be more tolerant than other species to crowding and high densities of other species. There was no correlation between year class strength and larval growth in the Great Lakes, however an inverse density-dependence of growth has been observed in some studies (Carlander 1997). Tank growth experiments showed young perch had faster growth rates when the volume of water per fish increased, implying density-dependent growth (Carlander 1997). This was corroborated by field data from Oneida Lakes where perch also grew faster when population densities were lower. Perch were stocked in enclosures in littoral areas at densities of 0.5, 1, and 2 times that observed in the field. The mean gut fullness dropped with density and was unaffected by pumpkinseed when mixed at the same density levels, implying that they did not compete.

In whole lake studies, yellow perch diet switched with a competitor present from benthos to zooplankton or vice versa (Bystrom *et al.* 1998). With a competitor (that is zooplankton-feeding), consumption of zooplankton decreased in young perch. Direct competition between zooplankton-eating stages resulted in increased mortality. If zooplankton abundances were low then larvae switched to benthic invertebrates earlier than usual, which may also have retarded growth. Others have observed that no significant density-dependent mortality occurred in the larval period during the 1st month and perch were unaffected by densities of 1, 2, and 4 individuals·m⁻² (Romare 2000). Larval densities of 6850 larvae·ha⁻¹ have been observed in the field, which translates to 0.7 ind·m². Under these densities, there was 8% survival from eggs to 1-week-old larvae, which is just after first feeding. It would be difficult to tease apart competitive effects on survival from habitat-based effects.

Other factors affected survival and growth in combination with density, such as high light intensity. When coupled with high larval density, good light conditions resulted in cannibalism. Mélard *et al.* (1996) determined that densities higher than a ratio of 7.5:1 larval: juvenile perch resulted in cannibalism in enclosure experiments. The specific growth rate of larvae in enclosures was related to temperature and the initial concentration of the food source (rotifers), which in turn, determined survival rates depending on initial larval densities.

Ontogenetic habitat shifts through first-year stages

Most references cited that all *Perca* larva have a pelagic existence in offshore areas and migrate to the littoral area by late summer, coincident with changes in food preferences from zooplankton to littoral benthic invertebrates and fish (Kelso 1976, Thorpe 1977, Craig 1987, Hayes 1990, Carlander 1997). They are found in the littoral zone just after hatching, then larval perch become pelagic until about 20 mm, at which point they move inshore to feed on benthic macroinvertebrates in shallow waters. Their spatial distribution is usually clustered and not uniform.

There are differences between lakes in the timing and distribution of larval and young-of-the-year fish. The following statements outline the most prevalent life history scenario but the actual spatial and temporal movements of fish are more than likely determined by a number of habitat and biotic interactions. At hatch, larvae are 4-7 mm (Hokanson and Kleiner 1974). At 8 mm, larvae have been documented as moving to the littoral zone in schools near vegetated edges. In Europe, larval perch are found in the littoral zone in the 1st week of July (Bystrom *et al.* 1998) but this varies in European lakes as well as in North America. Many studies suggest prolarvae remain in the spawning grounds for 3-4 days, at which point larvae became pelagic in the upper 6 m and are distributed by currents. Other studies quote 2-wk old larvae (~10 mm) in the littoral zone and an increase in abundance at 2 – 3.5 m depth contours (Perrone *et al.* 1983, Kornijow 1997).

At 3 weeks, or 12 mm in length, the densities of larvae in the pelagic and littoral zones were $6.7 \text{ ind}\cdot\text{m}^{-2}$ and $11.7 \text{ ind}\cdot\text{m}^{-2}$ respectively. Vertical bands appear on larvae at 20 mm, which may be an effective form of camouflage in vegetated areas but make them more apparent to predators in clear open water. However, fry (20-25 mm in length) were active at night during a continued epilimnetic phase and were vulnerable to predation by walleye in a Manitoba lake during the day (Kelso and Ward 1977). They schooled in midwater at 1.5 m and sank to bottom during disturbance. In smaller lakes, larval fish return to the littoral area when 25 mm long. Where littoral areas are sparse, perch became demersal more quickly.

The seeming lack of predictability of habitat use by larval yellow perch suggests two possibilities. One, there are several factors to consider when evaluating habitat use and distribution. Two, we have underestimated the plasticity of perch ontogenetic habit shifts. In either case, there may be some underlying generalisations that can be made about multidimensional habitat influences. The interaction between habitat characteristics and early life stage behaviour are reviewed below with the objective of defining this multidimensional space for larval and YOY perch separately.

Bathymetry & Age-0 Perch

A comparison of the depths at which larval perch are usually found differs between lakes but most literature cites areas shallower than 15 m. The majority of studies agree that perch become pelagic soon after hatching and even yolk-sac fry have been found in the pelagic zone. Larvae are thought to spend up to 2 months in open water, postlarval stages (YOY) are found in < 6 m with the highest densities in < 9 m (Thorpe 1997). In inland Ontario lakes, perch larvae were rarely below 3 m depth during their pelagic phase (Post and McQueen 1994), however the bulk of young perch move offshore to 3 - 4 m of water in late July and early August in most citations. In Europe, larvae spent their time in surface waters < 3 m for the 1st few weeks then became demersal until midsummer, and finally moved to the littoral zone at 4 m depth (Viljanen & Holopainen 1986). In Lake Erie, young are common to 11m and are mostly on the bottom, but some are midwater in summer. In southeastern Lake Michigan, age-0 yellow perch were collected in October 1998 at 15 m to 35 m eating a variety of benthic invertebrates depending on the depth. There may be environmental and biotic reasons for these depth preference discrepancies between locations. For example, predators have induced larvae to maintain a lower position in the water column (Jansen & MacKay 1992) and temperature and water movement may be confounding a direct preference for any particular water depth. An analysis of the predicted suitable thermal habitat locations is presented in this chapter.

Vegetation, Cover, Substrate & Age-0 Perch

Conflicting evidence for the importance of larval and YOY abundance relationships with vegetation make evaluation of this habitat feature difficult. Most literature indicated that YOY perch preferred vegetation; mainly medium-density submergents and emergents (Lane *et al.* 1996b). However, a European study stated that perch (8-100 mm) were found in vegetation, but stem density had no relationship to abundance (Diehl & Eklov 1995). Larvae supposedly became demersal after 4-5 weeks and lived in sheltered, nearshore areas with vegetation and gravel, rubble, sand, mud, and silt substrates (Thorpe 1977). However, low density vegetation did not differ from areas of no vegetation in the relative distribution of yellow perch. One explanation for the lack of predictability between vegetated habitat use and age-0 perch distributions may arise from a lack of size- or age-dependence in many observations and analyses. This may have confounded results if there are disparate habitat requirements of two different feeding stages in the first year of life. Pelagic and benthic forms are treated separately in this analysis.

The likely correlation with macrophytes in the littoral zone would indicate a vegetation preference and not a shallow water depth preference, which may be influenced by biotic interactions. The presence or absence of vegetation made no difference in larval European perch abundance in a study Jacobsen *et al.* (1997) unless piscivores were present. In which case, perch preferred macrophyte cover, and were absent from open water. The survival of young perch was affected by the abundance of yearling perch only at high predator densities with vegetative cover. Without cover, even small numbers of yearlings reduced survival.

In other systems, survival was greater in plankton-rich ponds compared to vegetated ponds, and possibly due to visibility (Carlander 1997). This would indicate that open water refugia may exist depending on water clarity. But there may be growth, as well as mortality factors, involved in habitat selection. Growth may have compensated for mortality loss in vegetated ponds because standing biomass was the same between pond types, indicating that growth rates were higher in vegetated areas. Or alternatively, there was size-selective mortality.

Wind, Waves and Exposure & Age-0 Perch

Age-0 perch (fry and YOY) are found in sheltered, inshore areas except during winter periods. Larval survival was proportional to wind velocity, and they preferred sheltered areas with more structure and exhibited schooling behaviour (Houde 1969). However, perch larvae (8.5mm) could maintain position during 0.76m waves along lee shores during storm conditions so some level of disturbance or exposure is tolerable. Smaller perch had a higher mortality rate in windier conditions (Carlander 1997). Wind also played a significant part in year class strength in Lake Oneida because wind-induced seiches caused thermal

shock (Clady & Hutchinson 1974) in addition to potential direct effects on mortality.

Wind and waves may also affect the survival of young perch by influencing food supply and bioenergetics for newly hatched fry. Turbulence can positively affect food availability (Megrey & Hinckley 2001). A moderate amount of turbulence can increase the catchability of food items, but the relationship is nonlinear. At higher water velocities (or turbulence), predation success can dramatically decrease. Therefore the mechanism by which exposure affects mortality directly or indirectly is unclear, as well as sublethal effects on growth. Beyond certain tolerance limits the distribution of larvae is thought to be wind-driven. Larvae were unable to maintain position in linear water velocities $> 2.5 \text{ cm}\cdot\text{s}^{-1}$ ($0.09 \text{ km}\cdot\text{hr}^{-1}$; Tyler & Clapp 1995). Therefore they may be passively distributed to areas that are less suitable.

Temperature & Age-0 Perch

Environmental conditions, but mainly ambient temperatures, affect the initial hatch size and subsequent growth increments in perch (Powles & Warlen 1988). Thermal tolerances ranged from 3-28 °C for age-0 perch (Hokanson 1977). In larval perch, the thermal preference did not differ significantly with developmental stage up to day-24 (Ross *et al.* 1977). An increase to 16-18 °C from hatch is optimal for prolarval survival and there was no survival at temperatures ≤ 10 °C. Other studies state that survival was greatest (63% over a 2 week period) at 20-21 °C (Thorpe 1977). Feeding was initiated at 12.5 °C while postlarval optimal feeding occurred at 20- 21 °C. Larvae were inactive at < 5.3 °C and no growth of larvae has been observed below < 10 °C. YOY temperature preference ranged around 23.3 ± 2.5 according to Hokanson (1977), which is slightly higher than feeding and survival optima stated.

Acclimation temperatures affect preferred temperatures of young yellow perch, which varied from 13 to 29 °C when ambient Lake Erie temperatures were 1-24 °C respectively. Larvae seem to prefer 21 to 24°C when acclimated at 20 to 25 °C (Ross *et al.* 1977). In laboratory experiments, *Perca* spp. exhibited a physiological optima at 25 °C and an upper lethal temperature between 29 to 35 °C depending on the species and the experimental conditions, or acclimation temperature (Hokanson 1977).

There are interactions between variables that affect overall recruitment, and possible indirect effects of temperature. Age-0 yellow perch were most abundant during years with more precipitation (higher water levels), less wind (less turbulence or exposure), and less variation in daily temperatures (Pope *et al.* 1996). Spring warming rate and regularity affected the strength of the perch year class in Saginaw Bay. However, Koonce *et al.* (1977) hypothesized that the observed correlation between temperature and year-class strength of yellow perch may not be the result of direct effects of the temperature regime on survivorship of early life

history phases, but indirectly on their food supply. Post and McQueen (1994) corroborate this hypothesis because the variability in young-of-the-year growth was explained by the availability of benthic or planktonic prey while mean annual water temperature and cumulative degree-days did not add to the explanatory power of the relationships.

Perhaps these metrics of thermal habitat may not capture the interaction between temporal and spatial thermal structure and larval dynamics accurately and may be obscured by larval behaviour because young fry did select water at optimal thermal conditions for growth at 23 °C. In laboratory experiments, larval fish chose locations based on thermal gradients first then food availability (Wildhaber & Crowder 1990). Under low food conditions, behavioural temperature modification can also improve survival. Unfed larvae survived 15 days at 19.8 °C and 65 days at 5.3 °C, much longer than survival estimates stated earlier of 9 days. Even so, a minimum amount of growth in the first year before over-wintering is required by young fish to survive until spring (Shuter & Post 1990).

Light, Turbidity and Age-0 Perch

Larvae are positively phototactic and after hatching become limnetic, then move inshore to a littoral zone depth <3 m and form shoals. Laboratory studies indicate that fry aggregated in bright diffuse light until 2 months after hatching, then they selected darker areas, ceased to be pelagic, and become demersal (Thorpe 1977). An increase in light during the demersal stage has been linked to a decreased survival, probably due to improved visibility for predators. Also, the size of ingested cladocerans increased with larval fish size and inversely with light intensity. However, fry need better light for feeding. The visual distance for young perch is 5-6 cm and they school by visual orientation (Craig 1987). Young fry do not have fully developed retina so prey items must be relatively close. However, young yellow perch are sensitive to short wavelengths and are able to use more of the light spectrum in order to search out food than adults (Loew 1991, 1993). In a summer study with 0.5 g fish, 28 °C was the growth optimum, however, growth was also dependent on photoperiod. Higher growth rates were observed under 16-hour light conditions versus 8-hour days in both 16 °C and 22 °C tests (Hokanson 1977). First year growth was negatively correlated with turbidity, especially in June, which also affected light availability (Carlander 1997). Growth and survival in the first 14 days after hatch was affected by illumination and prey contrast with background, which affects prey catchability. Until yellow perch are roughly 30 mm (age-0), their prey is not always recognizable (i.e. unfocussed or unclear), but is detectable up to a maximum distance of about 20 cm (Wahl 1993). Yellow perch move from pelagic to demersal waters when their visual acuity approaches adult values, as visual acuity improves, so does detection distance.

Other Physicochemical Factors & Age-0 Perch

Both growth and mortality of young perch can be affected by several other physicochemical factors than those listed above. Eutrophication positively affected growth, where growth rates were slower at low total phosphorus levels, but there was no change in growth rate beyond a threshold (Leach *et al.* 1977). Trophic status has been used in habitat suitability assessments of perch as an indicator of growth rate in different lakes because of increase primary productivity in these systems (Krieger *et al.* 1983).

Dissolved oxygen levels (DO) also plays a role in habitat suitability for perch, and may be linked to eutrophication in some areas. Below a minimum DO threshold can be detrimental to most fish. Dissolved oxygen distress for 0+ fish occurred at 7 ppm at 19 °C; with lethal limits at 1 ppm for perch fry (Petit 1973).

A2.1.4 Juvenile Stage

Perch are sexually immature juveniles for the first 2 to 3 years of life. Sexual differentiation occurs at 10-12 mm but the size is dependent on growth rates (Thorpe 1977, Craig 1982). Growth rates may differ between the sexes until maturation. Age-1 lengths ranged from 5.7 –12.7 cm (males) and 8.6-10.4 cm (females) in some studies. Maturation occurs at 2 years for males and 1-2 years later for females.

The habitat requirements of juveniles differ subtly from adults (and perhaps also between sexes), except during spawning, when adults have very different habitat requirements. The driving forces behind juvenile and adult differences may be a function of biological competitive interactions between fish as much as physical habitat preferences or relationships with vital rates.

Juvenile Food & Growth

Perch < 115 mm were almost exclusively zooplanktivorous with increasing benthos and fish consumed through the summer and fall. The size of prey increased with the size of fish. Piscivorous perch are gape-limited predators able to consume prey ≤ 60 mm. Early growth rates are important because there is size-selective mortality of smaller perch over winter (Johnson & Evans 1991, Radke & Eckmann 1999). Perch from stunted populations do not differ genetically from perch growing more rapidly (Carlander 1997), which may indicate physical habitat effects if genetic differences were not found.

Falk (1971) studied digestion rates and relationships to fish size, the structure of food items, and water temperature. Food consumption rates were based on diurnal feeding patterns and gastric digestion rates corresponded to stomach fullness and not to daylength and temperature (Falk 1971). Contrary to this finding, thermal effects on bioenergetic rates have been documented for different life stages of perch (Kitchell 1977; Post 1990). The contradictions indicate that the link between bioenergetic rates and physical habitat may not be direct.

Juvenile Predation, Competition & Density-dependence

A negative relationship between juvenile growth and abundance of older perch, muskellunge, walleye, and goldeye abundance was determined that may indicate competition (Diehl & Eklov 1996, Bystrom *et al.* 1998). There was no relationship between bluegill and pumpkinseed year class strength and juvenile perch growth, which could indicate a lack of competition of habitat segregation or both. Results from enclosure experiments with white perch (Parrish & Margraf 1993) indicated a density-dependent threshold for growth between these species. Behaviourally, immature perch stay several body lengths from adults or from pike (Eklov 1997). Young and juvenile perch schooled separately from mature fish in summer and remained nearshore in Lake Erie and size classes were also segregated by habitat in a Florida lake (Havens *et al.* 2001). It would be difficult without laboratory tests or controlled field experiments to determine if habitat requirements were different between age classes (fundamental niche) or if distribution differences were caused by competition or predation effects (realised niche). Although one could argue that based on ideal-free distribution ideal habitat is a combination of optimizing survival and growth and therefore optimal habitat strictly based on a physical conditions would become less suitable because of biotic interactions.

Water Depth & Juveniles

Scant information is available on juvenile perch depth preferences. Age-1 perch used the littoral zone in several studies, however older perch were found in the littoral as well. In contrast, yearling perch (age=1) have been found up to 31 m water depth. Age-2+ perch (some may be juveniles) were found at shallow and intermediate depths in Lake Michigan but no actual depth distribution was given (Wells 1977). Yellow perch feeding behaviour in the laboratory indicated that perch favoured prey on the bottom of experimental tanks and in the middle of the water column over higher-situated prey (Ansari 1989). For the most part, depth distribution differences between juvenile and adult habitats occurred during spawning because juveniles do not need to migrate to shallower waters in the spring. Therefore, they probably concentrate their activities on foraging, seeking preferred temperatures, and avoiding predation at this time, which may or may not overlap with the littoral zone during spawning in spring.

Vegetation, Cover, Substrate and Juveniles

In South Dakota lakes, presence or absence of submergent or emergent vegetation had no influence on juvenile fish abundance (Fisher *et al.* 1999). However, there were minor, positive effects of low level complexity of habitat on the predation efficiency of 4.4-6.7 cm perch (Mattila 1992). Individual invertebrate prey size was inversely related to age-1 Eurasian perch proportional use of vegetated habitat (Diehl &

Kornijow 1998) indicating size-selective predation on smaller food items in vegetated areas.

Juvenile abundance was low over coarse substrate in south Dakota lakes (Fisher *et al.* 1999). Substrate coarseness was also related with the relative abundance of fish in the nearshore during night and day surveys. This may indicate that bottom substrates are used for different reasons diurnally (i.e. separate feeding and refuge habitats). Feeding substrate preference is probably determined by benthivore or piscivore feeding behaviour and depends on the time of year and relative food availability.

Temperature & Juveniles

Juveniles are the most thermally tolerant of all the life stages. Juvenile preferences have been documented at 3 °C higher than adult preferences (Thorpe 1977). When acclimated to 24 °C, young perch selected warmer water than adults when permitted to distribute in a gradient from 14-29 °C. In both Lake St. Clair and the Grand River, young fish were found in 1-5 °C warmer water than adults between June and November (Danzmann *et al.* 1991). A physiological optimum of 25 °C has been measured for juvenile perch. During a fall-to-spring study using 5.2 – 23.7 g fish, 23 °C was the growth optimum, and 20-29 °C was the thermal range preferred (Hökanson 1977). Various lethal temperatures have been calculated for juveniles depending on size and acclimation temperature, from upper lethal temperatures of 29-30 °C after 24-83 hours (fish were acclimated to 22-25 °C and weighed 3 – 50 g). A chronic temperature maximum of 33-34 °C with 1 °C / day warming rates has also been determined.

A2.1.5 Adult Stage

In a literature review by Thorpe (1977), female perch matured between 2-4 years and males between 1-3 years; a broader range than stated by other authors. Male size at maturity has ranged from 5-16 cm and females were 12-24 cm in some studies (converted to biomass, adult males were 10-60 g and adult females 20-240 g). In Lake Erie, males (age-1) and females (age-2) have matured at 14.0-17.8 cm. Under hatchery conditions, sexual maturation can be precocious; recorded as early as 3.5 cm in females and 8.5 cm in males (Craig 1987). Alternatively, females may delay maturation if the year-class is strong (i.e. when densities are high) under natural conditions. Early high growth rates can affect maturation, and age at maturity is earlier at higher temperatures. This would indicate that the premature hatchery fish may not be a result of stress under too high densities but perhaps growth rates. Conversely, slow-growing fish mature later, which would indicate a size-dependent maturation and not an age-dependent relationship and perhaps be related to high competition if densities are high.

Generally, perch live in surface waters in spring and early summer with a gradual migration to deeper waters through the rest of the year.

After spawning each year, perch typically move to deeper, offshore waters near the thermocline. Older fish migrate first. Diurnal feeding is frequently reported for perch and they are considered opportunistic feeders with seasonal changes in feeding rates (Thorpe 1977). The maximum rates occur mid-summer, with maintenance feeding in fall, which is thought to be dependent on food availability and temperatures (Thorpe 1977b).

Food, Growth & Density-dependence in Adult Perch

Tesch (1955) suggested in Thorpe (1977) that optimal conditions for adult perch growth are large, moderately deep, weed-free, mesotrophic waters containing a substantial population of forage fish. Growth rates were subject to inverse density-dependence and summer water temperatures. Adult densities have been recorded at 312 ind·ha⁻¹ but the average densities of yellow perch varied from 0.5 – 2.2 ind·ha⁻¹. In Lake Erie, individual growth was inversely related to population size, however a lot of variation occurred between basins and between years (Henderson & Nepszy 1989).

Carlander (1997) cited that the average growth rates for yellow perch in the Great Lakes tended to be greater than other regions. For yellow perch, age 2 to 5 years in the late 1970s, May and July growth rates were higher in the central > eastern > western basins on the Canadian side of the lake. The ranks of size-at-age from 1968 to 1986 for the basins of Lake Erie and Lake St. Clair were central > western > eastern > Lake St. Clair and size-at-age declined over time at all sites; implying that growth rates were decreasing. On average, adult perch range from 15-20 cm at 0.2-0.3 kg in the Great Lakes (OMNR 2000).

Some perch appear to be migratory and others not. This has ramifications on the scale of habitat associations and perch if movement is great. The prevailing thought is that habitat drives movement and could be based on the depth of the thermocline, or a combination of dissolved oxygen levels, temperature, and light in the system (Craig 1987). Average distances travelled of marked fish were 1.9 to 3.9 km (Lac St. Louis, Québec), although 80-90 km have been recorded in Lake Michigan (Thorpe 1977). Perch can travel up to 100 km in 9 months but their home range is stated as 100 m. In contrast, some studies indicate that perch do not cover large distances and remain close to certain areas and have a tendency for homing (Hasler & Bardach 1949).

In Europe, large perch share a diet with several competitors (pike, pike-perch, and burbot), but feeding was separated temporally (diurnally or seasonally) between species reducing potential competition. Certain prey items may be selected by perch preferentially; although they are considered generalists. Diptera and zooplankton were more important to <100 mm fish, while larger fish were recorded as ingesting *Bythotrephes* as a major component of their diet when available in Lake Michigan (Baker *et al.* 1992) and even ingesting zebra mussels in Lake Erie

(Morrison *et al.* 1997). Therefore good related habitat specificity is probably low.

Mortality & Predation in Adult Perch

Different sources contribute to mortality rates, such as disease, starvation, predation, and fishing pressure. Cohort comparisons of mortality between 1975-80, ranked the basins of Lake Erie as follows: western (93% mortality) > central (86%) > eastern (62%). These figures were consistent with fishing pressure differences between basins: central, western, and eastern basins were ranked from 32.7%, 20.9%, and 7.5% fishing mortality, respectively (Henderson & Nepszy 1989). The average annual mortality proportion for exploitation of age-3+ fish in Lake Erie ranges between 0.35-0.77.

In North America, predators of perch include a wide range of species from warm to cold water fish. Bird predators include mergansers, loons, cormorants, and herring gulls. The maximum age for yellow perch reported in the literature ranges between 12-20 years (Carlander 1997). Although in another review, life span was recorded as 6 to 21 years depending on growth rates, which were linked to population mortality and reproduction rates, (m and k-related), and also susceptible to temperature fluctuations (Pauly 1980 in Craig 1987). The average adult life span in North America is 5-7 years, with a longer life in colder areas.

Water Depth and Adult Perch

Different sources quote varying correlations between perch presence and water depth that may be confounded with other habitat factors, as well as seasonal and diurnal behaviours. From February to May, most perch were found at 2-22 m, concentrating in mid to late May at <15 m on rocky bottoms to spawn, and returning to deep water (24 m) in early August (Thorpe 1977). Other sources cite spawning at 6-12 m depths with perch returning to deep water again by October. The depth distribution of perch increased in summer but was not related to temperature according to Henderson & Nepszy (1989). Perch had a wide vertical distribution, and were found to depths of 21 m in summer and 49 m in winter in Cayuga Lake. In fall, perch were rarely closer than the 6 m depth contour to shore. Older fish are usually found in deeper waters, and move to profundal areas during winter and inshore during spring, remaining there until autumn. In a compilation by Lane *et al.* (1996c) depth preferences were listed as 5+ m in fall. Yellow perch were found in Lake Michigan at 25 m or less (Hayes 1999) but mainly the 8-m contour in smaller inland lakes (Hayes *et al.* 1992). Yellow perch and white perch were found at 3.3 and 7.0 m depths, respectively, in an intensive survey of eastern Lake Erie (Parrish & Margraf 1994).

Migrations could be a major source of the discrepancies in depths recorded. In hydroacoustic surveys, fish > 5 cm in small Québec lakes were shown to migrate offshore in the afternoon in the 0-10 m zone (the migration is more pronounced in lakes with pelagic piscivores) but spend

the remainder of the time in the littoral zone. Perch showed highly clumped distributions along shore probably indicating habitat selection (Gaudreau & Boisclair 1998) or schooling behaviour. Adult perch were rarely found above 2.5 m when temperatures exceeded 26 °C in Florida. This type of behaviour would indicate a thermal preference or avoidance, and not a strict depth preference, that overrides optimal foraging behaviour.

In European lakes, all perch stages were found mainly in littoral areas (Viljanen & Holopainen 1982). Adult fish were mainly caught in fall at the 15m contour (the shallowest depth sampled) and very few at 25 and 35 m (Pothoven *et al.* 2000). Contrary to this finding, Bergman (1991) found Eurasian adult perch prefer 5-10 m depths, with no real seasonal differences. Hydroacoustic surveys in reservoirs (up to 40 m deep) in the Czech Republic showed most fish concentrated in the upper 0 – 5 m layer from the end of April through August (between 0-1 m depth layer under deoxygenated hypolimnion conditions) and were especially concentrated in the littoral zone (Kubecka & Wittingerova 1998). Schools of perch have been found just above the thermocline at 12 m in summer and at depths of 9-18 m under ice in winter. The variability in depth correlations might indicate that depth is not the driving factor for perch distributions, or it is mitigated by a combination of factors.

Vegetation, Cover & Adult Perch

Most studies state that perch prefer open water with moderate vegetation, while some state that adult perch do not inhabit vegetated areas (except during spawning). In Lake of the Woods, woody debris or vegetation over sandy bottoms was associated with perch distributions. Similarly, submerged vegetation or emergents in Lake Winnebago were associated with perch presence. In general, greater fish species richness has been linked, nonlinearly, with macrophyte density (Randall *et al.* 1996) and various reasons have been proposed. Most fish have difficulty penetrating dense macrophytes ($> 300 \text{ g dry weight} \cdot \text{m}^{-2}$; Perrow *et al.* 1999, Engel 1988) and may avoid moderately-dense macrophytes because of the predation risk.

Conversely, there is usually an increase in prey item density in vegetation. Macrophyte and macroinvertebrate densities were positively related (Diehl & Kornijow 1998, Cyr & Downing 1988), which is either due to reduced predation because of refugia provided by plants, or higher production in vegetated areas. Fish growth is usually higher in vegetated areas than non-vegetated; possibly indicating a greater food availability (Diehl & Kornijow 1998). The use of vegetated areas for foraging may be controlled by the fish species assemblage present and the relative predation risk to adult perch (Diehl & Eklov 1995). In Long Point Bay, there is a diverse fish species assemblage so the predation risk may be higher than in other systems, especially due to the presence of pike.

Substrate & Adult Perch

Perch presence has been associated with mud, sand, and gravel lake bottoms, however they are considered non-specific for substrate type as adults (Craig 1987). In literature reviews, adult perch were associated with vegetation, gravel, rubble, sand, mud, and silt (Thorpe 1977, Lane *et al.* 1996c). In Lake Mendota, fish moved inshore at sunset between May and October, then moved along shore at the 6m contour over muddy areas, with some stones and rocks, and within macrophyte proximity. In Delaware lakes, the greatest number of perch were on flat bottoms with small coarse gravel and clean swept sand. In controlled experiments, however, substrate type could not be used to discriminate site selection in perch (Jansen & Mackay 1992).

Seasonal use and diet complexity in yellow perch did not differ between cobble and rubble shoal sites and sand sites, where *Gammarus* spp. was the major prey item throughout (Danehy *et al.* 1991). Growth rates for perch were greater in cobble and rubble shoals compared to sandy substrate, which may indicate a hierarchy of suitability for growth potential, but females outnumbered males in these areas (Danehy *et al.* 1991). This may have introduced a bias in the results if growth rates differed between the sexes and were not corrected. Also, it is unclear how the authors accounted for movement, if any, between habitat types. If benthic invertebrates were the food source softer substrates would have a higher probability of success unless to fine, like clay-based sediments.

Temperature & Adult Perch

Fry (1947) described five major effects of temperature: controlling (setting the pace of development and metabolism), masking (affecting the expression of other environmental factors), limiting (influencing locomotory activity and hence distribution), directing (stimulating an orientation response), and finally as a lethal agent (chronic lethal minimum and maximum). Negus *et al.* (1987) listed factors which modify fish behaviour in thermal gradients: acclimation temperature, food, light & dissolved oxygen, season, turbulence, photoperiod, and the distribution of competitors and predators. Obviously, all these factors cannot be addressed at once, but temperature does play a key role in population dynamics of poikilotherms in many ways. Some conflicting reports of the effects of temperature on the life cycle and distribution of fish suggest that complex and multivariate interactions are at work, but this is consistent with the multidimensional definition of habitat.

Brandt *et al.* (1980) showed that different freshwater fish species segregate along temperature gradients with those patterns maintained despite rapid oscillations in thermocline location. It has been shown that some fish will even compete for favourable temperatures (Magnuson *et al.* 1979). Yellow perch are considered a cool water species. Predictions forecasted that thermal habitat during summer would increase for yellow perch in the central basin of Lake Erie due to climate warming (Magnuson *et al.* 1990) implying that thermal habitat may be limiting currently. The

association between temperature and perch distributions, growth, and mortality are discussed below.

Most thermal habitat assessments refer to the work by Magnuson *et al.* (1979) that defined a fundamental thermal niche as 'a range of temperatures around a species' final preferendum that defines the optimum conditions for activity and metabolism'. A temperature of 21 °C is listed as a preference for adult perch, although reports vary. Overall mean temperature over 24 hours was 20 °C in preference experiments (Craig 1987). Temperatures of 16-17 °C were selected predawn and 24 °C at dusk under normal light conditions in another experiment (Ross and Siniff 1982). In most cases, significantly lower temperatures were 'selected' in field surveys rather than laboratory experiments. A list of thermal ranges during different seasons in Lake Erie is shown in Table A2.1.

Table A2.1: Yellow perch seasonal thermal range of distribution in western Lake Erie (modified from Carlander 1997)

Stage	Winter	Spring	Summer	Autumn
YOY /Young	1-15 °C	17-25 °C	25-29 °C	24-31 °C
Adult	1-16 °C	10-16 °C	23-26 °C	13-25 °C

Temperature may be also be a cue for migration to feeding areas seasonally and affects schooling behaviour. Offshore migrations increased as surface water temperatures increased and the thermocline depth increased perhaps seeking preferred temperatures between feeding bouts. Swimming speed increased linearly with temperature but activity was linked to other behavioural factors as well. (For example, fish tend to be inactive at night, resting on the bottom.) The lowest swimming speeds were recorded at 0-5 °C and maximum speeds between 20-25 °C. Cruising speed decreased with reductions in oxygen content as well (Craig 1987). This increased mobility may improve foraging efficiency either individually or as a group. Individual fish swim half-speed as schools compared to single fish. Swimming speeds of schools increased from winter to summer, and seemed to be temperature-dependent as well. In summer, fish were evenly spaced within schools by about 15 cm between individuals and average swimming speed was 2.2 times body length per second (Hergenrader and Hasler 1967) but denser schools were formed at higher temperatures. Winter was spent in midwater in loose schools. Winter schools average 6.7 m from top to bottom, while in summer school depth was 2.5 m.

Conflicting findings for the effects of temperature on growth and mortality are abundant, perhaps indicating a complex set of relationships. Nevertheless, growth is linked to food intake, within genetic and physiological bounds, and modified by temperature (Kitchell 1977). Laboratory studies indicate there is an effect of temperature on growth

rates (Christie and Regier 1988) and temperature modifiers have been applied as coefficients in bioenergetics models (Kitchell 1977, Post 1990).

The length of the growing season (temperature and day length) has been suggested as a significant factor limiting perch growth, the optimal temperature for growth being 22.5 °C for adults for a 5-24 g perch. More rapid growth occurred at 22°C than 16 °C in the laboratory, but a photoperiod of 16 vs. 8 hours had a greater experimental effect. Growth maximums occurred at 21 °C when a temperature series was experimentally tested (Carlander 1997).

Analysis of yellow perch trawl data, showed growth was not related to average water temperatures or degree-days, but inversely to the abundance of year-classes (Henderson 1985), indicating that competitive or density-dependent effects were limiting. Hayward and Margraf (1987) hypothesized that within-lake, inter-basin growth differences in Lake Erie were due to food and not temperature differences. Although productivity is related to temperature and light, which could imply indirect or nonlinear temperature effects (masking). Indeed, Craig (1987) showed that adult perch growth was regulated by post-spawning fall temperatures and two-thirds of the variation in growth was accounted for by temperatures above 14 °C during the year. In Lake Superior, under a much different thermal regime than Lake Erie, perch are limited to warm water embayments and harvestable size is not reached until ≥ 4 years old. In contrast, Lake Erie perch reach harvestable size-at-age 2 or 3. This would imply a thermal habitat constraint on population dynamics.

Although behavioural experiments with yellow perch do not exist, minnows seemed to trade-off higher prey concentrations in a river for higher temperatures in shallow areas where they spent most of their time (Garner *et al.* 1998). It should be noted that guts were still full even though prey density was lower, which could indicate local depletion of food supply through top-down effects could be occurring but food was not limiting. Perhaps temperature acts secondarily to food availability, and becomes less important if food is not limiting.

Adult perch cannot survive for more than a few hours at 31 °C and the 30 °C summer isotherm marks the latitudinal boundary for their southern distribution (Thorpe 1977). In laboratory experiments, *Perca* spp. exhibited an upper lethal temperature between 29 to 35 °C depending on the acclimation temperature (Hokanson 1977; Table A2.2). Among the biotic, chemical and physical factors influencing temperature tolerance, acclimation temperature is probably the most critical. Acclimation only occurs at constant or very gradually changing water temperatures. Body core temperature is changed, but acclimation is not reached, when linear temperature changes of $0.3 \text{ }^\circ\text{C min}^{-1}$ occur (Beitinger *et al.* 2000).

Table A2.2: Acclimation temperatures and associated preferred, upper and lower avoidance temperatures in laboratory experiments with yellow perch (Hokanson 1977) including final preferenda.

Temperatures (°C)		Experiment 1					
Acclimation	8	10	15	20	25	30	Final preferendum
Preferred	18.6	19.3	23.0	23.1	24.5	26.7	24.2
		Experiment 2					
Acclimation	15	18	21	24	7-day upper lethal		
Lower avoidance	12	15	18	18	26		
Upper avoidance	21	27	27	29	Final preferendum		
Preferred Temp	19.2	20.4	21.1	22.4	21.4		

Most studies concentrate on determining the upper lethal limit of temperature, but more “cold” kills are reported than heat kills (Beitinger *et al.* 2000). Fish are able to increase their tolerance of high temperatures more quickly than cold and fish lose heat tolerance more slowly. High temperatures also induce frantic activity, which assists in fleeing, whereas cold induces lethargy. Upper temperature tolerances are well above ambient temperatures in most natural habitats but not so for lower lethal temperatures. Therefore both upper and lower limits should be considered in assessments.

Exposure, Wind, Waves & Adult Perch

The linear velocity that perch could resist was 10-15 times the square root of their body length (Houde 1969). Therefore perch would either actively avoid certain areas of high flow or be distributed by storm events. Modelling studies have shown a nonlinear relationship between turbulence and predator-prey encounters and catchability; greater success occurs at moderate disturbance levels (Megrey & Hinckley 2001). Although weather conditions are generally considered to be important in the distribution of fish, and potentially their growth and mortality, no relationship was found between the growth of perch and rainfall, sunshine or wind in Lake Erie in a study by Carlander (1997).

Turbidity, Light & Adult Perch

Adult perch require light but usually limit feeding to crepuscular times, remaining inactive at the bottom at night and forming shoals in morning and twilight in open water. Interestingly, walleye light optima coincide with a decrease in visual acuity for yellow perch in shallows during twilight (Thorpe 1977), which could make them more susceptible to predation at that time. Perch are also less adapted to turbid water than other fish. Perch retinas had no blue cones, like goldfish, which are

adapted to highly turbidity areas. Rod and cone configuration in yellow perch retina indicated that clear, shallow water would be optimal visually (Loew & Wahl 1991). This is corroborated by field evidence where turbidity or light transmission was inversely related to perch abundance. The higher the turbidity, the smaller the mean volume with less fish per school (Wahl et al. 1993).

Other physicochemical factors

Carlander (1997) concluded that the distributions of perch are limited by temperature, current speed, salinity and dissolved oxygen. Temperature and current speed have already been discussed in previous sections. In tagging experiments, perch have moved up to 10 km, and oriented to oxygen content as well as preferred temperatures. Lower dissolved oxygen limits were 0.4-0.9 ppm at 15.5 °C and 2.25 ppm at 20-25 °C. The preferenda for dissolved oxygen was 7 ppm at 20 °C (Fry 1957). In winter, perch moved upward from typical depths to just under the ice when oxygen concentrations fell to 0.5 mg O₂·L⁻¹ (Carlander 1997). Salinity tolerances ranged from 0.3-10.3‰ in freshwater. Also, water levels and growth of older perch were negatively correlated.

Appendix 2.2: Yellow perch habitat associations by life stage: egg, larva (includes fry, planktonic & demersal stages), juvenile & adult.

	Egg	Larva	Juvenile	Adult
Vegetation / Cover	<ul style="list-style-type: none"> • Medium-density submergent, mid-density emergent, rocks, brush & debris (Lane <i>et al.</i> 1996) • Random deposition on vegetation, rocks, brush, debris (Goodyear 1982) • Submergent vegetation & trees (Thorpe 1977) • Vegetation and debris (Collette 1977) • Aquatic macrophytes (Craig 1987) • Hatching success may be higher in areas of sparse aquatic vegetation than in areas of very dense vegetation (Kreiger 1983) • Eggs released near aquatic or inundated vegetation (Herman <i>et al.</i> 1964, Mansueti 1964, Scott & Crossman 1973, Clady & Hutchinson 1975, all in Kreiger <i>et al.</i> 1983) 	<ul style="list-style-type: none"> • Medium-density submergent, mid-density emergent, rocks, brush & debris (Lane <i>et al.</i> 1996) • Vegetation (Goodyear 1982) • Move to open water during first 2 months of life (Krieger 1983) • Presence / absence of submergent or emergent vegetation had no influence on fish abundance (Fisher 1999) • Difference in habitat selection for 0+ perch with presence/absence of piscivores during both day and night (prefer macrophyte cover when present, open water when absent; Jacobsen 1997) • 80-100mm Eurasian perch spent more time in simulated vegetated habitat compared to roach and rudd (Bean 1995) • Stem density had no relation to amount of time spent in vegetation for Eurasian perch 80-100mm (Bean 1995) • Stem density did affect vertical swimming heights of Eurasian perch they swim lower than roach and ruffe (Bean 1995) • With Predators, perch increased time spent in vegetation, but less difference at lowest stem densities (200 & 400 stems m⁻²; Bean 1995) 	<ul style="list-style-type: none"> • Presence or absence of submergent or emergent vegetation had no influence on fish abundance (Fisher 1999) • Minor effects of low level complexity on the predation efficiency of 4.4-6.7cm perch (Mattila 1992) • YOY and age-1 Eurasian perch - individual mass increase of prey was inversely related to their proportional use of the vegetation habitat (Diehl 1995). 	<ul style="list-style-type: none"> • Medium-density submergent, mid-density emergent (Lane <i>et al.</i> 1996; incl. juveniles) • Optimum habitat is weed-free (Tesch 1955) • Adults associated with shoreline, littoral areas, moderate vegetation used for cover and spawning habitat (Herman <i>et al.</i> 1964, Ward & Robinson 1974, Kitchell <i>et al.</i> 1977, Kreiger 1983) • River, moderate vegetation > 20% cover (Coots 1956, Kitchell 1977 in Krieger 1983) • Spawning nearshore on branches of <i>Potentilla</i> & <i>Carex</i> (Urho 1996) • Strongly selected intermediate vegetation densities (40-60 stems m⁻²; Eklov 1997) • Large perch stay close to habitats used as refuge by smaller prey fish (Eklov 1997) • Perch group size decreases as habitat becomes more vegetated (Eklov 1997) • Gut analysis had size-structure ratios similar to ratios found for invertebrate larvae in upper sediments at low and medium plant densities, may supplement diet when high vegetation is present (Kornijow 1997)
Trophic	<ul style="list-style-type: none"> • 	<ul style="list-style-type: none"> • Suggest that homogeneous lakes do not have the classic larval migration patterns (Fisher 1999) 	<ul style="list-style-type: none"> • 	<ul style="list-style-type: none"> • Mesotrophic water with substantial population of forage fish (Tesch 1955)

	Egg	Larva	Juvenile	Adult
Substrate	<ul style="list-style-type: none"> • Medium affinity for rubble, silt, clay; high affinity for gravel, sand (Lane <i>et al.</i> 1996) • Boulders, gravel, tree & branches (Craig 1987) • Found on gravel or rocky substrate (84%) with only rocky substrate being selected (LEI=0.124; Fisher 1996) • Most egg masses associated with some type of structure (92%), with a strong selection for a periphyton-free wood structure (LEI=0.917), strong selections made for human-constructed structures (LEI=0.833; Fisher 1996) • Egg masses associated with submerged tree branches, perch prefer freshly submerged wood as spawning substrate (Fisher 1996) 	<ul style="list-style-type: none"> • High affinity for gravel, sand, silt (Lane <i>et al.</i> 1996) • Associated with gravel, rubble, sand, mud, silt (Goodyear 1982) 	<ul style="list-style-type: none"> • Benthivore & piscivore, therefore substrate preference probability determined by feeding habitat • Abundance low over coarse substrate (Fisher 1999) • Night and day relative abundance of fish in nearshore is negatively correlated with substrate coarseness (Fisher 1999) 	<ul style="list-style-type: none"> • Low affinity for bedrock, boulder, cobble, rubble, clay; medium affinity for gravel; high affinity for sand & silt (Lane <i>et al.</i> 1996 incl. juveniles) • Cobble/rubble shoal > sand sites for growth (Danehy <i>et al.</i> 1991) • Rocks, sand and gravel used if submergent vegetation not available for eggs (see above for Kreiger <i>et al.</i> 1983) • Prey consumed more often on sandy bottoms than on cobble bottoms (Fullerton 1998)
Salinity	•	•	•	<ul style="list-style-type: none"> • Salinity tolerances 0.3-10.3 ‰ (Driver & Garside 1966) • 13 ppt brackish (Hildebrand & Schroeder 1928 in Krieger 1983) • Freshwater required for spawning (Scott & Crossman 1973)
Dissolved Oxygen	•	• Distress at 7 PPM (Petit 1973)	•	<ul style="list-style-type: none"> • Limits 0.4-0.9 PPM at 15.5 °C, 2.25 PPM at 20-25 °C, preference limit 7 PPM at 20 °C (Fry 1957) • 0.2 - 0.5 mg·L⁻¹ are lethal in winter (Moore 1942, Cooper & Washburn 1949, Magnuson & Karlen 1970 in Krieger 1983) • At 26 °C, DO < 3.1 mg·L⁻¹ is lethal (Moore 1942) but studies < 5 days so determined that 5 mg·L⁻¹ lower optimal limit (Krieger 1983)

	Egg	Larva	Juvenile	Adult
Bathymetry (Water Depth)	<ul style="list-style-type: none"> • 0-5+ m (Lane <i>et al.</i> 1996) • Littoral up to 21.6 m but mostly <9m (Goodyear 1982) • 0.5-3 m (Collette 1977) • 6-12 m; males first (Craig 1987) • 0.5-8 m (Craig 1987) • Eggs broadcast in 1-3.7 m (Harrington 1947, Herman <i>et al.</i> 1964, Benson 1973, Clady and Hutchinson 1975 in Krieger 1983) • Egg masses found within 30 m (94%) and 15 m (77%) of shore (Fisher 1996) • 75% of sectors with egg masses found at depths 0.6-0.9 m (Fisher 1996) • Spawns in shallow waters in spring, shortly after ice-out in dimictic lakes (Williamson 1997) 	<ul style="list-style-type: none"> • 0-5 m spring, 5+ in fall(overwinter), pelagic 4-5 wks; Lane <i>et al.</i> 1996) • Postlarvae < 6 m, pelagic; demersal stage littoral area up to 20 m, highest density at <9 m (Goodyear 1982) • Prolarvae are limnetic, demersal <3 m; overwinter in deeper water, midwater school 1.5 m (Kelso & Ward 1977) • With yolk sac in pelagic zone; 8 mm perch in littoral in aggregates at vegetated edges; 2wk (10mm) highest abundance at 2- 3.5m; 3wk old (12 mm), 6.7 ind·m⁻² pelagic; 11.7 littoral (Urho 1996). • Larva usually in surface waters (<2.5-3m) for the first weeks, after the young are in demersal and littoral habitat (Williamson 1997) • Age-0 yellow perch occupied water <4m deep, closely associated with nearshore areas (Bronte 1993) • Age-0 yellow found predominantly at depths of >2.5-3 m until mid-summer (then become demersal) (Wahl 1993) • Age-0 yellow perch consistently leave the pelagic zone midseason (Post 1997) • Fry hatch nearshore and moved offshore but use both areas until 18 mm in length, then to nearshore (Fisher 1997) • 80-100 mm Eurasian perch occupied a lower average vertical position when predator present (Bean 1995) 	<ul style="list-style-type: none"> • Preferred depths slightly shallower than adults (Krieger 1983) • Abundance negatively correlated with water depth (Fisher 1999) • Perch occupied the 4-7 m layer (strata; Jachner 1991) • Yellow perch favoured prey on the bottom of the tank and the middle of water column over higher situated prey (Ansari 1989) • Age-1 (75-150 mm TL) and adult fish shorter than 200 mm found all over the bay, usually in water 4-7 m deep (Bronte 1993) • Daytime relative abundance in nearshore negative & significant correlated with water depth (Fisher 1999) 	<ul style="list-style-type: none"> • 0-10+, all year (Lane <i>et al.</i> 1996) • Found in shallow water (Ali <i>et al.</i> 1977) • Deep water >18 m until spawning • Found at 3.3 and 7 m depth in eastern Lake Ontario (Danehy <i>et al.</i> 1991) • Optimal lake is not shallow (Tesch 1955) • Largest adults (>200 mm TL) mostly found in water 2 – 7 m deep (Bronte 1993) • 90% of adult perch caught in the 8-m contour (Hayes 1992) • Outer bay sites in Long Point had a higher proportion of larger fish than did the inner bay sites (Diana 1990) • Perch more abundant in shallower water, but age of fish not specified (Bergman 1991) • Large perch not commonly found in littoral zone (Eklov 1997)

	Egg	Larva	Juvenile	Adult
Turbidity / Light	<ul style="list-style-type: none"> • Treating perch eggs with UV-b and longer lengths of solar radiation can damage eggs in water <1m deep in lakes with low DOC; fish in these environments must lay their eggs in deep waters to avoid ultra violet radiation, lowering ambient temperature around the eggs, and reducing their chance of normally timed development (Williamson 1997) 	<ul style="list-style-type: none"> • Visual distance 5-6 cm during schooling (Disler & Smirnov 1977) • Fry aggregate in bright diffuse light until 2 mo. after hatching then darker areas when no longer pelagic and become demersal (Thorpe 1977) • High light intensity decreases survival (Hokanson 1977) • Activity peaks usually correspond to onshore migrations in evening and offshore in morning; diurnal behaviour (Helfman 1979) • Lens diameter increases with fish size, cone density is inversely related to fish size, young yellow perch need light to forage, more time spent during development periods where visual acuity is low (Wahl 1993) • Young perch are able to detect, locate and strike natural prey with only near-UV light (Loew 1993) 	<ul style="list-style-type: none"> • Growth dependent on photoperiod 16h days better than 8h day, (Hokanson 1977) • Juvenile yellow perch have at least 3 spectral mechanisms at short wavelengths: sensitive above 580 nm, maximally sensitive at 480-580 nm, and sensitive <450 nm, (~395-406 nm; Loew 1991) • Yellow perch move from pelagic to demersal waters when their visual acuity approaches adult values, as visual acuity improves, so does detection distance (Wahl 1993) • Until yellow perch are ~30 mm SL, their prey is detectable (yet not always recognisable) at max distances of <20cm (Wahl 1993) • Juveniles able to use more of the light spectra in order to search out food than adults (Loew 1993) 	<ul style="list-style-type: none"> • Higher turbid smaller schools, clear water (Ali et al 1977) • Abundance inversely related to turbidity (Scot and Crossman 1973, Nelson & Walburg 1977 in Krieger 1983) • peak activity at sunrise and sunset and very inactive in darkness (Scott 1955) • abundance of perch decreased in more productive lakes, related to competition with roach for zooplankton, and increased algae turbidity (Bergman 1991) • both light and temperature influence the vertical distribution of perch (Bergman 1991) • (adult perch insensitive to short wavelength light; Loew 1993) • Yellow perch (95-250 mm), visual methods of foraging fail in the evening, switch to a tactile method of foraging (Jansen 1992)
Exposure	<ul style="list-style-type: none"> • Eggs found in sheltered areas (Goodyear 1982) • No egg masses found in wind-protected bays, with cattail growth, most egg masses found in unprotected regions of main lake (Fisher 1996) 	<ul style="list-style-type: none"> • YOY found in sheltered areas (Goodyear 1982) • YOY perch are active for shorter length of the day than older perch and have a higher affinity for structure and to school (Helfman 1979) 	<ul style="list-style-type: none"> • Foraging efficiency in young fish linked to water turbulence (Megrey & Hinckley 2001) 	<ul style="list-style-type: none"> •
Current Speed	<ul style="list-style-type: none"> • Velocities above $25 \text{ cm}\cdot\text{s}^{-1}$ fragment egg strands (Coots 1956; in Krieger 1983) • Prefer sluggish and slow water especially during spawning (Harrington 1947 in Krieger 1983) • Spawning occurs in low velocities ($<5 \text{ cm}\cdot\text{s}^{-1}$; Harrington 1947) 	<ul style="list-style-type: none"> • Larvae (<9.5 mm) unable to maintain position in velocities $>2.5 \text{ cm}\cdot\text{s}^{-1}$ (Houde 1969) • Larval survival and wind velocity are inversely related (Clady 1976) • Most perch (< 6.5mm) ceased swimming movements when current $5 \text{ cm}\cdot\text{s}^{-1}$ (Houde 1969) 	<ul style="list-style-type: none"> • 	<ul style="list-style-type: none"> • Prefer pools or slow flow in rivers (Kitchell 1977 in Krieger 1983) • Adults found in moderate currents but prefer sluggish and slow water (Krieger 1983)

	Egg	Larva	Juvenile	Adult
Temperature	<ul style="list-style-type: none"> • Spawning between 7-22 °C (Lane <i>et al.</i> 1996) • 3-23 °C over entire spawning range; Max fecundity at 4-6 °C over >=185 d; Gamete viability highest 8-11°C; highest % hatch 9-15 °C; tolerance 3.7-21°C in early stages and 7-22.9 °C later egg stages; optimal survival with incubation 4.9-10 °C and 1 °C/day increase (Hokanson 1977) • Spawning peaks 6-12 °C (Goodyear 1982) • Highest egg viability adults acclimated 6-9 °C; egg incubation at 9-15 °C (Treasurer 1983) • Year class strength related to rate of warming during incubation & hatching (Hartman 1972, Kreiger <i>et al.</i> 1983) • 7-20 °C range for embryo incubation and hatching (Hokanson and Kleiner 1973) • 10 °C increasing 1°C/day to 20 °C for optimum embryo development (Kreiger 1983) • Spawning occurs at water temps of 7-11°C (Williamson 1997) • Areas with cooling water effluent usually >=10° C warmer than ambient induced early spawning over controls; Successful perch development 8-18 °C, optimum at 13°C; higher causes disintegration of egg strands (Sandstrom 1997) • Warmer temperatures, faster hatch (22 vs. 16 vs. 10°C); Otolith growth rates linked warmer temperatures (Powles 1988) 	<ul style="list-style-type: none"> • Production of swim-up larvae 9.8 °C; newly-hatched larvae tolerate 3-28 °C, inactive below 5.3 °C, optimum survival if 1 °C·day⁻¹ increase from hatching to 16-18 °C at prolarval stage; postlarval feeding optimum 21°C, no survival at ≤0 °C, feeding initiates 12.5 °C, survival of 63% at 20-21 °C for 3 wk. preferred temps 13-29 °C when ambient temp 1-24 °C; tolerate temperatures from 3-28 °C but inactive below 5.3 °C and survival is better at 20 °C than at 10 °C ; 0.5 g fish 28 °C was growth optimum (Hokanson 1977) • Young fry (before swim bladder formation) have a tendency to move to warm water areas (Krieger 1983) • 12 mm yellow perch swam with velocity 15.3 cm/sec in 18.3 °C water and 4.15cm/sec in 13 °C water (Houde 1969) • Perch had a daily ration in the laboratory between 24-27% of their dry body weight at 13 °C and between 45-51% of their dry body weight at 18 °C (Marmulla 1990) • Optimal temp for growth 23 °C (Fisher 1997) 	<ul style="list-style-type: none"> • Juveniles 3 °C higher than adult preference, lethal temps 29-34 °C depending on size and acclimation temp and °C/day change; 25 °C physiological optimum, 5.2-23.7 g fish 23 °C as growth optimum; upper incipient lethal temperature 29-35 °C (Hokanson 1977) • Juveniles selected temperatures of 20-23.3 °C (adults 17.6-20.1°C) in vertical temperature gradient 14-30 °C after 24 °C acclimation (McCauley & Read 1973) • Catch per trawl positively related to water temperature in offshore bottom night trawls (Fisher 1999) • 83-310 mm fish, seasonal pattern in daily rations correspond to seasonal growth, interaction water temp, food availability, gonad development (Nakashima 1978) • High spring temps stimulated piscivory in perch due to large size difference between predator and prey; growth rates lower when decrease piscivory (Mehner 1996) • 1+ yr perch activity rates higher in warmer lake (24% of consumption rates vs. 13%); mean weight 2X higher; growth rates 3.5x higher (2.9-8.0g wet vs. 1.9-3.7g wet) (Aubin-Horth 1999) • Temporal- sequential appearance of juveniles in open water (perch 3 wks before smelt, 10 wks before roach) (Jachner 1991) 	<ul style="list-style-type: none"> • 24.7 (physio-optimum), 29.2-34.0 (lethal), 33.4 (critical maximum); gonadal growth <12°C; spawning temp related to gonad mature temp (Hokanson 1977) • Swimming speed linear with temp (lowest 0-5 °C; max 20-25 °C; Hasler & Villemente 1953) • 24-25 °C optimum; upper lethal 30.9 °C after 12 h (acclimation temp 12.5 °C) temperature of; in field 16.7 °C at predawn 23.8 °C at dusk (April normal light conditions; Reynolds and Casterline 1979) • Temp above 14 °C accounts 2/3 of growth variation (Le Cren 1958) • Upper lethal 31 °C (Thorpe 1977) • Adults must be exposed to 4-10°C for 145-175 d to ensure egg ripening (Hokanson 1977) • Preferred 17.6-25°C (McCauley & Read 1973); 19-24°C optimum (Scott & Crossman 1973); growth initiated at 6-10°C (Nakashimo & Leggett 1978); upper lethal 32.3°C (Ferguson 1958) • Lab & wild fish spawned same time without <10 °C as in wild conditions (Hergenrader 1969) • Annual swimming activity (CPUE) correlated mostly to temperature and day-length (Neuman 1996) • Natural mortality & temp limiting stock L Superior (bay depth 8.6 m; Bronte 1993) • constant temp & photoperiod, 60 d decrease, slight temp and large photo increase induced spawning in fall (Kolkovski 1998)
			A-59	

	Egg	Larva	Juvenile	Adult
Water Levels	<ul style="list-style-type: none"> • Rising water levels during spawning increased terrestrial vegetation inundation and related to large year class strength (Kreiger 1983) • Reduction in water levels may lead to desiccation of eggs (Benson 1973) 	<ul style="list-style-type: none"> • 	<ul style="list-style-type: none"> • 	<ul style="list-style-type: none"> • Drawdown of Missouri River decreased perch abundance (Beckman and Elrod 1971, Nelson and Walburg 1977)
PH & Ions	<ul style="list-style-type: none"> • 	<ul style="list-style-type: none"> • In water that was free of Ca and included CO₂ (lateral line inhibitor) perch (and ruffe) did not respond to prey unless the prey touched part of the fish's mouth, nor did the fish respond to water jet streams (normal water induced both prey and water jet stream responses; Janssen 1997) 	<ul style="list-style-type: none"> • 	<ul style="list-style-type: none"> • Tolerance range pH 3.9-9.5 (Honson <i>et al.</i> 1977, Rahel 1983); reproductive success affected < pH 5.5 (Ryan and Harvey 1979); optimum range 6.5-8.5 for FW fish (Stroud 1967; all in Krieger 1983) • Fish (unknown age) from circumneutral lake stock performed better than fish from acidic lake stock in circumneutral water (pH 7.8), and no significant difference was found in acidic water (pH 4.0; Nelson 1989) • Perch have high tolerance to acidic water with low levels of Ca and high levels of labile Al; Low numbers of young fish in acidic lake perhaps poor reproduction (Hesthagen 1992) • Variable production, both weak & strong year-classes, lack of mature specimens, great variation between similar lakes for perch abundance (Hesthagen 1992)

Appendix 4.1: Comparison of different types of models used to evaluate different fish species, the level of habitat detail used, the habitat characteristics modelled, temporal resolution, model structure, and the main hypotheses and conclusions, including PercaSpace.

Model Reference	Model Type	Species	Habitat Detail	Habitat Characteristics	Temporal Resolution	Model Structure	Vital Rate Hypothesis	Conclusions
Bartsch <i>et al.</i> 1989	SE-IBM, movement	Herring	Spatially-explicit lattice	Hydrodynamics	40-minute	Early life IBM	Habitat effects on spatial distributions	Vertical migration patterns affect spatial distributions
Pulliam & Danielson 1991	Metapopulation, movement	Generic Fish	Simulated Habitat	Inferred source /sink habitat configuration	Annual?	Stage-structured	Reproductive site selection affects source/sink population dynamics	Selection of high-reproductive fitness habitat affected metapopulation persistence
DeAngelis <i>et al.</i> 1991	IBM, no movement	Smallmouth Bass	Simulated homogeneous	Water temperature, daylight	Seasonal, some daily	Life stage structure	Intrinsic factors that affect individual growth and survival	Hatch times at large population sizes important for survival & growth
SALMOD (Bartholow <i>et al.</i> 1993)	Habitat-based population model, movement	Salmonids	Variable patch size; WUA	Temperature, stream flow	Weekly	Life stage x length class	Mortality related to spatial and temporal variability in habitat at different scales	Pattern of flow is controlling and not the volume.
Jager <i>et al.</i> 1993 (IFIM)	IBM, movement	Smallmouth bass	SE dynamic cells/ patches	Stream flow, depth, substrate, food	Daily	Early life IBM	Physical habitat heterogeneity influences YOY growth & survival	
Minns <i>et al.</i> 1996	Population, no movement	Northern Pike	System Aggregate (WUA)	Depth, Substrate, Vegetation	Annual Static	3 stages (spawn, YOY, juvenile/adult)	Habitat carrying capacity limits life stage /population	Spawning habitat not limiting
Tyler & Rose 1997	SE-IBM	Yellow Perch	Simulated grid (open water/refuge)	Food and predator densities	Daily	YOY growing season	Relationship with prey/predator distributions and individual fitness	Predator distribution, juvenile abundance, and cell-departure rule affects cohort survival
Van Winkle <i>et al.</i> 1997	Bioenergetic, no movement	Rainbow Trout	Homogeneous	Temperature	Seasonal	Juvenile	Thermal effects on growth & survival	Model very sensitive to parameters

Model Reference	Model Type	Species	Habitat Detail	Habitat Characteristics	Temporal Resolution	Model Structure	Vital Rate Hypothesis	Conclusions
Jones <i>et al.</i> 1998	Partial population model with movement	Walleye	Patch Aggregate, some SE	Depth, water velocity, temperature, substrate	Daily, Variable	Early life stages	Effects of habitat on first year survival	Temporal mismatch between larval transport feeding habitat important
Shuter <i>et al.</i> 1998	Habitat based population	Lake trout	Static System Aggregate (WUA)	Lake area, total dissolved solids	Annual	Life Stage structure	Environmental effects on population characteristics	Lake size related to maximum fish size, age at maturity, mortality rates, yield
Bevers & Flathers 1999	Discrete reaction-diffusion model	Generic fish?	Simulated cellular grid	Inferred suitable and unsuitable	Undefined	Single stage	Habitat heterogeneity effects on dispersal mortality	Limiting habitat, strong preferences, low reproductive and dispersal rates, produce clustered distributions
PercaSpace 2004	SE super-individual, no movement	Yellow Perch	Dynamic, cellular aggregate	Temperature, Depth, Substrate, Exposure, Vegetation	Daily	Early life stage structure	Habitat interactions with spawning & early growth & survival	See Chapter 4 conclusions

Appendix 4.2: Definitions and units of coefficients and variables used in calculating bioenergetic consumption rates for yellow perch (Hanson *et al.* 1997).

Coefficient or Variable	Definition	Units
W	Weight	grams
C	Specific consumption rate	$\text{g prey} \cdot \text{g predator}^{-1} \cdot \text{day}^{-1}$
C_{\max}	Max feeding rate	$\text{g prey} \cdot \text{g predator}^{-1} \cdot \text{day}^{-1}$
p	Proportion of maximum consumption HSI-defined	
f(T)	Temperature-dependent function	
CQ	$\sim Q_{10}$	$^{\circ}\text{C}^{-1}$
CTO	Lab temp preferendum	$^{\circ}\text{C}$
CTM	Maximum temperature when consumption ceases (i.e. upper incipient lethal)	$^{\circ}\text{C}$

Appendix 4.3: Life stage specific coefficients used in calculating bioenergetic consumption rates for yellow perch (Hanson *et al.* 1997).

Coefficients	Fry	Juvenile	Adult
CA	0.51	0.25	0.25
CB	-0.42	-0.27	-0.27
CQ	2.3	2.3	2.3
CTO	29	29	23
CTM	32	32	28

Appendix 4.4: Coefficients for bioenergetic respiration rate calculations (Hanson *et al.* 1997).

Coefficients	Fry	Juvenile	Adult
RA	0.0065	0.0108	0.0108
RB	-0.2	-0.2	-0.2
RQ	2.1	2.1	2.1
RTO	32	32	28
RTM	35	35	33
ACT	4.4	1	1
SDA	0.150	0.172	0.172

Appendix 4.5: Definitions and units for coefficients and variables used in respiration and specific dynamic bioenergetic equations (Hanson *et al.* 1997)

Coefficient or Variable	Definition	Units
R	specific rate of respiration	$\text{g} \cdot \text{g}^{-1} \cdot \text{day}^{-1}$
f(T)	temperature dependence function	
S	proportion of energy lost to SDA (specific dynamic action)	
C	specific consumption rate	$\text{g prey} \cdot \text{g predator}^{-1} \cdot \text{day}^{-1}$
F	specific egestion rate	$\text{g} \cdot \text{g}^{-1} \cdot \text{day}^{-1}$
RQ	$\sim Q_{10}$	$^{\circ}\text{C}^{-1}$
RTO	optimal temperature for respiration	$^{\circ}\text{C}$
RTM	max or lethal water temperature	$^{\circ}\text{C}$
ACT	the activity multiplier is influenced by environmental factors	

Appendix 4.6: Annual totals table showing the number of potential spawning days that successfully reach each life stage, the minimum, maximum, mean and standard deviation for annual abundances at each stage for all the scenarios tested in PercaSpace.

Scenario	Statistic (nonzero)	Eggs Spawned	Survivors to Swim-up	YOY Survivors	Scenario	Statistic (nonzero)	Eggs Spawned	Survivors to Swim-up	YOY Survivors
S1E1L1	N (days)	365	228	208	S1E1L2	N (days)	365	228	174
	Min	400.00	0.11	0.001		Min	400.00	0.11	0.00
	Max	400.00	199.82	105.82		Max	400.00	199.82	78.59
	Mean	400.00	88.20	30.29		Mean	400.00	88.20	8.17
	SD	0.00	54.20	19.52		SD	0.00	54.20	16.72
S1E2L1	N (days)	365	228	208	S1E2L2	N (days)	365	228	174
	Min	400.00	0.10	0.001		Min	400.00	0.10	0.00
	Max	400.00	199.81	105.62		Max	400.00	199.81	78.50
	Mean	400.00	88.09	30.21		Mean	400.00	88.09	8.15
	SD	0.00	54.17	19.51		SD	0.00	54.17	16.71
S2E1L1	N (days)	365	223	186	S2E1L2	N (days)	365	223	143
	Min	145.22	0.001	0.001		Min	145.22	0.00	0.00
	Max	187.83	91.89	50.06		Max	187.83	91.89	41.81
	Mean	166.08	31.60	8.11		Mean	166.08	31.60	4.60
	SD	11.37	32.45	11.01		SD	11.37	32.45	9.16
S2E2L1	N (days)	365	223	186	S2E2L2	N (days)	365	223	143
	Min	145.22	0.001	0.001		Min	145.22	0.00	0.00
	Max	187.83	91.89	49.94		Max	187.83	91.89	41.78
	Mean	166.08	31.56	8.07		Mean	166.08	31.56	4.59
	SD	11.37	32.42	10.98		SD	11.37	32.42	9.15
S2*E1L1	N (days)	365	228	197	S2*E1L2	N (days)	365	228	154
	Min	399.99	0.00	0.00		Min	399.99	0.00	0.00
	Max	400.01	202.52	112.27		Max	400.01	202.52	93.11
	Mean	400.00	72.22	17.70		Mean	400.00	72.22	9.78
	SD	0.01	75.55	24.90		SD	0.01	75.55	20.13
S3E1L1	N (days)	184	126	116	S3E1L2	N (days)	184	126	62
	Min	0.35	0.01	0.01		Min	0.35	0.01	0.00
	Max	161.89	43.02	13.49		Max	161.89	43.02	1.81
	Mean	42.02	8.84	1.58		Mean	42.02	8.84	0.40
	SD	44.58	12.48	2.80		SD	44.58	12.48	0.50
S3E2L1	N (days)	184	126	116	S3E2L2	N (days)	184	126	62
	Min	0.35	0.01	0.01		Min	0.35	0.01	0.00
	Max	161.89	42.97	13.49		Max	161.89	42.97	1.81
	Mean	42.02	8.81	1.56		Mean	42.02	8.81	0.40
	SD	44.58	12.45	2.79		SD	44.58	12.45	0.50
S3*E1L1	N (days)	184	132	123	S3*E1L2	N (days)	184	132	65
	Min	399.99	0.09	0.04		Min	399.99	0.09	0.01
	Max	400.01	300.09	112.24		Max	400.01	300.09	10.03
	Mean	400.00	131.56	34.69		Mean	400.00	131.56	2.93
	SD	0.00	82.18	28.16		SD	0.00	82.18	2.62

Appendix 4.7: Table showing the number of potential spawning cells that successfully produced each life stage on the maximum abundance date, as well as the minimum, maximum, mean and standard deviation and total daily abundance at each stage for all the scenarios tested in PercaSpace.

Scenario	Statistic ($\neq 0$)	Eggs Spawned		Fry Hatched		Swim-up Survivors		YOY Survivors	
		Spring	Fall	Spring	Fall	Spring	Fall	Spring	Fall
S1E1L1	N(cells)	400	--	334	398	294	400	331	280
	Min	1000	--	81	377	10	328	1	248
	Max	1000	--	896	870	760	787	526	505
	Mean	1000.00	--	589.36	670.12	519.44	499.56	145.07	377.94
	SD	0.00	--	184.82	71.61	181.63	52.77	115.35	37.62
	Total	400000	--	196847	266706	152714	199823	48019	105822
	Date	Any Day	--	5/14/99	10/17/99	5/1/99	10/3/99	5/22/99	10/13/99
S2E1L1	N(cells)	320	--	292	318	294	320	278	276
	Min	976	--	24	215	7	140	1	104
	Max	312	--	606	567	593	533	192	401
	Mean	586.98	--	347.79	56.79	278.38	287.16	65.70	181.40
	SD	171.92	--	122.59	76.99	113.87	95.31	40.54	51.09
	Total	187834	--	101556	113459	81845	91893	18264	50065
	Date	7/12/99	--	4/30/99	10/17/99	5/3/99	10/3/99	5/15/99	10/12/99
S3E1L1	N(cells)	177	186	158	109	126	109	158	--
	Min	341	387	131	133	170	31	15	--
	Max	891	856	600	662	593	392	193	--
	Mean	511.22	582.72	330.00	419.28	341.42	257.78	85.33	--
	SD	121.66	117.38	80.47	92.26	87.78	67.72	39.48	--
	Total	90486	108386	52140	45702	43019	28098	13490	--
	Date	5/15/99	10/29/99*	5/15/99	10/30/99	5/3/99	10/30/99	5/15/99	--
S1E2L1	N(cells)	400	--	340	397	340	400	330	280
	Min	1000	--	64	38	47	79	1	137
	Max	1000	--	896	870	650	787	527	505
	Mean	1000.00	--	577.65	666.70	447.08	498.63	145.48	377.21
	SD	0.00	--	189.53	83.22	146.95	56.76	115.28	40.23
	Total	400000	--	196402	264678	152006	199451	48008	105620
	Date	Any Day	--	5/15/99	10/17/99	5/15/99	10/3/99	5/22/99	10/13/99
S2E2L1	N(cells)	320	--	290	317	293	320	278	276
	Min	976	--	2	18	2	25	1	82
	Max	312	--	606	567	593	533	193	401
	Mean	586.98	--	348.06	355.04	277.50	286.81	65.70	180.94
	SD	171.92	--	123.96	80.94	115.65	96.08	40.57	51.42
	Total	187834	--	100938	112548	81308	91778	18264	49940
	Date	7/12/99	--	4/30/99	10/17/99	5/3/99	10/3/99	5/14/99	10/12/99
S3E2L1	N(cells)	177	186	158	109	126	109	158	--
	Min	341	387	131	133	2	31	15	--
	Max	891	856	600	662	593	392	193	--
	Mean	511.22	582.72	330.00	419.28	339.1	257.78	85.36	--
	SD	121.66	117.38	80.47	92.26	92.76	67.72	39.46	--
	Total	90486	108386	52140	45702	42974	28098	13490	--
	Date	5/15/99	10/29/99*	5/15/99	10/30/99	5/3/99	10/30/99	5/15/99	--

Scenario	Statistic ($\neq 0$)	Eggs Spawned		Fry Hatched		Swim-up Survivors		YOY Survivors	
		Spring	Fall	Spring	Fall	Spring	Fall	Spring	Fall
S1E1L2	N(cells)	400	--	334	398	294	400	235	331
	Min	1000	--	81	377	10	328	1	89
	Max	1000	--	896	870	760	787	158	409
	Mean	1000.00	--	589.36	670.12	519.44	499.56	28.89	237.43
	SD	0.00	--	184.82	71.61	181.63	52.77	27.51	83.45
	Total	400000	--	196847	266706	152714	199823	6789	78587
	Date	Any Day	--	5/14/99	10/17/99	5/1/99	10/3/99	5/15/99	10/4/99
S2E1L2	N(cells)	320	--	292	318	294	320	199	312
	Min	976	--	24	215	7	140	1	30
	Max	312	--	606	567	593	533	78	315
	Mean	586.98	--	347.79	56.79	278.38	287.16	16.30	134
	SD	171.92	--	122.59	76.99	113.87	95.31	14.20	62.55
	Total	187834	--	101556	113459	81845	91893	3242	41808
	Date	7/12/99	--	4/30/99	10/17/99	5/3/99	10/3/99	5/9/99	10/3/99
S3E1L2	N(cells)	177	186	158	109	126	109	97	--
	Min	341	387	131	133	170	31	1	--
	Max	891	856	600	662	593	392	62	--
	Mean	511.22	582.72	330.00	419.28	341.42	257.78	18.67	--
	SD	121.66	117.38	80.47	92.26	87.78	67.72	10.55	--
	Total	90486	108386	52140	45702	43019	28098	1810	--
	Date	5/15/99	10/29/99*	5/15/99	10/30/99	5/3/99	10/30/99	5/2/99	--
S1E2L2	N(cells)	400	--	340	397	340	400	235	331
	Min	1000	--	64	38	47	79	1	51
	Max	1000	--	896	870	650	787	159	409
	Mean	1000.00	--	577.65	666.70	447.08	498.63	28.80	237.15
	SD	0.00	--	189.53	83.22	146.95	56.76	27.52	84.31
	Total	400000	--	196402	264678	152006	199451	6770	78498
	Date	Any Day	--	5/15/99	10/17/99	5/15/99	10/3/99	5/15/99	10/4/99
S2E2L2	N(cells)	320	--	290	317	293	320	198	312
	Min	976	--	2	18	2	25	1	6
	Max	312	--	606	567	593	533	78	315
	Mean	586.98	--	348.06	355.04	277.50	286.81	16.30	133.91
	SD	171.92	--	123.96	80.94	115.65	96.08	14.24	62.70
	Total	187834	--	100938	112548	81308	91778	3228	41779
	Date	7/12/99	--	4/30/99	10/17/99	5/3/99	10/3/99	5/9/99	10/3/99
S3E2L2	N(cells)	177	186	158	109	126	109	97	--
	Min	341	387	131	133	2	31	1	--
	Max	891	856	600	662	593	392	62	--
	Mean	511.22	582.72	330.00	419.28	339.1	257.78	18.7	--
	SD	121.66	117.38	80.47	92.26	92.76	67.72	10.52	--
	Total	90486	108386	52140	45702	42974	28098	1710	--
	Date	5/15/99	10/29/99*	5/15/99	10/30/99	5/3/99	10/30/99	5/2/99	--
S2*E1L1	N(cells)	320	--	298	318	298	320	287	253
	Min	412-811	--	190	493	124	309	1	263
	Max	1764-2285	--	1517	1301	1255	1175	447	795
	Mean	1250	--	800.94	818.26	636.38	632.87	145.16	443.75
	SD	205.86-	--	246.43	176.55	217.72	210.08	96.86	106.78
	Total	400000	--	238681	260206	189641	202517	41660	112270
	Date	Any Day	--	5/9/99	10/17/99	5/9/99	10/3/99	5/10/99	10/13/99

Scenario	Statistic ($\neq 0$)	Eggs Spawned		Fry Hatched		Swim-up Survivors		YOY Survivors	
		Spring	Fall	Spring	Fall	Spring	Fall	Spring	Fall
S3*E1L1	N(cells)	1-177	6-300	2	1	2	1	3	--
	Min	1239-	634-59653	179391	305494	146680	233206	34134	--
	Max	3468-	2001-	185264	305494	153406	233206	42928	--
	Mean	2259.88-	1333.33-	182327.5	305494	150043	233206	37412.33	--
	SD	0-	257.24-	4152.84	--	4756	0	4804.98	--
	Total	400000	400000	364655	305494	300086	233206	112237	--
	Date	4/4/99-	10/23/99-	6/15/99	10/10/99	6/15/99	10/10/99	7/14/99	--
S2*E1L2	N(cells)	320	--	298	318	298	320	206	309
	Min	412-811	--	190	493	124	309	1	74
	Max	1764-2285	--	1517	1301	1255	1175	184	646
	Mean	1250	--	800.94	818.26	636.38	632.87	38.56	301.34
	SD	205.86-	--	246.43	176.55	217.72	210.08	34.27	127.84
	Total	400000	--	238681	260206	189641	202517	7944	93113
	Date	Any Day	--	5/9/99	10/17/99	5/9/99	10/3/99	5/10/99	10/4/99
S3*E1L2	N(cells)	1-177	6-300	2	1	2	1	104	--
	Min	1239-	634-59653	179391	305494	146680	233206	1	--
	Max	3468-	2001-	185264	305494	153406	233206	343	--
	Mean	2259.88-	1333.33-	182327.5	305494	150043	233206	96.4	--
	SD	0-	257.24-	4152.84	--	4756	0	61.57	--
	Total	400000	400000	364655	305494	300086	233206	10026	--
	Date	4/4/99-	10/23/99-	6/15/99	10/10/99	6/15/99	10/10/99	5/2/99	--